HOLOCENE GLACIATION OF THE CENTRAL BROOKS RANGE, ALASKA

by

James M. Ellis

A dissertation submitted to the Faculty of the Graduate School of State University of New York at Buffalo in partial fulfillment of the requirements for the degree of Doctor of Philosophy

February 1982

ABSTRACT

The central Brooks Range was glacierized in higher, north-facing cirques during the past ~5000 yr. Lichenometric mapping of deposits downslope of over 50 cirque glaciers, along with five radiocarbon dates associated directly with Neoglacial moraines, defines seven major expansions of similar magnitude during this interval. The last major advance is dated at 390 ± 100 yr B.P. (A.D. 1410-1600). Initial recession from this advanced position was slow with the ice margins close to their maximum extents until A.D. 1640-1750. Retreat was most rapid after A.D. 1870 and decelerated after the mid 1900's based on historical photographs and lichenometry. Recession since this most recent Neoglacial expansion has covered 150-700 m and continues at present.

Radiocarbon analysis of dead moss that is emerging undisturbed from beneath a receding glacier toe dates a Neoglacial advance across the site at 1120 ± 180 yr B.P. The situation suggests that for the past millennium cirque glaciers were continuously in more advanced positions than they are under the present climatic regime. Three expansions dated lichenometrically (± 20% age reliability) and with radiocarbon methods at 1150 ± 200, 800 ± 150, and 390 ± 100 yr B.P. occurred during this glaciologically favorable time. However, from 1150 back to at least 1800 yr B.P. climatic conditions apparently were unfavorable for glaciers. Before 1800 yr B.P. four expansions are lichenometrically dated at ~1800 ± 400, 2900 ± 600, 3500 ± 700, and 4400 ± 1000 yr B.P. A climatic optimum ranges from early to

middle Holocene time based on a lack of cirque glacier deposits and stabilization of rock glacier surfaces in early Holocene time. The early Holocene age for rock glaciers is determined relatively from their advanced stage of lichen, soil, and boulder weathering development.

The cirque glacier advances in the central Brooks Range were of similar magnitude, accompanied by equilibrium-line altitude (ELA) depressions of 100 to 200 m below present. Reconstructions of Neoglacial maxima utilized an accumulation area ratio (AAR) of 0.67 and imply a lowering of ~1°C from present summer temperatures during major expansions. In the east-central Brooks Range these maxima ELA's rise northward across the mountain mass at ~5 m km^{-1}.

Although glaciers across the central Brooks Range have similar dimensions and orientations, varying environments promote formation of different types of Neoglacial moraines. Neoglacial moraines without ice cores occur in cirques with minimal bedrock exposed in cirque cliffs (~80 m) and extensive direct radiation energy during the ablation season (~92%). The lichenometric record is most distinct on these moraines because of substrate stability. Three out of four moraines studied are cored with glacial ice. The most important factor controlling formation of this type of ice deposit is amount of bedrock exposed in cirque cliffs (~170 m). Core preservation is also enhanced by receipt of only ~78% of the potential solar energy. Neoglacial moraines situated as transition zones upslope of older rock glaciers are environmentally and morphologically similar to glacier-cored moraines; however, some form where as

little as 1% direct radiation is received and vertical headwall exposures exceed 400 m.

Cirque glacier deposits in the granitic terrain of the Arrigetch Peaks of the west-central Brooks Range are more extensively glacier cored and in deeper cirques than those in the sedimentary terrain of Anaktuvuk and Atigun Passes farther to the east. Their cirque environments differ respectively in direct radiation energy received at the deposit (65 $\pm$ 20% versus 85 $\pm$ 10%), potential debris supply as measured by height of bedrock in cirque cliffs (245 $\pm$ 135 versus 130 $\pm$ 90 m), and ELA depression from present mean glacier altitude during Neoglacial maxima (130 $\pm$ 60 m in contrast with 70 $\pm$ 35 m). Nevertheless, lichenometric mapping of Neoglacial moraines across the central Brooks Range suggests similar glacial histories despite varying cirque environments and degree of coring by glacial ice.

ACKNOWLEDGEMENTS

I am most grateful to Dr. Parker Calkin for introducing geomorphology to me in 1976 and then for providing the environment and support necessary to produce this study. His involvement ranged from finagling critical helicopter rides in the field to guiding my publication efforts. Together we hiked to help unravel the Holocene glacial history of the Brooks Range.

I am also very appreciative to Dr. Thomas Hamilton who went out of his way to show me the central Brooks Range. His continual support expanded the scope of our research from a local study to one spanning a third of the mountain range. Between field seasons he kindly and thoroughly reviewed manuscripts and exchanged ideas freely.

My three field assistants deserve much thanks for their dedication, good humor, and combined help on surveying, logistics, and mapping. I especially thank Michael Bruen ('78) for setting a solid foundation on our glaciologic study, Steven Walti ('79) for helping to map the Arrigetch Peaks, and Thomas Lowell ('80) for pursuing soil studies in spite of adverse weather.

My gratitude is extended to Dr. Lawrence Onesti who arranged and provided the all-important base camp and vehicular transport within the oil pipeline corridor from 1977 to 1980; Christopher Smith assisted in '78 and '79. Along the corridor David Witt of the University of Alaska's Logistic Services (Division of Life Sciences), Alyeska, ALASCOM, Placid Oil, Northwest Pipeline, and CRREL provided invaluable logistical assistance. In particular the generous people

stationed at various construction camps on the Chandalar Shelf assured the success of this project.

I wish to thank Drs. Brian Whalley and Peter Birkeland for respectively encouraging me to examine the environments and soils of alpine moraines and rock glaciers. Our use of lichens for dating was enhanced by Dr. Patrick Webber, Dr. W. A. Weber, and David Cooper. The faculty and students at INSTARR, especially Drs. J. T. Andrews, W. N. Mode, and W. McCoy, provided encouragement and guidance during my semester stay in 1979. The assistance of Dr. Andre Roy and Lynn Doyle Ellis in multivariate analysis and computerization of data is greatly appreciated.

This study was funded by the National Science Foundation (Department of Polar Programs) through the Research Foundation of State University of New York. Funds for the photographic survey were largely provided by the Society of the Sigma Xi and the Graduate Resource Access Development project at State University of New York at Buffalo. In addition, the G.I. Bill provided substantial support to my graduate education.

Unending support and encouragement from my parents, Wright and Mary Ellis, and wife, Lynn Doyle Ellis, is gratefully acknowledged. They never gave up as the years rolled along.

CONTENTS

FIGURES

TABLES

PLATE

INTRODUCTION

The cirques and high mountain slopes of the Brooks Range, Alaska, in common with many other alpine glacial areas, display an assemblage of cirque glaciers and associated moraines as well as prominent rock glaciers. A basic goal of this study is to concentrate on the Holocene record furnished by cirque glaciers within the central Brooks Range in order to delineate climatic variations through time. This goal is approached by 1) characterizing past and present cirque glaciers, their environments, and distribution patterns with emphasis on distinguishing types of moraines and rock glaciers that may reflect differing orographic climatic controls, and 2) applying this physical analysis to help construct Holocene glacial and climatic histories and to determine the magnitude of Holocene glacial fluctuations in the central Brooks Range.

Determination of the history of Holocene glacial fluctuations has been aided by the development of lichenometry as an absolute dating tool in the central Brooks Range, supplemented by historical glacier photographs and relative dating methods related to weathering and soil properties. Such techniques, with reconstructions of previous equilibrium-line altitudes (ELA's), allow a detailed assessment of climatic change through the Holocene. In addition, the study provides a meaningful complement to glaciologic, climatic, palynologic, and dendrochronologic studies in northern Alaska and in other arctic and alpine regions of the world.

Three field areas within the central Brooks Range (Fig. 1) were

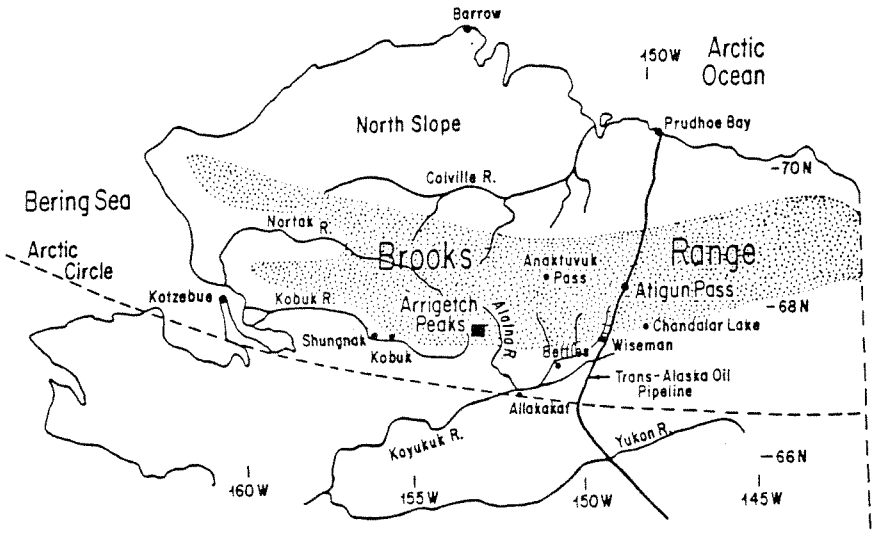

Figure 1. Location map of the central Brooks Range, northern Alaska.

studied in order to establish a chronology of glacial events. The Atigun Pass area (Fig. 2) was chosen for the main portion of the work because of easy access to a large number of glaciers and proximity to detailed climatic records associated with recent pipeline construction and operation. The centrally located Anaktuvuk Pass (Fig. 3) is significant because of previous reconnaissance work undertaken on deposits of cirque glaciers (Detterman and others, 1958; Porter, 1966). Glaciers in the Arrigetch Peaks (Fig. 4), the third area studied, are of special interest because of their different climatic and lithologic setting and because of a relatively long photographic record of glacial terminal positions (Hamilton, 1965a).

Some of the basic questions to be considered in this study are

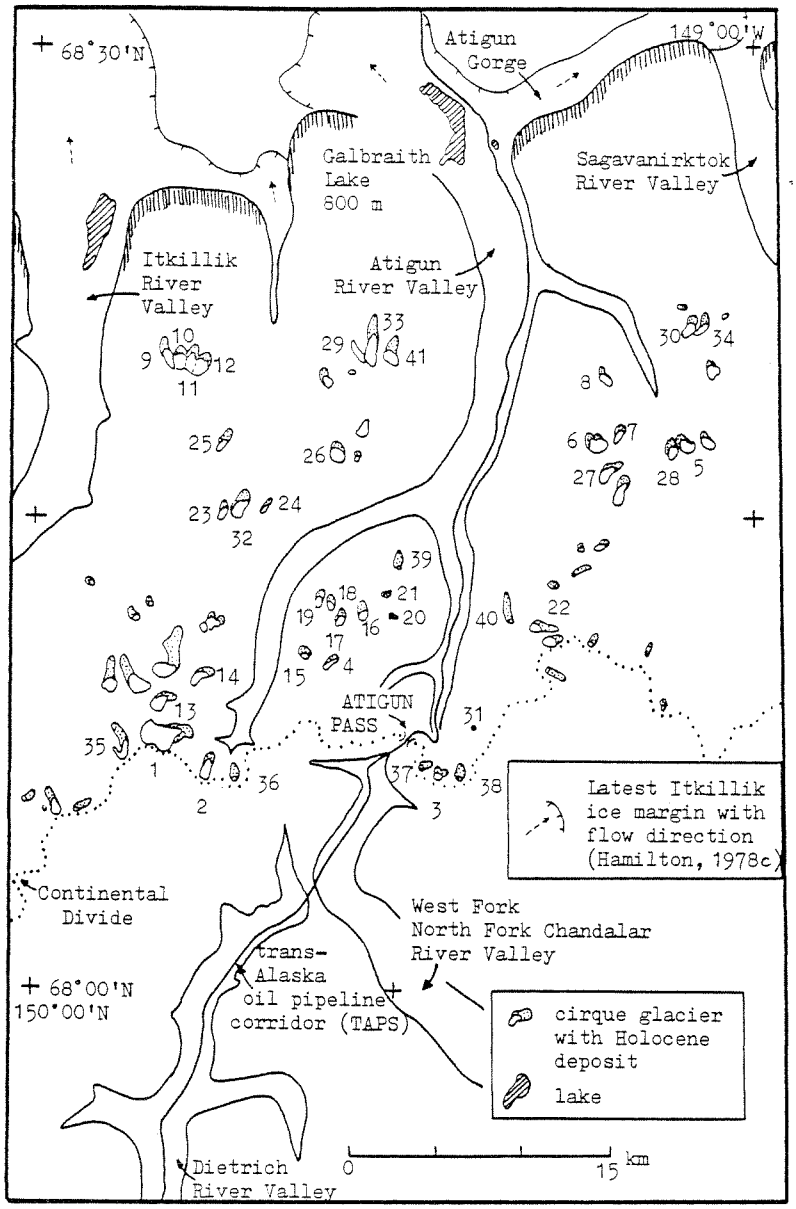

Figure 2. Location map of the Atigun Pass area, east-central Brooks Range. Glaciers studied are numbered and given informal names (Appendix A). Glaciers 1-12 have Neoglacial moraines largely without ice cores, 13-33 have moraines with cores of glacier ice, and those numbered 35-41 have Neoglacial moraines superimposed upslope of an older, rock glacier tongue.

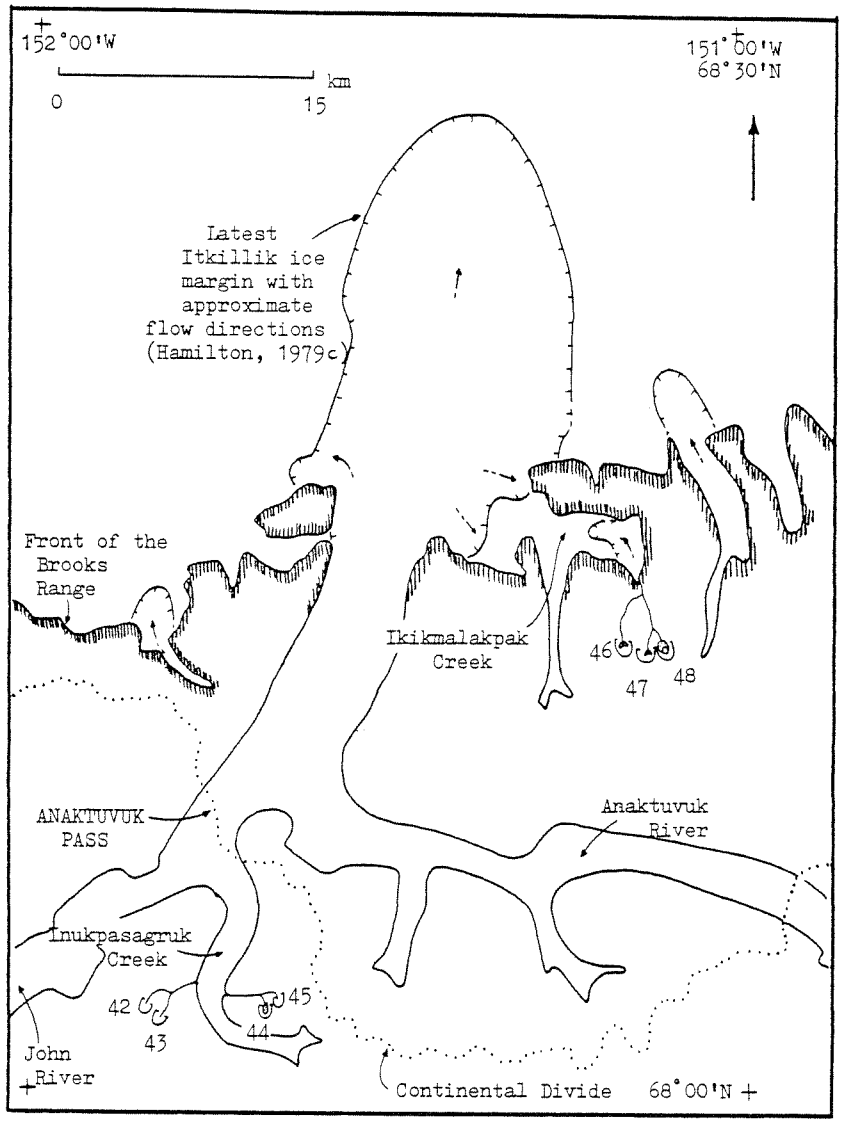

Figure 3. Location map of the Anaktuvuk Pass area, central Brooks Range. Empty cirques of Pleistocene age are noted as 42, 43, and 45; a tongue-shaped rock glacier with no visible glacier core is in cirque 44; lobate rock glaciers are located in cirques 46 and 47; and a cirque glacier fronted by a Neoglacial moraine with an ice core is in cirque 48 (see Appendix A).

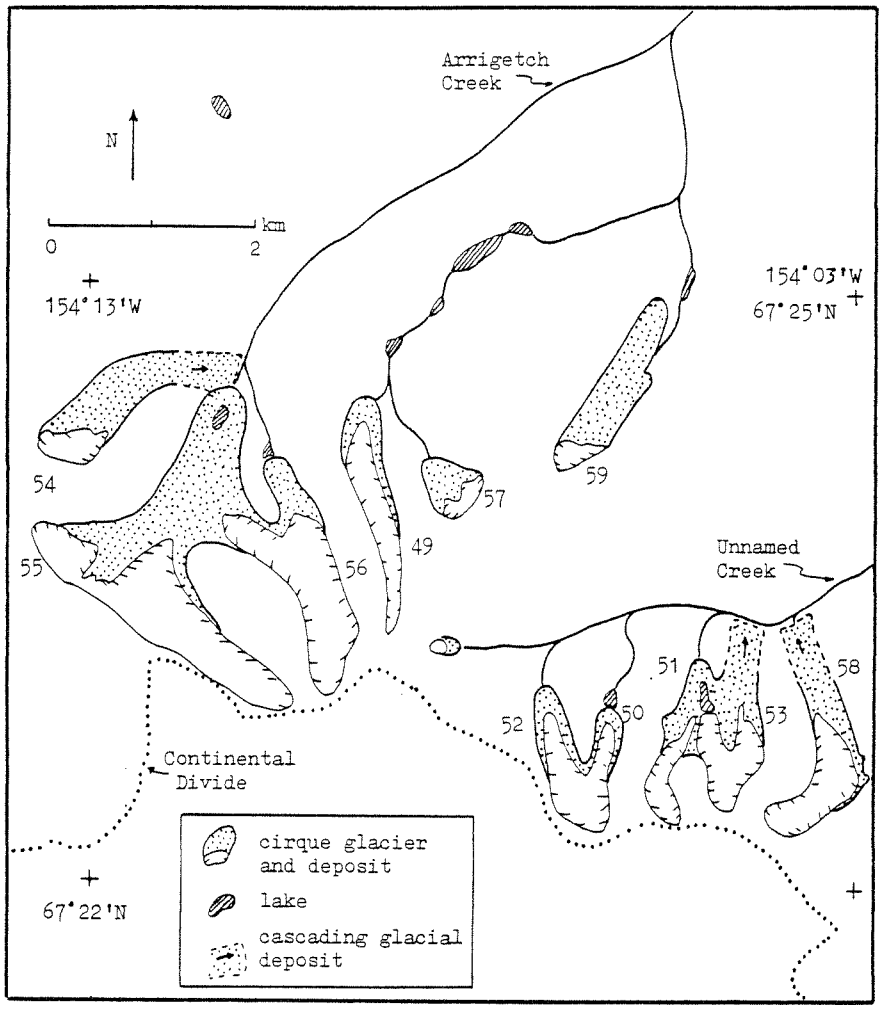

Figure 4. Location map of the Arrigetch Peaks, southwest-central Brooks Range. Glaciers 49-51 are fronted by Neoglacial moraines without ice cores; glaciers 52-58 have glacier-cored moraines; and a tongue-shaped rock glacier with an exposed glacier core and Neoglacial moraine upslope is numbered 59 (see Appendix A).

as follows:

a) Which environmental factors best discriminate between different types of cirque glacier deposits and which ones best explain the state of activity for rock glaciers?

b) Are chronologies derived for the various types of cirque glacier deposits significantly different?

c) Are there physical and chronological differences between cirque glacier deposits in the three different study areas across the central Brooks Range?

The extent of Quaternary glaciers in Alaska has been summarized by Karlstrom (1964), Coulter and others (1965), and Péwé (1975). Details of the central Brooks Range late Cenozoic glaciation and stratigraphy were reviewed more recently by Hamilton and Porter (1975) and Hamilton (1978a). During the last major Pleistocene event, the Itkillik Glaciation (Detterman, 1953), glaciers reached just beyond the mountain front (Detterman and others, 1958; Porter, 1964; Hamilton, 1969; Hamilton and Porter, 1975). Itkillik I moraines represent a maximum ice advance whose entire history may lie beyond the range of conventional radiocarbon dating (Hamilton, 1979a, 1979b, 1980a, 1980b). The northern terminus of the last and least intense Itkillik event, termed the "latest Itkillik" (Hamilton, 1978c, 1979c), is represented in Atigun and Anaktuvuk valleys by arcuate end moraines ~45 km north of the Continental Divide (Figs. 2, 3). This advance culminated about 13,000 to 12,500 yr B.P., and glacier tongues retreated from the area during the following 500 to 1000 yr interval. Contemporaneous retreat from the Itkillik Valley

is suggested, and radiocarbon dates in the Sagavanirktok Valley to the east (Fig. 2) demonstrate relatively ice-free conditions by 11,500-10,500 yr B.P.

Most valleys of the central Brooks Range were free of Pleistocene glaciers by the beginning of the Holocene (Hamilton and Porter, 1975), when streams generally were incising through glacial deposits to approach their modern levels (Hamilton, 1980c). Snowline has risen on the order of 600 m from the time of maximum Itkillik I advances (Hamilton and Porter, 1975).

Previous studies undertaken on glacial deposits at valley heads and relative to Holocene glaciation have been of a reconnaissance nature. Relatively undissected and unvegetated glacial deposits at thresholds of cirques were referred to the Fan Mountain Glaciation based on work in the Alapah Mountain area 60 km west of Atigun Pass (Detterman and others, 1958). Near Anaktuvuk Pass, Porter (1964, 1966) recognized two end moraines; an inner set within the cirques (Fan Mountain II) and an outer set (Fan Mountain I) lying within three kilometers of cirque thresholds. Porter and Denton (1967) considered these to be post-Hypsithermal (Neoglacial) in age and suggested that Fan Mountain moraines were probably built within the last several centuries. A two-stage, Fan Mountain record was suggested by Hamilton (1965a) for the Arrigetch Peaks area. Snowline was several hundred meters higher in the Neoglacial than in the Pleistocene.

Prior to glacial and glaciologic work associated with this study (Ellis, 1978; Ellis and Calkin, 1979; Bruen, 1980a; Calkin

and Ellis, 1980, 1981; Ellis and others, 1981), geomorphic work at the valley heads in the Atigun Pass area had largely been confined to general engineering mapping alongthe trans-Alaska oil pipeline and haul road corridor (TAPS; Fig. 1; Ferrians, 1971; Kachadoorian, 1971; unpub. Alyeska Pipeline Company data) and surficial geologic mapping (scale 1:250,000) by the U.S. Geological Survey (Hamilton, 1978b, 1978c). Surficial geologic maps have also been compiled at this scale for the Anaktuvuk Pass and the Arrigetch Peaks areas by Hamilton (1979c, 1980d, unpub. data). In addition, Hamilton (1979a, 1979b, 1980a, 1980b, 1980c) has done extensive stratigraphic work on episodic Holocene alluviation in the central Brooks Range.

Preliminary studies of cirque and cirque glacier distribution patterns have been undertaken by the U.S. Geological Survey (1978) for the Brooks Range (scale 1:250,000) and by Porter (1966) in the Anaktuvuk Pass area. Considerably more information can be extracted from the distribution of cirque glacier altitudes if the deposits immediately downslope are also analyzed (Ellis and Calkin, 1979). Similarly, a Holocene chronology of glacier expansions and retreats based on detailed lichenometric mapping (Calkin and Ellis, 1980) is much morecomplicated than envisioned by these earlier studies.

GEOGRAPHICAL SETTING AND CLIMATE

The Brooks Range is an east-west trending mountain mass lying above the Arctic Circle. This range has been repeatedly glaciated since early Pleistocene time (Hamilton, 1978a). The three study

areas are all above the limit of the boreal-spruce forest and within the zone of continuous alpine permafrost (Ferrians, 1965). Vegetation above tree line, at 600 to 700 m altitude, consists of shrubby tundra with alder and dwarf birches which gives way to a mixed, herbaceous tundra vegetation at higher elevations (Brown, 1980, p. 36). Bouldery, cirque glacier moraines are unvegetated where located near receding ice margins; however, lichens, algae, mosses, sedges, and grasses can cover these deposits and rock glaciers to varying degrees (Spetzman, 1959)..

Although records are sporadic and difficult to compare, climatic data from small villages at low altitudes along the south flank of the central Brooks Range show a general eastward decline in annual precipitation (Table 1; Ellis and others, 1981). In addition, summer temperature, annual snowfall, and total precipitation decrease with latitude across the central Brooks Range. However, snowfall and total precipitation increase with altitude (Fig. 5; Hamilton, 1966; Johnson and Hartman, 1969, p. 62-79; Haugen, 1979; Brown, 1980, p. 9-19; Calkin and Ellis, 1980). Areas marginal to cirque glaciers and downslope generally remain free of snow from late June through early August. Pleistocene and Holocene snowlines, abandoned cirques, and modern glaciers increase in altitude north- and eastward in the central Brooks Range (Porter, 1966; Péwé, 1975, p. 26-32; Ellis and Calkin, 1979; Hamilton, 1978c, 1979c, 1980d, unpub. data; Ellis and others, 1981).

TABLE 1. AVERAGE ANNUAL PRECIPITATION RECORDED IN VALLEYS ALONG SOUTH FLANK OF THE CENTRAL BROOKS RANGE[a]

Region	Stations (with altitudes in meters)	Average Annual Precipitation (millimeters)
Middle Kobuk	Kobuk (~50) Shungnak (~50)	400 - 430
Middle Koyukuk	Allakaket (105) Bettles (189)	330 - 360
Upper Koyukuk	Wiseman (366)	280 - 300
Upper Chandalar	Chandalar Lake (555)	230 - 280

[a]U.S. Weather Bureau (1915-1979); from Ellis and others (1981).

Atigun Pass Area

The work described in this study has been undertaken mostly near the Atigun Pass; within the headwaters of the Atigun, Itkillik, Sagavanirktok, and West Fork North Fork Chandalar rivers (Fig. 2). The area is underlain by thrust-faulted and steeply-folded marine and non marine sedimentary rocks of late Devonian through Permian age (Brosgé and others, 1979). Most of the higher peaks and glacierized cirques in this region are composed of siliceous conglomerates and sandstones or quartzites of the resistant Devonian Kanayut Conglomerate (Ellis, 1978). These peaks rise to altitudes of 2300 m, forming over 1000 m of relief above U-shaped valley floors. The northernmost portion of this region is made of a thick sequence of the crystalline Lisburne limestone. Less resistant, phyllitic

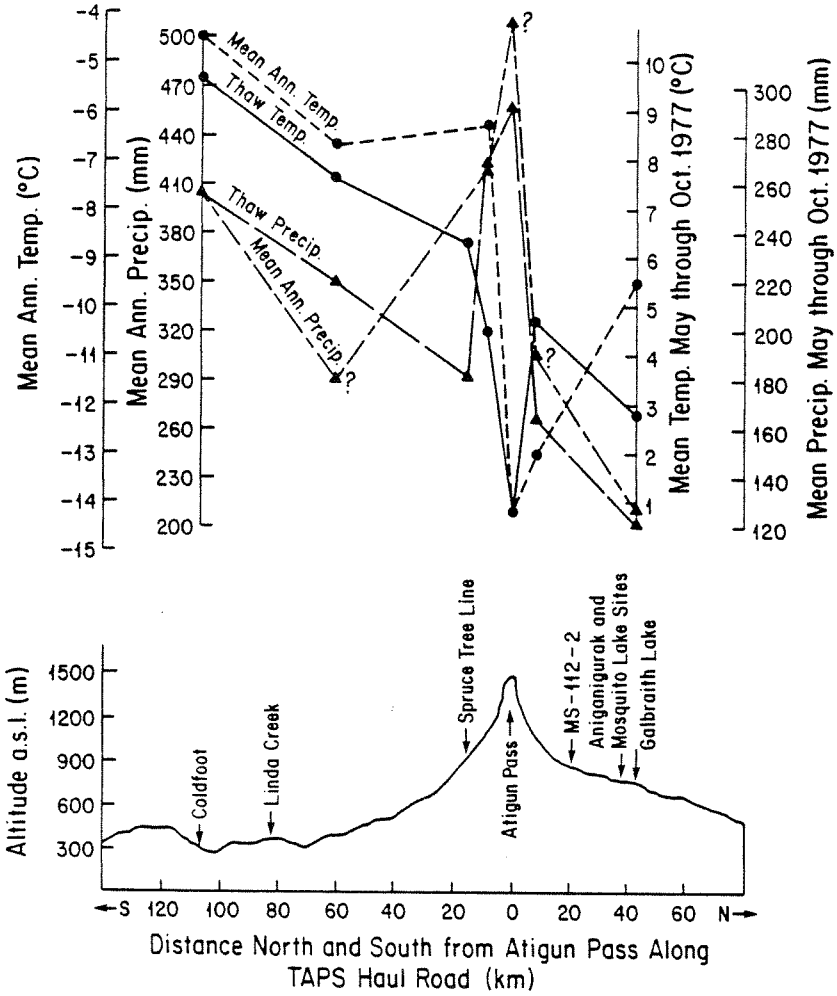

Figure 5. Temperature and precipitation transects along the trans-Alaska pipeline haul road (TAPS) between Coldfoot (south of Wiseman) and Galbraith Lake construction camps. Means are derived from measurements between 1975 and 1979. Question marks (?) show estimates of mean annual precipitation obtained by doubling thaw season (May through October) data. Adapted with minor modifications from Haugen (1979; from Calkin and Ellis, 1980).

Hunt Fork Shale dominates immediately south of the Divide; the Skagit Limestone and metamorphic rocks are found farther to the south (Brosgé and Reiser, 1974).

At least 130 cirque glaciers lie within this area; 97% of these occur north of the Continental Divide. Here the Pacific-Arctic drainage divide correlates with the transition zone between the continental climate of Alaska's interior with its temperature extremes, and the generally cooler arctic regime of the North Slope (Berg and others, 1978).

Climatic data collected along the TAPS corridor since 1975 (Haugen, 1979; Brown, 1980) indicate temperatures above freezing are attained in May through September in the Pass area, but low insolation during the rest of the year allows temperatures to reach -45°C. The mean annual temperature of Atigun Pass (1440 m a.s.l.) is about -14°C. June, July, and August mean temperatures at Atigun Pass averaged 2.1, 7.3, and 7.3°C, respectively, from 1976 through 1978 based on extrapolation of Cold Regions Research and Engineering Laboratory (CRREL) data (Haugen, 1979). CRREL data, combined with discontinuous records from Anaktuvuk Pass (Porter, 1966) and glacier snow pit studies (Bruen, 1980b), suggest annual precipitation at Atigun Pass ranges between 400 and 700 mm, of which about 50% is snow.

Anaktuvuk Pass Area

Anaktuvuk Pass is located in a ~5 km wide, U-shaped valley at an altitude of only 650 m (Figs. 1, 3; Porter, 1966). Field work

was undertaken in cirques incised within the Kanayut Conglomerate. These basins drain into Inukpasagruk and Itikmalakpak Creeks; tributaries to the south-flowing John and north-flowing Anaktuvuk rivers, respectively.

There are fewer glacierized cirques here than farther east around the higher Atigun Pass area (Porter, 1966, Fig. 20a; Ellis and Calkin, 1979, Fig. 8). Climatic data are meager but Porter (1966, p. 13-16) estimated that the mean annual temperature and annual precipitation at the Pass was about -10°C and 300 mm.

The Arrigetch Peaks

The Arrigetch Peaks occupy an area of about 110 km^2 on the south flank of the west-central Brooks Range (this section condensed from Ellis and others, 1981). Summits rise to altitudes of 2150 m, some to heights of 1200 m above valley floors. More than 40 deeply incised cirques surround individual peaks and line the north-facing walls of glacial troughs; 11 of these basins are occupied by glaciers to 2.2 km long (Fig. 4). Drainage toward the northwest, north, and east is via tributaries of the Alatna River, which flows south into the Koyukuk. Drainage southwest and south is through the headwaters of the Kobuk River west into Kotzebue Sound.

The Arrigetch consist of granitic orthogneiss of Cretaceous age (Nelson and Grybeck, 1980) which is characterized by nearly vertical slopes. These protrude as much as 1000 m above the more erodible limestone, shale, and schist of the surrounding terrain.

The moisture regime of the Arrigetch area appears to be transitional between the wetter maritime conditions of the western Alaskan coast and the relatively dry continental climate of interior Alaska. Winter snowfall is heavier and snow-avalanche activity appears to be greater than farther east in the central Brooks Range. Summers are short and generally cool; coastal storms commonly invade from the west via the broad Noatak and Kobuk rivers. The sparse climatic data (including Table 1) suggest the Arrigetch Peaks is slightly warmer and wetter than the more eastward Atigun Pass area.

METHODS

Planimetric and Distribution Analysis

Planimetric control in the Atigun Pass area was established by U.S. Geological Survey 1:80,000 aerial photographs (Series GS-VCIK, August, 1970) complemented by Chandalar Lake and Philip Smith Mountains 1:63,360 topographic sheets. In the Anaktuvuk Pass and the Arrigetch Peaks areas planimetry was based on oblique photographs and on U.S. Geological Survey 1:250,000 Chandler Lake and Survey Pass sheets. These sheets have not been field checked by the U.S. Geological Survey; on a few glaciers significant errors in contouring of glacial margins were corrected by hand, based on oblique photographs taken in the field.

Altitudes were taken from the 1:63,360 and 1;250,000 topographic sheets which display contour lines at 100 ft (30 m) intervals and 200 ft (60m) intervals, respectively. The accuracy of these

altitudes is estimated to average ± the interval. Mean altitudes for each glacier were measured at the topographic midpoint of ice that was relatively debris free. Altitudes for their downslope debris lobes were measured at the crest of the debris terminus or at cirque thresholds for cascading deposits. Altitudes for tongue and lobate rock glaciers were taken at the crest of the debris snout.

Orientations of glaciers, cirque headwalls, and snouts of moraines and rock glaciers were plotted to the nearest 10°. The mean of these orientations or the vector resultant was derived by vector summation (Evans, 1977). This method gives the general trend of the distribution, strength of the mean orientation (aspect), and allows numerical comparison with other distributions (Evans, 1969; Ellis and Calkin, 1979).

The concentration of aspects along the vector resultant, termed the vector strength (K), is obtained by dividing the length of the resultant (R) by the total length of the individual vectors (N). The vector strength (K) represents the degree of asymmetry for the distribution, for example the asymmetry tends to be high if the range of aspects about the mean is low. Degree of asymmetry is expressed in the following terms (Evans, 1977).

Vector Strength (K)	Degree of Asymmetry
80-100%	extremely asymmetric
60-80	strongly asymmetric
40-60	markedly asymmetric
20-40	weakly asymmetric
<20	symmetric

A laboratory study based largely on interpretation of aerial photographs and topographic sheets encompassed 133 glaciers and 573

rock glaciers in a ~4000 km^2 area around Atigun Pass (Plate 1). It emphasized spatial and directional characteristics of glaciers and rock glaciers (Ellis and Calkin, 1979).

Field data for this study were gathered at more than 50 cirque glaciers in the three field areas and on rock glaciers in the Atigun and Anaktuvuk Pass areas. The cirque glaciers and their deposits were analyzed for area, altitude, aspect, topographic horizon, direct radiation energy received, potential debris supply, and lichenometric patterns. All were planimetrically reconstructed to their previous shape during their Neoglacial maxima. Horizons, altitudes, aspects, and slopes of periglacial landforms, including tongue-shaped and lobate rock glaciers, were measured in the field.

Terrain Screening

The shadowing effect of surrounding mountainous terrain on glacial and periglacial landforms was initially analyzed in the field by plotting the horizon at 143 survey sites located on 116 landforms (Table 2, Appendix F). These horizon surveys were made at 015° increments (24 horizon inclinations per site) with a Brunton compass attached vertically to a tripod (Appendix J). Several landforms were mapped before this instrumentation was ready or when cloudbase was below the horizon; their horizons were estimated trigonometrically at 015° increments from the topographic sheets.

Each landform's horizon was superimposed upon the sun's 24 hr path at +20° declination (~24 July) to determine the times of sun

TABLE 2. DESIGNATIONS AND NUMBERS OF GLACIAL AND PERIGLACIAL LANDFORMS MEASURED FOR TERRAIN SCREENING

Landform Groups	Terrain Screening Designation (series)	Number of Landform Samples
Glacial groups		
Cirque glacier (CG)	000	8
Non glacier-cored moraine (M)	100	15
Ice-cored moraine (Mg)	200	19
Glacier-cored moraine (MG)	300	13
Glacier-cored transition zone upslope of rock glacier (TRGC)	400	8
Periglacial groups		
Tongue-shaped rock glacier (TRG)	500	5
Active lobate rock glacier (LRGa)	600	19
Partially active lobate rock glacier (LRGp)	700	9
Inactive lobate rock glacier (LRGi)	800	19
Empty cirque (C)	900	7
Fluvial valley (V, VH)	1000	4
		$\Sigma = 116$

[a] See Appendix F. As an example of the series usage, a site recorded as 312 is the 12th landform in the 300 series (glacier-cored moraines or MG).

appearance and disappearance (Fig. 6). This solar path (List, 1951) was chosen to best characterize the glacial ablation period.

Superimposing the landform's horizon upon the sun's path, as it would be on 24 July, establishes the duration of direct radiation received at each site during a typical part of the ablation season

(Fig. 6). The amount of direct radiation energy received at each landform during these times of sun appearance was then calculated (Appendix F), and this sum was compared to that measured at lat 68°N on unscreened horizontal surfaces under clear skies (Kondratyev, 1973, p. 304-305; Appendix F). This measured amount (~590 cal cm^{-2} day^{-1}) is treated as the potential unscreened energy and is assigned a value of 100%. The comparison of the actual amount of energy received to this potential energy provides a measure of the reduction in direct solar energy due to surrounding terrain at each landform. A similar study has been carried out with a theodolite on McCall Glacier at lat 70°N in the northeastern Brooks Range (Wendler and Ishikawa, 1974).

Increasing slope inclination in a more northerly aspect also markedly reduces solar insolation. This effect is amplified in upper latitudes (Table 3), beyond the values given in Wendler and Ishikawa (1974, Table II). The effects of aspect, slope, and terrain screening on incoming radiation receipt were combined to provide a measure of the total, direct radiation energy received at each survey site during a typical part of the ablation season. These energy values were then correlated with landform types.

GLACIERS, NEOGLACIAL MORAINES, AND ROCK GLACIERS

Cirque glaciers are fronted by different types of moraines in the central Brooks Range. The majority of cirque glaciers (CG; abbreviation refers to designation of landforms in subsequent figures, tables, and appendices) are associated with moraines which are cored

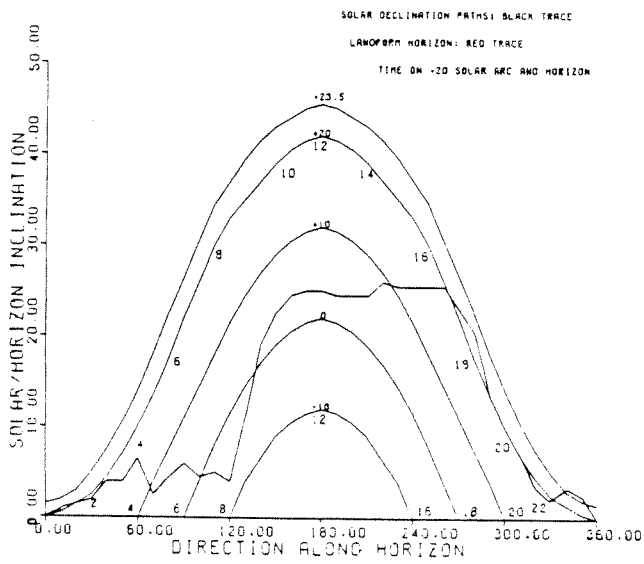

Figure 6. Topographic horizon of Grizzly Glacier (no. 3, Fig. 2; cover photograph) superimposed on paths of the sun at lat 68°N for different solar declinations (-10° = 20 October or 24 February, 0° = 21 March or 23 September, +10° = 16 April or 28 August, +20° = 21 May or 24 July, +23.5° = 21 June). In this study the +20° declination was used for terrain screening calculations as it represents a typical part of the ablation season. The hours of the day are plotted in two-hour increments along the trace of the +20° solar path. Sunrise(s) and sunset(s) are determined by following the horizon trace from due north (0.00° on the abscissa) through east, south, and west, returning to north (360.0°). When the horizon crosses and goes inside the solar path, it means the sun has just appeared above the horizon ("sunrise"). When the horizon crosses and goes outside the sun path, the sun is blocked from view ("sunset"). In this example, the sun initially appears at 1.6 hrs and radiation is received at the glacier until 16.9 hrs into the day when the sun is blocked by the landform's horizon. However, the sun reappears at 18.9 hrs and shines on the glacier until 22.2 hrs into the day. A total of 18.6 hours of sunshine is received on 24 July; this converts to 93% of the potential energy available during the 24 hr day to horizontal unscreened surfaces at lat 68°N. See Appendix F for data, computer programs to reduce the measurements and plot the horizon.

TABLE 3. MEAN DAILY DIRECT SOLAR RADIATION ENERGY AT LAT 68°N, + 20° DECLINATION [a]

Slope	Aspect				
	N	NE or NW	W or E	SE or SW	S
10	99	99	100	102	103
20	95	94	102	106	107
30	87	88	104	109	109

[a] Values expressed as a percentage of that received on an unscreened horizontal surface for a given aspect (direction of opening) and slope (L. Williams, written comm., 1979; from Ellis and others, 1981).

with ice (Mg). In many cases glacial ice is exposed beneath a thin cover of debris (MG). The remaining cirque glacier moraines either have formed without ice cores (M) or are situated as glacier-cored transition zones (TRGC) upslope of rock glacier tongues. Rock glaciers without exposed ice cores line valley walls and emanate from cirques; they are tongue- (TRG) or lobate- (LRG) shaped landforms.

Cirque Glaciers

Average slopes of 17° and lengths of 740 m characterize 133 cirque glaciers in the Atigun Pass area; average slopes of 16° and lengths of 1280 m were measured for 11 glaciers in the Arrigetch Peaks (Fig. 7; Appendix E). The Atigun Pass glaciers are all above 1500 m in altitude (Fig. 8). Those fronted by only morainal lobes occur on a trend surface rising from 1600 m south of the Continental

a)

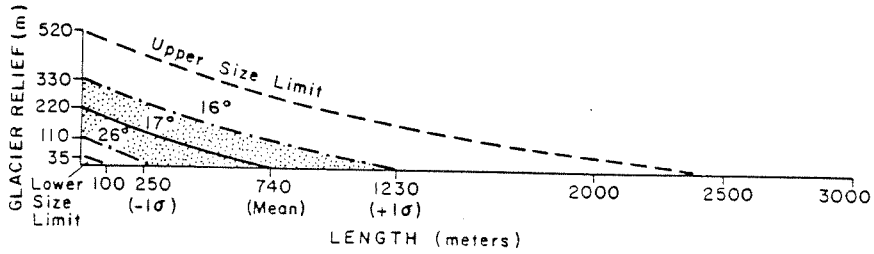

b)

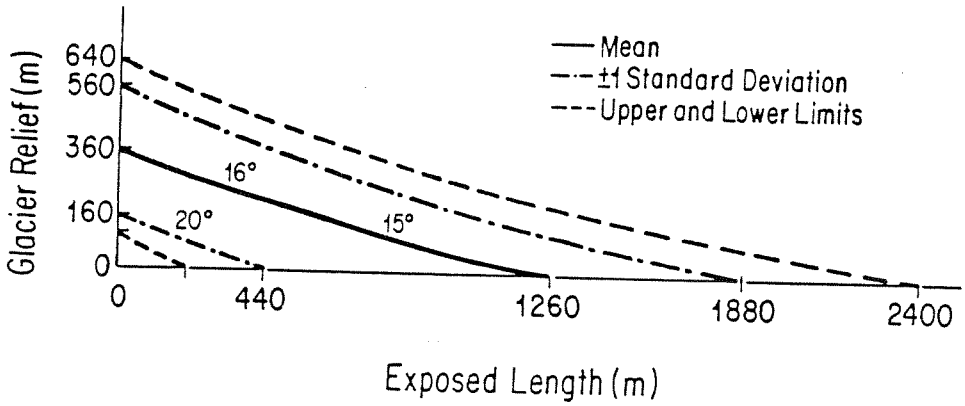

Figure 7. Generalized profile of 133 cirque glaciers in the Atigun Pass area (a) and 11 cirque glaciers in the Arrigetch Peaks (b). Profiles show mean relief and length with 68% zone of occurrence ($\pm 1\sigma$), upper and lower size limits, and slope of glacier surface.

Divide to 2000 m, 25 km farther north (Fig. 9). Glaciers that extend downslope into transition zones and rock glacier deposits occur on a parallel trend 100 m below. Both trend surfaces reflect depletion of moisture derived predominantly from southerly sources. In the Arrigetch, mean glacier altitude ranges from 1300 to 1750 m (Fig. 8).

The 133 ice bodies around Atigun Pass and the 11 in the Arrigetch

a)

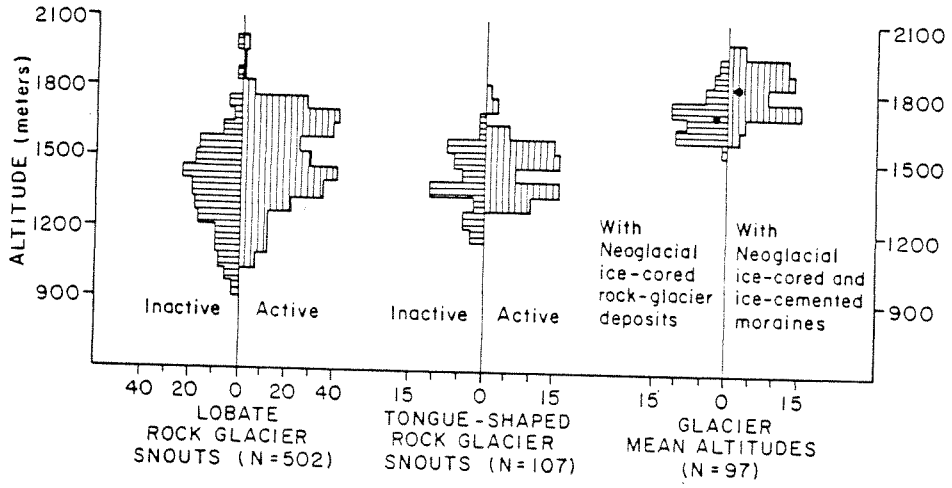

b)

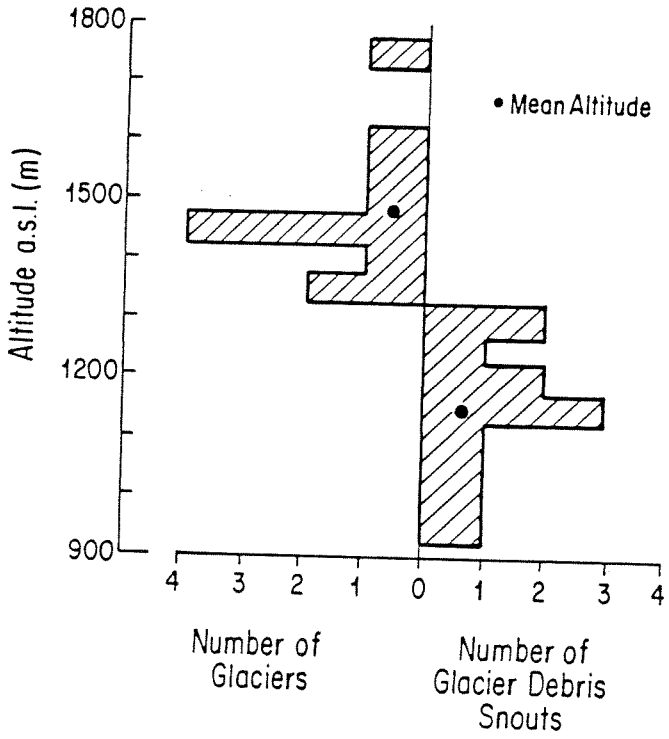

Figure 8. Summary of altitudinal distribution for glaciers and rock glaciers in the Atigun Pass area (a) and glaciers in the Arrigetch Peaks (b).

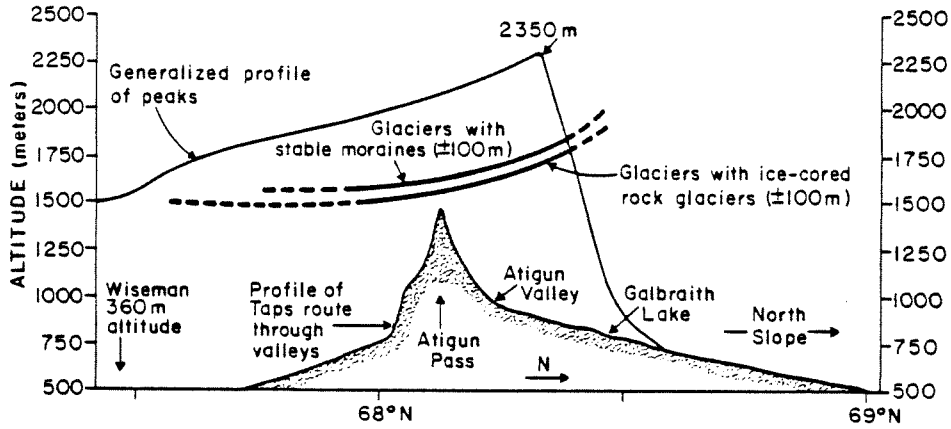

Figure 9. North-south profile through Atigun Pass with upper trend surface representing glaciers fronted by non ice-cored moraines and ice- or glacier-cored moraines (M, Mg, MG), and lower trend surface for glaciers with glacier-cored debris ridges (TRGC) forming a transition zone upslope of a rock glacier tongue. Each surface represents a zone ~200 m thick (see Plate 1).

area have mean aspects of 012° and 010° with extremely asymmetric strengths of 88% and 83%, respectively (Fig. 10). Their headwall aspects are slightly less asymmetric. Glaciers in both regions are oriented to minimize insolation as are glaciers elsewhere in the Brooks Range (Wendler, 1969). The aspect distribution pattern demonstrates marginal conditions and highly significant climatic control on glacierization during the Holocene time. This contrasts markedly with the symmetric orientation of Pleistocene glaciers and cirques (Fig. 11).

No significant differences in areas of glaciers and their deposits can be detected between the 42 ice masses in the sedimentary terrain of Atigun and Anaktuvuk Passes and the 11 glaciers in the

a) Atigun Pass area

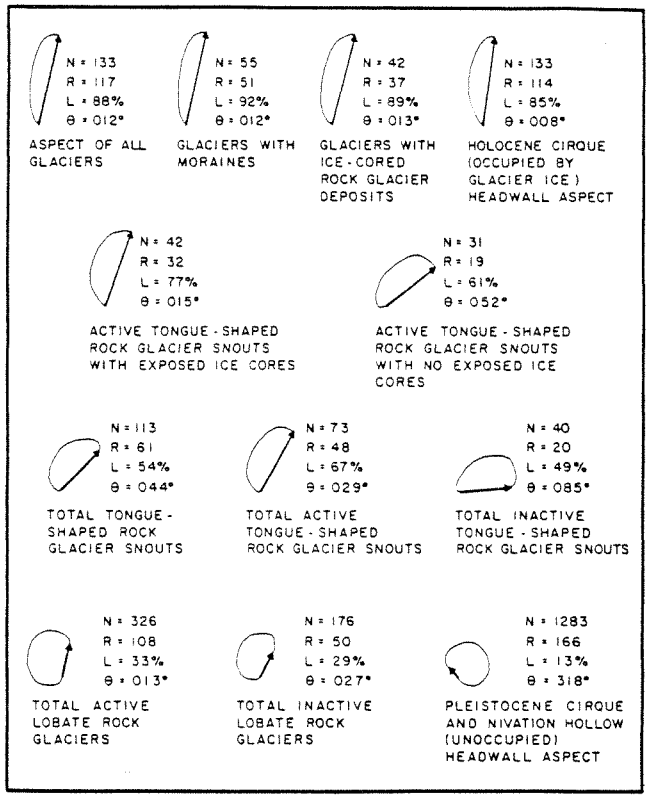

b) the Arrigetch Peaks

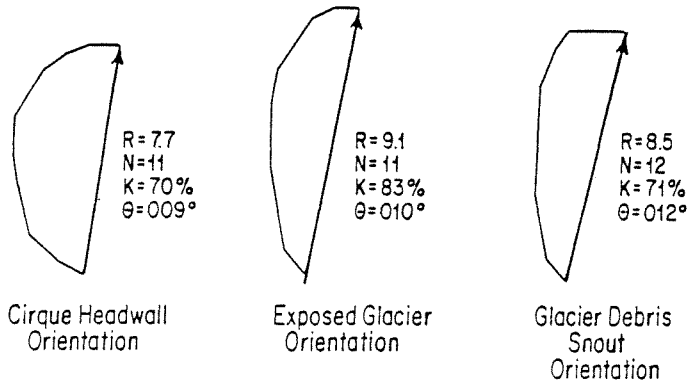

Figure 10. Graphical summary of aspect distribution data for the Atigun Pass area (a) and the Arrigetch Peaks (b). The concentration of aspects (strength K) along the vector resultant (R) is obtained by dividing the length of R by the total length of the individual vectors (N). Note absolute scale in (a) varies so that strength of mean vectors (K) are of equal lengths if K = 100%. K is shown by the thickened arrow.

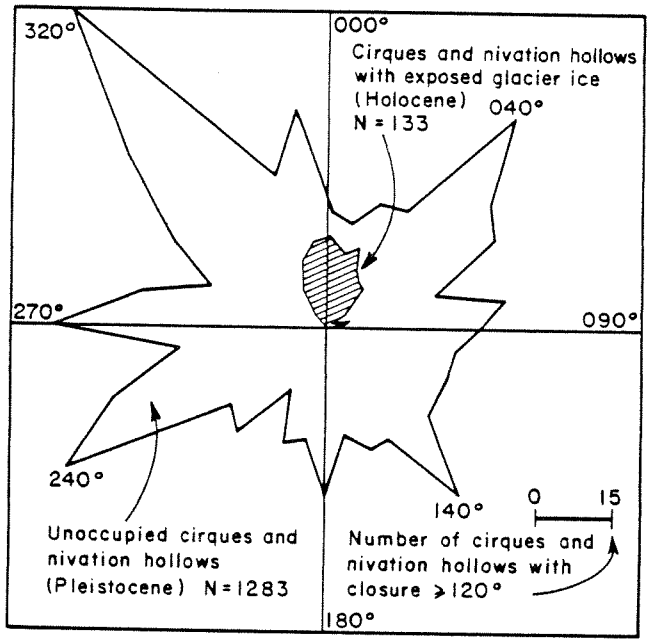

Figure 11. Orientation of cirques and nivation hollows in the Atigun Pass field area, east-central Brooks Range. Basins with glacier ice are labeled as Holocene, those without ice are assumed to have been actively cut only during Pleistocene glaciations.

granitic terrain of the Arrigetch Peaks (Table 4, Appendices B and E), largely because of excessive variance in the parameters measured. Relatively debris-free areas of glaciers in both regions average ~0.4 to 0.5 km^2; however, they range from 0.1 to over 2.0 km^2 in area. Glaciers tend to have more areal extent than their downslope deposits of Neoglacial age unless the deposit is a transition zone upslope of a rock glacier tongue. There the glacier core is typically inundated with debris from surrounding cirque walls (Table 4). The percent of glacier area increase during Neoglacial expansions

TABLE 4. PLANIMETRY OF CIRQUE GLACIERS AND THEIR DEPOSITS

(1) Type	(2) Area of Glacier (km^2)	(3) Neoglacial Area (km^2) [a]	(4) Percent Expansion (%)	(5) Neoglacial Debris (km^2) [a]	(6) ELA Depression (m) [b]	(7) Glacier Length (m)	(8) Relief (m)	(9) Exposed Headwall (m)	(10) Neoglacial Ice Thickness (m) [c]
M, Mg, MG, TRGC									
All (n=53)	0.45 ± 0.40	0.64 ± 0.64	88 ± 122	0.24 ± 0.20	82 ± 49	1032 ± 558	295 ± 143	153 ± 109	110 (88-145)
[d] Sedimentary (n=42)	0.44 ± 0.37	0.58 ± 0.42	85 ± 133	0.20 ± 0.12	70 ± 35	981 ± 533	275 ± 135	129 ± 89	112 (88-154)
[e] Granitic (n=11)	0.49 ± 0.50	0.87 ± 0.83	100 ± 72	0.37 ± 0.35	128 ± 62	1137 ± 702	353 ± 173	246 ± 134	108 (88-138)
M									
All (n=15)	0.58 ± 0.44	0.79 ± 0.54	42 ± 21	0.22 ± 0.13	78 ± 43	1186 ± 430	341 ± 95	72 ± 55	104 (84-137)
Sedimentary (n=12)	0.61 ± 0.49	0.82 ± 0.60	39 ± 21	0.21 ± 0.13	57 ± 24	1105 ± 285	315 ± 83	58 ± 49	105 (84-138)
Granitic (n=3)	0.45 ± 0.08	0.71 ± 0.23	55 ± 22	0.26 ± 0.15	148 ± 47	1510 ± 805	447 ± 64	100-180	102 (88-121

TABLE 4 (continued).

(1)	(2)	(3)	(4)	(5)	(6)	(7)	(8)	(9)	(10)
Mg									
All (n=18)	0.36 ± 0.20	0.53 ± 0.26	60 ± 37	0.17 ± 0.08	79 ± 35	930 ± 405	281 ± 139	148 ± 70	107 (87-138)
Sedimentary									
MG									
All (n=12)	0.55 ± 0.54	0.91 ± 0.86	86 ± 61	0.38 ± 0.33	119 ± 57	1130 ± 701	330 ± 173	190 ± 122	102 (84-130)
Sedimentary (n=5)	0.52 ± 0.49	0.77 ± 0.67	61 ± 26	0.29 ± 0.16	97 ± 54	1177 ± 848	302 ± 178	100 ± 0	98 (79-130)
Granitic (n=7)	0.55 ± 0.61	1.00 ± 1.00	104 ± 73	0.45 ± 0.42	135 ± 58	1096 ± 646	350 ± 181	247 ± 126	105 (87-133)
TRGC									
All (n=8)	0.28 ± 0.36	0.49 ± 0.43	240 ± 260	0.21 ± 0.12	40 ± 40	703 ± 802	154 ± 140	250 ± 139	152 (125-197) ?
Sedimentary (n=7)									

TABLE 4 (continued).

(1)	(2)	(3)	(4)	(5)	(6)	(7)	(8)	(9)	(10)
M, Mg, MG									
All (n=45)	0.48 ± 0.40	0.72 ± 0.57	61 ± 43	0.24 ± 0.21	89 ± 48	1069 ± 509	314 ± 136	137 ± 95	104 (86-133)
Sedimentary (n=35)	0.47 ± 0.37	0.59 ± 0.42	53 ± 32	0.20 ± 0.12	75 ± 35	1025 ± 451	296 ± 126	112 ± 70	104 (86-134)
Granitic (n=10)	0.53 ± 0.50	0.92 ± 0.84	89 ± 65	0.39 ± 0.36	139 ± 53	1220 ± 680	379 ± 158	226 ± 122	104 (88-127)

[a] Based on lichenometric mapping of debris lobes downslope of receding cirque glaciers.

[b] Measured from the present mean glacier altitude to the altitude of the ELA for the cirque glacier's Neoglacial maxima (Appendix B). ELA for the maxima is determined by the AAR = 0.67 method.

[c] Estimated from Weertman's (1971) cirque glacier formula ($h = \tau / 0.4 \rho g \sin\alpha$) where α equals the reconstructed glacier slope for the cirque glacier's Neoglacial maxima (Appendices B and E).

[d] Landforms in the Atigun and Anaktuvuk Pass areas (Fig. 1).

[e] Landforms in the Arrigetch Peaks area (Fig. 1).

cannot be consistently measured by comparison of the present glacier area to the downslope deposit because of variable inputs of supra-glacial debris and the ice-/glacier-cored nature of three out of four moraines studied. For morainal complexes, the estimated percent of glacier expansion during Neoglacial maxima as compared to present glacier area averages ~60 ± 40%.

Present Glacial Regime

Under the present climate, cirque glaciers across the central Brooks Range are wasting away (Porter, 1966; Ellis and Calkin, 1979; Bruen, 1980a). Glaciologic investigations during the 1978 field season at Grizzly Glacier (no. 3, Fig. 2; cover photograph) indicated a negative mass balance of -930 mm of water equivalent (Bruen, 1980b). The previous winter's accumulation (490 mm of H_2O) and an average of 1040 mm of ice had ablated over the entire surface. Between 11 June and 12 August 1978, the mean daily temperature and direct solar radiation were 3.6°C and 431 cal cm^{-2} day^{-1}, respectively. Based on the relationship of ablation to altitude, Bruen calculated the 1978 equilibrium-line altitude (ELA) to be ~1860 m, which is just above the glacier surface. For the Atigun and Anaktuvuk Pass areas, present ELA's are estimated to average ~1900 m and parallel the northward rising trend of cirque glaciers (Fig. 8). At the west-central Arrigetch Peaks present ELA's may be ~1500 m. These estimates are intermediate between the values of Porter (1966) and Péwé (1975).

Preliminary compilation of glaciologic observations from 1977 to 1980 on Buffalo, Marmot, and Grizzly glaciers (nos. 1, 2, 3 on

Fig. 2) indicates annual winter accumulation ranging from 250 to ~500 mm of H_2O (Ellis and Calkin, unpub. data). Summer precipitation at Grizzly Glacier was measured as 230 and 280 mm during 1979 and 1980, respectively. Ice ablation approached 2000 mm in 1979, but only 1100 mm in 1980 near the termini of the three glaciers.

Studies in other arctic areas indicate radiation is the dominating factor in the heat balance of central Brooks Range glaciers (see Patterson, 1969, p. 62). Radiation accounted for ~60% of ice and snow ablation at McCall Glacier, northeastern Brooks Range, during 1971 (Wendler and Weller, 1974). These glaciers may be classified cold because meltwater streams meander over their surfaces (Patterson, 1969, p. 178). They are defined as subpolar because the firn is saturated with water during the ablation season (Ahlmann, 1948), and internal ice temperatures averaged -1.1°C below 14 m depth at McCall Glacier (Orvig and Mason, 1963).

Neoglacial Moraines

Moraines Without Cores of Ice

Moraines which lack cores of ice (M) have subtle relief and are the most stable type of cirque glacier deposit (Fig. 12; see Østrem, 1964, p. 286-288). Moraines in the sedimentary environment of Atigun and Anaktuvuk Passes without extensive ice cores receive ~94% of the potential direct radiation energy on 24 July, while those in the Arrigetch Peaks gain only 85% (Table 5). In both terrains these deposits have low horizons (Table 5) and minimal bedrock

Figure 12. Vertical view of Buffalo Glacier (no. 1, Fig. 2) with a morainal deposit largely lacking an ice core (M). The ice-cemented ridges occur up to 700 m from the receding glacier snout. All vertical photographs reproduced in this study are from U.S. Geological Survey 1:80,000 GS-VCIK series.

Figure 13. Vertical view of Snow Bunting Glacier (no. 13, Fig. 2) fronted by an ice-cored moraine (Mg - no glacier core exposed). Note steep front ~200 m from glacier snout. Immediately downslope is an inactive rock glacier from an early Holocene (?) landslide.

TABLE 5. TERRAIN SCREENING OF GLACIAL LANDFORMS

(1) Type [a]	(2) Site Altitude (m)	(3) Sunshine Duration (hr) [b]	(4) Potential Energy Blocked (%) [b]	(5) Exposure Gain or Loss (%) [c]	(6) Total Direct Energy Received (%) [b]	(7) Mean Horizon (°)	(8) Maximum Horizon (°)
CG: 000 series							
All (n=9)	1711 ± 181	14.6 ± 2.3	-12.7 ± 5.9	-2.8 ± 2.2	84.5 ± 6.4	15.8 ± 2.9	29.2 ± 4.9
Sedimentary (n=7)	1795 ± 81	15.2 ± 2.3	-11.2 ± 5.7	-3.3 ± 2.2	85.5 ± 6.9	15.0 ± 2.8	27.6 ± 4.3
Granitic (n=2)	1400-1435	12.2-12.4	-16.1 to -20.2	-1	78.8-82.9	17.7-19.2	34.0-35.5
M: 100 series							
All (n=17)	1623 ± 201	17.1 ± 3.1	-6.6 ± 5.9	-1.3 ± 1.6	92.1 ± 6.2	13.5 ± 4.4	26.4 ± 5.6
Sedimentary (n=14)	1687 ± 126	17.9 ± 2.9	-4.8 ± 4.5	-1.4 ± 1.7	93.8 ± 5.2	12.0 ± 3.2	24.2 ± 3.1
Granitic (n=3)	1267 ± 29	13.8 ± 1.4	-14.8 ± 4.1	-0.7 ± 0.6	84.5 ± 4.6	20.3 ± 1.7	36.7 ± 0.8
Mg: 200 series							
All (n=20)	1675 ± 66	12.6 ± 2.2	-15.3 ± 7.2	-2.5 ± 2.2	82.3 ± 7.7	18.2 ± 2.4	30.7 ± 3.4
Sedimentary							

TABLE 5 (continued).

(1)	(2)	(3)	(4)	(5)	(6)	(7)	(8)
MG: 300 series							
All (n=17)	1429 ± 215	11.4 ± 3.5	-24.1 ± 15.1	-2.4 ± 1.8	73.5 ± 15.6	20.5 ± 5.2	36.1 ± 10.2
Sedimentary (n=9)	1608 ± 77	13.9 ± 2.2	-12.8 ± 6.1	-2.3 ± 1.7	84.9 ± 6.2	16.4 ± 3.3	28.0 ± 5.1
Granitic (n=8)	1227 ± 106	9.5 ± 2.2	-36.7 ± 11.4	-2.5 ± 2.1	60.8 ± 12.6	25.2 ± 1.5	45.2 ± 5.5
TRGC: 400 series							
All (n=16)	1490 ± 174	10.6 ± 3.8	-25.5 ± 25.4	-1.9 ± 1.8	72.6 ± 24.9	20.4 ± 4.9	33.4 ± 7.1
Sedimentary (n=14)	1541 ± 100	11.4 ± 3.0	-19.2 ± 16.3	-2.1 ± 1.9	78.8 ± 16.1	19.1 ± 2.9	31.5 ± 4.8
Granitic (n=2)	1000-1270	8.4-1.5	-41.6 to -99.0	-1 to 0	57.4 to ~1	23.7-34.5	44.0-50.5

[a] See Appendix F for data on individual landforms.

[b] See Figure 6 and Appendix F for procedure on determining duration and percent of direct radiation energy received.

[c] See Table 3 and Appendix F.

exposed in cirque cliffs (Table 4) as compared with ice- or glacier-cored moraines.

Ice-Cored Moraines

Ice-cored moraines (Mg) lack a visible ice core, yet have marked relief and sharp-crested fronts in the downvalley direction (Fig. 13). They may grade into zones without ice cores along continuous ridge systems, and contain either buried glacier ice (Goldthwait, 1951) or snowbank ice (Østrem, 1964) that may persist for thousands of years in this type of environment (Østrem, 1974).

Environments favoring the deposition of stable, ice-cored moraines may have the following characteristics (Barsch, 1971; Østrem, 1971; Whalley, 1974):

a) minimal lateral extent of surrounding cliffs

b) small headwall

c) deposition of the moraine on relatively horizontal terrain

d) low input of supraglacial debris

Ice-cored moraines were only mapped in the Atigun Pass field area (Fig. 2); in the other two areas glacier cores were exposed beneath the morainal debris surfaces. The ice-cored moraines (Mg) receive somewhat less solar radiation energy than non ice-cored moraines (M); however, their mean inclination to the horizon of 18 $\pm$ 2° is higher than that measured for M-type moraines which had horizons averaging 12 $\pm$ 3° (Table 5). In addition, potential debris input is greater for Mg moraines (148 $\pm$ 70 m) than for M deposits (72 $\pm$ 55 m, Table 4). The slopes of the bedrock that these relatively

stable moraines were deposited on is greater than that measured for older rock glacier tongues (Appendix E).

Glacier-Cored Moraines

Glacier-cored moraines (MG) are morphologically similar to ice-cored moraines (Mg) but reveal a glacier core (Fig. 14). In the sedimentary terrain of Atigun Pass there is considerable overlap between MG and Mg moraines in planimetric and terrain screening measurements (Tables 4, 5); therefore, subsequent analyses will group them together and consider glacier ice forms the cores of all these moraines. Vernon and Hughes (1966) designated these types of deposits in the Yukon Territory as debris-covered glaciers. They morphologically differentiated them from rock glaciers.

Cirque glacier deposits in the Arrigetch Peaks are more extensively cored with glacier ice than those studied in Atigun and Anaktuvuk. Ice-cored (Mg) and glacier-cored (MG) moraines in the sedimentary terrain acquire 83% of the potential solar energy. In contrast, eight glacier-cored moraines in the granitic terrain receive only 61% of the potential energy (Table 5). For these moraines, mean inclinations to their horizons are 16° and 25° in sedimentary and granitic terrain, respectively. This demonstrates that cirques are deeper in the granitic terrain of the Arrigetch. The potential debris supply available to glacier-cored moraines is also greater in the deeper cirques of the Arrigetch (245 $\pm$ 125 m of bedrock exposed in cirque cliffs) as compared to 140 $\pm$ 65 m for similar deposits in sedimentary terrain (Table 4).

a)

b)

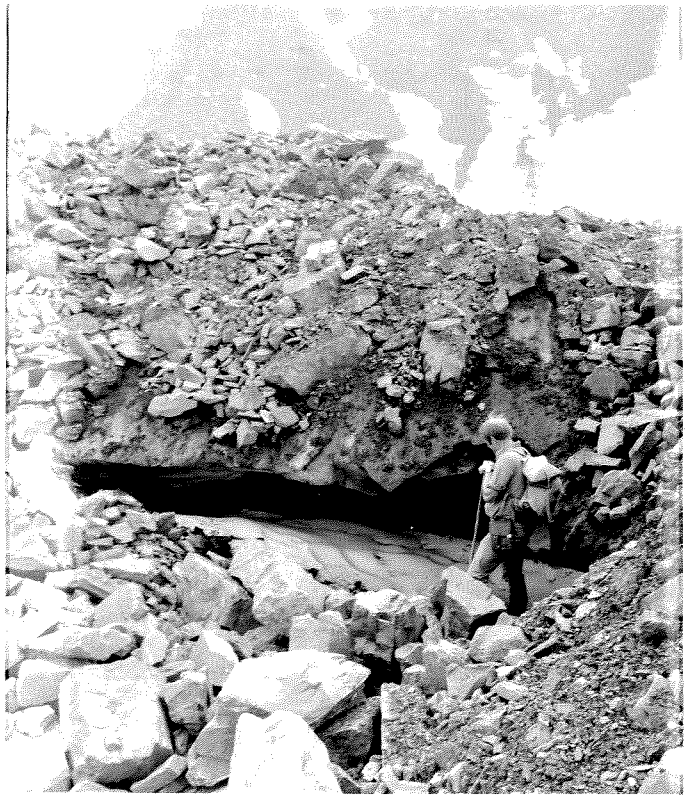

Figure 14. View south of glacier-cored moraines (MG) fronting Snowy Owl East Glacier (a; no. 34, Fig. 2) and Wolf Glacier (b; no. 31, Fig. 2), Atigun Pass area. The debris-covered terminus of Snowy Owl East is 50 m thick; in contrast, at Wolf Glacier the moraine is less than 10 m thick. Note thin cover of debris (<1 m thick) covering glaciers.

Glacier-Cored Rock Glaciers

Glacial deposits with surfaces and termini showing clear evidence of en mass downvalley movement and visible glacier cores are classified as glacier-cored, tongue-shaped rock glaciers (Fig. 15; Østrem 1974; Luckman and Crockett, 1978). These landforms are identified by criteria set forth by Wahrhaftig and Cox (1959) and White (1976). Although it had not been confirmed quantitatively, Whalley (1974) believes rock glaciers with ice cores occur where there are substantial cliffs above the glacier and a plentiful supply of debris (see Currey, 1969). Johnson (1980) proposes that debris supply is not a factor in glacier-cored rock glacier placement; rather, variations in cirque size and morphometry control the site of development. He regarded small confined cirques as optimum sites although he presents no evidence.

Glacier-cored, tongue-shaped rock glaciers are generally characterized by partially stable, looping ridges immediately downslope of an exposed ice core (Fig. 15). Transverse debris ridges override or abut downslope against an older rock glacier tongue. These types of deposits are classified as transitional, glacier-cored rock glaciers after Foster and Holmes (1965) who describe a similar morphology in the Alaska Range. The cresentic or looping ridges may be comparable to the modern glacial moraines depicted by Wahrhaftig and Cox (1959) that occur between glaciers and rock glacier tongues farther downslope (Johnson, 1980). However, these ridges have been interpreted as either ice-cored rock glacier or moraine deposits (Barsch, 1971; Østrem, 1971). In this study they are designated as

Figure 15. Vertical view of Mosquito Rock Glacier (no. 40, Fig. 2), a glacier-cored rock glacier with poorly expressed transitional zone of Neoglacial age (TRGC) upslope of an older rock glacier tongue. Debris front of rock glacier is active.

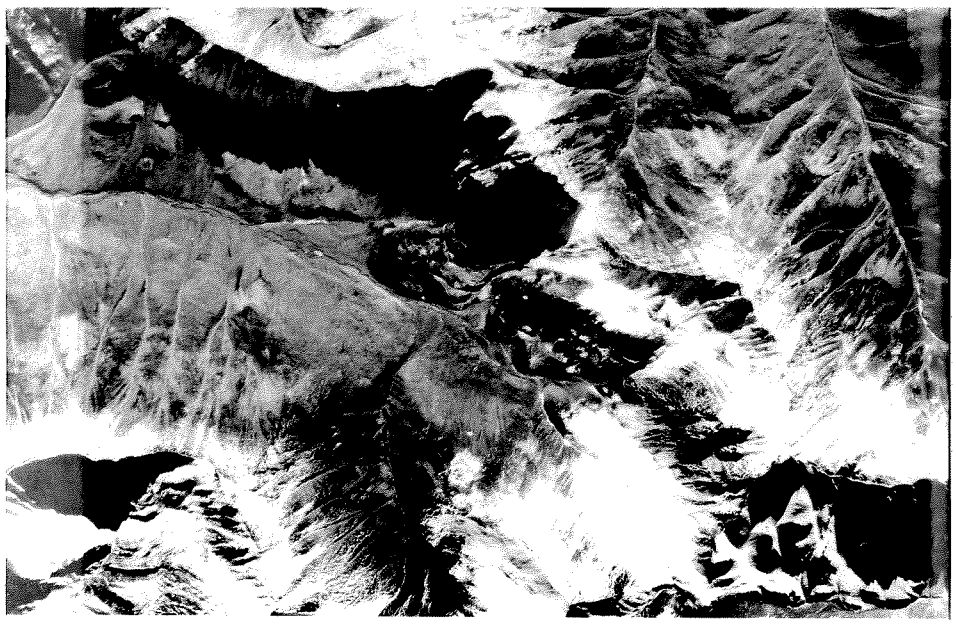

Figure 16. Vertical view of Spider Rock Glacier, Atigun Pass area, a tongue-shaped rock glacier with inactive debris front and no visible ice core (TRGi). Coalescing, lobate rock glaciers are upstream (left). Dark tone is due to lichen cover and it is indicative of stability since early Holocene time.

transition zones (TRGC) upslope of glacier-cored rock glaciers and are analyzed for comparability with glacier-cored moraines (MG).

Although the mechanism of behavior operating at the snouts of rock glaciers is unclear (Whalley, 1974), and some fresh steep snouts may result from a slow melting of the exposed front due to climatic amelioration (Thompson, 1957), it is generally believed that over-steepened fronts indicate an active (a) or partially active (p) rock glacier (Wahrhaftig and Cox, 1959). A rock glacier was recorded as inactive (i) if there was mature lichen growth over the upper surface and front, and rounded frontal lobes without a sharp break in slope at the snout. Regardless of activity state, most rock glaciers have cobbles and boulders on their upper surfaces covered with a mature growth of lichens. This indicates initial deposition of rock glaciers and stabilization of their upper surfaces beyond middle Holocene time (Calkin and Ellis, 1980).

Surface flow structures on downslope, glacier-cored rock glaciers may be initiated by normal glacier activity (Outcalt and Benedict, 1965; Johnson, 1980); however, after the period of glacial advance the rock glacier terminus may continue to deform (Johnson, 1980). The problems of mapping rock glaciers lichenometrically is emphasized by Haeverli and others (1979); they suggest the true lifetime of the landform since its origin from talus cones at valley walls may be on the order of the entire Holocene (Outcalt and Benedict, 1965; Luckman and Crockett, 1978, p. 547; Johnson, 1978, p. 1506, 1980, p, 203). Rock glaciers downslope of transition zones are not used to delineate a Neoglacial chronology in this study.

In the central Brooks Range, eight transition zones upslope of rock glacier tongues were mapped. They average 250 ± 140 m of bedrock exposed in cirque cliffs (Table 4). Terrain screening measurements along the longitudinal axes of glacier-transition zone-rock glacier complexes demonstrate mean horizons of 20 ± 5° and direct radiation energy received averaging 73 ± 25%. However, a few transition zone complexes form where as little as 1% solar energy is received and/or vertical headwall exposures exceed 400 m (Appendices E, F). In the east-central Brooks Range, glaciers fronted by transition zones (TRGC) that have partially overridden downslope, older rock glacier tongues are ~100 m lower in altitude than those glaciers fronted by only morainal loops (M, Mg, and MG deposits; Figs. 8, 9).

Rock Glaciers

Tongue-Shaped Rock Glaciers

The debris lobes of tongue-shaped rock glaciers are morphologically similar to glacier-cored tongues; however, there are no visible ice cores in these rock glaciers (TRG, Fig. 16). As with all rock glaciers the snout may be in an active (a), partially active (p), or inactive (i) state.

Five landforms of this type were mapped in the field near Atigun and Anaktuvuk Passes (Table 6). Terrain screening data show they average 12 hours of sunshine during which 77 ± 18% of the potential energy is received; no correlation was found between this incoming energy and the rock glacier's state of activity. Photo-

TABLE 6. TERRAIN SCREENING OF PERIGLACIAL LANDFORMS

(1) Type [a]	(2) Site Altitude (m)	(3) Sunshine Duration (hr) [b]	(4) Potential Energy Blocked (%) [b]	(5) Exposure Gain or Loss (%) [c]	(6) Total Direct Energy Received (%) [b]	(7) Mean Horizon (°)	(8) Maximum Horizon (°)
TRGa/i: 500 series							
All (n=5) Sedimentary	1436 ± 160	12.0 ± 3.0	-22.5 ± 17.5	-0.1 ± 2.3	77.4 ± 17.6	19.9 ± 3.4	35.0 ± 6.2
LRGa: 600 series							
All (n=19) Sedimentary	1489 ± 250	13.1 ± 2.7	-19.0 ± 13.3	-1.5 ± 4.3	79.0 ± 13.3	18.1 ± 2.9	35.1 ± 4.0
LRGp: 700 series							
All (n=10) Sedimentary	1247 ± 176	10.5 ± 2.5	-23.7 ± 10.5	+1.0 ± 3.8	77.4 ± 12.0	18.1 ± 1.8	37.2 ± 2.9
LRGi: 800 series							
All (n=19) Sedimentary	1352 ± 159	11.5 ± 2.1	-17.9 ± 9.7	+1.8 ± 5.8	82.9 ± 10.6	19.2 ± 2.3	35.7 ± 2.7

TABLE 6 (continued).

(1)	(2)	(3)	(4)	(5)	(6)	(7)	(8)
C: 900 series							
All (n=7) Sedimentary	1490 ± 116	12.4 ± 2.2	-19.2 ± 7.0	-0.7 ± 0.5	80.1 ± 7.0	20.5 ± 2.2	32.1 ± 1.8
V/VH: 1000 series							
All (n=4) Sedimentary	1285 ± 114	10.0 ± 3.5	-24.9 ± 16.0	-0.3 ± 1.5	74.8 ± 17.0	19.2 ± 5.2	29.9 ± 6.0

[a] See Appendix F for data on individual landforms.

[b] See Figure 6 and Appendix F for procedure on determining duration and percent of direct radiation energy received at each landform.

[c] See Table 3 and Appendix F.

graphic analysis of 71 tongue-shaped rock glaciers near Atigun Pass suggests about half are inactive (Fig. 8a; Ellis and Calkin, 1979), and that these inactive landforms have a more widely dispersed orientation pattern than active, tongue-shaped lobes (Fig. 10).

Tongue-shaped rock glaciers with active fronts and without exposed ice cores are so similar in their morphology, environment (Appendix G), aspect (Fig. 10), and altitudinal distribution (Ellis and Calkin, 1979, Table 3; Fig. 8a) to those with visible glaciers upslope that it may be assumed both have glacier cores. Those with inactive fronts, such as In-C rock glacier in the Anaktuvuk Pass area (no. 44, Fig. 3), may also have glacier cores in various states of deterioration (Fig. 16).

Lobate Rock Glaciers

The characteristics of lobate rock glaciers (LRG) as defined in this study are summarized by White (1976). They are broader than long downslope, and develop below taluses along valley walls including cirque walls. They are generally thought to lack glacial ice cores (Outcalt and Benedict, 1965), moving by creep of interstitial ice (Wahrhaftig and Cox, 1958). Lobate rock glaciers are differentiated from protalus ramparts or lobes (Richmond, 1962; Blagbrough and Breed, 1967) as these latter landforms grow by accumulation of debris at the base of snowbanks (see White, 1981)

Talus cones and rock glaciers often occur side-by-side along valley walls in the central Brooks Range. However, the rock glaciers, especially lobate-shaped ones, are localized directly beneath steep,

truncated bedrock spurs where there is a minimum of fluvial activity in the debris source area. Active, partially active, and inactive lobate rock glaciers are shown in Figures 17, 18, and 19, respectively. Large spoon-shaped depressions between the rock glacier and headward cliff suggest deteriorating ice cores within these rock glacier lobes (see White, 1976). Outcalt and Benedict (1965) did not see this feature in the lobate rock glaciers of the Colorado Front Range.

Forty-eight lobate rock glaciers in the Atigun and Anaktuvuk Pass regions were mapped in the field; these receive ~80% of the potential radiation energy and have mean horizons of ~19° (Table 6). Interpretation of aerial photographs around Atigun Pass suggest that most active lobate rock glaciers occur ~150 m higher than inactive ones (Fig. 8a). Both active and inactive lobate rock glaciers have aspects that face all directions (weakly asymmetric, Fig. 10a) demonstrating insensitivity to insolation. This aspect distribution may reflect their lower ice content relative to debris as compared to the other rock glacier and glacial landforms (Fig. 8a).

Discrimination and Classification of Neoglacial Moraines and Rock Glaciers

Morphological and environmental parameters were analyzed statistically in order to detect those that were capable of distinguishing and helping to explain the different glacial and rock glacier landforms (Tables 4 - 7). The study includes (see Appendix G for amplification):

Figure 17. View east of lobate rock glacier, Atigun Pass area, with an active front (LRGa). Note ponding of water in slight spoon-shaped depression and light tone of surface due to minimal lichen cover.

Figure 18. View south of lobate rock glacier, Atigun Pass area, with a partially active front (LRGp). Note stream at far toe of rock glacier is undercutting front, probably causing an active looking front in the background. The foreground lobes are well vegetated and have rounded crests. This rock glacier has significant depressions ponding water behind the debris crests, suggesting ice core deterioration; however, talus cones upslope are active. Grizzly Glacier (cover photo, no. 3, Fig. 2) is in far background.

Figure 19. View southwest of lobate rock glacier, Atigun Pass area, with an inactive front (LRGi). Dark tone is due to extensive cover of lichens on boulders. Debris front is well vegetated and stable in spite of stream running along toe. Headward talus cones of this rock glacier is inactive and well vegetated.

a) graphic display, linear correlation, and regression between two variables (Till, 1971),

b) linear discriminant analysis to distinguish between previously defined groups of glacial landforms (Klecka, 1975),

c) cluster analysis to classify previously undefined glacial and periglacial landforms, and to measure correlation coefficients between variables (Hartigan, 1977).

The concept that glacial and rock glacier landforms form a continuum or sequence of transitional facies (Currey, 1969; Madole,

TABLE 7. VARIABLES USED IN MULTIVARIATE ANALYSES OF LANDFORMS

Discriminant Analysis	Cluster Analysis	Explanation
NSUN	SUNENER	Direct radiation energy received (%)
NELA	-	Altitude of the ELA during Neoglacial maxima (m)
NHEAD	HEADEXP	Height of exposed bedrock in cirque headwall cliffs or potential debris supply (m)
NLAT	LAT	Latitude of the landform (°)
NDROP	ELADROP	Amount of ELA lowering during Neoglacial maxima as measured from present mean glacier altitude (m)
NAREA	NEOSIZE	Area involved during Neoglacial expansions (km^2)
	EXPANICE	Present area of relatively debris free ice compared to area involved during Neoglacial maxima (%)
	ICESLOPE	Slope of glacier surface (°)
	HEADINCL	Average inclination of horizon surrounding a landform (°)
	HEADMAX	Maximum inclination of horizon surrounding a landform (°)
	SUNHR	Duration of sunshine on ~24 July (hr)
	ALTITUDE	Altitude of terrain screening survey site (m)
	EXPOSURE	Gain or loss in direct radiation energy due to landform slope and aspect (Table 3; %)

1972; Whalley, 1974) was examined, and the 43 cirque glacier deposits mapped in the sedimentary terrain were compared to the 11 analyzed in the granitic terrain of the Arrigetch Peaks. The variables utilized in linear discriminant and cluster analyses are shown in Table 7. Those parameters associated with cirque glacier reconstructions and determination of ELA's during past Neoglacial maxima (Appendices B, E, Table 4), including "NELA, NDROP, and ELADROP", are derived and explained later under CLIMATIC ANALYSIS OF CIRQUE GLACIATION.

Glacial Landforms

A trend of decreasing solar energy received (92 to 73%) and increasing head- and side-walls (13 to 20°) generally characterizes the transition from non ice-cored moraines through glacier-cored moraines. However, many of the measurements made on glacier-cored rock glaciers with transition zones (TRGC) are dispersed within the M and Mg/MG groupings (Fig. 20). A more continuous transition from M through MG to TRGC is revealed within sedimentary and granitic terrain when direct radiation energy received is plotted against estimated height of bedrock in cirque cliffs (Fig. 21). In sedimentary terrain, moraines without cores of ice are favored where potential debris is <150 high in the cliffs and $>83\%$ of the potential solar energy is received. Transition zones can form in the most extreme cirque environments in this terrain with cliffs ~ 400 m and radiation receipt of $<30\%$ (Figs. 15, 21). Figure 21 also emphasizes the environmental difference between the glacier-cored moraines of the Arrigetch as compared to the glacier-cored moraines near

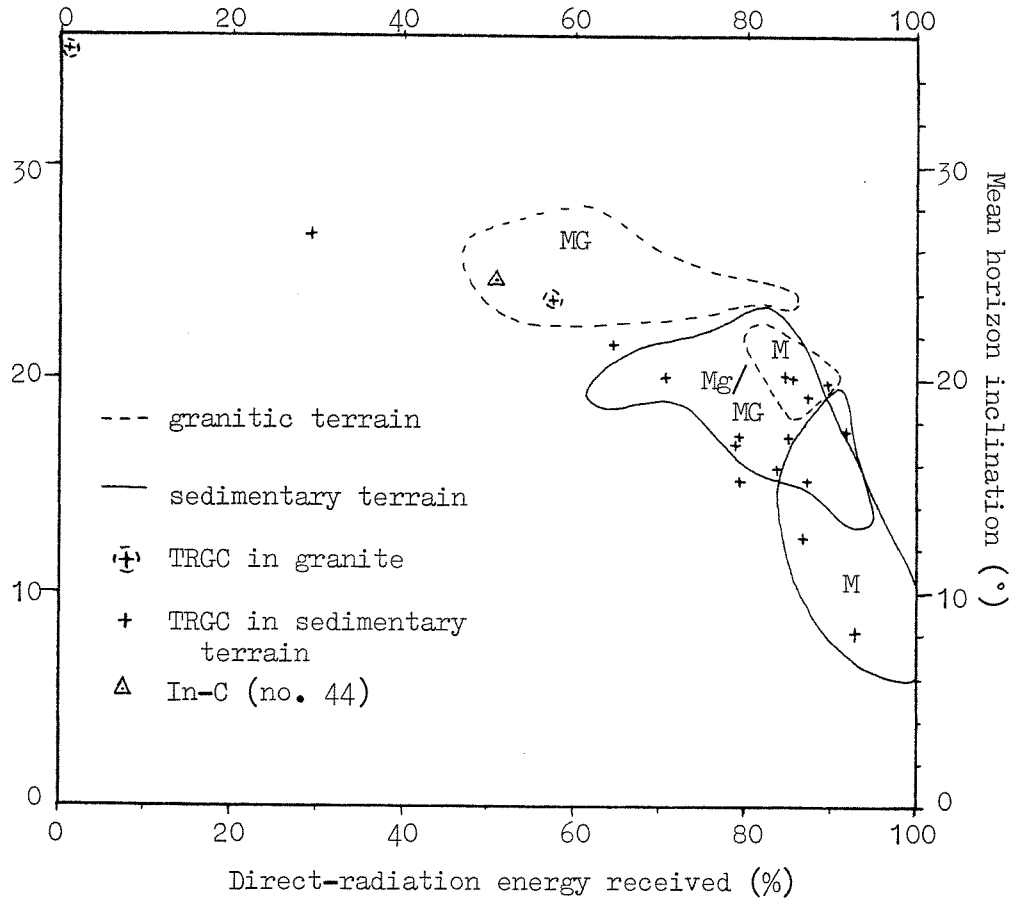

Figure 20. Plot of mean horizon inclination versus percent of direct radiation energy received for moraines without cores of glacial ice (M), moraines cored with ice (Mg), moraines visually cored with glacier ice (MG), and glacier-cored rock glaciers with transition zones upslope (TRGC). These landforms are distinguished according to location in the central Brooks Range (sedimentary terrain of Atigun and Anaktuvuk Passes or granitic terrain of the Arrigetch Peaks).

Atigun Pass and moraines without cores of ice.

The input of energy to empty cirque floors (C) is similar to that received by cirque glaciers and their glacier-cored deposits (Mg, MG, TRGC, Tables 5, 6). This suggests the thickness of glacial

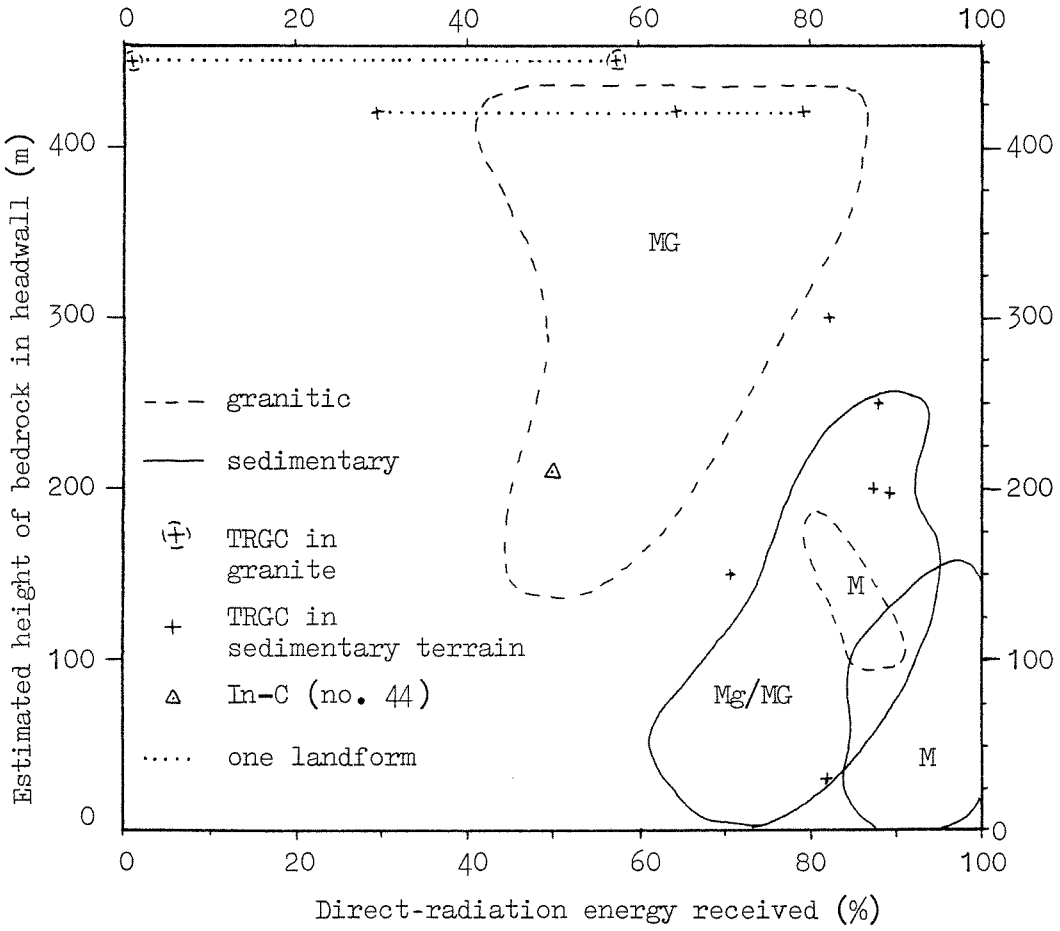

Figure 21. Plot of estimated height of bedrock exposed in cirque cliffs (potential debris supply) versus percent of direct radiation energy received for moraines without cores of glacial ice (M), moraines cored with ice (Mg/MG), and glacier-cored rock glaciers with transition zones (TRGC). These landforms are distinguished according to location in the central Brooks Range (sedimentary terrain of Atigun and Anaktuvuk Passes or granitic terrain of the Arrigetch Peaks).

ice in cirques is not substantial enough to lower the horizon; other variables such as latitude, altitude, and orientation determine whether a cirque is glacierized (Ellis, 1978; Ellis and Calkin, 1979).

Linear Discriminant Analysis 1 includes only those glacial landforms in sedimentary terrain (Fig. 22). It attempts to distinguish between moraines without ice cores (M), glacier-cored moraines (MG), and transition zones of tongue-shaped rock glaciers (TRGC) and to indicate the relative contribution of each variable to discriminating the three types of moraines. The analysis was based on four environmental and morphological variables (Table 7, Appendix G):

a) direct radiation energy received (NSUN),

b) altitude of ELA during Neoglacial maxima (NELA),

c) height of bedrock exposed in cirque cliffs (potential debris supply; NHEAD),

d) latitude (NLAT).

This analysis indicates that the ELA during Neoglacial maxima makes the largest relative contribution of the four variables in discriminating between the three morainal groups (Fig. 22). The higher in altitude the reconstructed ELA, the more easily fulfilled are the environmental conditions for moraines without cores of ice (M). TRGC and MG deposits have considerable overlap; however, the scatterplot (Fig. 22) demonstrates that a few TRGC moraines have markedly lower solar energy inputs and Neoglacial ELA's, and higher potential debris inputs than glacier-cored moraines (MG). The percent of "known" landforms correctly classified is 88% (Table 8), demonstrating the importance of these four variables, especially ELA, in controlling the deposition of the different glacial deposits.

Discriminant Analysis 2 used a) amount of ELA lowering from the present mean glacier altitude to Neoglacial maxima (NDROP) and

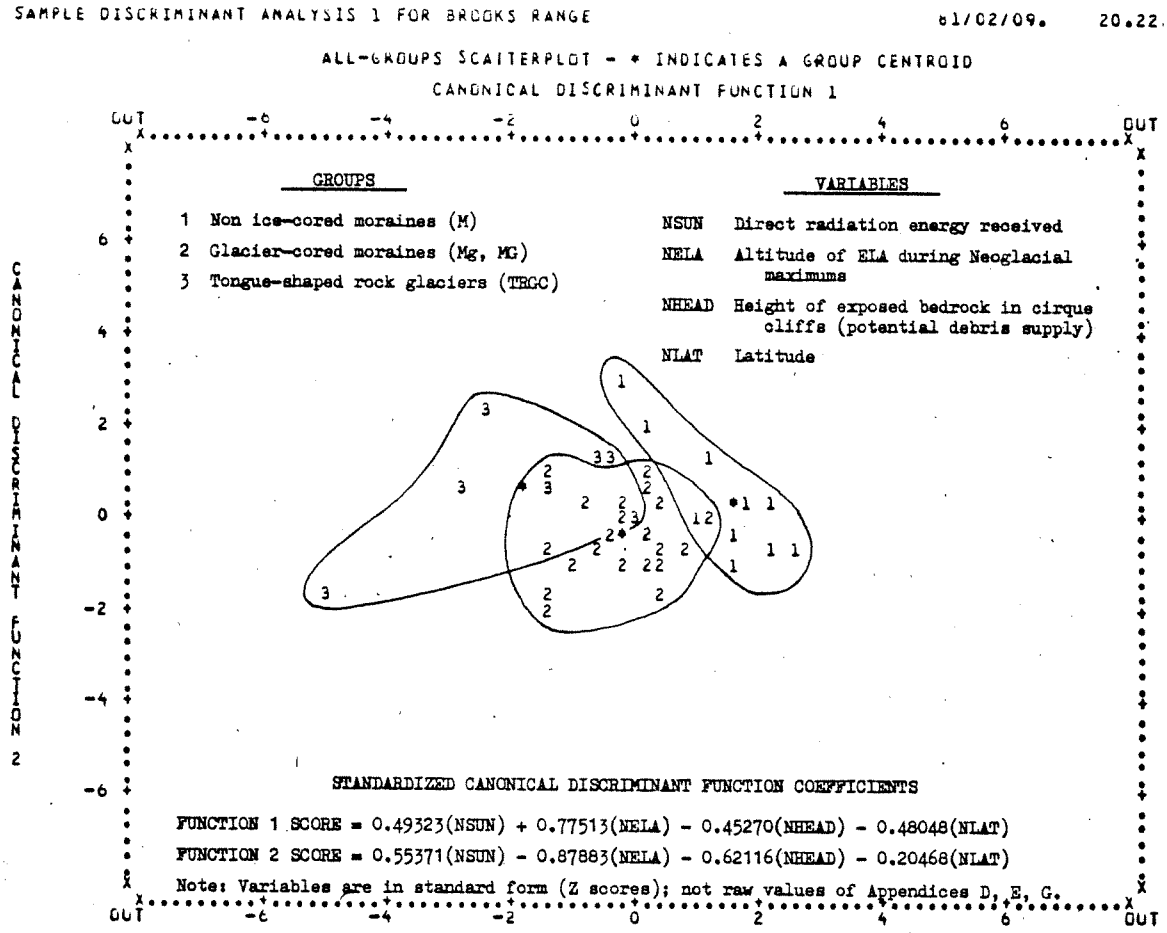

Figure 22. Scatterplot of Linear Discriminant Analysis 1 for glacial deposits in sedimentary terrain with groups, variables, and standardized coefficients for discriminant variables shown. These coefficients indicate the relative contribution of each variable to the function. Besides cirque environmental variables such as direct radiation energy received and potential debris supply, this analysis used geographically dependent variables latitude and altitude (see Table 8). The closer the coefficient is to $\pm$ 1.0, the larger the relative contribution of the variable to discriminating between the groups. Here the ELA for Neoglacial maxima (NELA) is the most important discriminant.

TABLE 8. LINEAR DISCRIMINANT ANALYSIS 1 OF GLACIAL LANDFORMS IN SEDIMENTARY TERRAIN: CLASSIFICATION RESULTS [a]

SAMPLE DISCRIMINANT ANALYSIS 1 FOR BROOKS RANGE [a]

CLASSIFICATION RESULTS -

ACTUAL GROUP		NO. OF CASES	PREDICTED GROUP MEMBERSHIP 1	2	3
GROUP 1 SUBFILE	MORAIN	12	11 91.7	0 0	1 8.3
GROUP 2 SUBFILE	GLAMCR	24	1 4.2	21 87.5	2 8.3
GROUP 3 SUBFILE	GLATRG	7	0 0	1 14.3	6 85.7

PERCENT OF GROUPED CASES CORRECTLY CLASSIFIED - 88.37

CLASSIFICATION PROCESSING SUMMARY

43 CASES WERE PROCESSED.
0 CASES WERE EXCLUDED FOR MISSING OR OUT-OF-RANGE GROUP CODES.
43 CASES WERE USED FOR PRINTED OUTPUT.

[a] See Figure 22 for scatterplot and Appendix G for data.

TABLE 9. LINEAR DISCRIMINANT ANALYSIS 2 OF GLACIAL LANDFORMS IN SEDIMENTARY TERRAIN: CLASSIFICATION RESULTS [a]

SAMPLE DISCRIMINANT ANALYSIS 2 FOR BROOKS RANGE

CLASSIFICATION RESULTS -

ACTUAL GROUP		NO. OF CASES	PREDICTED GROUP MEMBERSHIP 1	2	3
GROUP 1 SUBFILE	MORAIN	12	12 100.0	0 0	0 0
GROUP 2 SUBFILE	GLAMCR	24	0 0	18 75.0	6 25.0
GROUP 3 SUBFILE	GLATRG	7	0 0	1 14.3	6 85.7

PERCENT OF GROUPED CASES CORRECTLY CLASSIFIED - 83.72

CLASSIFICATION PROCESSING SUMMARY

43 CASES WERE PROCESSED.
0 CASES WERE EXCLUDED FOR MISSING OR OUT-OF-RANGE GROUP CODES.
43 CASES WERE USED FOR PRINTED OUTPUT.

[a] See Figure 23 for scatterplot and Appendix G for data.

b) area involved during this Neoglacial expansion (NAREA) in place of latitude and Neoglacial ELA maxima (Fig. 23). This study clearly discriminates non ice cored moraines (M) from the glacier-cored varieties, but there is even more intermixing of glacier-cored moraines (MG) and transition zones (TRGC). The potential debris supply is the most important environmental factor in determining the type of deposit formed; the less bedrock exposed in the headwall the more likely a moraine without an ice core will be formed.

Moraines that are cored with ice (Mg, MG) form in environments with variable inputs of solar energy and debris. The moraine downslope of Snow Bunting Glacier (Fig. 13) receives 92% of the potential solar energy, yet it has a substantial ice core apparently due to the high debris input from ~250 m of bedrock exposed in cirque walls. In the Arrigetch Peaks, the east arm of Arr-4 (no. 56, Fig. 4) leads into a glacier-cored moraine with minimal solar energy (53%) during the ablation season and relatively low input of debris.

Minimal depressions of ELA during Neoglacial maxima (Table 4) favor formation of TRGC and, for reasons unknown, M-type deposits. In addition, increased receipt of solar energy promotes deposition of non ice-cored moraines (Fig. 23). The application of these four non-geographic variables allows 100%-correct classification of moraines without cores of ice (Table 9).

A third discriminant analysis was applied between the glacial landforms mapped in sedimentary terrain and those of the granitic Arrigetch Peaks (Fig. 24, Appendix G). The environmental factors are nongeographical, the same as used in Linear Discriminant Analy-

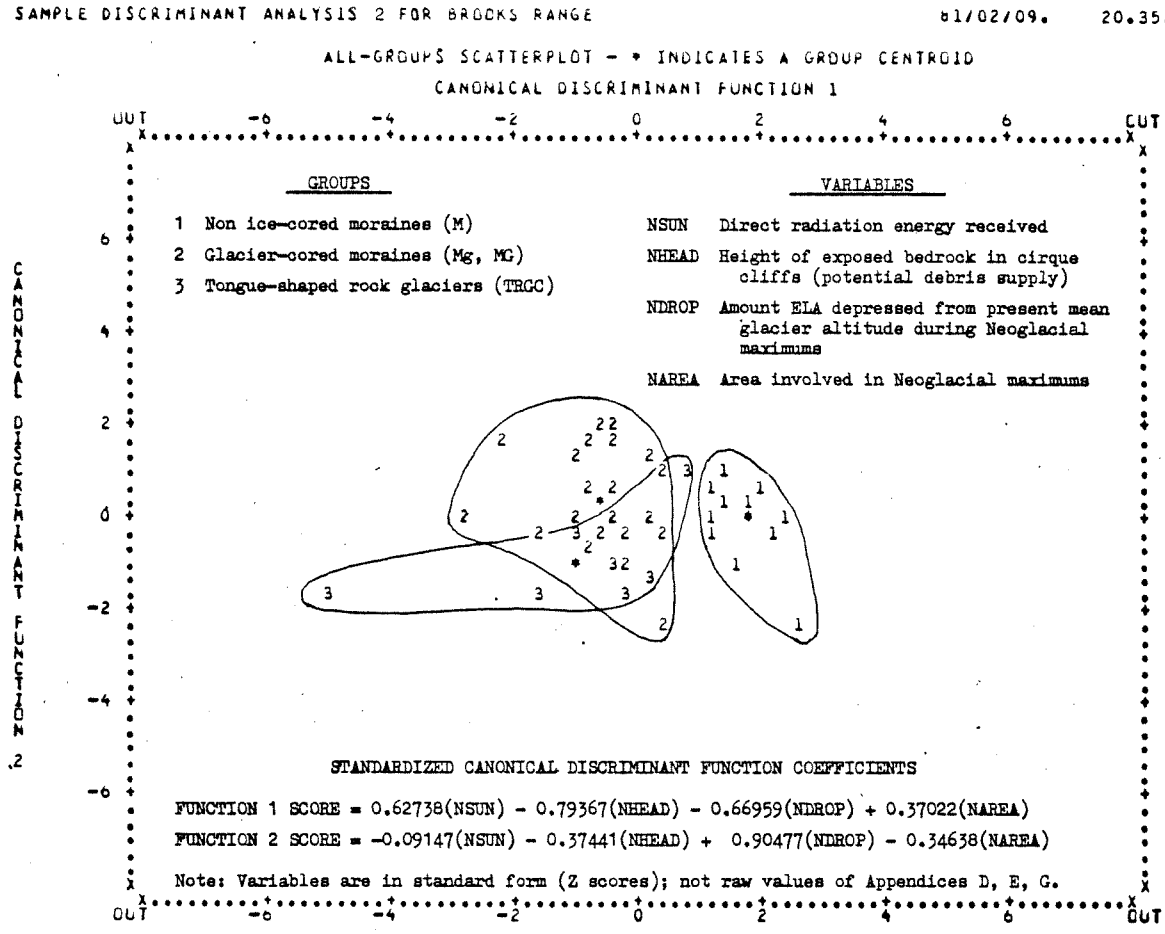

Figure 23. Scatterplot of Linear Discriminant Analysis 2 for glacial deposits in sedimentary terrain with groups, variables, and standardized coefficients given. Cirque environmental and landform morphological variables used in this analysis; these should be geographically independent (see Table 9). In this analysis, potential debris supply is the most important variable discriminating the morainal groups. Function 1 explains ~85% of the variance, emphasizing the importance of NHEAD (Appendix G).

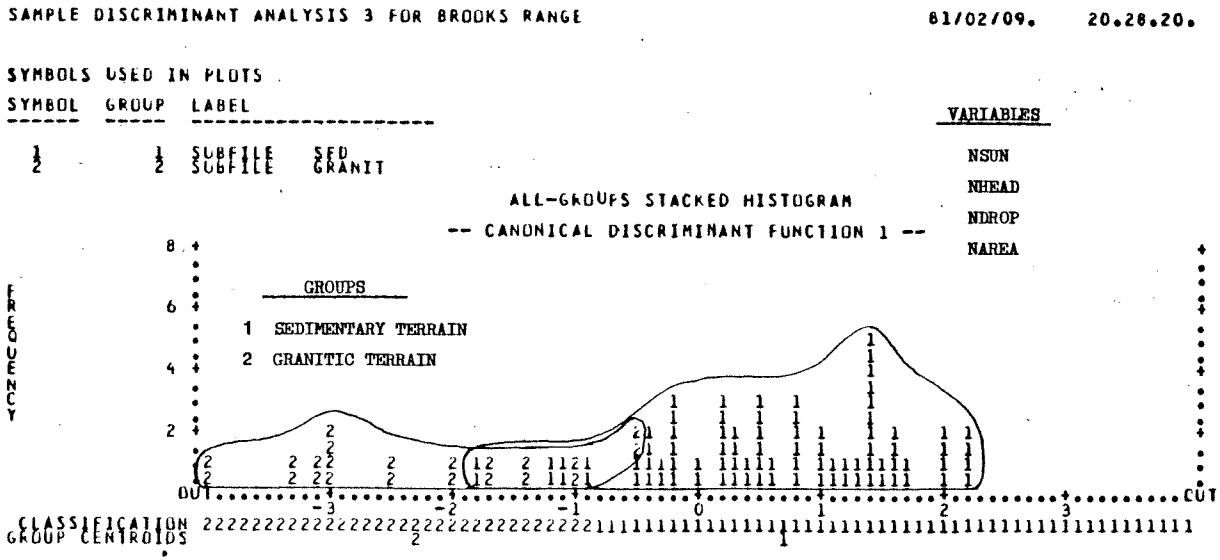

STANDARDIZED CANONICAL DISCRIMINANT FUNCTION COEFFICIENTS

FUNCTION 1 SCORE = 0.62388(NSUN) - 0.52452(NHEAD) - 0.90888(NDROP) + 0.11588(NAREA)

Note: Variables are in standard form (Z scores); not raw values of Appendices D, E, G.

Figure 24. Scatterplot of Linear Discriminant Analysis 3 for glacial deposits in sedimentary (Group 1) and granitic (Group 2) terrains. Cirque environmental and landform morphological variables used in Figure 23 are also used in this analysis to minimize geographical dependence (see Table 10). In this analysis the ELA depression during Neoglacial maxima as measured from the mean altitude of present-day glaciers is the most important factor discriminating the two groups.

sis 2 and are as follows:

a) percent of direct radiation energy received (NSUN),

b) height of bedrock exposed in cirque cliffs (NHEAD),

c) amount ELA lowered from present mean glacier altitude during Neoglacial maxima (NDROP),

d) area affected during Neoglacial maxima (NAREA)

The amount of ELA depression is by far the most important discriminant between the two terrains (Fig. 24); it is followed by the differences in solar energy received and potential debris supply. Why the ELA depression is so much greater in the west-central Brooks Range is uncertain; however, it may be related to the effects of probable greater annual precipitation, temperature, and cloudiness in the Arrigetch as compared to the more easterly Atigun Pass area. Because of this climatic difference, the glaciers may be more vigorous in the Arrigetch with increased erosive capabilities. The deeper cirques in the Arrigetch may be the result of this increased glacial erosion or the ability of the granite to stand with greater relief than sedimentary rocks. A direct result of either is markedly increased terrain screening of glacial landforms in the Arrigetch as compared to the Atigun Pass area (Table 5). These fundamental differences in cirque environments allow a 90%-correct classification of a glacial moraine into a granitic terrain of the west or a sedimentary cirque of the east, given only four non geographical variables (Table 10; see also Ellis and Calkin, in press).

Cluster Analysis 1 involved the 54 glacial deposits used in Linear Discriminant Analysis 3 (Fig. 24) but with nine environmental

TABLE 10. LINEAR DISCRIMINANT ANALYSIS 3 OF GLACIAL LANDFORMS IN SEDIMENTARY AND GRANITIC TERRAINS: CLASSIFICATION RESULTS [a]

SAMPLE DISCRIMINANT ANALYSIS 3 FOR BROOKS RANGE

CLASSIFICATION RESULTS -

ACTUAL GROUP		NO. OF CASES	PREDICTED GROUP MEMBERSHIP 1	2
GROUP 1 SUBFILE	SED	43	39 90.7	4 9.3
GROUP 2 SUBFILE	GRANIT	11	1 9.1	10 90.9

PERCENT OF GROUPED CASES CORRECTLY CLASSIFIED - 90.74

CLASSIFICATION PROCESSING SUMMARY

54 CASES WERE PROCESSED.
0 CASES WERE EXCLUDED FOR MISSING OR OUT-OF-RANGE GROUP CODES.
54 CASES WERE USED FOR PRINTED OUTPUT.

[a] See Appendix G for data and Figure 24 for scatterplot.

and morphological variables (Fig. 25, Table 11). The geographically dependent, Neoglacial maxima ELA and latitude were not considered in this analysis.

Cluster analysis does not use a priori classification of the individual landforms; it combines landforms with the greatest similarity between variables into groups (Parks, 1966; Appendix G). This analysis (Fig. 25) clusters glacier-cored moraines of the igneous Arrigetch Peaks (MGI) and the non ice-cored moraines of the sedimentary Atigun Pass area (MS) into individual groups, demonstrating statistical similarity. Moraines in the Arrigetch cirques that are without cores of ice (MI, Fig. 25) are environmentally most similar to glacier-cored moraines of the sedimentary Atigun and

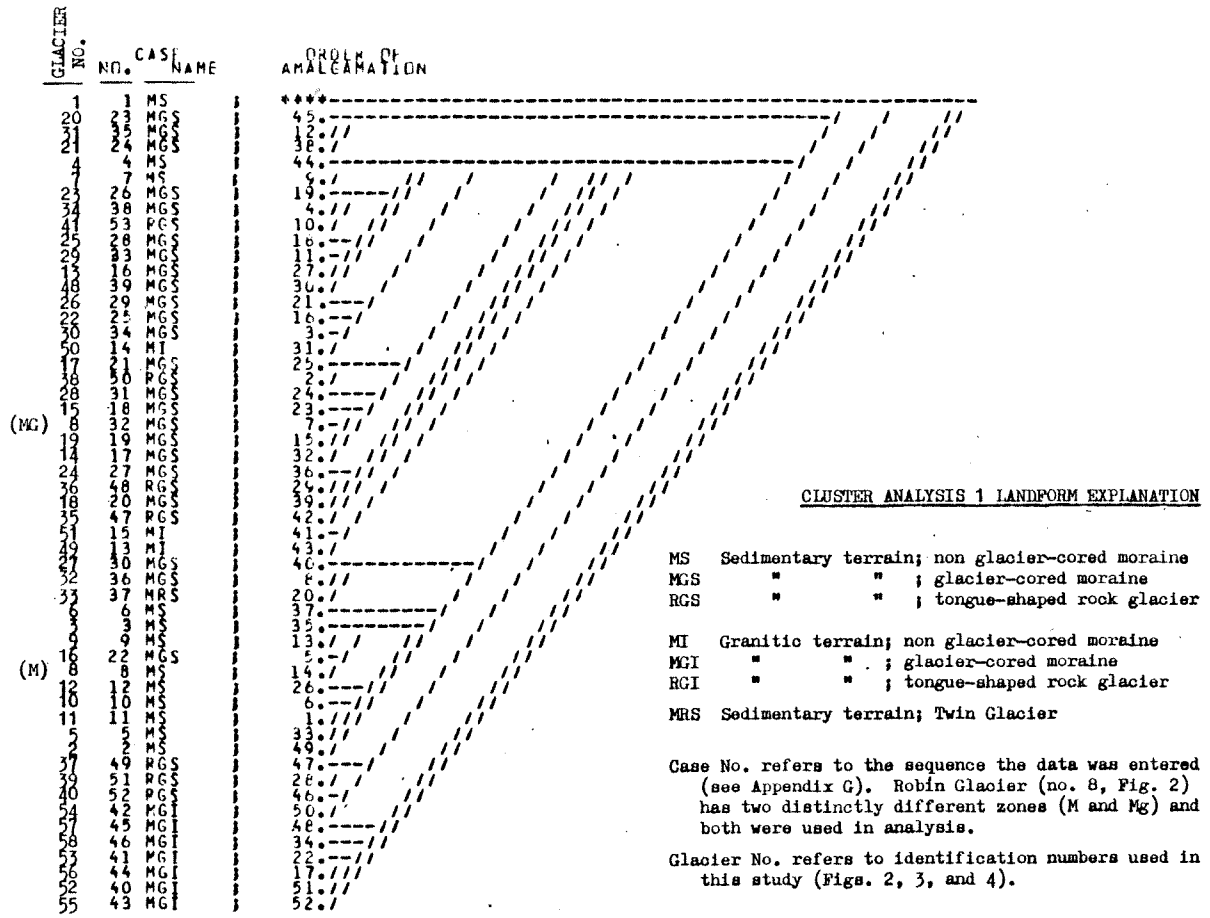

Figure 25. Plot of Cluster Analysis 1 of glacial landforms in sedimentary and granitic terrains using nine cirque-environmental and landform-morphological variables (see Table 11). Moraines without ice cores in sedimentary terrain (MS) and glacier-cored moraines in granitic terrain (MGI) are separated out of the 57 cases; however, the rest of the morainal deposits are intermixed indicating overall similarities based on the variables utilized for the analysis.

TABLE 11. CLUSTER ANALYSIS 1 OF GLACIAL LANDFORMS WITH NINE VARIABLES[a]

TREE PRINTED OVER CORRELATION MATRIX (SCALED 0-100).
CLUSTERING BY AVERAGE DISTANCE METHOD.

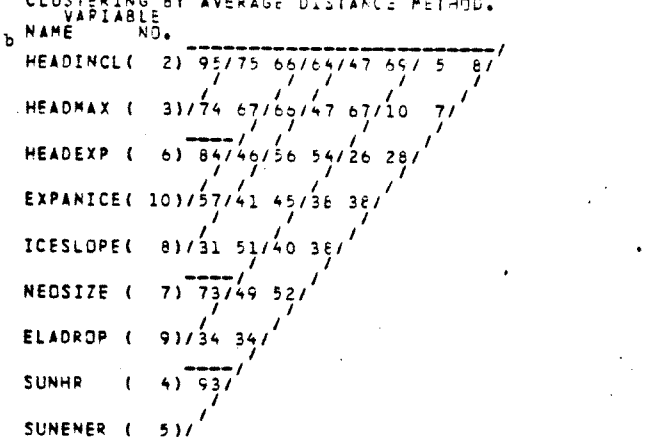

THE VALUES IN THIS TREE HAVE BEEN SCALED 0 TO 100 ACCORDING TO THE FOLLOWING TABLE

VALUE ABOVE	CORRELATION	VALUE ABOVE	CORRELATION
0	-1.000	50	.000
5	-.900	55	.100
10	-.800	60	.200
15	-.700	65	.300
20	-.600	70	.400
25	-.500	75	.500
30	-.400	80	.600
35	-.300	85	.700
40	-.200	90	.800
45	-.100	95	.900

[a]See Figure 25 for case cluster plot and Appendix G for data.

[b]See Table 2 for explanation of variables.

Anaktuvuk Pass areas (MGS, Fig. 25; see Fig. 21). The transition zone deposits on rock glaciers (RGS, Fig. 25) are interspersed throughout the sedimentary glacier-cored moraines (MGS) suggesting there are more similarities than differences between these two landforms when nine variables are considered.

The usefulness of the tree diagram (Fig. 25) for reevaluating field classification of glacial landforms is demonstrated with

Wolverine Glacier (no. 41, Fig. 2; Appendix B). Wolverine clusters closely with seven glacier-cored moraines (Fig. 25); however, field mapping revealed a small rock glacier tongue preserved downslope of the transition zone. This resulted in a field classification of Wolverine as a glacier-cored, tongue-shaped rock glacier deposit. The only substantial difference between glacier-cored rock glaciers (Fig. 15) and glacier-cored moraines (Figs. 13, 14) may be altitude (Fig. 9). Apparently, older rock glacier tongues are more typically preserved if the glacier is at a lower altitude because their ELA depression should be less vigorous than for glaciers at higher altitudes (Table 4). Higher altitude, glacier-cored rock glaciers probably did exist in some cirques before the Neoglacial. However, their surfaces were completely overrun and/or incorporated in a more significant glacial response to lowering of ELA, forming what are now defined as glacier-cored moraines. Glaciers at lower altitudes constructed debris ridges in transition zones which are environmentally and morphologically equivalent to glacier-cored moraines (Figs. 22, 23, 25). The particular response of a glacier core to Neoglacial climatic deteriorations has resulted in varying portions of the downslope rock glacier tongue being undisturbed.

Figure 11 combines the variables used in Cluster Analysis 1 with correlation coefficients (range -1.0 to +1.0) between the variables. It allows detection of highly correlated variables which can then be analyzed for cause and effect relationships, and poorly correlated variables which are desired for linear discriminant analysis (Figs. 22-25). In Figure 11, average headwall inclination (HEADINCL) and maximum headwall inclination (HEADMAX) have a positive

correlation (+0.95) as do hours of direct radiation (SUNHR) and energy received (SUNENER) (+0.93). However, of more importance to this study is the marked negative correlation (-0.85) between these two pairs of varibles; measuring only one of the four variables will explain most of the information included with the other three. For cirque glacier deposits an increase in mean or maximum horizon does result in a decrease in solar duration and energy received. In this study only one of these four parameters, direct radiation energy received (NSUN), was used for the linear discriminant analysis of glacial moraines.

Rock Glaciers

The state of activity for rock glaciers cannot be predicted based on analysis of topographic horizon and direct radiation received (Fig. 6, Table 6, Appendix F). A sample of 48 lobate rock glaciers studied near Atigun Pass showed that 16 were under cliffs of Hunt Fork Shale, 21 under the Kanayut Conglomerate, and the rest under other sandstones and limestones (Appendix G). There are no apparent correlations between landform activity, bedrock,and altitude (Fig. 26). In addition, Cluster Analysis 2 indicates no correlation to activity when exposure and latitude are also considered (Figs. 27, 10). Apparently the activity state of rock glaciers is most dependent upon the availability of debris from headwall cliffs, a parameter difficult to quantify.

The relationships between seven variables are examined in Cluster Analysis 2 (Table 12). The correlations between mean and

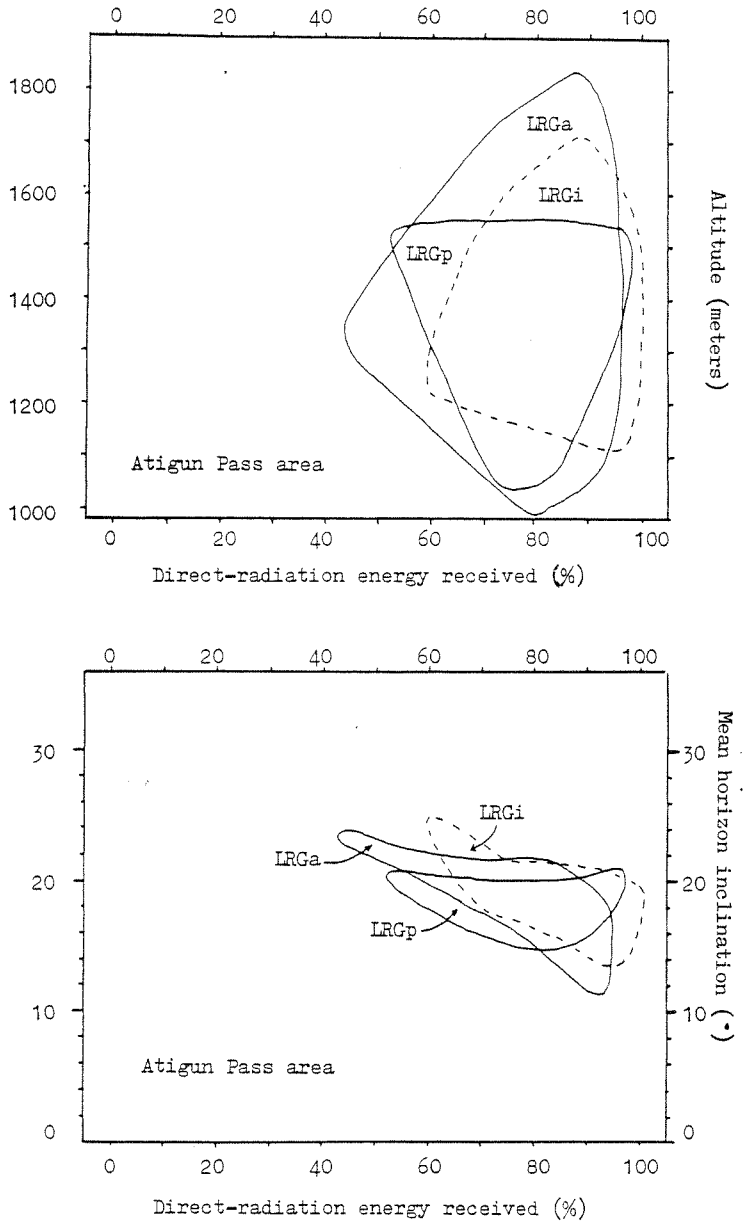

Figure 26. a) Plot of direct radiation energy received versus altitude for 48 lobate rock glaciers in active (LRGa), partially active (LRGp), and inactive (LRGi) states: no differences are evident.
b) Plot of direct radiation energy received versus mean horizon for 48 lobate rock glaciers: no differences are evident.

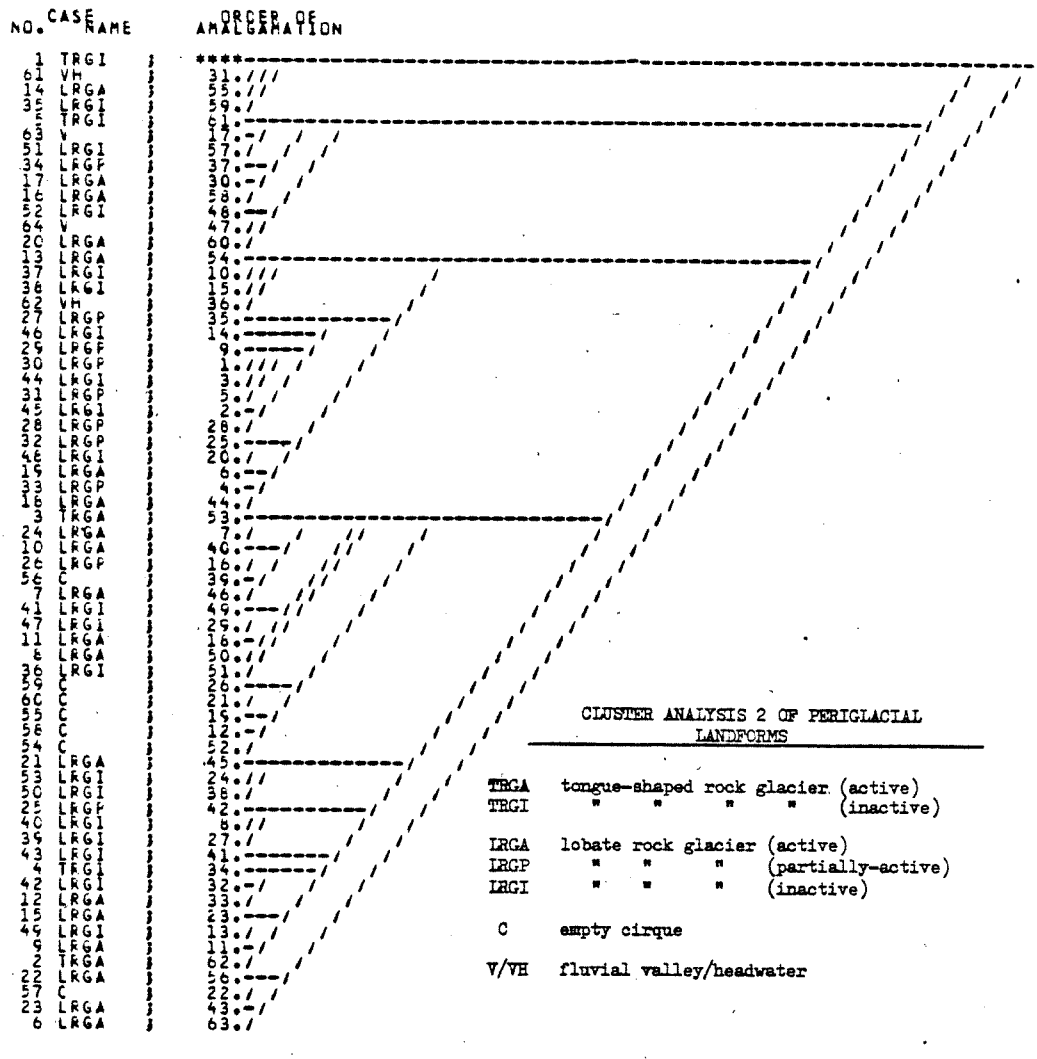

Figure 27. Plot of Cluster Analysis 2 of periglacial landforms in sedimentary terrain of Atigun and Anaktuvuk Passes using five terrain screening variables, latitude, and altitude of the horizon survey sites (see Table 12, Appendix F). Although empty cirques (C) are fairly well separated from the other periglacial landforms most of these landforms and rock glaciers in various states of activity are intermixed indicating similar alpine environments.

TABLE 12. CLUSTER ANALYSIS 2 OF PERIGLACIAL LANDFORMS WITH SEVEN VARIABLES [a]

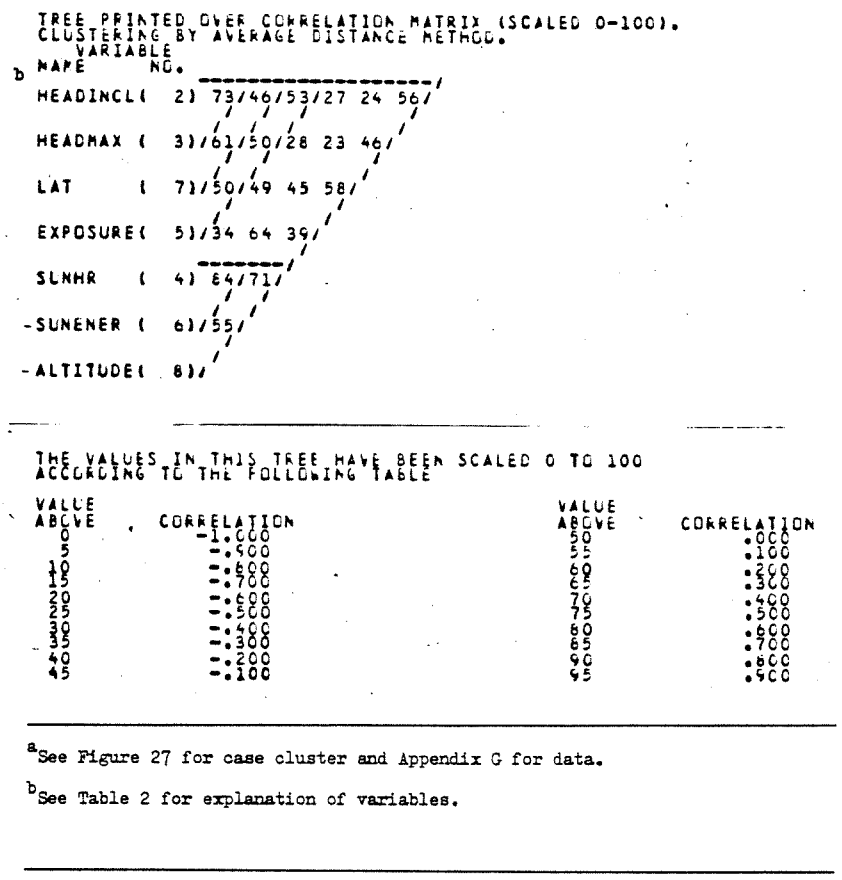

[a] See Figure 27 for case cluster and Appendix G for data.

[b] See Table 2 for explanation of variables.

maximum headwall inclination and solar duration and energy are far less than for glacial landforms (Table 11). In contrast to cirque glacier deposits, an increase in rock glacier horizon does not necessarily result in a decrease in solar energy received (Table 12). An aspect distribution that is more variable (Fig. 10), and/or increased importance of shading by terrain across valley probably accounts for the lack of correlation between rock glacier horizon and solar energy received.

DEVELOPMENT OF A HOLOCENE GLACIAL CHRONOLOGY

Lichenometry

Lichenometry is a dating technique that uses certain lichen species to obtain relative and/or absolute ages of rock substrates (Beschel, 1961). It is especially useful in arctic and alpine environments where ubiquitous, long-lived species are common (Webber and Andrews, 1973). The technique was pioneered by Beschel (1950) and is based on the general assumptions that: 1) rock debris is free of lichens when deposited; 2) rock stabilization and succeeding colonization occurs shortly after deposition; 3) subsequent lichen growth as expressed by increase in diameter occurs with a predicatable pattern; and 4) within an area of similar macroclimate, growth is a function of time passed since colonization (Calkin and Ellis, 1980). Therefore, the diameter of the largest lichen thallus is proportional to the age of the surface in question, if it may be assumed that the lichen is one that colonized shortly after glacial recession or other initial surface formation, and that the lifespan of the species utilized is greater than the age of the surface. Karlén (1979) suggests that during cold periods large areas of a glacial deposit could be covered by semi-permanent snowbanks, and underlying lichens killed or at least cease growing actively (Koerner, 1980). Therefore, only minimum ages can be determined with the lichenometric technique.

Lichenometry's basic concepts and limitations as a dating tool, as well as major elements in the technique's development, are well discussed in papers by Beschel (1950, 1961), Andrews and Webber (1964), Jochimsen (1966), Benedict (1967, 1968), Orwin (1970), Miller and Andrews (1972), Worsley (1973), Haerberli and others (1979), and Locke and others (1979). Lichenometry has been applied to construct Holocene chronologies in many areas of the world (Webber and Andrews, 1973; Miller, 1973a; Karlén, 1979; Porter, 1981). In Alaska it has been used in the central Alaska Range (Reger and Péwé, 1969) and in the St. Elias and Wrangell Mountains farther south (Denton and Karlén, 1973a, 1973b).

How long lichens can live is unknown. It is extremely difficult to determine the end of the active growth or arrival of senescence for lichens (Llano, 1956, cited in Reger and Péwé, 1969). The ultimate lifespan of some Rhizocarpon species apparently can be in excess of 9000 years (Denton and Karlén, 1973b; Andrews and Barnett, 1979).

Lichen Species Utilized

Six lichen species were selected as dating tools based on their wide distribution in the field area and elsewhere in the arctic, their characteristic morphologies, and consistent growth rates. Four of them were introduced to us by P.J. Webber (see Ellis, 1978) and are among the species studied on Baffin Island since 1950 (Hale, 1954; Andrews and Webber, 1964, 1969; Miller and Andrews, 1972; Miller, 1973b; Andrews and Barnett, 1979). The four species are

Alectoria minuscula Nyl., Alectoria pubescens (L.) Howe, Umbilicaria proboscidea (L.) Schrad, and Rhizocarpon geographicum (L.) DC. The first three are fast growing; the last, R. geographicum, is a cosmopolitan, slow growing,and long living lichen used in more than 40 published lichenometric studies (Webber and Andrews, 1973). The other species used in dating were Rhizocarpon eupetraeoides (Nyl.) Blomberg and Forsell and Rhizocarpon inarense (Vainio) Vainio (see Calkin and Ellis, 1980 for botanical descriptions, voucher speciman information, and photographs of the species).

R. geographicum is a rather variable species (Thomson, 1967) so its name has been used in the general sense (s.l.) in this study, as it has in most lichenometric studies to date (Andrews and Webber, 1964; Birkeland, 1973). References to R. geographicum generally can be applied to R. eupetraeoides/inarense for thallus diameters to 150 mm (see Calkin and Ellis, 1980 for interspecific ratio data, p. 249-250).

Measurement Techniques

Lichenometric mapping involved the recording of thallus diameters of the six species on mappable geomorphic units while traversing as much area as possible. Only the maximum diameter of the largest lichen thallus is used as an indicator of substrate age, because it is assumed to be the oldest and possess the optimum growth rate for the site being studied (Beschel, 1950). However, if the maximum diameter of this largest thallus was found to be ~20% above the next largest diameter or a cluster of diameters, it was generally dis-

counted and assumed to have been inherited from a pre-existing surface. Only lichens with distinct, slightly elliptical to circular shapes were measured, and these to the nearest 1 mm.

The search for lichens involved scrutinizing all sides and upper surfaces of boulders and cobbles for measurable lichen thalli while recording the state of development of other relative age indicators; for example, weathering, soil development, and horizontal stratigraphic position. Time limits on sampling, and short selective traverses across the terrain (Rampton, 1970; Birkeland, 1973) or other areally-limiting sampling techniques (Andrews and Webber, 1964; Matthews, 1974; Locke and others, 1979) provide data which are useful for statistical treatment of lichen diameters but limit the effectiveness of mapping and study of overall glacial history (Karlén, 1973; Miller, 1973a, p. 522; Calkin and Ellis, 1980).

Maximum diameters of the lichen species that characterized the age of a map unit or landform were compared to determine interspecific ratios (see Andrews and Webber, 1964). This determined the relative growth rates between the three fast growing species and Rhizocarpon geographicum s.l., enabling potential diameter and age relationships found for one species to be transferred to the other three (Ellis, 1978). In particular, it enables the transfer of growth rates determined from direct observations of the fast growing Alectoria minuscula and A. pubescens to the R. geographicum curve. It also allows comparison to the work done on Baffin Island (Andrews and Webber, 1964, 1969; Miller and Andrews, 1972; Miller, 1973b).

Construction of an Absolute Lichen-Dating Curve

Growth rate is not constant over a lichen's life span (Benedict, 1967). It is initially rapid over a great growth period lasting from 40 to 500 years, but decelerates with time until a generally linear, long term growth rate is attained (Fig. 28). Webber and Andrews (1973) compiled the growth rates (lichen factors) of 29 R. geographicum curves and concluded that high precipitation, long growing seasons, and high temperatures favor more rapid growth. That this climatic control strongly affects the rate and duration of the initial great growth period has been well shown by Beschel (1961) from Greenland. Meager climatic data across the central Brooks Range (Table 1) suggest the Arrigetch Peaks may be slightly warmer and wetter than the Atigun Pass area. This climatic difference may enable lichens to grow slightly faster in the Arrigetch as compared to those 225 km farther eastward.

However, Miller and Andrews (1972) suggest that climatic differences may have less control on the long term growth rate of R. geographicum since those of Baffin Island, the Colorado Front Range (Benedict, 1967), and Swedish Lapland and southern Alaska (Denton and Karlén, 1973b) have growth rates approximating 3 mm per century (Fig. 28). As a first approximation, the central Brooks Range growth curve for R. geographicum s.l. should resemble those from other regions with similar climatic regimes. The climatic regime of the central Brooks Range may be similar to that recorded for central Baffin Island (Andrews and Webber, 1964) where mean annual temperature is -10°C and annual precipitation is about 370 mm (Fig. 28).

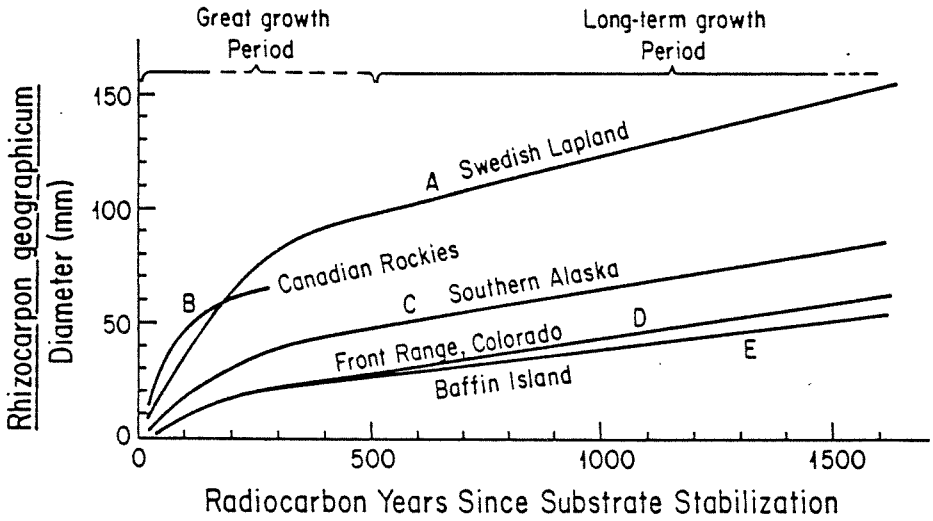

Figure 28. Selected Rhizocarpon geographicum growth curves showing the impact of climate. Generally decreasing precipitation, temperature, and length of growing season result in slower growth rate. Curves are from: A - Denton and Karlén (1973b); B - Luckman (1977); C - Denton and Karlén (1973b); D - Benedict (1967); and E - Miller and Andrews (1972).

In addition to this climatic control, direct measurements of the growth rate of fast growing lichens were able to be transferred to the R. geographicum species because interspecific ratios have been developed for the region (Ellis, 1978). Absolute dating control for the calculation of lichen growth rates was obtained from radiocarbon, dendrochronologic, and historic records; the latter includes abandoned gold mines, archeologic sites, and sequential glacier photographs dating from 1911.

Variations in Lithology, Stability, and Macroenvironment. The effects of lithologic variations on lichen growth are not clearly

understood, and studies usually minimize this potential problem by measuring lichens on rocks of similar composition. In the Atigun and Anaktuvuk Pass areas (Fig. 1) the siliceous Kanayut Conglomerate provides a relatively uniform and extensive lithology upon which to base the lichenometric dating curve. Varying amounts of silica do not seem to noticably affect the lichen growth. The granitic terrain of the west-central Arrigetch Peaks apparently provides a comparable base for growth.

The lichens used in this study are very rarely associated with limestones (see Osborn and Taylor, 1975). The only exceptions are where growth occurs on associated chert nodules. This becomes a critical problem for lichenometry in the glacierized cirques north of the Anaktuvuk Pass area (Porter, 1966) and eastward 30 km in the Alapah and Fan Mountain regions where type locations for the Neoglacial in the Brooks Range are presently located (Detterman and others, 1958); both areas are extensively underlain by limestones.

Lichens used in this study are able to grow on a variety of rock substrates, including the metamorphic rocks at the Arrigetch and the mining district near Wiseman (Fig. 1). In addition, they populate the shales and phyllites of the Hunt Fork formation which generally crop out south of the Continental Divide in the central and east-central Brooks Range (Porter, 1966; Brosgé and others, 1979). However, R. geographicum typically are limited to diameters of less than 25 mm on easily weathered, shaley substrates. In contrast, on tough orthoquartzitic conglomerates R. geographicum attain diameters in excess of 250 mm. The largest thalli found that appar-

ently belonged to this species measured 325 x 245 mm; it was growing on a two meter boulder situated at the front of an inactive, lobate rock glacier downslope of Raven Glacier, Atigun Pass area (no. 21, Fig. 2). On massive granitic bedrock and boulders located outside of Neoglacial deposits in the Arrigetch Peaks, we have measured R. geographicum ~250 mm in diameter.

Substrate stability is a major limiting factor in the application of lichenometry. The maximum lichen diameters on glacial drift are less reliable for determining the age of initial ridge construction where there has been a shifting of the surface due to melting of ice cores or rock glacier creep has occurred. At the Arrigetch Peaks, it may be the destabilizing effects of melting glacier-ice cores that cause lichens to be relatively sparse and inconsistent in size (Fig. 29) as compared with the cover in sedimentary terrain. In addition, the aerial green algae with hematochromatic pigment identified by R. Zander (pers. comm., 1980) as Trentepohlia iolithus (L.) Wallr is widespread in the Arrigetch Peaks; it may further inhibit lichen cover as it precedes lichen colonization (D. Cooper, pers. comm., 1980). When other relative dating parameters point to an older age for the deposit than indicated by maximum lichen diameters, it is suggested that the surface has been too unstable for "normal" lichen colonization and/or the surface has been subjected to semi-permanent snow cover in the past (Karlén, 1979).

Recorded observations of glaciers in the central Brooks Range date to 1911, when Philip S. Smith of the U.S. Geological Survey explored Arrigetch Creek and photographed the glaciers at its head

Figure 29. View southeast on 15 August 1979 toward east glacier arm and associated glacier-cored moraine of Arr-4 and combined terminal moraine of Arr-2, -3, and -4 (nos. 55, 56 of Fig. 4). Dotted line shows approximate ice margin in 1911 (Smith, 1912, 1913; Ellis and others, 1981). A bedrock divide marked by a glacial spillway (S) separates Arr-4's east and west arms. A thin veneer of drift over bedrock left on the divide and along the interlobate area (B) during deglaciation provides an optimum substrate for lichenometry.

(Smith, 1912, 1913). Sequential photographs in 1962 by T.D. Hamilton (1965a) and in 1979 by Hamilton and Ellis (Ellis and others, 1981, Figs. 6, 7) of the receding Arrigetch Peaks cirque glacier complex Arr-2,-3, and -4 (nos. 55, 56, Fig. 4; shown in Fig. 29) enabled stability of lateral and terminal ridges associated with two glacier-cored moraines to be assessed. The interiors of these debris lobes which are cored with glacial ice subsided appreciably from 1962 to

1979. Even more intense subsidence was recorded for the 51 year interval between 1911 and 1962. However, the distinct lateral and terminal ridges at the perimeters of these lobes support overall stability along the margin during the 20th century (Fig. 29). Stability is also indicated by the dark tonal quality of the margins imparted by a widespread cover of Trentepohlia iolithus algae. This cover intensified from 1911 to 1962 (Hamilton, 1965a), perhaps with algal colonization of the granitic substrate, but it has remained relatively uniform since 1962.

The maintenance of peripheral stability, despite the collapse of the interior glacier core, is favorable for lichenometric dating which depends on substrate stability. It suggests that lichenometric records preserved along the margins of glacier-cored moraines and debris ridges of transition zones may be similar to those found on stable moraines without cores of ice if glacial expansions were synchronous in both cirque environments.

Reger and Péwé (1969) considered the most important microenvironmental controls in the central Alaska Range 500 km south of Atigun Pass to be the availability of sunlight and moisture, and stability of the substratum. Rock faces hosting the largest lichen thalli there displayed a dominant southwest orientation in contrast to the Front Range (Birkeland, 1973) or the Swiss Alps (Haerberli and others, 1979) where R. geographicum is absent from south-facing rock surfaces. No strong relationships between lichen growth and orientation or height above the moist ground surface showed up in this study. Substrate stability and the presence or absence of the algae,

Trentepholia iolithus, are suggested as the strongest influences of lichen development on cirque glacier deposits in the central Brooks Range, assuming the snow-free period is equivalent on the deposits.

Direct Measurement of Lichen Thalli. The relative growth rates between the three fast growing lichens (Alectoria minuscula, A. pubescens, and Umbilicaria proboscidia) and Rhizocarpon geographicum show the rates of the fast growing species as relatively similar; all grow about seven times faster than R. geographicum (Ellis, 1978; Calkin and Ellis, 1980, Table 1). Our data on cirque glacier deposits suggest that the species colonize and/or become visible to the unaided eye contemporaneously.

Thalli of A. minuscula and A. pubescens ranging in maximum diameters from 30.0 to 71.3 mm were traced in early August 1977 and remeasured in early August 1979 allowing growth rates to be computed for thalli of this diameter range. The lichens were located on bouldery Neoglacial drift associated with Grizzly Glacier at an altitude of 1680 m, about 1 km east of Atigun Pass (cover photograph). Changes in thallus diameters were determined from these tracings by the planimetric method (diameter = $2.0 \left(\text{area} / \pi \right)^{\frac{1}{2}}$) with results that show a progressively decreasing growth rate with increasing diameter for both Alectoria species (Table 13). These direct measurements were extrapolated to the indirectly controlled growth curve of the slow growing R. geographicum by use of the 7:1 interspecific ratio. This suggests as diameters increase from 5.0 to 10.1 mm, the growth rate of R. geographicum decreases from ~25 mm 100 yr^{-1} to ~14 mm 100 yr^{-1} (Table 13).

TABLE 13. DIRECT GROWTH MEASUREMENT DATA FOR *ALECTORIA MINUSCULA/PUBESCENS* EXTRAPOLATED TO *RHIZOCARPON GEOGRAPHICUM*

A. minuscula and *A. pubescens*		*R. geographicum*	
Maximum Diameters (mm) 1977	Planimetrically Determined Diameter Change ($mm\ yr^{-1}$) [a] 1977 - 1979	Extrapolated Great Growth Rate ($mm\ 100\ yr^{-1}$)	Effective Diameter Range (mm)
30.0	+1.8		
31.5	+1.7	25	5.0 - 5.5
35.0	+1.2		
35.5	+1.9		
42.5	+1.6		
47.3	+1.8	24	6.0 - 6.7
63.0	+1.3		
64.0	+1.4	18	9.0 - 9.7
68.0	+1.0		
71.3	+1.0	14	10.1

[a] Diameter = 2.0 $(area/\pi)^{\frac{1}{2}}$ from tracings made in early August of 1977 and 1979.

Absolute Control Points for the Lichen Growth Curve. Eleven control points were found in the central Brooks Range; they encompassed abandoned mines, archeological sites, glacier photographs, radiocarbon ages, and dendrochronology (see Calkin and Ellis, 1980 for details). Abandoned gold placer mines and shafts occur 85 km south of Atigun Pass at Linda Creek (Fig. 5), just north of Wiseman (Fig. 2). The production and abandonment of these mining operations is documented by Maddren (1910, 1913), Cobb and Kachedoorian (1961),

and Cobb (1976).

R. geographicum attain maximum diameters of 10 mm on stones in tailings associated with shafts abandoned in 1909 (Calkin and Ellis, 1980, Fig. 5). This species attains maximum diameters of 12 mm on handworked placer deposits abandoned soon after 1901. Since the summers are warmer in this low altitude, southern mining district than near Atigun Pass (Brown, 1980), these lichen diameters should be considered as maximum values for the growth curve constructed for use primarily on higher altitude, cirque glacier deposits.

At an abandoned Nunamiut Eskimo village named Aniganigurak (Fig. 2), rifle cartridges were recovered indicating occupation no earlier than 1873, and abandonment between 1880 and 1890 (Corbin, 1971, p. 272-296). R. geographicum attain diameters of 12 mm on a few siliceous erratics used to build campfire and tent rings.

Sequential photographs taken in 1911, 1962, and 1979 of the receding cirque glacier Arr-4 (Fig. 29) provide clues to lichen colonization and growth rates (Hamilton, 1965a,; Ellis and others, 1981, Fig. 7). The lag period between substrate stabilization and initial lichen colonization of A. minuscula/pubescens and R. geographicum is ill defined, but the glacial geologic literature suggests that it ranges from 10 to 50 yr (Webber and Andrews, 1964; Benedict, 1968; Rampton, 1971; Miller and Andrews, 1972; Beschel and Weidick, 1973; Karlén, 1973). At glacier Arr-4 the area deglaciated since 1911 is approximately delineated on Figure 29. A bedrock divide marked by a glacial spillway (S) separates Arr-4's east and west arms. This spillway was ice- or snow-filled in 1911

(Smith, 1912). In 1962 and 1979 the ice margin was well upslope of this spillway. A thin, bedrock-cored veneer of glacial drift left on the divide and along the interlobate area (B, Fig. 29) provides an optimum substrate for lichenometric measurements.

No visible lichens were found in the ice marginal zone exposed since 1962; this provides a minimum time of 17 years for colonization. However, R. geographicum thalli progressively increase in diameter to at least 9 mm with distance from the retreating glacier within the area apparently exposed in the 51 years between 1911 and 1962. Some attained diameters of 11 mm where found on boulders deposited directly on bedrock. Alectoria pubescens reached diameters of 62 mm and R. eupetraeoides/inarense reached 10 mm diameters in associated areas deglaciated since the 1911 photograph (Fig. 29).

A fresh surface was carved during 1950 into lichen covered bedrock located at ~1000 m altitude, ~100 km northwest of the Arrigetch Peaks. In 1979 it was photographed for analysis of lichen colonization rates in the region (Brosgé, pers. comm., 1979). Most of the 29 year old inscription lacked lichen growth; however, R. geographicum thalli ranging to 2.0 mm were measured on the 1979 photograph. This places colonization time at somewhat less than 29 years; the Arrigetch Peaks photographs bracket it between 17 and 68 years. Based on this and the literature range of 10 to 50 years, the lichen growth curves generated for the central Brooks Range have an assumed colonization period of 30 years.

Four radiocarbon dates obtained on deposits in the Atigun Pass area could be correlated with maximum R. geographicum thalli occurring

on the overlying surficial deposits (Table 14, Fig. 30). The designation on Figure 30, the radiometric age, and the maximum thallus diameters associated with the four control points are as follows: a) 210 ± 90 yr B.P. = 12 mm; b) 320 ± 100 yr B.P. = 20 mm; g) 800 ± 90 yr B.P. = 33 mm; and i) 1300 ± 100 yr B.P. = 50 mm (see Ellis and Calkin, 1980 for amplification).

The white spruce tree line is located 15 km south of and 750 m below Atigun Pass along the TAPS corridor (Fig. 30). The oldest tree on an alluvial fan there displayed 310 rings; the largest R. geographicum thallus on associated boulders was 26 mm in diameter. White spruce in three small channels on another alluvial fan provide ages from 100 to 106 years, R. geographicum on boulders in the same channels commonly attain diameters to 10 mm. In the Linda Creek placer gold mining area a white spruce adjacent to a relatively recent shaft tailing pile was 39 years old. Diameters of the R. geographicum on the surrounding stones reached 7 mm.

Growth Curve Construction. Climatic, historic, radiocarbon, direct measurement, and dendrochronologic controls allow construction of a Rhizocarpon geographicum s.l. growth curve for the central Brooks Range (Fig. 31). From 0 to 1300 years the curve is fitted among the 11 control points discussed in the preceding paragraphs. A colonization period of 30 years is incorporated into the curve. All control points are adjusted to A.D. 1979, and are given in radiocarbon years on Figure 31. With each radiocarbon date some estimate of the time lag between death and burial of vegetation and stabilization of the lichen bearing rock surface had to be incorpo-

TABLE 14. RADIOCARBON DATES

Sample	Age yr B.P.	Location (Fig. 30)	Description
BGS 547	210 ± 90	a	Peat layer at 0.65 m depth in an alluvial fan at 900 m altitude in the TAPS corridor (Alyeska Material site MS-112-2). Associated with R. geographicum on the fan's aggradational surface ≤12 mm in diameter.
BGS 522	320 ± 100	b	Woody vegetation preserved in bedrock joints underneath the lateral margin of Buffalo Glacier's (no. 1, Fig. 2) outermost, non glacier-cored moraine (Calkin and Ellis, 1980, Fig. 6). Located at 1615 m altitude; associated with R. geographicum ≤20 mm and A. minuscula ≤140 mm in diameter that grow on the upper surface of the moraine.
BGS 671	380 ± 90	c	Peat layer at 1.5 m depth in an alluvial fan at 1070 m altitude in TAPS corridor. Dates beginning of aggradation on fan surface.
BGS 549	480 ± 140	d	Plant fragments from the interface between an older rock glacer lobe and an overriding ice-cored Neoglacial moraine ~30 m thick. Sample may date advance of Wolverine Glacier (no. 41, Fig. 2) over the rock glacier.
BGS 613	540 ± 180	e	Grassy plant fragments from the interface of the cirque threshold and Ram Glacier's (no. 16, Fig. 2) ice cored moraine. Sample dates advance of the glacier or mass wasting of steep front of the moraine.
BGS 513	740 ± 100	f	Top of massive peat layer in floodplain deposits of Atigun Valley. Used to aid in pollen analysis of section (W. Mode, written comm., 1980).

TABLE 14 (continued).

BGS 548	800 ± 90	g	Peat layer 0.95 m depth in an alluvial fan at 1220 m altitude near Alyeska Material Site MS-110.2. Maximum R. geographicum of 33 mm were measured on boulders at the fan surface in the vicinity of the dated material.
BGS 614	1120 ± 180	h	Emergent mosses collected in situ from around boulders being exposed by the receding Golden Eagle Glacier (no. 7, Fig. 2; Fig. 44). Dates glacier's last Neoglacial advance over this cirque threshold site (Calkin and Ellis, 1981, Fig. 3).
BGS 670	1300 ± 100	i	Peat layer at 0.85 m depth in an alluvial fan at 1130 m altitude in the TAPS corridor. Maximum R. geographicum of 50 mm were measured on boulders at the fan surface in the vicinity of the dated material.
BGS 615	1500 ± 150	j	Plant fragments from the interface of the bedrock cirque threshold and ice-cored terminal moraine of Kid Glacier (no. 18, Fig. 2). Sample may date advance of glacier or mass wasting event at front of steep moraine.
BGS 512	2510 ± 110	f	Base of massive peat layer in floodplain deposit of Atigun Valley near Galbraith Lake. Provides basal date for pollen analysis done by W. Mode.
BGS 616	5870 ± 160	k	Basal peat layer exposed in terrace 9.5 m high of Atigun Valley. Peat alternates with lacustrine silt. Oldest age yet determined for aggradation in the Atigun River valley (Hamilton, 1979b).

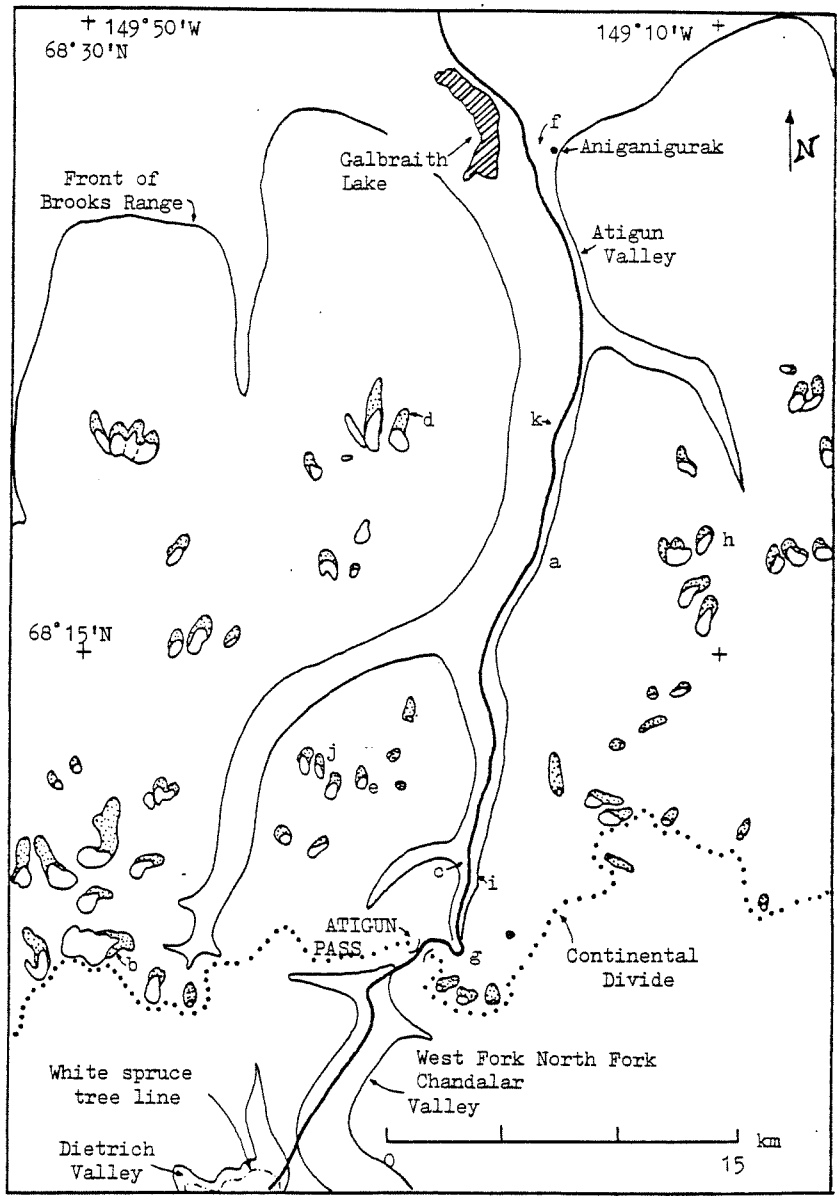

Figure 30. Radiocarbon sites in the Atigun Pass area (a-k, see Table 14 for description and age obtained at each site.

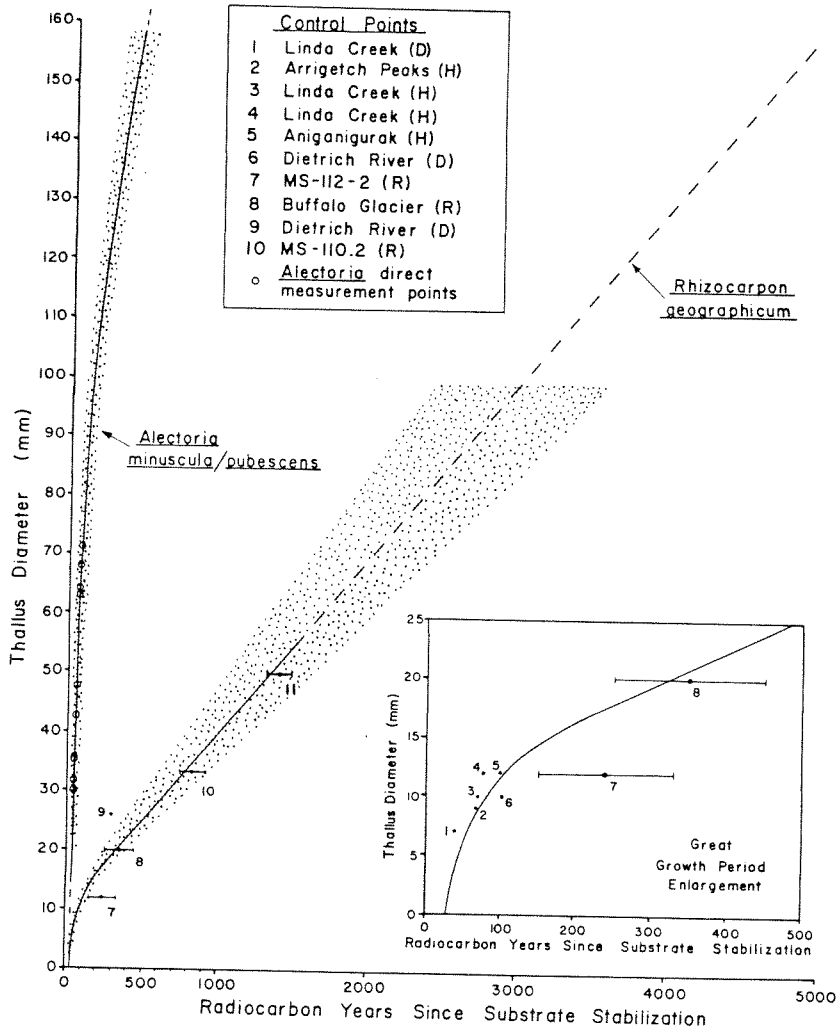

Figure 31. Rhizocarpon geographicum and Alectoria minuscula/pubescens growth curves, central Brooks Range. See Table 13 for direct growth measurement data on Alectoria taxa. Shaded zone indicates qualitative ± 20% age reliability for the growth curves. Colonization is assumed to occur 30 years after substrate stabilization as shown by the growth curve placement. Control points 1-10 are indicated as dendrochronologic (D), historic (H), or radiocarbon (R). Control point 11 is based on a radiocarbon age (Table 14).

rated into the curve. This results in the curve being offset to the left (younger part) of the points themselves. Direct A. minuscula/pubescens thallus measurements over two growing seasons were extrapolated to assist in constructing the R. geographicum curve for the first 400 years by using the interspecific ratio 7:1 (Table 13). A qualitative ± 20% age reliability is shown by the shaded zone about these growth curves. This estimate of age reliability is speculative, but is included to emphasize the limitations of lichenometric dates (see Miller and Andrews, 1972; Miller, 1973a).

The R. geographicum growth curve can be applied with reservation to R. eupetraeoides/inarense for thallus diameters less than 150 mm. A. minuscula and A. pubescens can be reliably used for dating deposits to 400 years age. The R. geographicum curve from 0 to 1300 years indicates a great growth period lasting for 200 years which is followed by a linear growth approximating 3 mm per century. This curve is extrapolated beyond the 1300 ± 100 yr B.P. radiocarbon control point to 5000 yr B.P. (Fig. 31). The linear extrapolation is not based directly on data from the Brooks Range; it is inferred from measurements of R. geographicum obtained in other parts of the world that are controlled by radiocarbon dates ranging from 1050 to 9000 yr. B.P. (Benedict, 1967; Miller and Andrew, 1972; Denton and Karlén, 1973b; Andrews and Barnett, 1979).

One point of indirect evidence supporting this growth curve extension beyond 1300 yr B.P. may be drawn from correlations between Holocene stream terraces and cirque glacier deposits of the central Brooks Range. Hamilton (1980c) suggests that a relatively mild cli-

matic interval during the middle Holocene terminated about 4000 yr B.P. This was followed by intensification of cold climate processes and a significant and radiocarbon-dated episode of terrace alluviation downstream of cirques occupied by large ice masses (Hamilton, 1979b). Lichenometric mapping of Neoglacial cirque moraines in the region reveals stable deposits bearing R. geographicum with thallus diameters to 145 mm (Fig. 32; Calkin and Ellis, 1980). These are the oldest, lichenometrically dated moraines yet found in the central Brooks Range; they may be associated with initiation of this ~4000 yr B.P. terrace building event.

Lichenometric Mapping of Cirque Glacier Moraines

Moraines downslope of 41 cirque glaciers were lichenometrically mapped in the Atigun Pass area (Fig. 2; Appendix C: 1-41). Although seven cirques were mapped in the Anaktuvuk Pass area (Fig. 3), only one cirque had a deposit with a visible glacier upslope (Appendix C: 48). The lichen record on this debris lobe (no. 48, Fig. 3) was grouped with the Atigun Pass data as they all are at approximately the same latitude, altitude, and in similar sedimentary terrain (Fig. 33). In the Arrigetch Peaks six depositional complexes were mapped; these form nine distinct morainal lobes downslope of glacier tongues (Fig. 4; Appendix C: 50-59).

Only lichens measured on moraines (M, Mg, MG), including transition zone deposits (TRGC) upslope of rock glacier tongues, were used in the subsequent Neoglacial chronology. All thallus measurements refer to R. geographicum. To clearly delineate an age as licheno-

Figure 32. View looking south at large boulder on the stable moraine associated with Triple East Glacier, Atigun Pass area (no. 12, Fig. 2). Boulder hosts Rhizocarpon geographicum s.l. thalli to 145 mm in diameter. This is the oldest Neoglacial moraine yet discovered in the central Brooks Range. In the background is younger debris and the glacier.

metrically determined, (L) is placed before the derived age, followed by the ± 20% age reliability range. Ages derived from the lichen growth curve date the beginning of glacial retreat from advanced ice positions and stabilization of debris ridges, not strictly the times of maximum glacier expansions and ridge construction (Andrews

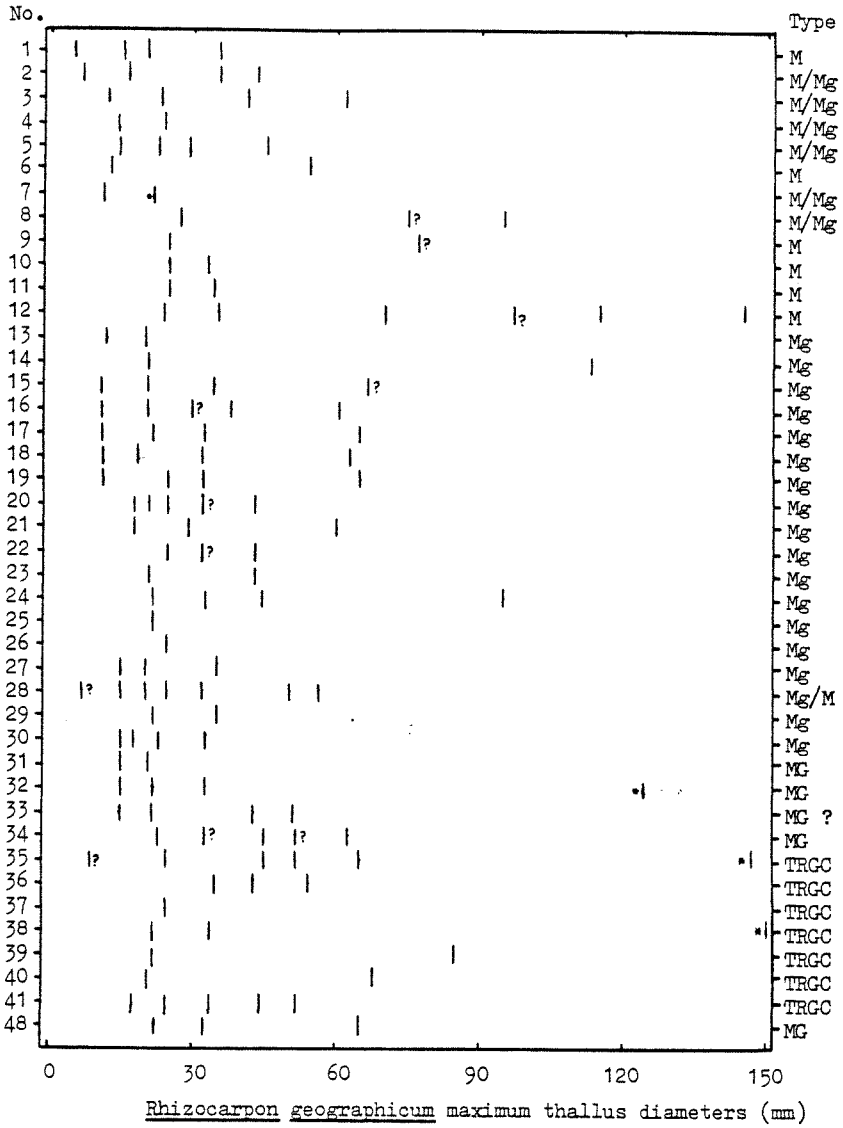

Figure 33. Maximum thallus diameters of R. geographicum characterzing moraines downslope of cirque glaciers in the sedimentary terrain of Atigun and Anaktuvuk Passes. Those diameters that were found on thin drift over bedrock are shown by (•); those thalli found on rock glacier tongues downslope of transition zones were not used in the subsequent Neoglacial chronology (*). The glaciers' identification numbers and type of moraine are indicated (Table 2).

and Barnett, 1979).

Atigun Pass Area. Twelve morainal complexes were deposited with minimum cores of ice (M-type, nos. 1-12, Figs. 2, 33). Their lichenometric record is the most distinct for all cirque glacier deposits because of their increased substrate stability.

The largest lichens found on a Neoglacial moraine in the central Brooks Range were at Triple East Glacier (Figs. 32, 34). The most complete and oldest lichen record was found on the east side where the concentration of shale is the lowest. There clusters of lichens maximizing at 24, 35, 70, 97(?), 115, and 145 mm characterize ridges on this stable debris lobe. These represent stabilization events at (L) 450, 850, 2000, 3000, 3500, and 4500 yr B.P. ($\pm$ 20% age reliability). On the west side of the morainal loop where shale dominates, increased instability and easily weathered substrates prevent large lichens from developing (Fig. 34).

Eighteen glacial deposits are extensively cored with ice (Mg) as compared to M-type moraines. Within this Mg-group, Fox, Ram, Ewe, Kid, and Vole Glaciers (nos. 15-19, Fig. 2) show very similar lichen records (Fig. 33). Major ridge building events terminated about (L) 1900 $\pm$ 400, 800 $\pm$ 200, and 350 $\pm$ 80 yr B.P., and a recessional glacier-cored ridge system dated at (L) 100 $\pm$ 20 yr B.P. is also present. Similar glacier sizes and shapes (Appendix B) along with relatively similar cirque environments (Fig. 25; Appendices E, G) may reinforce the effects of geographical closeness. Lichen thalli indicative of stabilization beyond 2000 yr B.P. are rare on ice-cored moraines; however, some dating to (L) 3500 $\pm$ 700 yr B.P. are

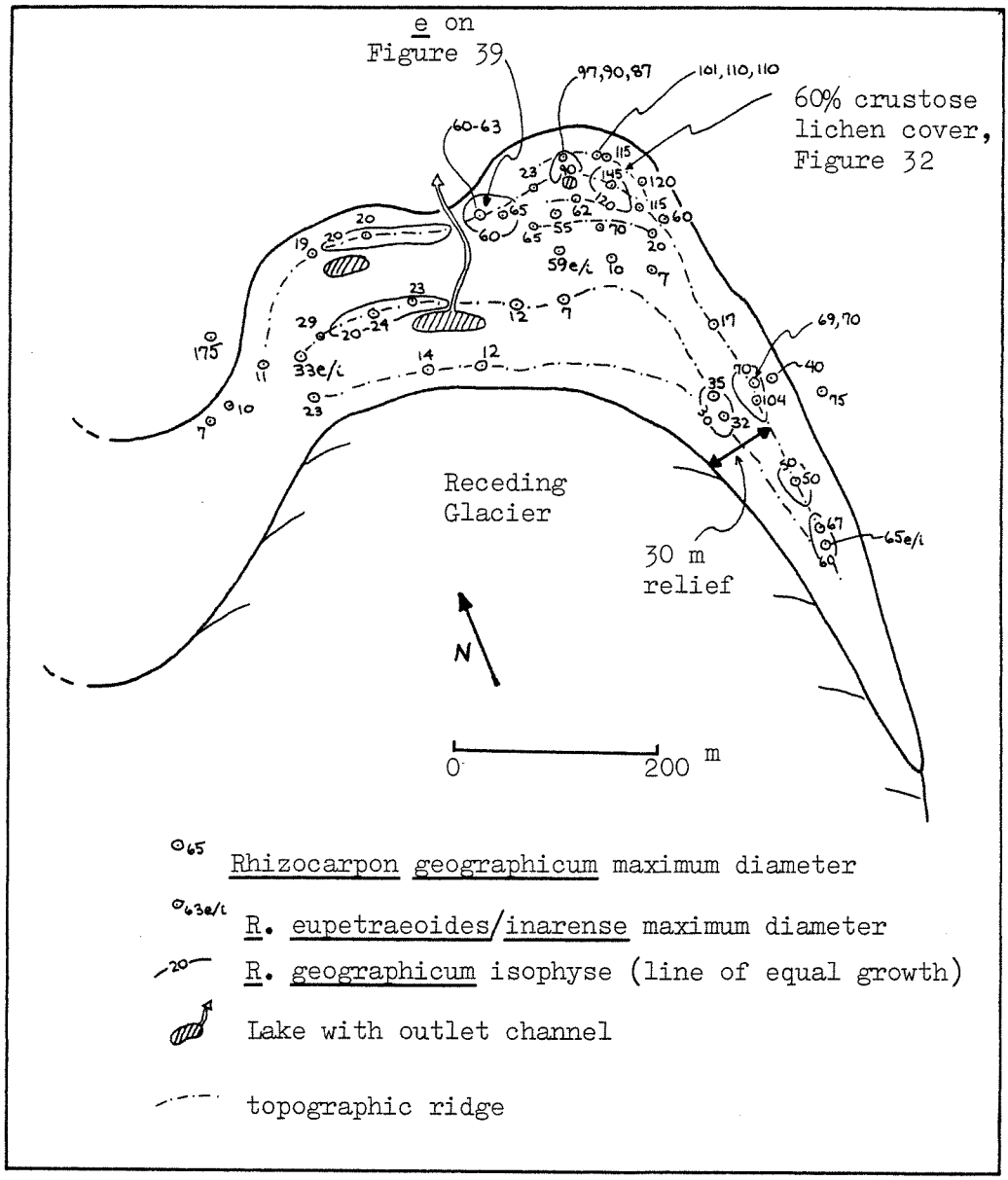

Figure 34. Lichenometric map of Neoglacial moraine complex (M) downslope of Triple East Glacier (Fig. 33, no. 12). The location of Figure 32 is shown; letter e refers to a photographic site in Figure 39.

preserved on a lateral ridge at Snow Bunting Glacier (no. 14, Figs. 2, 13) and at Arctic Char Glacier (no. 24, Fig. 2) a distal debris lobe dates to (L) 2900 ± 600 yr B.P.

Four glacier-cored moraines (MG) were mapped in the Atigun Pass region. Snowy Owl East Glacier (no. 34, Figs. 2, 14a) drains into the Sagavanirktok River; it provides an example of a stable debris cover less than 1 m thick over a glacier (Fig. 35). The lichenometric pattern becomes progressively older towards the periphery of the moraine. It is characterized by constructional ridges dated as (L) 1800 ± 360, 1200 ± 240, 800 ± 160, and 390 ± 80 yr B.P. (Fig. 33). However, there is a zone near the terminus where lichen sizes are intermixed and maximum lichens on individual boulders date to one of these four expansion periods preserved elsewhere as ridges of debris. This intermixing of lichen sizes without topographic expression implies that during phases of ridge construction, glacier-cored debris can be selectively overturned, exposing fresh surfaces for lichen colonization, thereby recording the time of expansion.

Seven glacier-cored, tongue-shaped rock glaciers were studied in the Atigun Pass area (see Ellis, 1978; Bruen, 1980a). Harlequin Duck Rock Glacier, which drains into the Itkillik River (no. 35, Fig. 2; Ellis and Calkin, 1979, Fig. 4d), displays a prominent glacier-cored transition zone characterized by stabilization ages of (L) 1800 ± 400, 1400 ± 300, 1200 ± 250, and 480 ± 100 yr B.P. (Fig. 36). The largest lichen found on the downslope rock glacier surface was 147 mm, but this yields only a minimum age based on other relative dating criteria (Fig. 36).

Radiocarbon Ages. While lichenometrically mapping cirque and valley deposits, 12 radiocarbon ages were obtained on buried organic

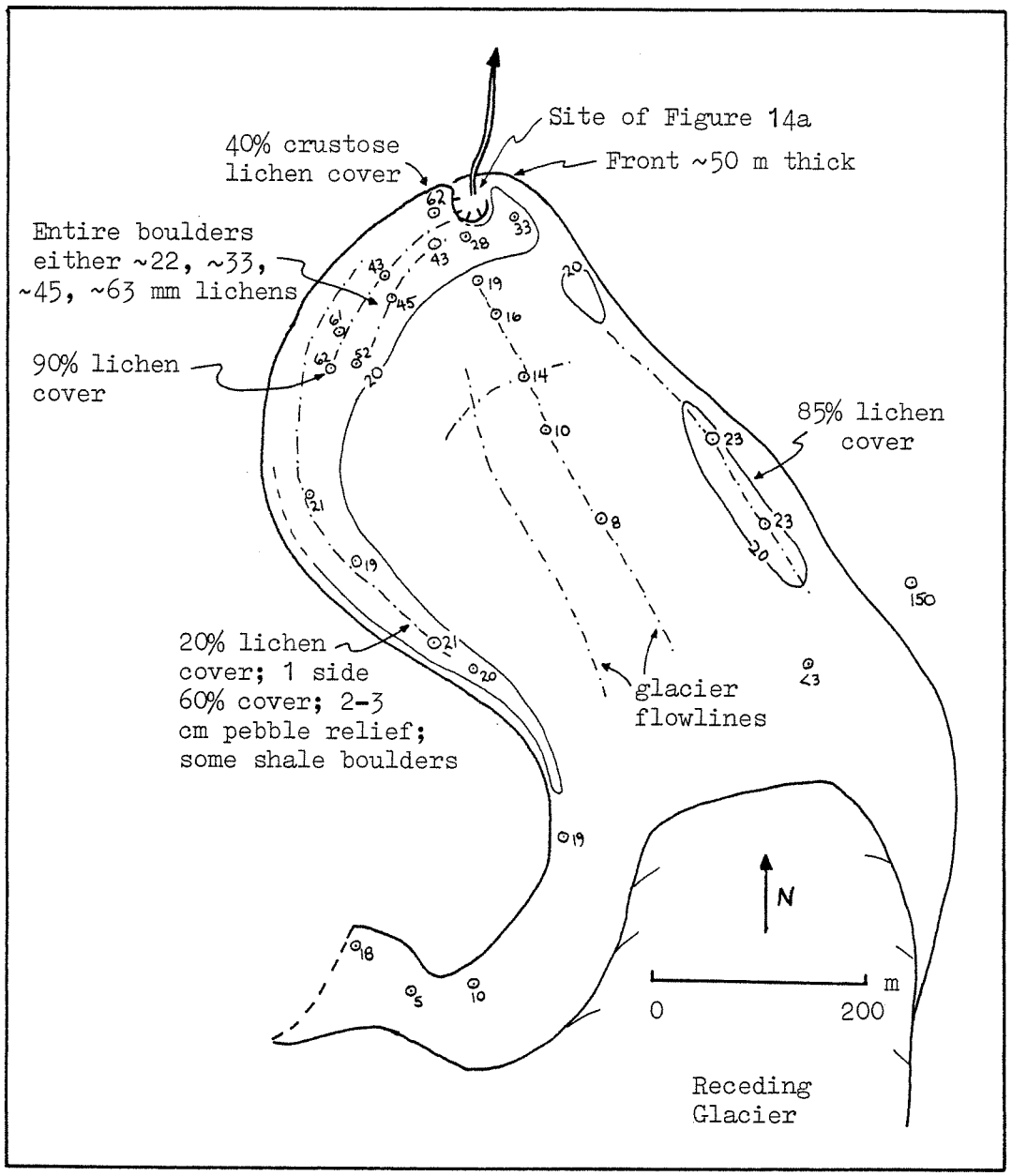

Figure 35. Lichenometric map of the glacier-cored moraine (MG) associated with Snowy Owl East Glacier (no. 34, Fig. 2). Photographic site for Figure 14a shown. Debris covering glacier is less than 1 m thick; the glacier extends to the moraine terminus and is exposed.

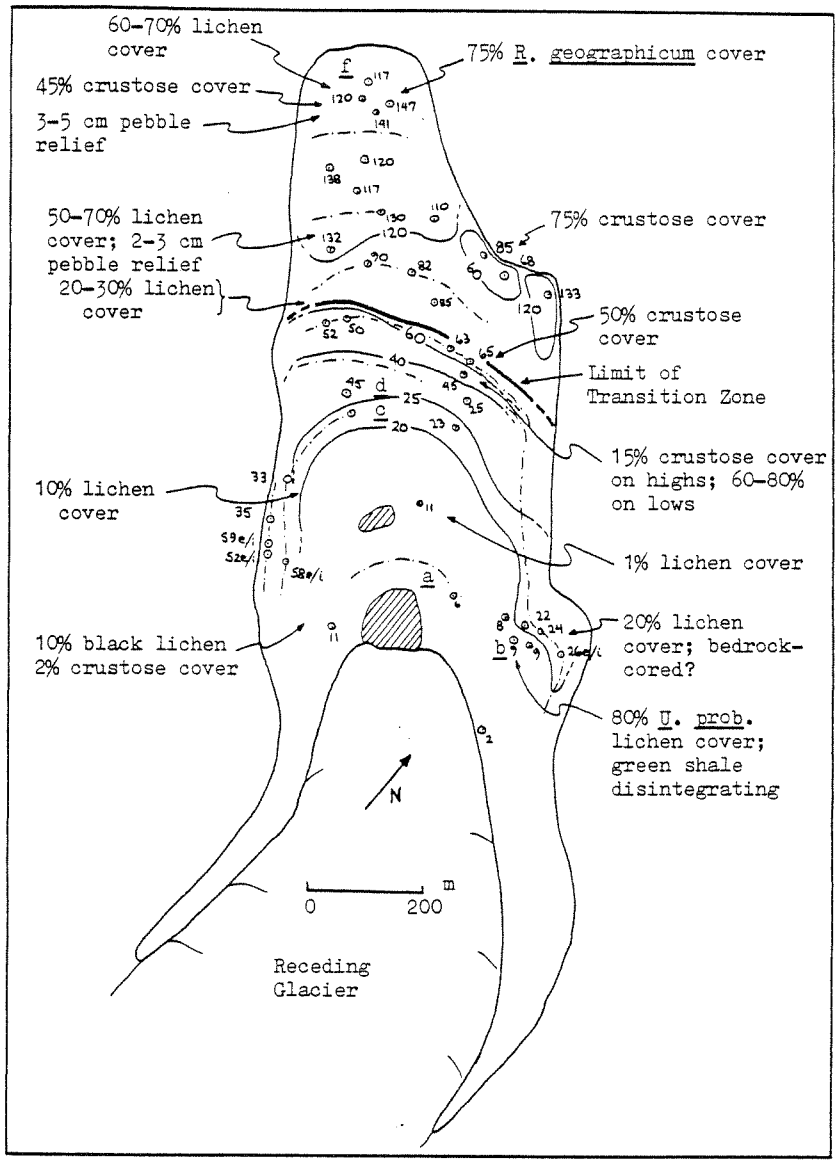

Figure 36. Lichenometric map of a glacier-cored rock glacier with a transition zone (TRGC) of Neoglacial debris ridges downslope of the receding Harlequin Duck Glacier (no. 35, Fig. 2). Letters a - d and f refer to photographs of lichen development with time in Figure 39. Lichen cover noted as "black" refers to Alectoria and Umbilicaria taxa while "crustose" means Rhizocarpon taxa.

material in the Atigun Pass area (Fig. 30). Five of these dates were directly associated with Neoglacial cirque deposits (Table 14). Problems with the interpretation of radiocarbon dates, as discussed by Griffey and Matthews (1978) and Karlén (1979), include mean residence time of buried soils, root contamination, and mean time of deposition for peats. These factors can result in the radiocarbon ages representing either maxima or minima. Conversions of radiocarbon B.P. ages to calender A.D. ages follows the detailed correlation curve in Oeschger (1975, Fig. 6) to A.D. 1200. For older dates the correlation curve in Ralph and Michael (1974) can be used.

The most significant radiocarbon ages for a late Holocene glacial chronology are those directly associated with cirque deposits. A major expansion at Buffalo Glacier (Fig. 5) is dated at 320 $\pm$ 100 yr B.P. or A.D. 1450-1650. Terminal moraines with substantial ice cores at Ram and Kid Glaciers (e and j, Fig. 30) apparently overran their bedrock cirque thresholds around 540 $\pm$ 180 and 1500 $\pm$ 150 yr B.P., respectively. At the glacier-cored rock glacier named Wolverine (d, Fig. 30) organic material may have been overrun by a younger, upslope debris lobe that formed the terminus of the transition zone; it provides an age of 480 $\pm$ 140 yr B.P. The radiometric ages obtained from buried organic material recovered at the toe of steep-fronted, ice-/glacier-cored moraines may represent a mass movement event or slow creep of the morainal lobe downslope; the age may not be related to a glacial advance. Nevertheless, taken together the four radiometric ages indicate a wideapread phase of cirque glacier expansion from 720 to 220 yr B.P. and perhaps an advance 1000 years

earlier.

Alluvial fan aggradation may be related to cirque glacier expansions at valley heads in the sameway terrace alluviation appears to be contemporaneous with increased cirque glacier activity (Hamilton, 1979b, 1980c). Layers of peat were located beneath four aggradational fan surfaces. The provided radiometric dates of 210 ± 90, 380 ± 90, 800 ± 90, and 1300 ± 100 yr B.P. (Table 14; a, c, g, i on Fig. 30).

The thick peat accumulation at the northern end of Atigun Valley (f, Fig. 30; Hamilton, 1979b, Fig. 10) spans ~2000 years. This massive peat corresponds to a period of continued, active alluviation farther up Atigun Valley. Pollen samples were collected here and analyzed by W.N. Mode (written. comm., 1980).

A basal date of 5870 ± 160 yr B.P. for peat interbedded with lacustrine silt (k, Fig. 30) was determined ~7 km upstream from the massive peat layer; it is the earliest age yet found in the moraine dammed Atigun Valley Basin. Hamilton (1979b) notes the initial episode of alluviation within the Atigun basin may have culminated about 5000-4500 yr B.P., but it cannot be correlated to regional geologic or climatic events.

Soil Development and Other Relative-Dating Tools. Twenty-three soils on moraines and rock glaciers that date from 0 to ~12,500 yr B.P. were examined in the Atigun Pass region. The major data collected included color, horizon thickness, and pH (Appendix H). Glacial deposits in alpine environments can be dated relatively by differences in these properties (Richmond, 1962; Morrison, 1967; Mahaney,

1974). Of particular interest to this study is the rapid weathering and soil formation reported for Holocene deposits in other alpine environments (Birkeland and Shroba, 1974; Birkeland and others, 1979).

On recent recessional moraines and glacial outwash, studies on soil evolution demonstrate pH declines from ~8.0 to 5.0 in 75 years for a coastal, southern Alaska site (Crocker and Major, 1955; Ugolini, 1968) and from 8.0 to ~6.0 in 200 years at a drier, Yukon Territory site (Jacobsen and Birks, 1980). The lowering of pH is related to the rate of leaching and build-up of organic matter, organic acids, and carbonic acid produced by respiration of plant roots and microorganisms (Birkeland, 1974).

Pedogenic investigations undertaken in northern Alaska since the early 1950's (see Brown, 1966) are confined to the arctic coastal plain (Everett and Parkinson, 1977; Parkinson, 1978; Everett, 1980); foothills; or relatively low, Pleistocene age valleys of the Brooks Range (Ugolini and Tedrow, 1963; Brown and Tedrow, 1964; Brown, 1966, 1980). In the valleys Brown (1966) noted the pH values of well-drained soils increased with depth; the most acid values of pH 4.5 to 5.0 were found in the upper solum, and pH values approaching 6.0 were found in the lower solum and C horizons. Tedrow and Brown (1962) and Brown (1966) suggested a weakening of soil forming processes with increasing altitude in the mountains. To my knowledge, no soil analysis has been done in the area of the valley heads on cirque glacier moraines and rock glaciers in the Brooks Range.

As part of this study, I have developed a very preliminary

chronosequence of soil development in diamicton sediments of cirque glaciers, rock glaciers, and late Pleistocene valley glaciers (Fig. 37). Soil pits were located on crests of moraines or rock glacier lobes where drainage was unimpeded during the thaw season. The deposits incorporate bedrock from a variety of sedimentary units around Atigun Pass, including the Hunt Fork Shale, the Kanayut Conglomerate, the Kayak Shale, and locally the Lisburne limestone. A Munsell color chart was used to determine moist colors in the field and dry colors in the laboratory; dry colors were used in the subsequent chronosequence (Birkeland, 1974, p. 250). PH was determined in the field by colormetric methods. The soil profiles were correlated to lichenometric ages for cirque glacier moraines, relative ages for rock glacier deposits, and radiocarbon ages for late Pleistocene moraines in the Atigun and West Fork North Fork Chandalar valleys (Fig. 2; Hamilton, 1979b).

Neoglacial moraines in sedimentary terrain yield pH soil values from 7.5-8.0 and chromas of ~2 for newly deposited till and unoxidized horizons at depth (Fig. 37). Thin (~1 cm) organic horizons and oxidation to depths of 15 cm develop in less than 400 lichenometric years. On moraines lichenometrically dated at ~2000 yr B.P., the organic horizons reach 3 cm thicknesses, A horizons extend to depths of 10 cm with pH values ~6.2, and oxidized C horizons from 20 to <50 cm. Thicker A horizons, development of a B horizon, chromas of ~3, and soil pH values of 4.8-6.4 help distinguish early (?) Holocene rock glacier tongues from the upslope Neoglacial moraines.

Soils on latest Itkillik drift (~12,500 yr B.P. in age) are

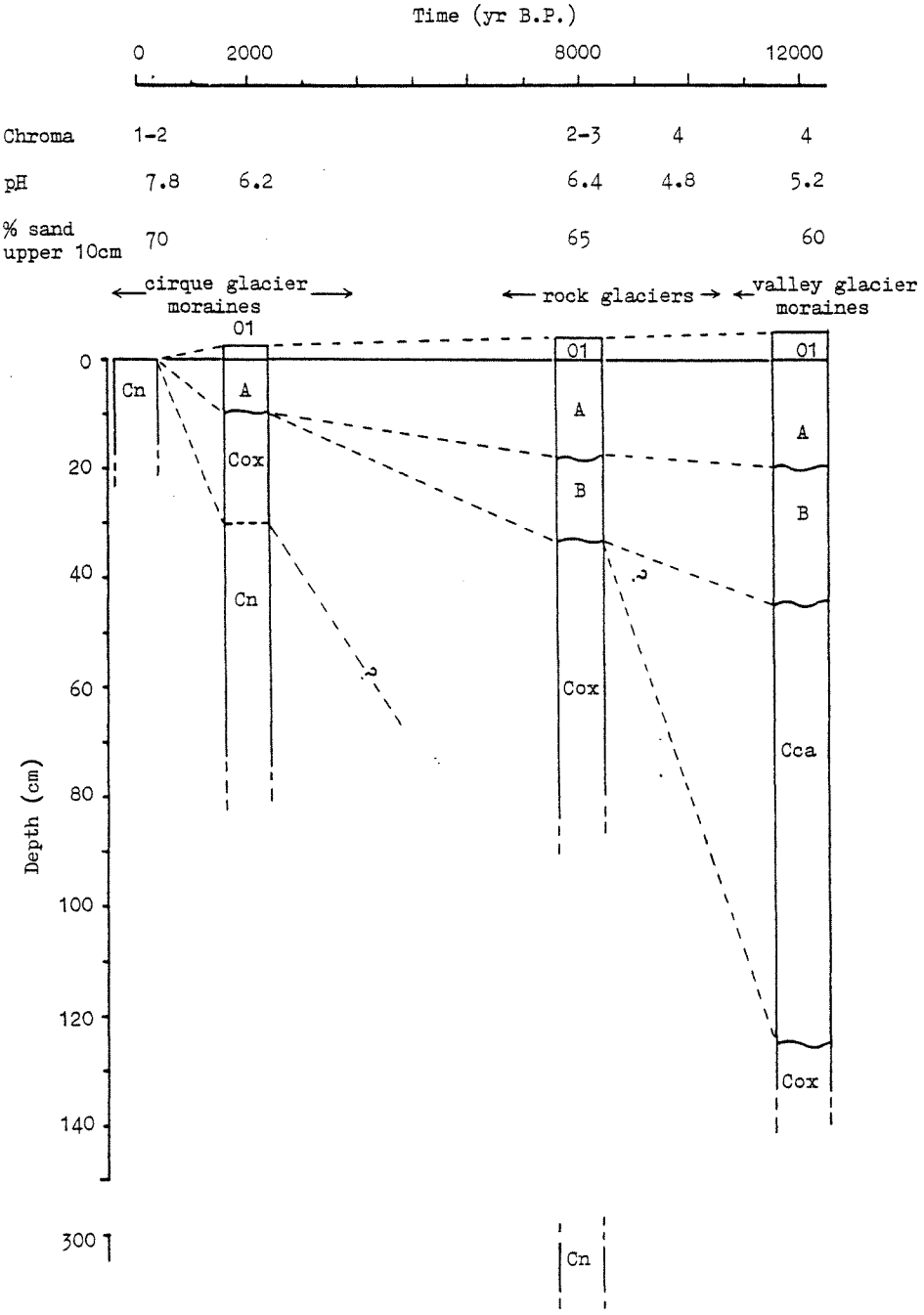

Figure 37. Generalized schematic of soil development from 0 to ~12,500 yr B.P. on moraines and rock glaciers of the Atigun Pass area. The parent material is till derived from sedimentary rocks (see Appendix H for soil profiles). An oxidized C horizon is designated by "Cox" and a seemingly unweathered C horizon by "Cn" (Birkeland, 1974). Development of a calcium carbonate (Cca) horizon apparently depends on influx of calcareous loess.

more uniformily well-developed than those on rock glaciers, and have pH values ranging from 4.7-5.4. In the northern Atigun Valley, the late Pleistocene moraines typically have organic horizons to 7 cm depth, A horizons from 20 to 25 cm thick, color B horizons, chromas to 4, and in one case a calcium carbonate build-up below 60 cm. On the south side of the Continental Divide soils exposed within two pits in latest Itkillik drift displayed pH values from 5.0 to 5.4, color chromas of 4, and massive caliche build-up below 25 cm (see Appendix H). Calcareous loess derived from extensive exposures of limestone along the south flank of the east-central Brooks Range may cause this caliche build-up. It is not commonly reported in soils of arctic regions (see Everett and other, 1981, p. 147-151).

An attempt to use weathering rinds in the sandstones and conglomerates of the Kanayut Conglomerate as a relative dating tool was made on Holocene and late Pleistocene deposits around Atigun Pass (Fig. 2; Appendix I). This method has been shown to be an effective measure of relative age on lithologically- and texturally-uniform basalts and granites (Porter, 1975; Coleman, 1976; Birkeland, 1978; Burke and Birkeland, 1979) and quartzarenites (Anderson and Anderson, 1981). Chinn (1981) indicates successful absolute age determination with highly indurated quartzofeldspathic sandstones.

A related technique using the degree of weathering as a measure of relative age involved measuring relief of highly resistant chert pebbles and quartz veins above the general rock surface; this was termed pebble relief. Three other relative dating techniques (percent lichen cover, disintegration of a distinctive shale, and percent

of boulder exposed above the terrain) were used locally; they are depicted in Appendix I.

Variations in texture, composition, and the nature of the cementing agent cause marked differences in the rate of weathering rind development (Fig. 38 a-c). Tough orthoquartzitic conglomerates and sandstones can show no weathering rind development after 12,500 years of exposure. Those samples with higher percentages of iron oxide as estimated visually in fresh surfaces develop weathering rinds most rapidly (Fig. 38c). Those samples estimated to have intermediate percentages of iron oxide (Fig. 38b) are somewhat consistent in separating late Holocene moraines (~1 mm rind thickness) from early Holocene/late Pleistocene deposits (~5 mm thickness).

The height of pebble relief above the surface of Kanayut stones may be more consistent than weathering rinds as a relative dating tool (Fig. 38d). Late Holocene drift had pebble relief clustering about 1 mm, while early Holocene/ late Pleistocene surfaces displayed about 6 mm of relief.

Very preliminary results with the other relative dating techniques (Appendix I) suggest the following:

a) Percent of lichen cover generally increases from 0 to ~20% on surfaces ranging from 0 to 400 lichenometric years (Fig. 39 a-c), except on those boulders inundated with Umbilicaria taxon. On Neoglacial surfaces from 400 to~5000 lichenometric years of age, percent of lichen cover varies over a wide range (Fig. 39 d-e); it has not been developed or analyzed in the field area to the degree necessary for relative dating. Beyond middle Holocene time, percent cover is

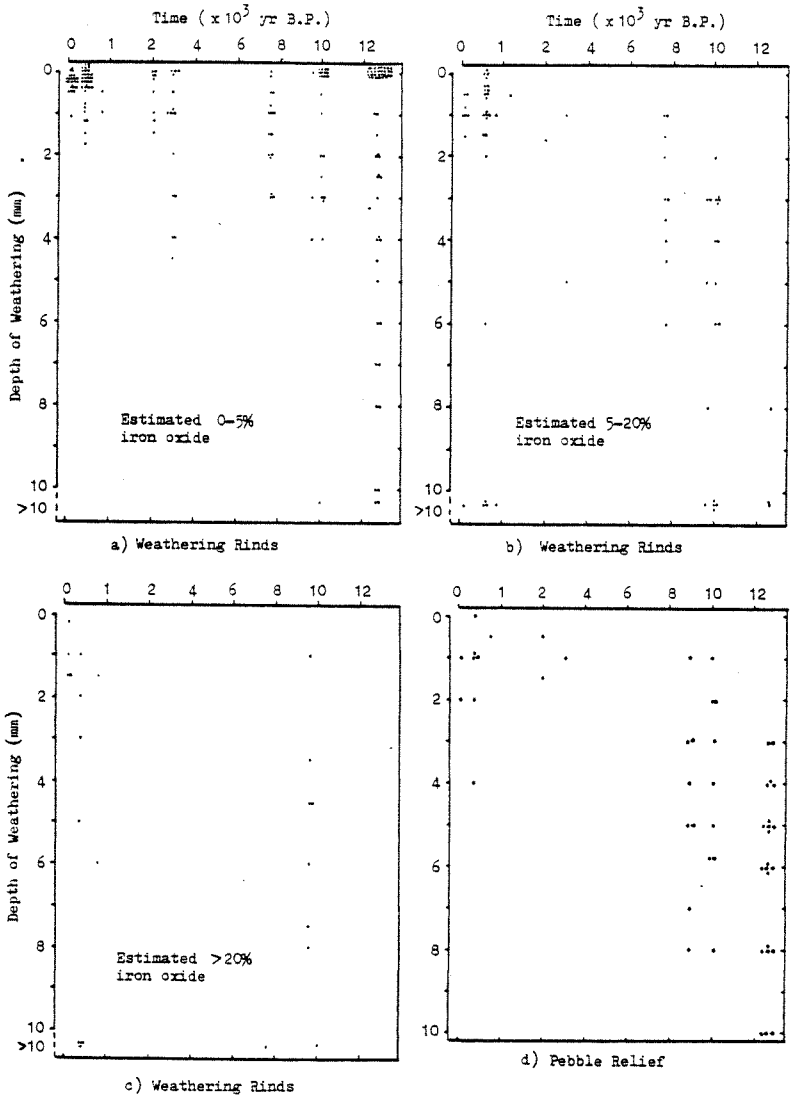

Figure 38. Generalized schematic showing weathering rind development (a-c) and pebble relief (d) with time from 0 to ~12,500 yr B.P. (see Appendix I). The percentage of iron oxide was visually estimated from fresh surfaces of the Kanayut Conglomerate samples. Samples chronologically placed from 0 to ~3000 yr B.P. are lichenometrically aged and located at cirque glacier moraines. Those clustered from ~7000 to ~10,000 yr B.P. are located on rock glaciers, and those grouped at ~12,500 yr B.P. are from valley glacier moraines.

a)

b)

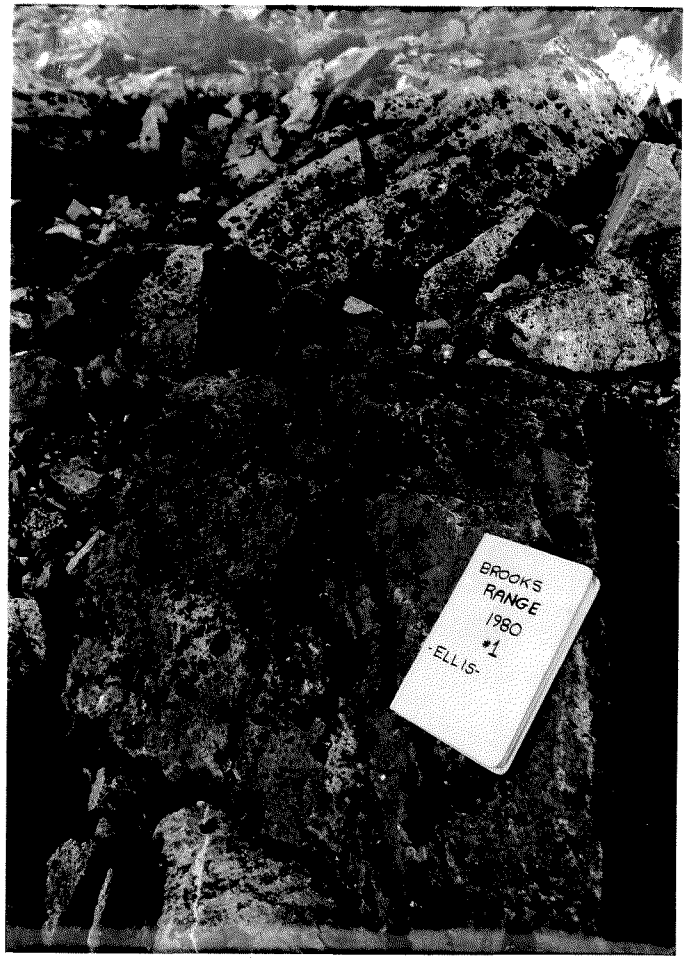

Figure 39. Development of lichens and weathering with time in sedimentary terrain of Atigun Pass (a-h).

a) <10 years of exposure (Fig. 36).

b) ~80 lichenometric years of exposure (Fig. 36).

c)

d)

Figure 39 (con't). c) ~400 lichenometric years of exposure (Fig. 36).
d) ~1200 lichenometric years of exposure (Fig. 36).

e)

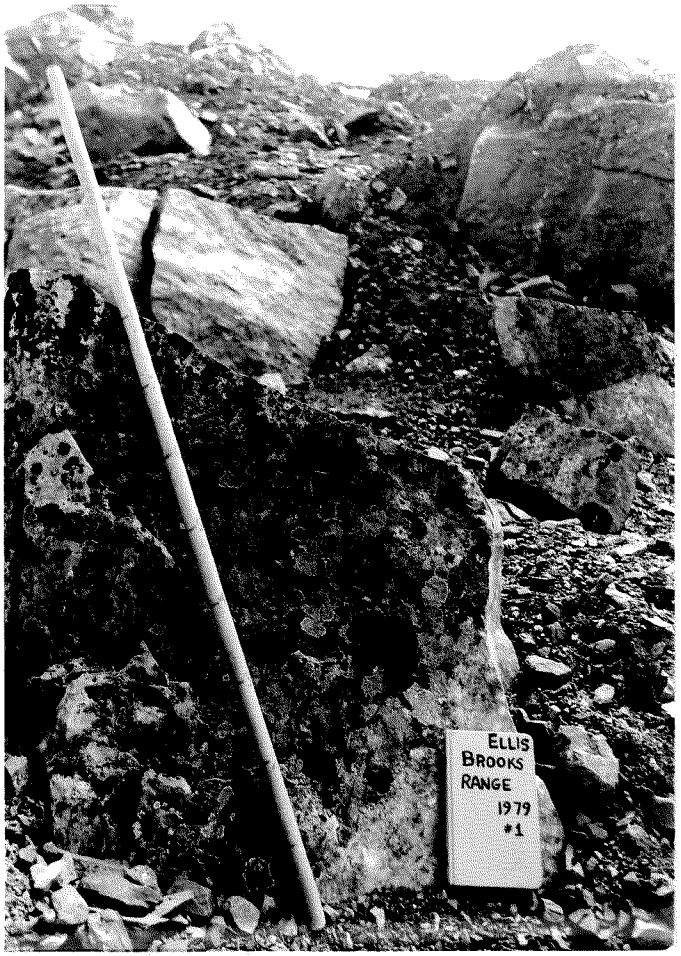

f)

Figure 39 (con't). e) ~2000 lichenometric years of exposure (Fig. 34).
f) ~early Holocene in age (Fig. 36).

g)

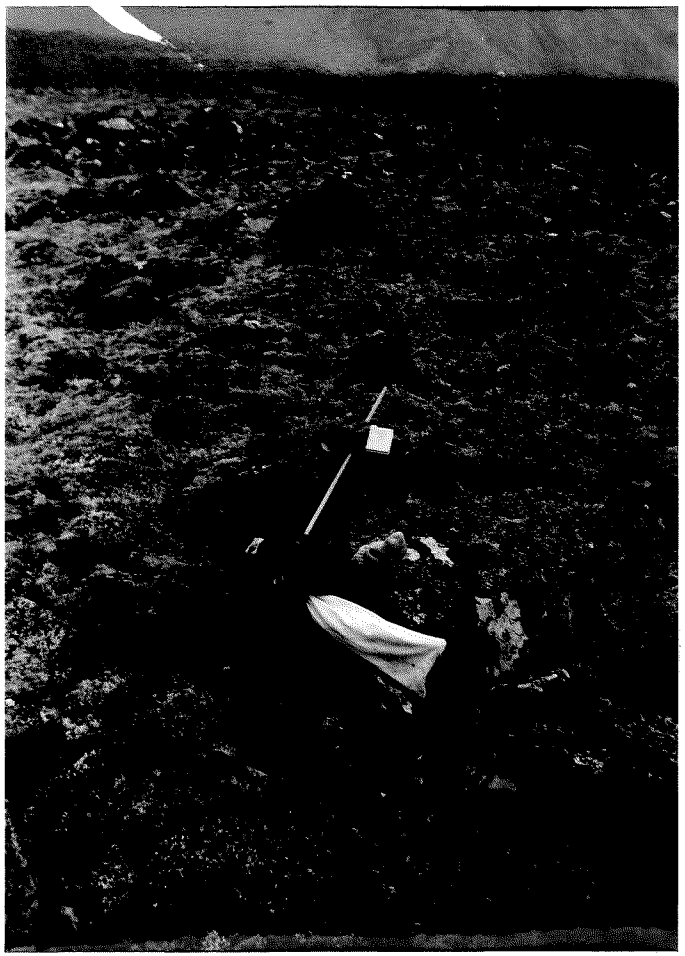

h)

Figure 39 (con't). g) ~early Holocene rock glacier surface.
h) late Pleistocene (~12,500 yr B.P.) end moraine surface, Atigun Valley (Fig. 2).

nearly constant or reflects boulder disintegration; generally over 70% of the rock is covered with crustose lichen (Fig. 39 f-g).

b) The disintegration of red and green shale boulders from the middle member of the Kanayut takes place in less than 500 lichenometric years (Fig. 39 a).

c) Boulder exposure is estimated at ~90% on the older Neoglacial moraines (Fig. 39 e), ~50-70% on early Holocene rock glaciers (Fig. 39 f-g), and ~30-50% on late Itkillik moraines (Fig. 39 h).

Anaktuvuk Pass Area. It-C Glacier (no. 48, Fig. 3) is fronted by a glacier-cored moraine with a lichen record characterized by maximum R. geographicum thallus diameters of 23, 33, and 65 mm (Fig. 33); these date to (L) 420 ± 90, 800 ± 160, and 1800 ± 360 yr B.P. Preserved along a distal portion of this moraine is a rock glacier (?) lobe (Appendix C); it has crustose lichen cover approaching 70%, coalescing Rhizocarpon thalli, and lichens of 152-157 mm.

Lichenometric mapping in two tributaries of Inukpasagruk Creek (Fig. 3; Porter, 1966, Fig. 18) demonstrates that the Neoglacial or Fan Mountain Glaciation was not as extensive as previously described (Fig. 40a). The two tributaries hang above Inukpasagruk Creek with subtle, late Pleistocene (Alapah Mountain) morainal accumulations at their mouths (Porter, 1964, Fig. 5, 1966, Plate 11; Hamilton, 1979c). R. geographicum in excess of 250 mm, boulders with rounded corners, hollows weathered to depths of 4 cm on Kanayut stones, and lichen cover to 95% along the length of both branches of the west tributary (Fig. 40b) indicate that the two empty cirques and tributary floor

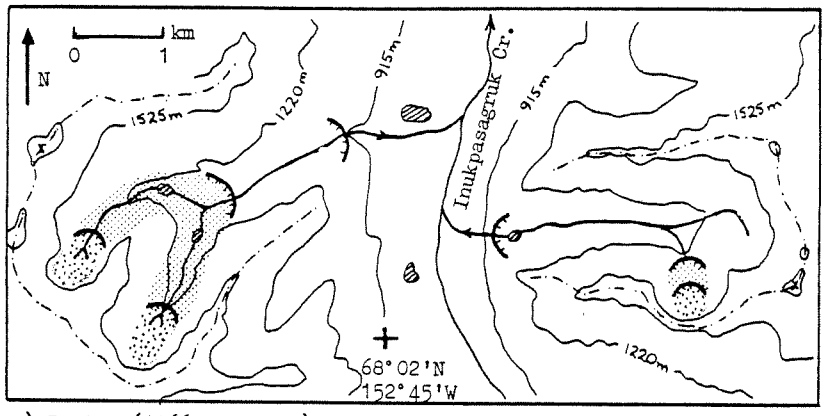

a) Porter (1966, Fig. 18).

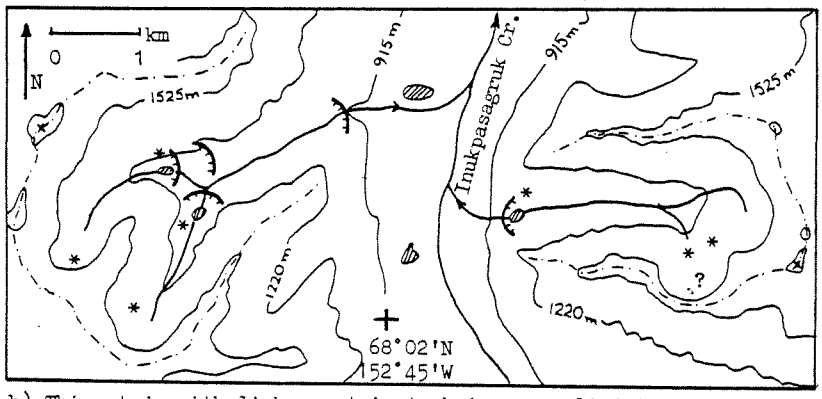

b) This study with lichenometric techniques applied to mapping.

Fan Mt. II Moraines

Fan Mt. I Moraines

* R. geographicum thalli 200–270 mm in diameter

Alapah Mt./Latest Itkillik Drift (late Pleistocene age)

Lake

Drainage divide

Figure 40. Four cirques draining into Inukpasagruk Creek, Anaktuvuk Pass area (Fig. 3) with Porter's (1966) and this study's interpretations of Neoglacial events. This study's analysis is based on lichenometry and physical analyses of cirque environments (case no. 5, 54-56, Fig. 27; 505a, 901-903, Appendix F). Together these methods show very limited evidence of Neoglacial climatic deteriorations because these cirques are too low in altitude for ~68°N latitude.

date to late Pleistocene time.

A cirque deposit in the west cirque of Mount Ahgook (In-C, no. 44, Figs. 3, 40), previously identified as superimposed moraines of Fan Mountain age (Porter, 1966, Plate 13), is reclassified as a probable, glacier-cored rock glacier. Its altitude of $\leq$1350 m is well below the altitude of the lowest, glacier-cored rock glacier at Atigun Pass (Fig. 9), but similar to inactive, tongue-shaped rock glaciers without exposed cores of ice (Appendix F; Fig. 8a).

Rock glacier In-C has a kettled surface, longitudinal debris ridges, and rounded stable frontal lobes covered with vegetation. The surface of the lower lobe (previously dated as Fan Mountain I) is stable, has an ~80% lichen cover, and hosts R. geographicum s.l. from 171-195 mm. Farther upslope the second debris lobe bears lichens in excess of 155 mm along its crest. However, with proximity to the cirque headwall the rock glacier surface is more disturbed and lichen diameters become progressively smaller. The Neoglacial affected less than five percent of this rock glacier's surface (Fig. 40b). The ELA depression during the Neoglacial maxima was insufficient to reactivate this buried core of ice because of its low altitude.

The Arrigetch Peaks. Nine distinct moraines downslope of glacier termini in the Arrigetch were mapped (Fig. 41). The destabilizing effects of melting, glacier-ice cores are marked there and cause lichens to be more sparse and inconsistent in size than in the sedimentary terrain farther east. In addition, the ubiquitous Trentepohlia iolithus algae may further inhibit lichen development.

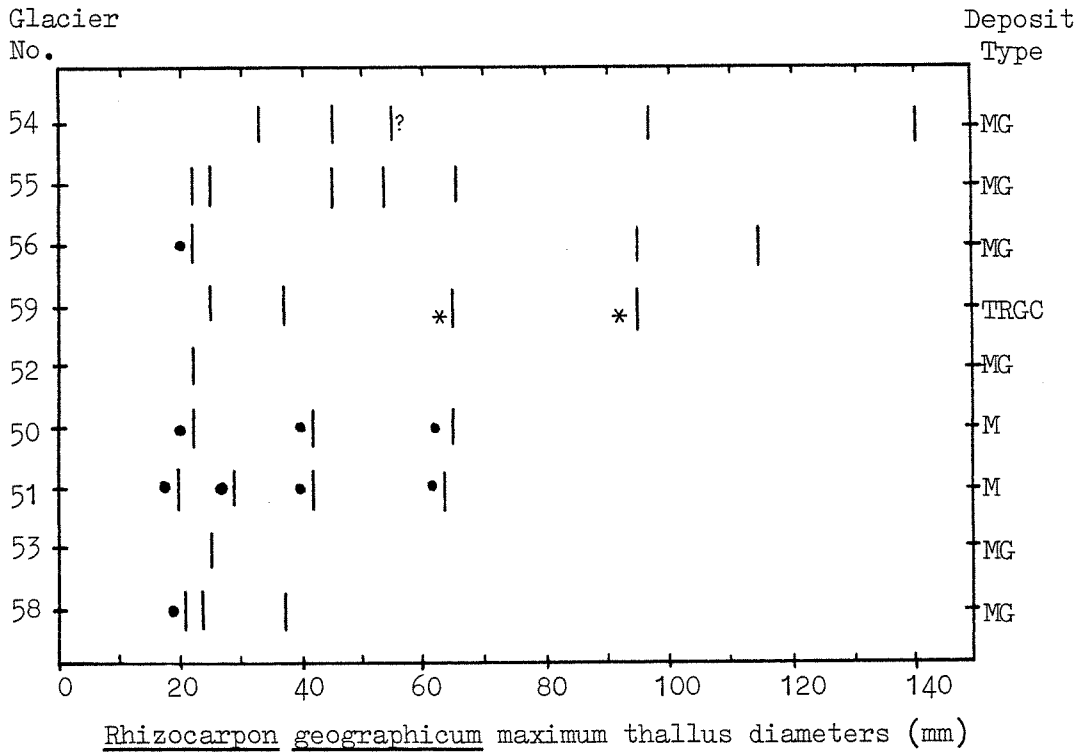

Figure 41. Maximum thallus diameters of R. geographicum characterizing nine morainal lobes that were lichenometrically mapped downslope of cirque glacier tongues in the west-central Arrigetch Peaks (Fig. 4). Those diameters that were found on thin drift over bedrock are shown by (•); those thalli found on rock glacier surfaces downslope of Neoglacial transition zones are shown by (*) and disregarded in the subsequent Neoglacial chronology. The glaciers' identification numbers and types of moraines are indicated (Table 2).

Stable, thin drift sheets have been deposited directly on bedrock behind terminal moraines of several cirque glaciers in the Arrigetch (Fig. 41). These terminal moraines date to the last major Neoglacial advance of (L) 390 ± 90 yr B.P. Lichen development on tne stable boulders deposited between these terminal ridges and the present ice margins allow deglaciation rates to be determined from

the most recent expansion.

Initial recession from the (L) 390 ± 90 yr B.P. maximum was slow, as most of the deglaciated areas are characterized by lichens less than or equal to 16 mm in diameter (Fig. 42). This lichen size suggests that the ice margins remained close to the maximum extent until ~(L) 170 ± 40 yr B.P. or about A.D. 1640-1750, when marked recession commenced. At Arr-10 West (no. 51, Fig. 4) the ice margin has retreated 200 to 300 m since A.D. 1640-1750. At Arr-4 (Fig. 29), lichenometric mapping and sequential photographs suggest deglaciation was most rapid after ~A.D. 1870. Hamilton (1965a) estimated that both arms of Arr-4 retreated 200 m upvalley and 100 m higher in altitude during the period A.D. 1911 to 1962. No lichens were found within 15 m of the ice margin; this distance may represent deglaciation during the ~30 years assumed necessary for lichen colonization (Fig. 42). The 15 m distance indicates the recession rate has slowed since the 1950's.

The Neoglacial expansion of (L) 390 ± 90 yr B.P. is well represented by continuous ridges in the Arrigetch (Fig. 41) as elsewhere in the central Brooks Range (Fig. 33). It disturbed large segments of the older, glacier-cored lichenometric record; however, nested debris ridges without cores of ice were preserved along the perimeter of some moraines. These continuous morainal ridges host lichens with maximum diameters suggesting stabilization at (L) 1120 ± 300 and 1800 ± 400 yr B.P. At four morainal complexes there are discontinuous, glacier-cored surfaces that stabilized between (L) 540 and 870 (± 20%) yr B.P. The range of lichen sizes on these discontinuous

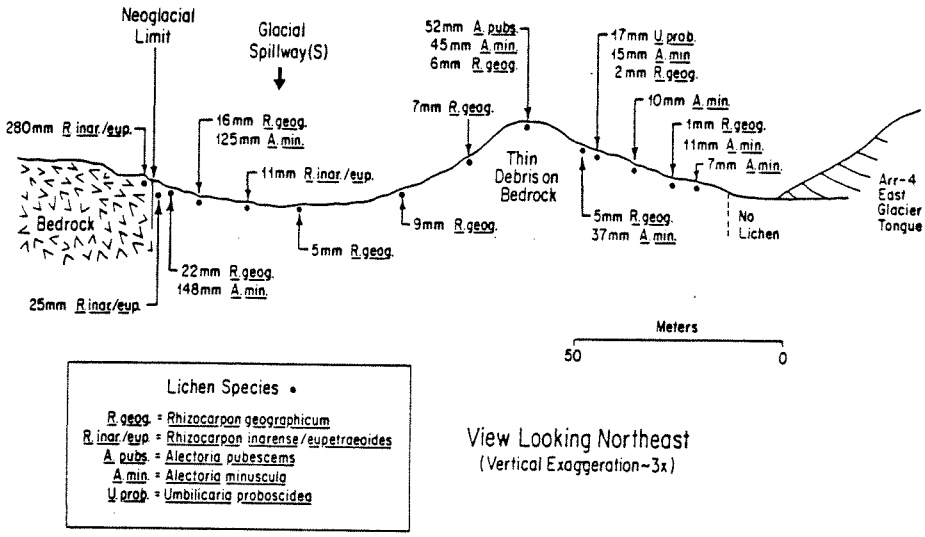

Figure 42. View northeast of the bedrock divide separating the east and west arms of Arr-4 (no. 56, Figs. 4, 29). This field sketch depicts the glacial spillway (S, Fig. 29) that was ice- or snow-filled in 1911 (Hamilton, 1965a). No lichen thalli were found within 15 m of the ice margin; this suggests only ~15 m was deglaciated within the past ~30 years.

surfaces may relate more to varying degrees of surface stability than unsynchronous times of glacial growth.

Evidence for major glacial activity prior to (L) 2000 yr B.P. occurs beyond the ridges considered above as stable patches of drift bearing lichens that indicate ages to (L) 4400 $\pm$ 900 yr B.P. (Ellis and others, 1981, Fig. 9). Interpretation and dating of these surfaces is difficult due to poor geomorphic expression (Fig. 29) and uncertainties with the older part of the lichen growth curve.

Holocene Glacier and Rock Glacier Chronology

Summation of Lichenometric Frequency Data

Maximum thallus diameters of Rhizocarpon geographicum s.l. recorded for individual morainal ridges and map units are plotted in Figures 33 and 41. These are replotted as frequency histograms in Figure 43 (a, b) in order to develop a lichenometric chronology for the central Brooks Range.

The Atigun/Anaktuvuk and Arrigetch histograms (Fig. 43 a, b) show similar concentrations of moraines characterized by lichens in the 20 to 70 mm range and small clusters of moraines hosting R. geographicum >90 mm in diameter. In the more easterly sedimentary terrain (Fig. 1) there is evidence for ridge stabilization during overall glacial recession since 20 mm lichen time as numerous moraines host ~18, 15, and 11-12 mm lichens (Fig. 43a). However in the Arrigetch Peaks where historical photographs and thin, stable, recessional drift sheets are formed this evidence is absent. There glacial recession was rapid after 16 mm lichen time, apparently accelerating ~12 mm lichen time (Fig. 42). Therefore it is difficult to base broad climatic implications on recessional ridges with maximum lichens <20 mm in diameter.

The similarity of the lichen data from the three study areas suggests: a) the ice masses reacted synchronously to climatic changes, b) lichen colonization times do not vary significantly with lithology or substrate stability, and/or c) the lichenometric method is too imprecise to distinguish colonization differences or slight

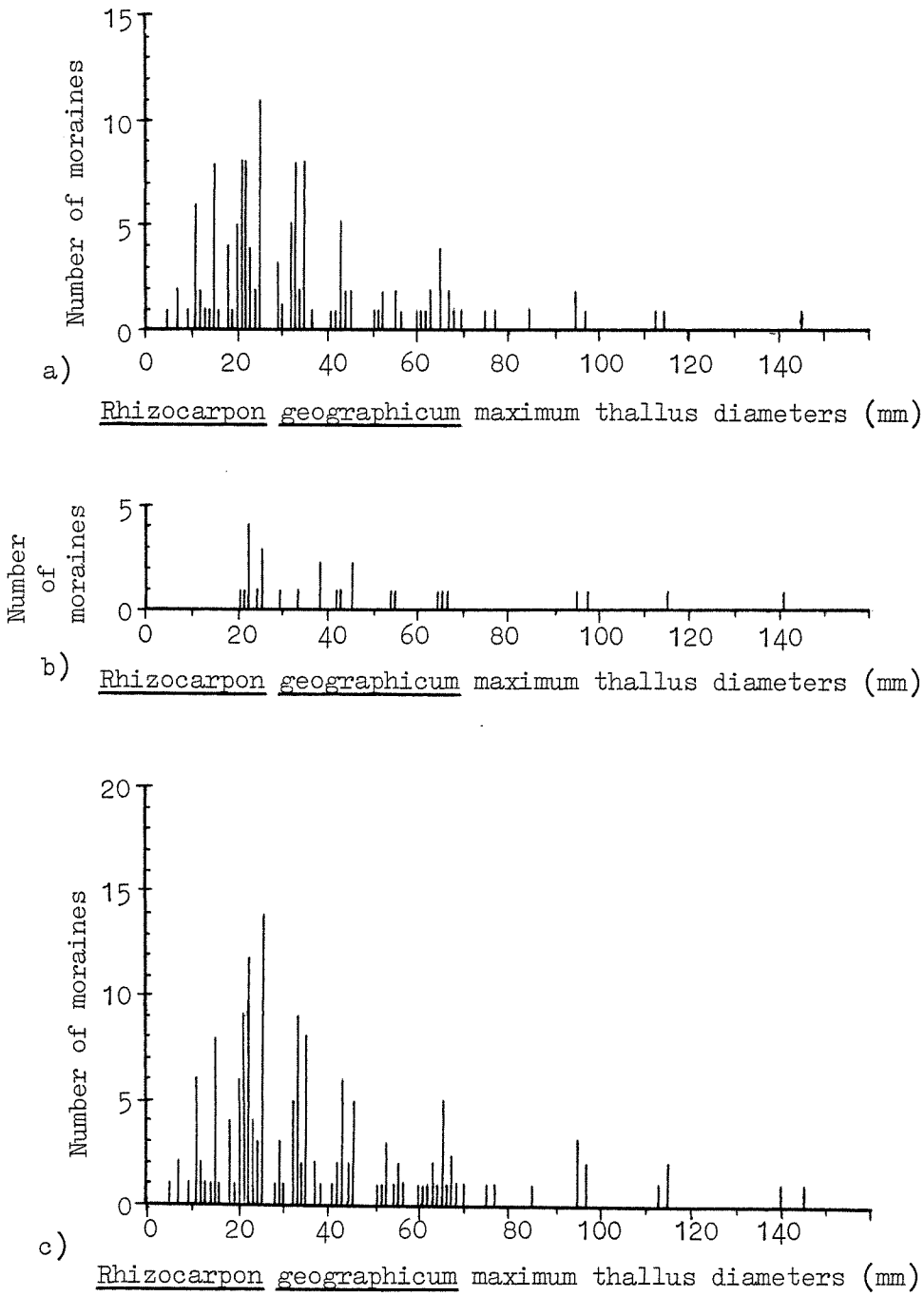

Figure 43. Frequency histograms of occurrences of R. geographicum maximum thallus diameters that characterize individual moraines or map units on Neoglacial deposits (M, Mg, MG, TRGC; Figs. 33 and 41).

changes in climate across 225 km of the central Brooks Range. In addition, both the granitic and sedimentary Neoglacial records demonstrate a progressively decreasing number of morainal surfaces with larger R. geographicum thalli (Fig. 43). This suggests that each advance disturbed approximately the same amount of older drift; therefore, major cirque glacier expansions during the Neoglacial may have been on the same order of magnitude.

The Golden Eagle Glacier Chronology

At the gently sloping toe of Golden Eagle (no. 7, Fig. 2; Fig. 44), glacial retreat has exposed an area of about 800 m^2 bearing undisturbed, nonsorted patterned ground; and in situ patches of unidentified dead mosses partially enveloping hundreds of lichen-covered boulders and cobbles ranging to 1.5 m across (Calkin and Ellis, 1981). The arrangement of the crustose lichens and mosses suggests that the hosting stones were largely undisturbed by the glacier that overrode them. Near the ice margin, the relict lichens are brightly colored and morphologically undamaged. The emergence of vegetation (Arnold, 1965; Collins, 1976; Lowden and Blake, 1970) from beneath glaciers is well documented in polar areas. On Baffin Island, emergent mosses have been dated at 350 $\pm$ 75 yr B.P. (I-1204, Falconer, 1966).

The Golden Eagle site is unique in the Atigun Pass area because the overrun surface on the east side was not buried under a continuous sheet of drift during the most recent recession (Calkin and Ellis, 1981, Fig. 2). Debris input is apparently very low as glacial

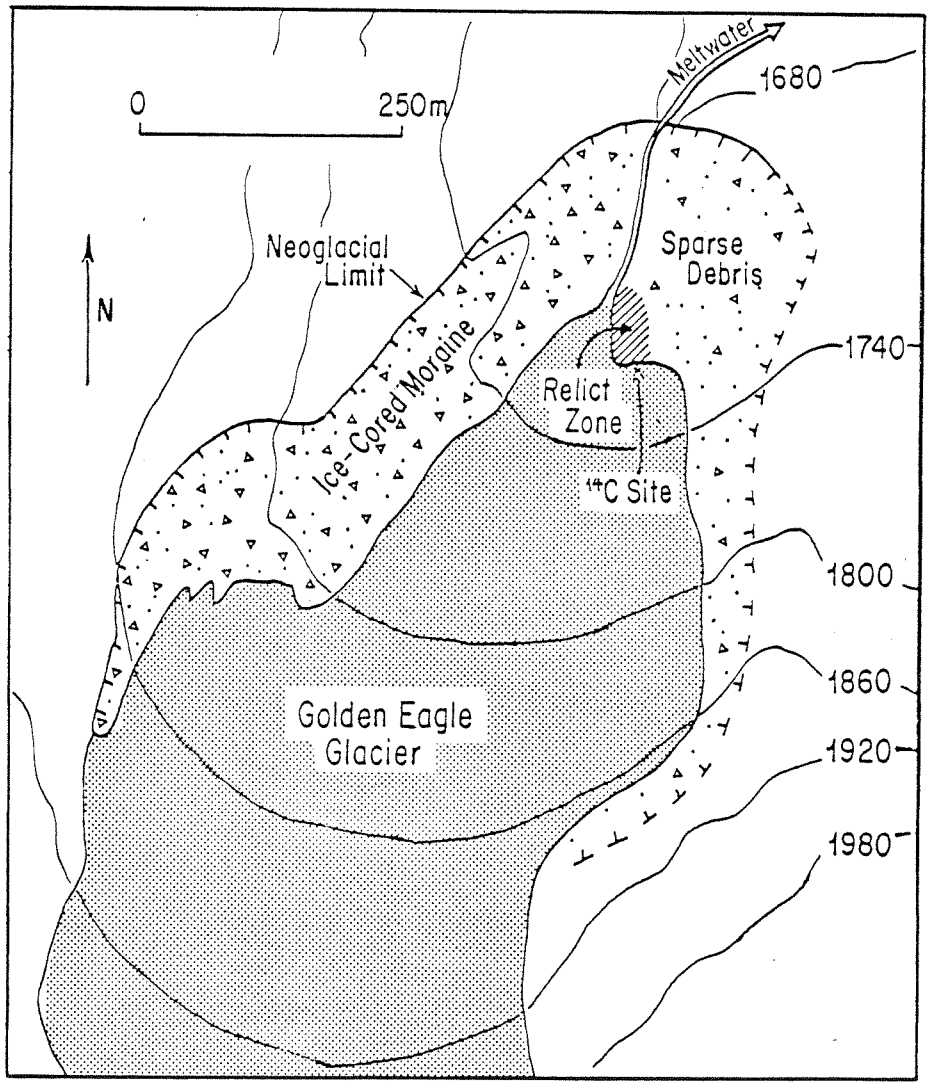

Figure 44. Golden Eagle Glacier (no. 7, Fig. 2) is the site of relict patterned ground, mosses and lichen covered boulders emerging undisturbed from beneath the receding glacial toe (see Table 14, radiocarbon site h). This glacier advanced across the relict site about 1120 ± 180 yr B.P. and continuously cover the site until present-day.

ice covers the headwall nearly to the crest; it was estimated only ~10 m of bedrock is exposed (Appendix E).

At the site a radiocarbon age of 1120 ± 180 yr B.P. was obtained for the dead mosses surrounding the undisturbed, lichen-covered boulders (h, Fig. 30, Table 14). The sample was obtained within 1 m of the July 1979 ice margin (Fig. 44). This dates a Neoglacial advance across the presently deglaciated site. The advance overran and preserved the patterned ground and vegetation under apparent cold-based conditions, or the glacier may have initially advanced through the mechanism of accumulation rather than by active downhill movement. The latter type of advance would normally have removed evidence of former vegetation or patterned ground.

The length of the preceding, ice-free episode is inferred from lichenometric measurements of R. geographicum s.l. found on the emergent boulders. The largest, well-defined thalli had maximum diameters ranging from 62 to 72 mm, suggesting a minimum duration of 2000 ± 500 years for an ice-free interval at the site prior to the 1120 yr B.P. advance (see Calkin and Ellis, 1981 for lichenometric data). The terminal moraine is 250 m downslope of the present ice margin and is composed of sparse boulders perched on the cirque threshold, dated at (L) A.D. 1500-1600 ± 100 . The lichenometric pattern of the western lateral moraine suggest deglaciation from this advance was not uniform but was most rapid after (L) A.D. 1750 ± 30.

A Holocene Chronology

The age groupings of Neoglacial moraines found on the 53 glacial debris lobes across the central Brooks Range are derived from correlation of moraine-frequency distributions (Fig. 43c) to the growth curve for Rhizocarpon geographicum (Fig. 45). The lichen diameters are grouped into seven major clusters corresponding to mean lichenometric ages ± 20% in Table 15.

There is less geomorphic evidence preserved in cirque glacier deposits with increasing age, resulting in a steady decrease in the number of morainal ridges found with larger-size lichens. The 28-30 mm and 50-56 mm lichen groups representing ages of (L) 630 ± 150 and 1450 ± 350 yr B.P., respectively, have been eliminated from the major groupings based on their relatively minor representation.

Of concern is the approximate nature of older lichenometric ages with their subjective ± 20% age reliability. This reliability range is increased beyond 20% of the mean thallus size because each of the seven major stabilization events incorporates a range of thallus diameters; their low and high ± 20% dating errors are considered in the age determinations. The most reliable lichenometric dates are those less than 2000 years in age because of the large number of morainal surfaces represented (Fig. 44) and reasonable control of the R. geographicum growth curve (Fig. 31). The events older than 2000 years or based on thalli greater than 70 mm may be best considered as representing three stabilization events spanning the period 5500 to 2500 yr B.P.

Maximum R. geographicum thalli on tongue- and lobate-shaped rock glaciers appear to be developed well beyond the range of the

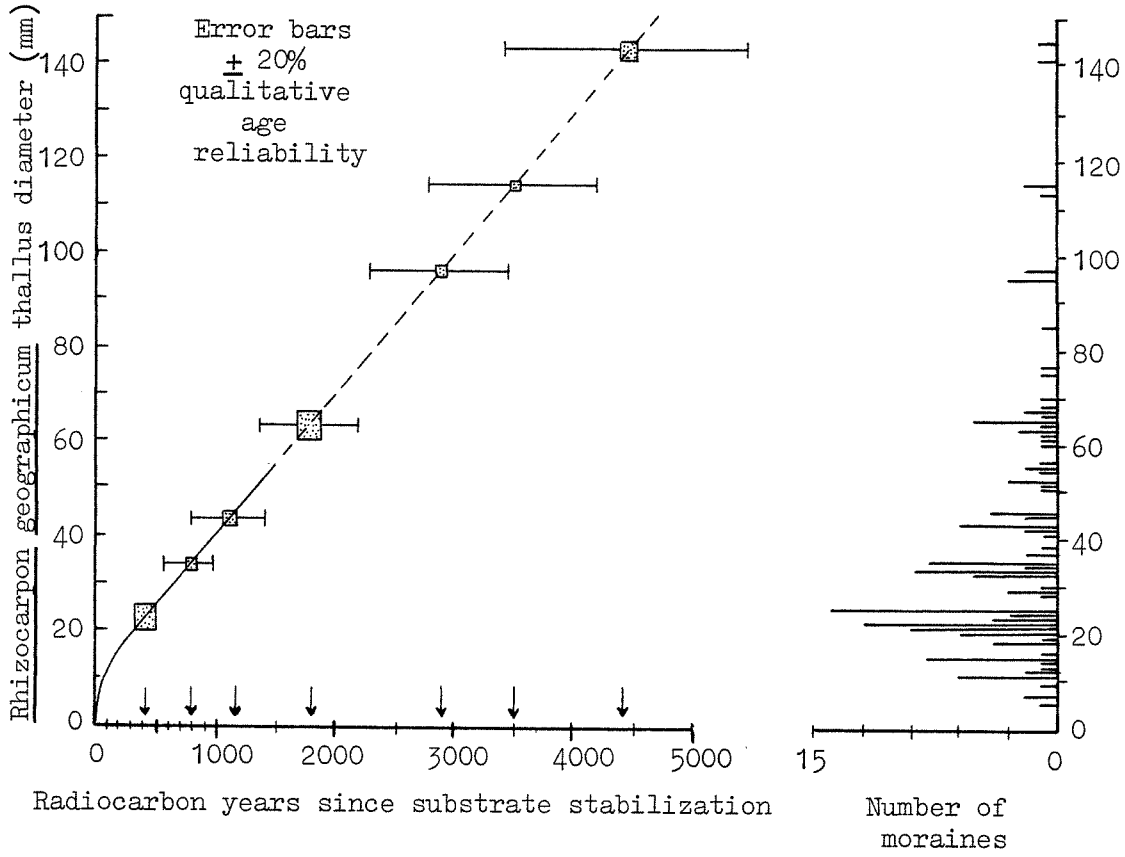

Figure 45. The frequency histogram of R. geographicum maximum thallus diameters for the cirque glacier deposits of the central Brooks Range (Fig. 44c) correlated with the R. geographicum growth curve (Fig. 31). Seven major clusters of similar size thalli from this histogram are shown on the growth curve as rectangles drawn to indicate each cluster's age and size range. Estimated ± age reliability is drawn as error bars. Arrows along growth curve's abscissa point to mean age of the seven lichen size concentrations. The curve is not fixed to any given year. To convert radiocarbon years given on the abscissa to radiocarbon yr B.P. (before A.D. 1950), subtract A.D. 1950 from the current A.D. date and deduct this value from the graph's radiocarbon age.

TABLE 15. SUMMARY OF LICHENOMETRIC MAPPING

Number of Morainal Ridges	Maximum Thallus Size (mm)	Lichenometric Age (L) (± 20%)
48	20 - 25	390 ± 100 yr B.P. ≈ A.D. 1410-1600
24	32 - 35	800 ± 200
15	42 - 45	1150 ± 300
12	60 - 66	1800 ± 400
5	95 - 97	2900 ± 600
3	113 - 115	3500 ± 700
2	140 - 145	4400 ± 1000

present lichen growth curve. Areal position and other relative dating techniques must be applied in order to establish a chronology for rock glaciers. Soil profiles show a progressive decrease in pH values from ~8.0 for newly deposited till in cirques to < 5.0 for late Pleistocene moraines downvalley; rock glaciers have intermediate values of 4.8-6.4. The largest thalli found during this study that apparently belonged to the R. geographicum s.l. species was located on an inactive rock glacier lobe. The height of chert pebbles and quartz veins (Fig. 38d) on late Holocene drift in cirques clusters ~1 mm while for valley moraines it averages ~6 mm; rock glacier values are intermediate at ~4 mm. Together this preliminary data indicates that a majority of rock glaciers had formed and at least portions of their upper surfaces had stabilized by early Holocene time.

Rock glaciers were probably initiated by increased mass wasting in cirques and valleys during late Pleistocene deglaciation. Headward ice cores and spoon-shaped depressions (Figs. 15-19) suggest that glacier ice is within many rock glaciers of the central Brooks Range. This ice is probably of late Pleistocene age (a remnant of valley deglaciation) or incipient early Holocene ice. The continuous permafrost condition enhanced preservation of these cores through Holocene time (Østrem, 1959; Loomis, 1970; Whalley, 1974, Fig. 2) allowing debris surfaces to stabilize.

The importance of this mass wasting in preserving glacial cores at lower altitudes through the Holocene is shown by comparison of empty, north-facing cirques to cirques at similar altitudes containing rock glacier tongues. The empty cirques are environmentally similar to those with rock glaciers (Fig. 27; S-901, 904-907 in Appendix F maps); however, a lack of mass wasting left receding, late Pleistocene ice unprotected. This ice disappeared in early to middle Holocene time. Neoglacial deteriorations were not severe enough to regenerate glacial ice in these empty cirques that are ~100 m below cirques with Neoglacial moraines. However, the debris-protected, headward ice cores of rock glacier tongues (also ~100 m below glaciers fronted by Neoglacial moraines, Fig. 9) were rejuvenated to varying degrees during the late Holocene depending largely on altitude.

A Holocene chronology encompassing moraines and rock glaciers in the central Brooks Range (Fig. 46) is developed by combining the lichenometric (Table 15), radiocarbon (Table 14), and relative dating

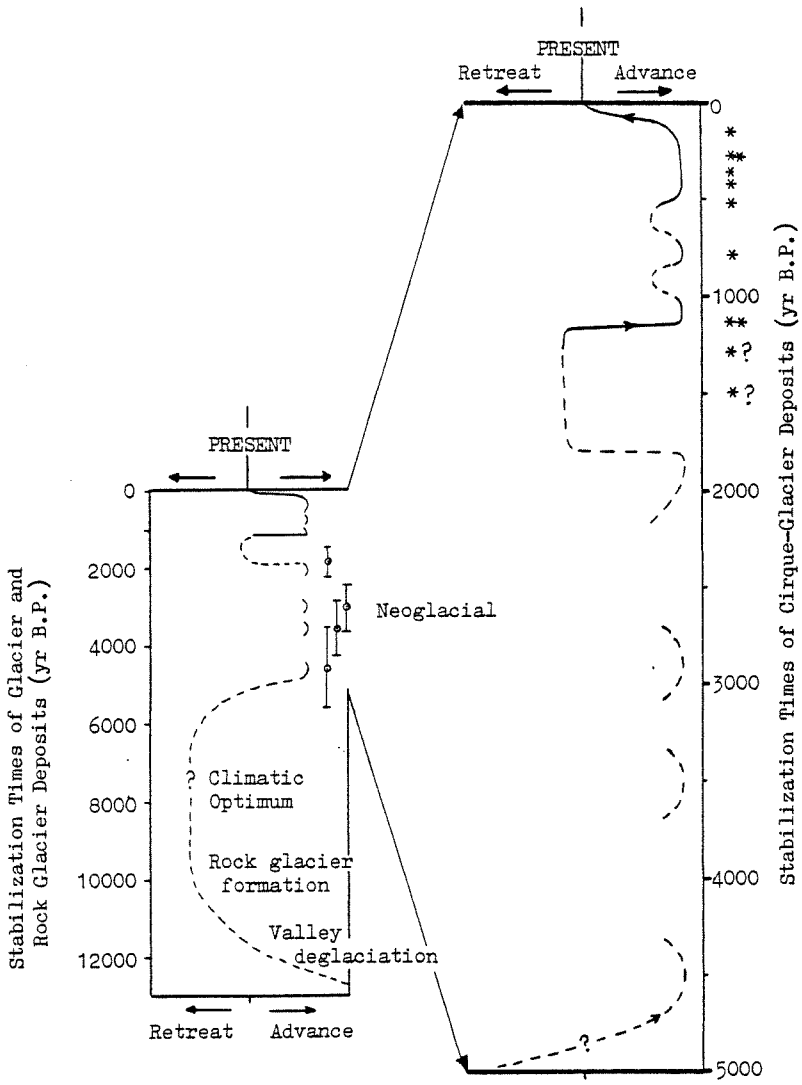

Figure 46. Holocene glacier chronology for the central Brooks Range based on lichenometric, radiometric and relative dating criteria. Seven periods of cirque glacier expansions followed by moraine stabilization are depicted. The four vertical error bars parallel to the time line on the left (5500-1400 yr B.P.) are assumed age reliability ranges of ± 20% about the mean lichen ages. Radiocarbon ages (Table 14) are depicted by asterisks (*); all were interpreted as being related more to glacial advances than retreats. Two radiocarbon dates (**) of 320 ± 100 and 1120 ± 180 yr B.P. are exceptionally reliable as indicators of glacial expansions.

ages (Figs. 37-39). The last major Neoglacial expansion is lichenometrically dated as (L) 390 ± 90 yr B.P. (A.D. 1410-1600) with radiocarbon dates directly associated with deposits ranging from 320 ± 100 to 540 ± 180 yr B.P. (A.D. 1200-1650). The well documented and widespread lichenometric range is chosen to represent the culmination of the last major expansion. Ice margins remained close to this advanced position until ~(L) 170 ± 40 yr B.P. or about A.D. 1640-1750 when marked recession commenced. Deglaciation was most rapid after ~A.D. 1870; however, the rate has slowed since the 1950's.

A major glacial advance, radiocarbon dated at 1120 ± 180 yr B.P. and lichenometrically dated at (L) 1150 ± 300 yr B.P., is well established for the central Brooks Range. Culmination of this advance may have occurred ~1150 ± 200 yr B.P. based on combining the above evidence. There may have been a subsequent readvance ~(L) 800 ± 200 yr B.P. that resulted in alluvial fans undergoing aggradational events, one radiocarbon dated at 800 ± 90 yr B.P. Combining these ages provides a culmination date of ~800 ± 150 yr B.P.

The state of glaciers between the three most recent expansion phases is unknown; however, the evidence at Golden Eagle Glacier suggests that during the past 1120 ± 180 years, glaciers did not recede as far into their cirques as they have at present. Climatic conditions in the summers for the past millennium may have been colder, cloudier, or snowier as compared with present.

Beyond 1200 yr B.P. the chronology is based only on lichenometric measurements of R. geographicum and relative dating criteria. Figure 46 has a subjective ± 20% age reliability depicted for the

four advances older than 1200 yr B.P. to emphasize the limited and decreasing resolution with time this older portion of the chronology has built into it.

There is much lichenometric evidence based on live lichens for a moraine stabilization phase at (L) 1800 ± 400 yr B.P. However, at Golden Eagle Glacier lichenometric measurements on emergent but relict lichens suggest a preceding ice-free period to ~(L) 3000 ± 600 yr B.P. for the cirque gloor site. Either a) the lichenometric growth curve is already unreliable at this age which is unlikely as there is a radiocarbon control point at 1300 ± 100 yr B.P. (Fig. 31), b) measuring relict lichens is not a valid technique for determining the length of a preceding ice-free episode, or c) Golden Eagle Glacier did not react to a regional climatic deterioration that was recorded lichenometrically at numerous other cirque glaciers. There is no environmental or morphological reason why Golden Eagle should react differently; it is a typical cirque glacier (Appendix B). This local evidence for an extensive ice-free interval cannot be resolved at this time with the widespread evidence for a glacial advance ~1800 yr B.P. The proposed Neoglacial chronology of the central Brooks Range (Fig. 46) includes the advance of 1800 ± 400 yr B.P. age; the contradictory relict evidence at Golden Eagle is disregarded.

Lichenometric measurements on ten preserved ridges of debris in the Atigun Pass and Arrigetch Pass areas suggest cirque glacier moraines stabilizing at (L)2900 ± 600, 3500 ± 700, and 4400 ± 1000 yr B.P. There is little evidence of expansion periodicity during

the Neoglacial interval. In addition, there is little morphological evidence of younger deposits breaking through older moraines in the central Brooks Range. The debris ridges and zones that form individual lateral and end moraines lichenometrically dated from middle to late Holocene time tend to be closely nested within a belt less than 50 m wide along the margin of Neoglacial deposits (see Appendix C). This concentration of terminal positions along the perimeter indicates that the major Neoglacial expansions were on the same order of magnitude. A climatic optimum ranges from early Holocene time to 4400 $\pm$ 1000 yr B.P. based on a lack of glacial deposits and stabilization of rock glacier surfaces during this time interval in the central Brooks Range (Fig. 46).

The term Fan Mountain Glaciation (Detterman and others, 1958) is still retained to describe cirque glacier deposits in the central Brooks Range of Neoglacial age for continuity with the literature. However, contrary to previous reports of this area (Detterman and others, 1958; Hamilton, 1965a; Porter, 1966) this glaciation is not composed of two stages, and it does not include ice-free cirques with Fan Mountain moraines. Misinterpretation of coalescing lobate rock glaciers (probably early Holocene in age) as Fan Mountain moraines in ice-free cirques may have occurred during previous reconnaissance studies (see type locality photograph in Detterman and others, 1958, Fig. 10). This type locality is about 60 km west of Atigun Pass near Fan Mountain; it has never been closely mapped, the sites are not specified in the literature, and it is relatively inaccessible.

It is proposed that the type locality for the Fan Mountain

Neoglaciation in the central Brooks Range be changed to four cirque glaciers and their deposits in the Atigun Pass area. Large scale surficial/lichenometric maps have been or are being published for these four reference sites:

a) Buffalo Glacier (Fig. 12) in Calkin and Ellis (1980, Fig. 8),

b) Golden Eagle Glacier (Fig. 44) in Calkin and Ellis (1981, Fig. 1),

c) Triple East Glacier (Fig. 34) in Ellis and Calkin (in prep.),

d) Harlequin Duck Rock Glacier (Fig. 36) in Calkin and Ellis (in press, Fig. 5).

These cirque glacier deposits span the Neoglacial time interval, two have critical radiocarbon ages, and all are relatively accessible due to proximity to the trans-Alaska oil pipeline haul road (Fig. 2).

CLIMATIC ANALYSIS OF CIRQUE GLACIATION

Climatic Sensitivity of Cirque Glaciers

It is generally acknowledged that glaciers in the Brooks Range are the least active in the United States because of the combined effects of high latitude and remoteness from the primary source of precipitation, the Pacific Ocean (Meier and others, 1971). The response time of glaciers in the central Brooks Range to changes of input (climate and debris supply) is presently unknown. Andrews and others (1971) suggest cirque glaciers may respond recognizably to changes of input on a time scale of 10-100 years (see also Miller,

1973a; Tangborn and others, 1977; Gordon, 1981); more rapidly to climatically induced snout retreats than to snout advances (Sugden and John, 1976).

The distribution of glacier area by altitude can significantly affect a glaciers's response to environmental changes (Ahlmann, 1948). The shape of cirque glaciers in the central Brooks Range (Appendix B) demonstrates high sensitivity to climatic change. As an example, Yellowjacket Glacier (no. 22, Fig. 2) was planimetrically reconstructed to its Neoglacial maxima and a steady-state ELA of 1630 m calculated (procedure explained below in Holocene Changes in Glacier Mass). Twenty-five percent of the glacier's surface area is concentrated around the reconstructed ELA. Sixty-seven percent of the surface area is upslope of this Neoglacial maxima ELA forming a substantial accumulation zone (AAR = 0.67, Fig. 47). This area-altitude distribution pattern is typical for cirque glaciers in the central Brooks Range (Appendix B). By raising the ELA only 90 m to 1720 m altitude, the accumulation area to ablation area ratio is reversed from 2:1 to 1:2 (AAR = 0.33, Fig. 47). Such a modest change in ELA would conspicuously shrink the glacier. When this typical glacier shape is combined with the markedly northward orientation pattern of these glaciers (Fig. 10), it is evident that cirque glaciers in the central Brooks Range are very sensitive to climate and should react rapidly to climatic changes.

Holocene Changes in Glacier Mass

Reconstruction of 53 cirque glaciers to their Neoglacial maxima

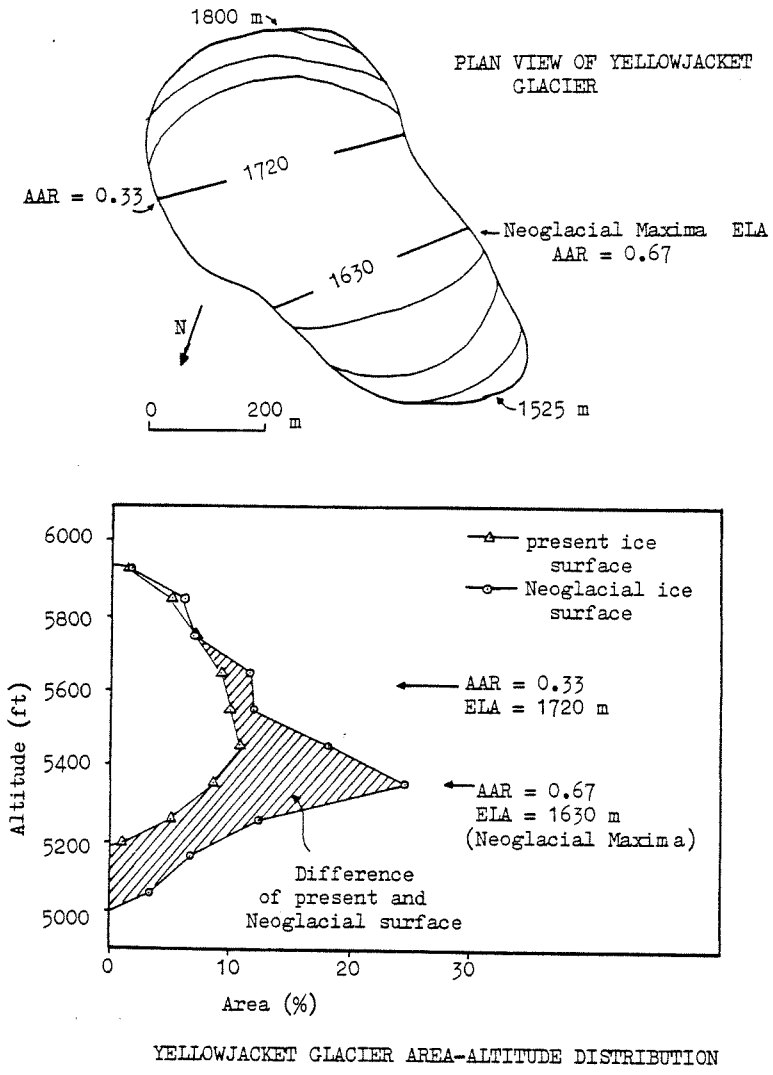

Figure 47. Reconstruction of Yellowjacket Glacier (no. 22, Fig. 2) showing typical climatic sensitivity of cirque glaciers in the central Brooks Range to changes in ELA. Plan view of reconstructed Neoglacial maxima and area-altitude distribution of present glacier and Neoglacial maxima depicted with ELA = 1630 m for maxima when accumulation area ratio (AAR) = 0.67. AAR reverses to 0.33 with an ELA rise of only 90 m from the Neoglacial maxima.

was based on geomorphic and lichenometric mapping of the downslope moraines and involved the entire Neoglacial deposit for simplicity and consistency. The results are applicable to the seven Neoglacial maxima as the more recent and older moraines are closely nested along the perimeter of most Neoglacial deposits in the central Brooks Range. Although some older deposits may form rigid barriers to subsequent glacier expansions, thereby changing glacier morphometry during subsequent advances, most older deposits are cored with glacial ice that is continuous upslope to the receding glacier. The response of these buried ice cores and their cover of debris to subsequent Neoglacial expansions is not clearly understood (see Figs. 14, 35) and is disregarded in the reconstructions.

Determination of Equilibrium-Line Altitudes (ELA's)

Determination of cirque glacier, steady-state ELA's was accomplished planimetrically by application of an assumed accumulation area to ablation area ratio of 2:1 or a ratio of accumulation area to total glacial area (AAR) of 0.67. The contour line on the reconstructed glacier that coincides with the steady-state ELA is one that defined the change in contour shape from concave in the accumulation zone to convex in the ablation zone (Østrem, 1966; Appendix B).

The AAR = 0.67 was chosen on the basis of extensive investigations of snowline in glacierized areas of the Alps (Gross and others, 1976; see also Miller and others, 1975). In addition, Meier and Post's (1962) observation of AAR's between 0.5 and 0.8; Zubok's

(1975) and Porter's (1975) AAR calculation of 0.67 and 0.6, respectively, for maritime coastal glaciers in northwestern North America; and Porter's (1970) suggestion of AAR = 0.65 ± 0.05 for cirque glaciers support use of AAR = 0.67 in this study. The ELA's derived by this planimetric 2:1 method form the basis of this study; however, these values were compared to estimates determined from the altitude of the upper limits of lateral moraines and the altitude three-fifths of the way between the backwall and end moraine of the reconstructed glacier (Andrews, 1975, p. 54-55).

ELA's reconstructed for the Neoglacial maxima with AAR = 0.67 average 1755 ± 70 m for cirque morainal deposits (M, Mg, MG) and 1640 ± 80 m for rock glacier transition zones (TRGC) in the Atigun Pass area (Figs. 22, 48). However, most glacier-cored rock glaciers in the Atigun Pass area are in the lower southern part of the field area (Fig. 2, Plate 1). These east-central, sedimentary terrain ELA's are significantly higher than those found in the Arrigetch Peaks where ELA's for glaciers fronted by glacier-cored moraines averaged 1345 ± 30 m and for one leading downslope into a rock glacier tongue was at 1320 m (Appendix E). Across the central Brooks Range the upper limit of the lateral moraines gave ELA values 50 ± 40 m higher and the three-fifths altitude calculations provide ELA's 10 ± 30 m higher than those found with the AAR = 0.67 method (Appendix E).

The lowering of ELA from the mean altitude of present glaciers (NDROP, ELADROP, Table 7) fronted by moraines (excluding those in rock glacier transition zones) was 75 ± 35 m around Atigun and Anaktuvuk Passes and 140 ± 55 m in the more westerly Arrigetch (Fig. 24,

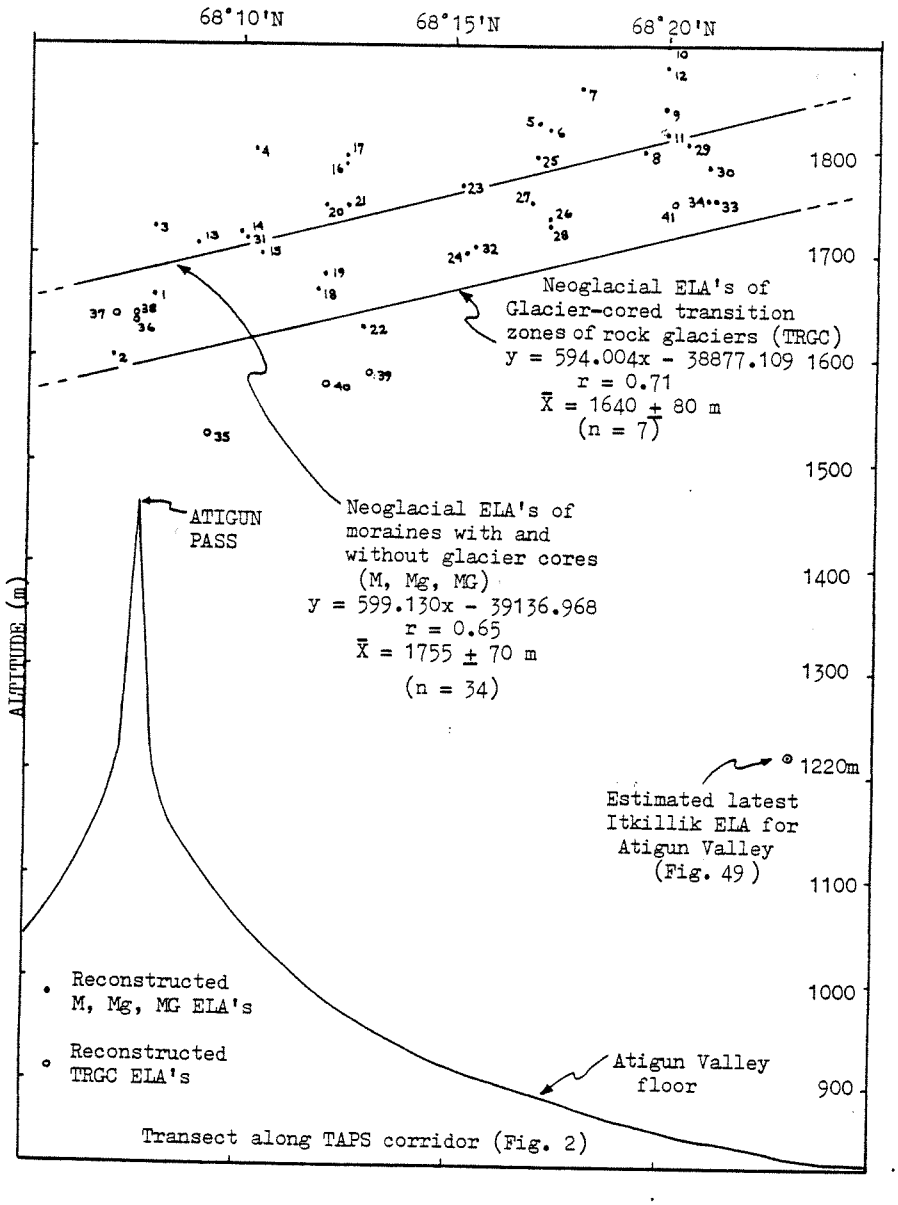

Figure 48. North-south transect through Atigun Pass showing altitudes of ELA's during Neoglacial maxima. The upper trend surface represents ELA's for glaciers fronted by moraines without ice cores (M) and moraines with ice- or glacier-cores (Mg/MG). The lower trend surface represents ELA's for cirque glaciers fronted by transitional zones (TRGC) upslope of rock glacier tongues. These ELA's rise northward ~5 m km^{-1} showing predominant moisture from southerly sources.

Table 4). Although this difference is not statistically significant at the 95% confidence level, it is when compared with glaciers fronted by transition zone moraines. There the ELA lowered only 40 $\pm$ 40 m during Neoglacial maxima. Regardless of deposit type and location, during major Neoglacial advances an average lowering of ELA from the mean altitude of present glaciers was topographically reconstructed for 53 glaciers in the central Brooks Range as ~80 $\pm$ 50 m (Table 4).

When the reconstructed ELA's for Neoglacial maxima calculated for the Atigun Pass area are plotted along a north-south transect, a trend rising to the north is easily seen (Fig. 48). In addition, when these Neoglacial maxima ELA's are associated with type of deposit, a trend representing glaciers fronted by only morainal deposits is approximately 115 m higher than one for glaciers leading into transition zone moraines upslope of rock glaciers. However, both rise ~100 m over a northward distance of 19 km for an ELA gradient of ~5 m km^{-1}.

Moraines without cores of ice (M, nos. 1-12, Fig. 48) are concentrated along the upper altitudinal range of the trend surfaces (Fig. 22). This implies their localization in cirques of higher altitude which would favor cirque environments with lower topographic horizons, less debris, and greater solar energy inputs (see Figs. 21-23). The steady-state ELA's for glacier-cored moraines in the east-central Brooks Range (Mg, MG, nos. 13-34, Fig. 48) are above those reconstucted for glaciers fronted by rock glacier transition zones (TRGC, nos. 35-41, Fig. 48). This may have allowed for the greater amount of ELA depression and Neoglacial expansion associated with

higher altitude Mg/MG deposits (Fig. 9); otherwise, the deposits are essentially the same (Figs. 22, 23, 25).

A preliminary reconstruction of the area covered by the latest Itkillik valley glacier (~12,500 yr B.P.) in the Atigun drainage basin was made to approximate the difference in ELA during maximum cirque and latest valley glaciations (Fig. 49). Using an AAR = 0.67 the latest Pleistocene ELA was determined at 1220 m and located over the northern portion of the valley at lat 68°23'N. Eighty percent of the Atigun drainage basin was glacierized, and the valley glacier covered ~610 km^2. A rise in ELA of ~500 m separates this last valley glaciation from the maximum Neoglacial fluctuations.

Past and Present Cirque Glacier Thicknesses

Field estimates of ice thickness and ablation since the last major Neoglacial expansion were made with an optical range finder and a Brunton compass level. The heights from present glacier surfaces to crests of Neoglacial lateral moraines were measured, providing an estimate that ~30 m (range 27-39 m) of glacial ice has ablated since the last major advance. Estimates of cirque glacier thicknesses during this most recent Neoglacial maximum were made at snouts of ice- and glacier-cored moraines (see Fig. 35). Here the glacier core is well protected from ablation by a cover of debris (Fig. 14); therefore, its thickness may provide an estimate of the size attained during maxima farther upslope. Many morainal snouts had thicknesses averaging ~65 m (range 10-75 m). These field estimates of past thickness and subsequent ablation imply only ~35 m

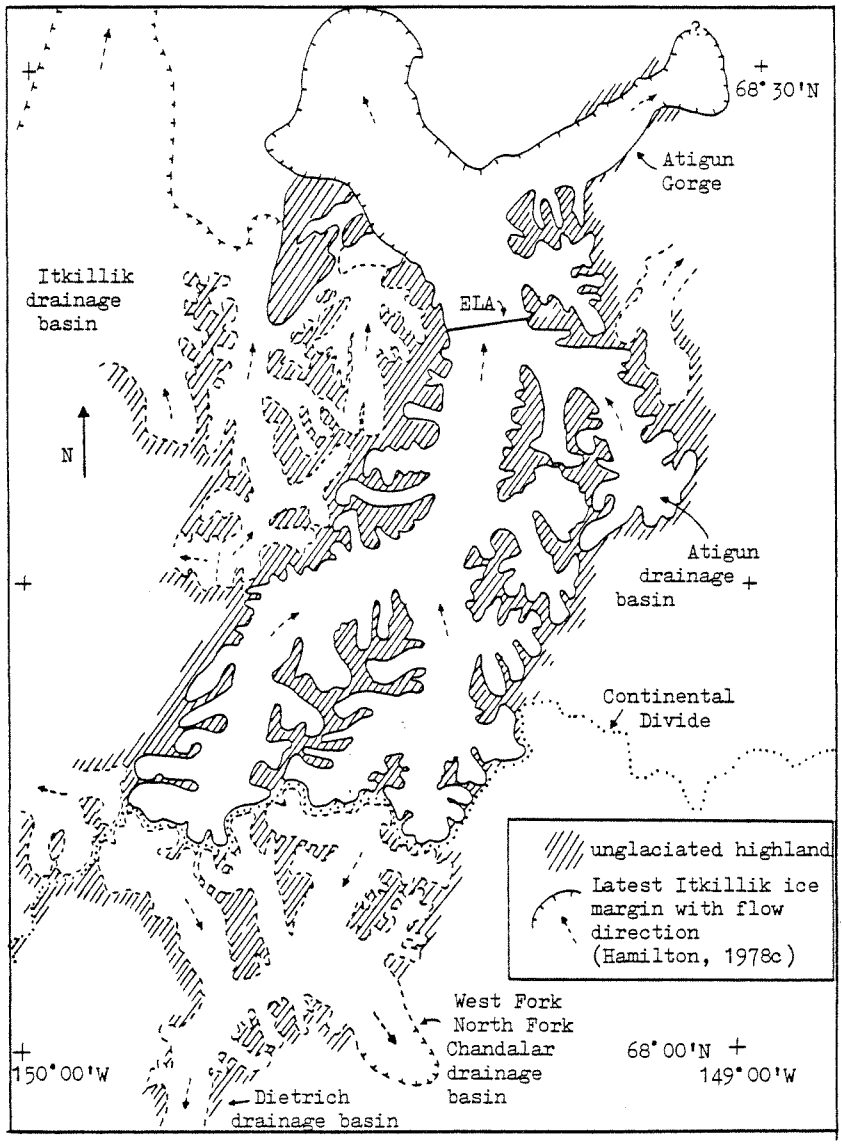

Figure 49. Preliminary planimetric reconstruction of the latest Itkillik valley glacier (~12,500 yr B.P.) in the Atigun drainage basin (see Fig. 2). Equilibrium-line altitude of 1220 m (4000 f) is based on an accumulation area to ablation area ratio of 2:1. This reconstructed ELA is ~500 m below the Neoglacial maxima at lat 68 23'N (see Fig. 48).

of ice may remain in many glacierized cirques.

Weertman's (1971) theoretical formula for steady-state cirque glaciers was applied to check the field-estimated, minimum thickness of 65 m during Neoglacial maxima. This formula uses a basal shear stress value of $\tau = 0.4 \rho g h \sin\alpha$ which when applied with $\tau = 1$ bar, $\rho = 0.9$ g cm^{-2}, and $g = 980$ cm sec^{-2} provides cirque glacier thickness (h) in meters (K. Brugger, pers. comm., 1981): $h = \tau / 0.4 \rho g \sin\alpha = 1 / (0.4)(0.0892)(\sin \alpha)$. A mean glacier slope ($\alpha$) of 15°, reconstructed from Neoglacial maxima (Appendix B), was used with Weertman's formula to provide a theoretical thickness of ~110 m for cirque glaciers during steady-state expansions in the central Brooks Range.

There is little change in glacier slopes between present (Fig. 7) and reconstructed glaciers (Table 4). The steepest reconstructed slope of 22° was determined for Raptor Glacier (no. 6, Fig. 2) giving a steady-state ice thickness of 75 m. In contrast, the largest glacier in the Atigun Pass area, Buffalo Glacier (Fig. 12) was found to have the most gentle reconstructed slope of 8° (Appendix B), suggesting a Neoglacial steady-state thickness of 200 m with Weertman's formula. However, Buffalo Glacier is the result of three coalescing cirques and its motion downslope may be more related to valley glacier flow (Nye, 1965) than to rigid-body rotation (Weertman, 1971). Using Nye's valley-shape factor = 0.7, the recalculated thickness that treats Buffalo Glacier as a small valley body is 115 m. There are no differences between reconstructed ice thicknesses for the different types of glacial deposits or the Arrigetch and Atigun/Anaktuvuk terrains (Table 4), except for glacier-cored rock glaciers.

For the latter, estimation of glacier slope is hindered by excessive debris.

Climatic Implications

Determining the climate that accompanied Neoglacial ELA depressions is difficult (see Porter, 1975). ELA's are the result of interacting climatic parameters such as air temperature, annual and summer snowfall, cloudiness, snow drift accumulation (wind), and frequency/duration of storm activity. These factors are integrated by the ice body; the altitude where the mass balance equals zero (ELA) is the reflection of this integration of a short- and long-term basis (Sugden and John, 1976).

Equilibrium-line altitude is estimated to have risen 100 to 200 m across the central Brooks Range since (L) A.D. 1410-1600. At Grizzly Glacier (cover photograph) the ELA rise since this time has been measured glaciologically as 130 m for A.D. 1978 (Bruen, 1980a). This climatic ELA change is different than the topographically determined ELA change (NDROP, ELADROP, Table 7) utilized by necessity throughout this study. The topographically determined ELA change is an easily obtained, standardized measurement used in the statisical comparisons of glacial landforms. It was calculated as the difference between the topographically determined mean altitude of present glaciers and the reconstructed Neoglacial maxima ELA. The climatic ELA change is based on minimal glaciological data (Ellis and Calkin, unpub. data, 1977-1981) and is estimated as the difference between the present ELA and the reconstructed Neoglacial maxima

ELA. Although this latter calculation is only approximate, it is useful for estimating the magnitude of climatic change that accompanied glacier expansions.

If the climatic ELA depression of 100 to 200 m from present ELA was solelya function of temperature lowering during Neoglacial maxima, a reduction from present summer temperature of only ~1° C would account for the maximum Neoglacial advances with a lapse rate of 0.6°C/100 m (see Porter, 1966 for lapse rate calculation). This temperature lowering is probably a maximum value because of the numerous factors involved in determining climatic ELA's. Atmospheric circulation patterns that bring moist air masses and increased summer snowfall markedly enhance glacier growth, resulting in lower ELA's in the northeastern Brooks Range (Fahl, 1973, 1975). In addition, an increase in the number of cloudy days during the summer would contribute to a lowering of ELA there (Wendler and Weller, 1974) as it would in the central Brooks Range because radiation is probably the most significant factor in the ablation of these glaciers (Fig. 10).

Comparison to Other Holocene Chronologies

Regional Studies

Studies of climatic history from within and around the Brooks Range landmass corroborate the Holocene chronology presented in this study. They support a climatic optimum in early to middle Holocene time followed by deteriorating conditions in middle to late Holocene

time (Fig. 50). On a more detailed scale, this study indicates cirque glaciers were near their maximum expansions from A.D. 1410 to 1750, deglaciation accelerated after the 1870's, and decelerated by the 1950's (Fig. 46). This is substantiated by the following a) a period of stream terrace alluviation within the past 500-200 years (Hamilton, 1980c); b) depression of rates of forest growth in central Alaska during several distinct intervals, notably the mid 1600's and early 1800's (Haugen and Brown, 1978); c) tree line chronologies for the Noatak and Arrigetch valleys (Fig. 1) suggesting that cold spells occurred in the mid 1500's and late 1600's and warming conditions from the late 1800's to the 1900's (G. Jacobi, pers. comm., 1979); d) a rise of ~2°C from A.D. 1830 based on tree ring data from the Alatna River valley (Fig. 1; Garfinkel and Brubaker, 1980); and e) interpretation of a composite Alaskan temperature record as rising a net 1°C from the 1800's to 1941, followed by a decreasing mean annual temperature (Hamilton, 1965b, Fig. 9).

Neoglacial events prior to this most recent advance are compatible with alternating building and downcutting of alluvial terraces in valleys of the central Brooks Range (no. 12, Fig. 50; Hamilton, 1980c). Lake sediment samples collected along the Atigun River (f, Fig. 30, Table 14) were analyzed for their pollen content by W. N. Mode (written comm., 1980; no. 14, Fig. 50). His analysis was climatically inconclusive (see also Walker and others, 1981); however, his work indicates a wetter tundra vegetation from ~2500 to 1200 yr B.P., approximately the same interval of time that nearby Golden Eagle Glacier (Fig. 44) was in a shrunken state based on

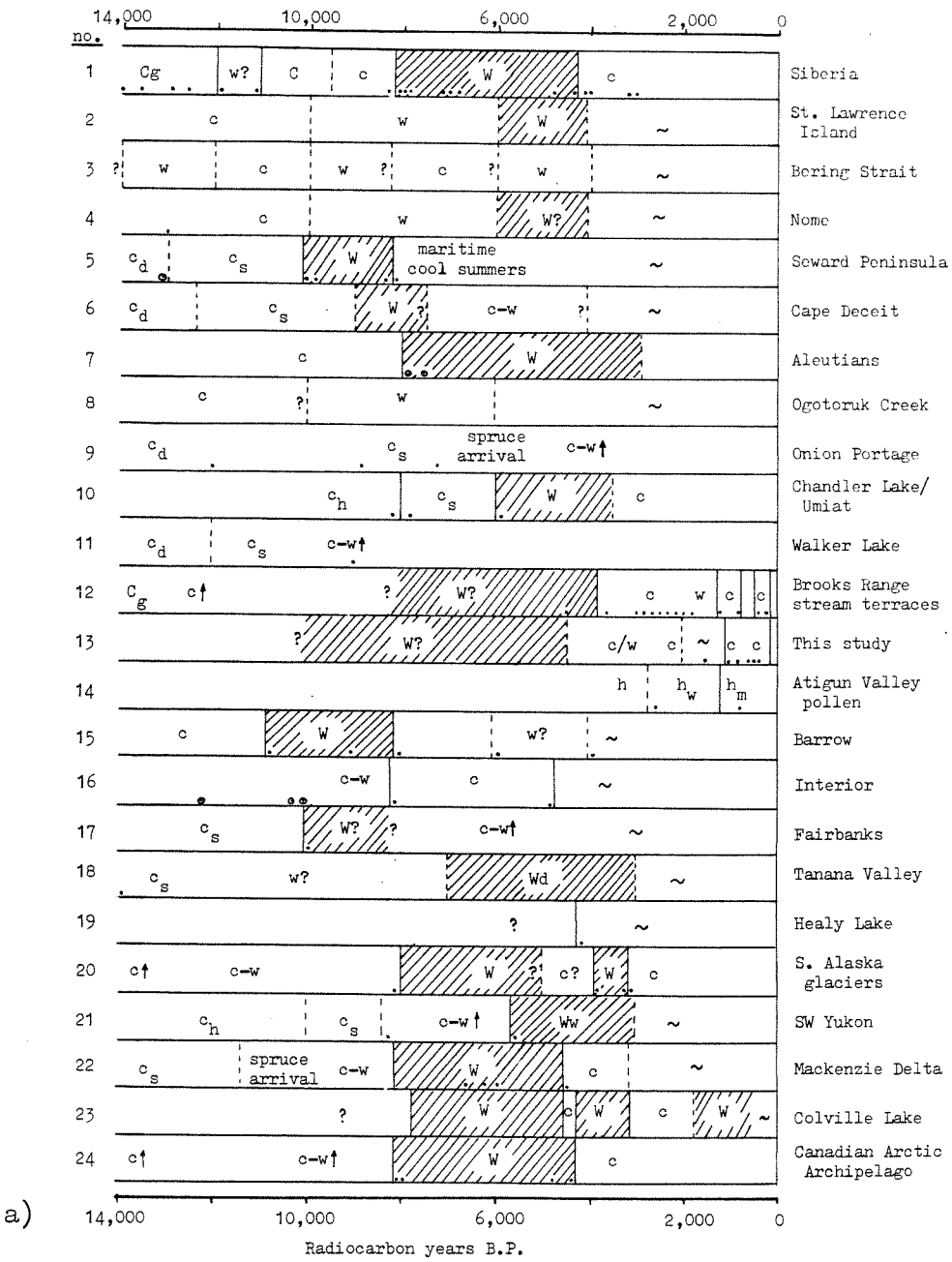

Figure 50. a) Regional climatic indicators within and around the central Brooks Range with map (b), legend (c), and references (d) shown on facing page.

b)

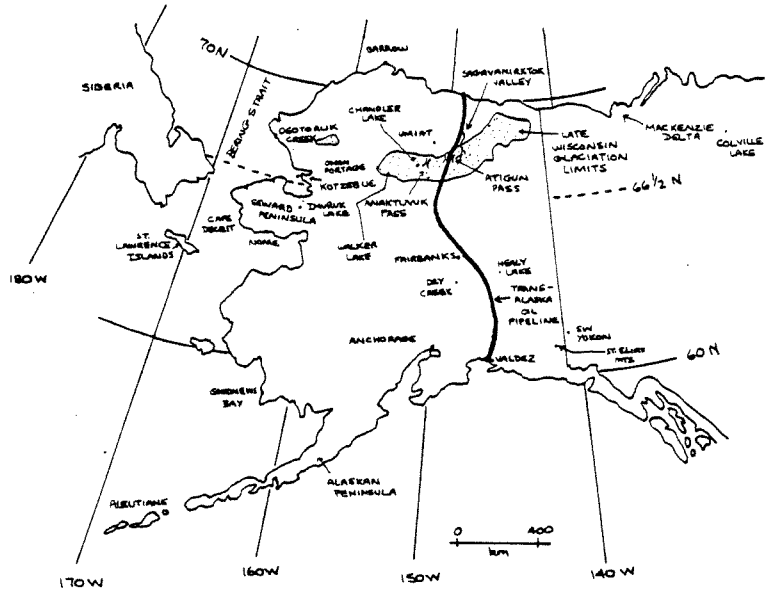

c) LEGEND FOR FIGURE

Symbol	Explanation
Wd	warmer than recent , dry
Ww	warmer than recent, wet
W	warmer than recent
w	moderately warm
c	moderately cold
c-w	moderating climate
c/w	changable climate
C	cold
C_g	cold glacial
c_d	cold steppe tundra, dry
c_s	cold shrub tundra
c_h	cold herbaceous tundra
c-w	warming out of cold
c	warming out of glacial
w	warming to maximum
h	herbaceous tundra
h_w	wet herbaceous tundra
h_m	mesic herbaceous tundra
·	radiocarbon control date
⊙	archeologic site with radiocarbon date
~	same climate as recent

d) REFERENCES FOR FIGURE

No.	References
1	Kind, 1967.
2	Heusser, 1965; Colinveaux, 1967.
3	Hopkins, 1967.
4	Heusser, 1965.
5	McCulloch and Hopkins, 1966; McCulloch, 1967; Hopkins, 1972.
6	Matthews, 1974a.
7	Black, 1976.
8	Heusser, 1965.
9	Schweger, 1971.
10	Livingstone, 1955, 1957; Colinveaux, 1965.
11	Brubaker, 1979.
12	Hamilton, 1980c.
13	this study.
14	Mode, W. N., pers. comm., 1980.
15	Douglas and Tedrow, 1960; Tedrow and Walton, 1964; Brown, 1965, 1969; Black, 1969, Tedrow, 1972.
16	Thorson and Hamilton, 1977.
17	Brown and others, 1969; Matthews, 1970, 1974b; Péwé, 1975.
18	Ager, 1975.
19	Anderson, 1973.
20	Denton and Karlén, 1977.
21	Rampton, 1971.
22	Mackay and Terasmae, 1963; Ritchie, 1972; Ritchie and Hare, 1971; Hyvarinen and Ritchie, 1975.
23	Nichols, 1972.
24	Blake, 1972.

Figure 50 continued.

lichenometric measurements of relict lichens. The pollen site also records a change to a mesic tundra about 1200 yr B.P., approximately the same time that cirque glaciers strongly readvanced (Fig. 46). This pollen record is difficult to coincide with glacier retreat and expansion unless it reflects a change in local drainage conditions as the climate changed.

Rising permafrost tables (Brown, 1965; Kind, 1967), pingo development (Hyvarinen and Ritchie, 1975), spruce tree line retreat (Ritchie, 1972), and changes in pollen (Heusser, 1965; Colinveaux, 1967; Parrish, 1980) substantiate a severe climate returning to the Brooks Range between 4500 and 3000 yr B.P. after a climatic optimum spanning early to middle Holocene time (Fig. 50). This climatic optimum within and around the Brooks Range is demonstrated by a) alder prominences in pollen cores (Livingstone, 1955, 1957), b) thaw lake (Black, 1969) and poplar (Detterman, 1970) expansion on the North Slope, c) bog formation (Parrish, 1980, d) northward migration of the spruce tree line (Ritchie, 1972; Péwé, 1975), e) lower permafrost tables (Douglas and Tedrow, 1964; Brown, 1965; Tedrow, 1972), f) stable slopes and peat formation (Hamilton, 1978c), and g) archeological evidence (Hamilton, 1978d).

Glacial Studies

Extensive compilation of Holocene glacial records by Grove (1979) and global Neoglacial moraines by Davis (1980, p. 73-74) demonstrate the synchrony of the last major Neoglacial expansion throughout the world; however, the evidence available at present suggests a lack of synchroneity or a failure of dating methods to delineate syn-

chronous events beyond 500 years in age (Grove, 1979). The central Brooks Range sequence is similar in form to those from most other regions (see Davis, 1980, p. 73-74), including Baffin Island (Miller, 1973a), the eastern Alps (Heuberger, 1974), Patagonia (Mercer, 1976), and New Zealand (Burrows, 1975). These all show five or more pulsations from middle to late Holocene time which are non cyclic.

The magnitudes of each of the major late Holocene advances in the central Brooks Range were similar (Fig. 46). This situation was also found in detailed studies of the Alps (summarized in Grove, 1979), southern Alaska (Denton and Karlén, 1973b, 1977), and Scandinavia (Karlén, 1973). However, Miller (1973a) notes the most recent Neoglacial advance as the maximum in Baffin Island. Benedict (1973) suggests a middle Holocene advance in the central Rockies as the largest of the Neoglacial there. Mercer (1976) indicates the first Neoglacial advance (4600-4200 yr B.P.) in Patagonia as the most extensive; he reports that the most recent (< 300 yr B.P.) advance as the smallest.

Rock glacier formation was the main glacial event during early Holocene time in the central Brooks Range. Rock glaciers were also formed during this interval in the Canadian Rockies (Luckman and Crockett, 1978; Johnson, 1980), the Colorado San Juan Mountains (Carrara and Andrews, 1976), and the Swiss Alps (Haerberli and others, 1979).

A comparison of the central Brooks Range ELA depression (estimated from present ELA to Neoglacial maxima) to other glacierized alpine regions is as follows (see Porter, 1975, Fig. 9, Table 2):

a) 140 m	Southern Alps of New Zealand
b) 100-200 m	Cascades (Scott, 1974)
c) 150 m	Columbian Andes (Herd, 1974)
d) 100-200 m	Alps (Heuberger, 1968)
e) 100-200 m	central Brooks Range (this study)

The similarity of Neoglacial ELA depressions on a worldwide scale, including the central Brooks Range, suggests a worldwide climatic deterioration of similar magnitude. In the central Brooks Range of northern Alaska this climatic deterioration occurred approximately seven times during the past ~5000 years.

CONCLUSIONS

1) Comparison of cirque glaciers in the west-central Arrigetch Peaks to those in the sedimentary terrain of Atigun and Anaktuvuk Passes demonstrates similar glacier shapes, dimensions, and aspects. However, the moraines downslope of the Arrigetch glaciers are much less stable, more extensively glacier cored, and ~300 m lower in altitude.

2) The granitic Arrigetch cirques are substantially deeper than those in sedimentary terrain farther east. Their cirque environments differ respectively in mean inclinations to the horizon for non ice-cored moraines (~20° versus ~12°), glacier-cored moraines (~25° versus ~17°), and transition zone deposits upslope of rock glaciers (~30° as compared with ~19°).

3) The state of activity for tongue- and lobate-shaped rock glaciers as determined by vegetation development and morphology of

debris fronts has little relation to altitude, aspect, topographic horizon, or direct radiation energy received. Apparently their activitystate is largely dependent upon the availability of debris from headwall cliffs.

4) Lichenometry has proved to be the most useful tool for absolute and relative dating of Holocene glacial deposits in portions of the central Brooks Range dominated by sandstone, conglomerate, and granite. The growth curve for Rhizocarpon geographicum s.l. includes a colonization period of 30 years, a great growth period of about 200 years, a long term linear phase approximating 3 mm per century, and a subjective ± 20% age reliability.

5) Lichenometric patterns and maximum lichen diameters mapped on the various Neoglacial deposits located across the central Brooks Range are remarkably similar, suggesting a) the ice masses reacted synchronously to climatic changes, b) lichen colonization times do not vary significantly with lithology or substrate stability, and/or c) the lichenometric method is too imprecise to detect colonization differences between different types of moraines and slight climatic differences across 225 km of the central Brooks Range.

6) Weathering and soil development, including soil pH, complement lichenometry and help differentiate Holocene deposits in sedimentary terrain. Soil pH values of 7.5-8.0 were found for freshly deposited till, 4.8-6.4 for rock glacier tongues downslope of Neoglacial cirque moraines, and 4.7-5.4 for late Pleistocene moraines farther downvalley.

7) Preservation of an early Holocene rock glacier tongue downslope of glacier cores is largely a function of altitude. Ice cores

at lower altitudes were unable to respond vigorously to Neoglacial climatic deteriorations and were unable to completely overrun their downslope rock glacier tongues; therefore, they formed Neoglacial moraines situated in transition zones upslope of the older rock glaciers. During Neoglacial maxima in the east-central Brooks Range, glaciers forming these transition zones averaged ELA depressions of only 40 $\pm$ 40 m as measured from the mean altitudes of the present-day glaciers. In contrast, glaciers fronted by solely morainal deposits are ~100 m higher and had ELA's depressed 90 $\pm$ 50 m from the mean altitudes of the present-day ice masses. They obliterated any evidence of a previous rock glacier lobe emanating from the cirque.

8) Cirque glaciers demonstrate significant climatic sensitivity as much of their surface area is concentrated around the reconstructed ELA's of Neoglacial maxima. An ELA rise of only 150 m from the Neoglacial maxima altitude severely reduces if not eliminates the accumulation area of cirque glaciers in the central Brooks Range.

9) Neoglacial advances in the central Brooks Range were of similar magnitude. The expanded cirque glaciers averaged only ~0.65 km^2 in area and reached steady-state thicknesses of ~65-100 m.

10) The Atigun Pass area is proposed as the new type locality for the Fan Mountain Neoglaciation in the central Brooks Range, superceding previous type localities. Four cirque glaciers and their Neoglacial deposits that have had large scale surficial/lichenometric maps recently published are specified as reference sites within the Atigun Pass type locality. These deposits span the Neoglacial, two have critical radiocarbon ages, and all are relatively accessible.

REFERENCES CITED

Ager, T. A., 1975, Late Quaternary pollen record from Birch Lake, Tanana Valley, Alaska: Geological Society of America Abstracts with Programs, v. 7, p. 289-290.

Ahlmann, H. W., 1948, Glaciological research on the North Atlantic coasts: Royal Geographical Society Research Service, v. 1, 83 p.

Anderson, J. H., 1975, A palynological study of late Holocene vegetation and climate in the Healy Lake area, Alaska, in Weller, G. and Bowling, S. A., eds., Climate of the Arctic: Twenty-fourth Alaska Science Conference Proceedings, Fairbanks, Alaska, August, 1973: Fairbanks, Geophysical Institute, University of Alaska, p. 334-338.

Anderson, L. W. and Anderson, D. S., 1981, Weathering rinds on quartz arenite clasts as a relative-age indicator and the glacial chronology of Mount Timpanogos, Wasatch Range, Utah: Arctic and Alpine Research, v. 13, no. 1, p. 25-31.

Andrews, J. T., 1975, Glacial systems - an approach to glaciers and their environments: North Scituate, Mass., Duxbury Press, 191 p.

Andrews, J. T. and Webber, P. J., 1964, A lichenometrical study of the northwestern margin of the Barnes Ice Cap: a geomorphological technique: Geographical Bulletin, no. 22, p. 80-104.

_____1969, Lichenometry to evaluate changes in glacial mass budgets: as illustrated from north-central Baffin Island, N. W. T.: Arctic and Alpine Research, v. 1, p. 181-194.

Andrews, J. T., Barry, R. G., and Draper, L., 1970, An inventory of

the present and past glacierization of Home Bay and Okoa Bay, east Baffin Island, N. W. T., Canada, and some climatic and paleoclimatic considerations: Journal of Glaciology, v. 9, no. 57, p. 337-362.

Andrews, J. T. and Estabrook, G., 1971, Application of information and graph theory to multivariate geomorphological analyses: Journal of Geology, v. 79, no. 2, p. 207-221.

Arnold, K. C., 1965, Aspects of the glaciology of Meighen Island, Northwest Territories, Canada: Journal of Glaciology, v. 5, p. 399-410.

Barsch, D., 1971, Rock glaciers and ice-cored moraines: Geografiska Annaler, v. 59A, p. 203-206.

Benedict, J. B., 1967, Recent glacial history of an alpine area in the Colorado Front Range, U. S. A. I. establishing a lichen-growth curve: Journal of Glaciology, v. 6, p. 817-832.

_____1968, Recent glacial history of an alpine area in the Colorado Front Range, U. S. A. II. dating the glacial deposits: Journal of Glaciology, v. 7, p. 77-87.

_____1973, Chronology of cirque glaciation, Colorado Front Range: Quaternary Research, v. 3, p. 584-599.

Berg, R., Brown, J., and Haugen, R., 1978, Thaw penetration and permafrost conditions associated with the Livengood to Prudhoe Bay road, Alaska, in Proceedings of Third International Conference on Permafrost, July 10-13, Edmonton, Alberta, Canada, Volume 1: Ottawa, National Research Council of Canada, p. 616-621.

Beschel, R. E., 1950, Flecten als Altermassstab rezenter Moraien:

Zeitschrift für Gletscherkunde und Glazialgeologie, v. 1, p. 152-161. (Translated by W. Barr, 1973, as Lichens as a measure of the age of recent moraines: Arctic and Alpine Research, v. 5, p. 303-309).

_____1961, Dating rock surfaces by lichen growth and its application to glaciology and physiography (lichenometry), in Raasch, G. O., ed., Geology of the Arctic, Volume II, Toronto, University of Toronto Press, p. 1044-1062.

Birkeland, P. W., 1973, Use of relative age-dating methods in a stratigraphic study of rock glacier deposits, Mt. Sopris, Colorado: Arctic and Alpine Research, v. 5, p. 401-416.

_____1974, Pedology, weathering, and geomorphological research: New York, Oxford University Press, 285 p.

_____1978, Holocene glacial stratigraphy, southern Alps, New Zealand: Geological Society of America Abstracts with Programs, v. 10, no. 7, p. 367.

Birkeland, P. W. and Shroba, R. R., 1974, The status of the concept of Quaternary soil-forming intervals in the western United States, in Mahaney, W. C., ed., Quaternary environments - Proceedings of a symposium: York University - Atkinson College (Toronto) Geographical Monograph, no. 5, p. 241-274.

Birkeland, P. W., Burke, R. M., and Walker, A. L., 1979, Variation in chemical parameters of Quaternary soils with time and altitude, Sierra Nevada, California: Geological Society of America Abstracts with Programs, v. 11, p. 388.

Black, R. F., 1969, Geology, especially geomorphology of northern Alaska: Arctic, v. 22, p. 283-299.

_____1976, Geology of Umnak Island, eastern Aleutian Islands as related to the Aleuts: Arctic and Alpine Research, v. 8, p. 7-35.

Blagbrough, J. W. and Breed, W. J., 1967, Protalus ramparts on Navajo Mountain, southern Utah: American Journal of Science, v. 265, p. 759-772.

Blake, W., Jr., 1972, Climatic implications of radiocarbon-dated driftwood in the Queen Elizabeth Islands, Arctic Canada, in Vasari, Y., Hyvärinen, H., and Hicks, S., eds., Climatic changes in arctic areas during the last ten-thousand years: Finland, University of Oulu, p. 77-104.

Brosgé, W. P. and Reiser, H. N., 1964, Geologic map and section of the Chandalar Quadrangle: U. S. Geological Survey Miscellaneous Geologic Investigations Map I-375, scale 1:250,000.

Brosgé, W. P., Reiser, H. N., Dutro, J. T., Jr., and Detterman, R. L., 1979, Bedrock geologic map of the Philip Smith Mountains quadrangle, Alaska: U. S. Geological Survey Miscellaneous Field Studies Map MF-879-B, scale 1:250,000, 2 sheets.

Brown, J., 1965, Radiocarbon dating, Barrow, Alaska: Arctic, v. 18, p. 36-48.

_____1966, Soils of the Okpilak River Region, Alaska: U. S. Army Cold Regions Research and Engineering Laboratory Research Report 188, 49 p.

_____1969, Ionic concentration gradients in permafrost, Barrow, Alaska: Hanover, New Hampshire, U. S. Army Cold Regions Research and Engineering Laboratory Research Report 272, 25 p.

_____1980, The road and its environment, in Brown, J. and Berg, R. L., eds., Environmental Engineering and Ecological baseline

investigations along the Yukon River-Prudhoe Bay haul road: Hanover, New Hampshire, U. S. Cold Regions Research and Engineering Laboratory Report 80-19, p. 3-52.

Brown, J. and Tedrow, J. D. F., 1963, Soils of the northern Brooks Range, Alaska. 4 well-drained soils of glaciated valleys: Soil Science, v. 97, p. 187-195.

Brown, J., Gray, S., and Allen, R., 1969, Late Quaternary evolution of a valley fill, Fairbanks, Part I, Geochemistry and stratigraphy of the permafrost: Hanover, New Hampshire, U. S. Cold Regions Research and Engineering Laboratory Technical Note, 18 p.

Brubaker, L., 1979, Vegetational history of the central Brooks Range, Alaska (abstract): Eighth Annual Eastern Canadian Arctic Workshop, Institute of Arctic and Alpine Research, University of Colorado.

Bruen, M. P., 1980a, Morphology and process of a cirque glacier and rock glaciers at Atigun Pass, Brooks Range, Alaska (M. A. thesis): State University of New York at Buffalo, 95 p.

_____1980b, Past and present climatic regimes of a cirque glacier and rock glaciers, Atigun Pass, Alaska: Geological Society of America Abstracts with Programs, v. 12, no. 2, p. 27.

Burke, R. M. and Birkeland, P. W., 1979, Reevaluation of multiparameter relative dating techniques and their application to the glacial sequence along the eastern escarpment of the Sierra Nevada, California: Quaternary Research, v. 11, p. 21-51.

Burrows, C. J., 1975, Late Pleistocene and Holocene moraines of the Cameron Valley, Arrowsmith Range, Canterbury, New Zealand: Arctic and Alpine Research, v. 7, p. 125-140.

Calkin, P. E. and Ellis, J. M., 1980, A lichenometric dating curve and its application to Holocene glacier studies in the central Brooks Range, Alaska: Arctic and Alpine Research, v. 12, p. 245-264.

_____1981, A cirque glacier chronology based on emergent lichens and mosses: Journal of Glaciology, v. 27, p. 511-515.

_____in press, Development and application of a lichenometric dating curve, Brooks Range, Alaska, in Mahaney, W. C., ed., Quaternary Dating Methods: Stroudsberg, Pennsylvannia, Milo Dowden.

Carrara, P. E. and Andrews, J. T., 1976, Holocene glacial/periglacial record; northern San Juan Mountains, southwestern Colorado: Zeitschrift für Gletscherkunde und Glazialgeologie, v. 11, p. 155-174.

Chinn, T. J. H., 1981, Use of rock weathering-rind thickness for Holocene absolute age-dating in New Zealand: Arctic and Alpine Research, v. 13, p. 33-45.

Cobb, E. H., 1976, Summary of references to mineral occurrences (other than fuel and construction materials) in the Chandalar and Wiseman quadrangles , Alaska: U. S. Geological Survey Open File Report, 76-340, 200 p.

Cobb, E. H. and Kachadoorian, R., 1961, Index of metallic and non-metallic mineral deposits of Alaska compiled from published reports of Federal and state agencies through 1959: U. S. Geological Survey Bulletin 1139, 363 p.

Colinveaux, P. A., 1965, Pollen from Alaska and the origin of ice ages: Science, v. 147, p. 633.

_____1967, Quaternary vegetational history of arctic Alaska, in Hopkins, D. M., ed., The Bering Land Bridge, Stanford University Press, California, p. 207-231.

Collins, N. J., 1976, The development of moss-peat banks in relation to changing climate and ice cover on Signey Island in the maritime Antarctic: British Antarctic Survey Bulletin, v. 43, p. 85-102.

Corbin, J. E., 1971, Aniganigurak (S-67): A final contact period Nunamiut Eskimo village in the Brooks Range, in Cook, J. P., ed., Final Report of the Archeological Survey and Excavations along the Alyeska Pipeline Service Company Pipeline Route: Department of Anthropology, University of Alaska, p. 272-296.

Coulter, H. W., Hopkins, D. M., Karlstrom, T. N. V., Péwé, T. L., Wahrhaftig, C., and Williams, J. R., 1965, Map showing extent of glaciations in Alaska: U. S. Geological Survey Miscellaneous Geological Investigations Map I-416, scale 1:2,500,000.

Crocker, R. L. and Major, J., 1955, Soil development in relation to vegetation and surface age at Glacier Bay, Alaska: Journal of Ecology, v. 43, p. 427-448.

Currey, D. R., 1969, Neoglaciation in southwestern United States (Ph.D. dissertation): University of Kansas, Lawrence.

Davis, J. C., 1973, Statistics and data analysis in geology: New York, John Wiley, 550 p.

Davis, P. T., 1980, Late Holocene glacial, vegetational, and climatic history of Pangirtunk and Kingnait fiord area, Baffin Island, N. W. T., Canada (Ph.D. dissertation): University of Colorado.

Denton, G. H. and Karlén, W., 1973a, Holocene climatic variations - their pattern and possible cause: Quaternary Research, v. 3, p. 155-205.

_____1973b, Lichenometry: its application to Holocene moraine studies in southern Alaska and Swedish Lapland: Arctic and Alpine Research, v. 5, p. 347-372.

_____1977, Holocene glacial and tree line variations in the White River Valley and Skolai Pass, Alaska and Yukon Territory: Quaternary Research, v. 7, p. 63-111.

Detterman, R. L., 1953, Sagavanirktok-Anaktuvuk region, northern Alaska, in Péwé, T. L. and others, Multiple glaciations in Alaska: U. S. Geological Survey Circular no. 289, p. 11-12.

_____1970, Early Holocene warm interval in northern Alaska: Arctic, v. 23, p. 130-132.

Detterman, R. L., Bowsher, A. L., and Dutro, J. T., Jr., 1958, Glaciation on the Arctic Slope of the Brooks Range, Alaska: Arctic, v. 11, p. 43-61.

Douglas, L. A. and Tedrow, J. C. F., 1960, Tundra soils of arctic Alaska: Transactions of the seventh International Congress of Soil Science, Madison, Wisconsin, v. 4, p. 291-304.

Ellis, J. M., 1978, Neoglaciation of the Atigun Pass area, east-central Brooks Range, Alaska (M. A. thesis): State University of New York at Buffalo, 113 p.

Ellis, J. M. and Calkin, P. E., 1979, Nature and distribution of glaciers, Neoglacial moraines, and rock glaciers, east-central Brooks Range, Alaska: Arctic and Alpine Research, v. 11, p. 403-420.

_____in press, Environments and soils of Holocene moraines and rock glaciers, central Brooks Range, Alaska, in Evenson, E. and Schlüchter, Ch., eds., Morainic Deposits in an Alpine Environment: Rotterdam, A.A. Balkema.

Ellis, J. M., Hamilton, T. D., and Calkin, P. E., 1981, Holocene glaciation of the Arrigetch Peaks, Brooks Range, Alaska: Arctic, v. 34, no. 2, p. 158-168.

Evans, I. S., 1969, The geomorphology and morphometry of glacial and nival areas, in Chorley, R. J., ed., Water, Earth, and Man: A Synthesis of Hydrology, Geomorphology, and Socioeconomic Geography: London, Methuen, p. 369-380.

_____1977, World-wide variations in the direction and concentration of cirque and glacier aspects: Geografiska Annaler, v. 59A, p. 151-175.

Everett, K. R., 1980, Distribution and variability of soils near Atkasook, Alaska: Arctic and Alpine Research, v. 12, p. 433-446.

Everett, K. R. and Parkinson, R. J., 1977, Soil and landform associations, Prudhoe Bay area, Alaska: Arctic and Alpine Research, v. 9, p. 1-19.

Everett, K. R., Vassiljevskay, V. D., Brown, J., and Walker, B. D., 1981, Tundra and analogous soils, in Bliss, L. C., Cragg, J. B., Heal, D. W., and Moore, J. J., eds., Tundra Ecosystems: A Comparative Analysis, International Biological Programme 25: Cambridge University, p. 139-179.

Fahl, C. B., 1973, Relationships between glaciers and climate in Alaska (Ph.D. dissertation): University of Alaska, 191 p.

_____1975, Mean sea level pressure patterns relating to glacier

activity in Alaska, in Weller, G. and Bowling, S. A., eds., Climate of the Arctic: Twenty-fourth Alaska Science Conference Proceedings, Fairbanks, Alaska, August, 1973: Fairbanks, Geophysical Institute, University of Alaska, p. 339-346.

Falconer, G., 1966, Preservation of vegetation and patterned ground under a thin ice body in northern Baffin Island, N. W. T.: Geographical Bulletin, v. 8, p. 194-200.

Ferrians, O. J., Jr., 1965, Permafrost map of Alaska: U. S. Geological Survey Miscellaneous Field Studies Map I-445, scale 1:2,500,000.

_____1971, Preliminary engineering maps of the proposed trans-Alaska pipeline route, Philip Smith Mountains quadrangle: U. S. Geological Survey Open File Map 492, scale 1:125,000.

Foster, H. L. and Holmes, G. W., 1965, A large transitional rock glacier in the Johnson River area, Alaska Range: U. S. Geological Survey Professional Paper 525-B, B112-B116.

Garfinkel, H. L. and Brubaker, L. B., 1980, Modern climate-tree growth relationships and climatic reconstruction in sub-arctic Alaska: Nature, v. 286, p. 872-874.

Gordon, J. E., 1981, Glacier margin fluctuations during the 19th and 20th centuries in the Ikamiut Kangerdluarssuat area, West Greenland: Arctic and Alpine Research, v. 13, p. 47-62.

Griffey, N. J. and Matthews, J. A., 1978, Major Neoglacial glacier expansion episodes in southern Norway: evidence from moraine ridge stratigraphy with ^{14}C dates on buried paleosols and moss layers: Geografiska Annaler, v. 60A, p. 73-90.

Gross, G., Kerschner, H., and Patzelt, G., 1976, Methodische Unter-

suchungen über die Schneegrense in Alpinen Gletschergebieten (Methodical investigations on the snowline in glacierized areas of the Alps): Zeitschrift für Gletscherkunde und Glazialgeologie, v. 12, p. 223-251.

Grove, J. M., 1979, The glacial history of the Holocene: Progress in Physical Geography, v. 3., p. 1-54.

Haerberli, W, King, L., and Flotron, W., 1979, Surface movement and lichen-cover studies at the active rock glacier near the Grubengletscher, Wallis, Swiss Alps: Arctic and Alpine Research, v. 11, p. 421-441.

Hale, M. E., 1954, Lichens from Baffin Island: American Midland Naturalist, v. 51, p. 232-264.

Hamilton, T. D., 1965a, Comparative photographs from northern Alaska: Journal of Glaciology, v. 5, p. 479-487.

_____1965b, Alaskan temperature fluctuations and trends: an analysis of recorded data: Arctic, v. 18, p. 105-117.

_____1966, Geomorphology and glacial history of the Alatna Valley, northern Alaska (Ph.D. dissertation): University of Washington, Seattle, 264 p.

_____1969, Glacial geology of the lower Alatna Valley, Brooks Range, Alaska: Geological Society of America Special Paper 123, INQUA Volume, p. 181-223.

_____1978a, Late Cenozoic stratigraphy of the south-central Brooks Range, in Johnson, K. M., ed., The U. S. Geological Survey in Alaska - Accomplishments during 1977: U. S. Geological Survey Circular, no. 772-B, B36-B38.

_____1978b, Surficial geology of the Chandalar quadrangle, Alaska: U. S. Geological Survey Miscellaneous Field Investigations Map MF-878-A, scale 1:250,000.

_____1978c, Surficial geology of the Philip Smith Mountains quadrangle, Alaska: U. S. Geological Survey Miscellaneous Field Investigations Map MF-879-A, scale 1:250,000.

_____1978d, Geologic perspectives on early man in Alaska (abstract): Fifth Biennial Meeting, American Quaternary Association, Edmonton, Canada, p. 123-125.

_____1979a, Quaternary stratigraphic sections with radiocarbon dates, Chandalar quadrangle, Alaska: U. S. Geological Survey Open File Report 79-751, 10 p.

_____1979b, Radiocarbon dates and Quaternary stratigraphic sections, Philip Smith Mountains quadrangle, Alaska: U. S. Geological Survey Open File Report 79-866, 43 p.

_____1979c, Surficial geologic map of the Chandler Lake quadrangle, Alaska: U. S. Geological Survey Miscellaneous Field Studies Map MF-1121, scale 1:250,000.

_____1979d, Surficial geologic map of the Wiseman quadrangle, Alaska: U. S. Geological Survey Miscellaneous Field Studies Map MF-1122, scale 1:250,000.

_____1980a, Quaternary stratigraphic sections with radiocarbon dates, Chandler Lake quadrangle, Alaska: U. S. Geological Survey Open File Report 80-790, 28 p.

_____1980b, Quaternary stratigraphic sections with radiocarbon dates, Wiseman quadrangle, Alaska: U. S. Geological Survey Open File Report 80-791, 53 p.

_____1980c, Episodic Holocene alluviation in the central Brooks Range - chronology, correlations, and climatic implications, in Albert, N. R. D. and Hudson, T., eds., The U. S. Geological Survey in Alaska - Accomplishments during 1979: U. S. Geological Survey Circular 823-B.

_____1980d, unpublished data, Surficial geologic map of the Survey Pass quadrangle, Alaska: U. S. Geological Survey Miscellaneous Field Studies Map MF- .

Hamilton, T. D. and Porter, S. C., 1975, Itkillik glaciation in the Brooks Range, northern Alaska: Quaternary Research, v. 5, p. 471-497.

Hartigan, J., 1977, Cluster analysis of variables/cluster analysis of cases, in Dixon, W. J., ed., Biomedical Computer Programs (BMDP), P-Series: University of California Press, p. 621-651.

Haugen, R. K. and Brown, J., 1978, Climatic and dendroclimatic indices in the discontinuous permafrost zone of the central Alaska uplands, in Proceedings of the Third International Conference on Permafrost: Edmonton, Alberta, National Research Council of Canada, p. 392-398.

Haugen, R. K., 1979, Climatic investigations along the Yukon River to Prudhoe Bay haul road, Alaska, 1975-1978. Informal extract from final Federal Highway Administration contract report environmental engineering investigations along the Yukon River-Prudhoe Bay haul road, Alaska: Hanover, New Hampshire, U. S. Army Cold Regions Research and Engineering Laboratory, 23 p.

Herd, D. G., 1974, Glacial and volcanic geology of the Ruiz-Tolima volcanic complex Cordillera Central, Columbia (Ph.D. disserta-

tion): University of Washington, Seattle.

Heuberger, H., 1968, Die Alpengletscher im Spät- und Postglazial: Eiszeitalter und Gegenwart, v. 19, p. 270-275.

_____1974, Alpine Quaternary environments, in Ives, J. D. and Barry, R. G., eds., Arctic and Alpine Environments: London, Methuen, p. 318-338.

Heusser, C. J., 1965, A Pleistocene phytogeographical sketch of the Pacific Northwest and Alaska, in Wright, H. E., Jr. and Frey, D. G., eds., The Quaternary of the United States, Princeton University Press, p. 469-483.

Hopkins, D. M., 1967, The Bering Land Bridge: Sanford University Press, California, p. 464-475.

_____1972, The paleogeography and climatic history of Beringia during late Cenozoic time: Inter-Nord, v. 12, p. 121-150.

Hyvarinen, H. and Ritchie, J. C., 1975, Pollen stratigraphy of Mackenzie Pingo sediments, N. W. T., Canada: Arctic and Alpine Research, v. 7, p. 261-272.

Jacobsen, G. L., Jr. and Birks, H. J. B., 1980, Soil development on recent end moraines of the Klutan Glacier, Yukon Territory, Canada: Quaternary Research, v. 14, p. 87-100.

Jochimsen, M., 1966, Ist die Grösse des Flechten thallus wirklich ein brauchbarer Massstab zür Datierung von glazialmorphologischen Relikten:Geografiska Annaler, v. 48A, p. 157-164 (Translated by W. Barr, 1973, as Does the size of lichen thalli really constitute a valid measure for dating relict glacial deposits?: Arctic and Alpine Research, v. 5, p. 417-424).

Johnson, P. G., 1978, Rock glacier types and their drainage systems, Grizzly Creek, Yukon Territory: Canadian Journal of Earth Sciences, v. 15, p. 1496-1507.

_____1980, Glacier-rock glacier transition in the southwest Yukon Territory, Canada: Arctic and Alpine Research, v. 12, p. 195-204.

Johnson, O. R. and Hartman, C. W., 1969, Environmental atlas of Alaska: Fairbanks, University of Alaska Institute of Water Resources, 111p.

Kachadoorian, R., 1971, Preliminary engineering geologic maps of the proposed trans-Alaska pipeline route, Wiseman and Chandalar quadrangles: U. S. Geological Survey Open File Map 486, scale 1:125,000.

Karlén, W., 1973, Holocene glacier and climatic variations, Kebnekaise Mountains, Swedish Lapland: Geografiska Annaler, v. 55A, p. 29-63.

_____1976, Lacustrine sediments and tree line variations as indications of Holocene climatic fluctuations in Lappland, northern Sweden: Geografiska Annaler, v. 58A, p. 1-33.

_____1979, Glacier variations in the Svartisen area, northern Norway: Geografiska Annaler, v. 61A, p. 11-28.

Karlstrom, T. N. V. and others, 1964, Surficial geology of Alaska: U. S. Geological Survey Miscellaneous Geologic Investigations Map I-357, scale 1:1,584,000.

Kind, N. V., 1967, Radiocarbon chronology in Siberia, in Hopkins, D. M., ed., The Bering Land Bridge: Stanford University Press, California, p. 172-192.

Klecka, W. R., 1975, Discriminant analysis, in Nie, N. H. and others, eds., Statistical Package for the Social Sciences (2nd edition): New York, McGraw-Hill, p. 434-467.

Koerner, R. M., 1980, The problem of lichen-free zones in arctic Canada: Arctic and Alpine Research, v. 12, p. 87-94.

Kondratyev, K. YA., ed., 1973, Radiation characteristics of the atmosphere and the earth's surface: New Dehli, Amerind Publishing Co. Pvt. Ltd., p. 269-311.

List, R. J., ed., 1951, Smithsonian Meteorological Tables (sixth revision): Smithsonian Miscellaneous Collections, v. 114, Publications 4014, p. 504-512.

Livingstone, D. A., 1955, Some pollen profiles from arctic Alaska: Ecology, v. 36, p. 587-600.

_____1957, Pollen analysis of a valley fill near Umiat, Alaska: American Journal of Science, v. 255, p. 254-260.

Locke, W. W., Andrews, J. T., and Webber, P. J., 1979, A manual for lichenometry: British Geomorphological Research Group, Technical Bulletin no. 26, 47 p.

Loomis, S. R., 1970, Morphology and ablation processes on glacier ice, in Bushnell, V. C. and Ragle, R. H., eds., Ice Field Ranges Research Project, v. 2: Arctic Institute of North America Research Paper 57, p. 1-65.

Lowden, J. A. and Blake, W., Jr., 1970, Geological Survey of Canada radiocarbon dates IX: Radiocarbon, v. 12, p. 46-86.

Luckman, B. H., 1977, Lichenometric dating of Holocene moraines at Mount Edith Cavell, Jasper, Alberta: Canadian Journal of Earth Sciences, v. 14, p. 1809-1822.

Luckman, B. H. and Crockett, K. J., 1978, Distribution and characteristics of rock glaciers in the southern part of Jasper National Park, Alberta: Canadian Journal of Earth Sciences, v. 15, p. 540-550.

MacKay, J. R. and Terasmae, J., 1963, Pollen diagrams in the Mackenzie Delta area, N. W. T.: Arctic, v. 16, p. 229-238.

Maddren, A. G., 1910, The Koyukuk-Chandalar gold region, in Brooks, A. H. and others, Mineral Resources of Alska: U. S. Geological Survey Bulletin 442, p. 284-315.

_____1913, The Koyukuk-Chandalar region, Alaska: U. S. Geological Survey Bulletin 532, 119 p.

Madole, R. F., 1972, Neoglacial facies in the Colorado Front Range: Arctic and Alpine Research, v. 4, p. 119-130.

Mahaney, W. C., 1974, Soil stratigraphy and genesis of Neoglacial deposits in the Arapaho and Henderson Cirques, central Colorado Front Range, in Mahaney, W. C., ed., Quaternary Environments - Proceedings of a Symposium: York University - Atkinson College (Toronto) Geographical Monograph, no. 5, p. 197-240.

Matthews, J. A., 1973, Lichen growth on an active medial moraine, Jotunheimer, Norway: Journal of Glaciology, v. 12, p. 305-313.

_____1974, Families of lichenometric dating curves from the Storbreen Gletschervorfeld, Jotunheimen, Norway: Norsk Geografisk Tidsskrift, v. 28, p. 215-235.

Matthews, J. V., 1970, Quaternary environmental history of interior Alaska: pollen samples from organic colluvium and peats: Arctic and Alpine Research, v. 2, p. 241-251.

_____1974a, Quaternary environments of Cape Deceit (Seward Peninsula, Alaska: evolution of a tundra ecosystem): Geological Society of America Bulletin, v. 85, p. 1353-1384.

_____1974b, Wisconsin environment of interior Alaska: pollen and macrofossil analysis of a 27 meter core from the Isabella Basin (Fairbanks, Alaska): Canadian Journal of Earth Sciences, v. 11, p. 828-841.

May, R. W., 1972, The application of linear discriminant analysis to investigation of tills, in Yatsu, E. and Falconer, A., eds., Research Methods in Pleistocene Geomorphology: Second Guelph Symposium on Geomorphology, 1971, University of Guelph, Canada, p. 135-147.

McCulloch, D. S., 1967, Quaternary geology of the Alaskan shore of the Chukchi Sea, in Hopkins, D. M., ed., The Bering Land Bridge, Stanford University Press, California, p. 91-120.

McCulloch, D. S. and Hopkins, D. M., 1966, Evidence for a warm interval 10,000 to 8,000 years ago in northwestern Alaska: Geological Society of America Bulletin, v. 77, p. 1089- 1108.

Meier, M. F. and Post, A. S., 1962, Recent variations in mass net budgets of glaciers in western North America: Commission of Snow and Ice Symposium of Obergurgl, 1962, International Association of Scientific Hydrology, Publication No. 58, p. 63-77.

Meier, M. F., Tangborn, W. V., Mayo, L. R., and Post, A. S., 1971, Combined ice and water balances of Gulkana and Wolverine glaciers, Alaska, and South Cascade Glacier, Washington, 1965 and 1967 hydrologic years: U. S. Geological Survey Professional Paper 715-A, 23 p.

Mercer, J. H., 1976, Glacial history of southernmost South America: Quaternary Research, v. 6, p. 125-166.

Miller, G. H., 1973a, Late Quaternary glacial and climatic history of northern Cumberland Peninsula, Baffin Island, N. W. T., Canada: Quaternary Research, v. 3, p. 561-583.

_____1973b, Variations in lichen growth from direct measurements: preliminary curves for Alectoria minuscula from eastern Baffin Island, N. W. T., Canada: Arctic and Alpine Research, v. 5, p. 333-339.

Miller, G. H. and Andrews, J. T., 1972, Quaternary history of northern Cumberland Peninsula, east Baffin Island, N. W. T., Canada. Part IV: preliminary lichen growth curve for Rhizocarpon geographicum: Geological Society of America Bulletin, v. 83, p. 1133-1138.

Miller, G. H., Bradley, R. S., and Andrews, J. T., 1975, The glaciation level and lowest equilibrium line altitude in the high Canadian Arctic: maps and climatic interpretation: Arctic and Alpine Research, v. 7, p. 155-168.

Morrison, R. B., 1967, Principles of Quaternary soil stratigraphy, in Morrison, R. B. and Wright, H. E., eds., Quaternary Soils, Proceedings of the Seventh Congress International Association for Quaternary Research, September, 1965, Volume 9: Desert Research Institute, University of Nevada, p. 1-70.

Nelson, S. W. and Grybeck, D., 1980, Geologic map of the Survey Pass quadrangle, Alaska: U. S. Geological Survey Miscellaneous Field Studies Map MF-1176-A, scale 1:250,000.

Nichols, H., 1972, Summary of the palynological evidence for late Quaternary vegetational and climatic change in the central and eastern Canadian Arctic, in Vsari, Y., Hyvärinen, H., and Hicks, S., eds., Climatic Changes in Arctic Areas during the Last Ten-Thousand Years: Finland, University of Oulu, p. 309-340.

Nye, J. F., 1965, The flow of a glacier in a channel of rectangular, elliptical, or parabolic cross-section: Journal of Glaciology, v. 5, p. 661-690.

Oeschger, H., 1975, Die C14 - Daterierung im Gletschervorfeld, in Messerli, B. and others, Die Schwankungen des Unteren Grindelwaldgletschers seit sem Mittelalter: Zeitschrift für Gletscherkunde und Glazialgeologie, v. 11, p. 61.

Orvig, S. and Mason, R. W., 1963, Ice temperatures and heat flux, McCall Glacier, Alaska: Commission of Snow and Ice, International Association of Scientific Hydrology, Publication No. 61, p. 181-188.

Orwin, J., 1970, Lichen succession on recently deposited rock surfaces: New Zealand Journal of Botany, v. 8, p. 452-477.

Osborn, G. and Taylor, J., 1975, Lichenometry of calcareous substrates in the Canadian Rockies: Quaternary Research, v. 6, p. 111-120.

Østrem, G., 1959, Ice melting under a thin layer of moraine and the existence of ice cores in moraine ridges: Geografiska Annaler, v. 41, p. 228-230.

_____1964, Ice cored moraines in Scandinavia: Geografiska Annaler, v. 46, p. 282-337.

_____1966, The height of the glaciation limit in southern British Columbia: Geografiska Annaler, v. 48A, p. 126-138.

_____1971, Rock glaciers and ice-cored moraines, a reply to D. Barsch: Geografiska Annaler, v. 53A, p. 207-213.

_____1974, Present alpine ice cover, in Ives, J. D. and Barry, R. G., eds., Arctic and Alpine Environments: London, Methuen, p. 246-247.

Outcalt, S. I. and Benedict, J. B., 1965, Photointerpretation of two types of rock glacier in the Colorado Front Range, U. S. A.: Journal of Glaciology, v. 5, p. 849-856.

Parks, J. M., 1966, Cluster analysis applied to multivariate geologic problems, in Cubitt, J. M. and Henley, S., eds., 1978, Statistical Analysis in Geology: Benchmark Papers in Geology, v. 37, Stroudsburg, Pennsylvania, Dowden, Hutchinson & Ross, p. 49-57.

Parkinson, R. J., 1978, Genesis and classification of Arctic coastal plain soils, Prudhoe Bay, Alaska: Institute of Polar Studies, Ohio State University, Report No. 68, 147 p.

Parrish, L. L., 1980, A record of Holocene climatic changes from St. George Island, Pribilof Islands, Alaska: Institute of Polar Studies Report No. 75, The Ohio State University, 45 p.

Paterson, W. S. B., 1975, The physics of glaciers: Oxford, Pergamon Press, 250 p.

Péwé, T. L., 1975, Quaternary geology of Alaska: U. S. Geological Survey Professional Paper 835, 145 p.

Porter, S. C., 1964, Late Pleistocene glacial chronology of north-central Brooks Range, Alaska: American Journal of Science, v. 262, p. 446-460.

_____1966, Pleistocene geology of Anaktuvuk Pass, central Brooks

Range, Alaska: Arctic Institute of North America Technical Paper 18, 100 p.

_____1970, Quaternary glacial record in Swat Kohistan, west Pakistan: Geological Society of America Bulletin, v. 81, p. 1421-1446.

_____1975, Equilibrium-line altitudes of late Quaternary glaciers in the southern Alps, New Zealand: Quaternary Research, v. 5, p. 27-47.

_____1981, Alpine rockfall hazards: American Scientist, v. 69, p. 67-75.

Porter, S. C. and Denton, G. H., 1967, Chronology of Neoglaciation in the North American Cordillera: American Journal of Science, v. 265, p. 177-210.

Ralph, E. K. and Michael, H. N., 1974, Twenty-five years of radiocarbon dating: American Scientist, v. 62, p. 553-560.

Rampton, V., 1970, Neoglacial fluctuations of the Nataxhat and Klutlan Glaciers, Yukon Territory, Canada: Canadian Journal of Earth Sciences, v. 7, p. 1236-1263.

_____1971, Late Quaternary vegetational and climatic history of the Snag Klutlan area, southwestern Yukon Territory, Canada: Geological Society of America Bulletin, v. 82, p. 959-978.

Reger, R. D. and Péwé, T. L., 1969, Lichenometric dating in the central Alaska Range, in Péwé, T. L., ed., The Periglacial Environment: Montreal, McGill-Queens University Press, p. 223-247.

Richmond, G. M., 1962, Quaternary stratigraphy of the La Sal Mountains, Utah: U. S. Geological Survey Professional Paper 324, 135 p.

Ritchie, J. C., 1972, Pollen analysis of late-Quaternary sediments from the Arctic tree line of the Mackenzie River Delta region, Northwest Territories, Canada, in Vasari, Y., Hyvärinen, H., and Hicks, S., eds., Climatic Changes in Arctic Areas during the Last Ten-Thousand Years: Finland, University of Oulu, p. 253-271.

Ritchie, J. C. and Hare, F. K., 1971, Late Quaternary vegetation and climate near the arctic tree line of northwestern North America: Quaternary Research, v. 1, p. 331-342.

Schweger, C. E., 1971, Late-Quaternary paleoecology of the Onion Portage region, northwesten Alaska: Geological Society of America Abstracts with Programs, v. 3, no. 6, p. 413.

Scott, W. E., 1974, Quaternary glacial and volcanic environments, Metolius River area, Oregon (Ph.D. dissertation), University of Washington.

Smith, P. S., 1912, Glaciation in northwesten Alaska: Geological Society of America Bulletin, v. 24, p. 563-570.

_____1913, The Noatak-Kobuk region, Alaska: U. S. Geological Survey Bulletin 536, 160 p.

Soil Survey Staff, 1975, Soil taxonomy, a basic system of soil classification for making and interpreting soil surveys: Soil Conservation Service, U. S. Department of Agriculture Handbook No. 436, 754 p.

Spetzman, L. A., 1959, Vegetation of the Arctic Slope of Alaska: U. S. Geological Survey Professional Paper 302-B, 58 p.

Sugden, D. E. and John, B. S., 1976, Glaciers and landscape - a geomorphological approach: New York, John Wiley, 376 p.

Tangborn, W. V., Mayo, L. R., Scully, D. R., and Krimmel, R. M., 1977, Combined ice and water balances of Maclure Glacier, California, South Cascade Glacier, Washington, and Wolverine and Gulkana Glaciers, Alaska, 1967 hydrologic year: U. S. Geological Survey Professional Paper 715-B, 20 p.

Tedrow, J. C. F., 1972, Soil morphology as an indicator of climatic changes in the arctic areas, in Vasari, Y., Hyvärinen, H., and Hicks, S., eds., Climatic Changes in Arctic Areas during the Last Ten-Thousand Years: University of Oulu, Finland, p. 61-74.

Tedrow, J. C. F. and Brown, J., 1962, Soils of the Brooks Range, northern Alaska. 1. weakening of soil forming potential at high arctic altitudes: Soil Science, v. 93, p. 254-261.

Tedrow, J. C. F. and Walton, G. F., 1964, Some Quaternary events of northern Alaska: Arctic, v. 17, p. 268-271.

Till, R., 1974, Statistical methods for the earth scientist: New York, John Wiley, p. 83-103.

Thompson, H. R., 1957, The old moraines of Pangnirtung Pass, Baffin Island: Journal of Glaciology, v. 3, p. 42-49.

Thomson, J. W., 1967, Notes on Rhizocarpon in the arctic: Nova Hedwigia, v. 14, p. 421-481.

Thorson, R. M. and Hamilton, T. D., 1977, Geology of the Dry Creek site; a stratified early man site in interior Alaska: Quaternary Research, v. 7, p. 149-176.

Trabant, D., Harrison, W. D., and Benson, C., 1975, Thermal regime of McCall Glacier, Brooks Range, northern Alaska, in Weller, G. and Bowling, S. A., eds., Climate of the Arctic: Twenty-fourth Alaska Science Conference Proceedings, Fairbanks, Alaska, August

1973: Geophysical Institute, University of Alaska, p. 347-349.

Ugolini, F. C., 1968, Soil development and alder invasion in a recently deglaciated area of Glacier Bay, Alaska, in Trappe, G. M. and others, eds., Biology of Alders: U. S. Forest Service, Pacific NW Forest and Range Experiment Station, Portland, Oregon, p. 115-140.

Ugolini, F. C. and Tedrow, J. C. F., 1963, Soils of the Brooks Range, Alaska. 3. Rendzina of the Arctic: Soil Science, v. 96, p. 121-127.

U. S. Geological Survey, 1978, unpublished data, Brooks Range glacier inventory: scale 1:250,000. Available from: World Data Center - A for Glaciology (Snow and Ice), Institute of Arctic and Alpine Research, University of Colorado.

U. S. Weather Bureau, 1915-1979, Climatological data, Alaska; annual summaries: Washington, D. C., U. S. Department of Commerce, Weather Bureau, v. 1-65, p. 13.

Vernon, P. and Hughes, O. L., 1966, Surficial geology of Dawson, Larsen Creek, and Nash Creek map-area, Yukon Territory: Geological Survey of Canada Bulletin, v. 46, p. 216-231.

Wahrhaftig, C. and Cox, A., 1959, Rock glaciers in the Alaska Range: Geological Society of America Bulletin, v. 70, p. 383-436.

Walker, D. A., Short, S. K., Andrews, J. T., and Webber, P. J., 1981, Late Holocene and present-day vegetation, Prudhoe Bay and Atigun River, Alaskan Arctic Slope: Arctic and Alpine Research, v. 13, p. 153-172.

Webber, P. J. and Andrews, J. T., 1973, Lichenometry: a commentary: Arctic and Alpine Research, v. 5, p. 295-302.

Weertman, J., 1971, Shear stress at the base of a rigidly rotating cirque glacier: Journal of Glaciology, v. 10, p. 31-38.

Wendler, G., 1969, Characteristics of the glaciation of the Brooks Range, Alaska: Archiv für Meteorologie, Geophysik und Bioklimatologie, Serie B, v. 17, p. 85-92.

Wendler, G. and Ishikawa, N., 1974, The effect of slope, exposure, and mountain screening on the solar radiation of McCall Glacier, Alaska: A contribution to International Hydrological Decade: Journal of Glaciology, v. 13, no. 68, p. 213-225.

Wendler, G. and Weller, G. 1974, A heat-balance study of McCall Glacier, Brooks Range, Alaska: A contribution to International Hydrological Decade: Journal of Glaciology, v. 13, no. 67, p. 13-25.

Wendler, G., Benson, C., Fahl, C., Ishikawa, N., Trabant, C., and Weller, G., 1975, Glacio-meteorological studies on McCall Glacier, in Weller, G. and Bowling, S. A., eds., Climate of the Arctic: Twenty-fourth Alaska Science Conference Proceedings, Fairbanks, Alaska, August 1973: Geophysical Institute, University of Alaska, p. 334-338.

Whalley, B. 1974, Rock glaciers and their formation: as part of a glacier debris-transport system: University of Reading, Department of Geography, Geographical Papers, no. 24, 60 p.

White, S. E., 1976, Rock glaciers and block fields, review and new data: Quaternary Research, v. 6, p. 77-97.

_____1981, Alpine mass movement forms (noncatastrophic): classification, description, and significance: Arctic and Alpine Research, v. 13, p.127- 137.

Worsley, P. 1973, An evaluation of the attempt to date the recession of Tundsbergdalsbreen, southern Norway, by lichenometry: Geografiska Annaler, v. 54A, p. 137-141.

Zubok, O. M., 1975, Half decade study of mass balance at Sentinel Glacier, B. C., Canada: Snow and Ice Symposium, Proceedings of the Moscow Symposium, August, 1971, IAHS - AISH Publication No. 104, p. 202-207.

APPENDIX A. GLACIER INVENTORY

Unofficial Name	Type of Deposit [a]	Lat/Long	U. S. Geological Survey Designation [b]	This Study's Designation [c]
Atigun Pass area, east-central Brooks Range (Fig. 2)				
Buffalo	M	68 08'N/149 49'W	1111526	1
Marmot	M/Mg	68 07'N/149 46'W	1111525	2
Grizzly	M/Mg	68 07'N/149 26'W	-	3
Coyote	M/Mg	68 10'N/149 36'W	1111522	4
Caribou	M/Mg	68 17'N/149 05'W	1111504	5
Raptor	M	68 17'N/149 13'W	1111508	6
Golden Eagle	M/Mg	68 18'N/149 11'W	1111507	7
Robin	M/Mg	68 20'N/149 12'W	1111502	8
Lemming	M	68 20'N/149 49'W	1120110	9
Triple West	M	68 20'N/149 48'W	1120110	10
Triple Mid	M	68 20'N/149 47'W	1120110	11
Triple East	M	68 20'N/149 46'W	1120110	12
Dall Sheep	Mg	68 09'N/149 50'W	1111527	13
Snow Bunting	Mg	68 10'N/149 46'W	1111528	14
Fox	Mg	68 11'N/149 38'W	1111523	15
Ram	Mg	68 12'N/149 33'W	1111519	16
Ewe	Mg	68 12'N/149 35'W	1111520	17
Kid	Mg	68 12'N/a49 36'W	-	18
Vole	Mg	68 12'N/149 37'W	1111521	19
Sparrow	Mg	68 12'N/149 29'W	-	20
Raven	Mg	68 13'N/149 31'W	-	21

APPENDIX A. (continued)

Yellowjacket	Mg	68 13'N/149 17'W	1111514	22
Burbot	Mg	68 15'N/149 44'W	1120118	23
Arctic Char	Mg	68 15'N/149 41'W	1120116	24
Grayling	Mg	68 17'N/149 44'W	1120113	25
Cisco	Mg	68 17'N/149 35'W	1120105	26
Moose	Mg	68 17'N/149 12'W	1111509	27
Musk-Ox	Mg/M	68 17'N/149 08'W	1111505	28
Arctic Tern	Mg	68 20'N/149 34'W	1120101	29
Snowy Owl West	Mg	68 21'N/149 05'W	1111496	30
Wolf	MG	68 09'N/149 23'W	-	31
Lake Trout	MG	68 15'N/149 43'W	1120117	32
Twin	MG	68 21'N/149 32'W	1111534	33
Snowy Owl East	MG	68 21'N/149 04'W	1111496	34
Harlequin Duck	TRGC	68 08'N/149 53'W	1120124	35
Ptarmigan	TRGC	68 07'N/149 44'W	1111524	36
Pika	TRGC	68 07'N/149 28'W	1111516	37
Jaeger	TRGC	68 07'N/149 26'W	-	38
Parka Squirrel	TRGC	68 13'N/149 30'W	1111517	39
Mosquito	TRGC	68 12'N/149 21'W	1111515	40
Wolverine	TRGC	68 20'N/149 30'W	1111533	41

Anaktuvuk Pass area, central Brooks Range (Fig. 3)

In-A	C	68 03'N/151 50'W	-	42
In-B	C	68 02'N/151 49'W	-	43
In-C	TRG	68 02'N/151 40'W	-	44

APPENDIX A. (continued)

In-D	C	68 03'N/151 39'W	-	45
It-A	LRG	68 13'N/151 09'W	1120403	46
It-B	LRG	68 13'N/151 08'W	1120402	47
It-C	MG	68 13'N/151 06'W	1120401	48

The Arrigetch Peaks, west-central Brooks Range (Fig. 4)

Arr-5	M/Mg	67 24'N/154 09'W	1250107	49
Arr-9 East	M	67 23'N/154 06'W	1250104	50
Arr-10 West	M	67 23'N/154 05'W	1250103	51
Arr-9 West	MG	67 23'N/154 06'W	1250104	52
Arr-10 East	MG	67 23'N/154 05'W	1250103	53
Arr-1	MG	67 25'N/154 13'W	1250110	54
Arr-2,-3,-4	MG	67 24'N/154 12'W	1250109	55
Arr-4 East	MG	67 24'N/154 10'W	1250108	56
Arr-6	MG	67 24'N/154 08'W	1250106	57
Arr-11	MG	67 23'N/154 03'W	1250102	58
Arr-7	TRGC	67 24'N/154 06'W	1250105	59

[a] See Table 2 where M = moraine without an ice core; Mg = ice-cored moraine; MG = glacier-cored moraine; TRGC = transition zone of a glacier-cored, tongue-shaped rock glacier; TRG = tongue-shaped rock glacier without an exposed glacier core; LRG = lobate rock glacier; and C = empty cirque of late Pleistocene age.

[b] See U. S. Geological Survey, 1978, unpublished data (scale 1:250,000).

[c] See Figs. 2, 3, and 4 for locations.

APPENDIX B. PHYSICAL ANALYSIS OF CIRQUE GLACIERS AND THEIR DEPOSITS

The analyses include area-altitude distributions, horizon plots (Appendix F), present-day topography from U. S. Geological Survey topographic sheets (contours in ft) and field mapping, and reconstructions of ice masses based on lichenometry and surficial geologic mapping (Appendix C). The steady-state ELA for the Neoglacial maxima was determined using an assumed accumulation area to ablation area ratio of 2:1. Locations for photographic panoramas (Appendix D) are shown on the present topography map by an encircled dot. Separation of continuous ice masses that flow downslope into different debris lobes, especially horseshoe-shaped glaciers, was accomplished by dividing the headward portion of the glacier along a flowline that was perpendicular to the contours. Cirque glaciers 50 and 52 are shown together (Arr-9) and cirque glaciers 51 and 53 (Arr-10) are also depicted on one diagram.

APPENDIX B. (continued)

Legend for Cirque Glaciers at Present and Neoglacial Maximum

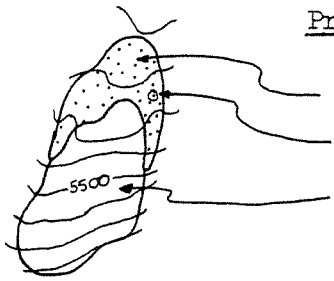

Present ice surface with deposit (contours in ft)

Deposit

Site of photographic panorama (Appendix D)

Cirque glacier

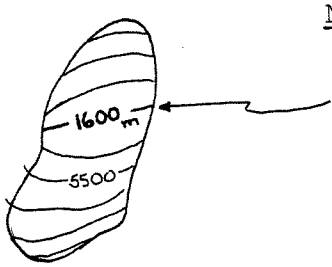

Neoglacial maximum surface

ELA shown in meters; other contours in ft

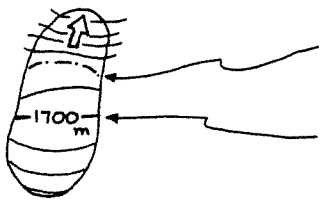

Cascading Neoglacial maximum surface

Downslope limit of Neoglacial area/altitude used in reconstructions

ELA (in meters) during Neoglacial maximums

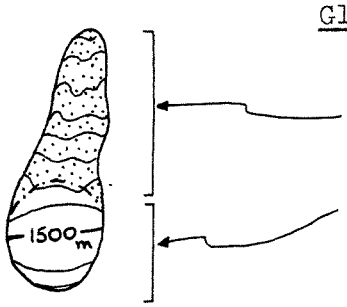

Glacier-cored rock glacier deposit

Undisturbed, early Holocene rock glacier tongue

Area disturbed during Neoglacial expansions including transition zone (TRGC)

APPENDIX B. PHYSICAL INVENTORY (Buffalo Glacier, no. 1)

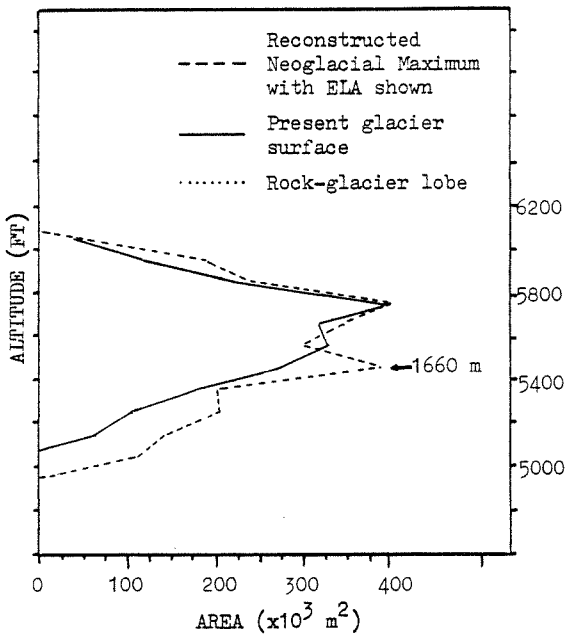

NEOGLACIAL MAXIMUM AND PRESENT AREA-ALTITUDE DISTRIBUTIONS

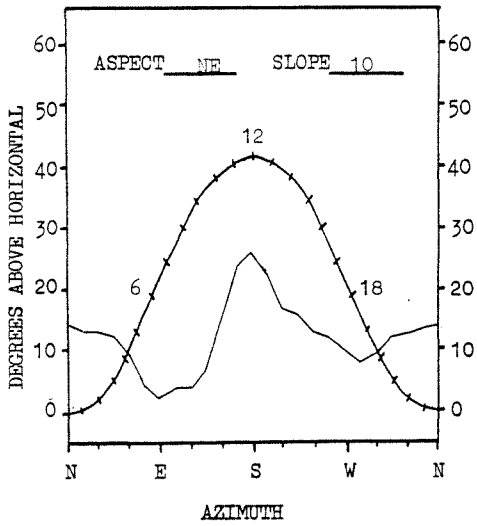

LANDFORM HORIZON (S- 101a) WITH +20° SOLAR DECLINATION

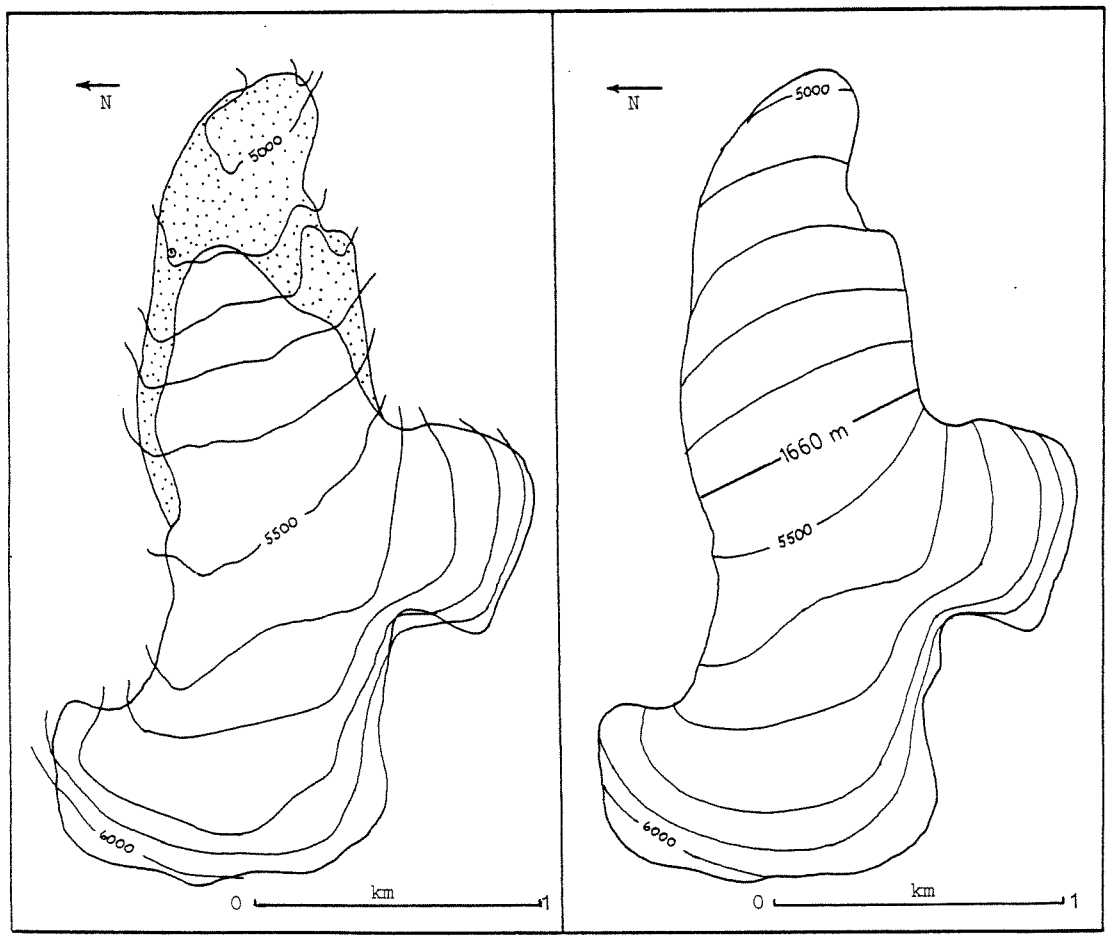

PRESENT ICE SURFACE WITH DEPOSIT

NEOGLACIAL MAXIMUM SURFACE

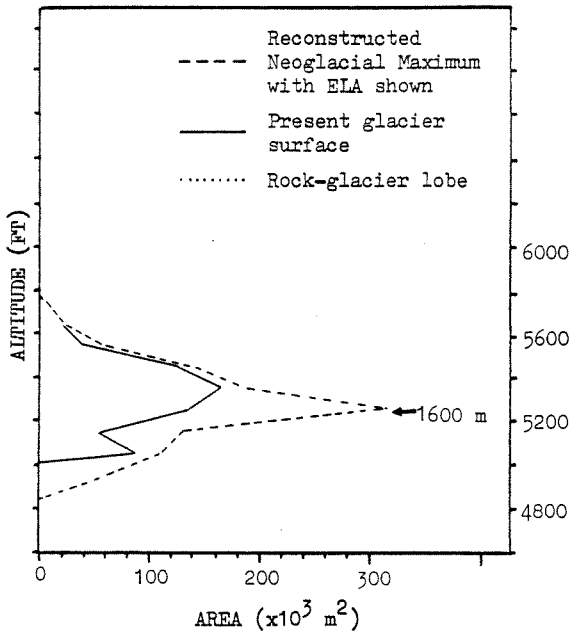

NEOGLACIAL MAXIMUM AND PRESENT AREA-ALTITUDE DISTRIBUTIONS

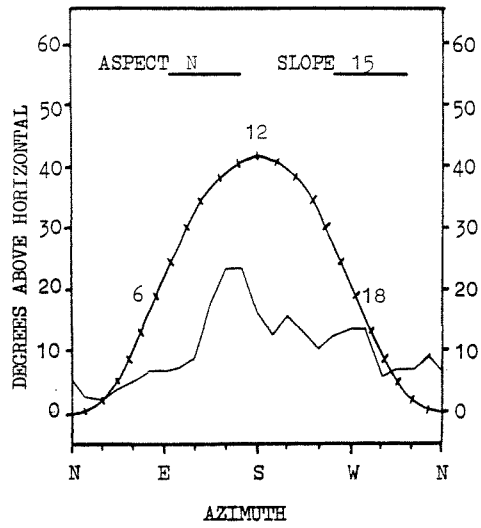

LANDFORM HORIZON (S-102a) WITH +20° SOLAR DECLINATION

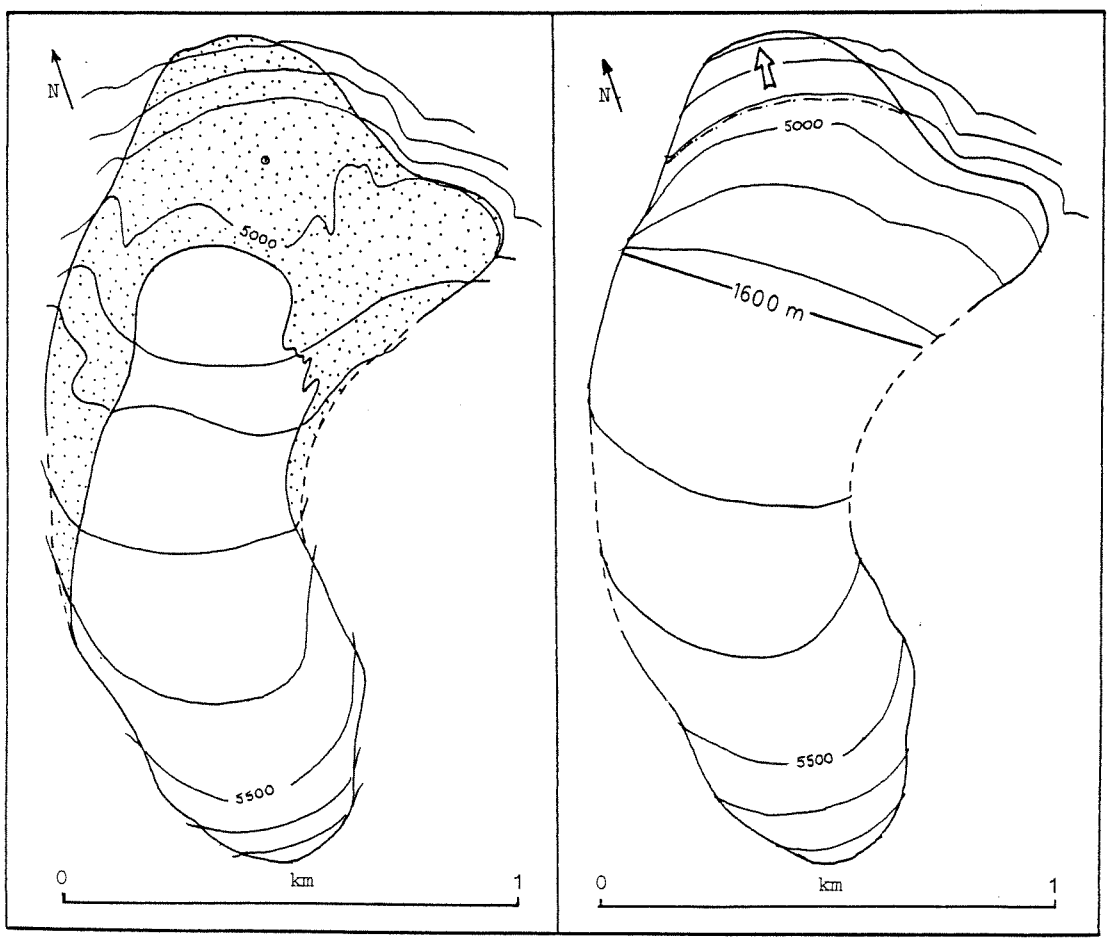

PRESENT ICE SURFACE WITH DEPOSIT

NEOGLACIAL MAXIMUM SURFACE

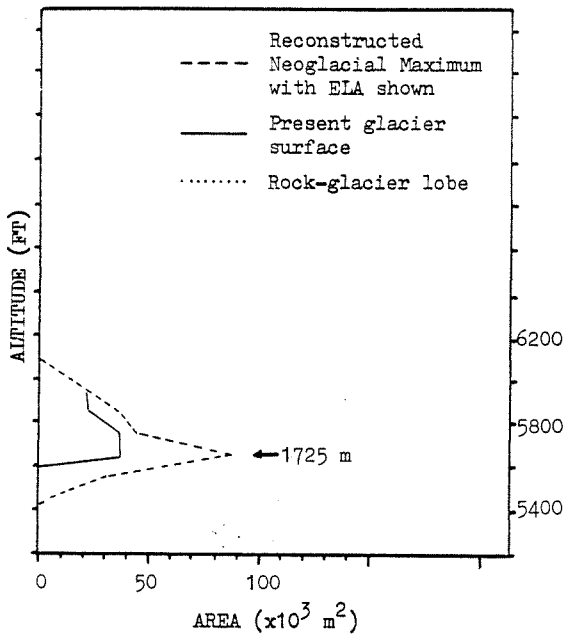

NEOGLACIAL MAXIMUM AND PRESENT AREA-ALTITUDE DISTRIBUTIONS

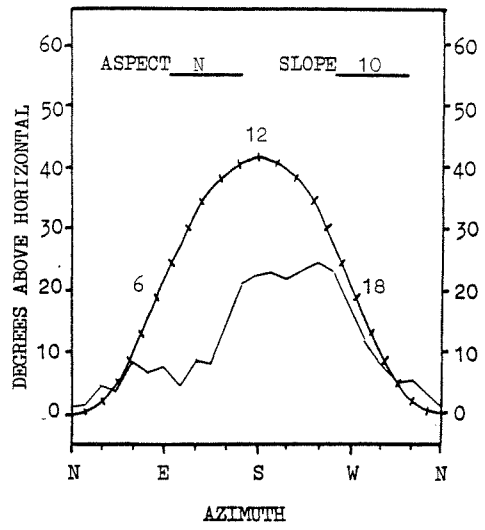

LANDFORM HORIZON (S- 003b) WITH +20° SOLAR DECLINATION

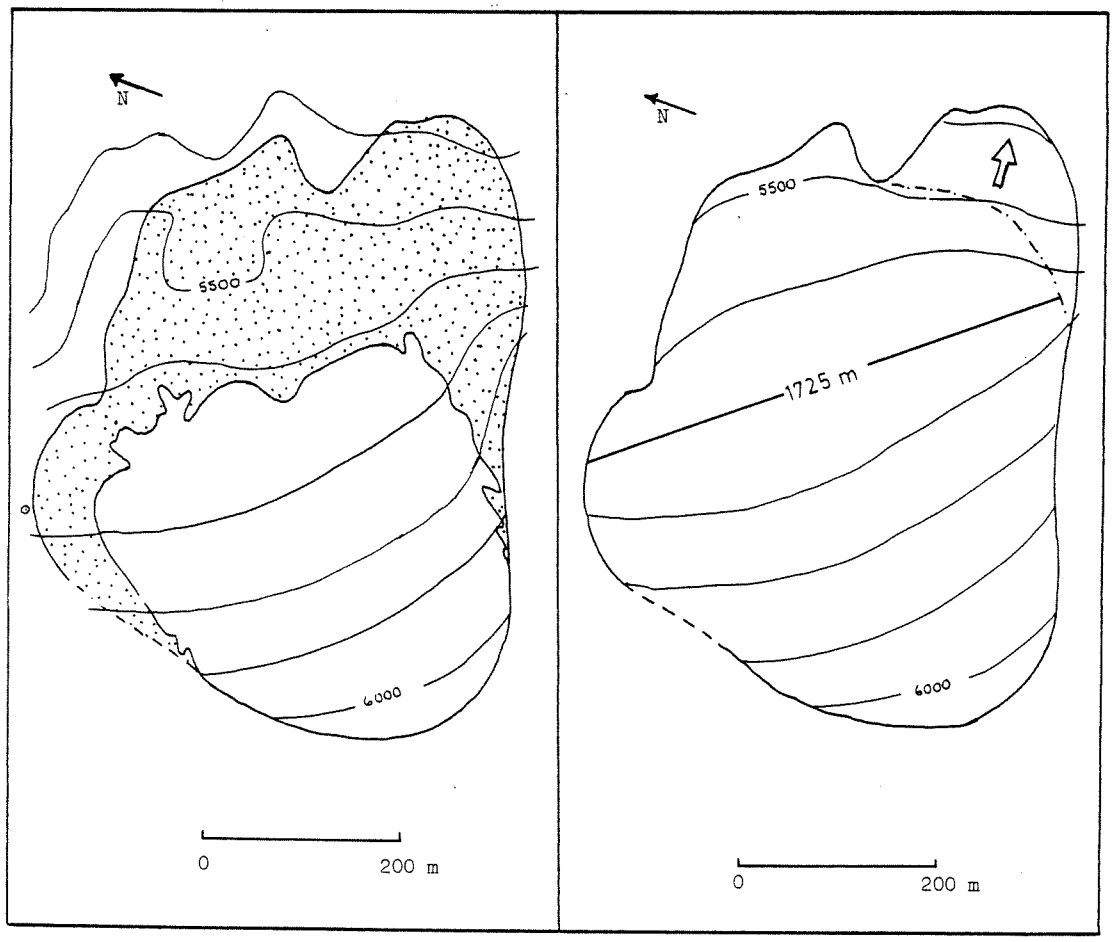

PRESENT ICE SURFACE WITH DEPOSIT

NEOGLACIAL MAXIMUM SURFACE

APPENDIX B. PHYSICAL INVENTORY (Coyote Glacier, no. 4)

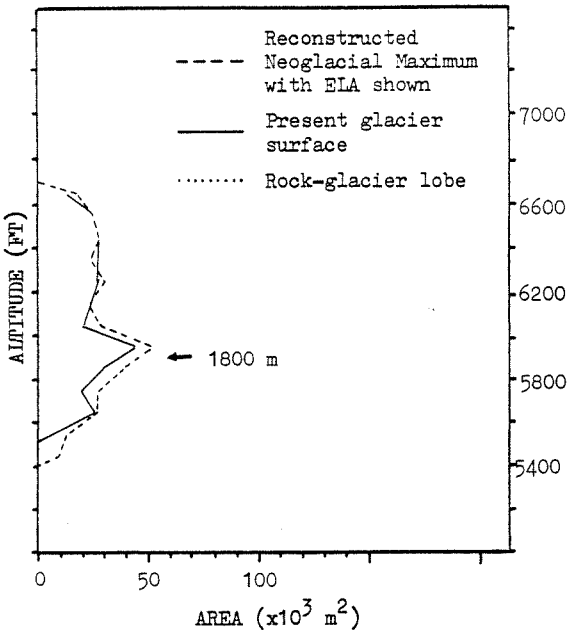

NEOGLACIAL MAXIMUM AND PRESENT AREA-ALTITUDE DISTRIBUTIONS

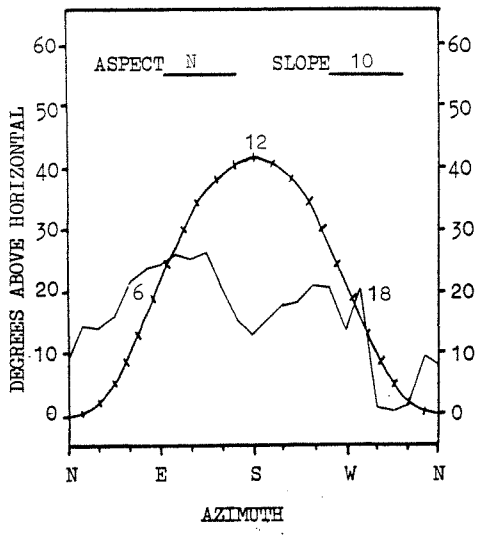

LANDFORM HORIZON (S- 104)
WITH +20° SOLAR DECLINATION

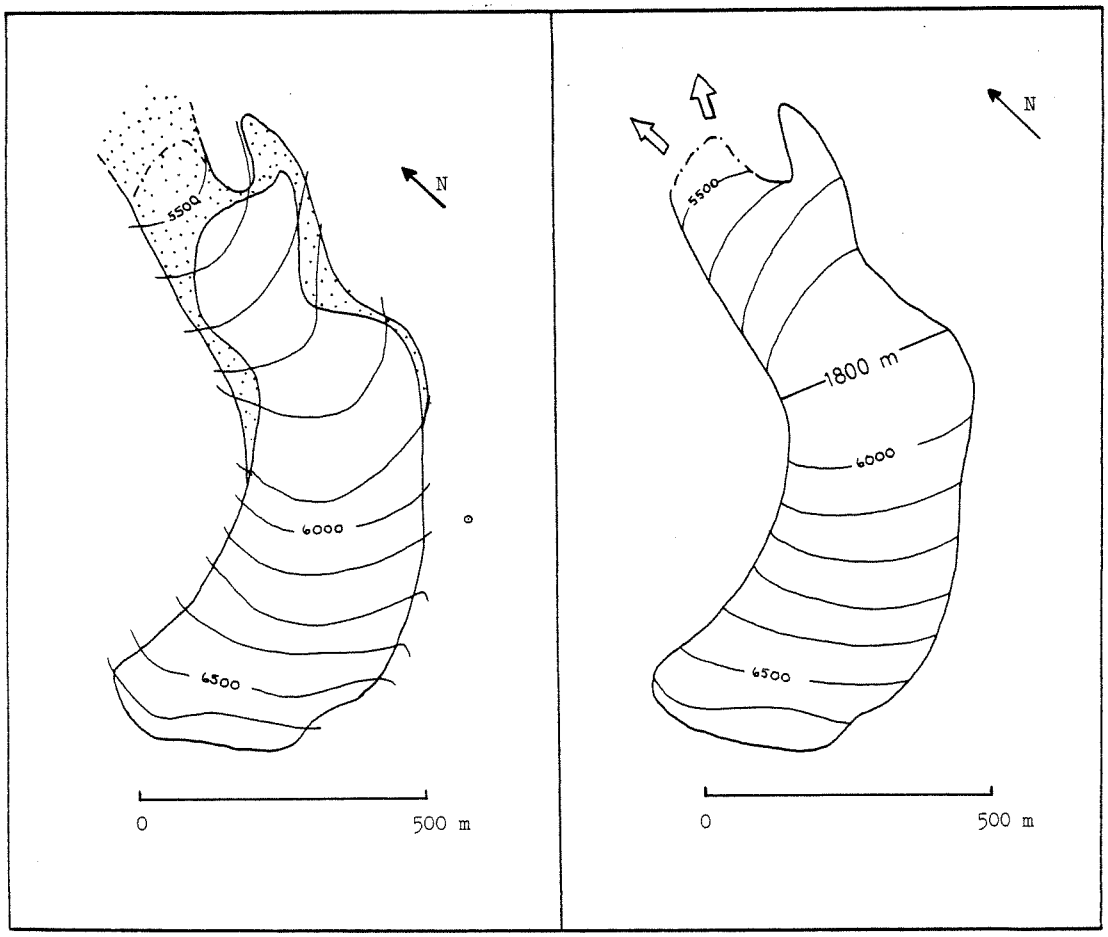

PRESENT ICE SURFACE WITH DEPOSIT

NEOGLACIAL MAXIMUM SURFACE

APPENDIX B. PHYSICAL INVENTORY (Caribou Glacier, no. 5)

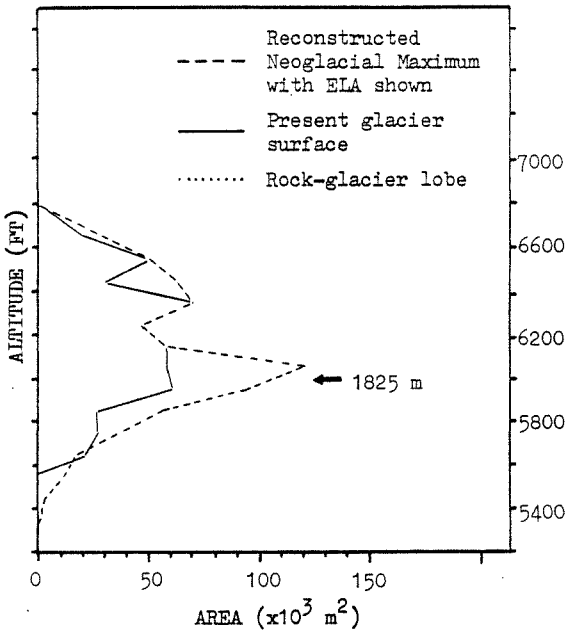

NEOGLACIAL MAXIMUM AND PRESENT AREA-ALTITUDE DISTRIBUTIONS

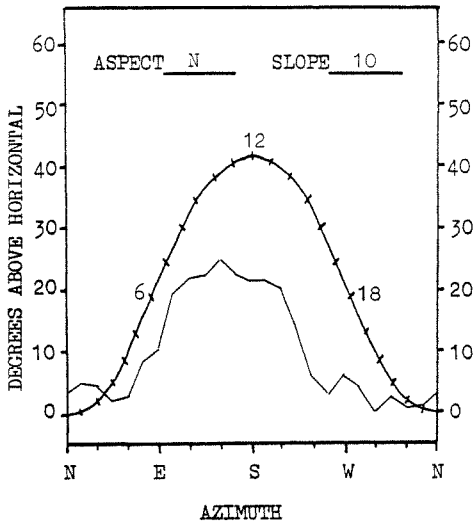

LANDFORM HORIZON (S- 105)
WITH +20° SOLAR DECLINATION

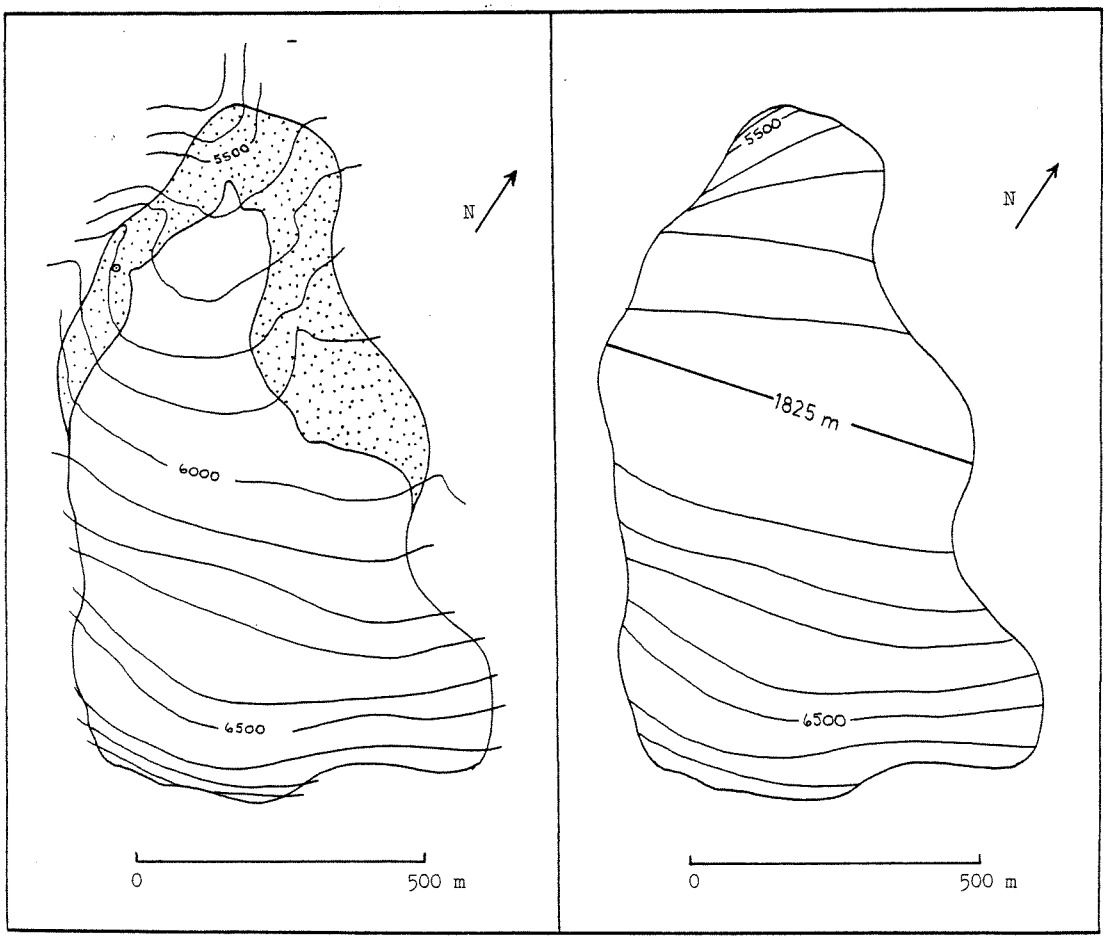

PRESENT ICE SURFACE WITH DEPOSIT

NEOGLACIAL MAXIMUM SURFACE

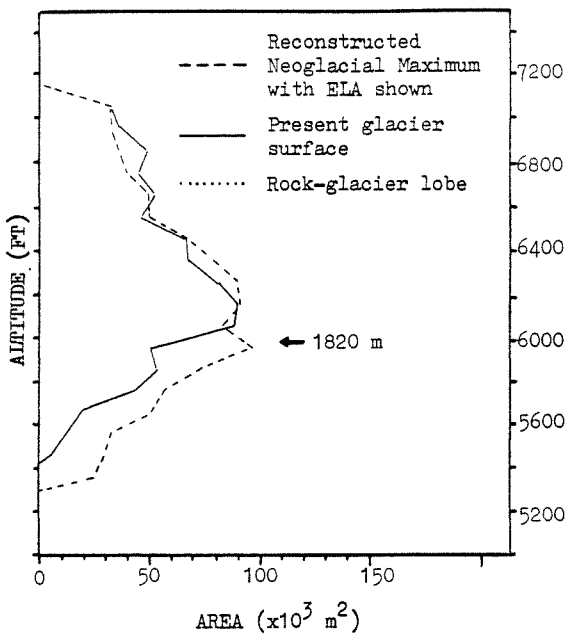

NEOGLACIAL MAXIMUM AND PRESENT AREA-ALTITUDE DISTRIBUTIONS

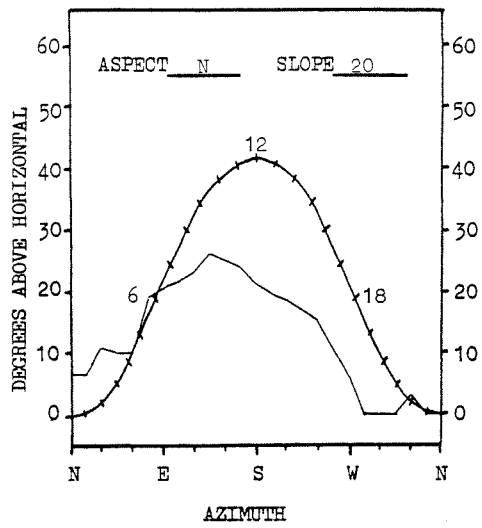

LANDFORM HORIZON (S-106) WITH +20° SOLAR DECLINATION

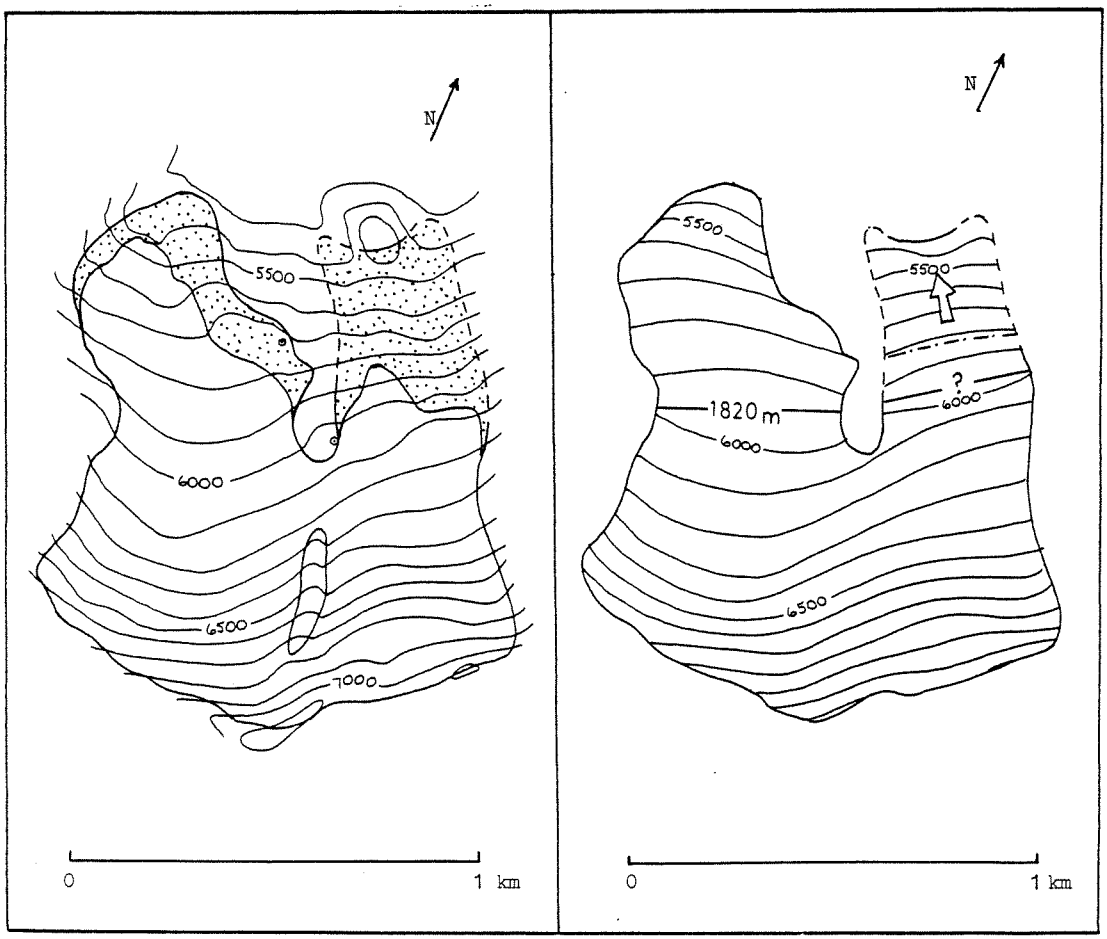

PRESENT ICE SURFACE WITH DEPOSIT

NEOGLACIAL MAXIMUM SURFACE

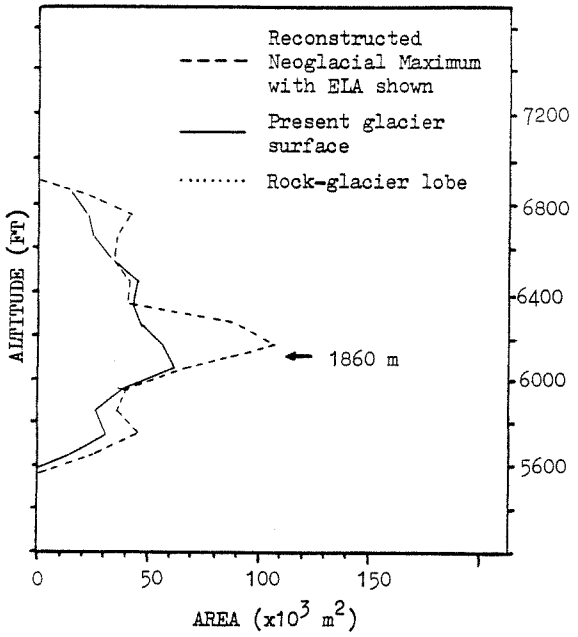

NEOGLACIAL MAXIMUM AND PRESENT
AREA-ALTITUDE DISTRIBUTIONS

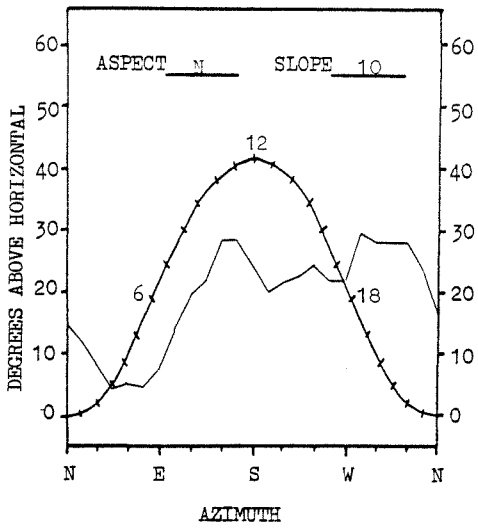

LANDFORM HORIZON (S- 107)
WITH +20° SOLAR DECLINATION

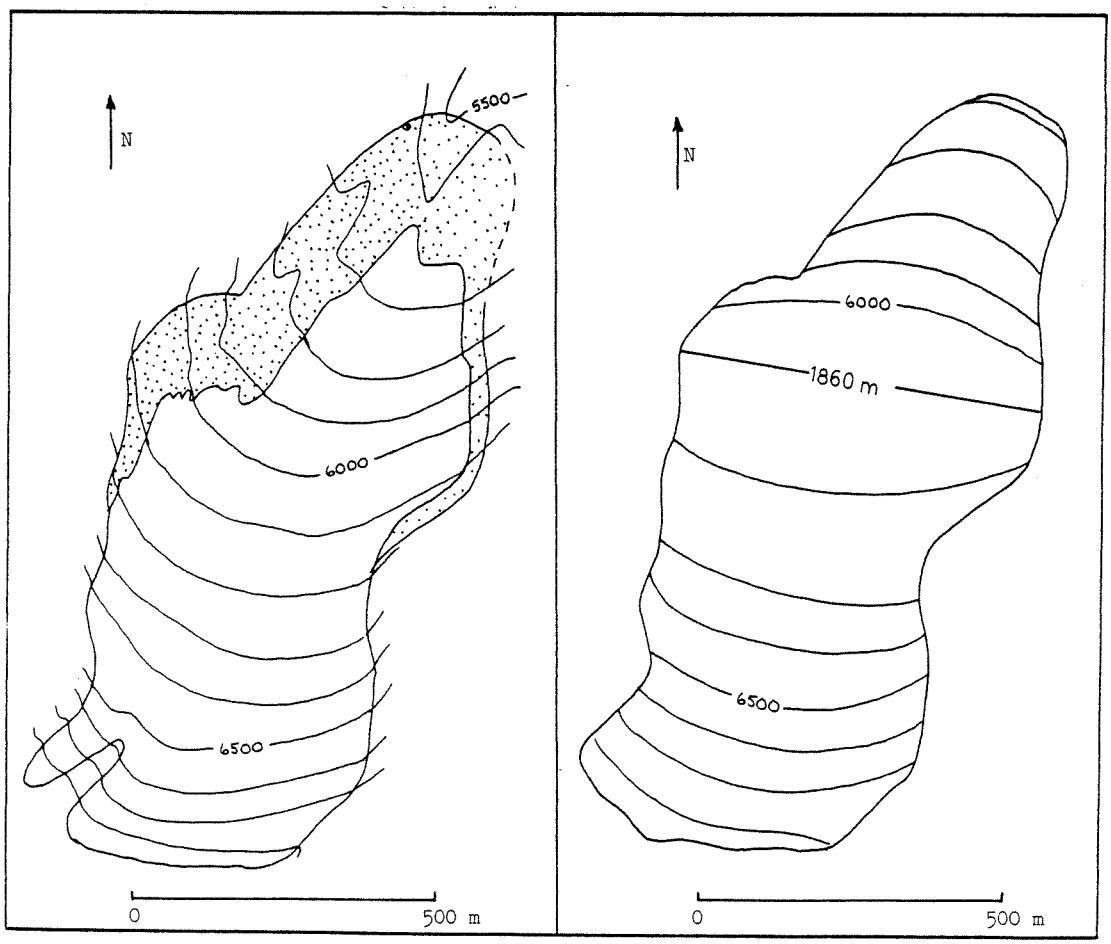

PRESENT ICE SURFACE WITH DEPOSIT

NEOGLACIAL MAXIMUM SURFACE

APPENDIX B. PHYSICAL INVENTORY (Robin Glacier, no. 8)

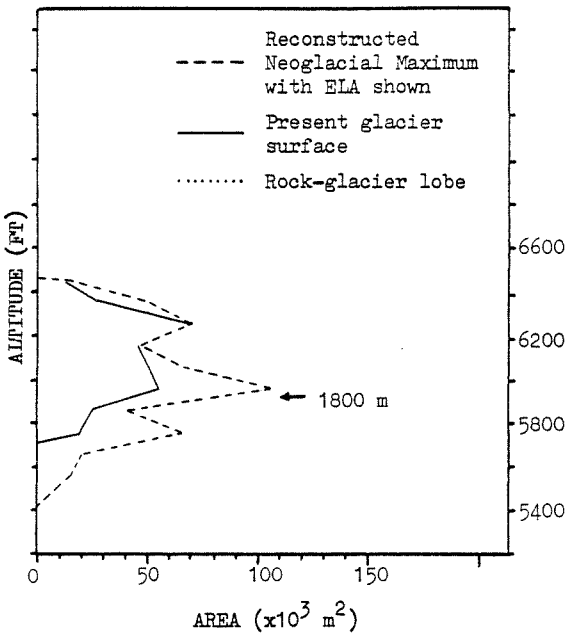

NEOGLACIAL MAXIMUM AND PRESENT AREA-ALTITUDE DISTRIBUTIONS

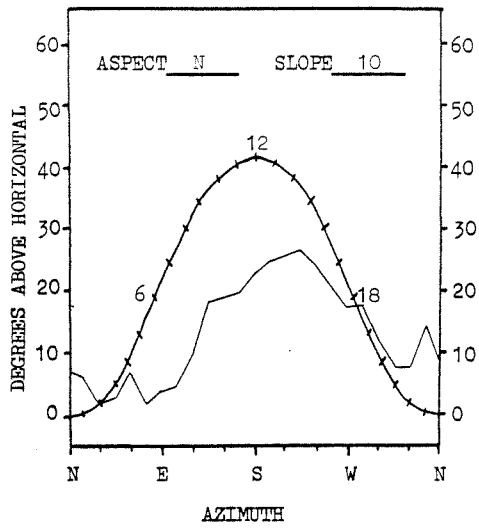

LANDFORM HORIZON (S- 108)
WITH +20° SOLAR DECLINATION

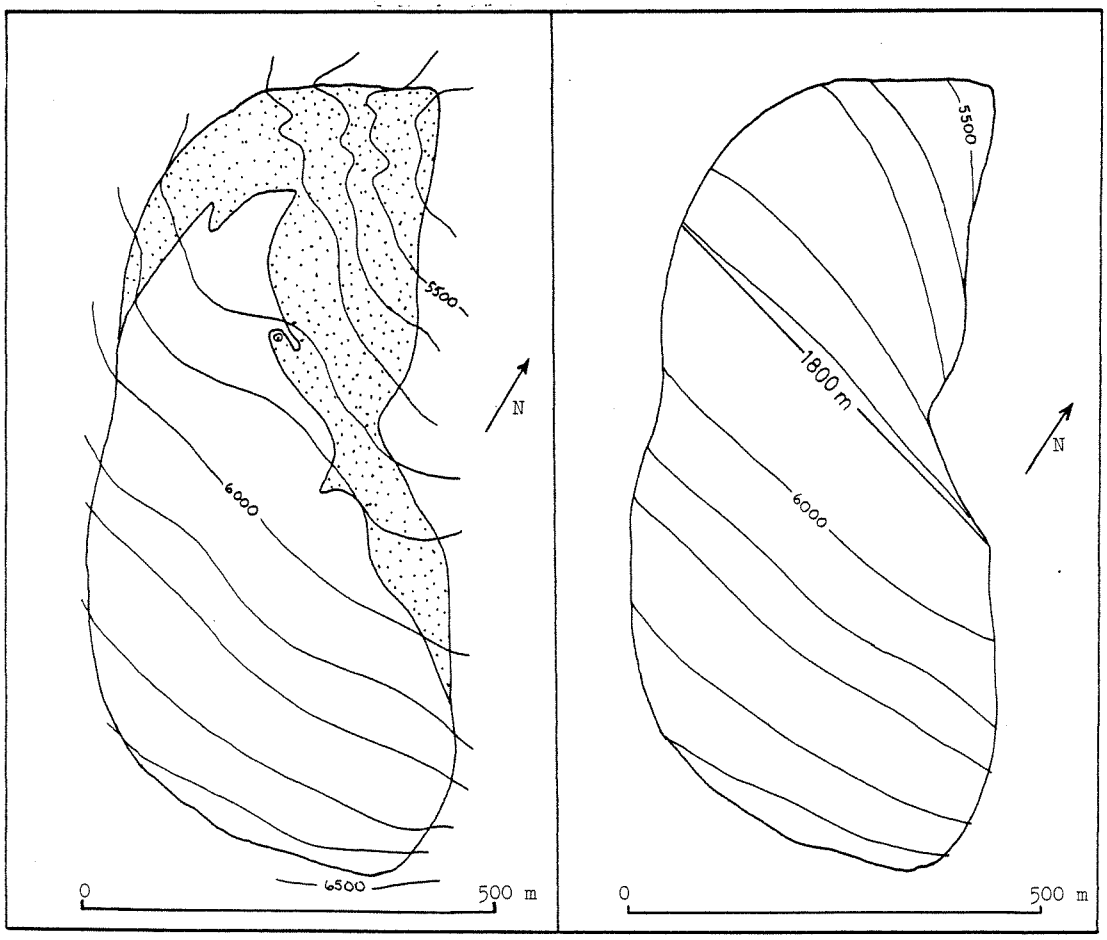

PRESENT ICE SURFACE WITH DEPOSIT

NEOGLACIAL MAXIMUM SURFACE

APPENDIX B. PHYSICAL INVENTORY (Lemming Glacier, no. 9)

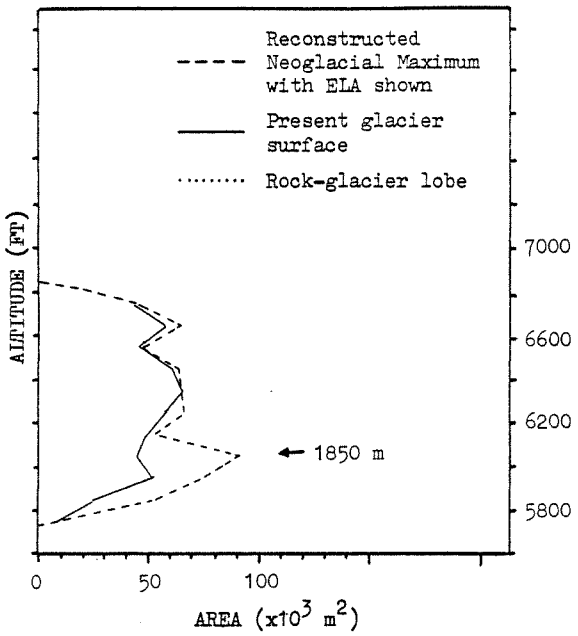

NEOGLACIAL MAXIMUM AND PRESENT AREA-ALTITUDE DISTRIBUTIONS

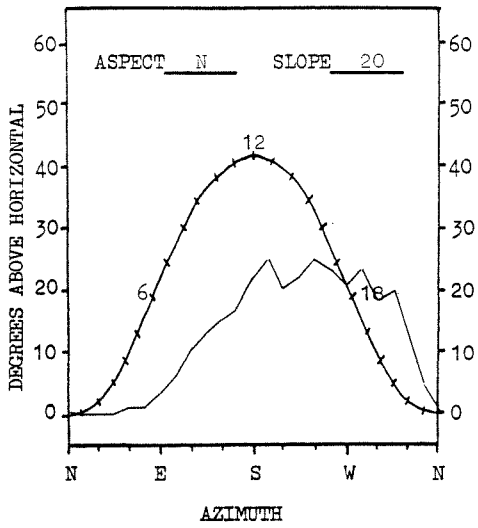

LANDFORM HORIZON (S- 109)
WITH +20° SOLAR DECLINATION

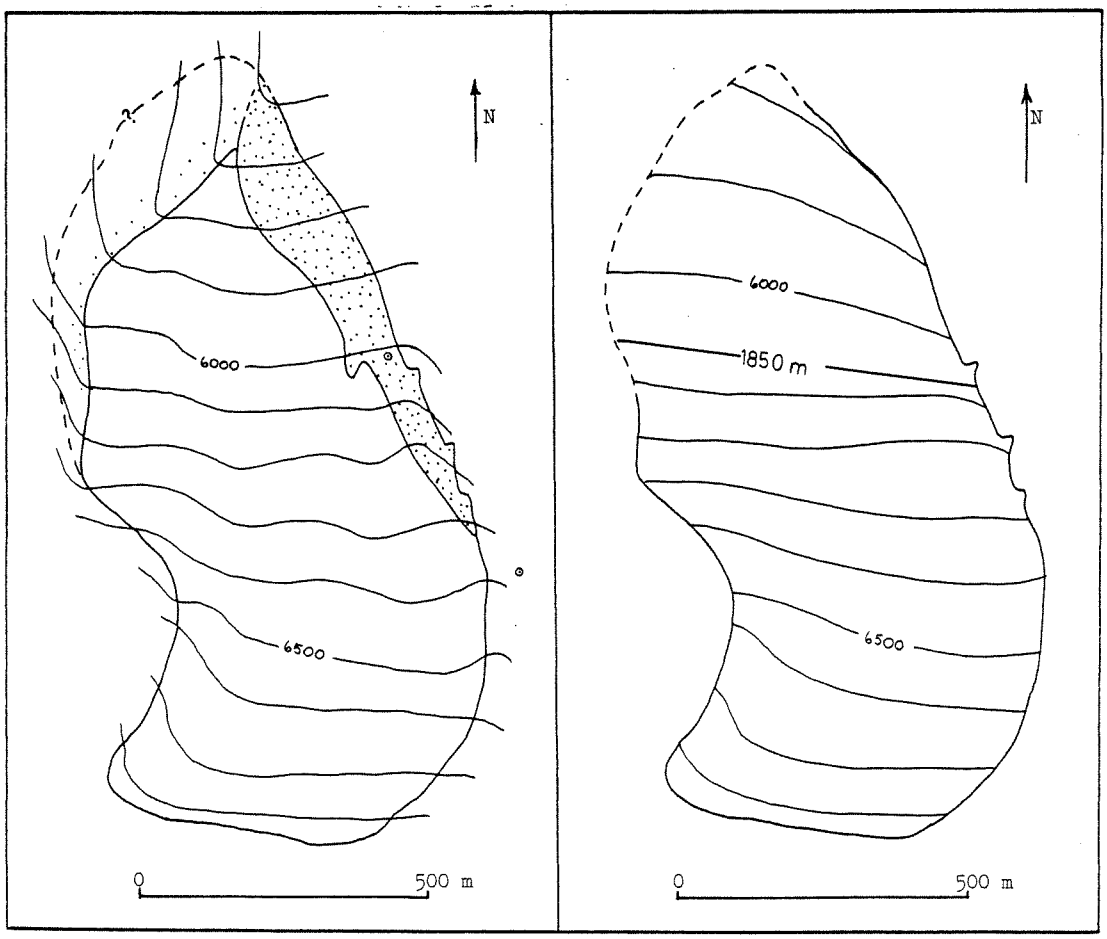

PRESENT ICE SURFACE WITH DEPOSIT

NEOGLACIAL MAXIMUM SURFACE

APPENDIX B. PHYSICAL INVENTORY (Triple West Glacier, no. 10)

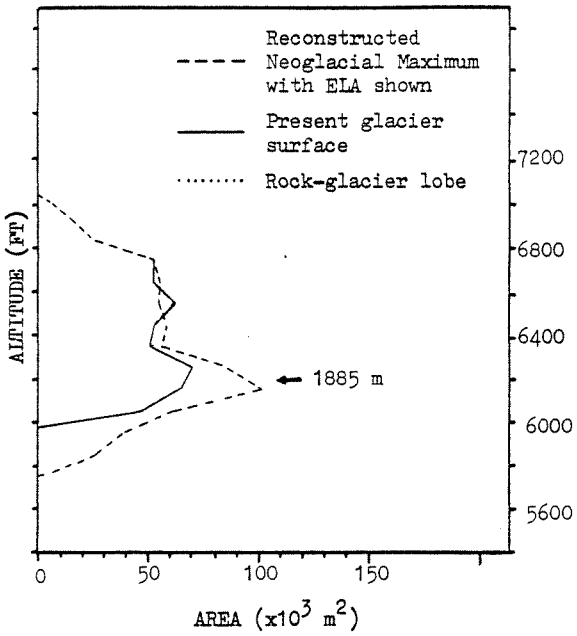

NEOGLACIAL MAXIMUM AND PRESENT AREA-ALTITUDE DISTRIBUTIONS

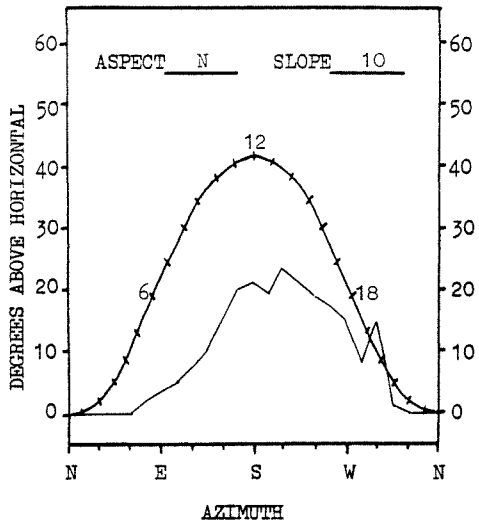

LANDFORM HORIZON (S- 110) WITH +20° SOLAR DECLINATION

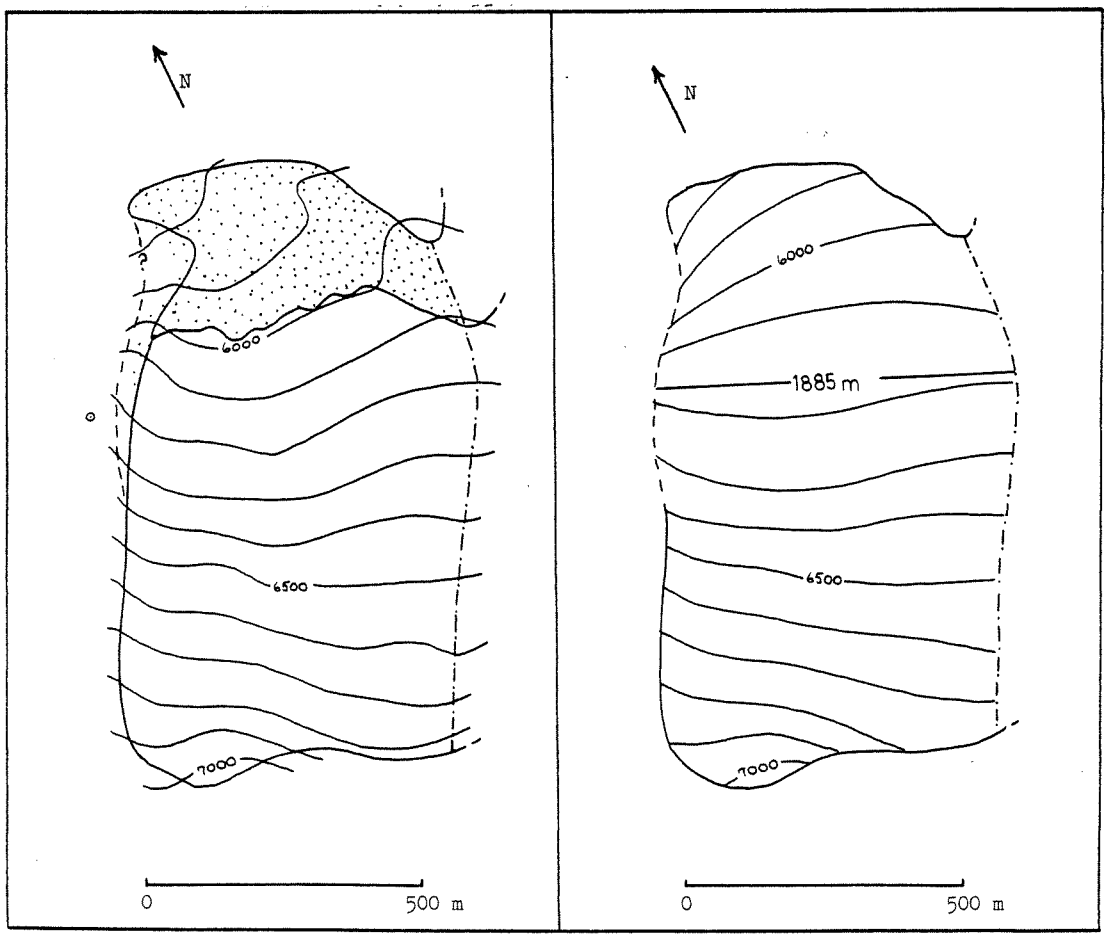

PRESENT ICE SURFACE WITH DEPOSIT

NEOGLACIAL MAXIMUM SURFACE

APPENDIX B. PHYSICAL INVENTORY (Triple Middle Glacier, no. 11)

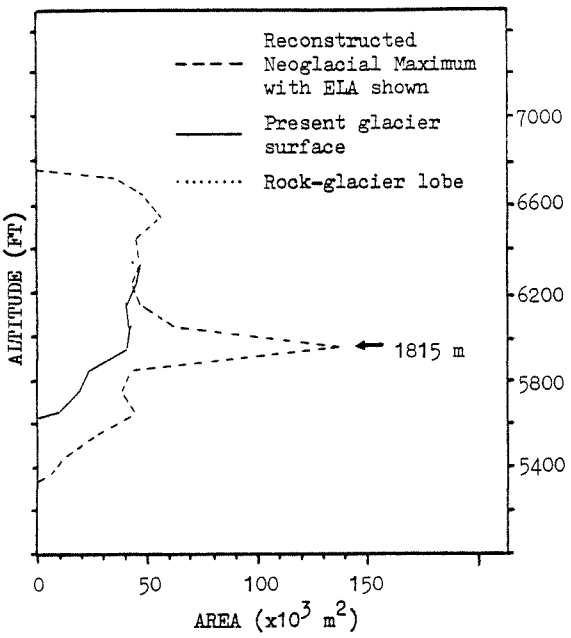

NEOGLACIAL MAXIMUM AND PRESENT AREA-ALTITUDE DISTRIBUTIONS

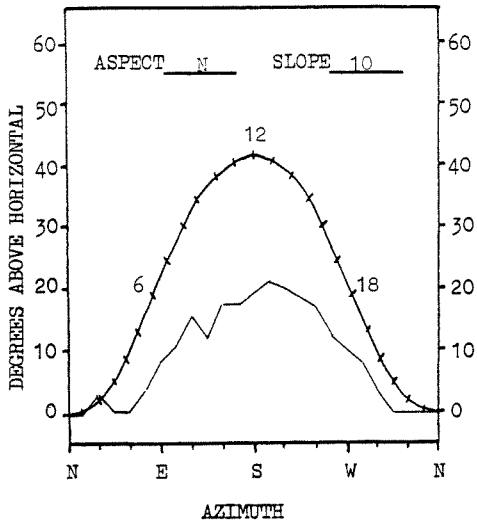

LANDFORM HORIZON (S- 111)
WITH +20° SOLAR DECLINATION

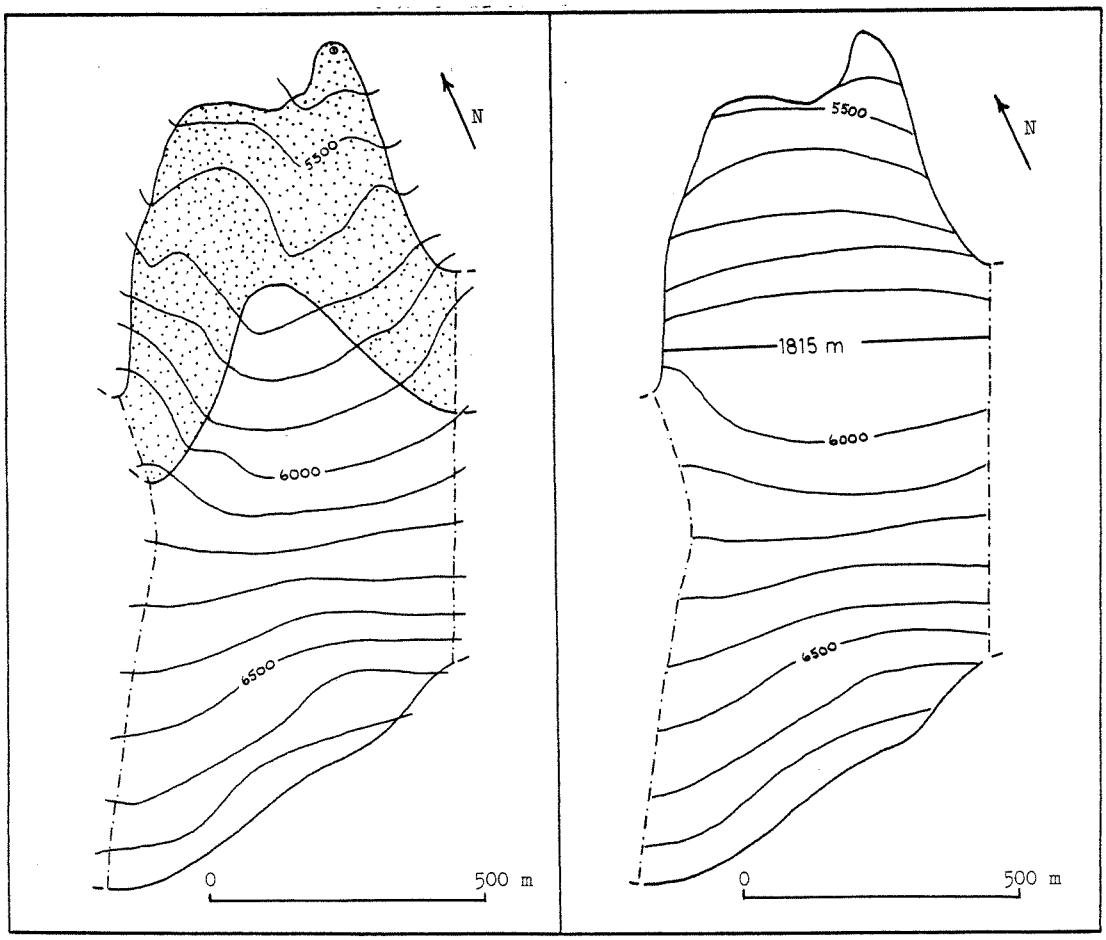

PRESENT ICE SURFACE WITH DEPOSIT

NEOGLACIAL MAXIMUM SURFACE

APPENDIX B. PHYSICAL INVENTORY (Triple East Glacier, no. 12)

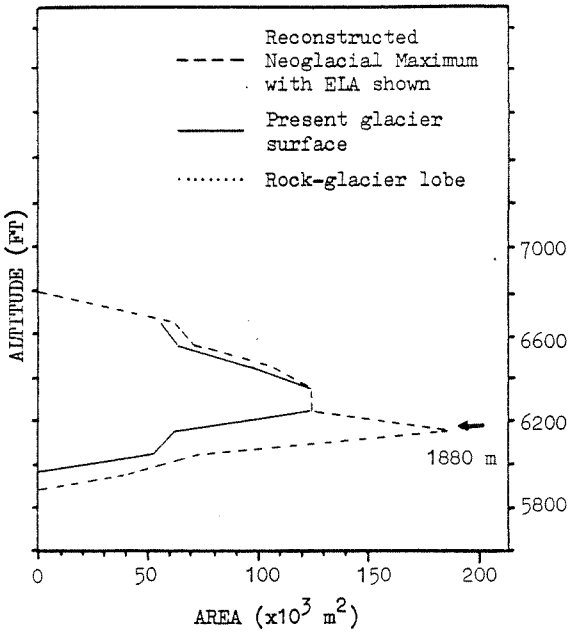

NEOGLACIAL MAXIMUM AND PRESENT AREA-ALTITUDE DISTRIBUTIONS

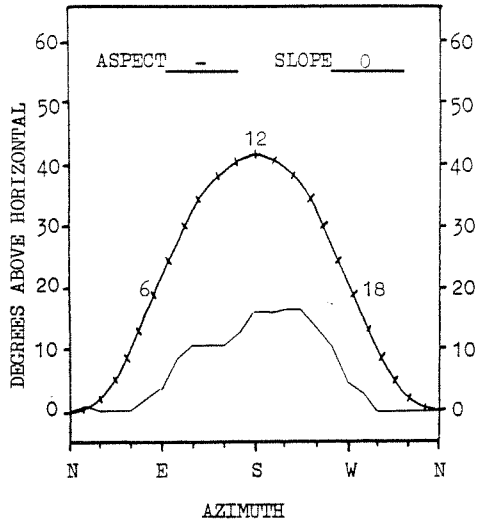

LANDFORM HORIZON (S- 112)
WITH +20° SOLAR DECLINATION

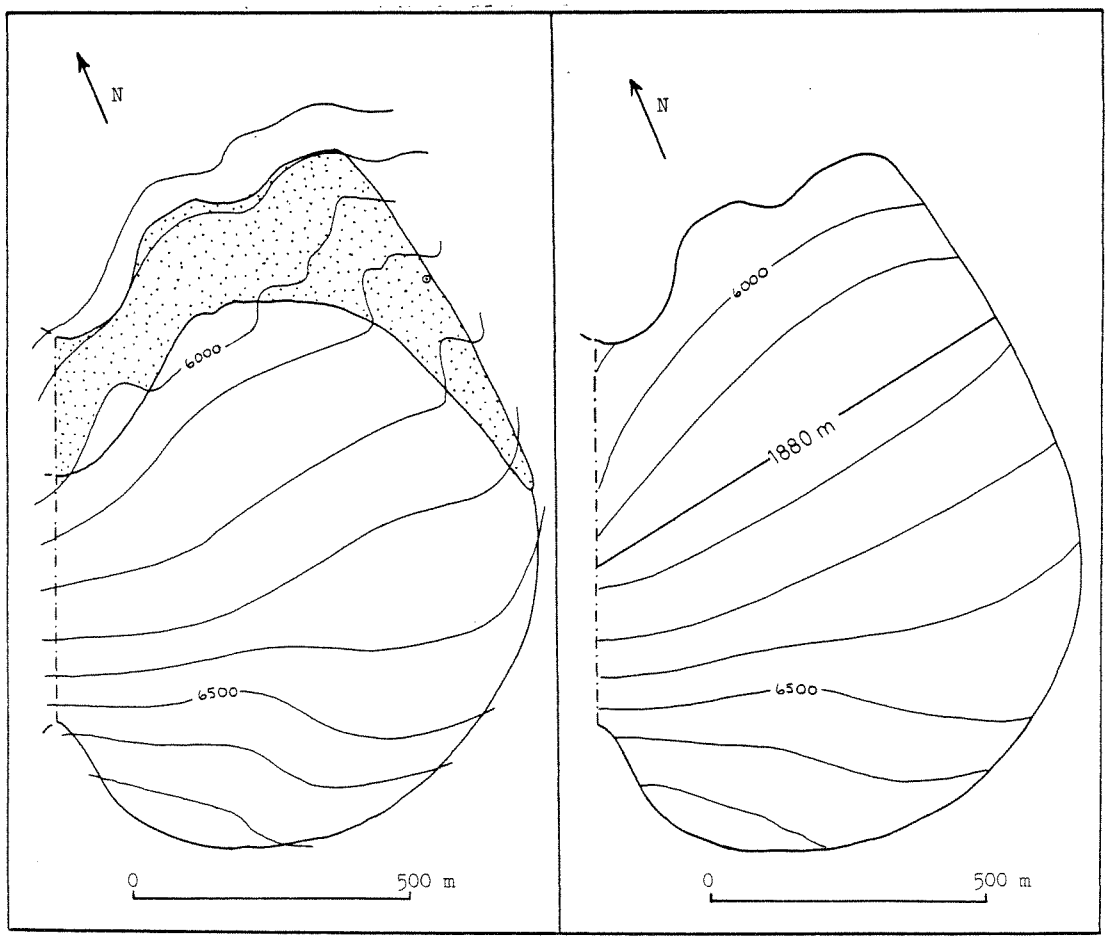

PRESENT ICE SURFACE WITH DEPOSIT

NEOGLACIAL MAXIMUM SURFACE

APPENDIX B. PHYSICAL INVENTORY (Dall Sheep Glacier, no. 13)

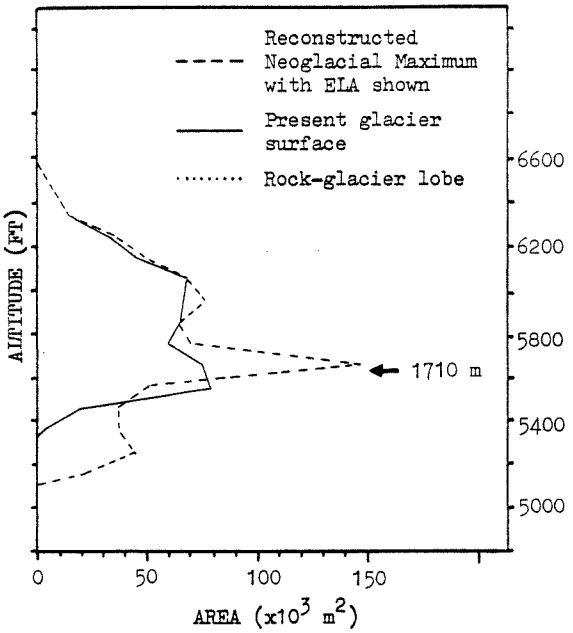

NEOGLACIAL MAXIMUM AND PRESENT AREA-ALTITUDE DISTRIBUTIONS

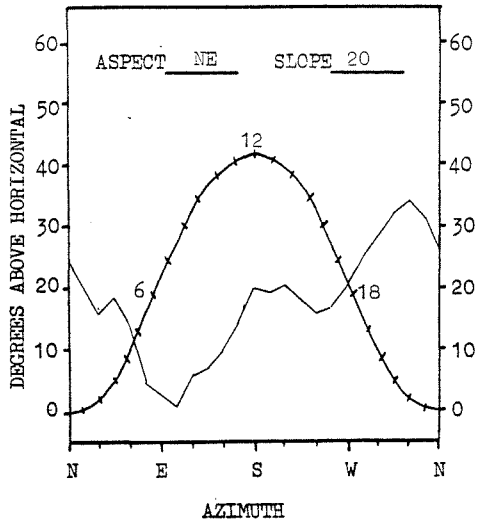

LANDFORM HORIZON (S- 201)
WITH +20° SOLAR DECLINATION

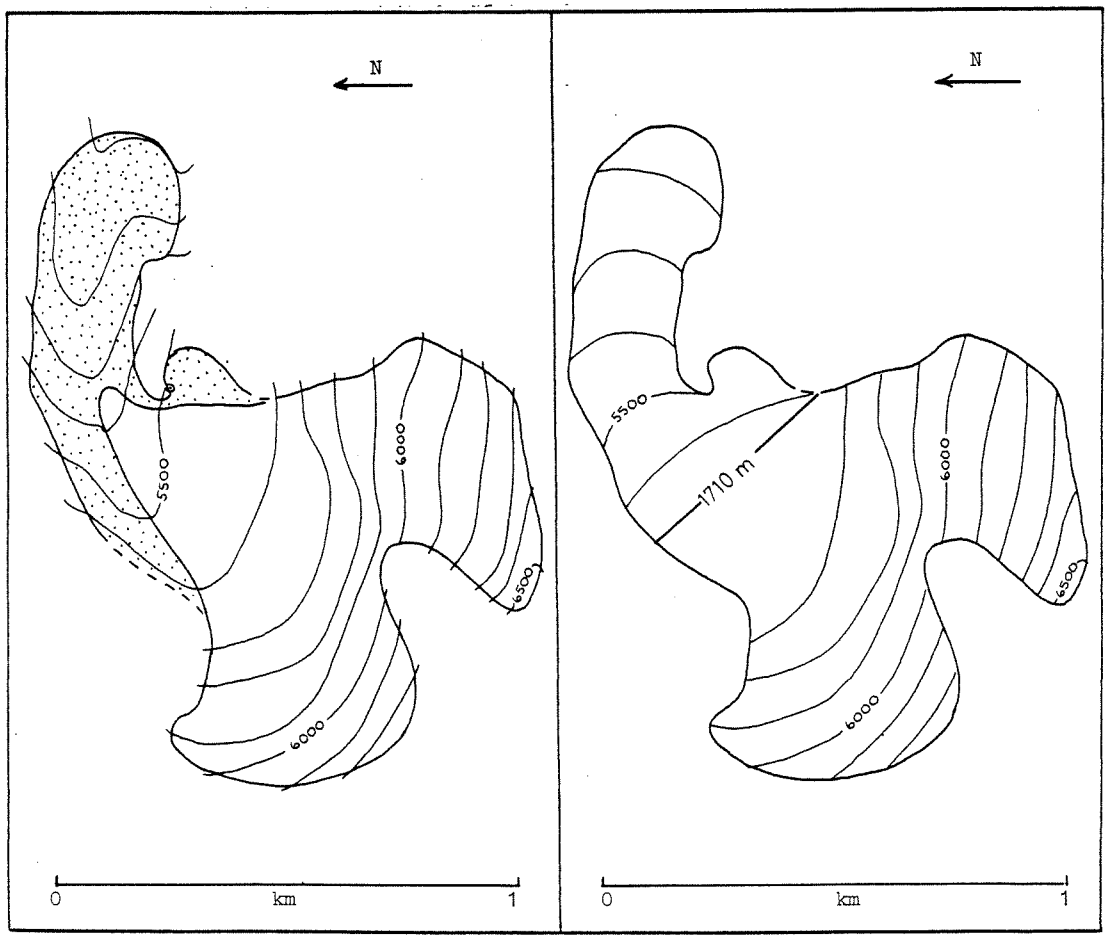

PRESENT ICE SURFACE WITH DEPOSIT

NEOGLACIAL MAXIMUM SURFACE

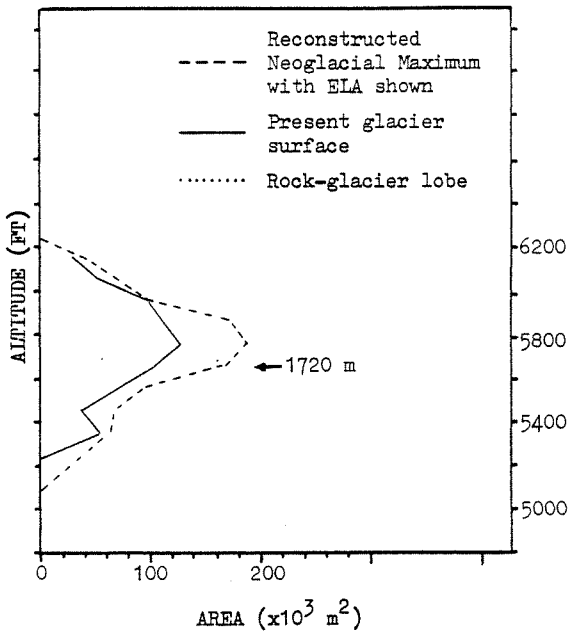

NEOGLACIAL MAXIMUM AND PRESENT AREA-ALTITUDE DISTRIBUTIONS

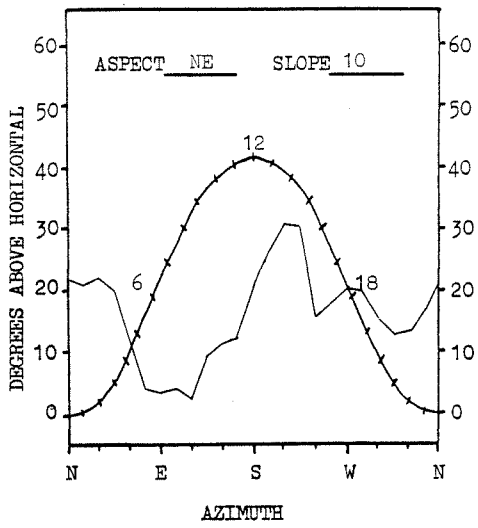

LANDFORM HORIZON (S- 202)
WITH +20° SOLAR DECLINATION

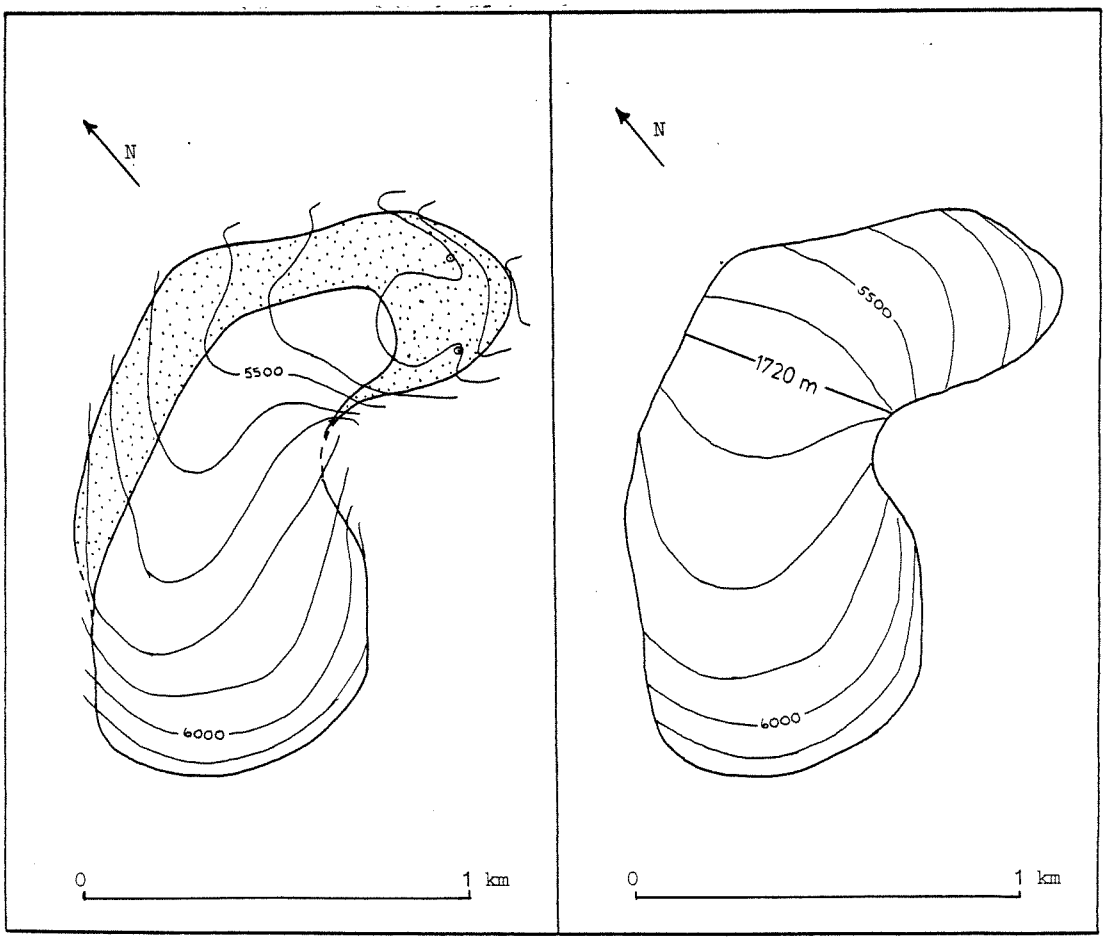

PRESENT ICE SURFACE WITH DEPOSIT

NEOGLACIAL MAXIMUM SURFACE

APPENDIX B. PHYSICAL INVENTORY (Fox Glacier, no. 15)

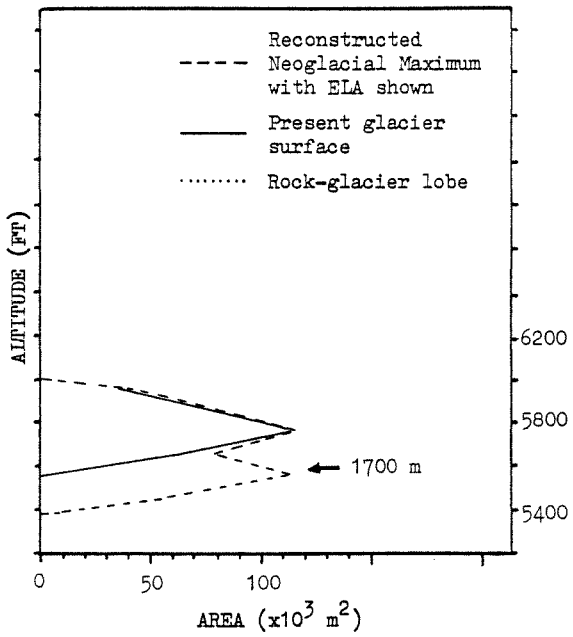

NEOGLACIAL MAXIMUM AND PRESENT AREA-ALTITUDE DISTRIBUTIONS

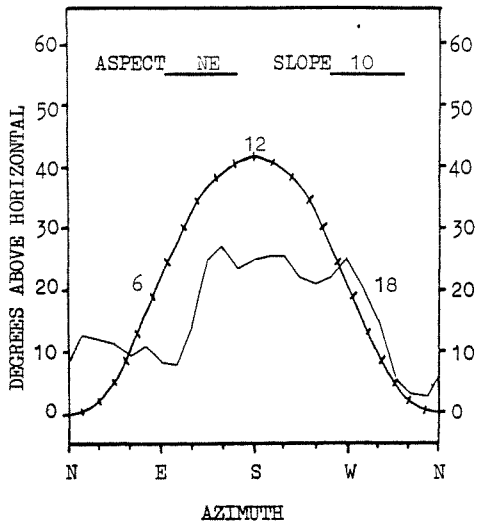

LANDFORM HORIZON (S- 203)
WITH +20° SOLAR DECLINATION

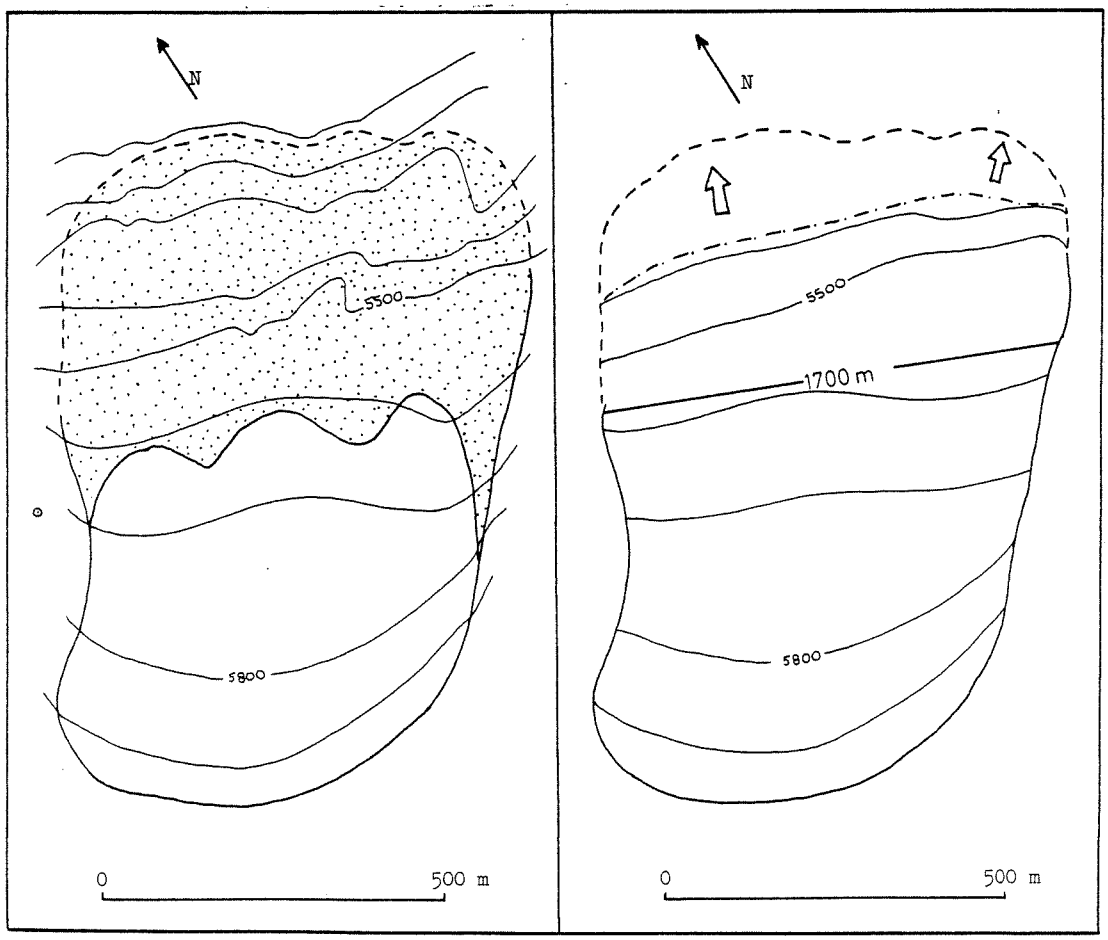

PRESENT ICE SURFACE WITH DEPOSIT

NEOGLACIAL MAXIMUM SURFACE

APPENDIX B. PHYSICAL INVENTORY (Ram Glacier, no. 16)

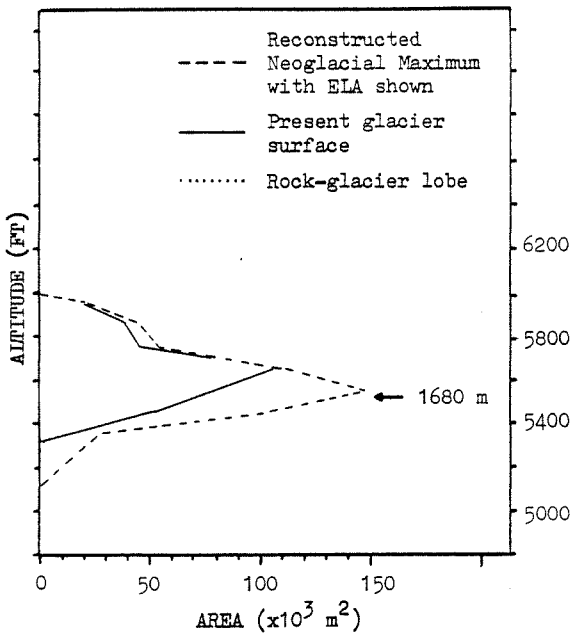

NEOGLACIAL MAXIMUM AND PRESENT AREA-ALTITUDE DISTRIBUTIONS

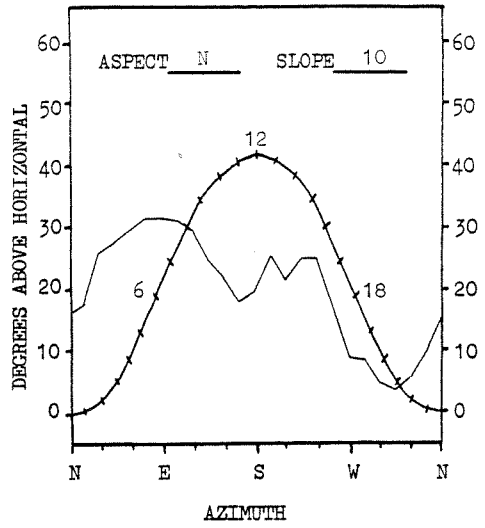

LANDFORM HORIZON (S- 204)
WITH +20° SOLAR DECLINATION

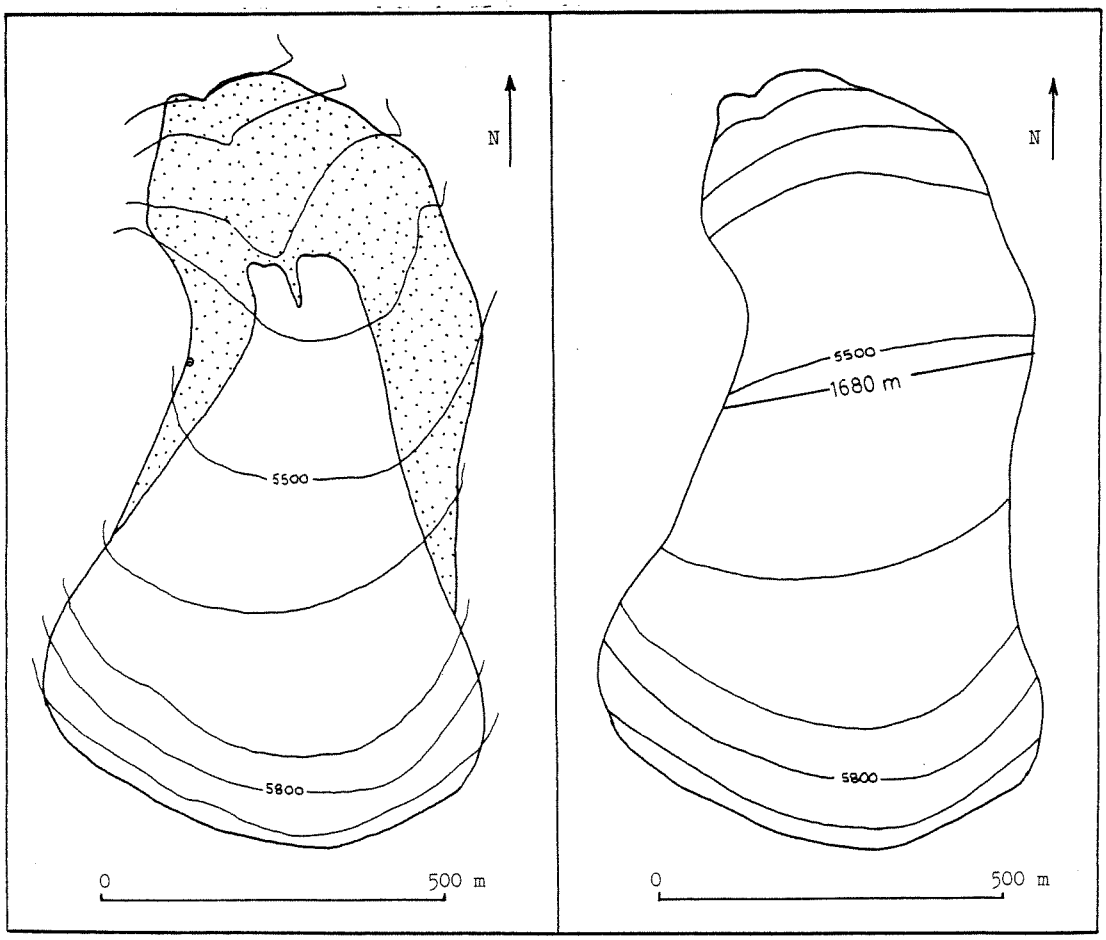

PRESENT ICE SURFACE WITH DEPOSIT

NEOGLACIAL MAXIMUM SURFACE

APPENDIX B. PHYSICAL INVENTORY (Ewe Glacier, no. 17)

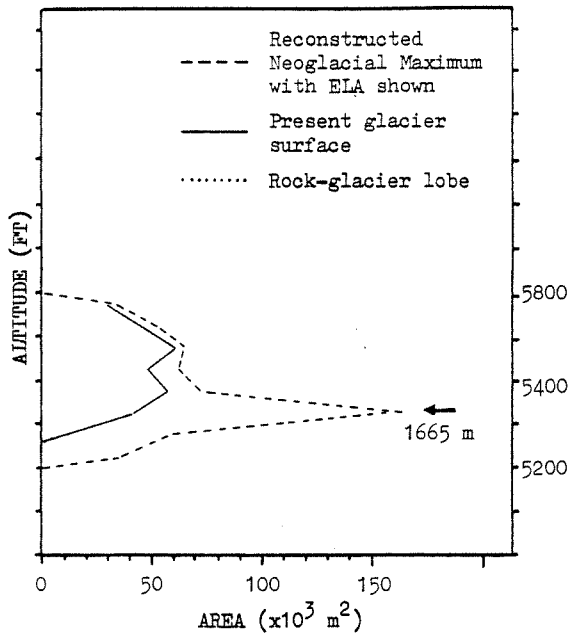

NEOGLACIAL MAXIMUM AND PRESENT AREA-ALTITUDE DISTRIBUTIONS

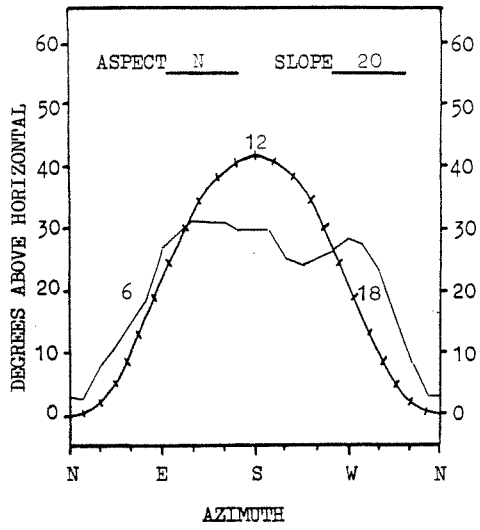

LANDFORM HORIZON (S- 205) WITH +20° SOLAR DECLINATION

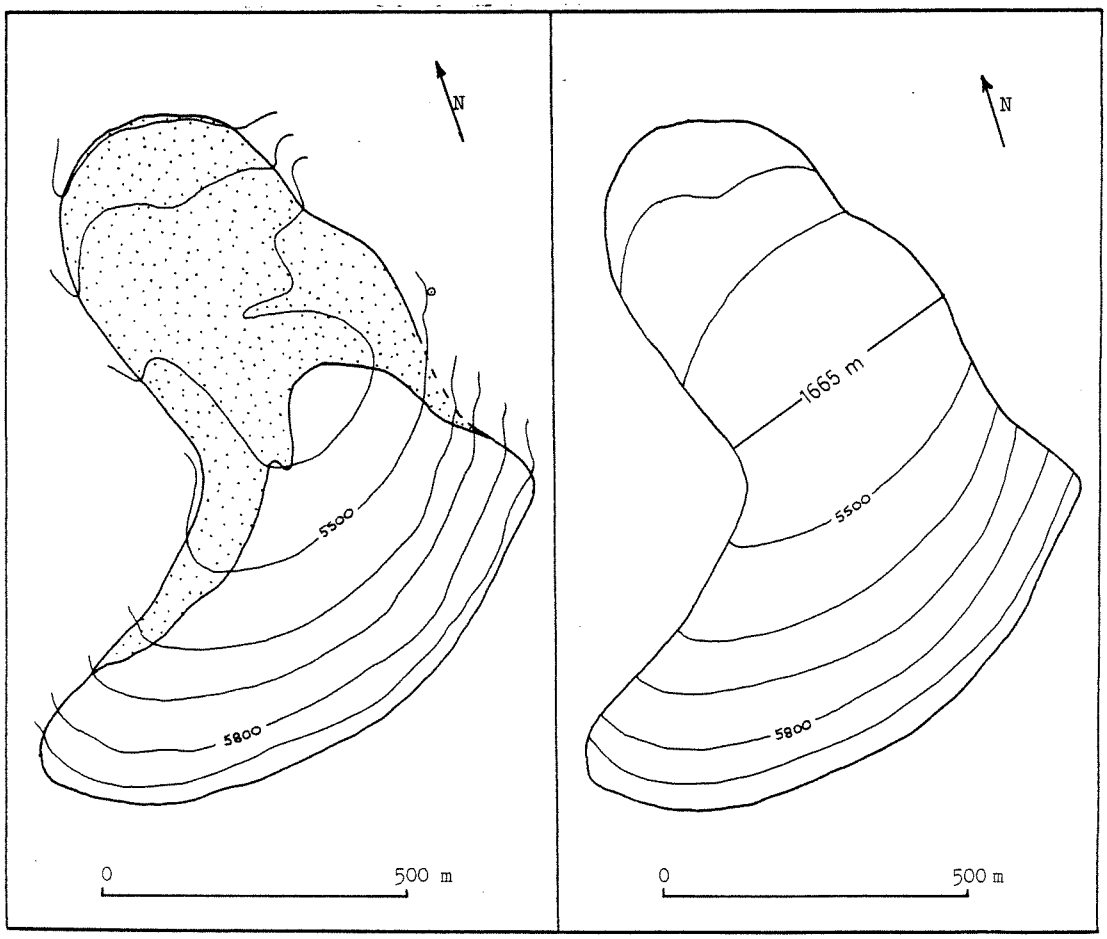

PRESENT ICE SURFACE WITH DEPOSIT

NEOGLACIAL MAXIMUM SURFACE

APPENDIX B. PHYSICAL INVENTORY (Kid Glacier, no. 18)

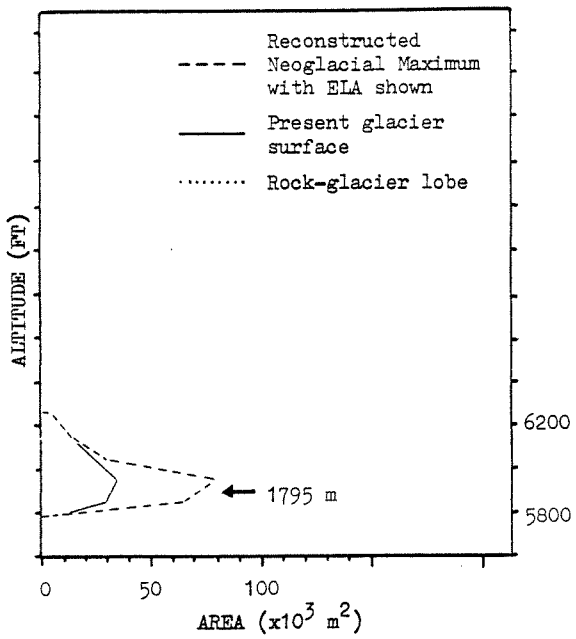

NEOGLACIAL MAXIMUM AND PRESENT AREA-ALTITUDE DISTRIBUTIONS

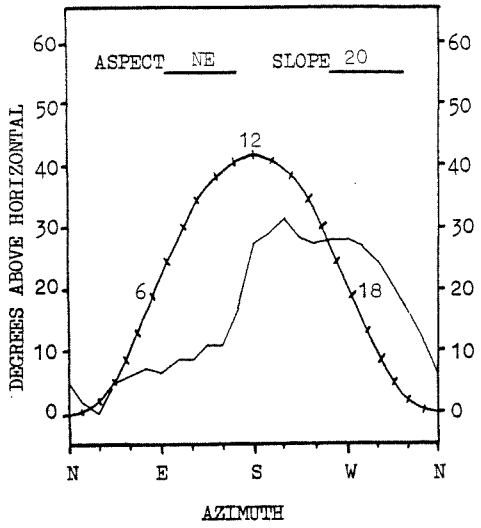

LANDFORM HORIZON (S-206)
WITH +20° SOLAR DECLINATION

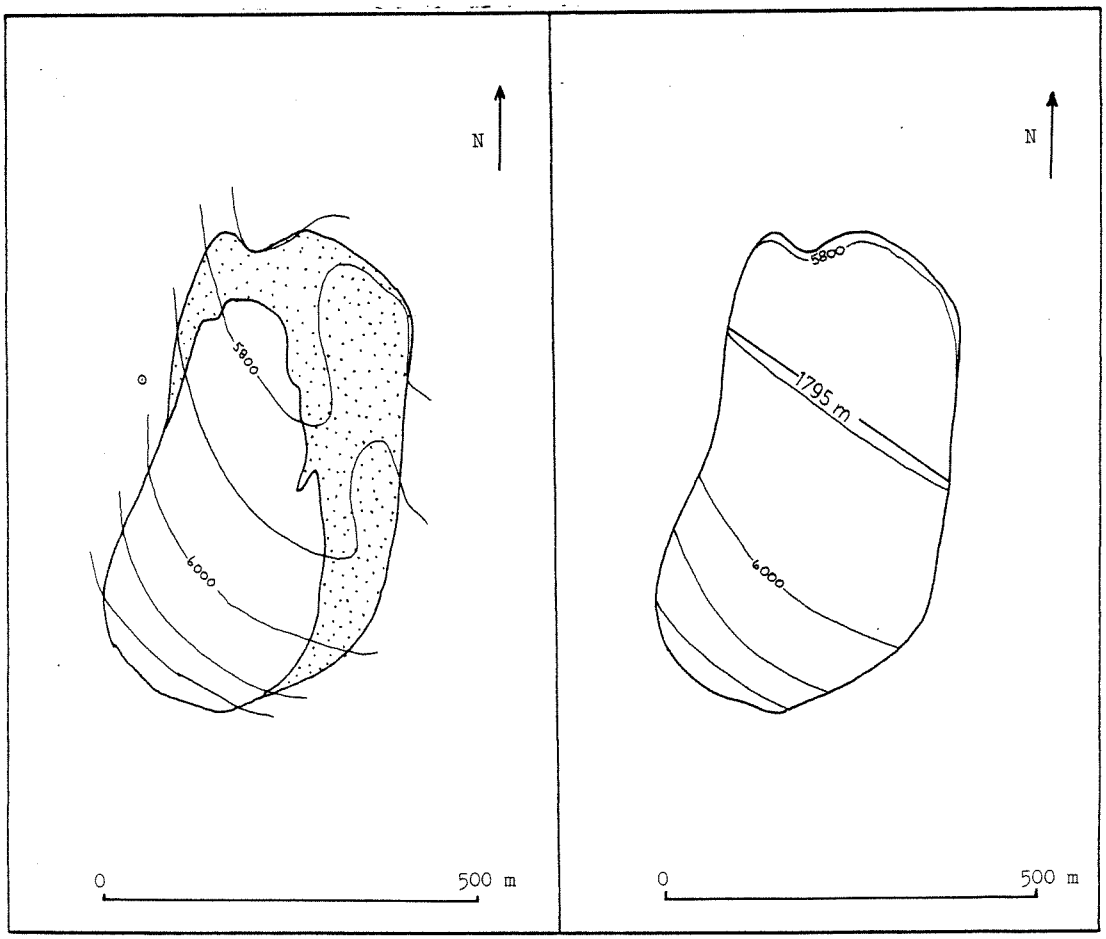

PRESENT ICE SURFACE WITH DEPOSIT

NEOGLACIAL MAXIMUM SURFACE

APPENDIX B. PHYSICAL INVENTORY (Vole Glacier, no. 19)

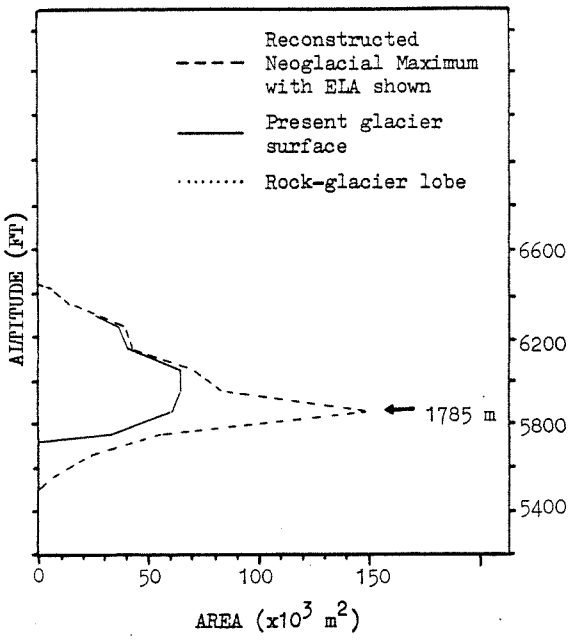

NEOGLACIAL MAXIMUM AND PRESENT AREA-ALTITUDE DISTRIBUTIONS

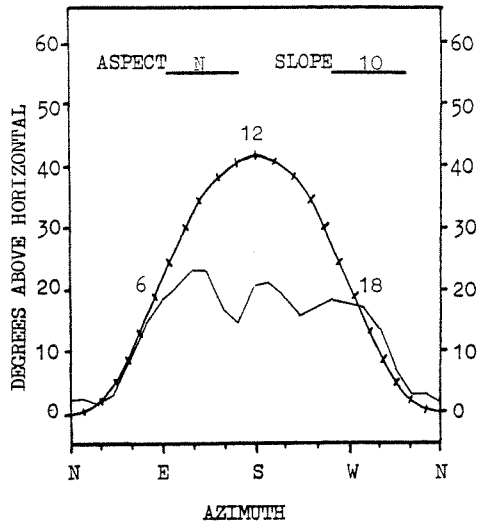

LANDFORM HORIZON (S- 207)
WITH +20° SOLAR DECLINATION

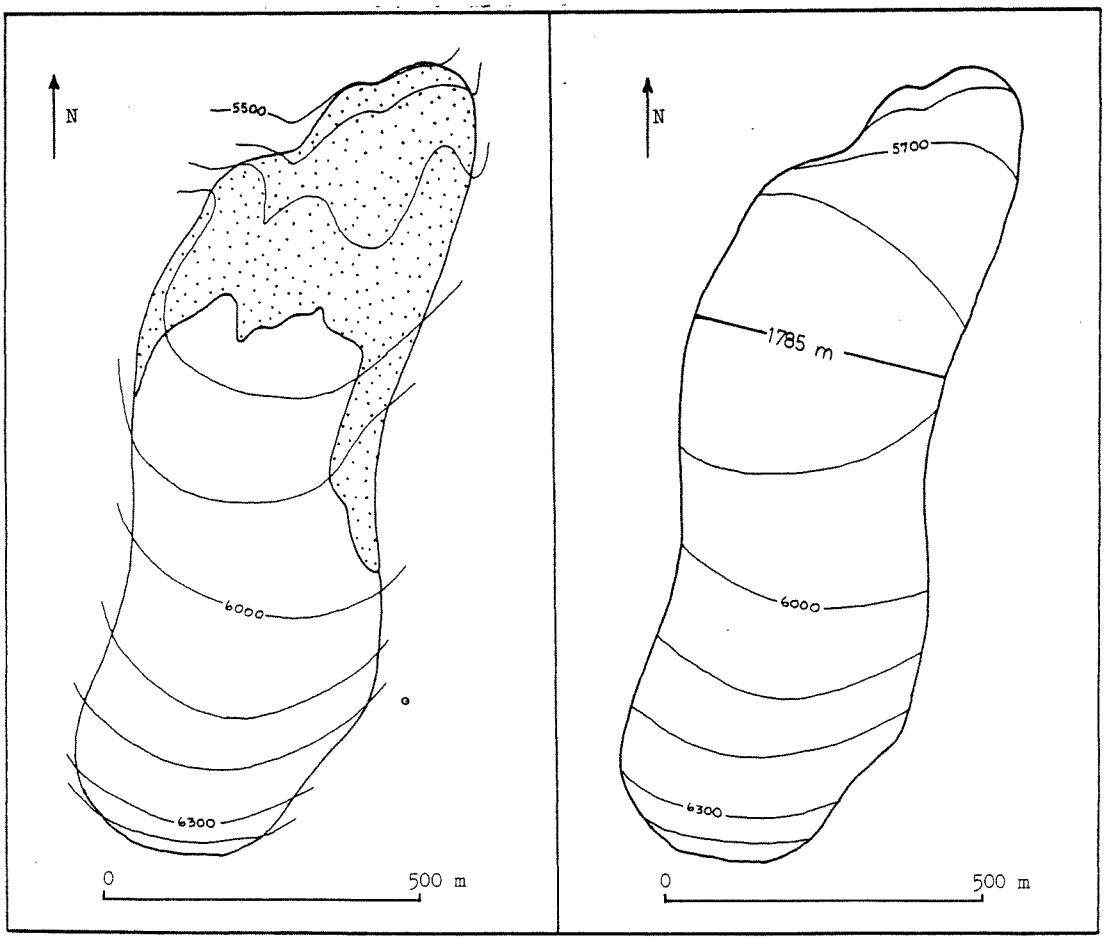

PRESENT ICE SURFACE WITH DEPOSIT

NEOGLACIAL MAXIMUM SURFACE

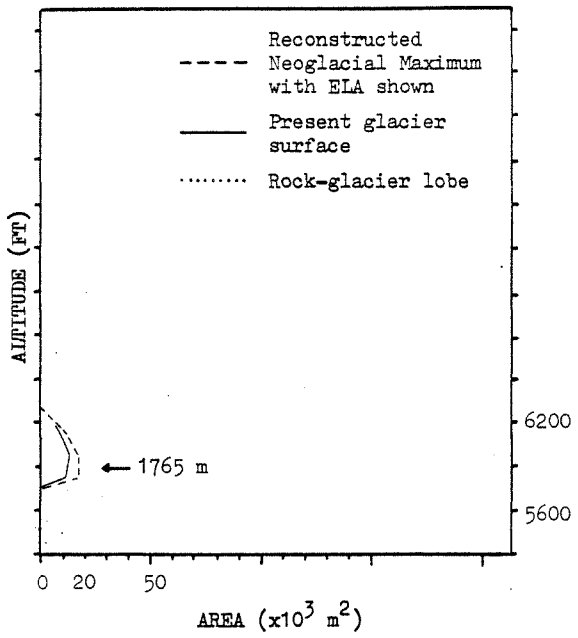

NEOGLACIAL MAXIMUM AND PRESENT AREA-ALTITUDE DISTRIBUTIONS

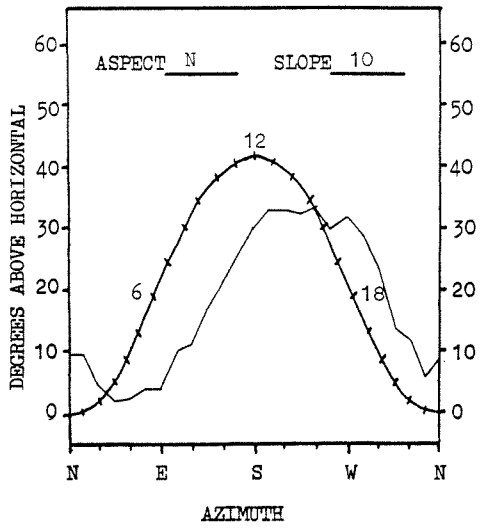

LANDFORM HORIZON (S- 208)
WITH +20° SOLAR DECLINATION

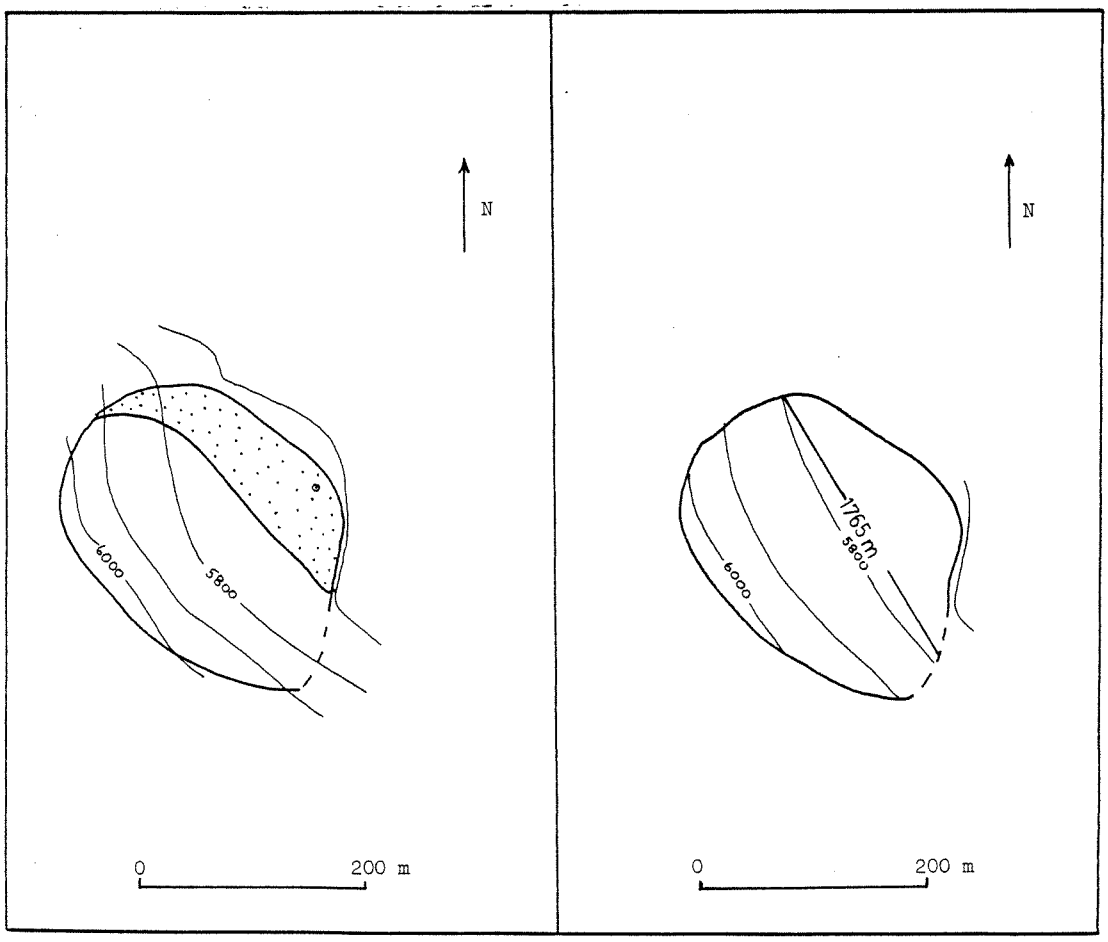

PRESENT ICE SURFACE WITH DEPOSIT

NEOGLACIAL MAXIMUM SURFACE

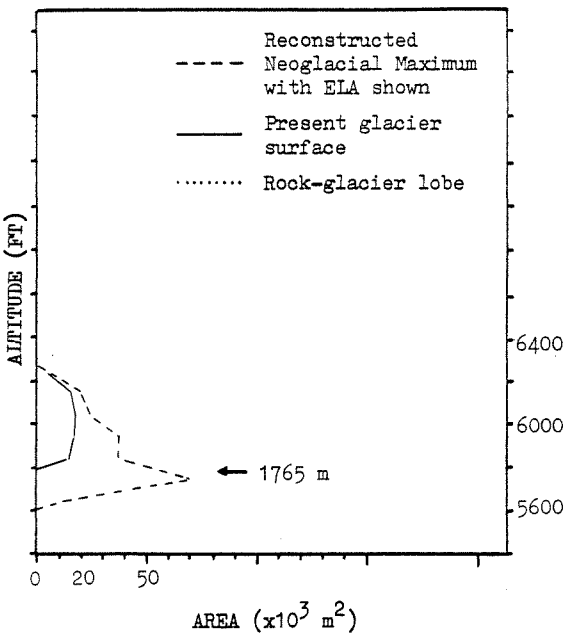

NEOGLACIAL MAXIMUM AND PRESENT AREA-ALTITUDE DISTRIBUTIONS

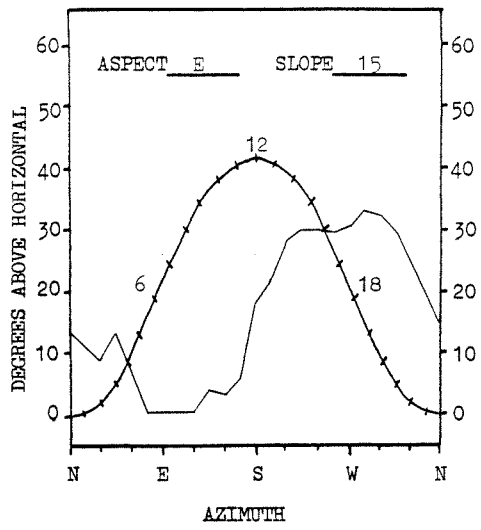

LANDFORM HORIZON (S- 209) WITH +20° SOLAR DECLINATION

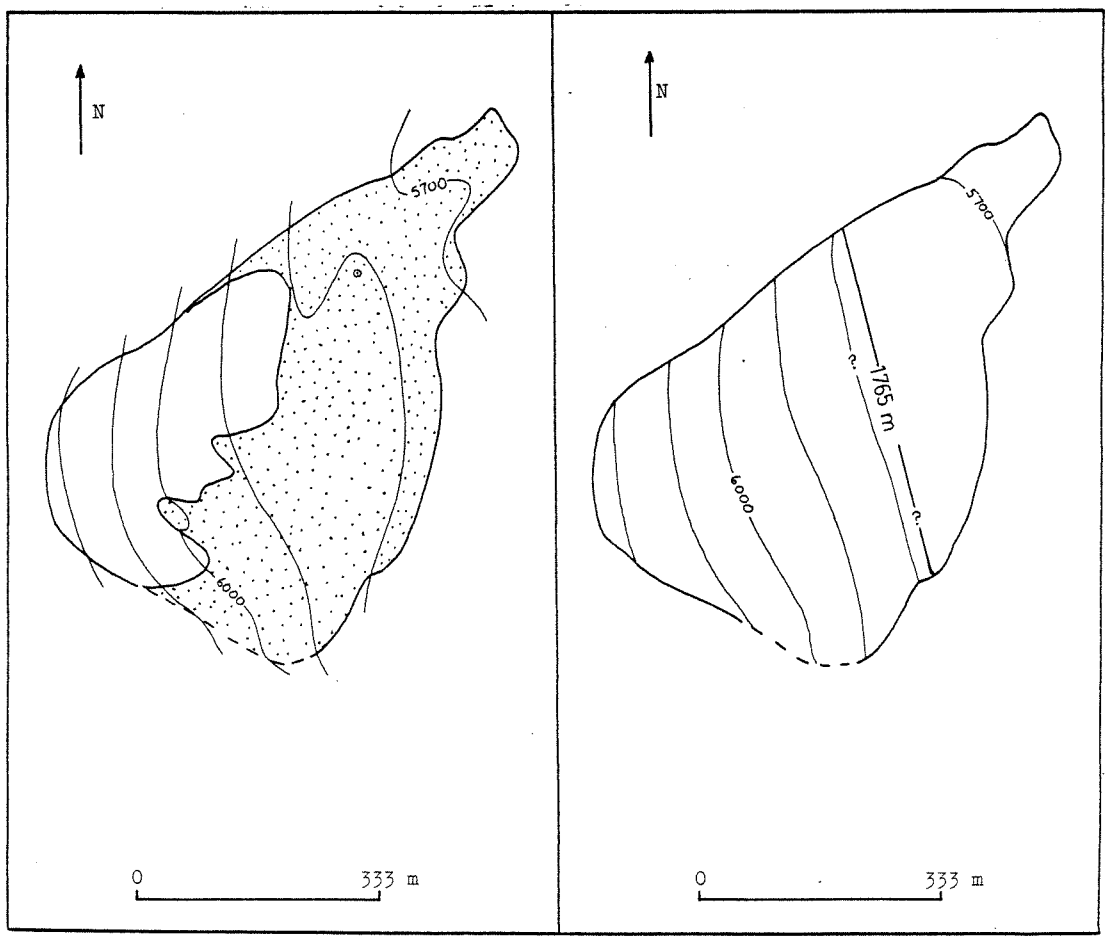

PRESENT ICE SURFACE WITH DEPOSIT

NEOGLACIAL MAXIMUM SURFACE

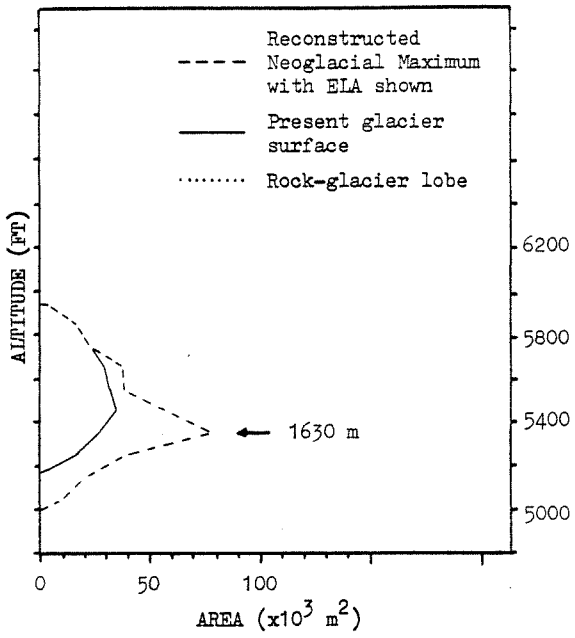

NEOGLACIAL MAXIMUM AND PRESENT AREA-ALTITUDE DISTRIBUTIONS

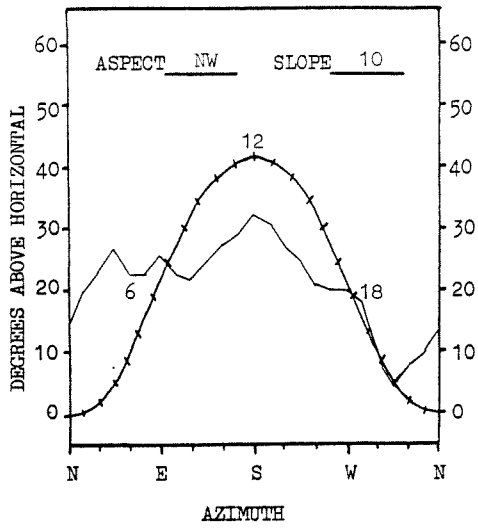

LANDFORM HORIZON (S-210b) WITH +20° SOLAR DECLINATION

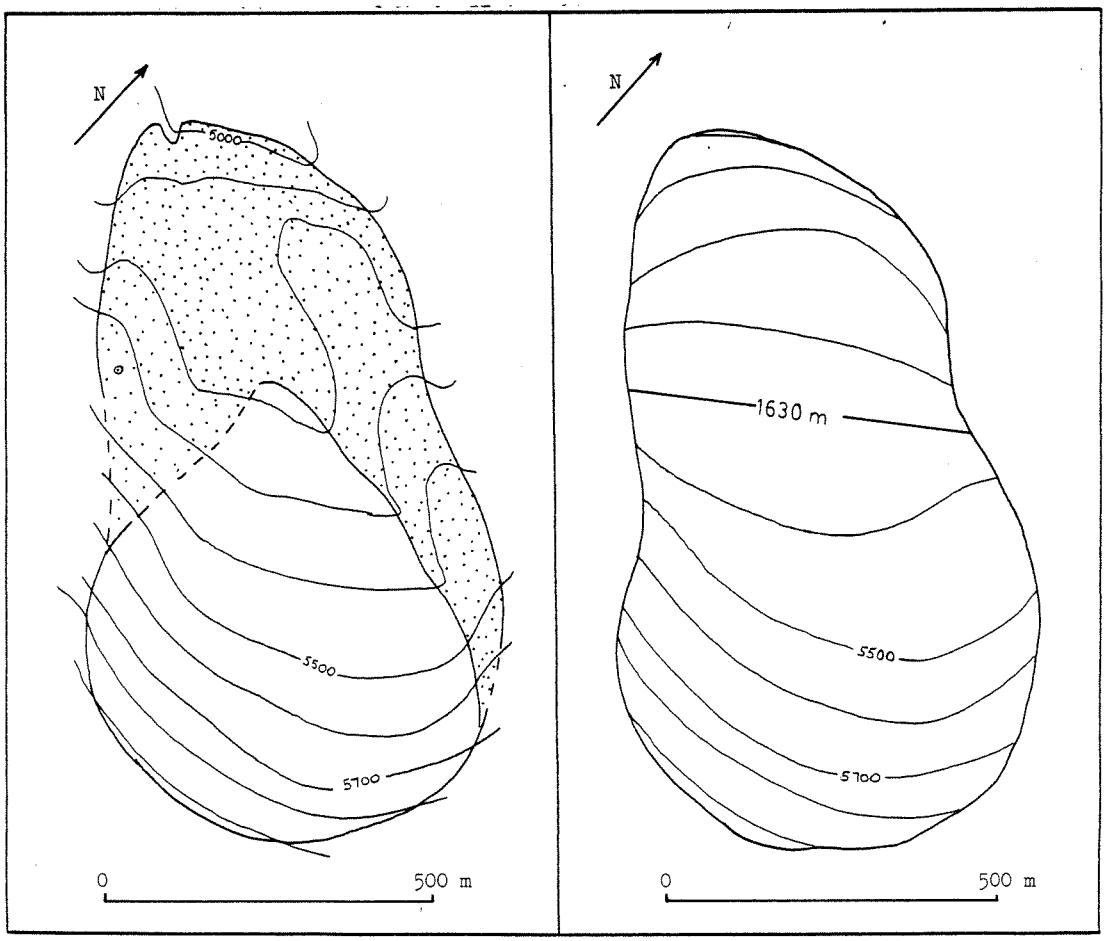

PRESENT ICE SURFACE WITH DEPOSIT

NEOGLACIAL MAXIMUM SURFACE

APPENDIX B. PHYSICAL INVENTORY (Burbot Glacier, no. 23)

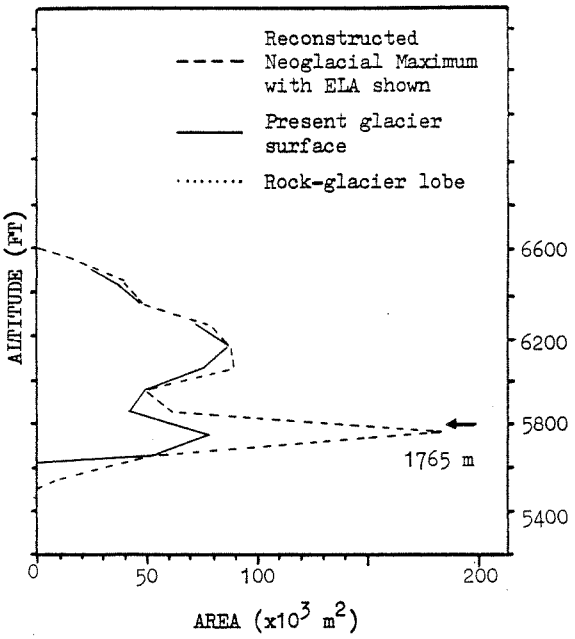

NEOGLACIAL MAXIMUM AND PRESENT AREA-ALTITUDE DISTRIBUTIONS

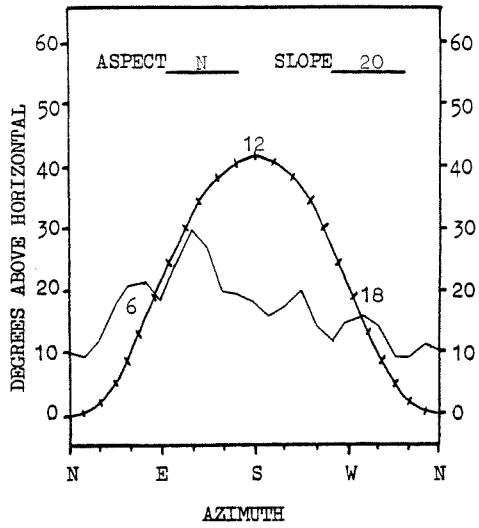

LANDFORM HORIZON (S- 211)
WITH +20° SOLAR DECLINATION

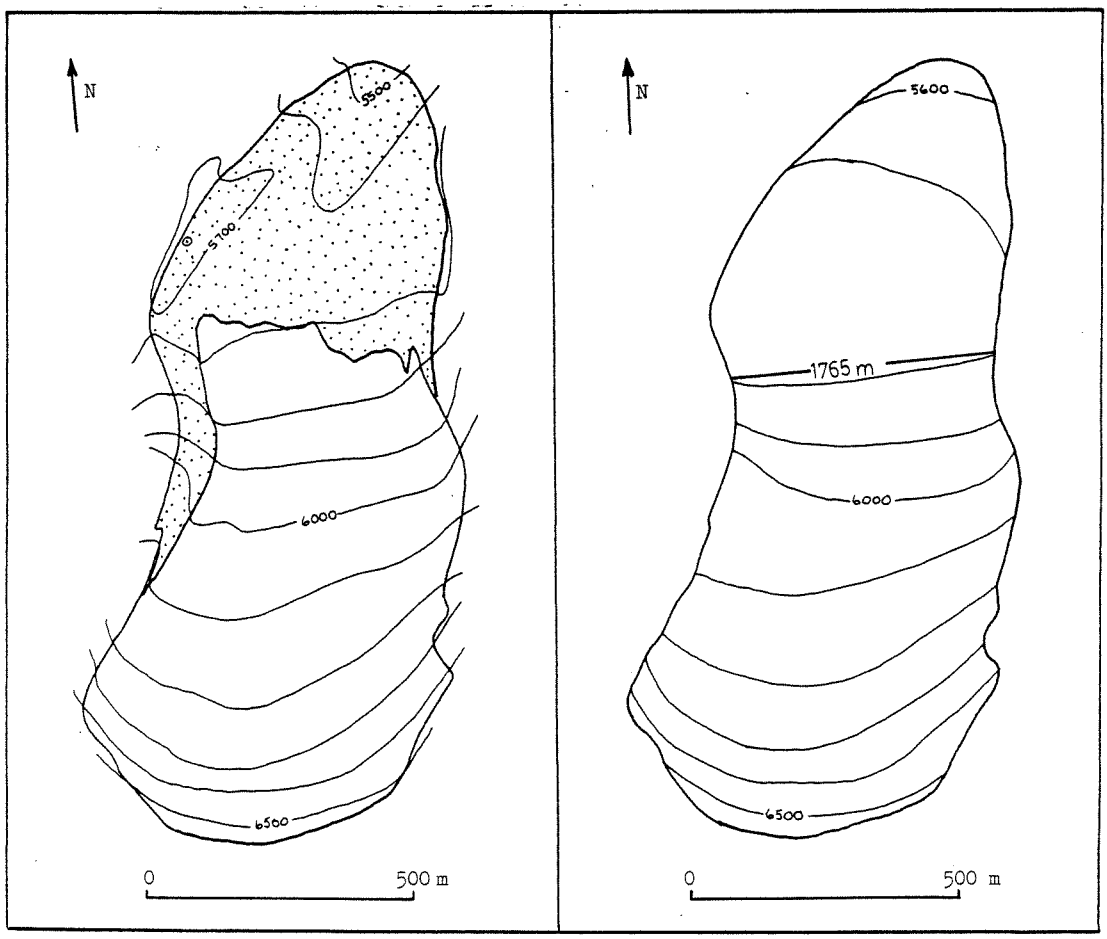

PRESENT ICE SURFACE WITH DEPOSIT

NEOGLACIAL MAXIMUM SURFACE

APPENDIX B. PHYSICAL INVENTORY (Arctic Char Glacier, no. 24)

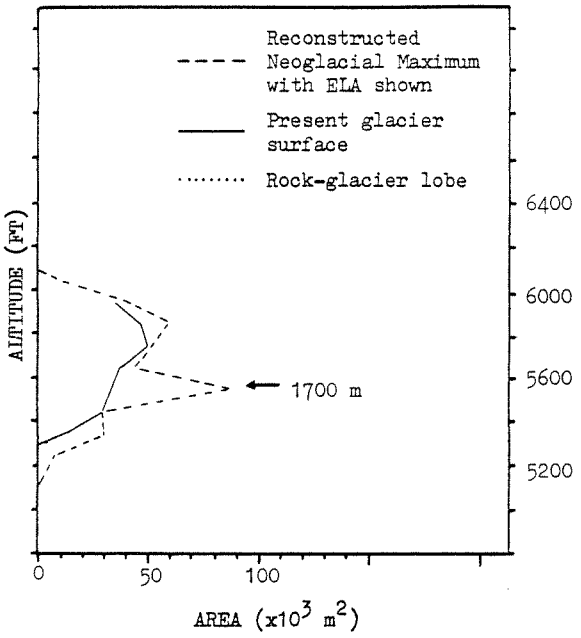

NEOGLACIAL MAXIMUM AND PRESENT AREA-ALTITUDE DISTRIBUTIONS

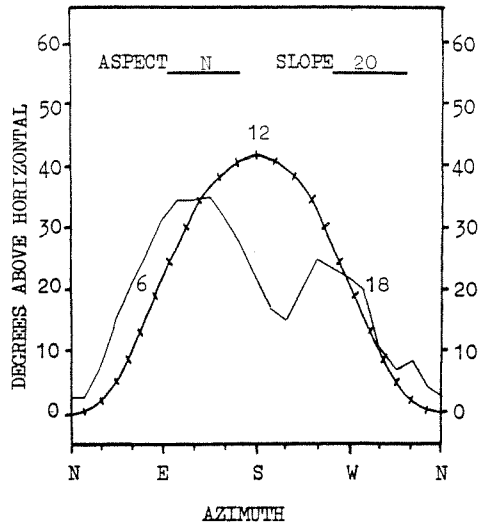

LANDFORM HORIZON (S- 212) WITH +20° SOLAR DECLINATION

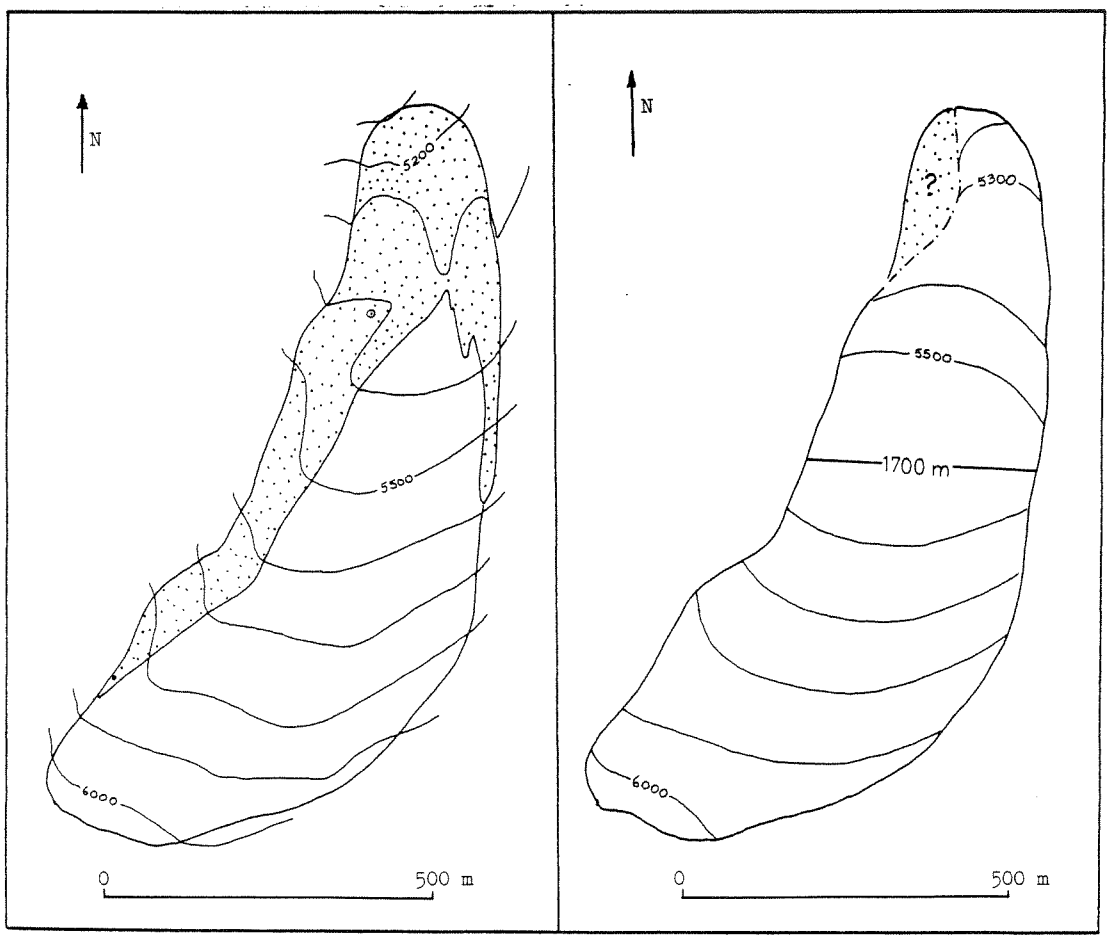

PRESENT ICE SURFACE WITH DEPOSIT

NEOGLACIAL MAXIMUM SURFACE

APPENDIX B. PHYSICAL INVENTORY (Grayling Glacier, no. 25)

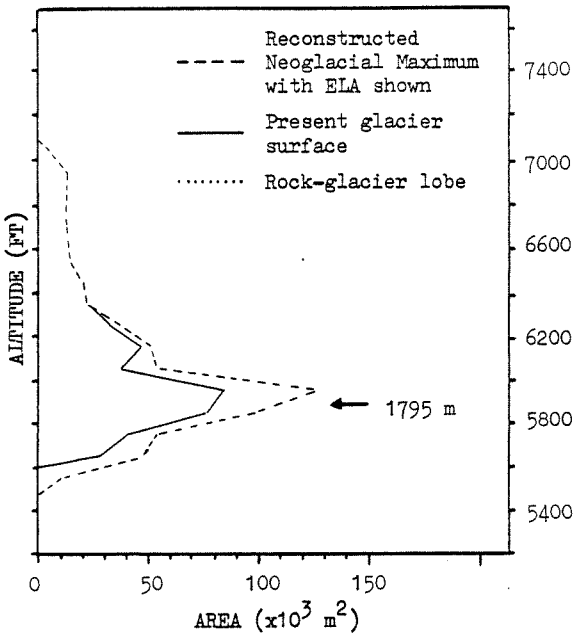

NEOGLACIAL MAXIMUM AND PRESENT AREA-ALTITUDE DISTRIBUTIONS

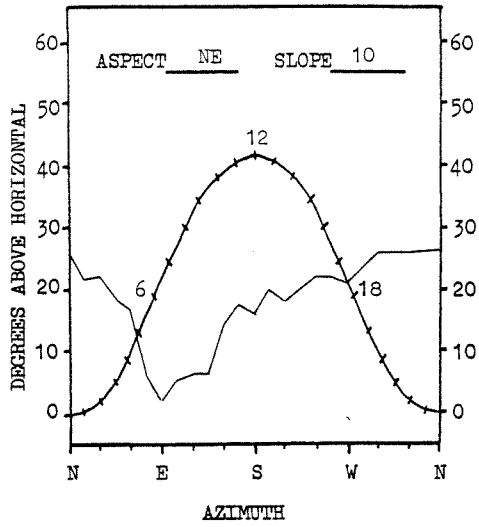

LANDFORM HORIZON (S- 213)
WITH +20° SOLAR DECLINATION

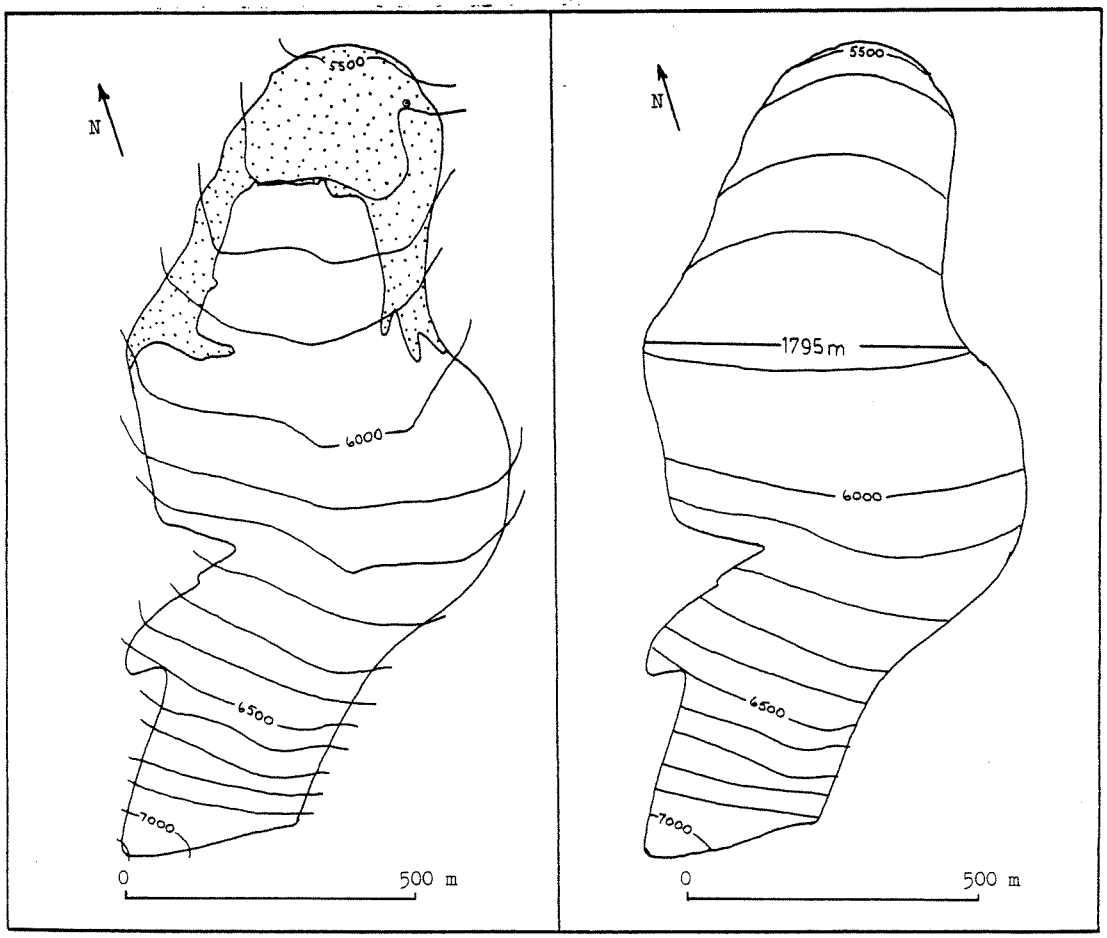

PRESENT ICE SURFACE WITH DEPOSIT

NEOGLACIAL MAXIMUM SURFACE

APPENDIX B. PHYSICAL INVENTORY (Cisc o Glacier, no. 26)

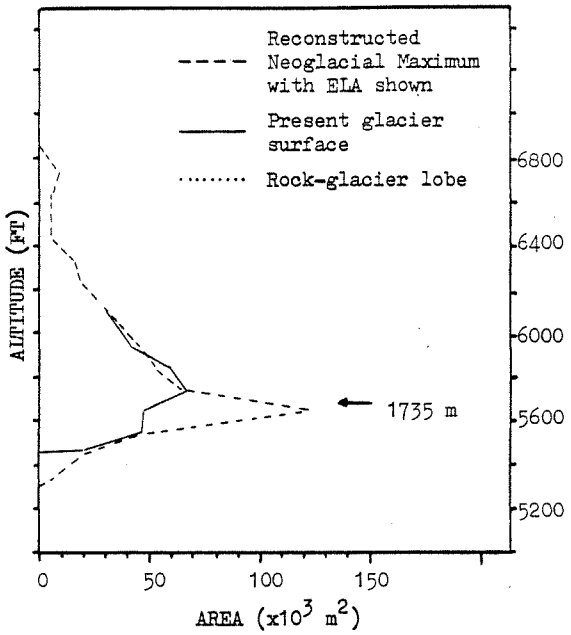

NEOGLACIAL MAXIMUM AND PRESENT AREA-ALTITUDE DISTRIBUTIONS

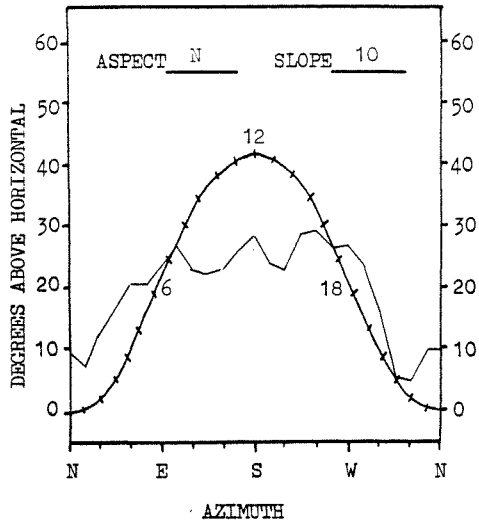

LANDFORM HORIZON (S- 214)
WITH +20° SOLAR DECLINATION

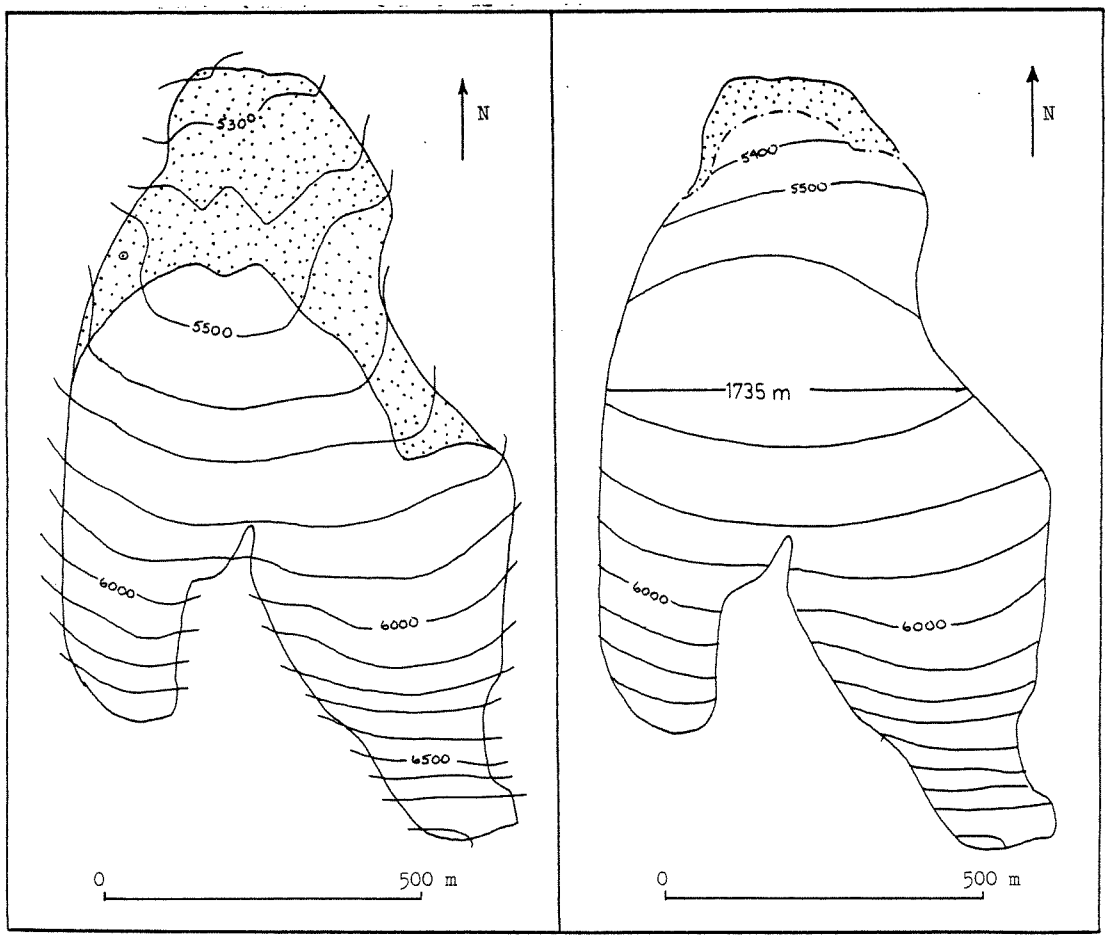

PRESENT ICE SURFACE WITH DEPOSIT

NEOGLACIAL MAXIMUM SURFACE

APPENDIX B. PHYSICAL INVENTORY (Moose Glacier, no. 27)

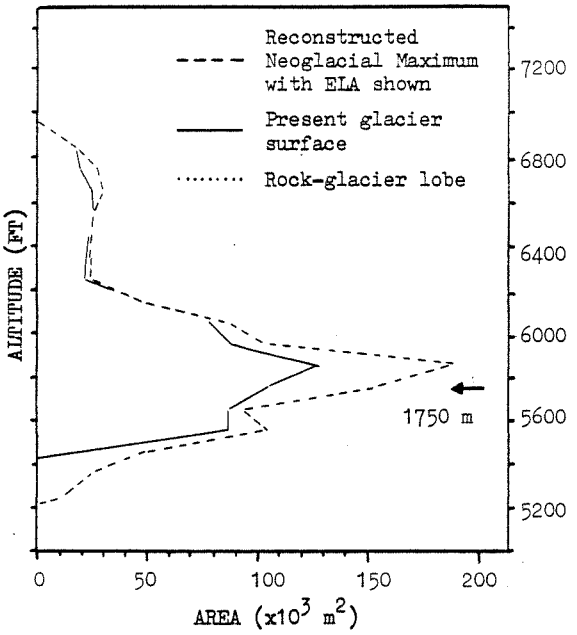

NEOGLACIAL MAXIMUM AND PRESENT AREA-ALTITUDE DISTRIBUTIONS

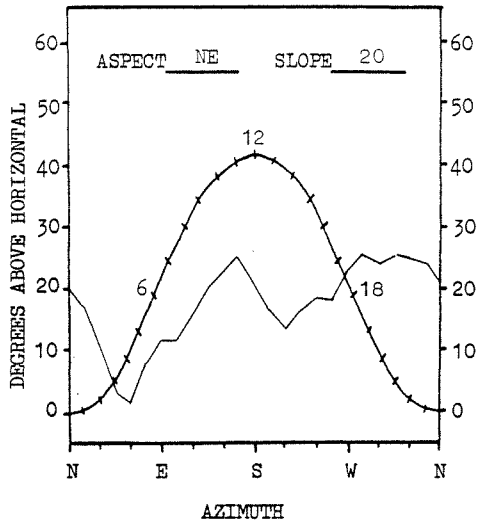

LANDFORM HORIZON (S-215)
WITH +20° SOLAR DECLINATION

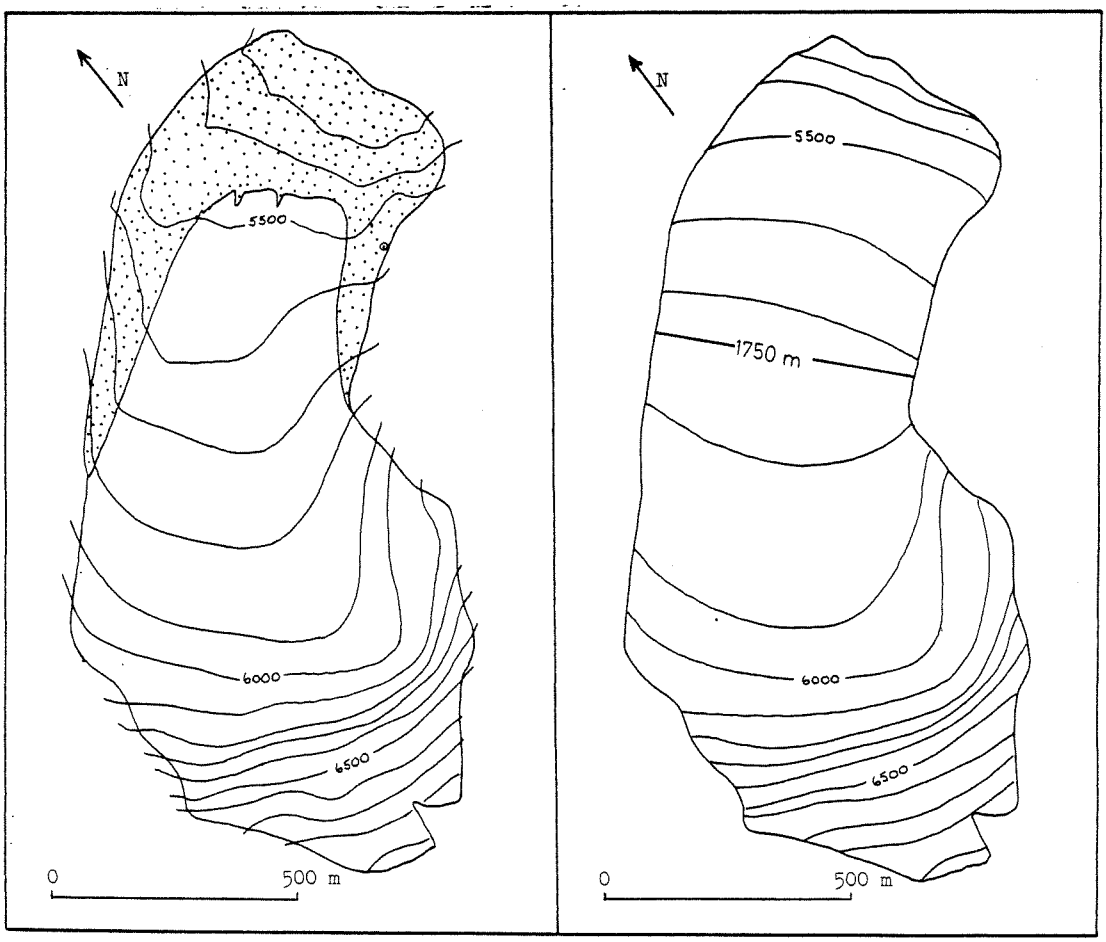

PRESENT ICE SURFACE WITH DEPOSIT

NEOGLACIAL MAXIMUM SURFACE

APPENDIX B. PHYSICAL INVENTORY (Musk-Ox Glacier, no. 28)

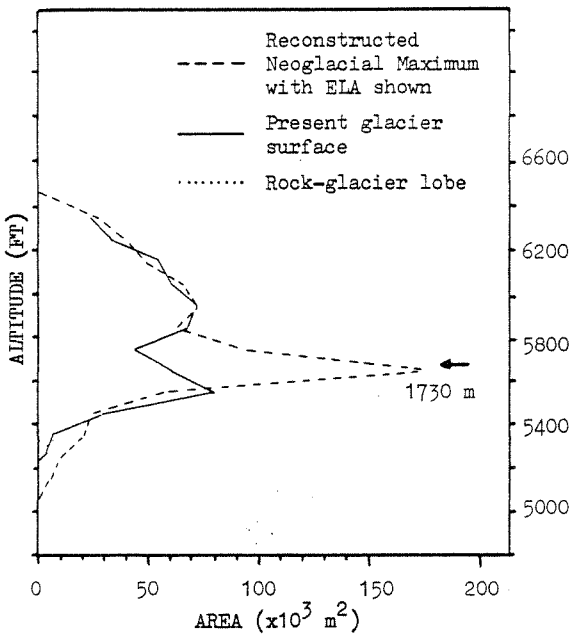

NEOGLACIAL MAXIMUM AND PRESENT AREA-ALTITUDE DISTRIBUTIONS

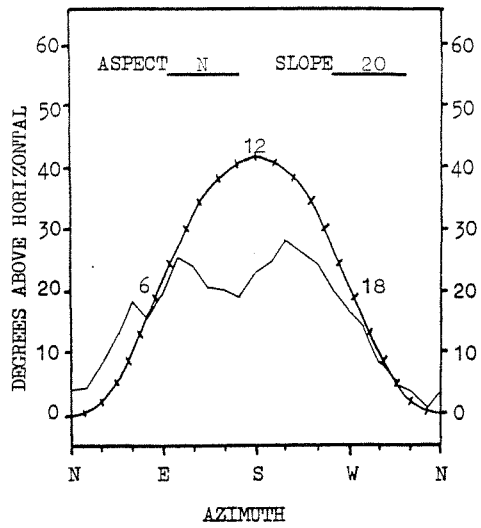

LANDFORM HORIZON (S- 216) WITH +20° SOLAR DECLINATION

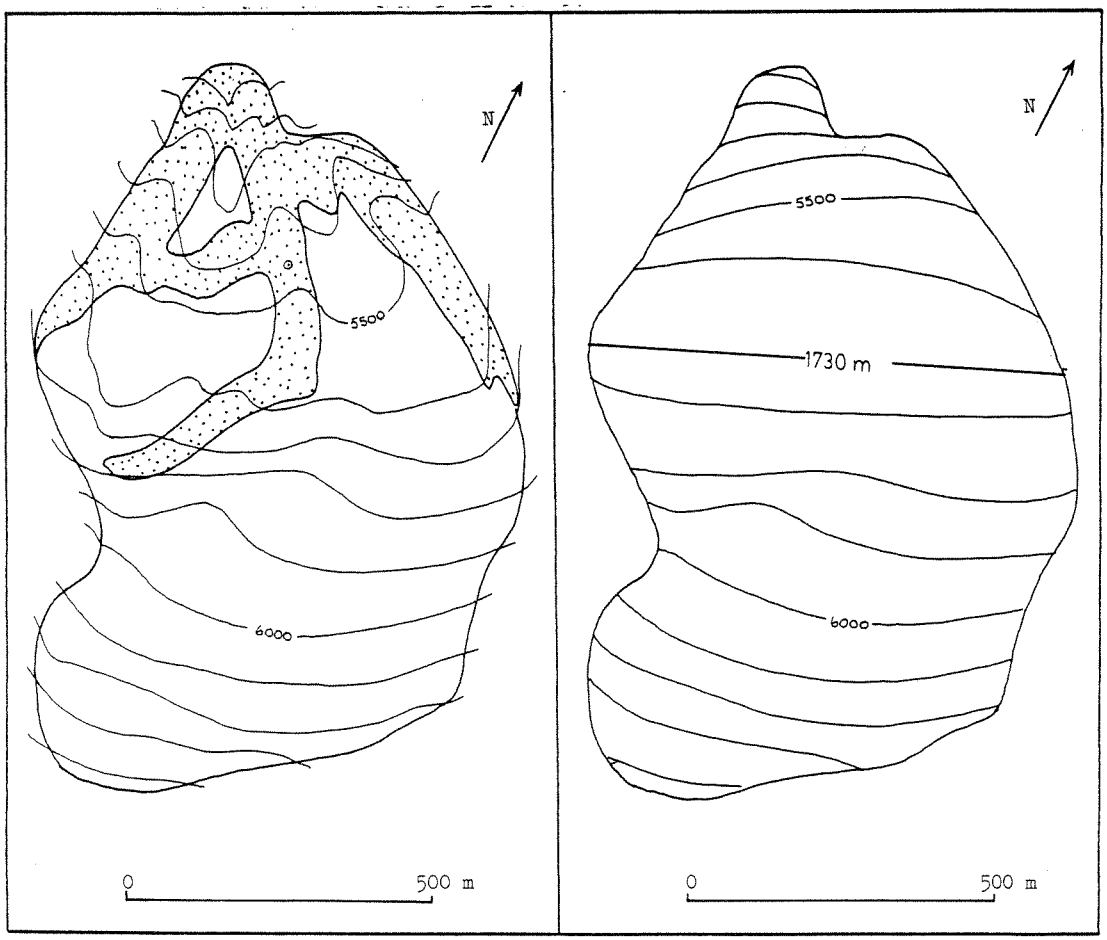

PRESENT ICE SURFACE WITH DEPOSIT

NEOGLACIAL MAXIMUM SURFACE

APPENDIX B. PHYSICAL INVENTORY (Arctic Tern Glacier, no. 29)

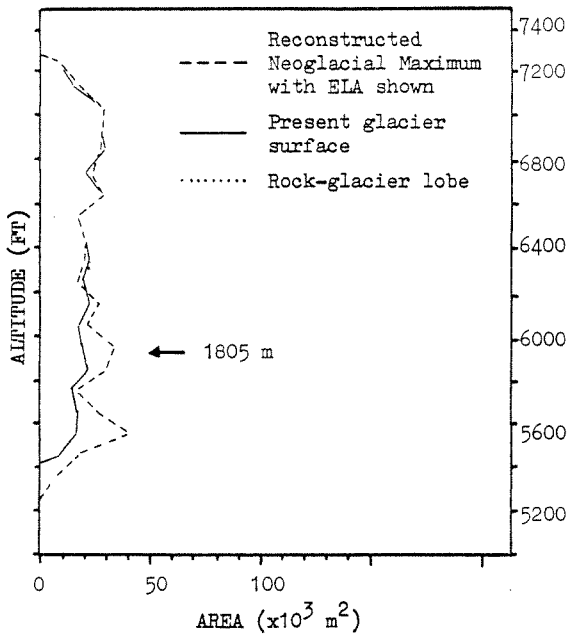

NEOGLACIAL MAXIMUM AND PRESENT AREA-ALTITUDE DISTRIBUTIONS

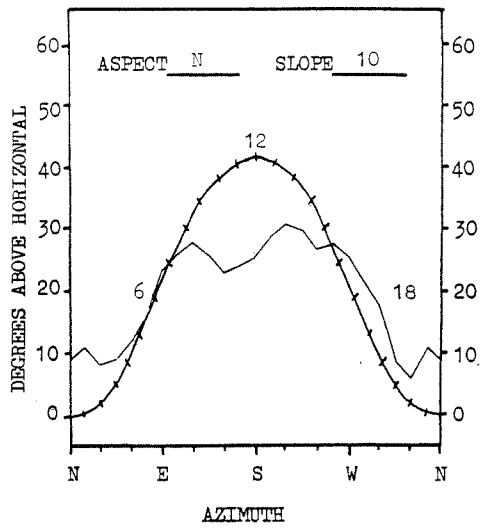

LANDFORM HORIZON (S- 218) WITH +20° SOLAR DECLINATION

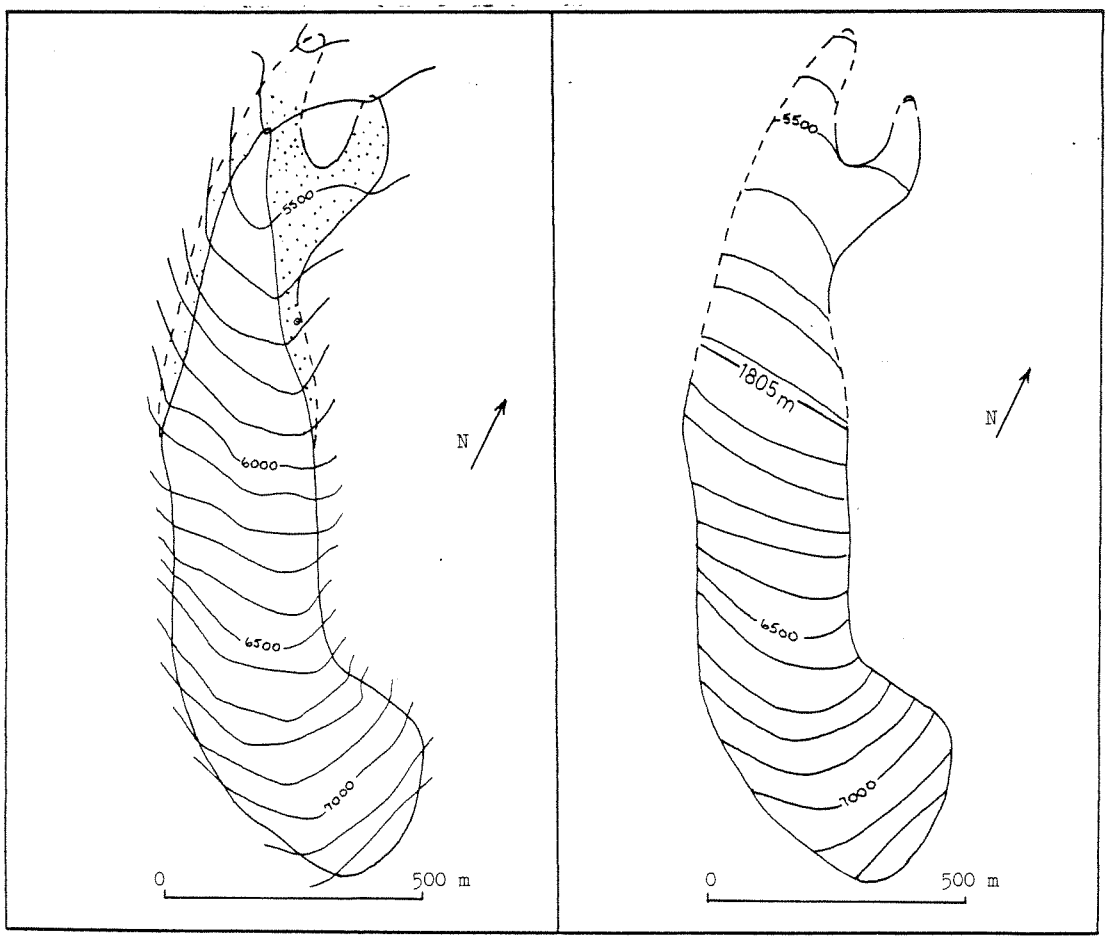

PRESENT ICE SURFACE WITH DEPOSIT

NEOGLACIAL MAXIMUM SURFACE

APPENDIX B. PHYSICAL INVENTORY (Snowy Owl West, no. 30)

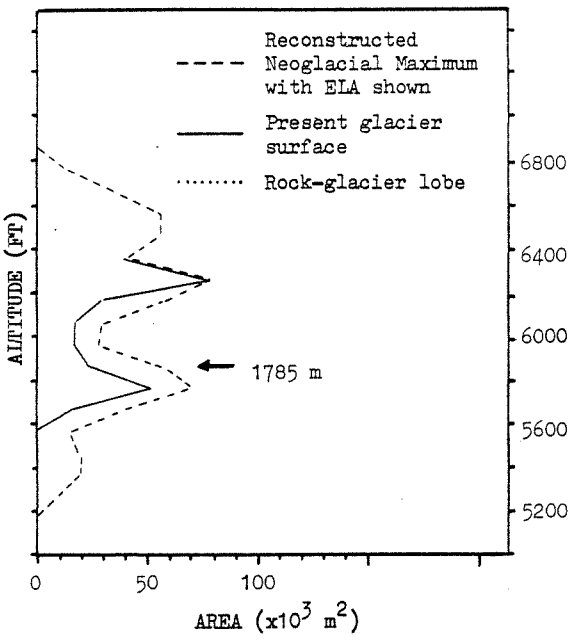

NEOGLACIAL MAXIMUM AND PRESENT AREA-ALTITUDE DISTRIBUTIONS

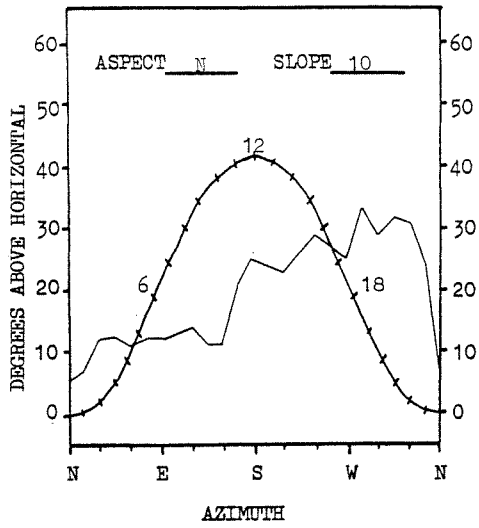

LANDFORM HORIZON (S- 219)
WITH +20° SOLAR DECLINATION

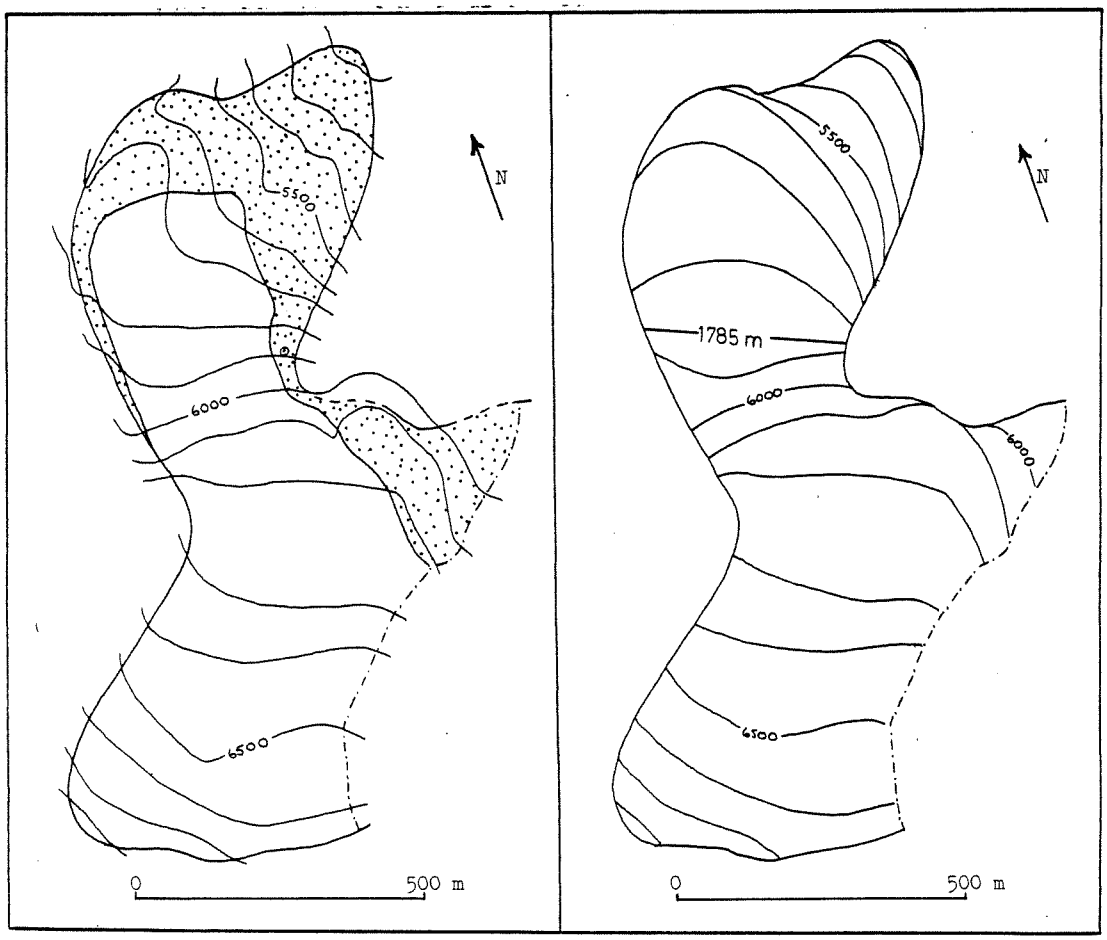

PRESENT ICE SURFACE WITH DEPOSIT

NEOGLACIAL MAXIMUM SURFACE

APPENDIX B. PHYSICAL INVENTORY (Wolf Glacier, no. 31)

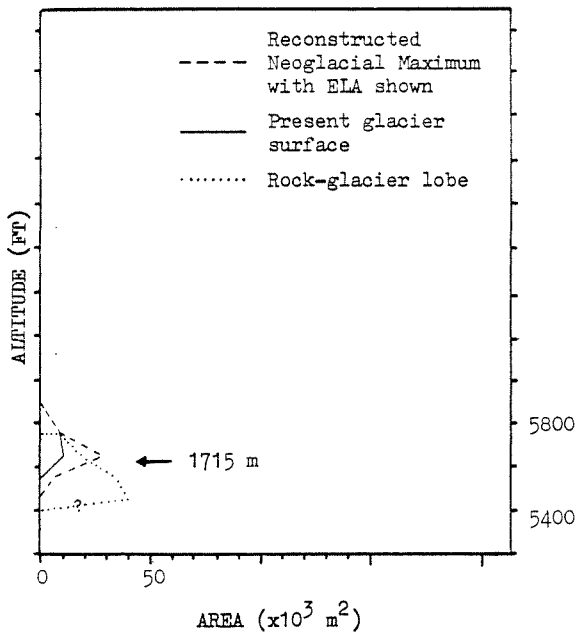

NEOGLACIAL MAXIMUM AND PRESENT AREA-ALTITUDE DISTRIBUTIONS

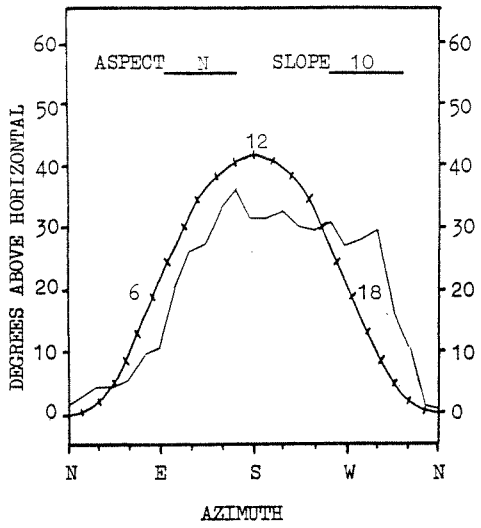

LANDFORM HORIZON (S- 301a) WITH +20° SOLAR DECLINATION

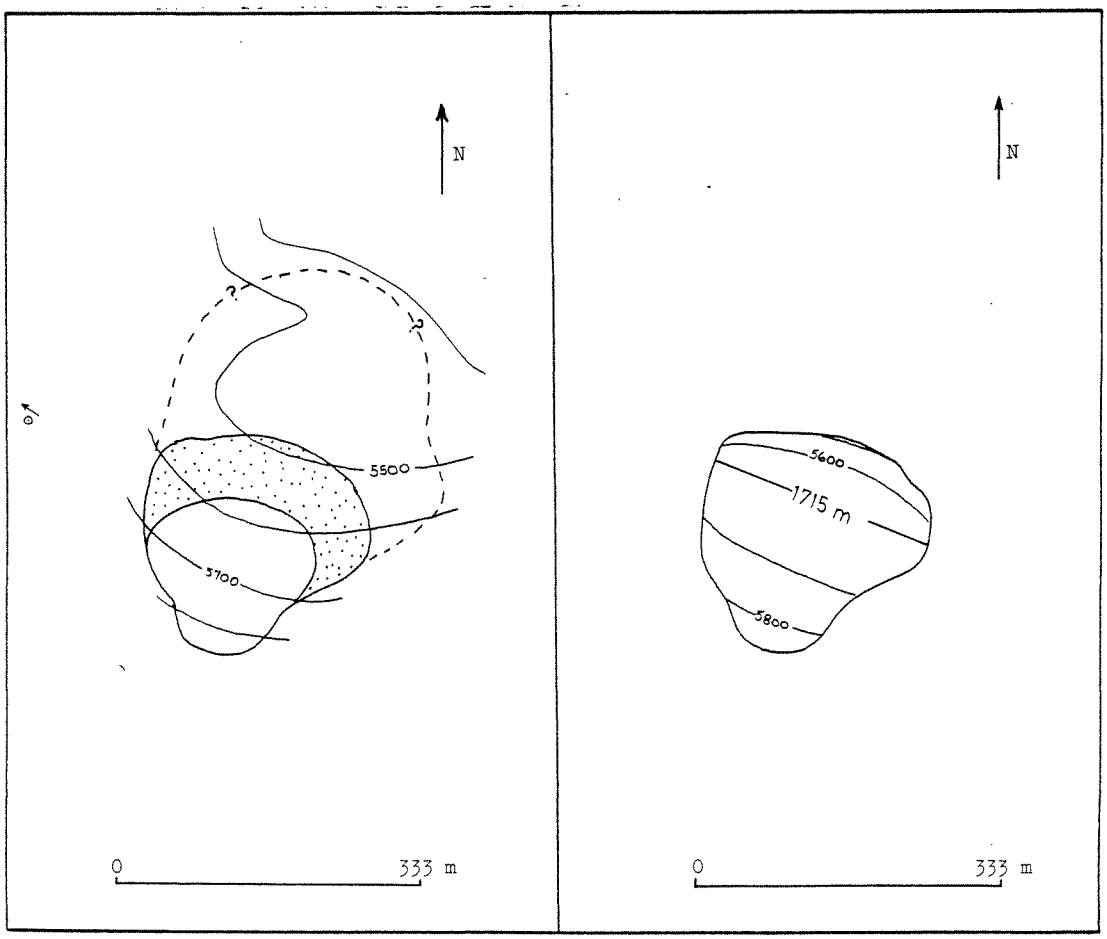

PRESENT ICE SURFACE WITH DEPOSIT

NEOGLACIAL MAXIMUM SURFACE

APPENDIX B. PHYSICAL INVENTORY (Lake Trout Glacier, no. 32)

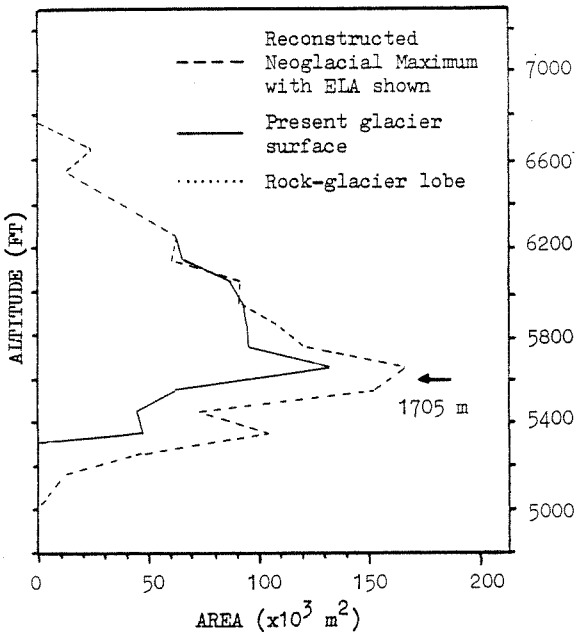

NEOGLACIAL MAXIMUM AND PRESENT AREA-ALTITUDE DISTRIBUTIONS

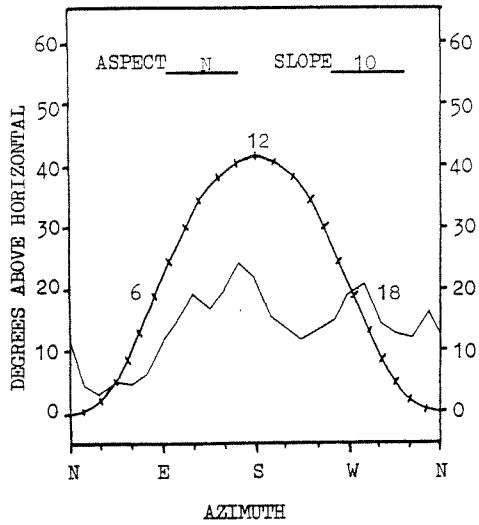

LANDFORM HORIZON (S- 302) WITH +20° SOLAR DECLINATION

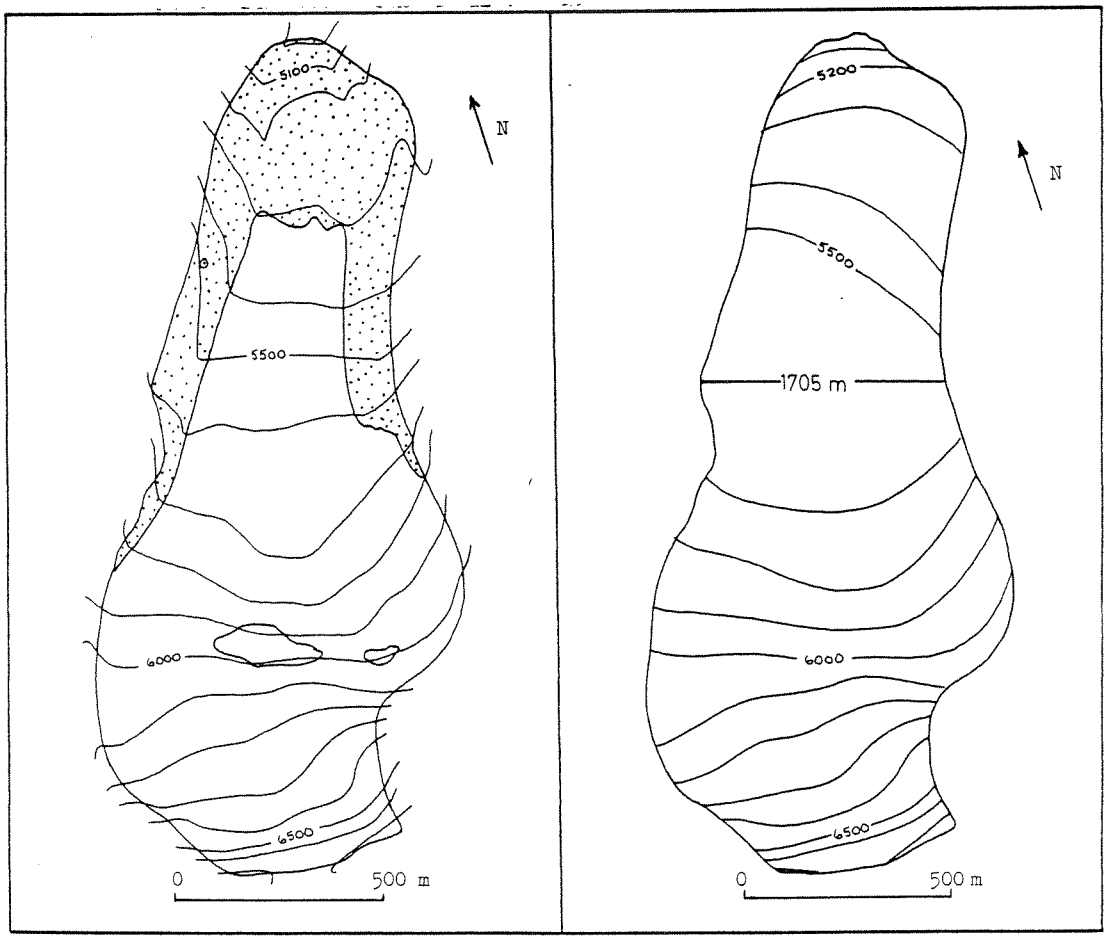

PRESENT ICE SURFACE WITH DEPOSIT

NEOGLACIAL MAXIMUM SURFACE

APPENDIX B. PHYSICAL INVENTORY (Twin Glacier, no. 33)

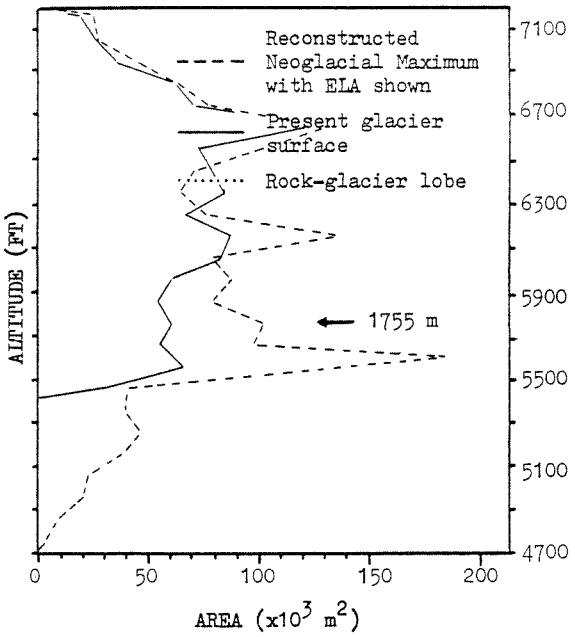

NEOGLACIAL MAXIMUM AND PRESENT
AREA-ALTITUDE DISTRIBUTIONS

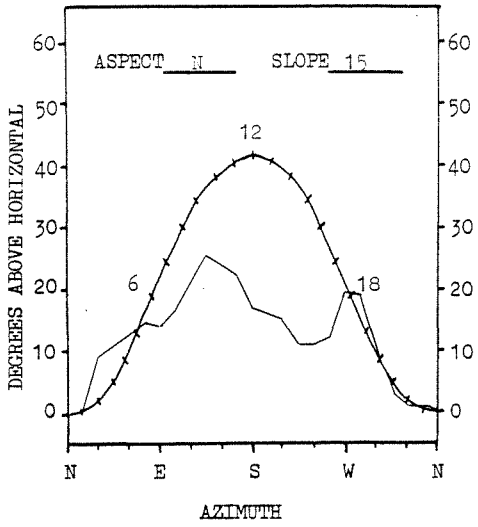

LANDFORM HORIZON (S- 303b)
WITH +20° SOLAR DECLINATION

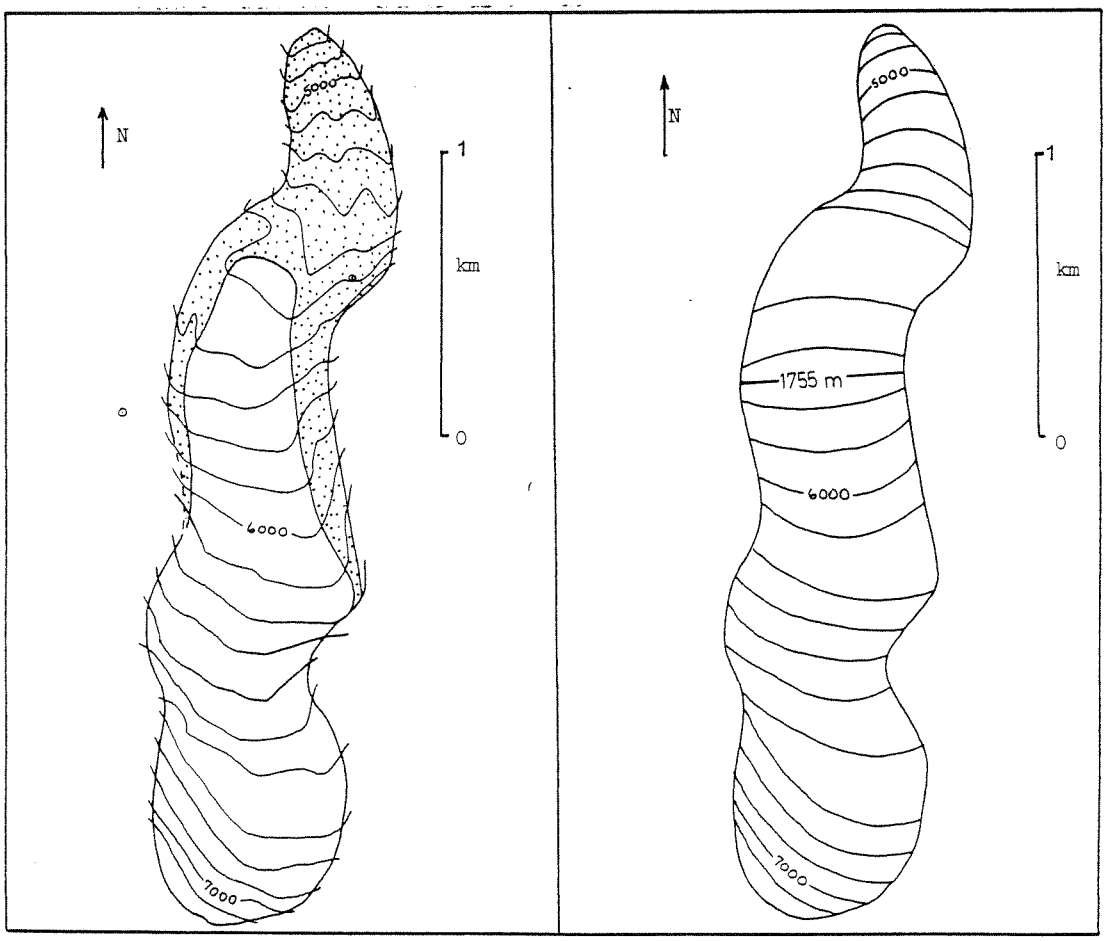

PRESENT ICE SURFACE WITH DEPOSIT

NEOGLACIAL MAXIMUM SURFACE

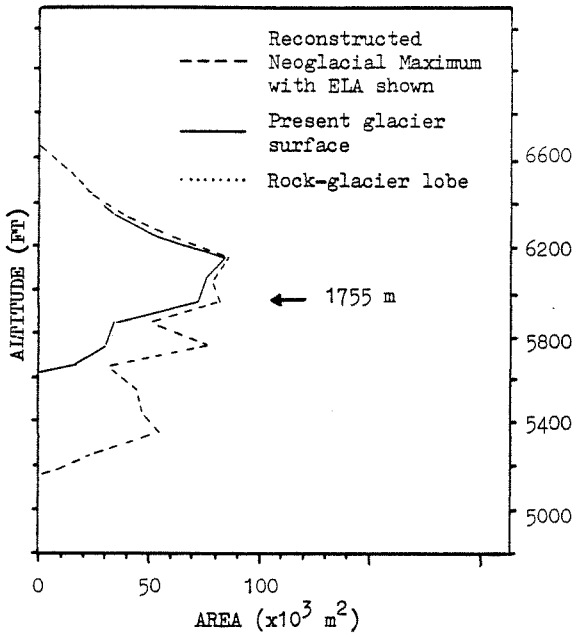

NEOGLACIAL MAXIMUM AND PRESENT AREA-ALTITUDE DISTRIBUTIONS

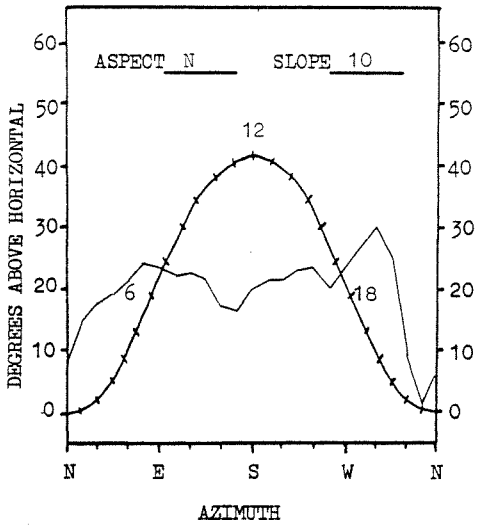

LANDFORM HORIZON (S- 304b) WITH +20° SOLAR DECLINATION

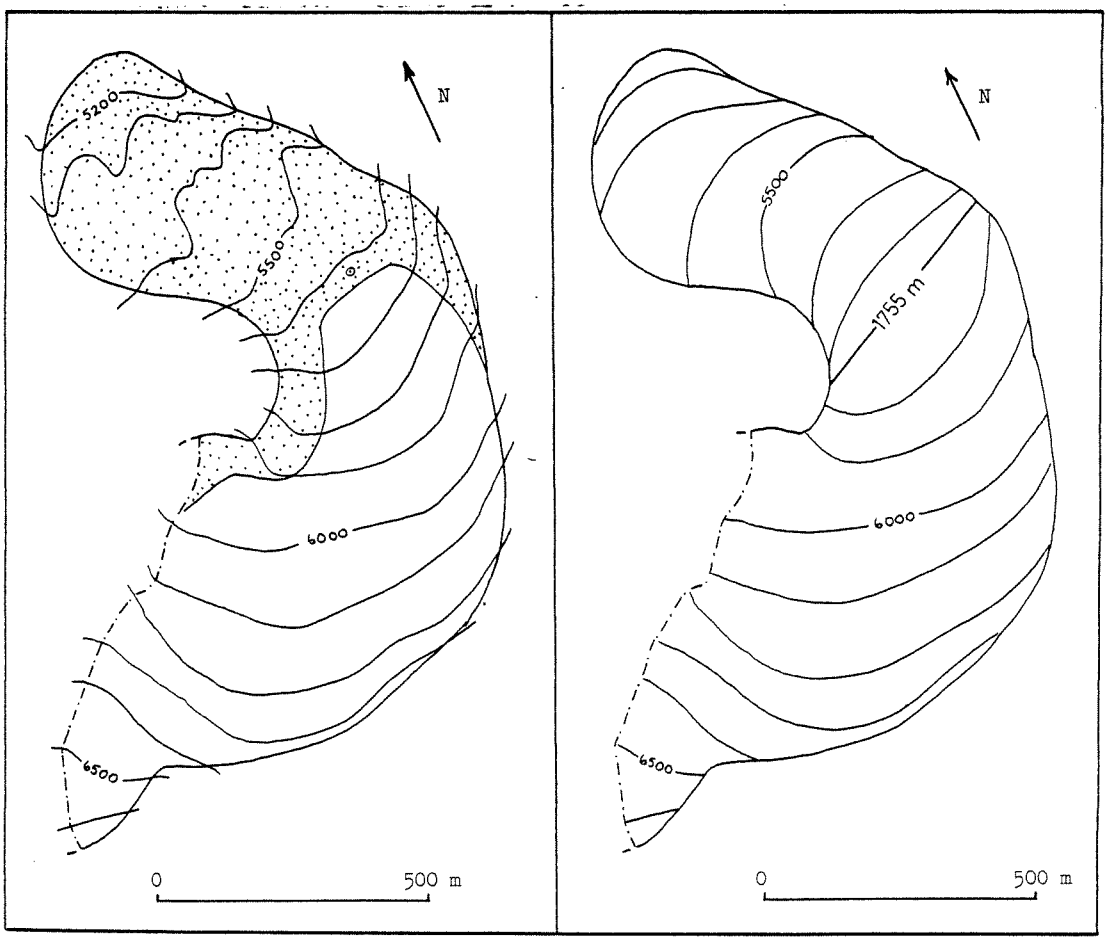

PRESENT ICE SURFACE WITH DEPOSIT

NEOGLACIAL MAXIMUM SURFACE

APPENDIX B. PHYSICAL INVENTORY (Harlequin Duck Rock Glacier, no. 35)

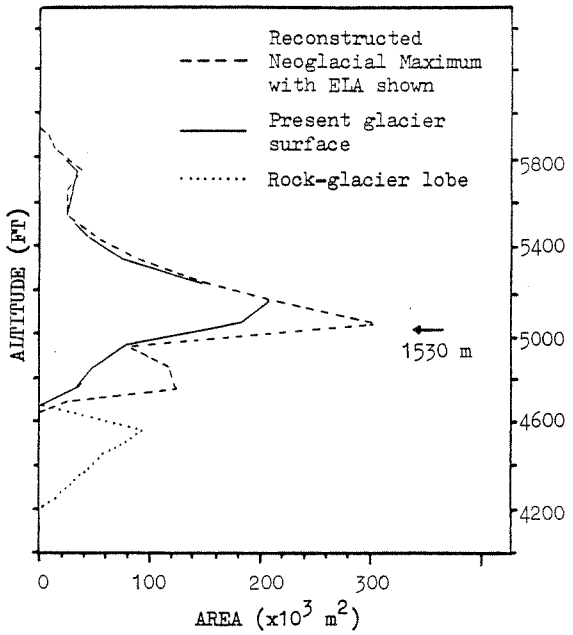

NEOGLACIAL MAXIMUM AND PRESENT AREA-ALTITUDE DISTRIBUTIONS

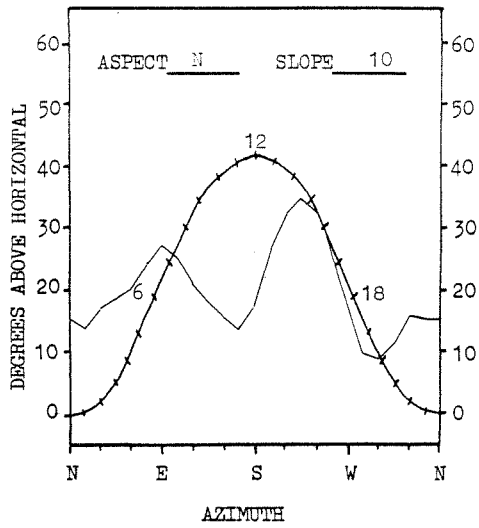

LANDFORM HORIZON (S- 401a) WITH +20° SOLAR DECLINATION

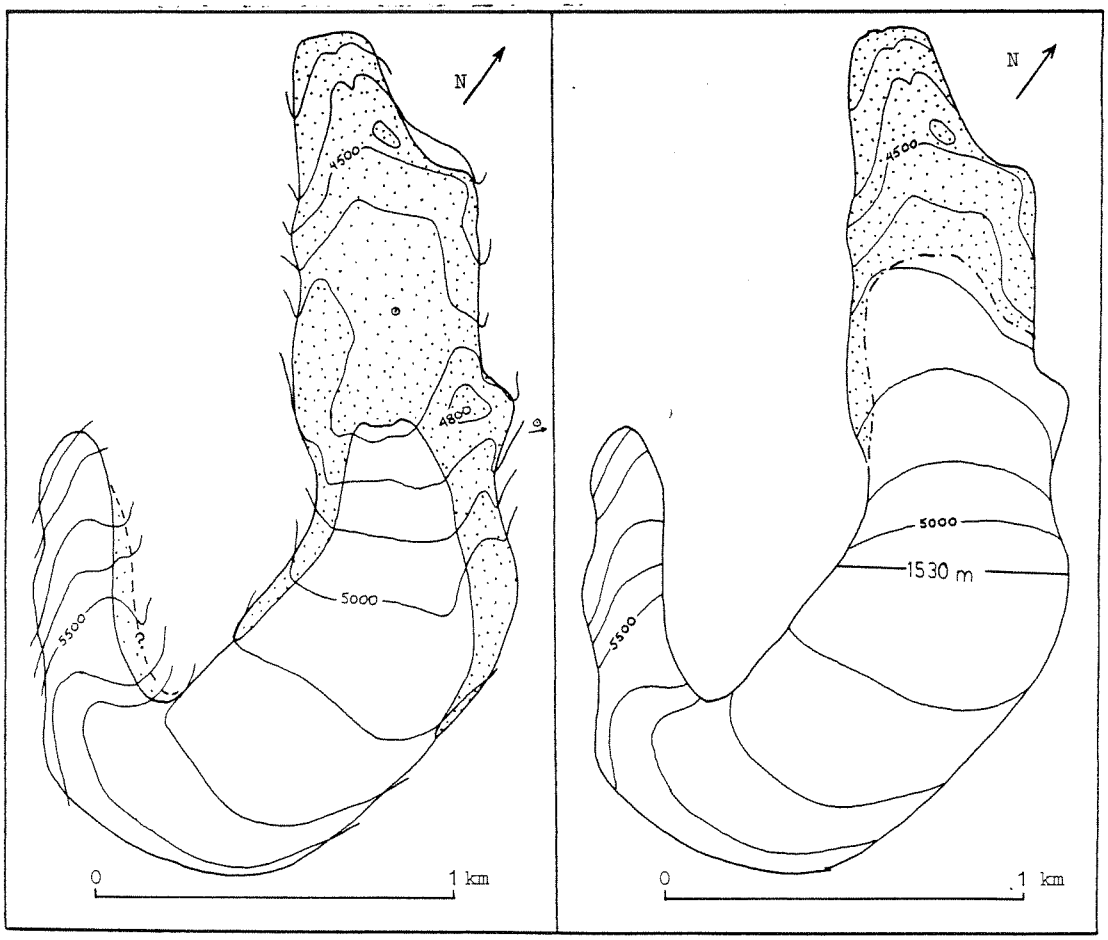

PRESENT ICE SURFACE WITH DEPOSIT

NEOGLACIAL MAXIMUM SURFACE

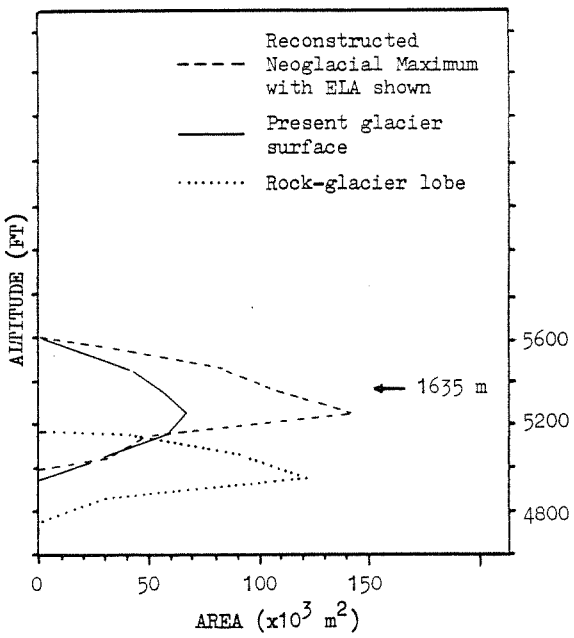

NEOGLACIAL MAXIMUM AND PRESENT AREA-ALTITUDE DISTRIBUTIONS

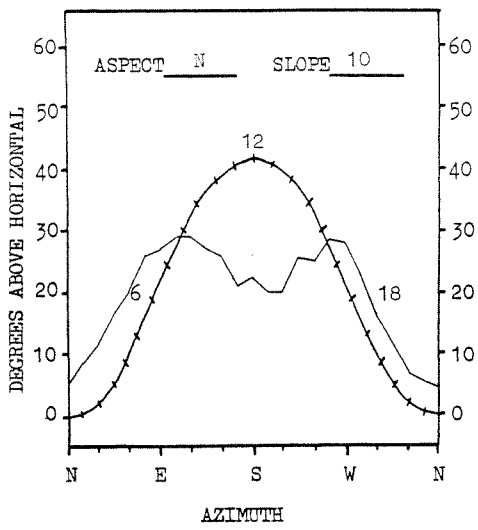

LANDFORM HORIZON (S- 402)
WITH +20° SOLAR DECLINATION

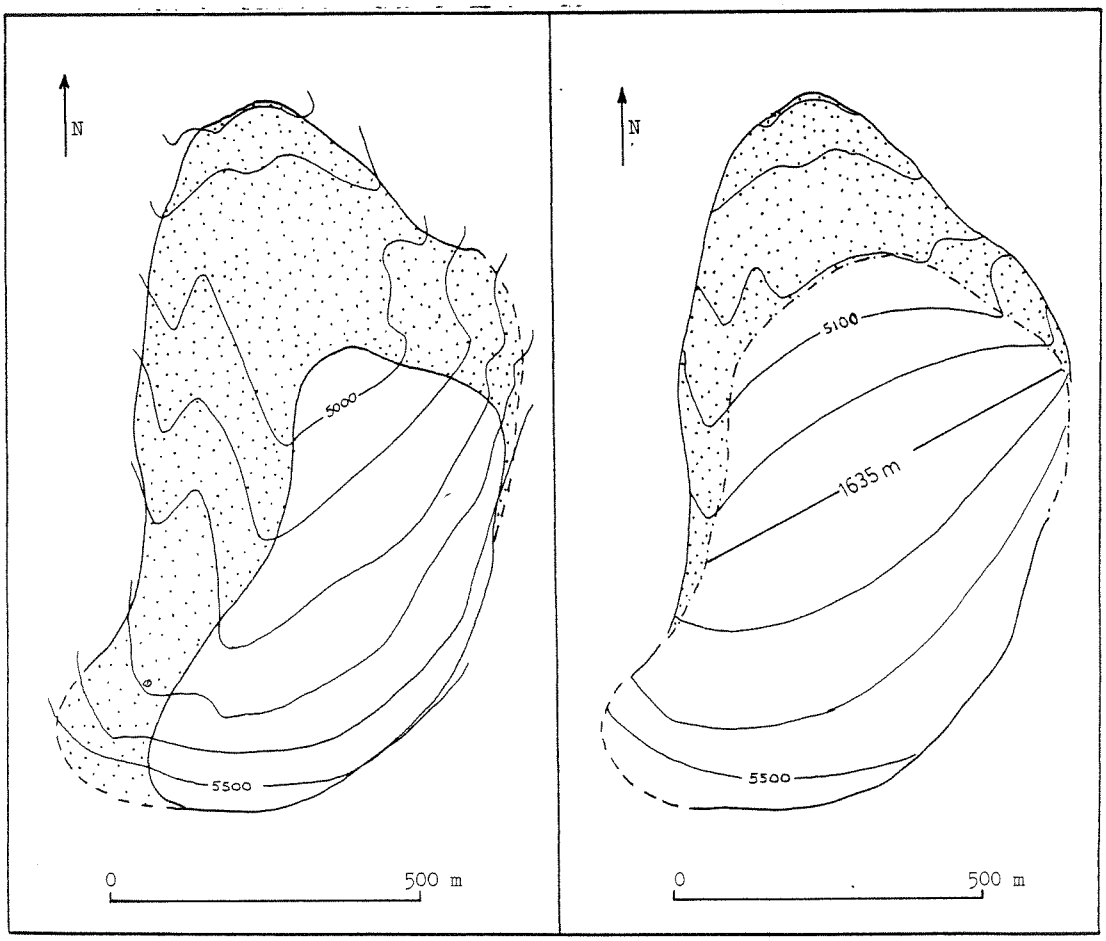

PRESENT ICE SURFACE WITH DEPOSIT

NEOGLACIAL MAXIMUM SURFACE

APPENDIX B. PHYSICAL INVENTORY (Pika Rock Glacier, no. 37)

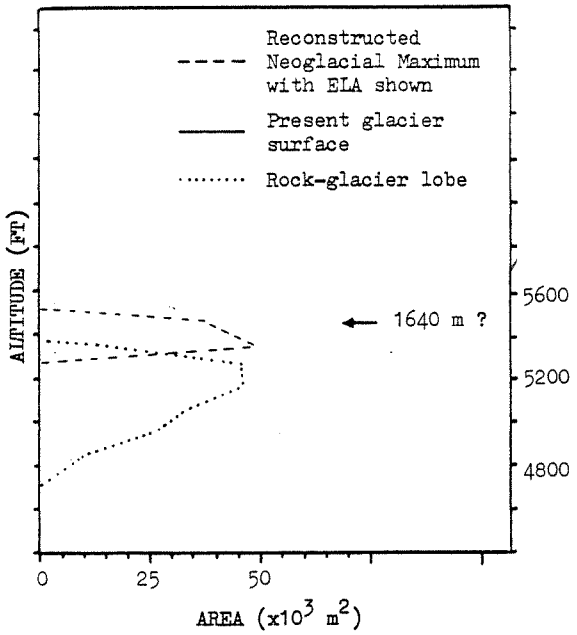

NEOGLACIAL MAXIMUM AND PRESENT AREA-ALTITUDE DISTRIBUTIONS

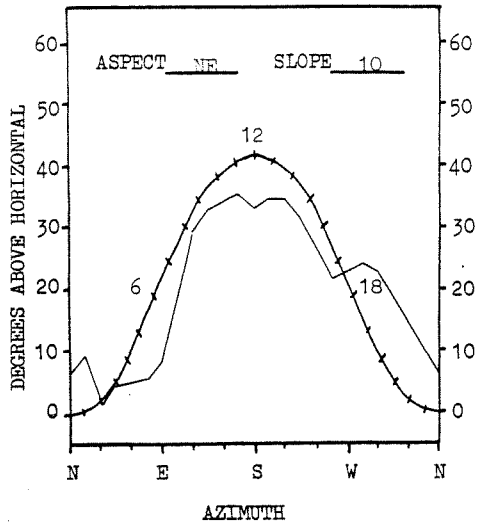

LANDFORM HORIZON (S- 403a) WITH +20° SOLAR DECLINATION

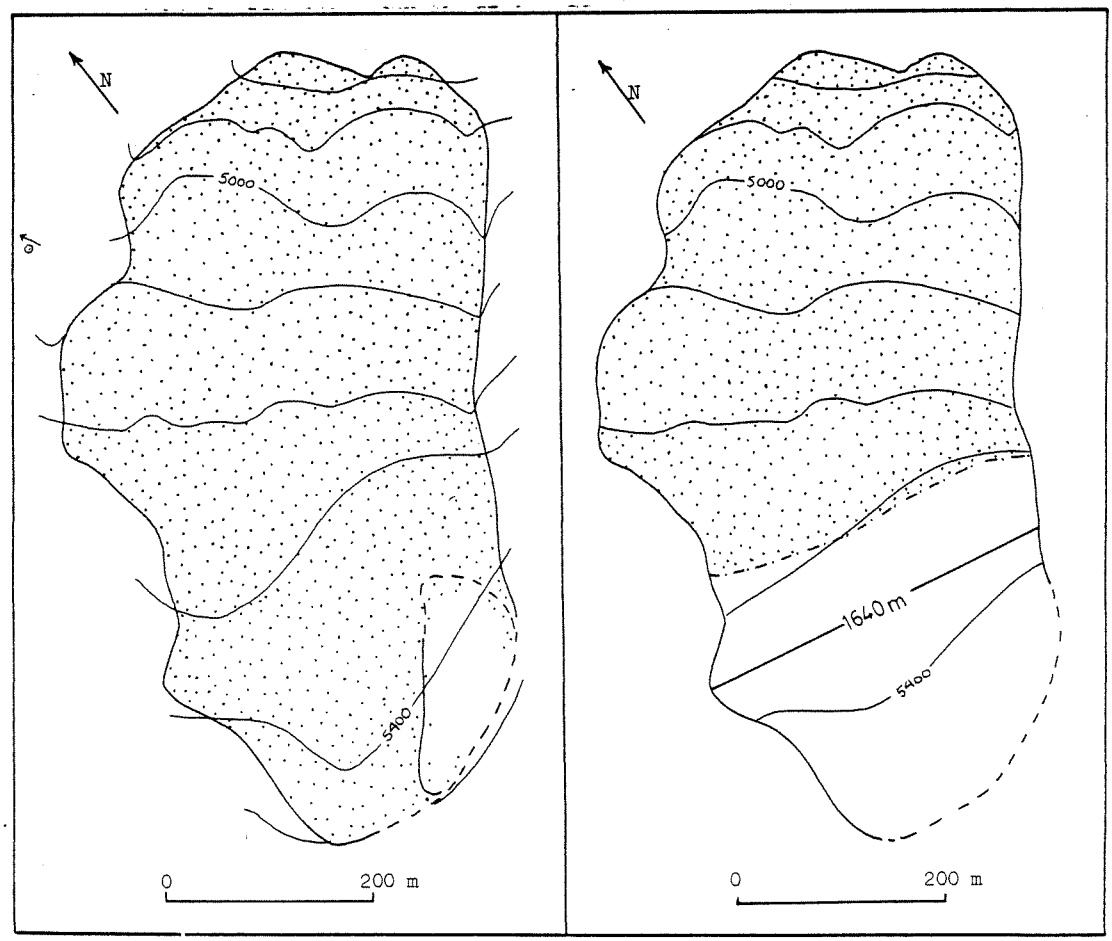

PRESENT ICE SURFACE WITH DEPOSIT

NEOGLACIAL MAXIMUM SURFACE

APPENDIX B. PHYSICAL INVENTORY (Jaeger Rock Glacier, no. 38)

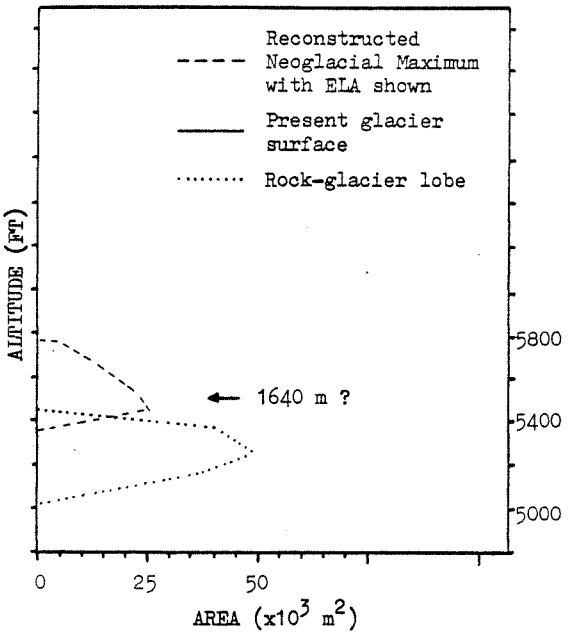

NEOGLACIAL MAXIMUM AND PRESENT AREA-ALTITUDE DISTRIBUTIONS

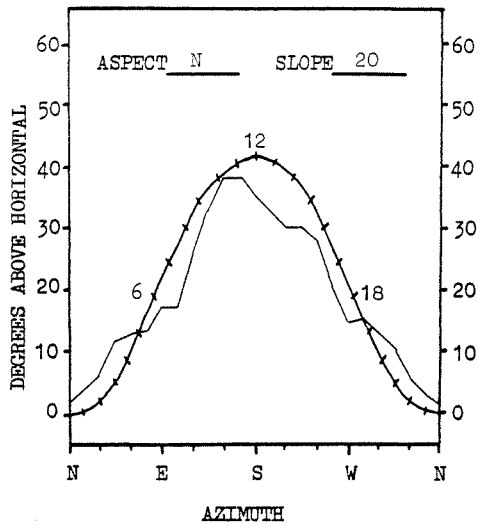

LANDFORM HORIZON (S- 404a) WITH +20° SOLAR DECLINATION

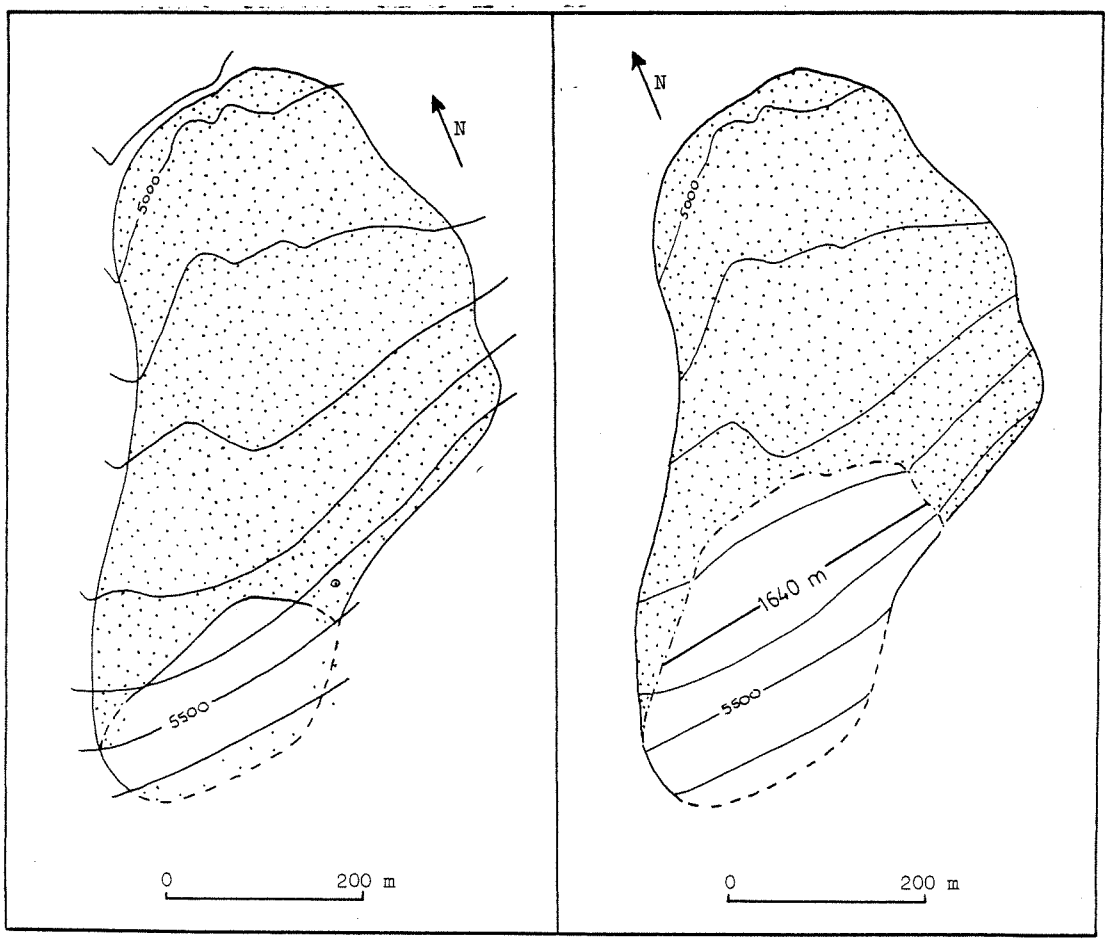

PRESENT ICE SURFACE WITH DEPOSIT

NEOGLACIAL MAXIMUM SURFACE

APPENDIX B. PHYSICAL INVENTORY (Parka Squirrel Rock Glacier, no. 39)

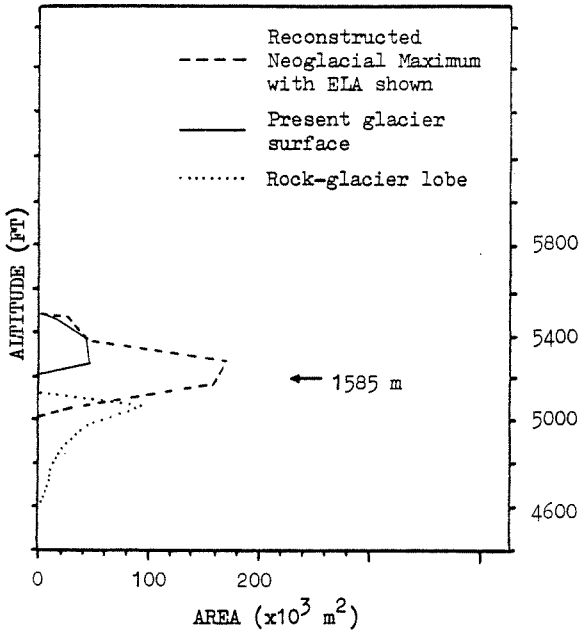

NEOGLACIAL MAXIMUM AND PRESENT AREA-ALTITUDE DISTRIBUTIONS

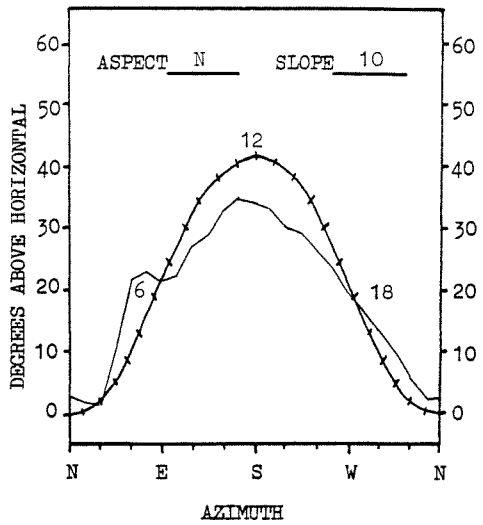

LANDFORM HORIZON (S- 405a) WITH +20° SOLAR DECLINATION

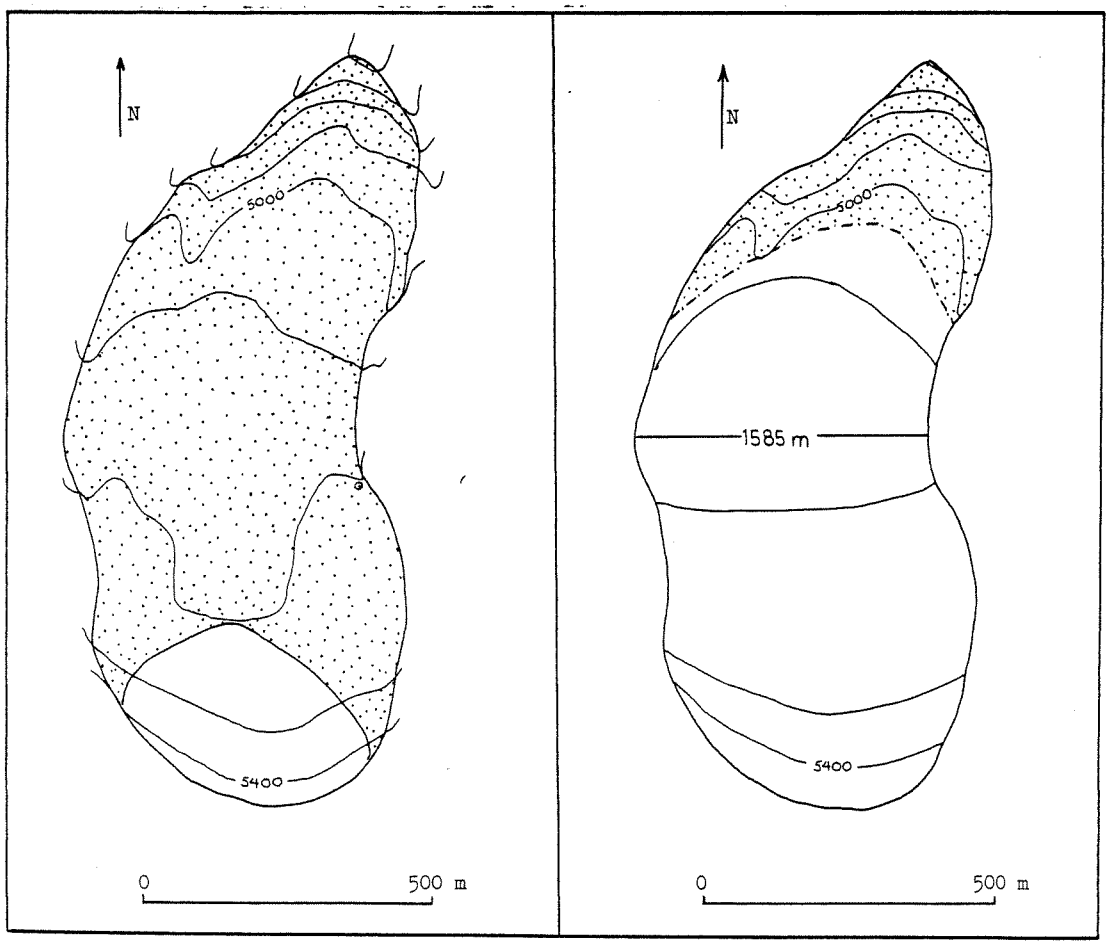

PRESENT ICE SURFACE WITH DEPOSIT

NEOGLACIAL MAXIMUM SURFACE

APPENDIX B. PHYSICAL INVENTORY (Mosquito Rock Glacier, no. 40)

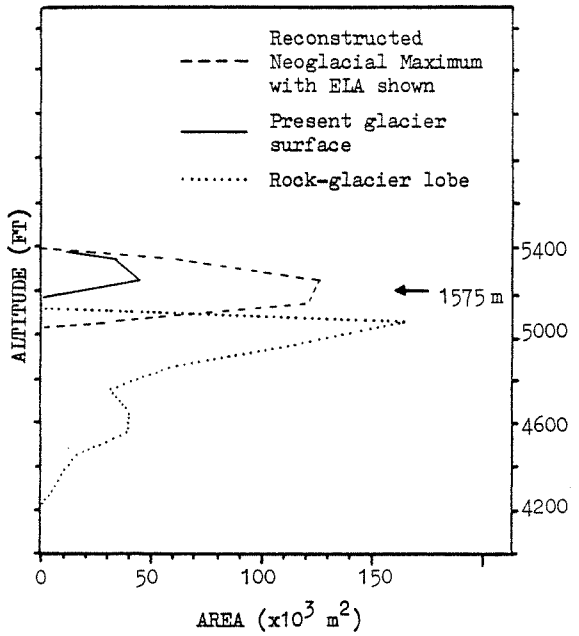

NEOGLACIAL MAXIMUM AND PRESENT AREA-ALTITUDE DISTRIBUTIONS

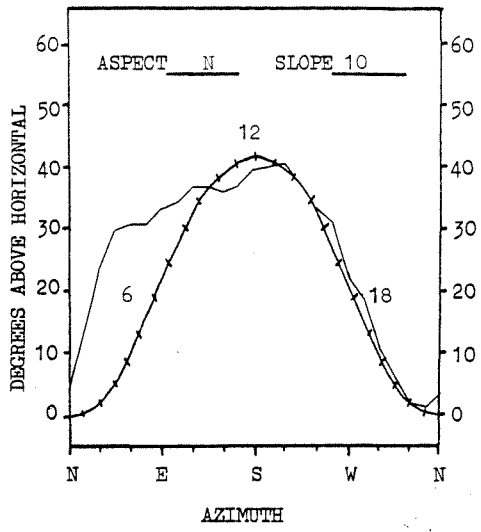

LANDFORM HORIZON (S- 406a) WITH +20° SOLAR DECLINATION

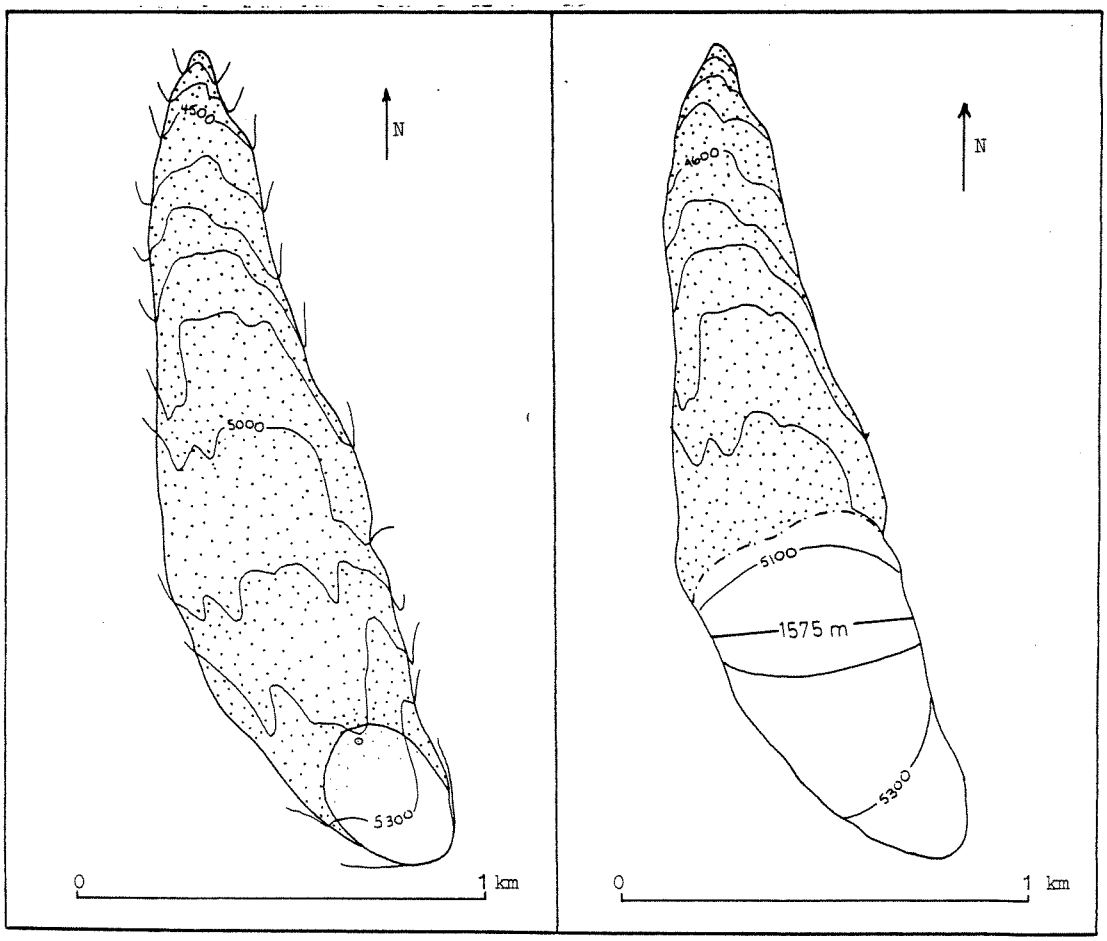

PRESENT ICE SURFACE WITH DEPOSIT

NEOGLACIAL MAXIMUM SURFACE

APPENDIX B. PHYSICAL INVENTORY (Wolverine Glacier, no. 41)

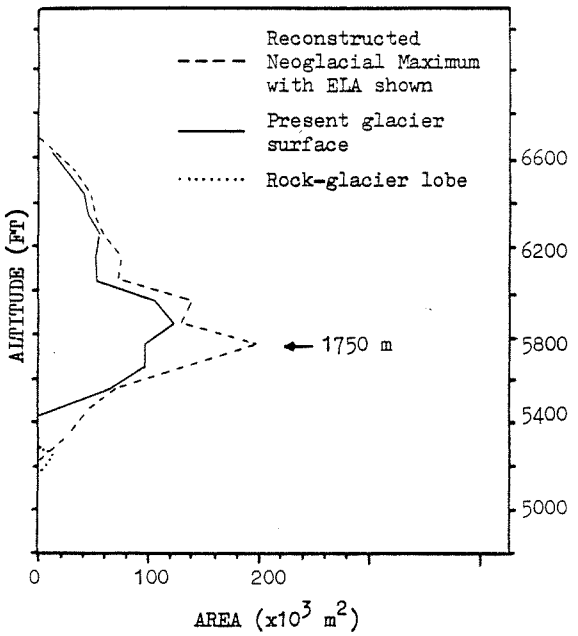

NEOGLACIAL MAXIMUM AND PRESENT AREA-ALTITUDE DISTRIBUTIONS

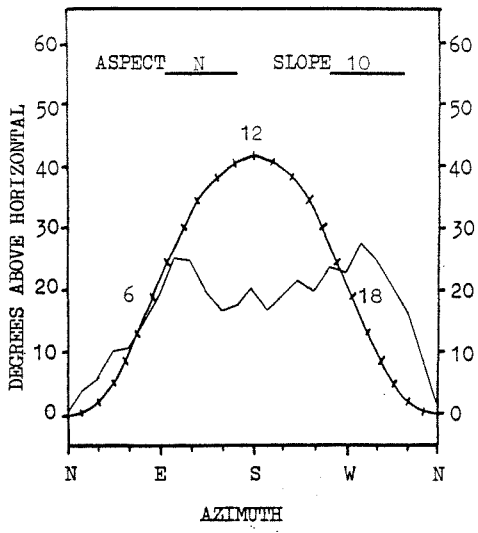

LANDFORM HORIZON (S- 407a) WITH +20° SOLAR DECLINATION

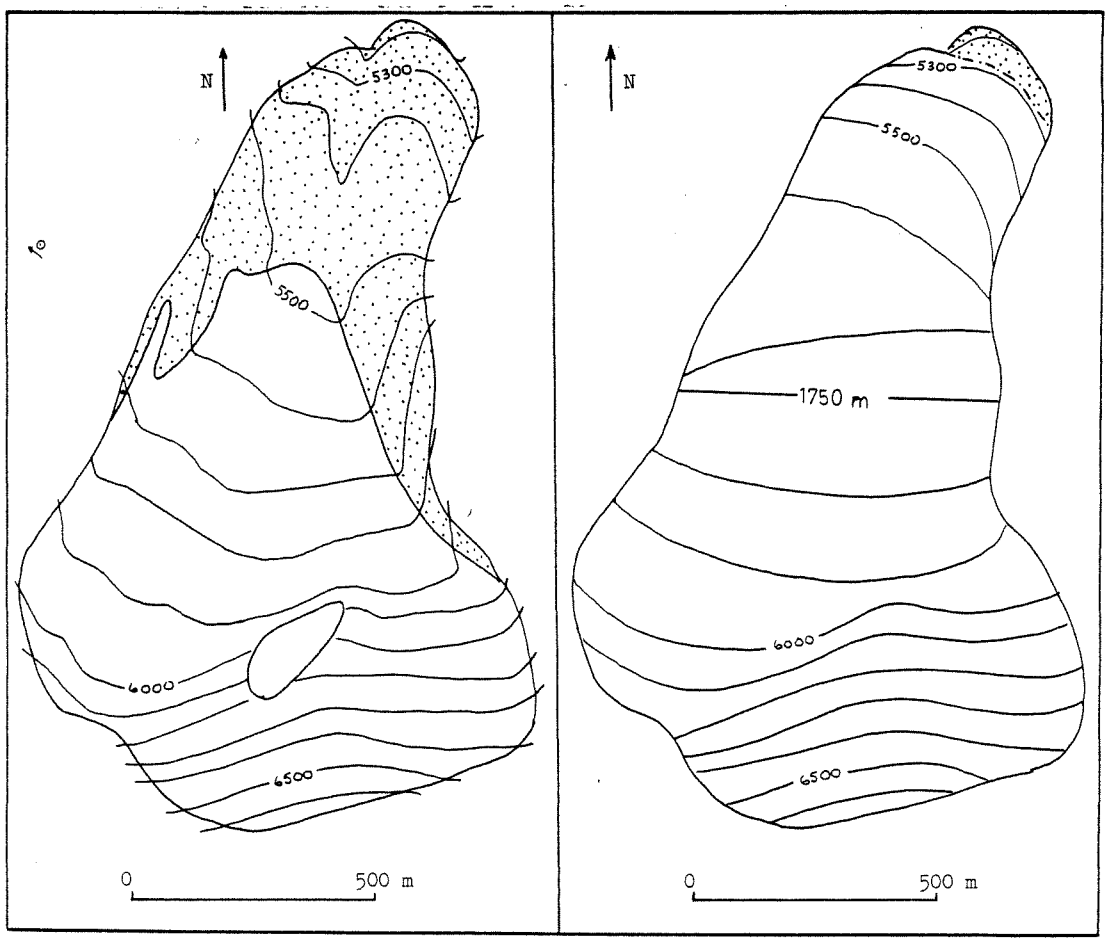

PRESENT ICE SURFACE WITH DEPOSIT

NEOGLACIAL MAXIMUM SURFACE

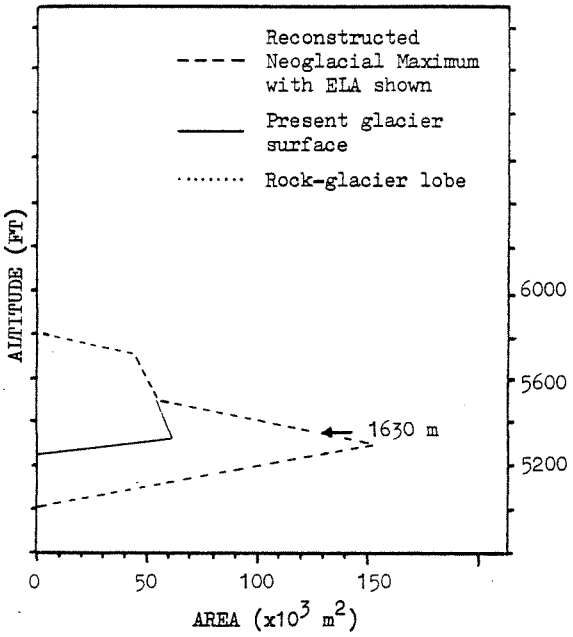

NEOGLACIAL MAXIMUM AND PRESENT AREA-ALTITUDE DISTRIBUTIONS

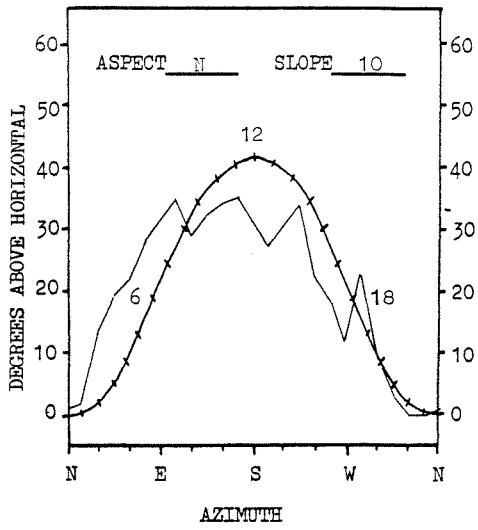

LANDFORM HORIZON (S- 305)
WITH +20° SOLAR DECLINATION

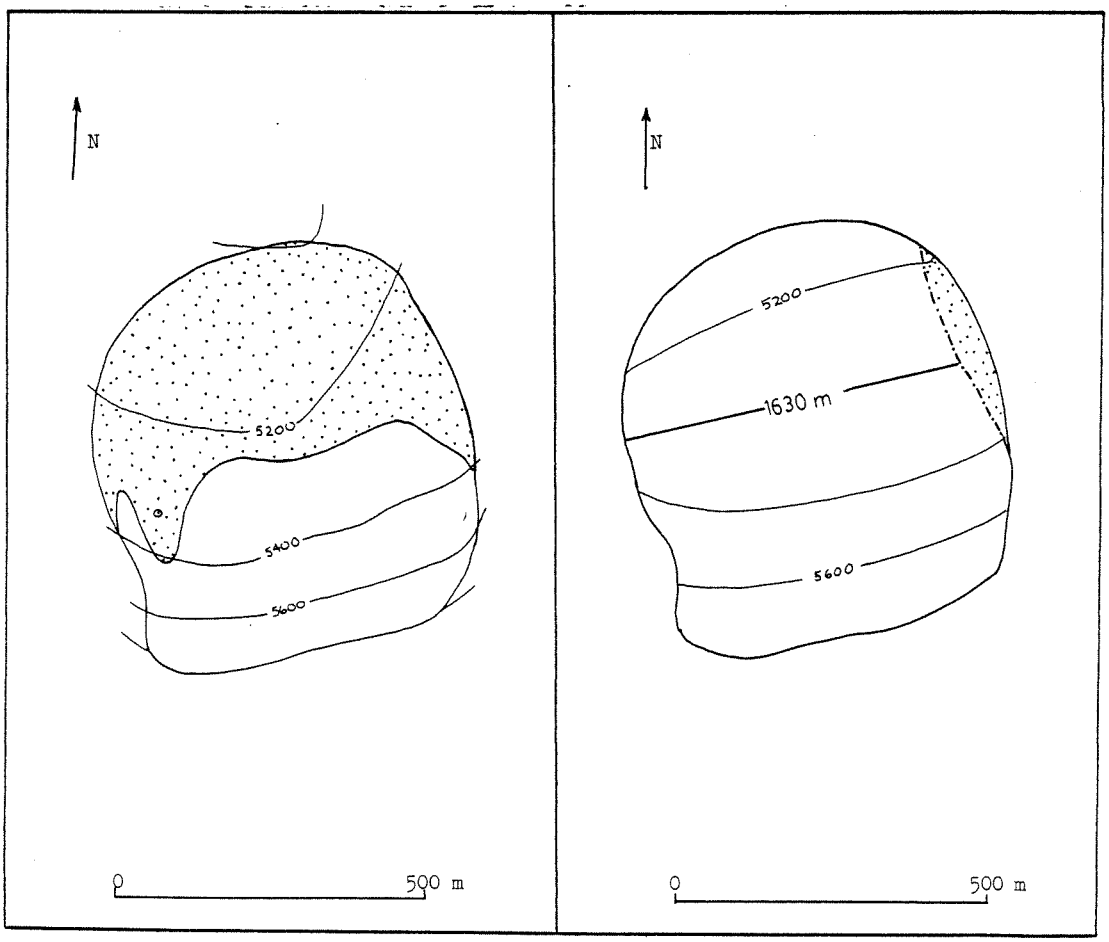

PRESENT ICE SURFACE WITH DEPOSIT

NEOGLACIAL MAXIMUM SURFACE

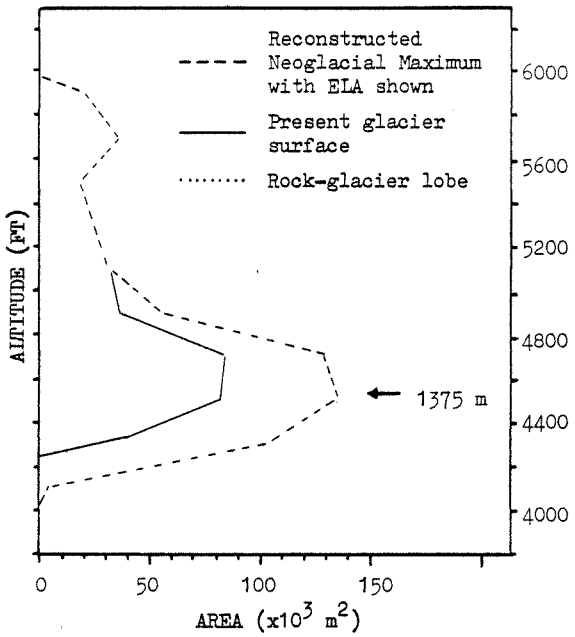

NEOGLACIAL MAXIMUM AND PRESENT AREA-ALTITUDE DISTRIBUTIONS

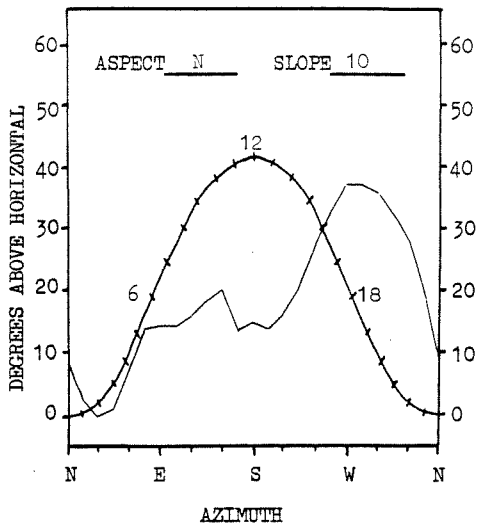

LANDFORM HORIZON (S- 113) WITH +20° SOLAR DECLINATION

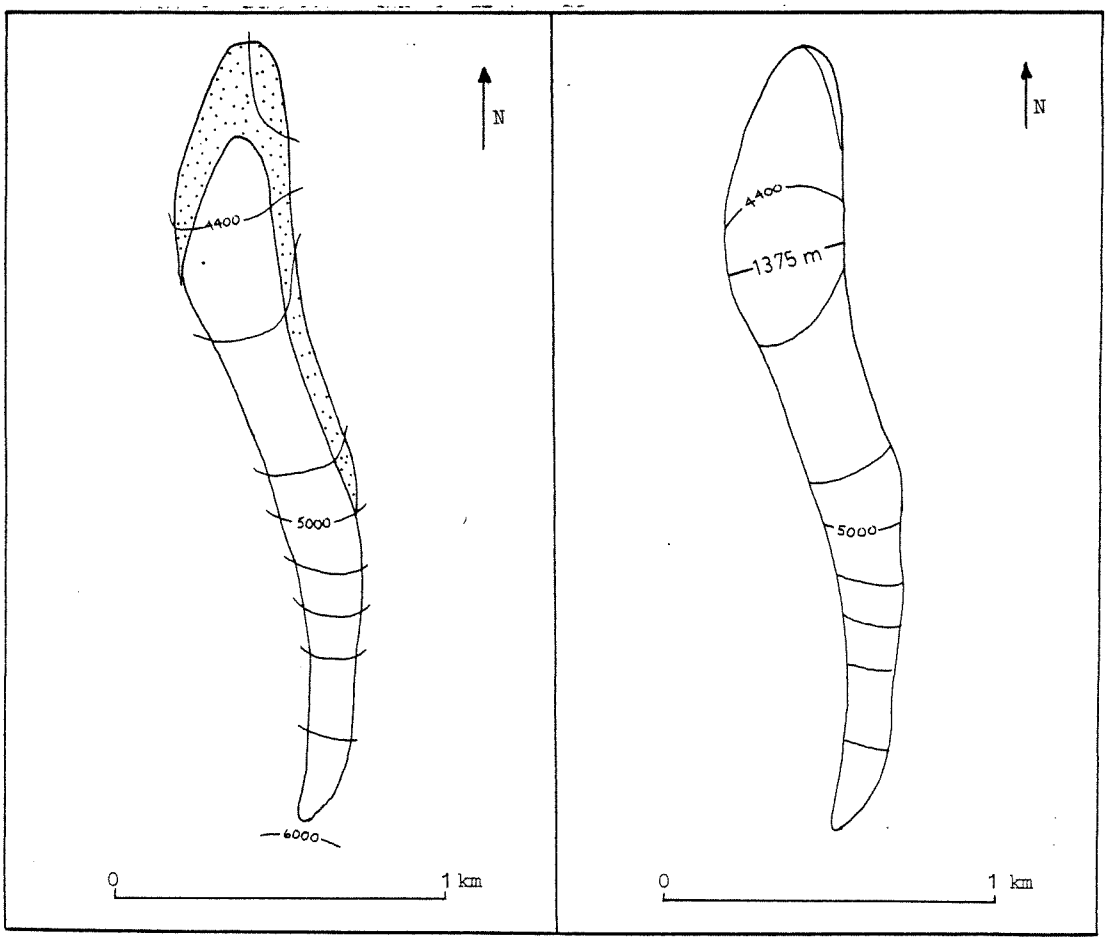

PRESENT ICE SURFACE WITH DEPOSIT

NEOGLACIAL MAXIMUM SURFACE

APPENDIX B. PHYSICAL INVENTORY (Arr-9 East, no. 50; Arr-9 West, no. 52)

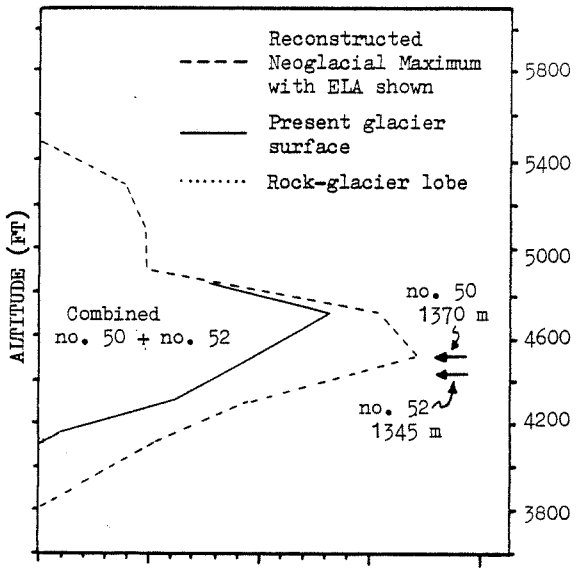

NEOGLACIAL MAXIMUM AND PRESENT AREA-ALTITUDE DISTRIBUTIONS

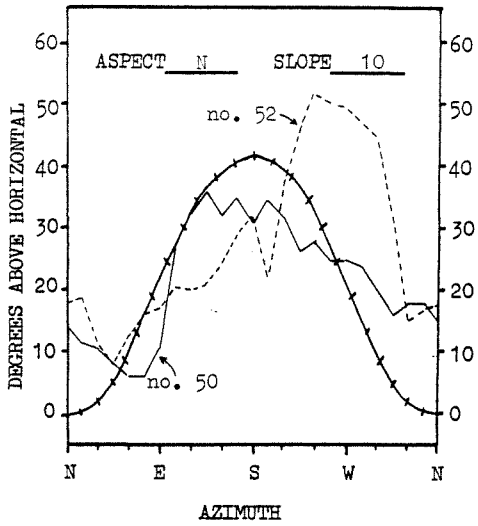

LANDFORM HORIZON (S- 114, 311) WITH +20° SOLAR DECLINATION

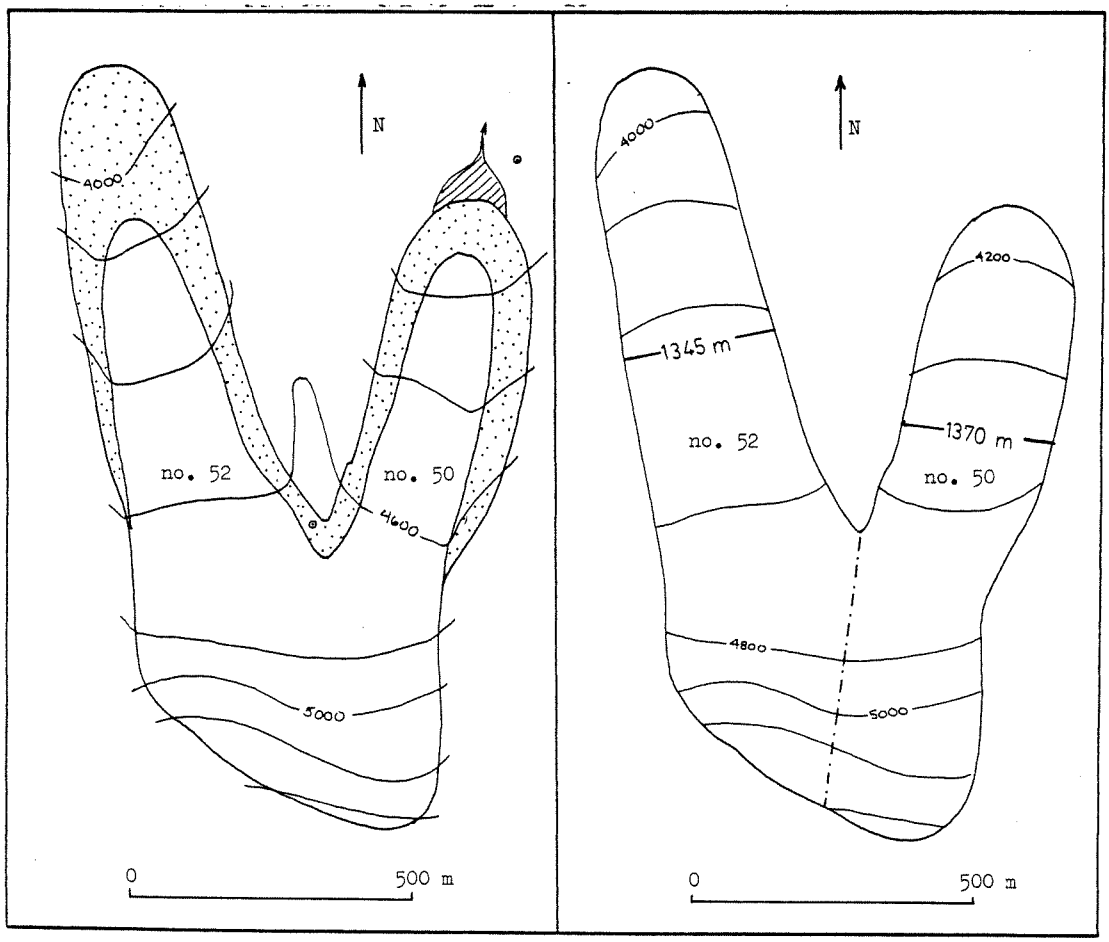

PRESENT ICE SURFACE WITH DEPOSIT

NEOGLACIAL MAXIMUM SURFACE

APPENDIX B. PHYSICAL INVENTORY (Arr-10 West, no. 51; Arr-10 East, no. 53)

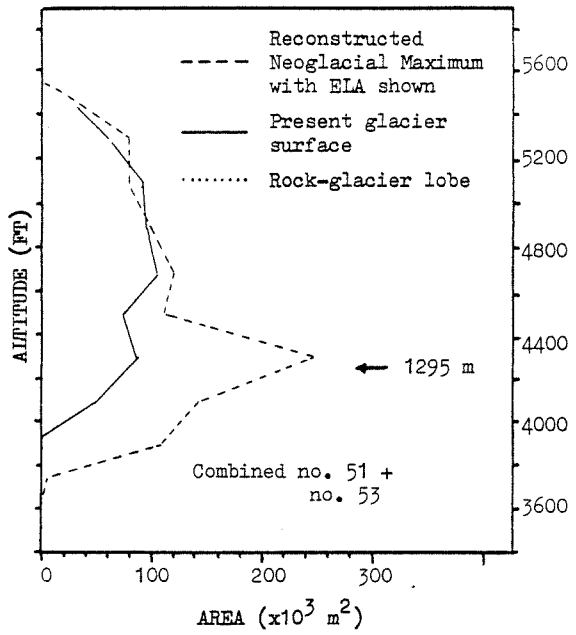

NEOGLACIAL MAXIMUM AND PRESENT AREA-ALTITUDE DISTRIBUTIONS

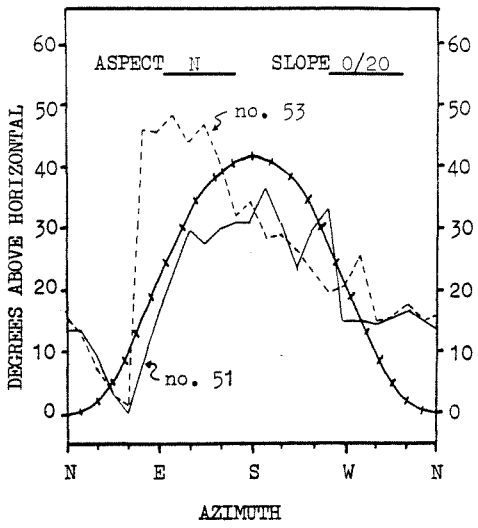

LANDFORM HORIZON (S- 115, 312) WITH +20° SOLAR DECLINATION

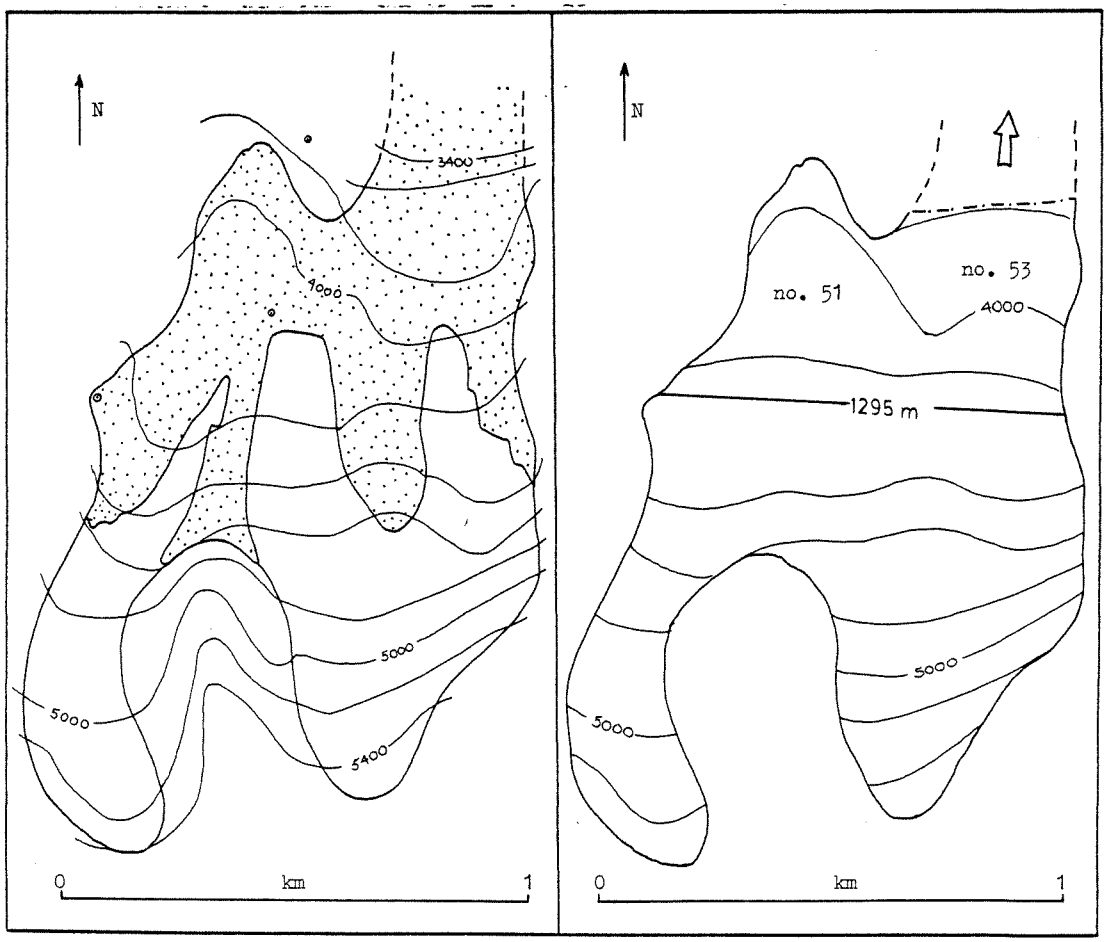

PRESENT ICE SURFACE WITH DEPOSIT

NEOGLACIAL MAXIMUM SURFACE

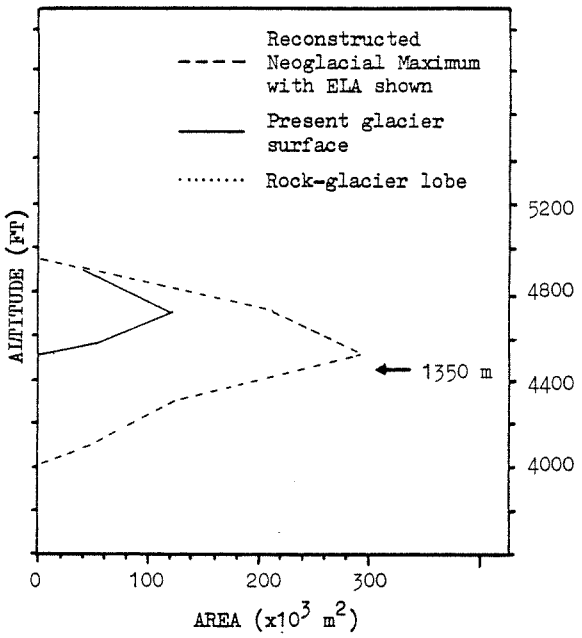

NEOGLACIAL MAXIMUM AND PRESENT AREA-ALTITUDE DISTRIBUTIONS

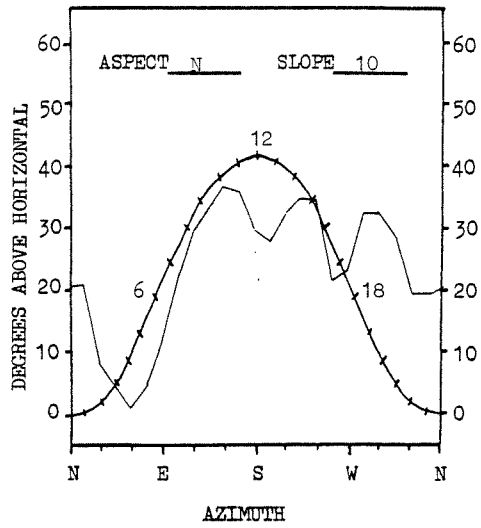

LANDFORM HORIZON (S- 306) WITH +20° SOLAR DECLINATION

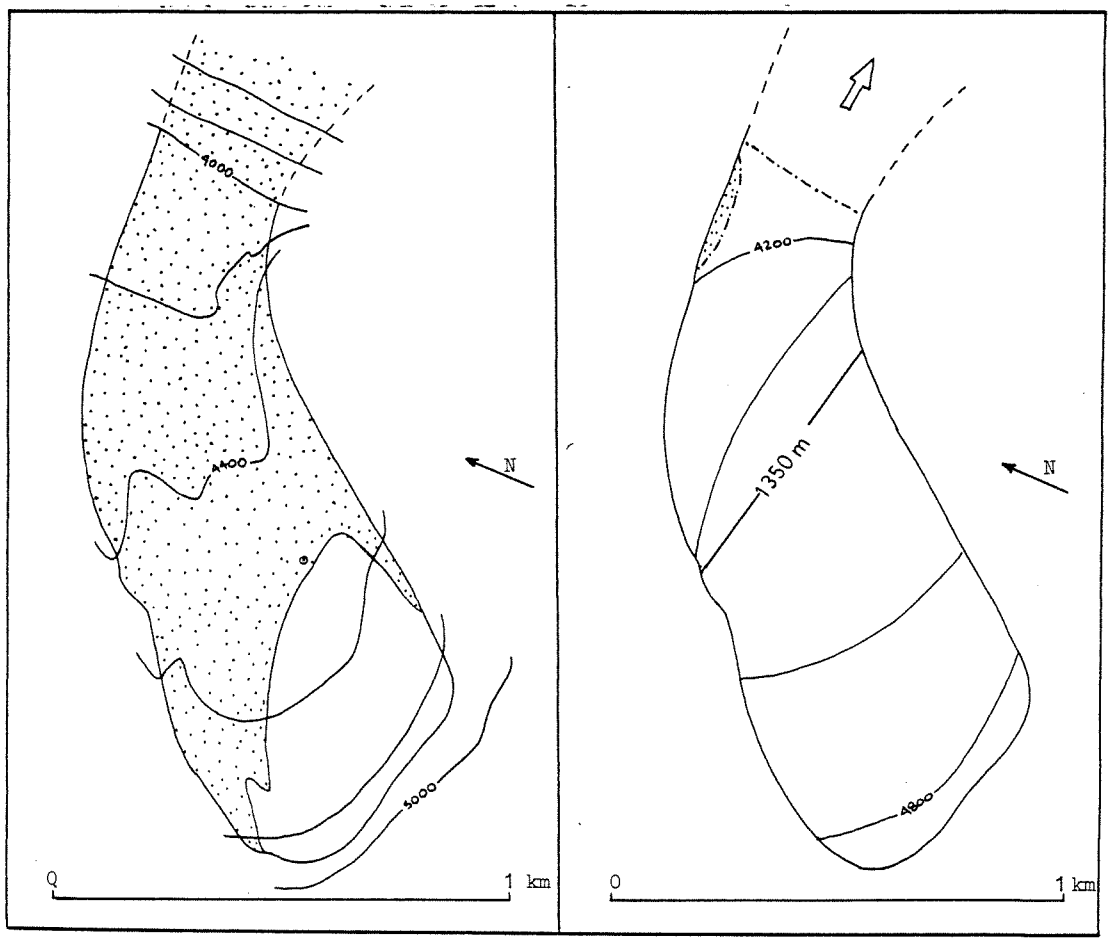

PRESENT ICE SURFACE WITH DEPOSIT

NEOGLACIAL MAXIMUM SURFACE

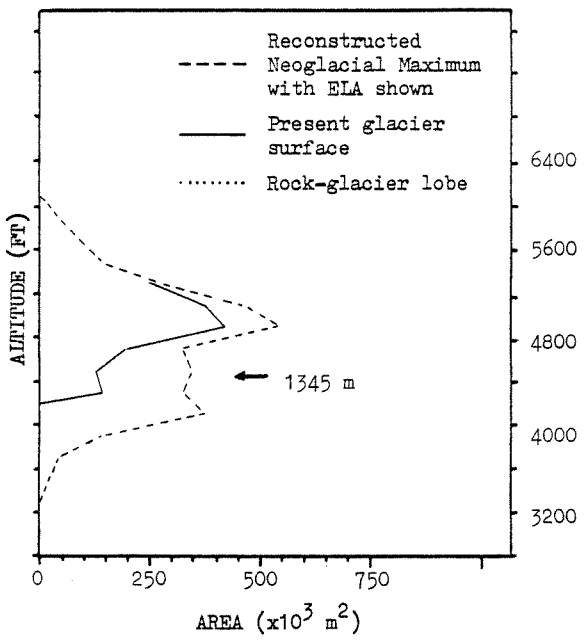

NEOGLACIAL MAXIMUM AND PRESENT AREA-ALTITUDE DISTRIBUTIONS

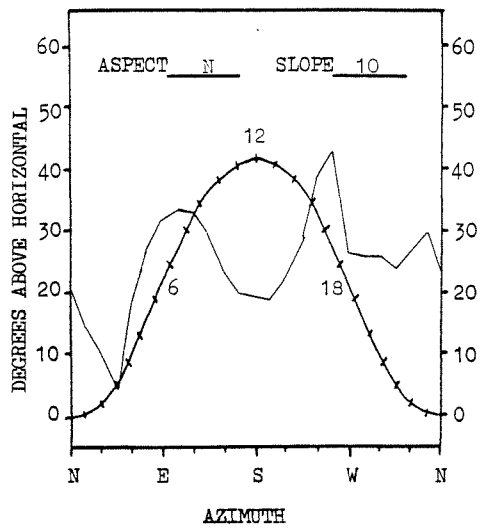

LANDFORM HORIZON (S- 308) WITH +20° SOLAR DECLINATION

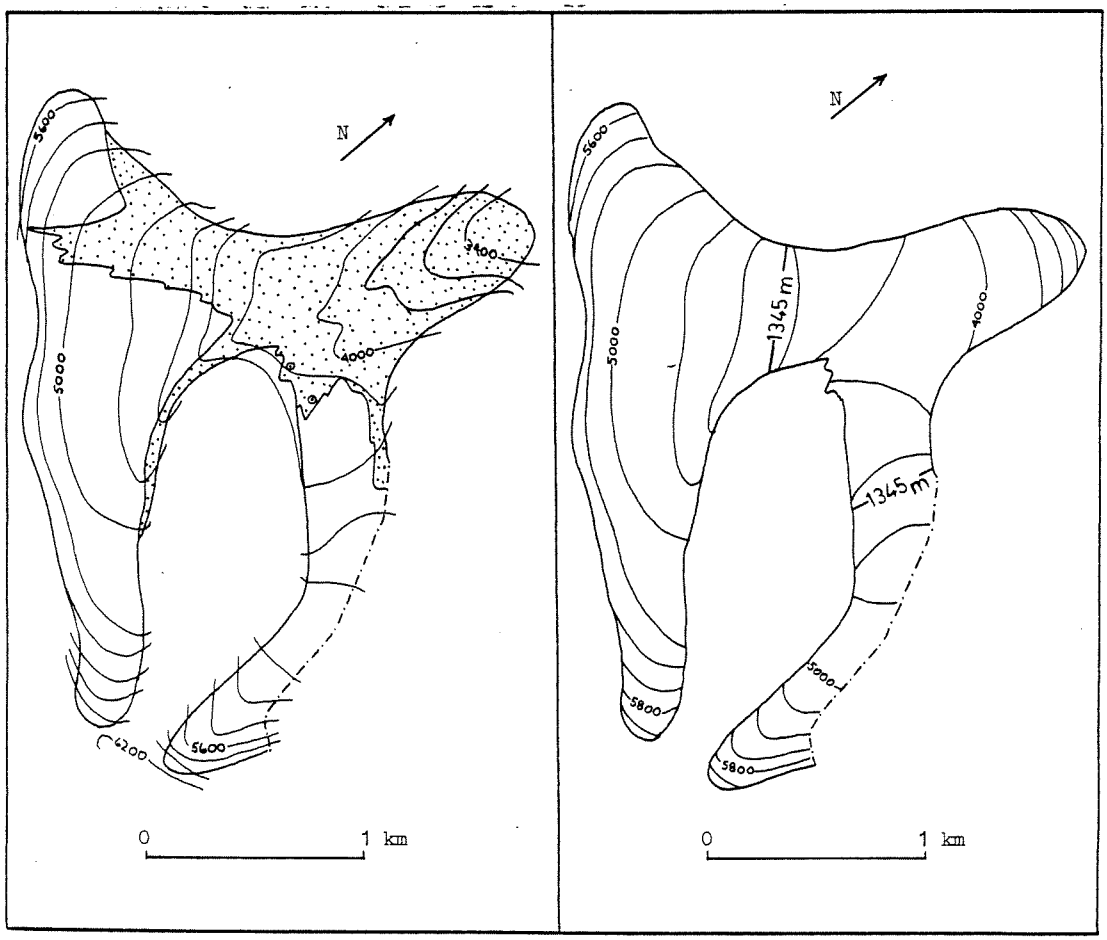

PRESENT ICE SURFACE WITH DEPOSIT

NEOGLACIAL MAXIMUM SURFACE

APPENDIX B. PHYSICAL INVENTORY (Arr-4 East, no. 56)

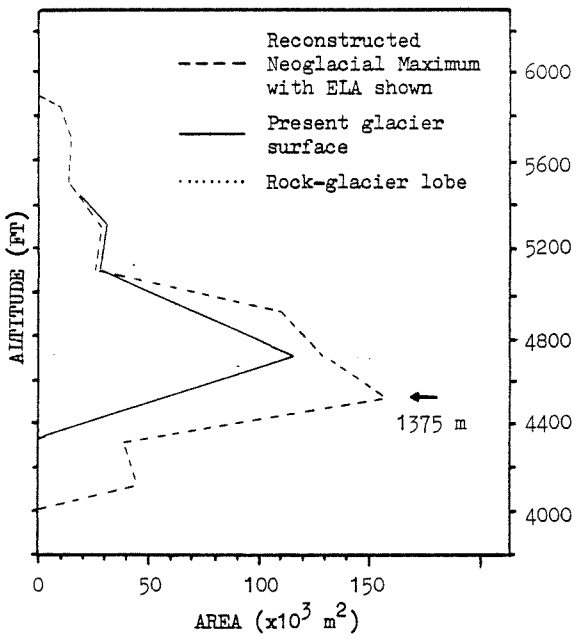

NEOGLACIAL MAXIMUM AND PRESENT AREA-ALTITUDE DISTRIBUTIONS

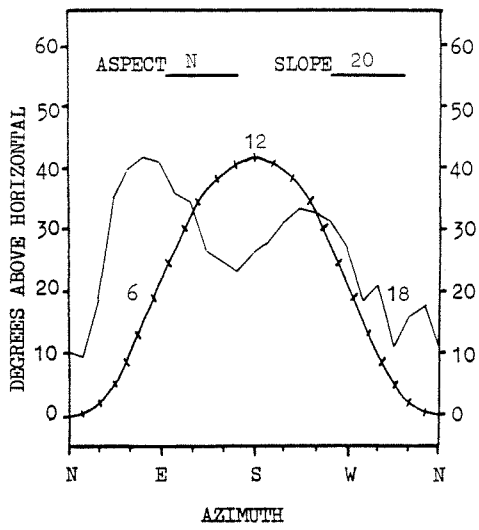

LANDFORM HORIZON (S- 309)
WITH +20° SOLAR DECLINATION

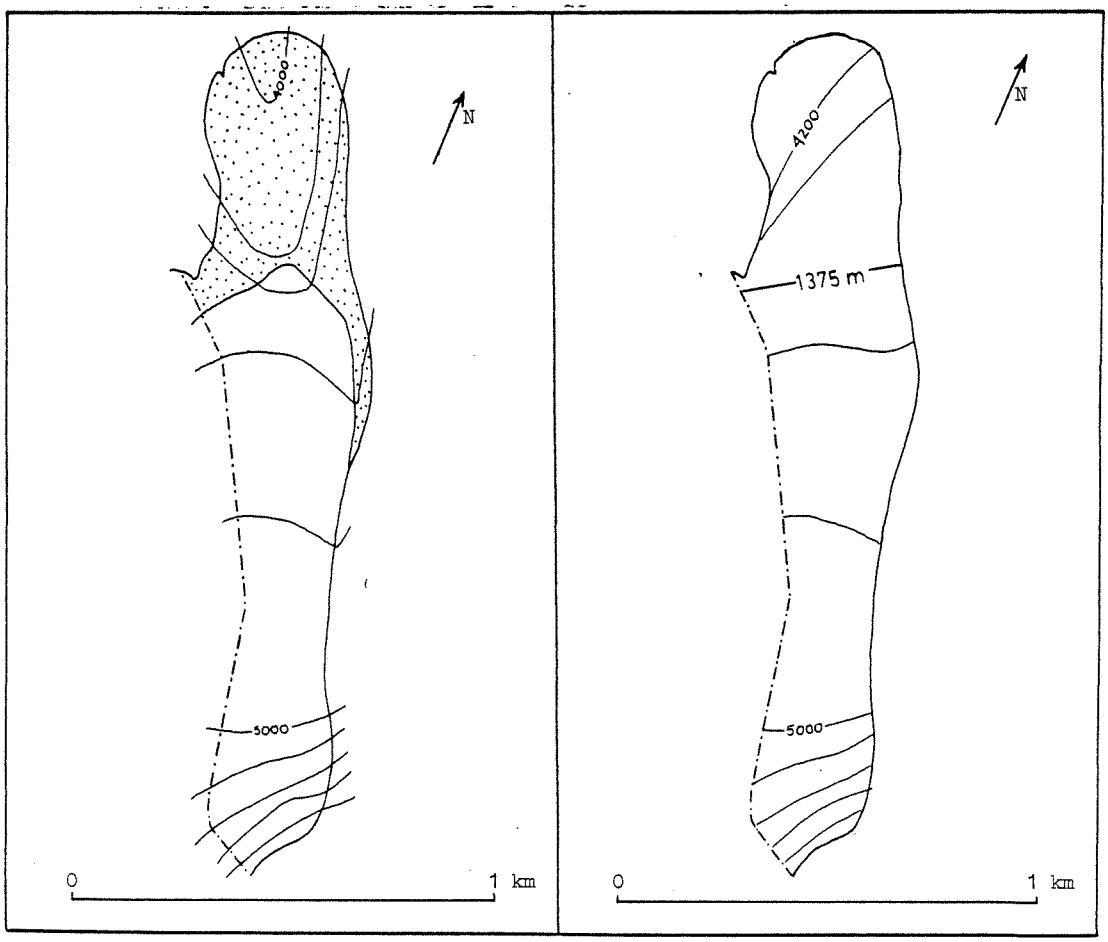

PRESENT ICE SURFACE WITH DEPOSIT

NEOGLACIAL MAXIMUM SURFACE

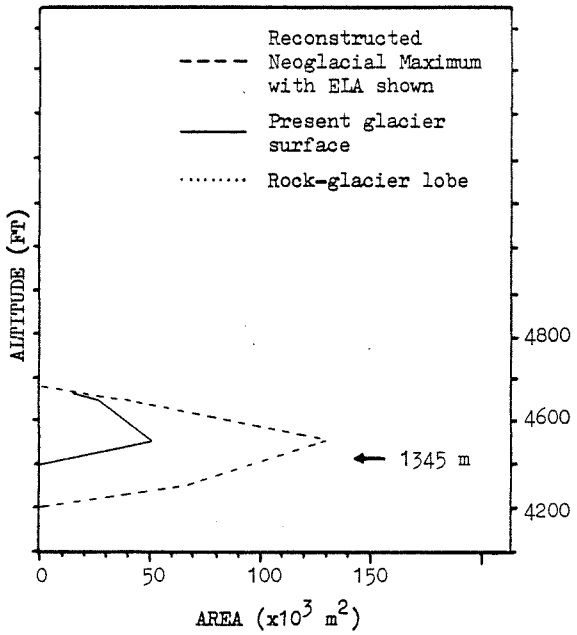

NEOGLACIAL MAXIMUM AND PRESENT AREA-ALTITUDE DISTRIBUTIONS

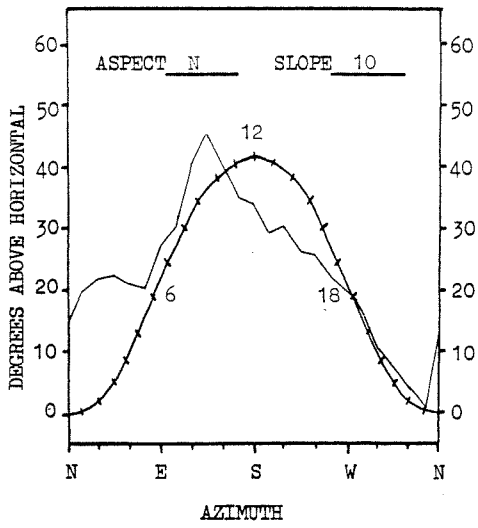

LANDFORM HORIZON (S- 310)
WITH +20° SOLAR DECLINATION

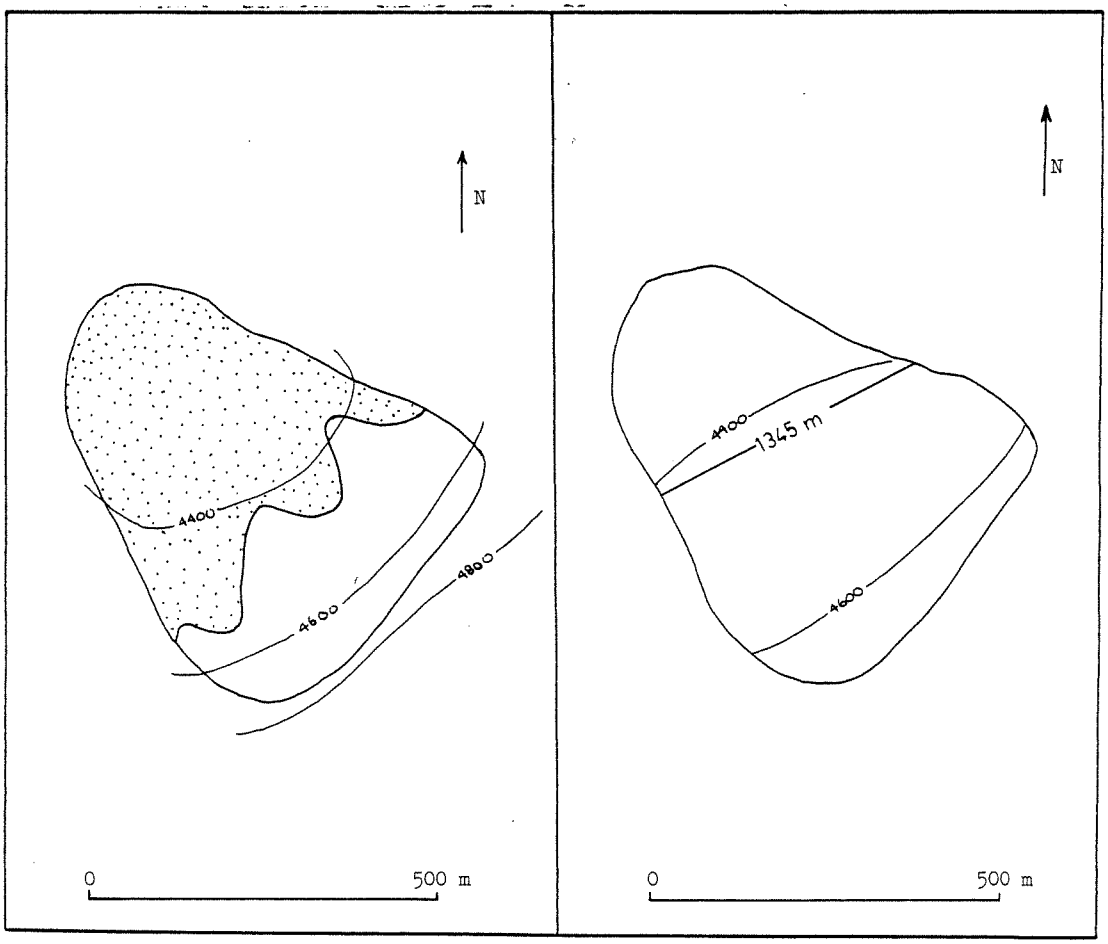

PRESENT ICE SURFACE WITH DEPOSIT

NEOGLACIAL MAXIMUM SURFACE

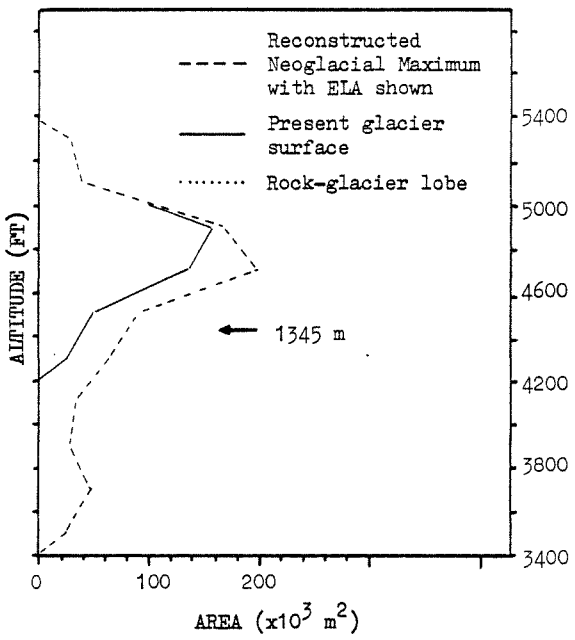

NEOGLACIAL MAXIMUM AND PRESENT AREA-ALTITUDE DISTRIBUTIONS

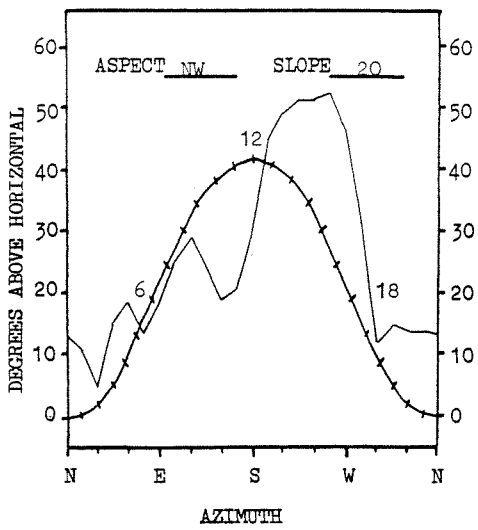

LANDFORM HORIZON (S- 313)
WITH +20° SOLAR DECLINATION

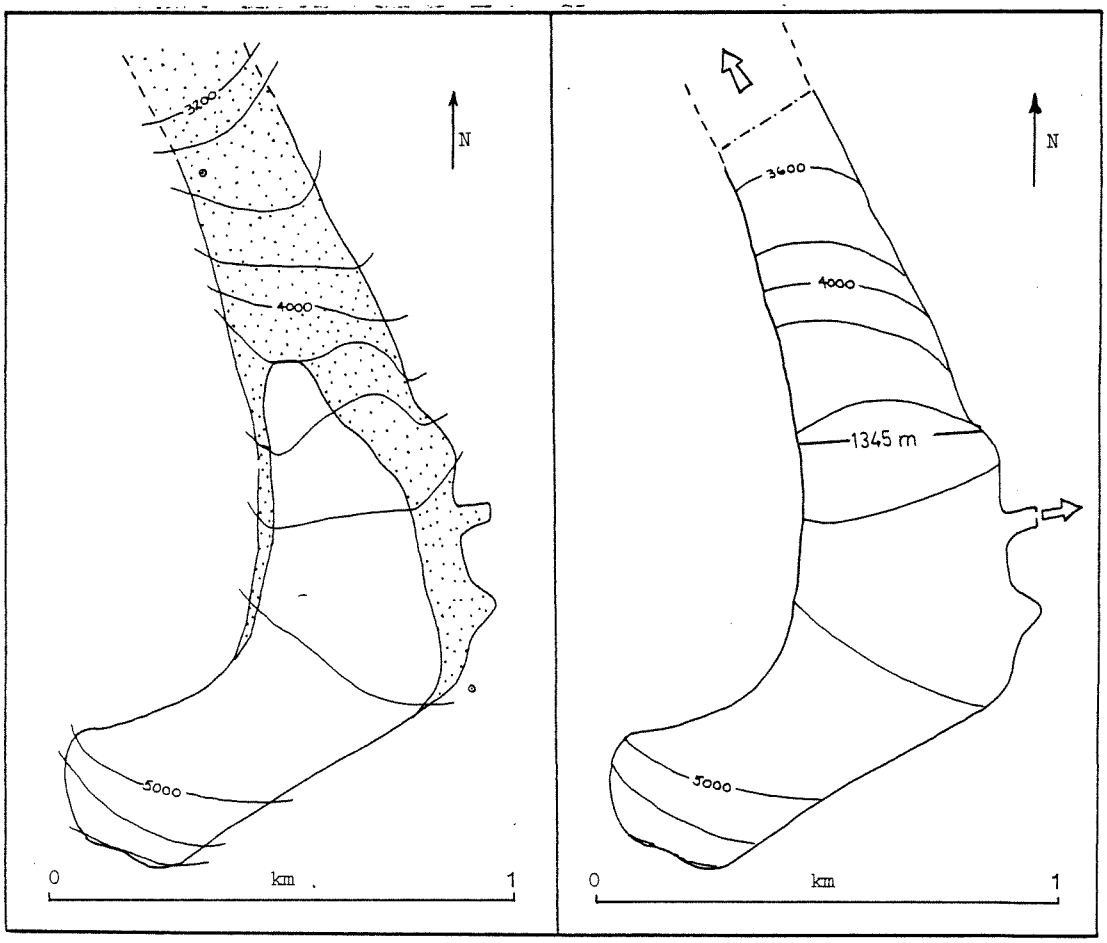

PRESENT ICE SURFACE WITH DEPOSIT

NEOGLACIAL MAXIMUM SURFACE

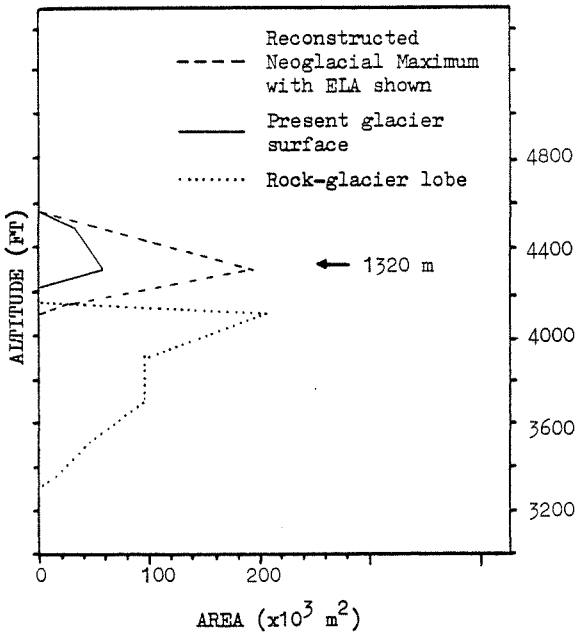

NEOGLACIAL MAXIMUM AND PRESENT
AREA-ALTITUDE DISTRIBUTIONS

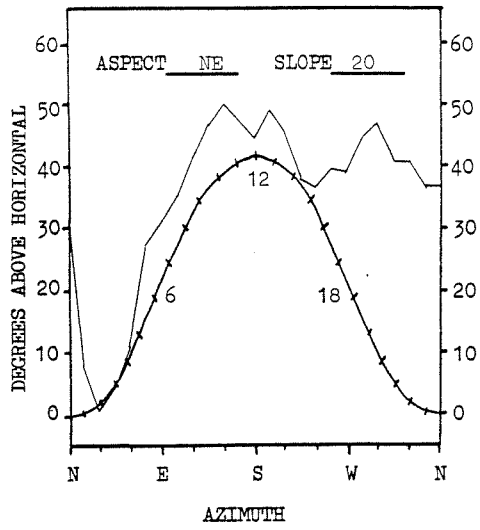

LANDFORM HORIZON (S- 408a)
WITH +20° SOLAR DECLINATION

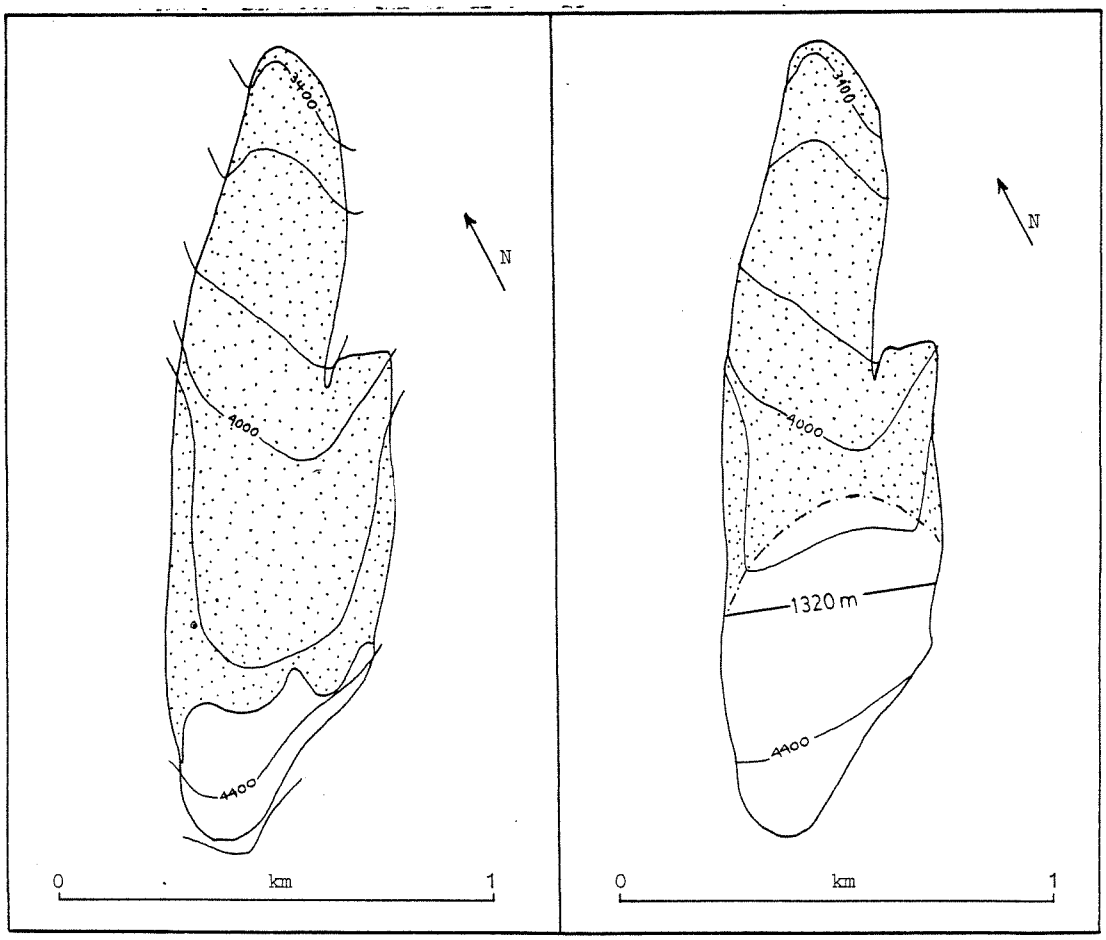

PRESENT ICE SURFACE WITH DEPOSIT

NEOGLACIAL MAXIMUM SURFACE

APPENDIX C. LICHENOMETRIC MAPS OF CIRQUE GLACIER DEPOSITS

Isolines connect surfaces with Rhizocarpon geographicum thalli of equal diameters (in mm) on these maps. Maximum thallus diameters characterizing a morainal ridge or map unit are shown as points with the thallus diameter (in mm). The lichenometric record preserved on each debris lobe and used in the glacial chronology (Figs. 33, 41) is summarized for each map. The isophyses refer only to the lichen species R. geographicum s.l. In some cases additional thallus measurements are shown for other species: R. eupetraeoides/inarense are annotated "e/i" and Alectoria minuscula/pubescens are noted with "A".

The maps are annotated as to percent lichen cover and lithology in some locations. Measurements from downslope rock glacier surfaces or valley substrates are shown, but are not used in the glacial chronology (Figs. 45, 46). The lichenometric maps for the following glaciers are modified from Ellis (1978): 1, 2, 4, 6, 13, 14, 21, and 39; and from Bruen (1980a): 3, 37, 38. Cirque glaciers 49 and 57 were not lichenometrically mapped.

Legend for Lichenometric Maps of Cirque-Glacier Deposits

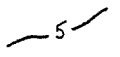

5 mm Rhizocarpon geographicum s.l. isophyse

5 mm R. geographicum s.l. site

21 mm Rhizocarpon eupetraeoides/inarense site

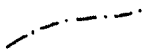

Topographic ridge

Lake with outlet stream

Cascading glacial deposit or talus (shows direction)

APPENDIX C. LICHENOMETRIC MAPS

Buffalo Glacier (no. 1).

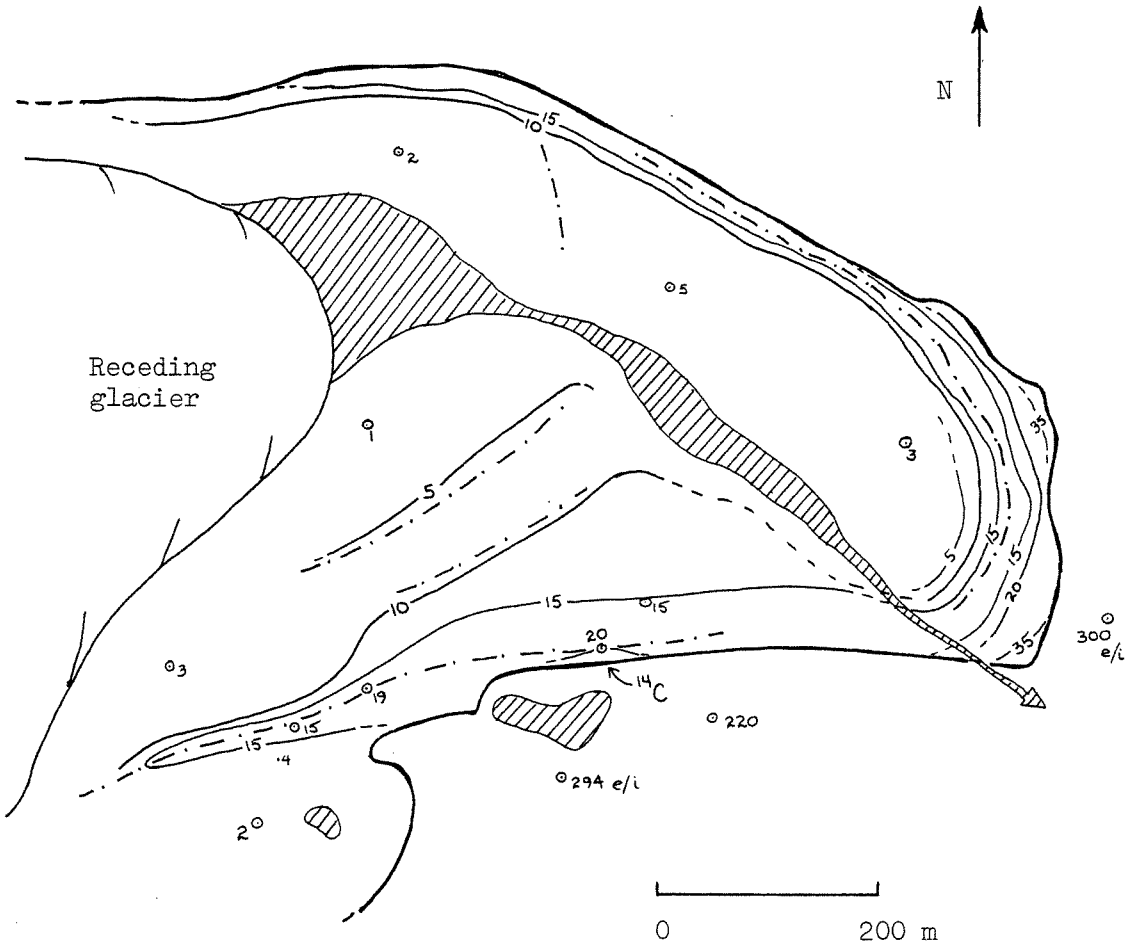

Maximum diameters of Rhizocarpon geographicum s.l. that characterize the debris lobe: 5, 15, 20, 35 mm.

APPENDIX C. LICHENOMETRIC MAPS

Marmot Glacier (no. 2).

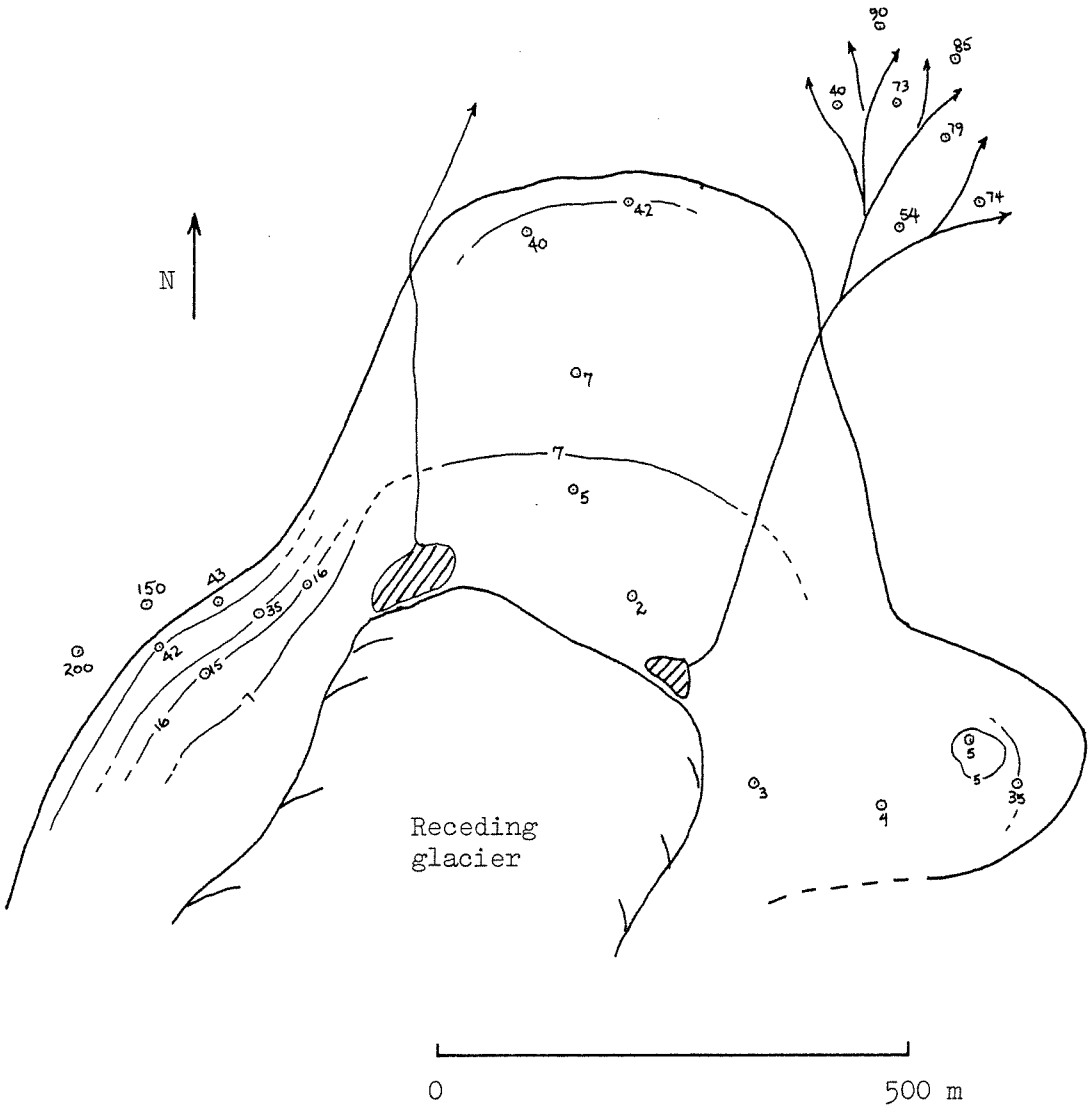

Maximum diameters of Rhizocarpon geographicum s.l. that characterize the debris lobe: 7, 16, 35, 43 mm.

APPENDIX C. LICHENOMETRIC MAPS

Grizzly Glacier (no. 3).

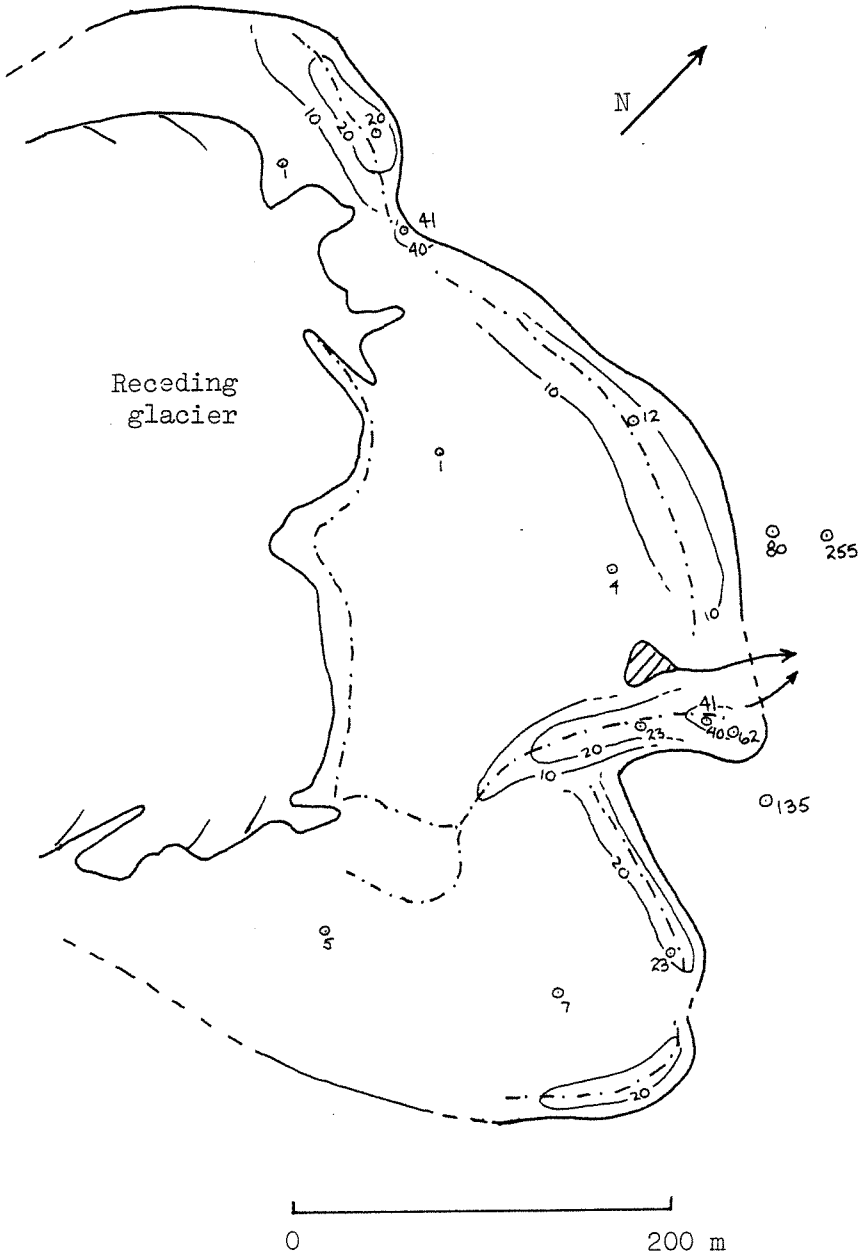

Maximum diameters of Rhizocarpon geographicum s.l. that characterize the debris lobe: 12, 23, 41, 62 mm.

APPENDIX C. LICHENOMETRIC MAPS

Coyote Glacier (no. 4).

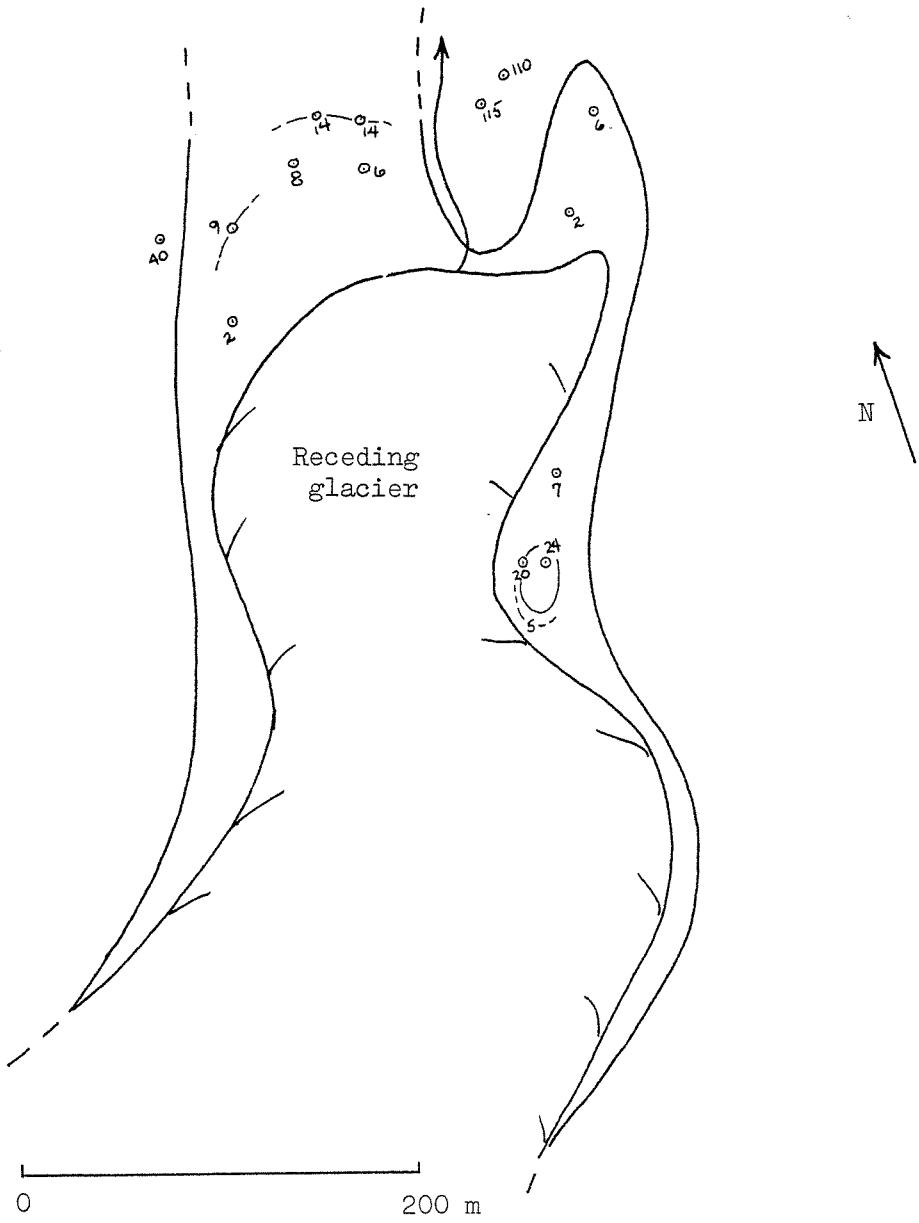

Maximum diameters of Rhizocarpon geographicum s.l. that characterize the debris lobe: 14, 24 mm.

APPENDIX C. LICHENOMETRIC MAPS

Caribou Glacier (no. 5).

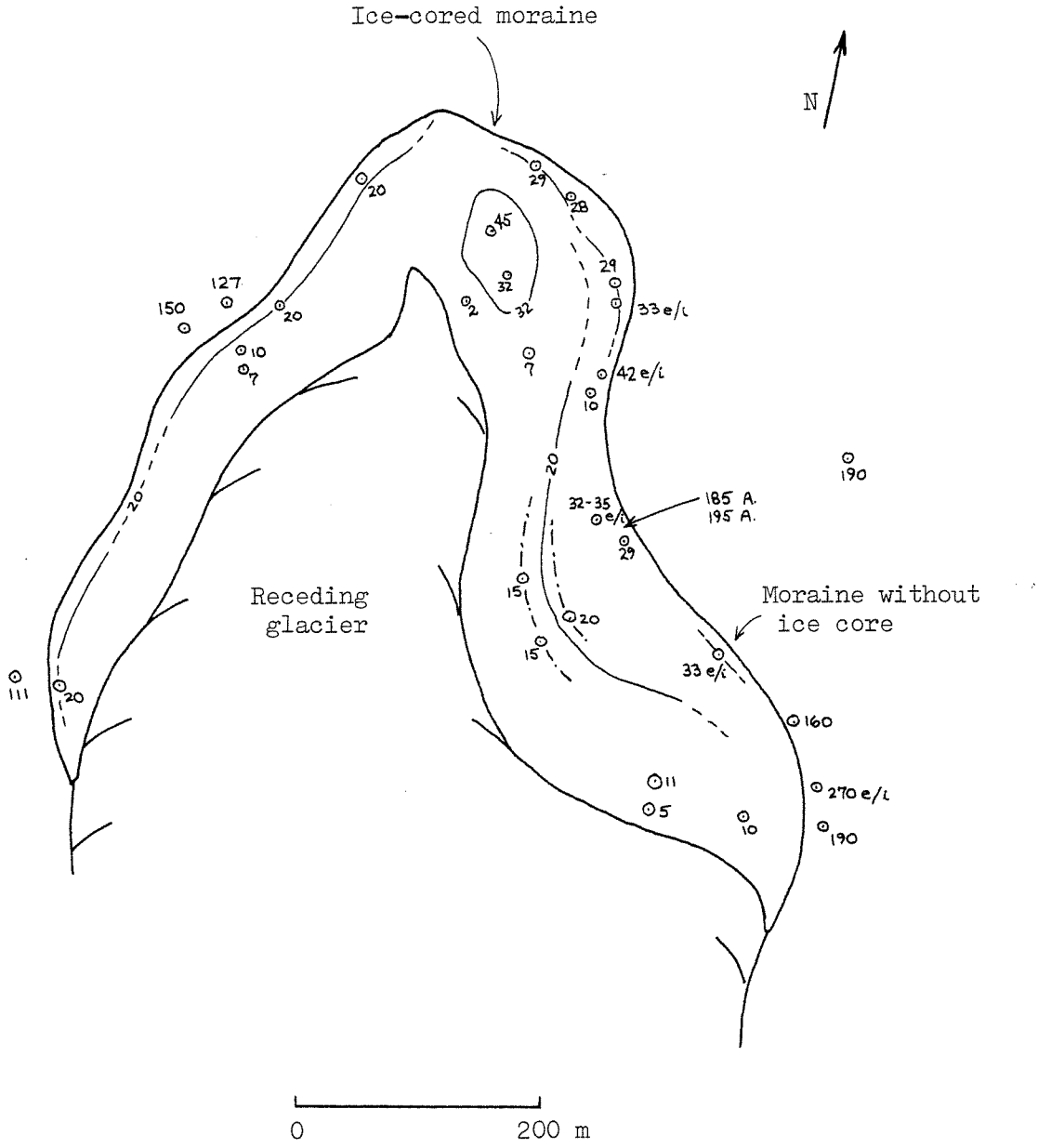

Maximum diameters of Rhizocarpon geographicum s.l. that characterize the debris lobe: 15, 20, 29, 45? mm.

APPENDIX C. LICHENOMETRIC MAPS

Raptor Glacier (no. 6).

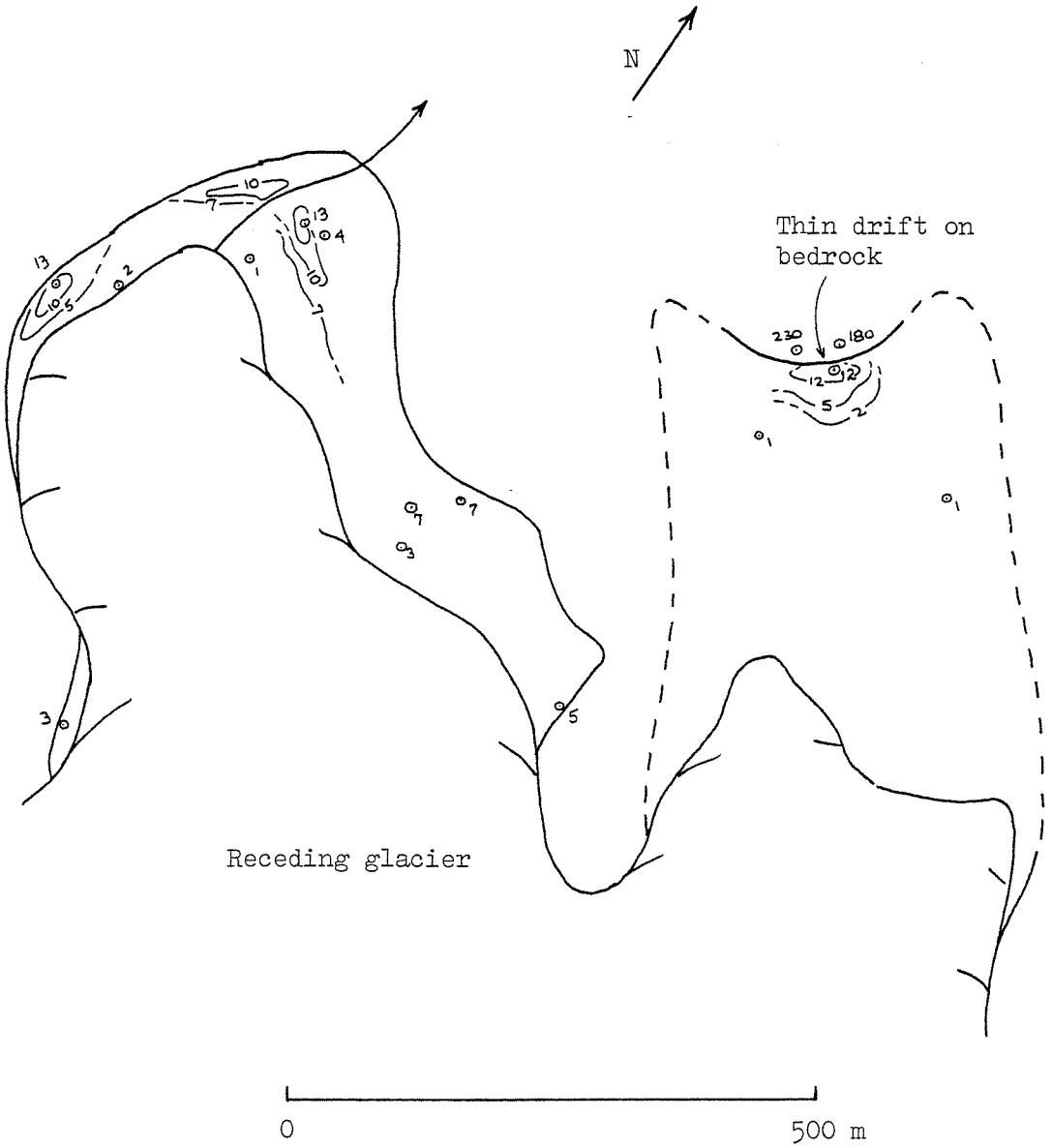

Maximum diameters of Rhizocarpon geographicum s.l. that characterize the debris lobe: 13 mm.

APPENDIX C. LICHENOMETRIC MAPS

Golden Eagle Glacier (no. 7).

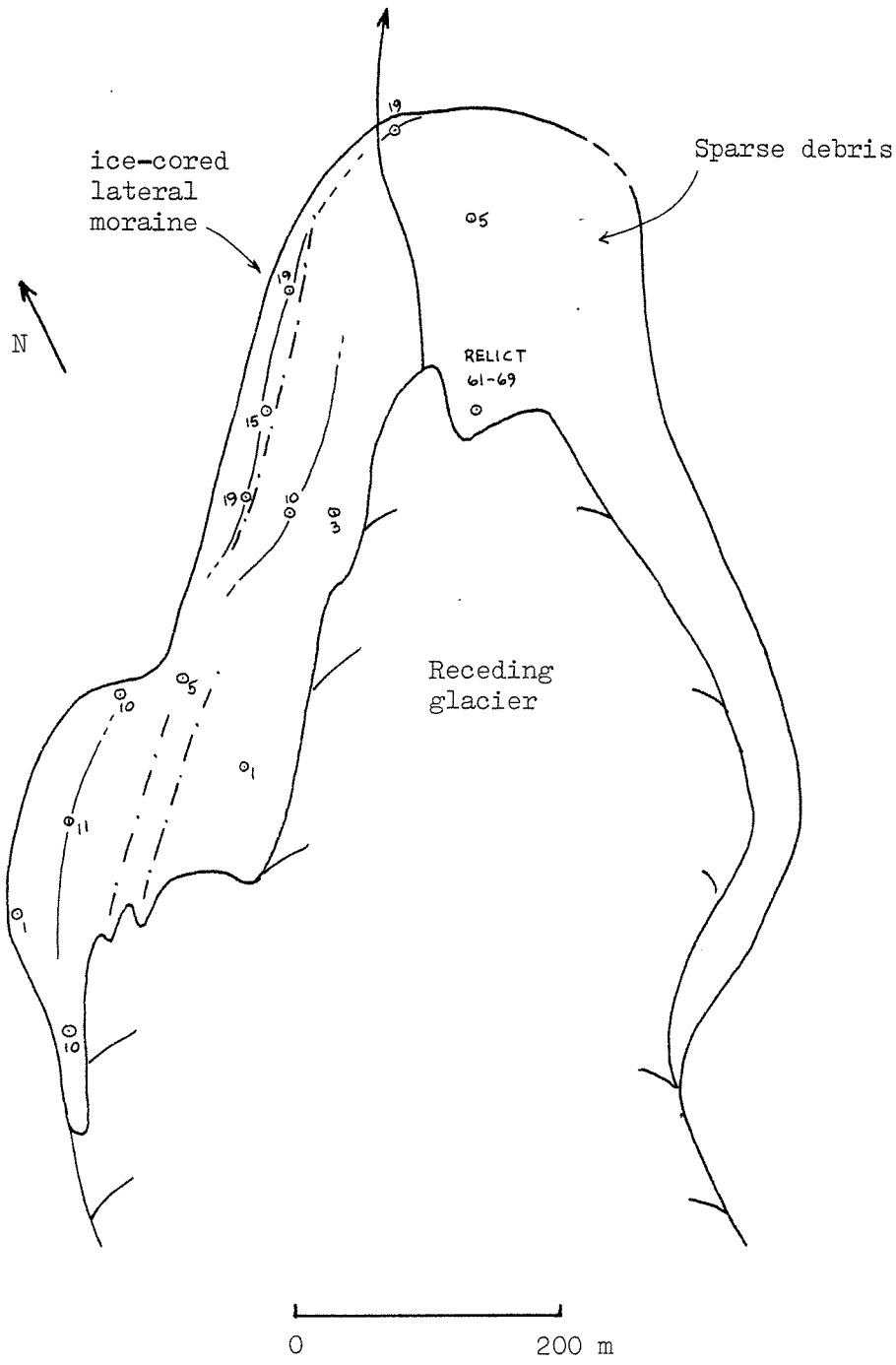

Maximum diameters of Rhizocarpon geographicum s.l. that characterize the debris lobe: 11, 19 mm.

APPENDIX C. LICHENOMETRIC MAPS

Robin Glacier (no. 8).

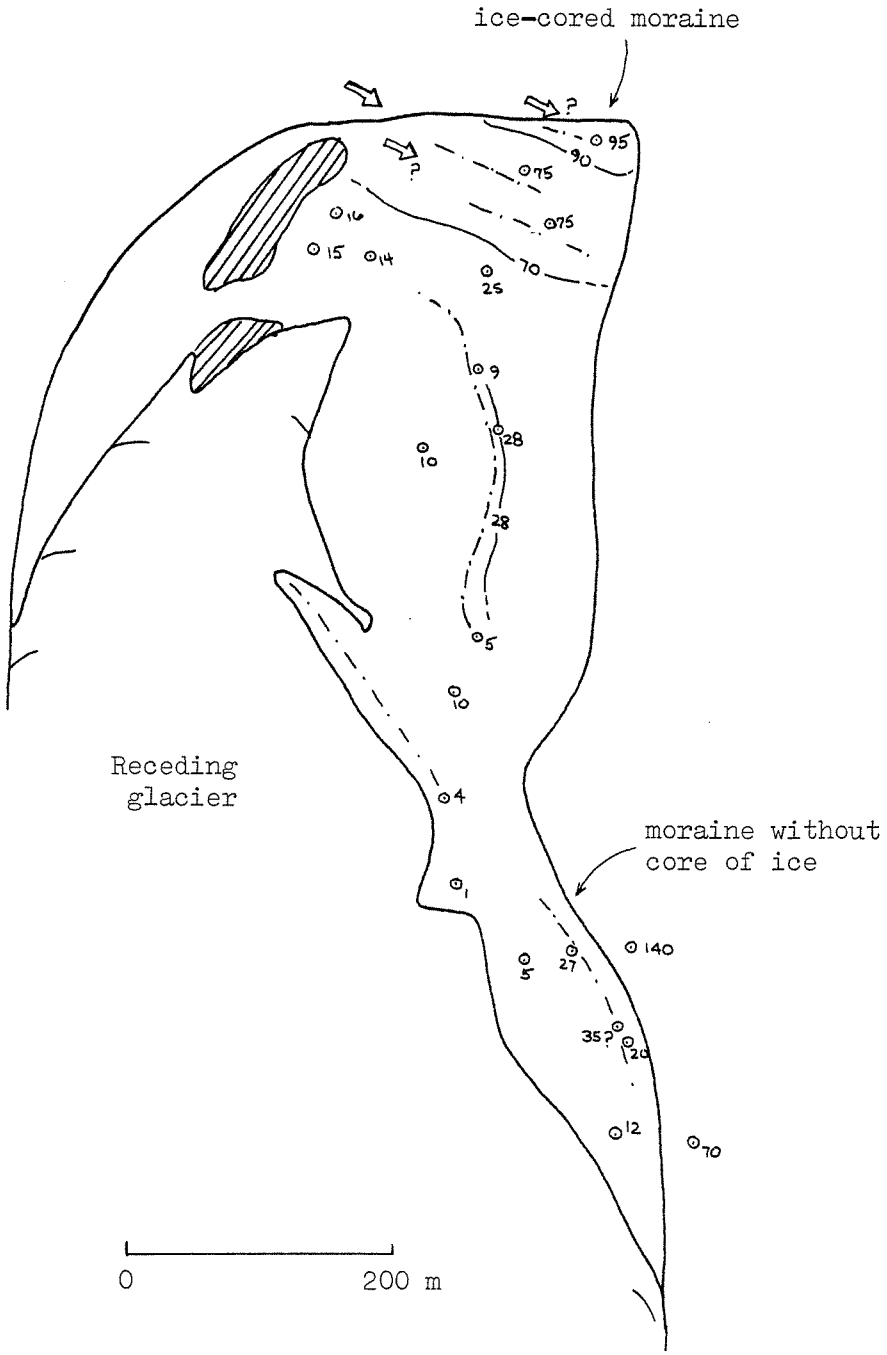

Maximum diameters of Rhizocarpon geographicum s.l. that characterize the debris lobe: 28, 75?, 95? mm.

APPENDIX C. LICHENOMETRIC MAPS

Lemming Glacier (no. 9).

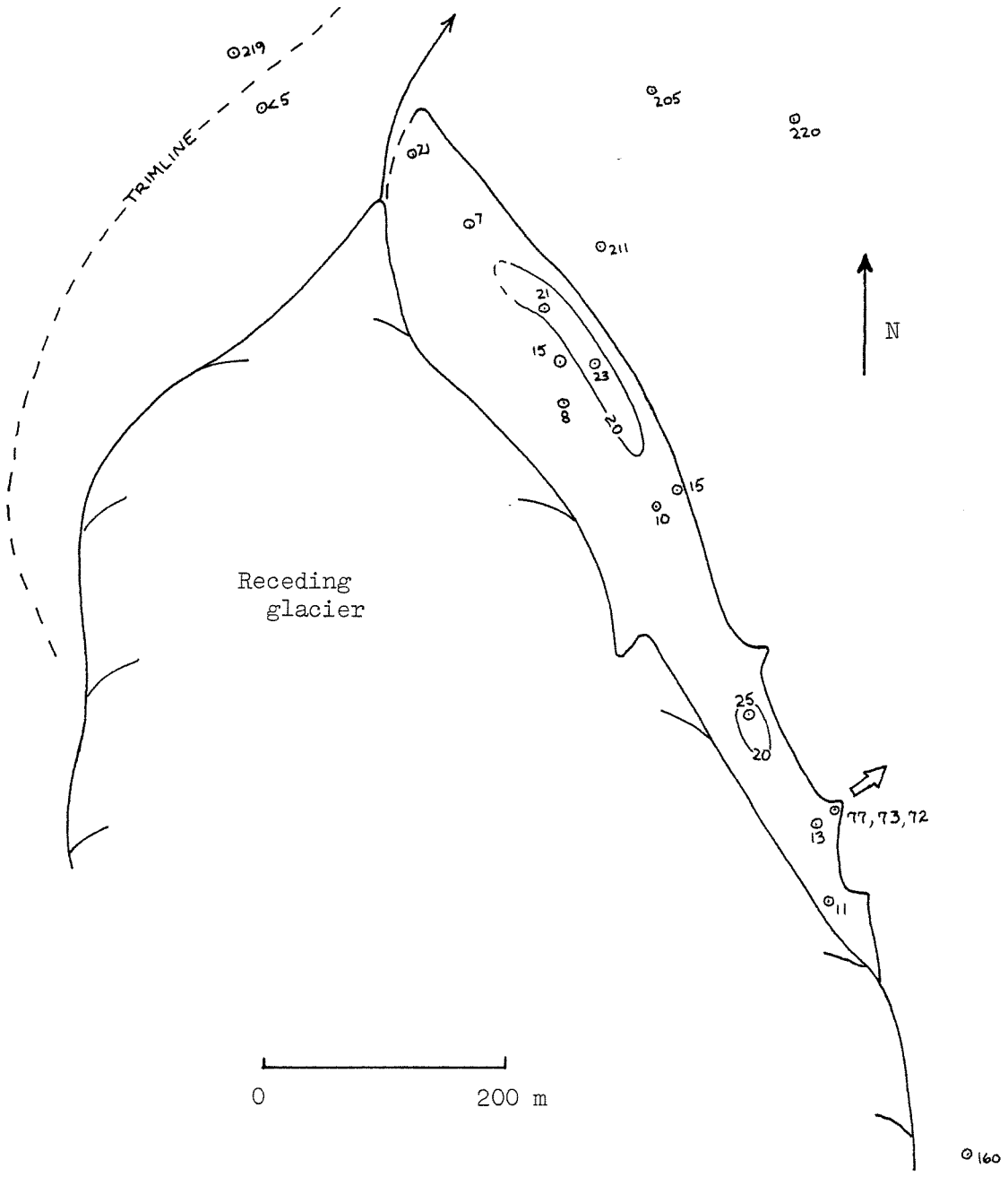

Maximum diameters of Rhizocarpon geographicum s.l. that characterize the debris lobe: 25, 77? mm.

APPENDIX C. LICHENOMETRIC MAPS

Triple West Glacier (no. 10).

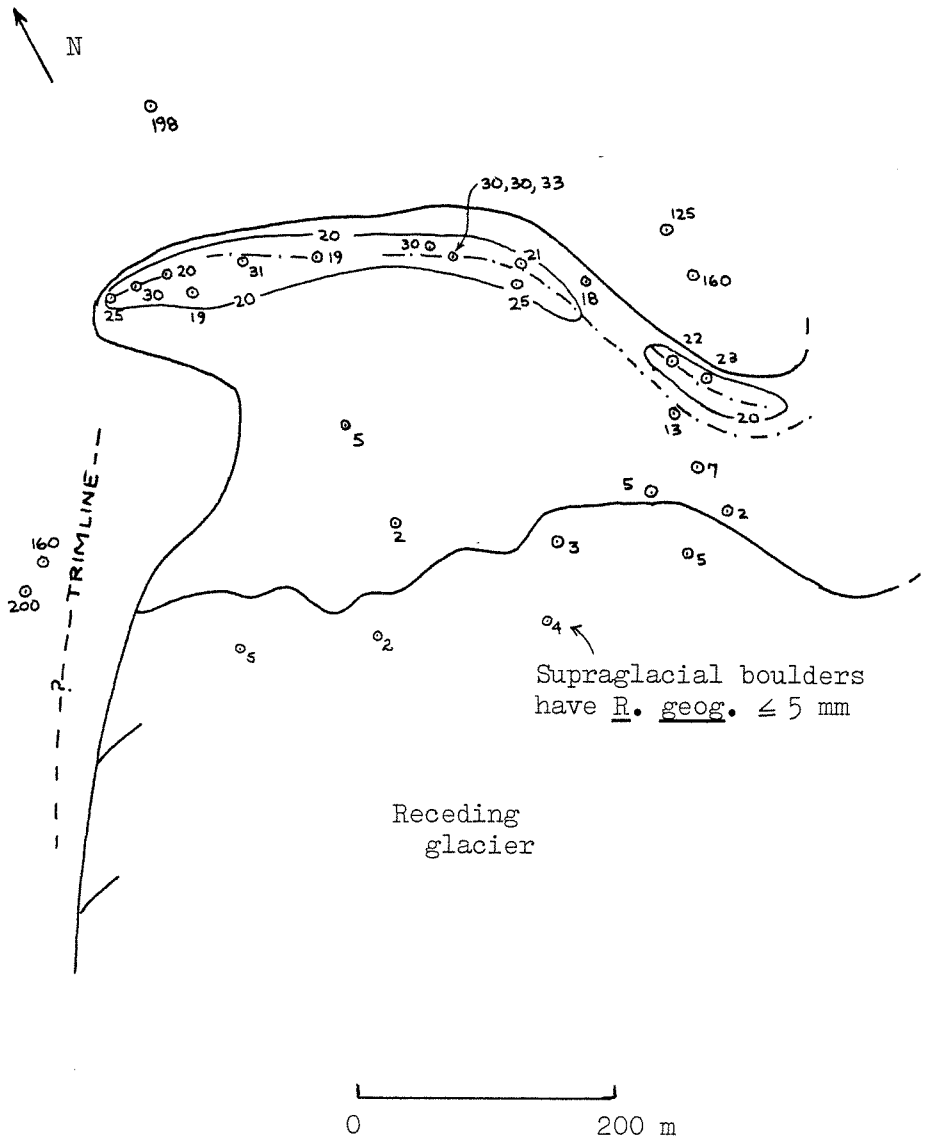

Maximum diameters of Rhizocarpon geographicum s.l. that characterize the debris lobe: 25, 33 mm.

APPENDIX C. LICHENOMETRIC MAPS

Triple Middle Glacier (no. 11).

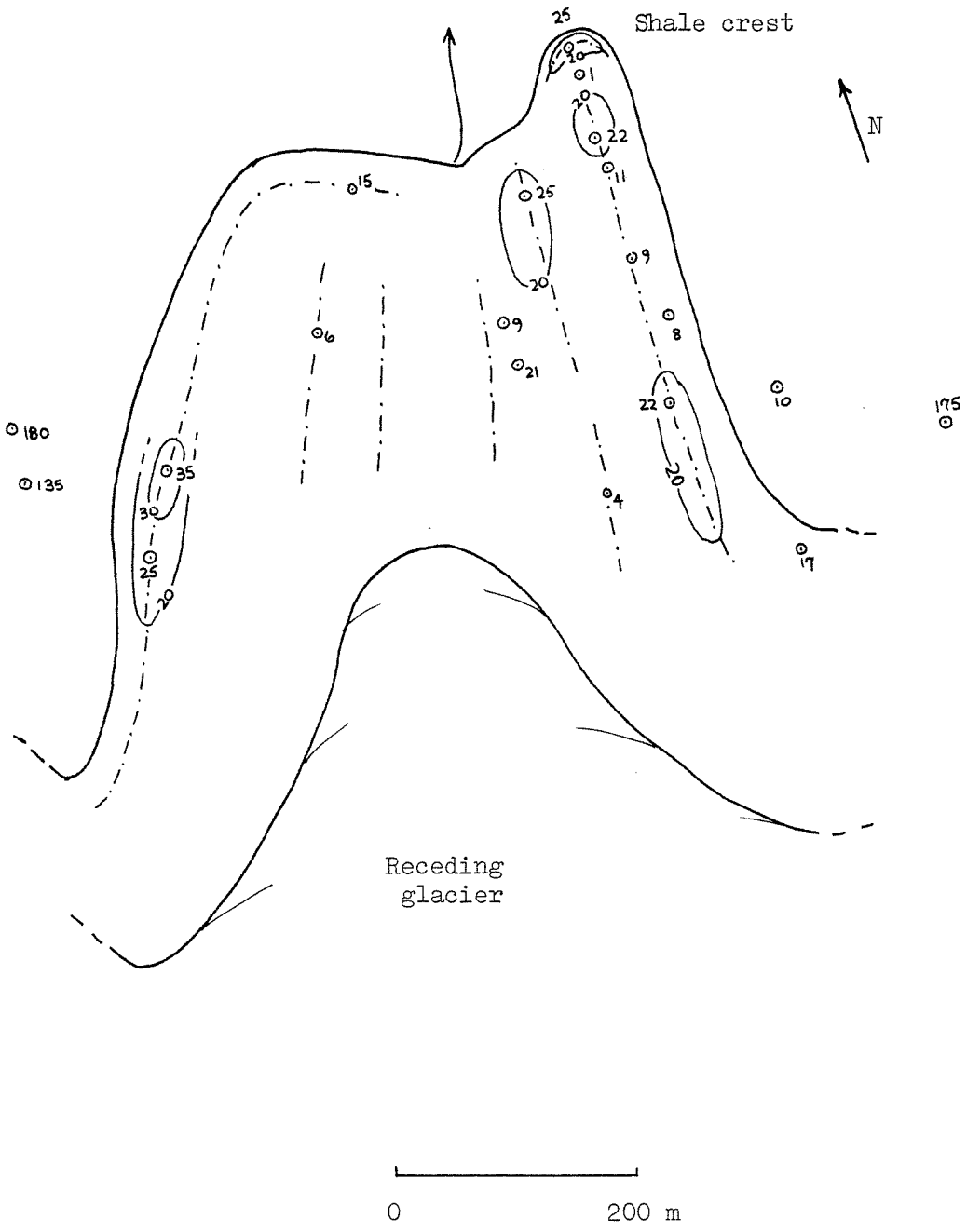

Maximum diameters of Rhizocarpon geographicum s.l. that characterize the debris lobe: 25, 35 mm.

APPENDIX C. LICHENOMETRIC MAPS

Triple East Glacier (no. 12).

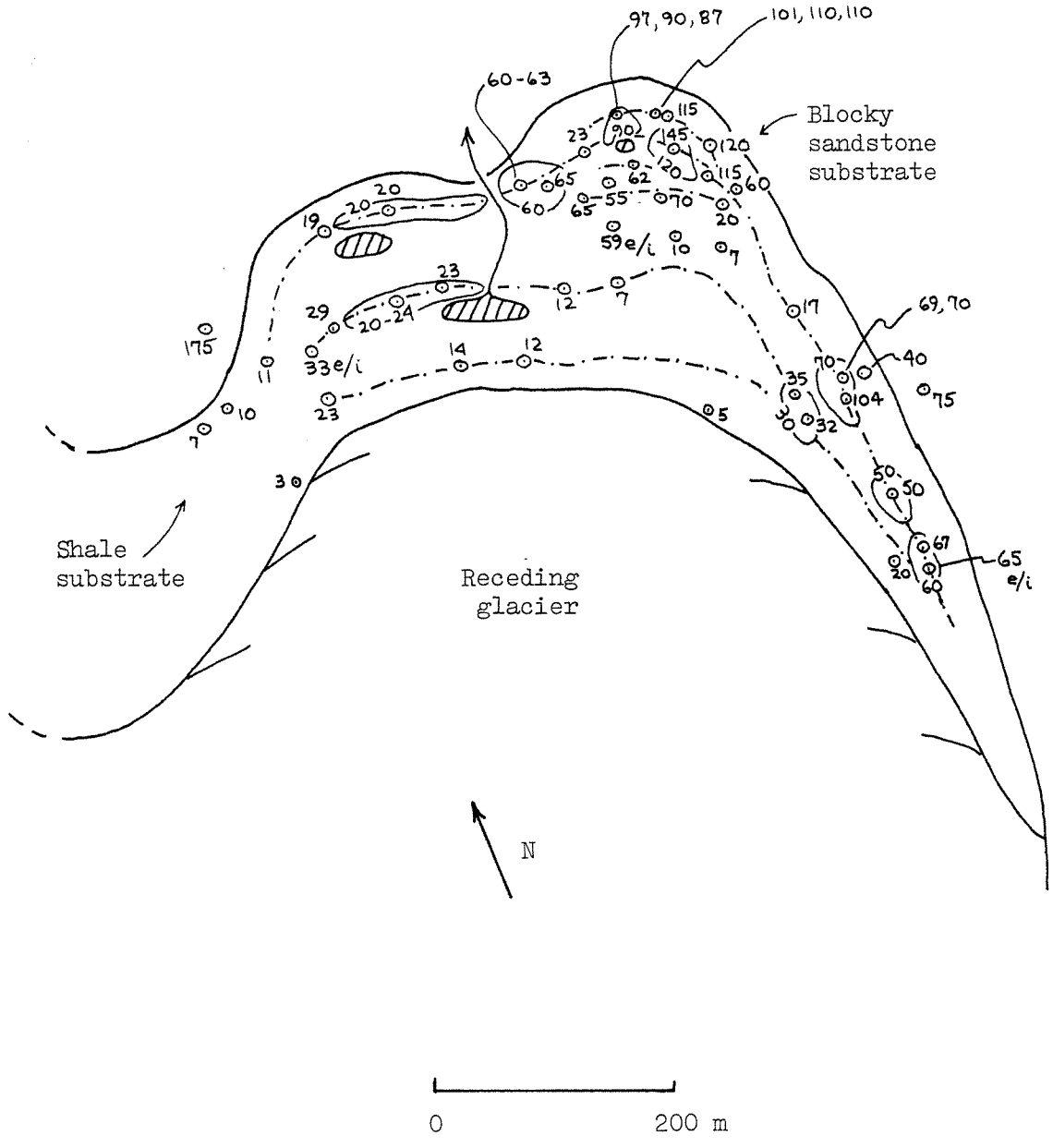

Maximum diameters of Rhizocarpon geographicum s.l. that characterize the debris lobe: 24, 35, 70, 97?, 115, 145 mm.

APPENDIX C. LICHENOMETRIC MAPS

Dall Sheep Glacier (no. 13).

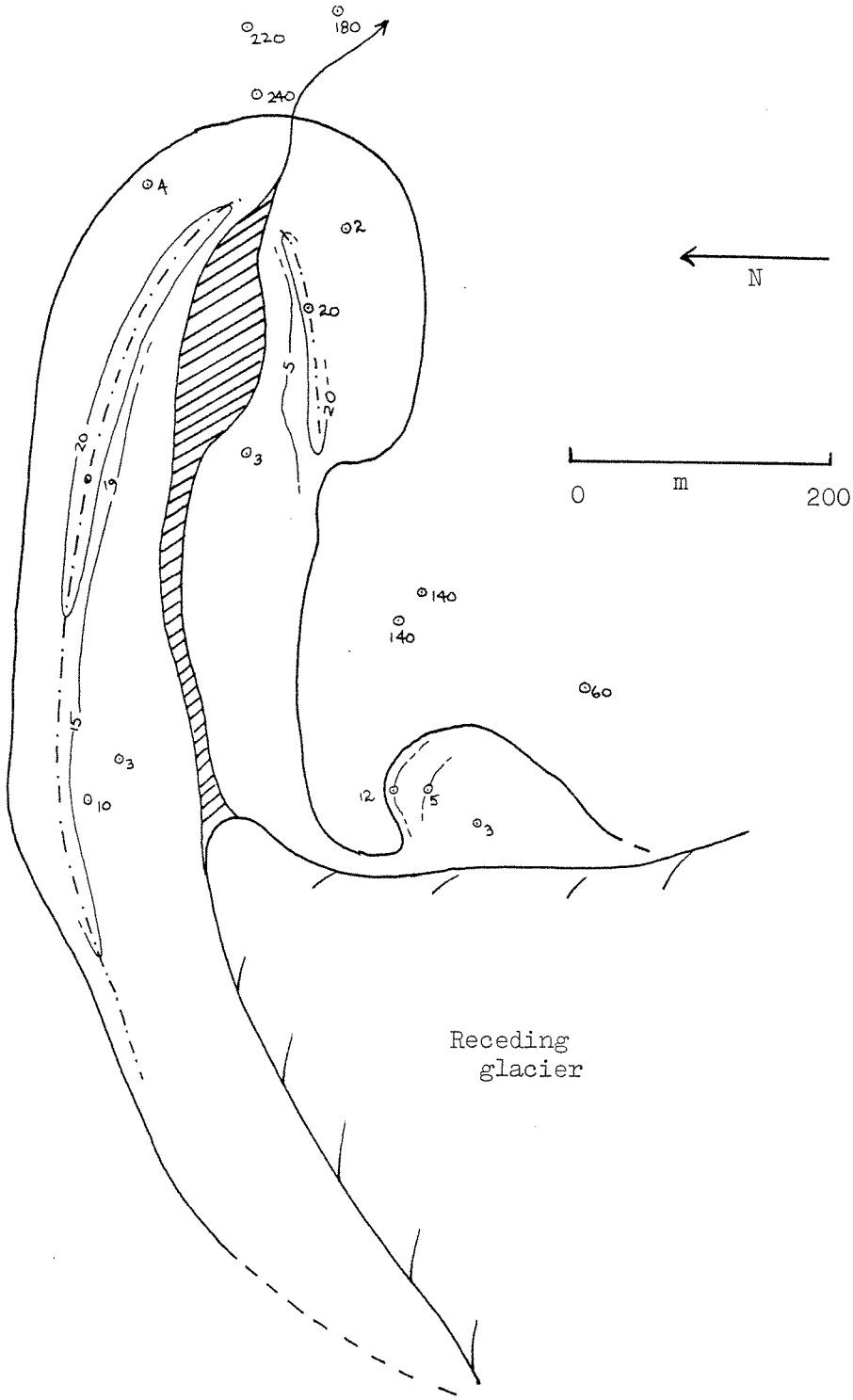

Maximum diameters of Rhizocarpon geographicum s.l. that characterize the debris lobe: 12, 20 mm.

APPENDIX C. LICHENOMETRIC MAPS

Snow Bunting Glacier (no. 14).

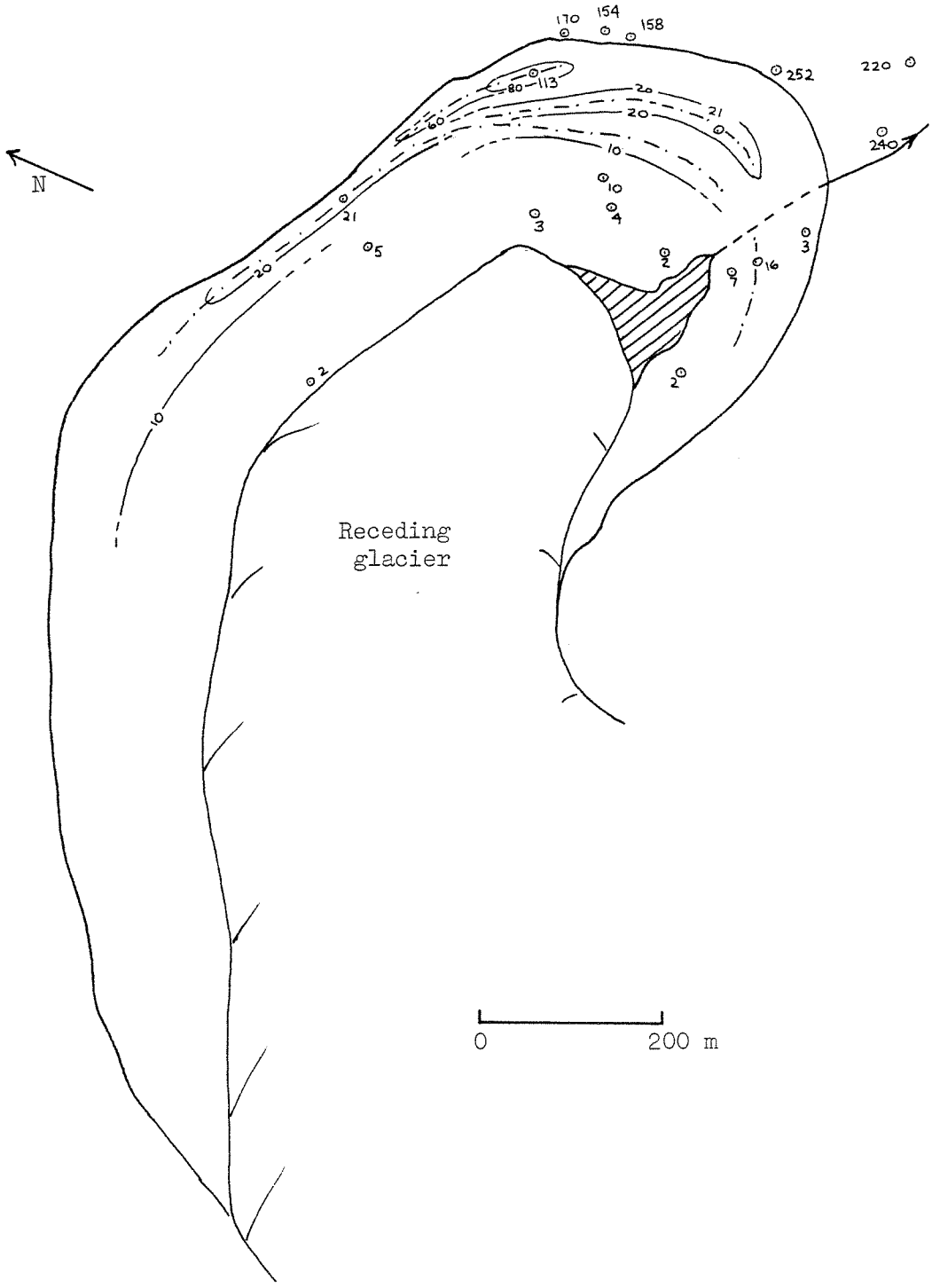

Maximum diameters of Rhizocarpon geographicum s.l. that characterize the debris lobe: 21, 113 mm.

APPENDIX C. LICHENOMETRIC MAPS

Fox Glacier (no. 15).

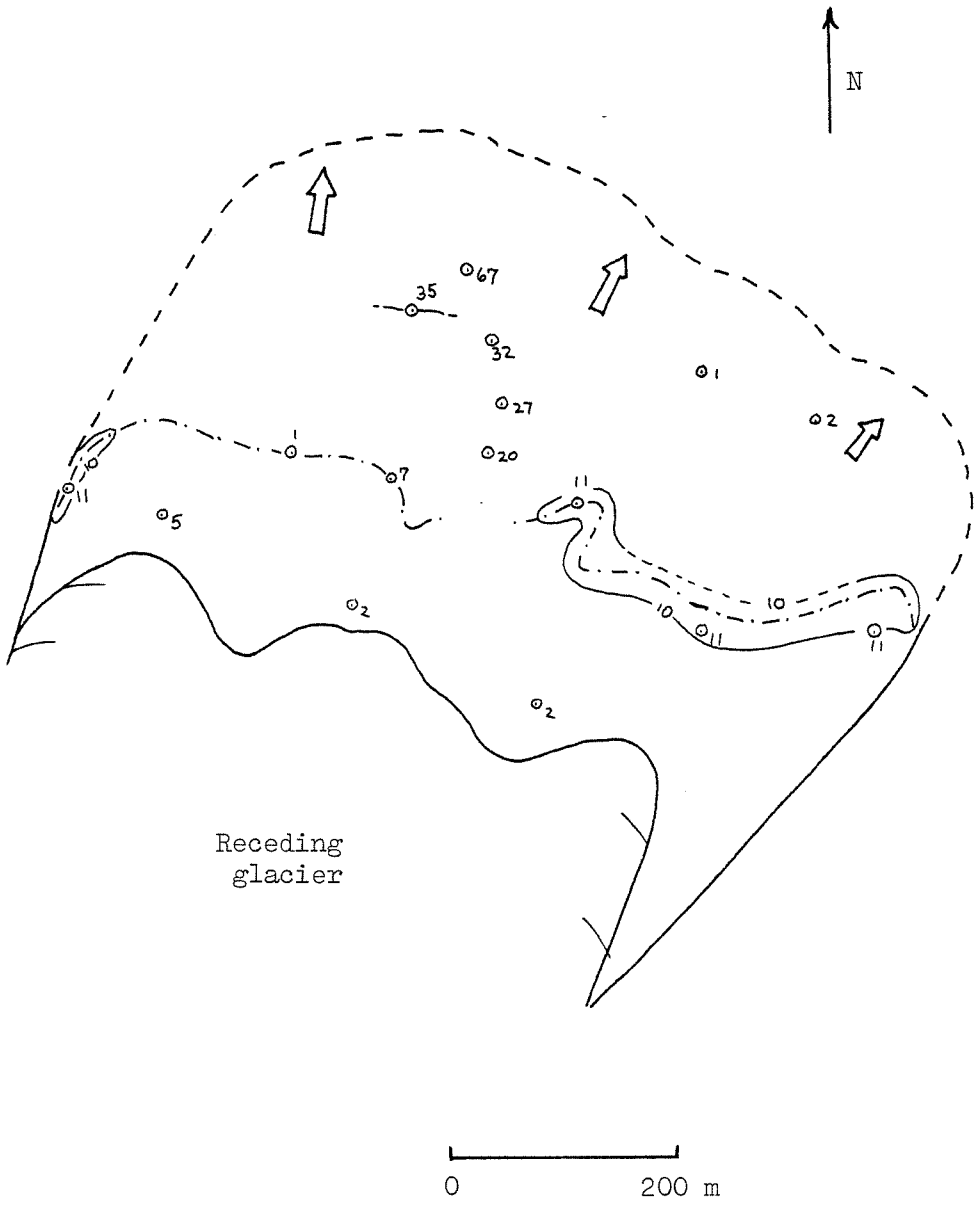

Maximum diameters of Rhizocarpon geographicum s.l. that characterize the debris lobe: 11, 21, 35, 67? mm.

APPENDIX C. LICHENOMETRIC MAPS

Ram Glacier (no. 16).

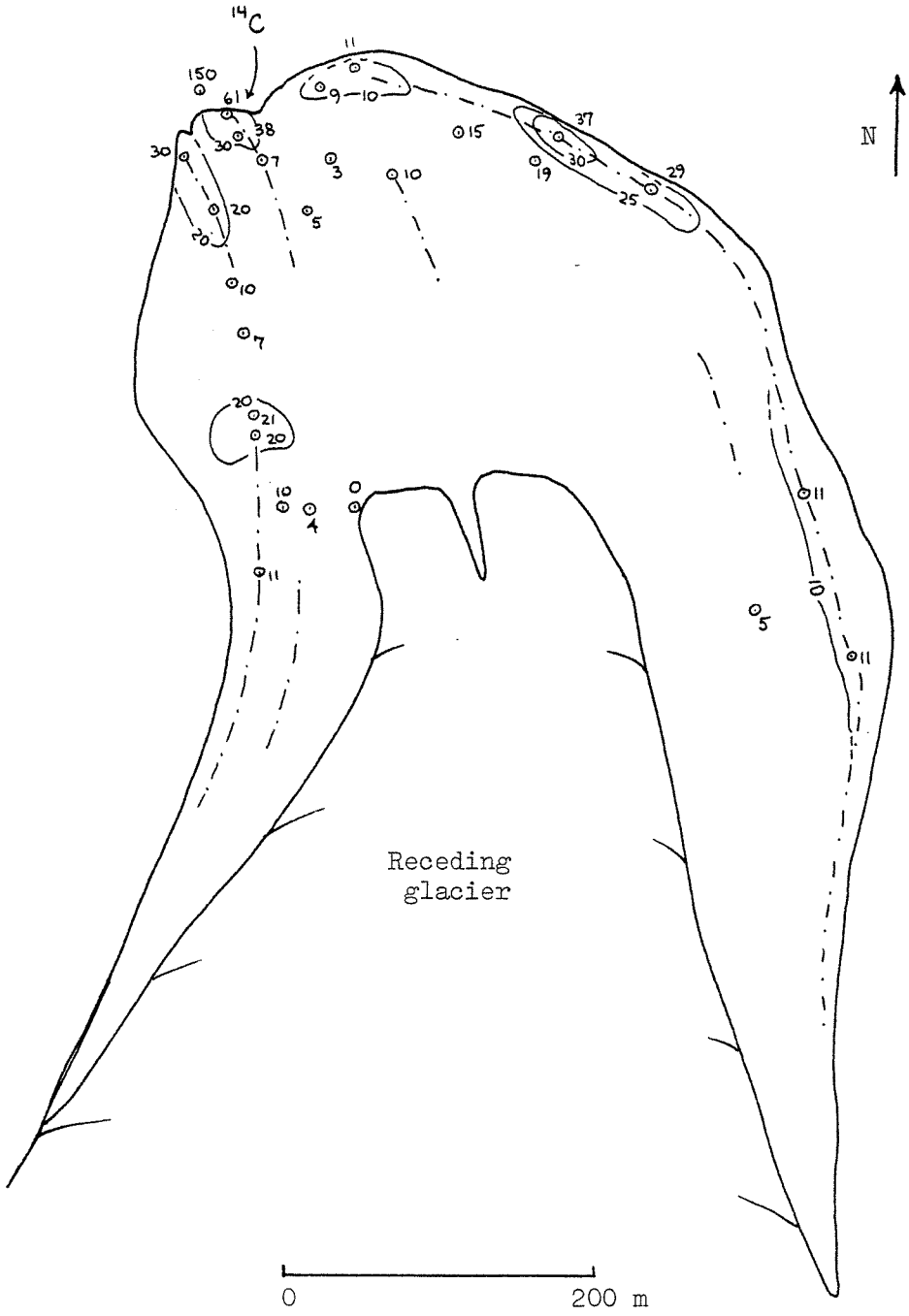

Maximum diameters of Rhizocarpon geographicum s.l. that characterize the debris lobe: 11, 21, 30?, 38, 61 mm.

APPENDIX C. LICHENOMETRIC MAPS

Ewe Glacier (no. 17).

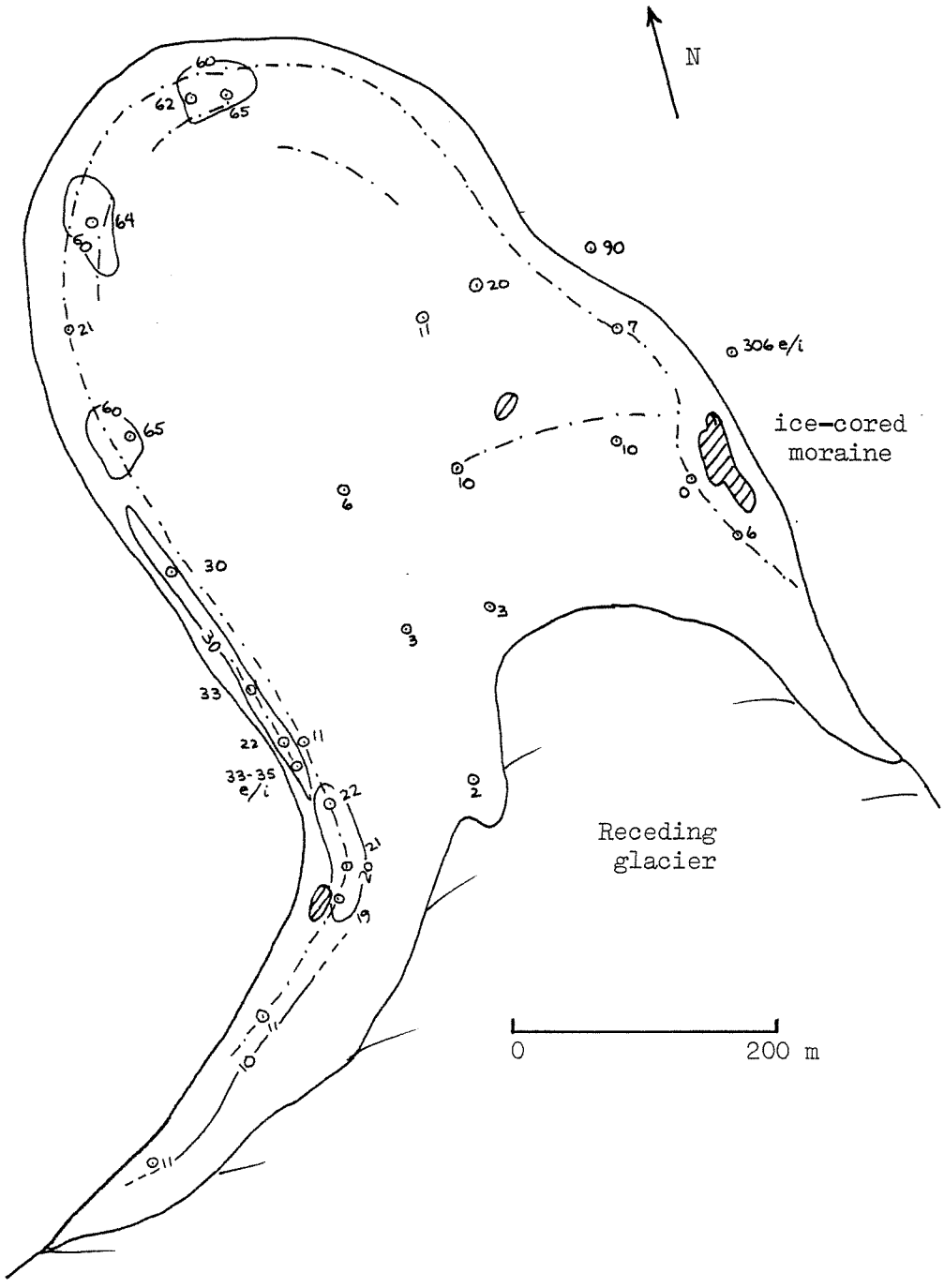

Maximum diameters of Rhizocarpon geographicum s.l. that characterize the debris lobe: 11, 22, 33, 65 mm.

APPENDIX C. LICHENOMETRIC MAPS

Kid Glacier (no. 18).

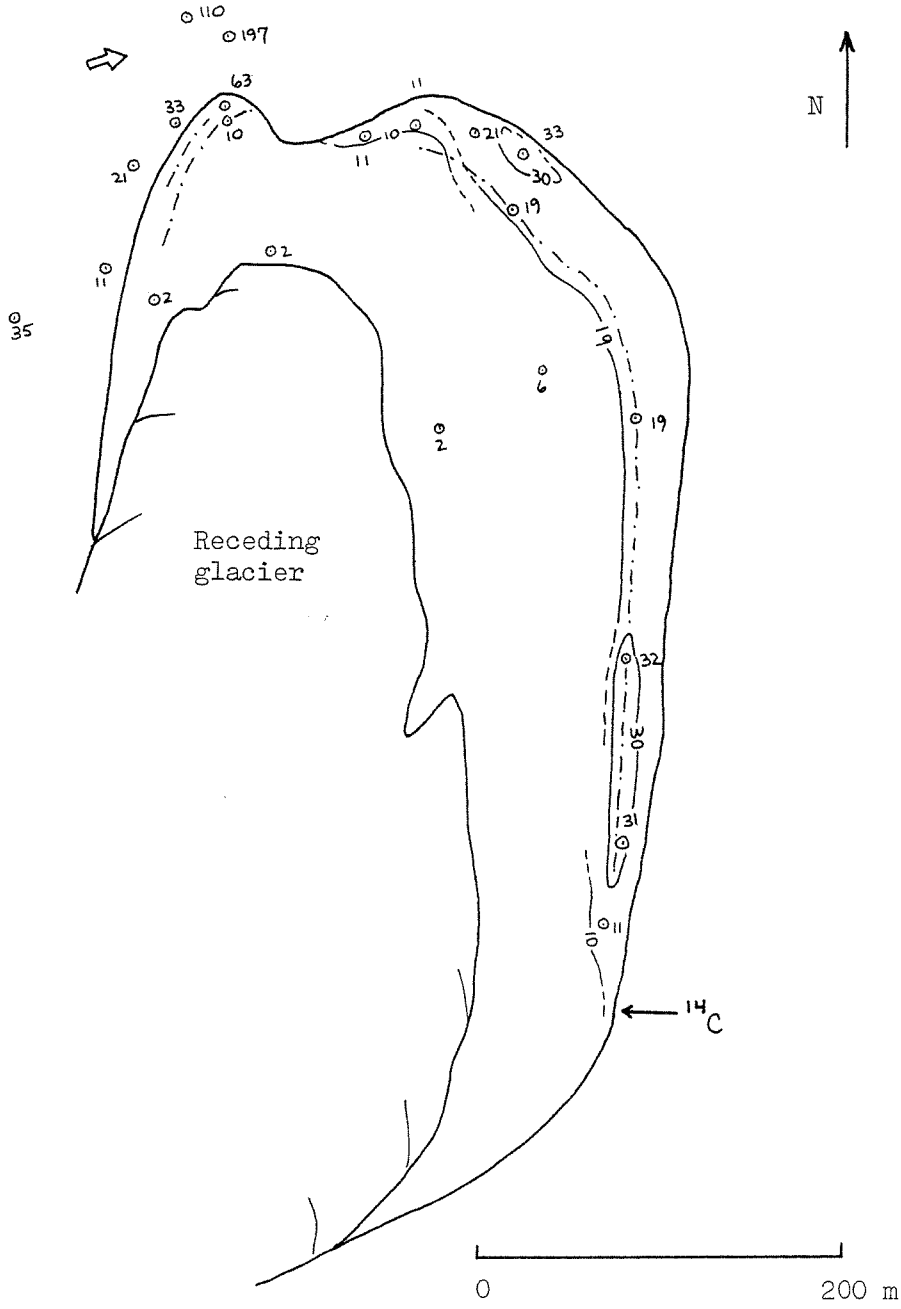

Maximum diameters of Rhizocarpon geographicum s.l. that characterize the debris lobe: 11, 19, 32, 63 mm.

APPENDIX C. LICHENOMETRIC MAPS

Vole Glacier (no.19).

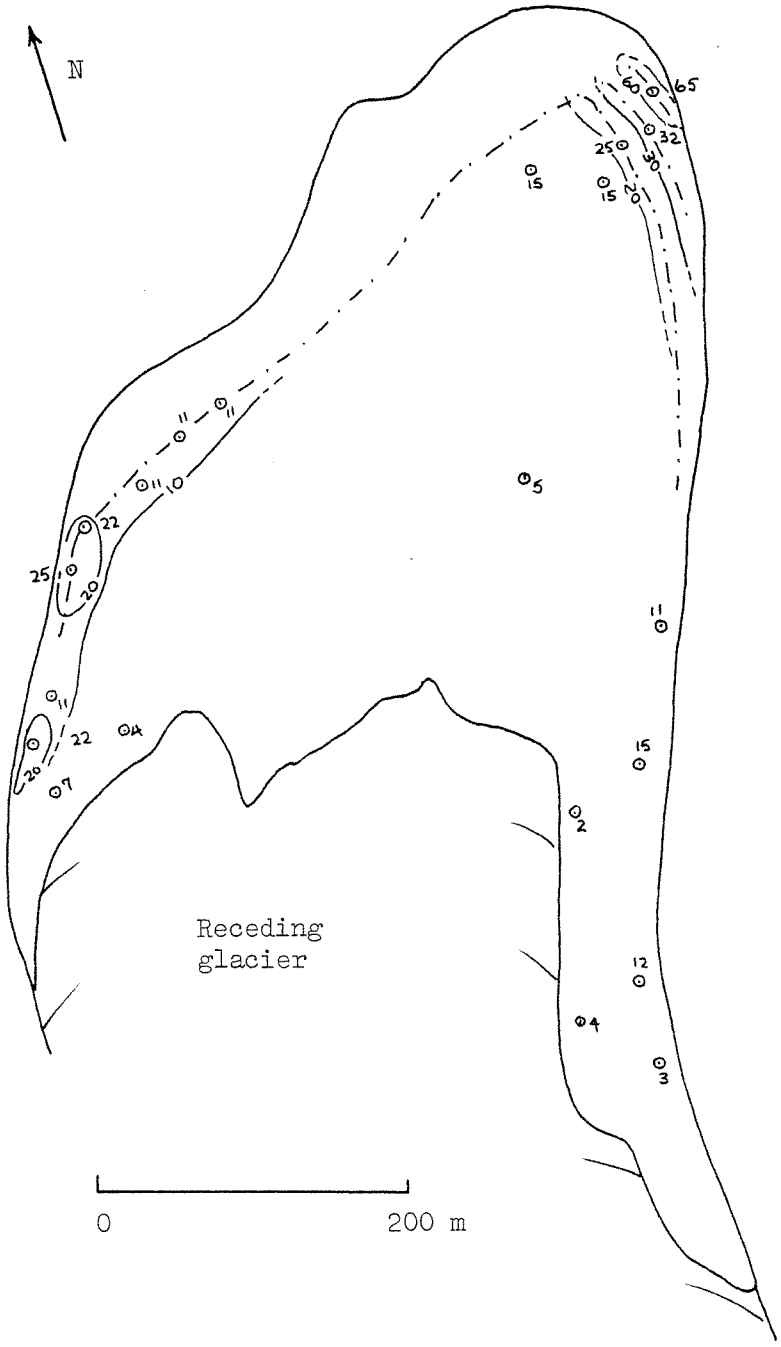

Maximum diameters of Rhizocarpon geographicum s.l. that characterize the debris lobe: 11, 25, 32, 65 mm.

APPENDIX C. LICHENOMETRIC MAPS

Sparrow Glacier (no. 20).

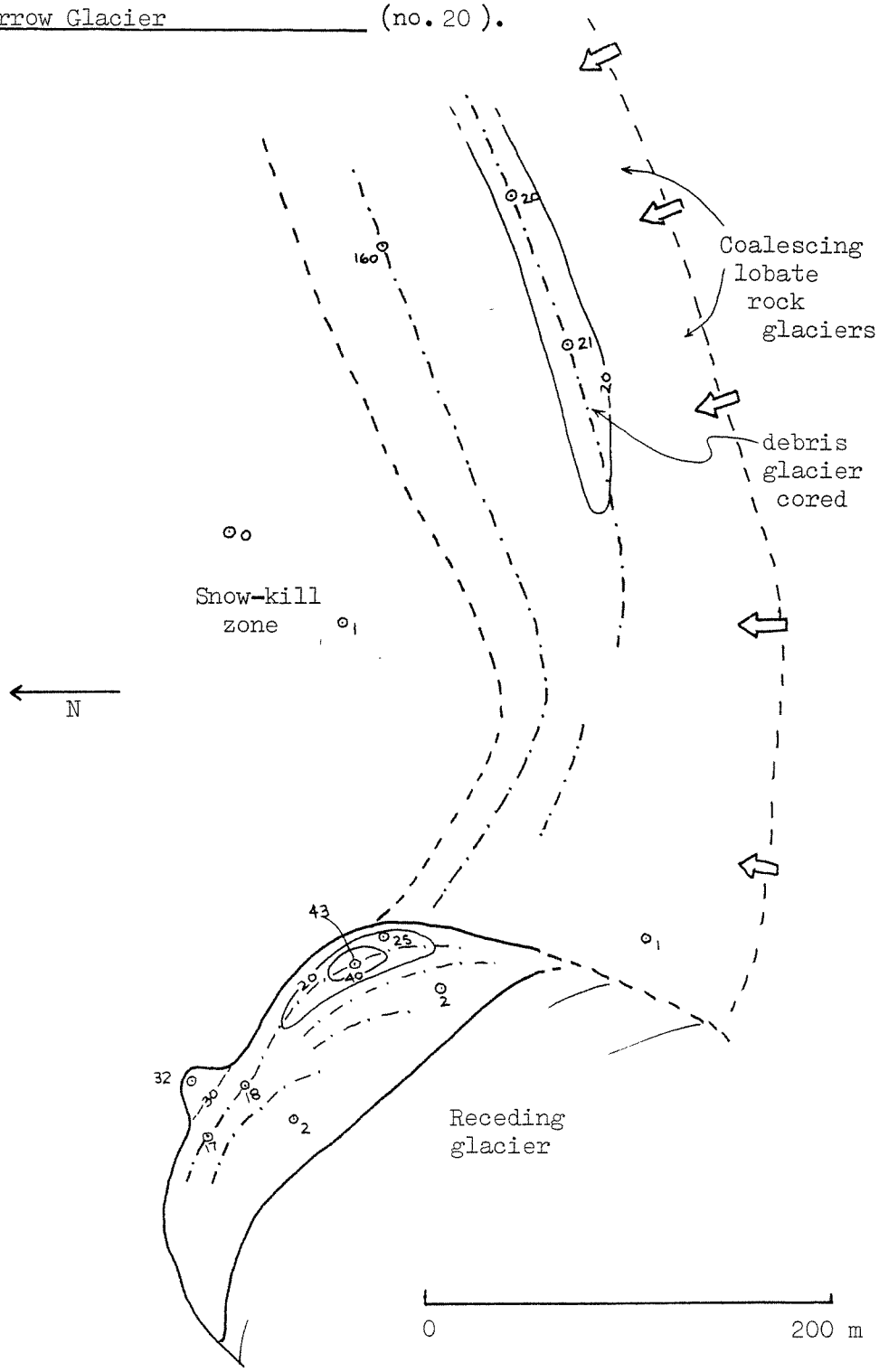

Maximum diameters of Rhizocarpon geographicum s.l. that characterize the debris lobe: 18, 21, 25, 32?, 43 mm.

APPENDIX C. LICHENOMETRIC MAPS

Raven Glacier (no. 21).

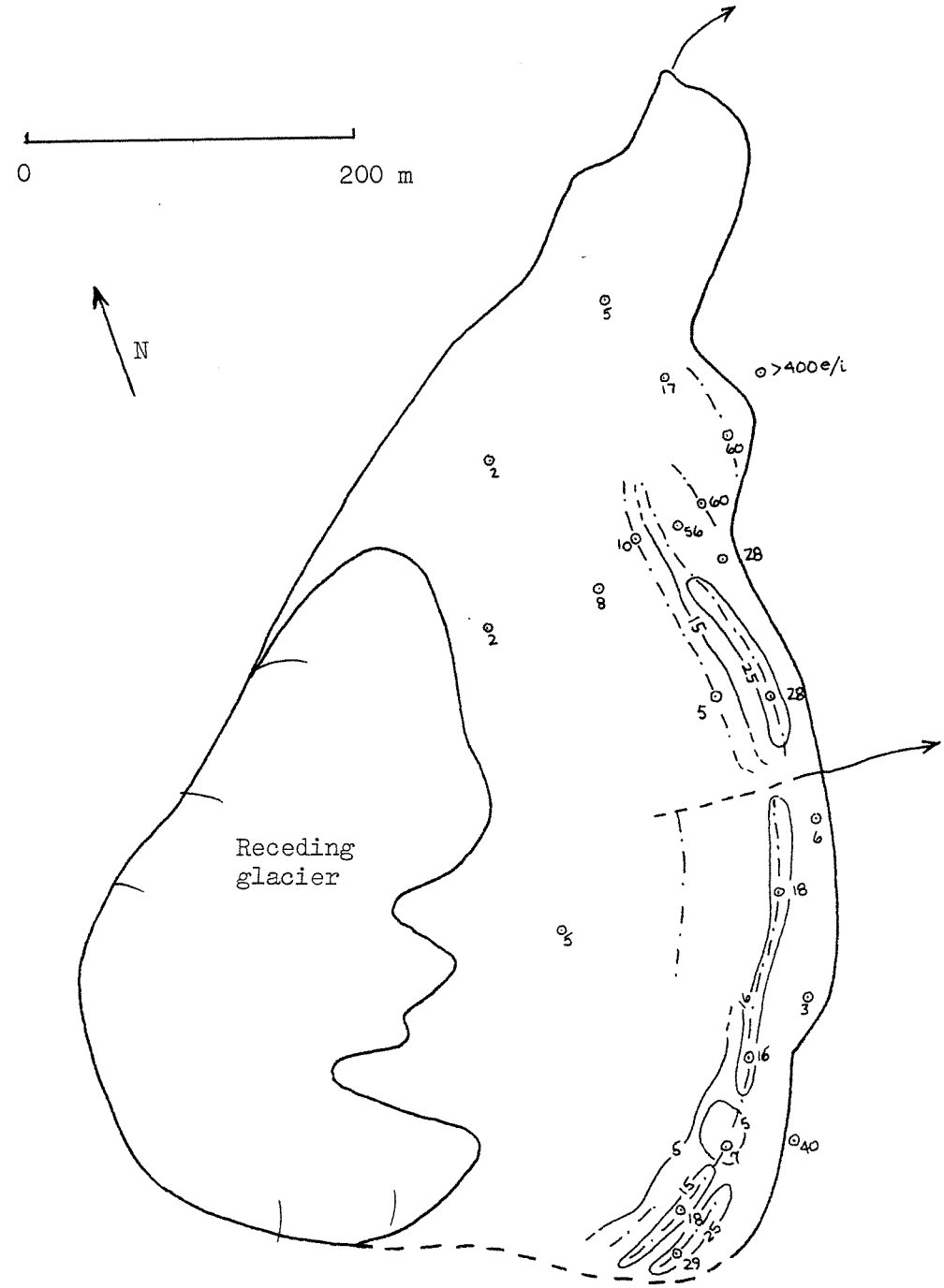

Maximum diameters of Rhizocarpon geographicum s.l. that characterize the debris lobe: 18, 29, 60 mm.

APPENDIX C. LICHENOMETRIC MAPS

Yellowjacket Glacier (no. 22).

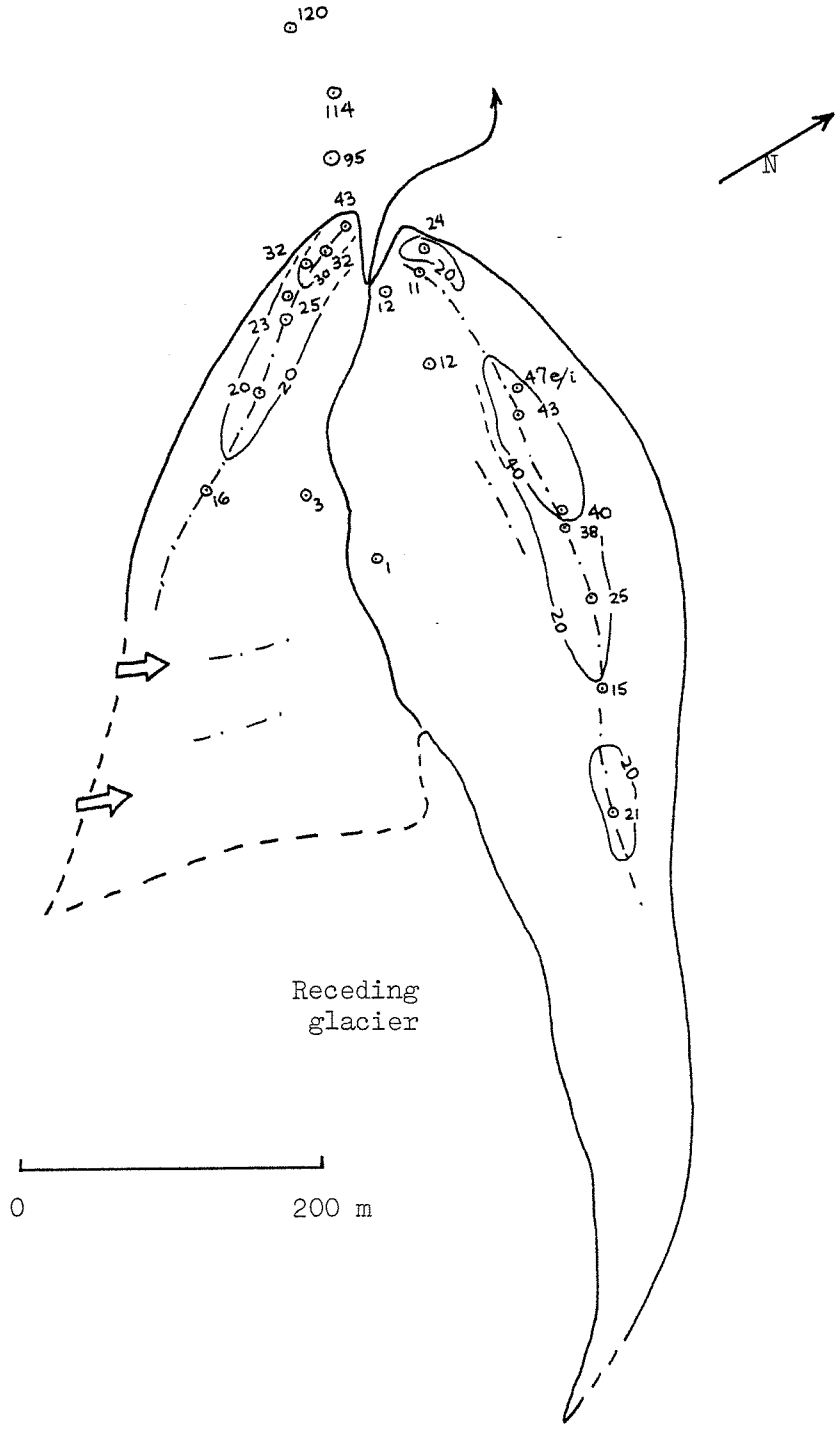

Maximum diameters of Rhizocarpon geographicum s.l. that characterize the debris lobe: 25, 32?, 43 mm.

APPENDIX C. LICHENOMETRIC MAPS

Burbot Glacier (no. 23).

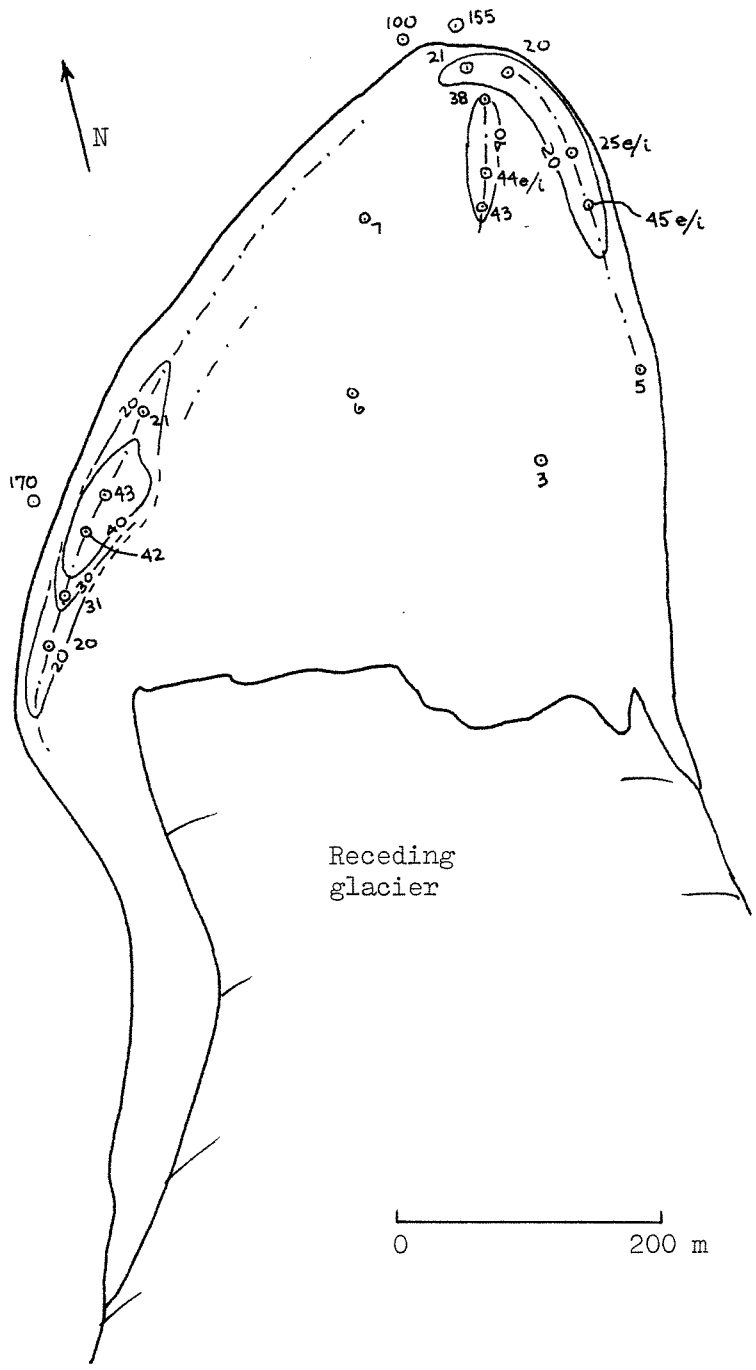

Maximum diameters of Rhizocarpon geographicum s.l. that characterize the debris lobe: 21, 43 mm.

APPENDIX C. LICHENOMETRIC MAPS

Arctic Char Glacier (no. 24).

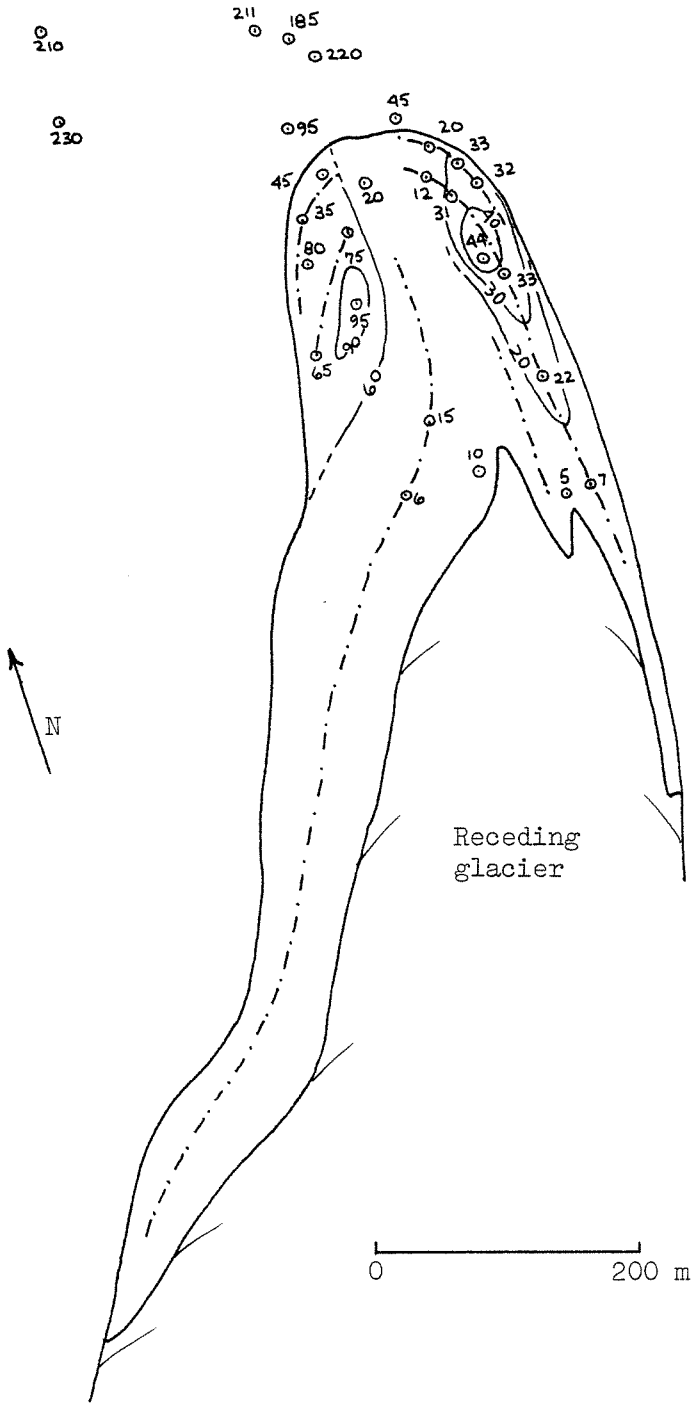

Maximum diameters of Rhizocarpon geographicum s.l. that characterize the debris lobe: 22, 33, 44, 95 mm.

APPENDIX C. LICHENOMETRIC MAPS

Grayling Glacier (no. 25).

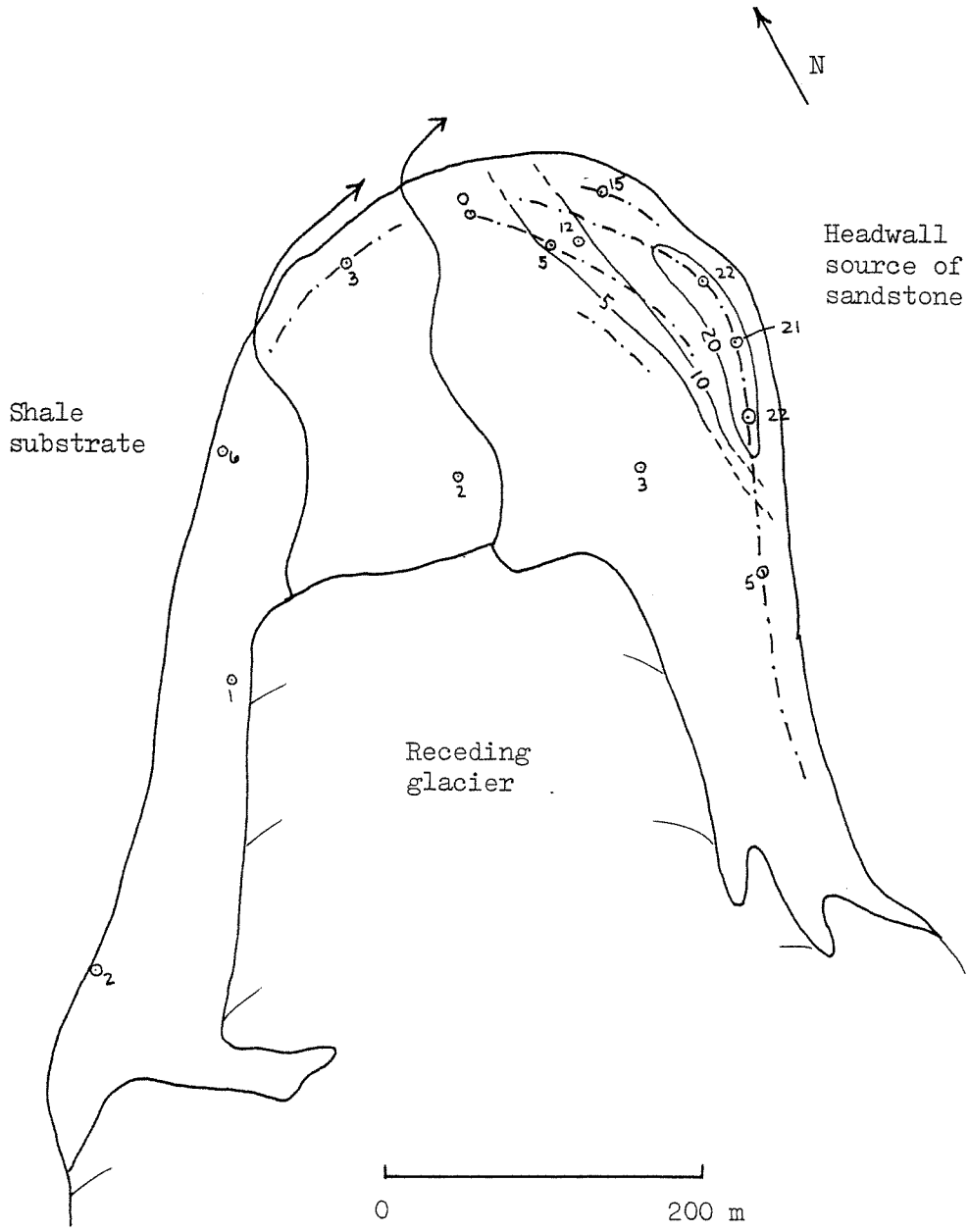

Maximum diameters of Rhizocarpon geographicum s.l. that characterize the debris lobe: 22 mm.

APPENDIX C. LICHENOMETRIC MAPS

Cisco Glacier (no. 26).

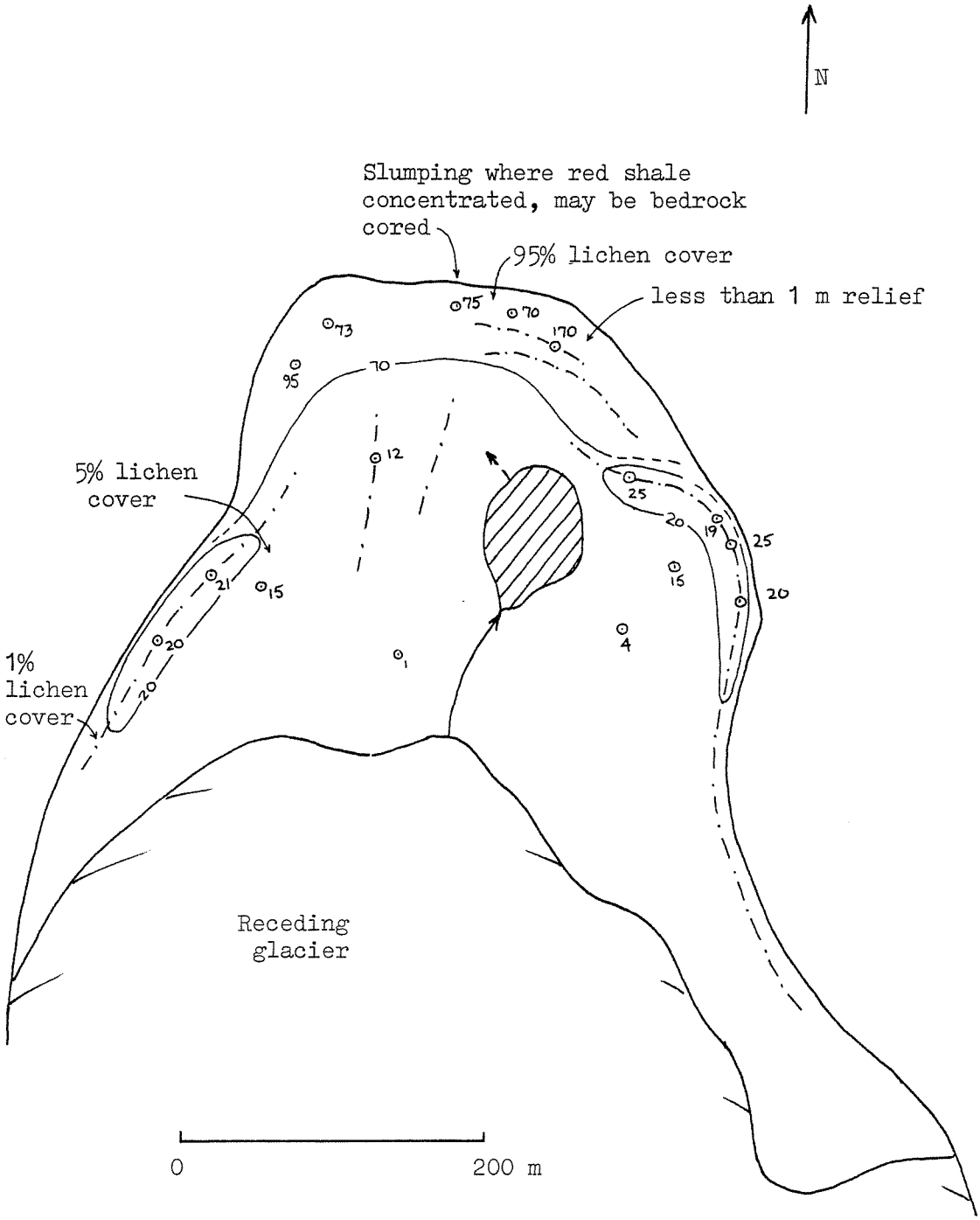

Maximum diameters of Rhizocarpon geographicum s.l. that characterize the debris lobe: 25 mm.

APPENDIX C. LICHENOMETRIC MAPS

Moose Glacier (no. 27).

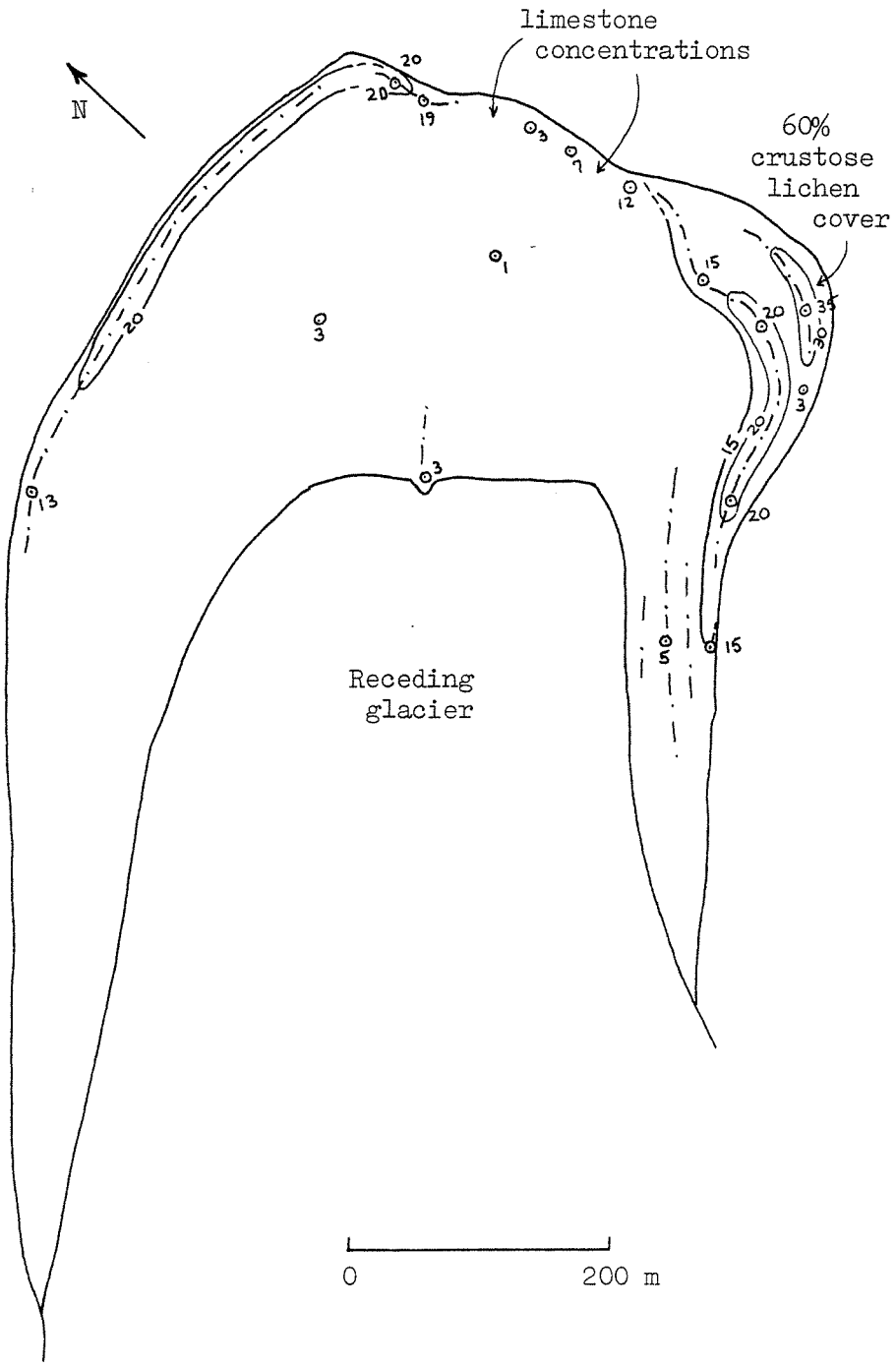

Maximum diameters of Rhizocarpon geographicum s.l. that characterize the debris lobe: 15, 20, 35 mm.

APPENDIX C. LICHENOMETRIC MAPS

Musk-Ox Glacier (no. 28).

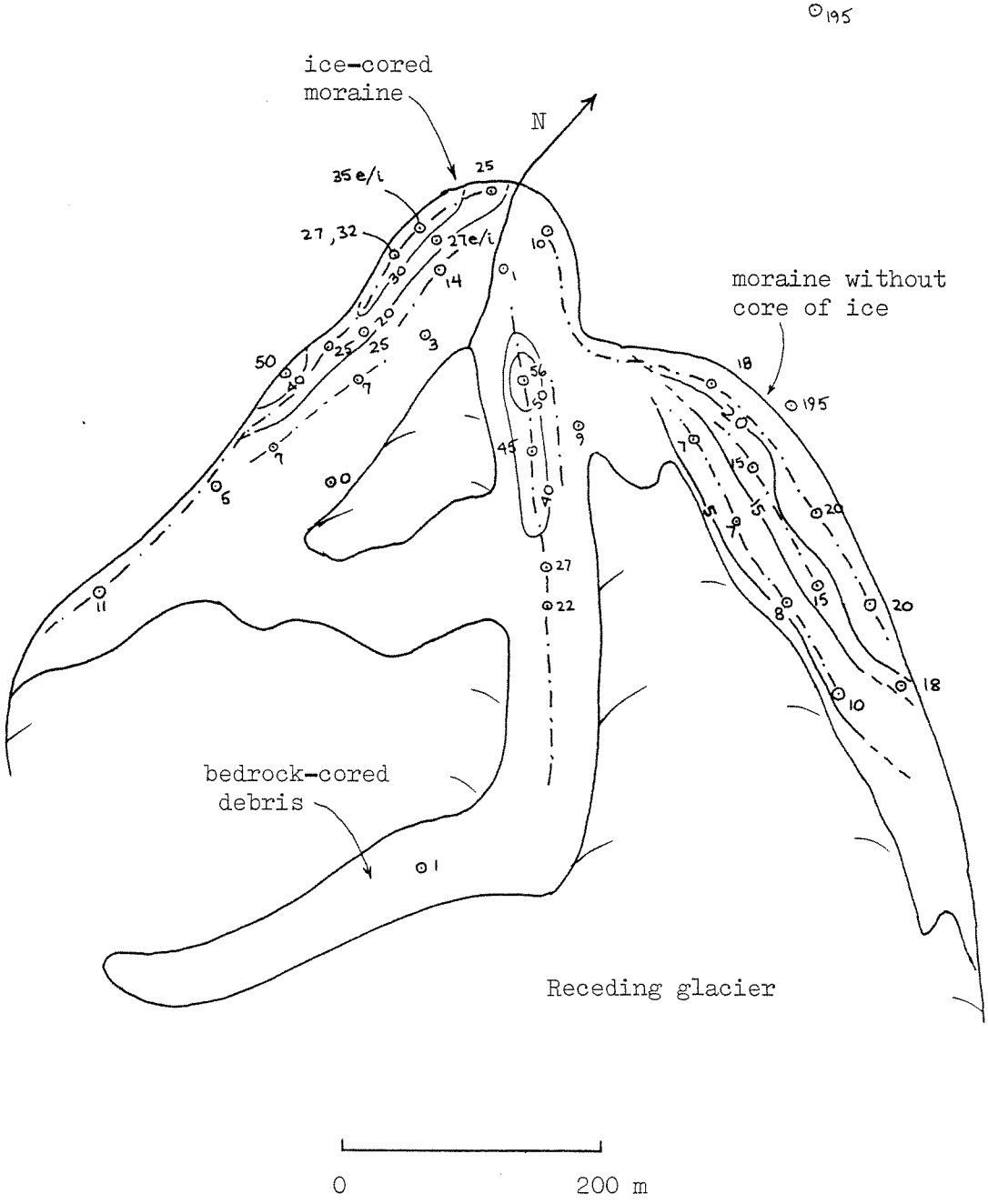

Maximum diameters of Rhizocarpon geographicum s.l. that characterize the debris lobe: 7?, 15, 20, 25, 32, 50, 56 mm.

APPENDIX C. LICHENOMETRIC MAPS

Arctic Tern Glacier (no.29).

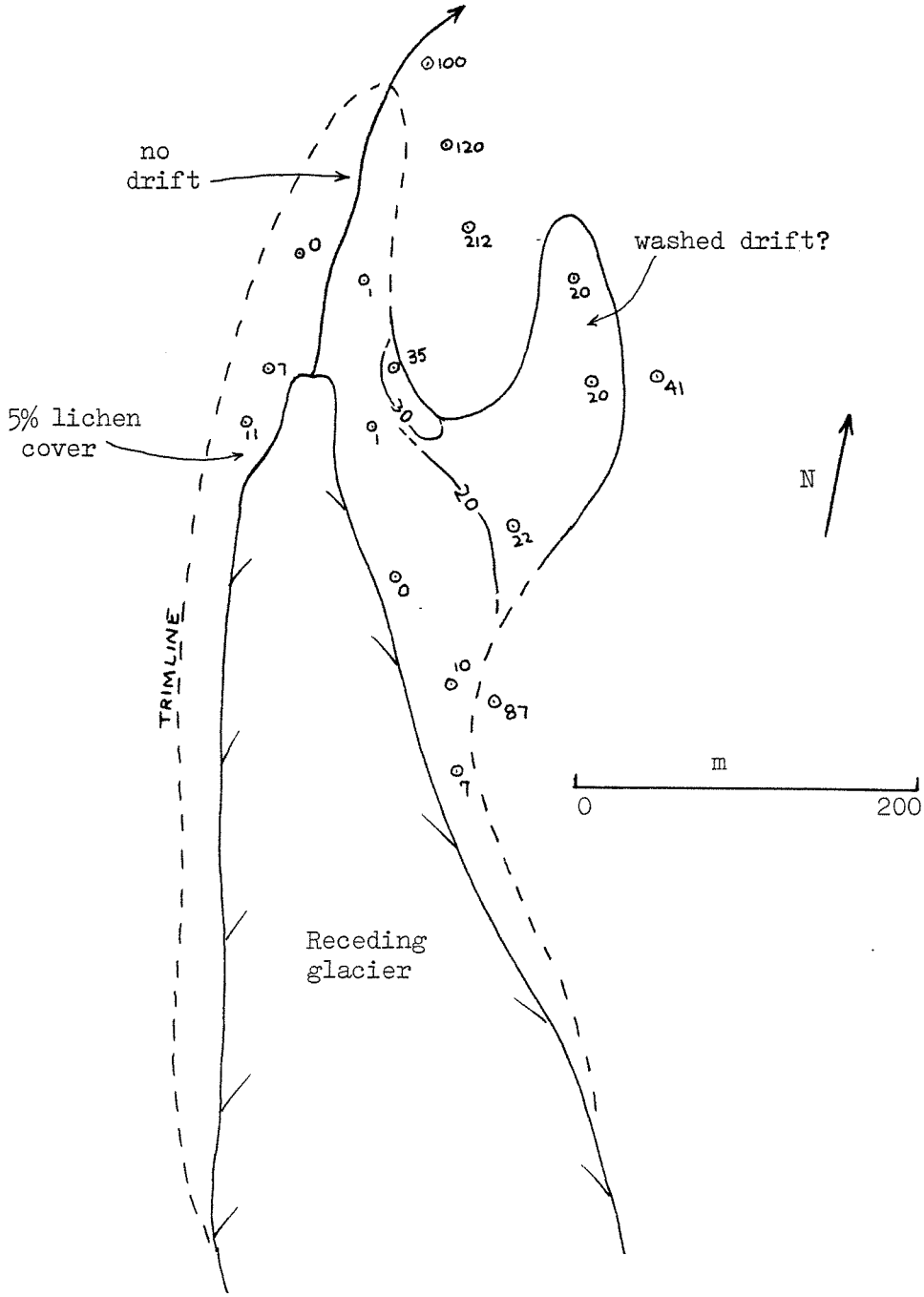

Maximum diameters of Rhizocarpon geographicum s.l. that characterize the debris lobe: 22, 35 mm.

APPENDIX C. LICHENOMETRIC MAPS

Snowy Owl West Glacier (no. 30).

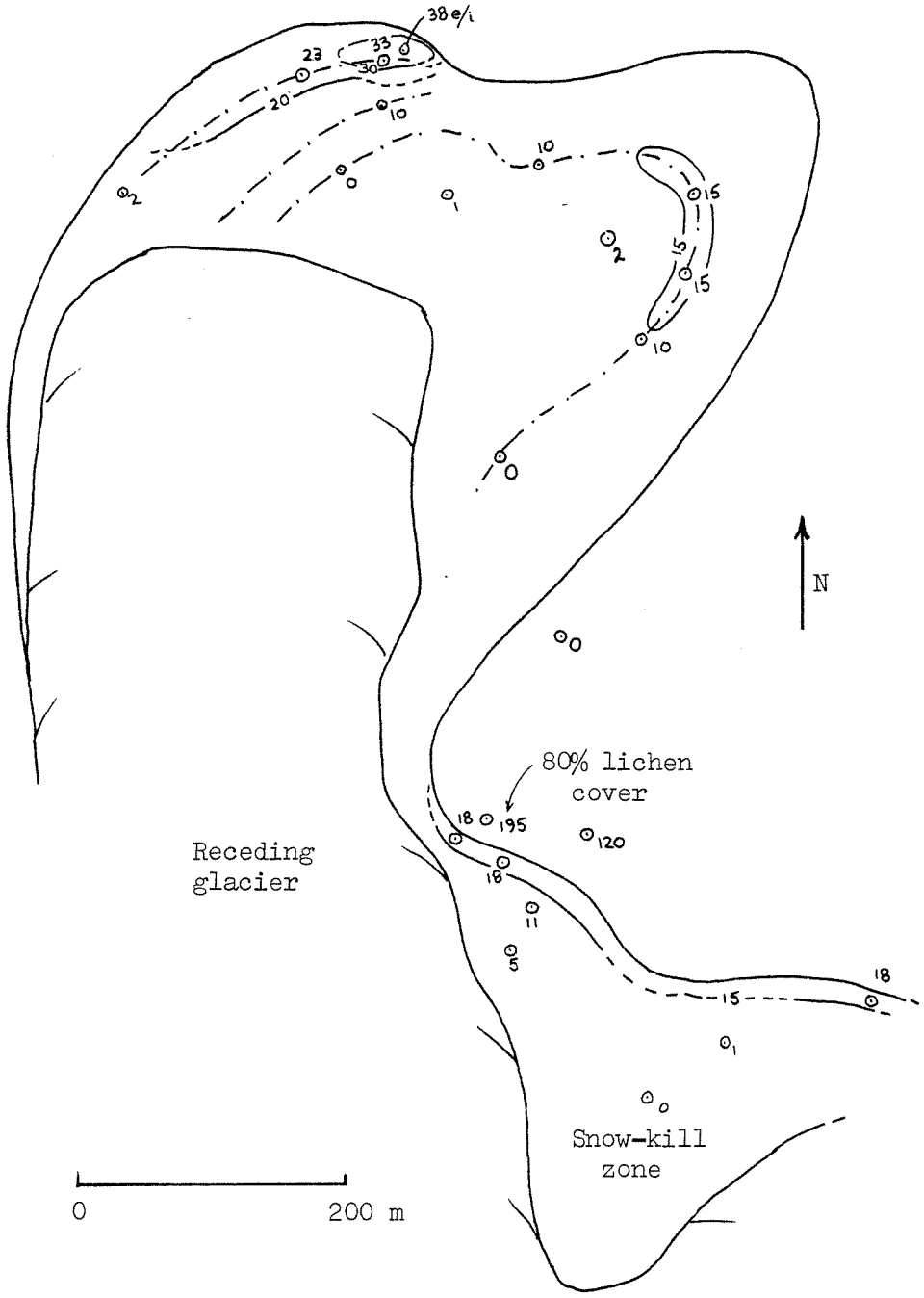

Maximum diameters of Rhizocarpon geographicum s.l. that characterize the debris lobe: 15, 18, 23, 33 mm.

APPENDIX C. LICHENOMETRIC MAPS

Wolf Glacier (no. 31).

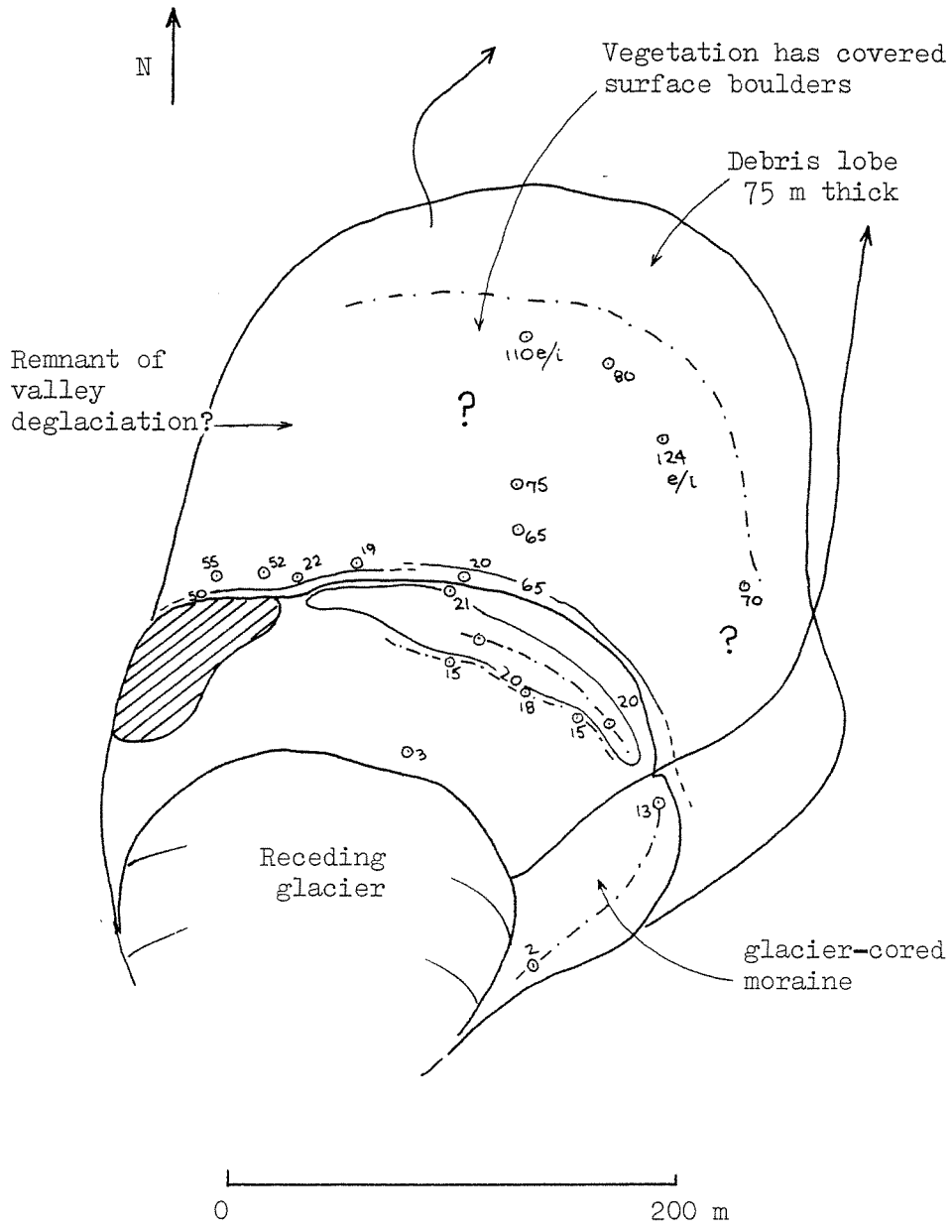

Maximum diameters of Rhizocarpon geographicum s.l. that characterize the debris lobe: 15, 21 mm.

APPENDIX C. LICHENOMETRIC MAPS

Lake Trout Glacier (no. 32).

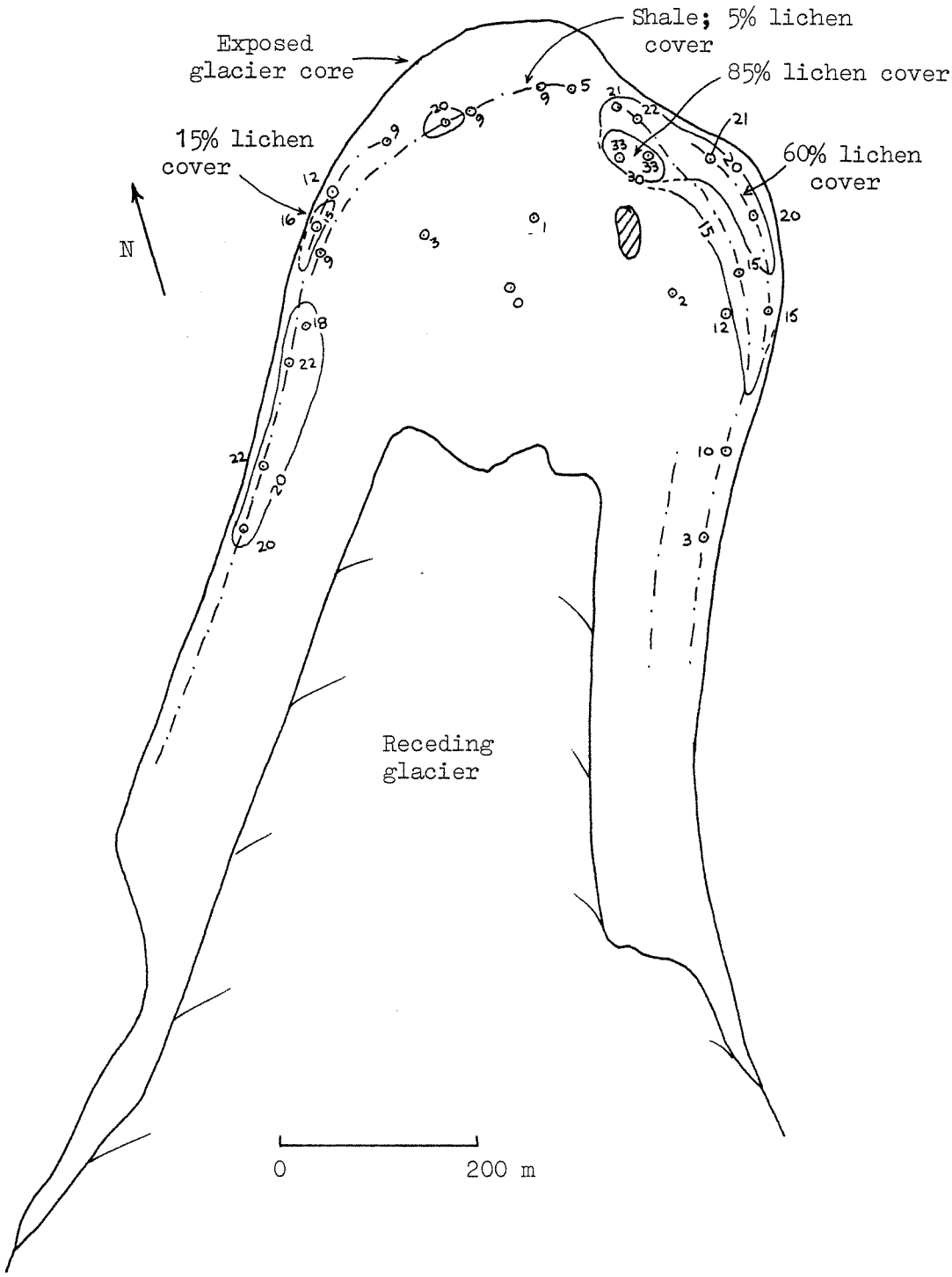

Maximum diameters of Rhizocarpon geographicum s.l. that characterize the debris lobe: 15, 22, 33 mm.

APPENDIX C. LICHENOMETRIC MAPS

Twin Glacier (no. 33).

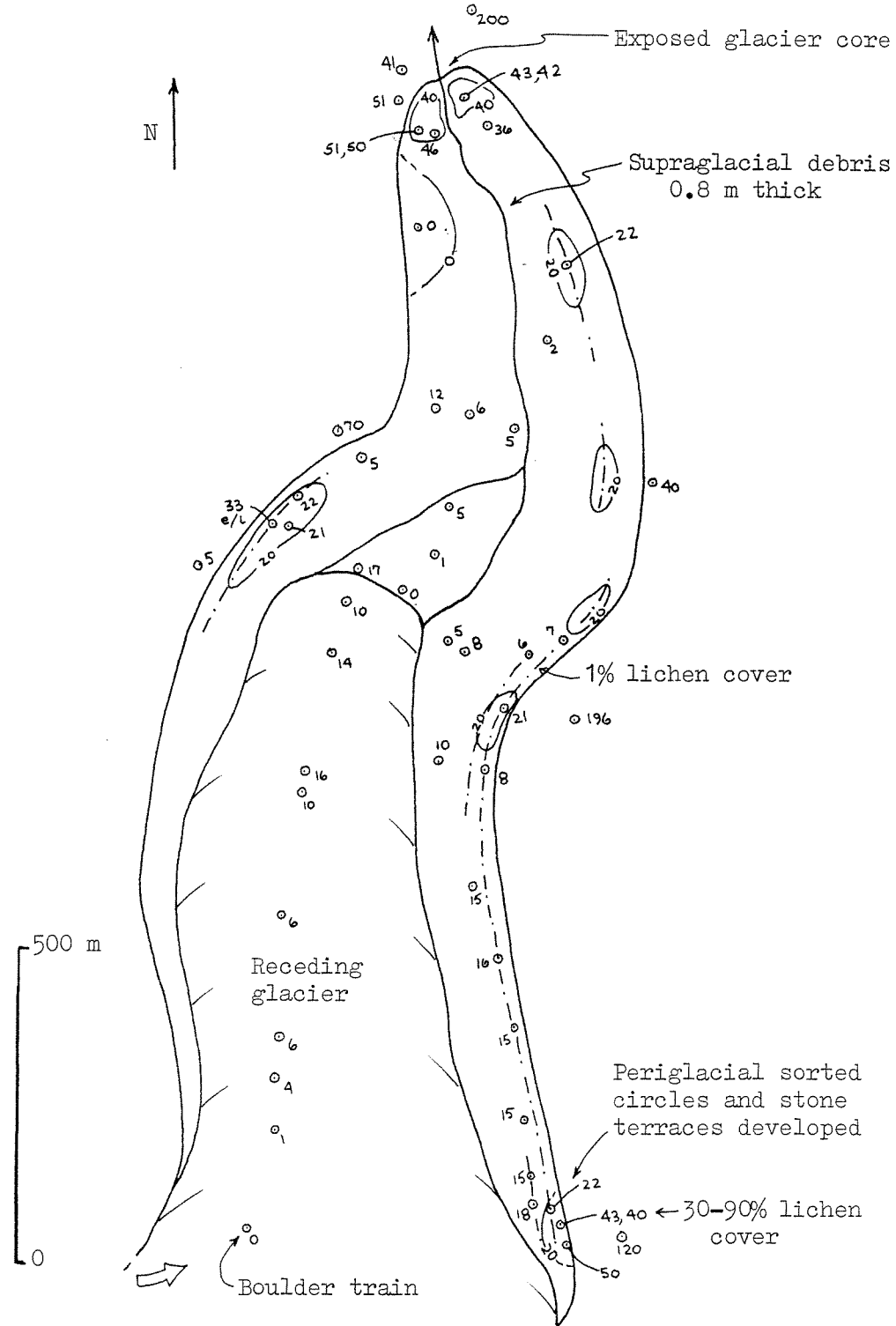

Maximum diameters of Rhizocarpon geographicum s.l. that characterize the debris lobe: 15, 22, 43, 51 mm.

APPENDIX C. LICHENOMETRIC MAPS

Snowy Owl East Glacier (no. 34).

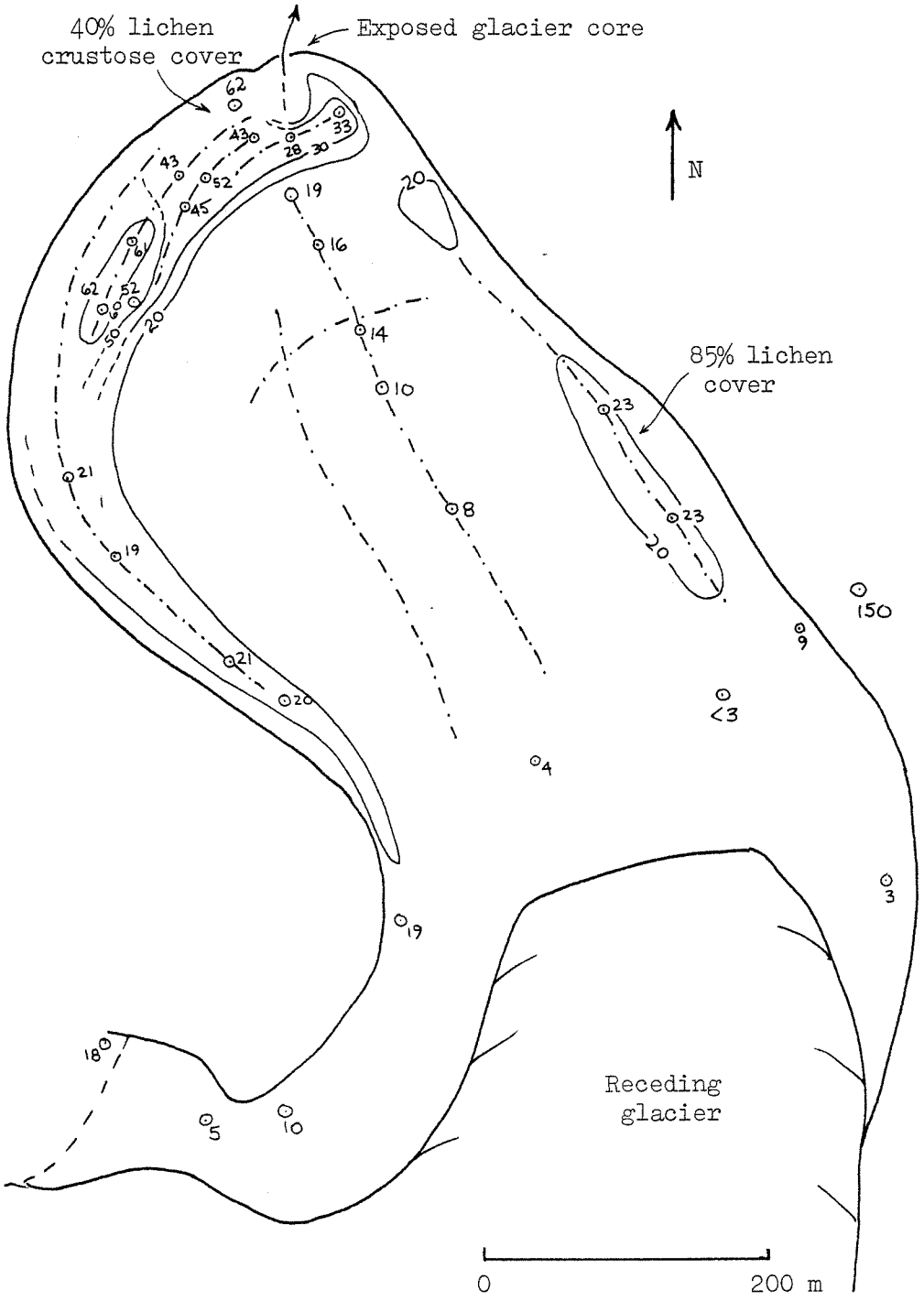

Maximum diameters of Rhizocarpon geographicum s.l. that characterize the debris lobe: 23, 33?, 45, 52?, 63 mm.

APPENDIX C. LICHENOMETRIC MAPS

Harlequin Duck Rock Glacier (no. 35).

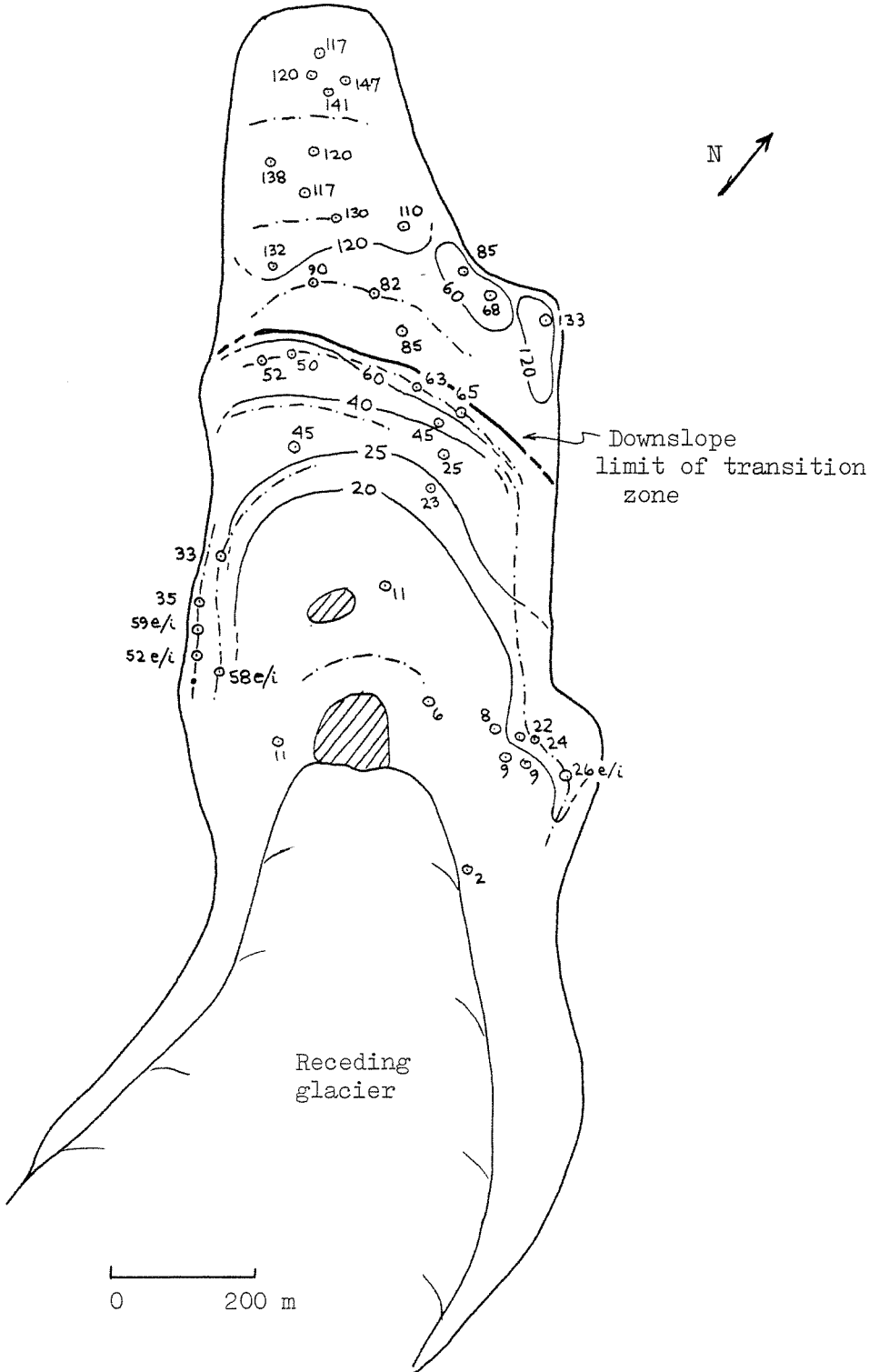

Maximum diameters of Rhizocarpon geographicum s.l. that characterize the debris lobe: 9?, 25, 45, 52, 65 mm.

APPENDIX C. LICHENOMETRIC MAPS

Ptarmigan Rock Glacier (no. 36).

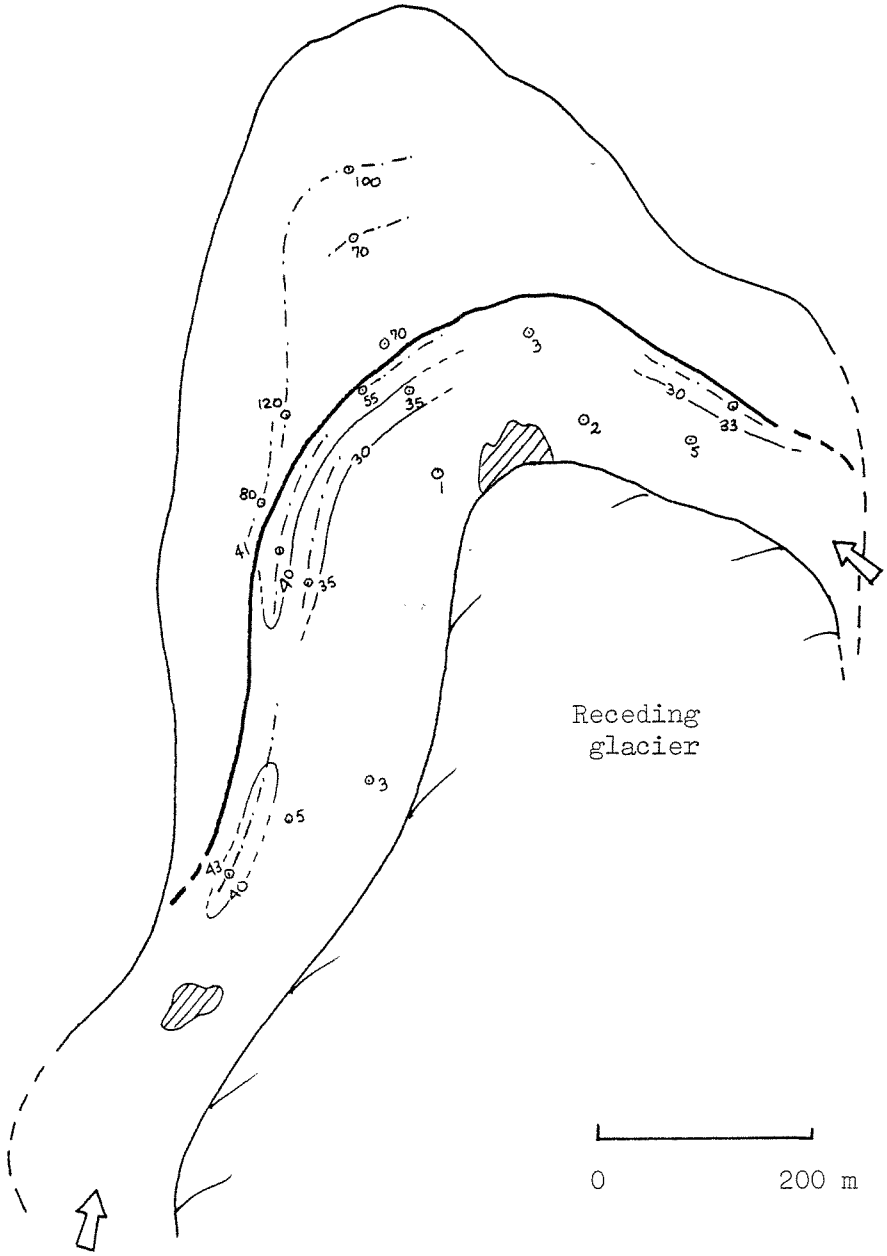

Maximum diameters of Rhizocarpon geographicum s.l. that characterize the debris lobe: 35, 43, 55 mm.

APPENDIX C. LICHENOMETRIC MAPS

Pika Rock Glacier (no. 37).

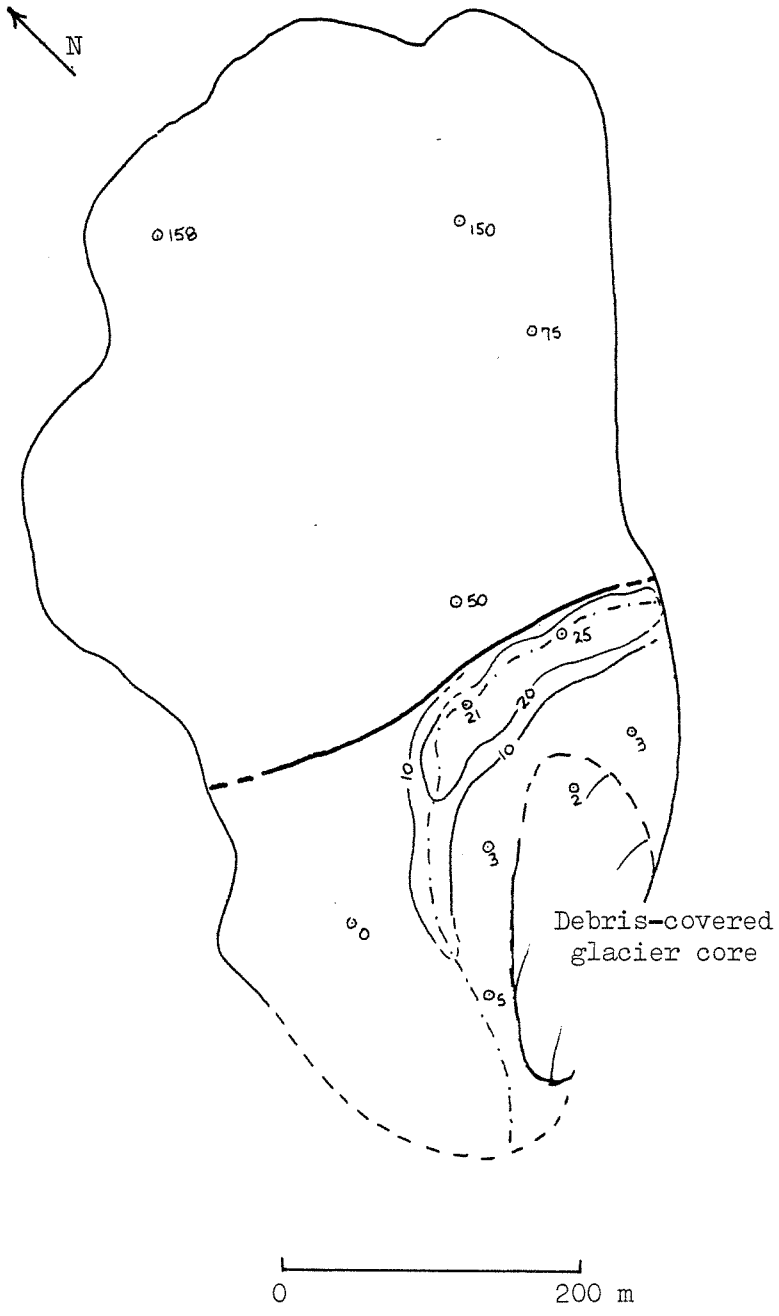

Maximum diameters of Rhizocarpon geographicum s.l. that characterize the debris lobe: 25 mm.

APPENDIX C. LICHENOMETRIC MAPS

Jaeger Rock Glacier (no. 38).

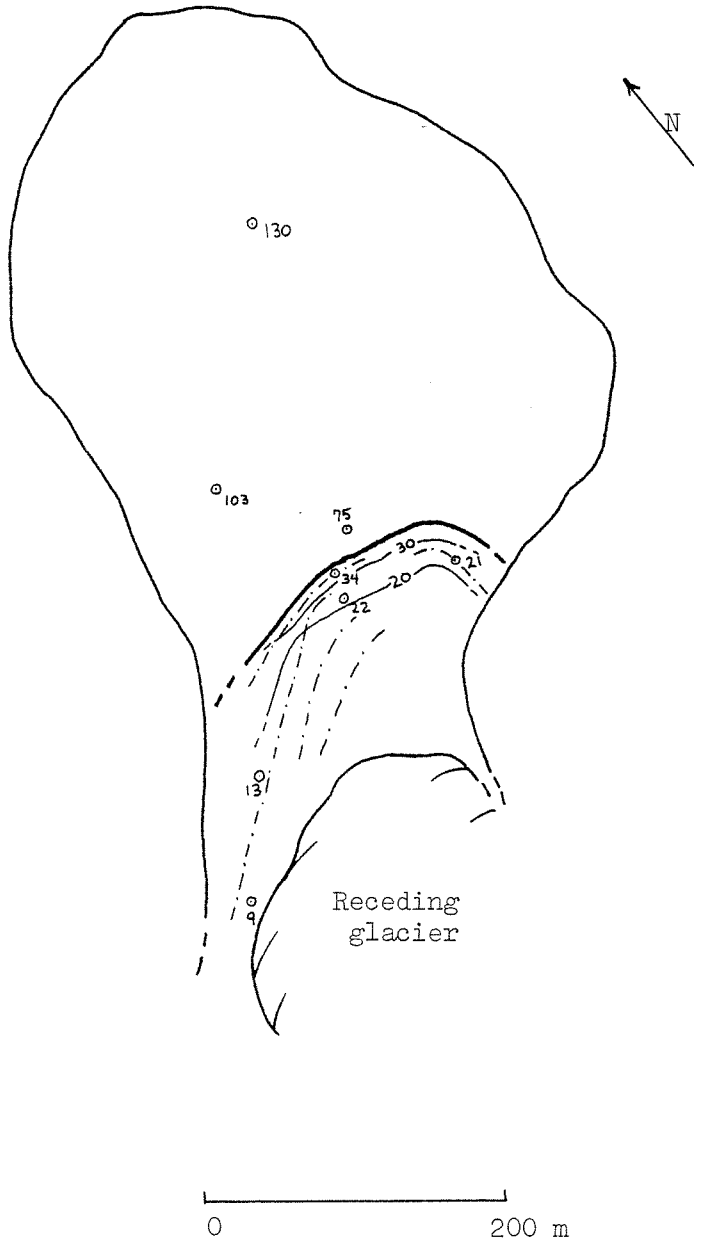

Maximum diameters of Rhizocarpon geographicum s.l. that characterize the debris lobe: 22, 34 mm.

APPENDIX C. LICHENOMETRIC MAPS

Parka Squirrel Rock Glacier (no. 39).

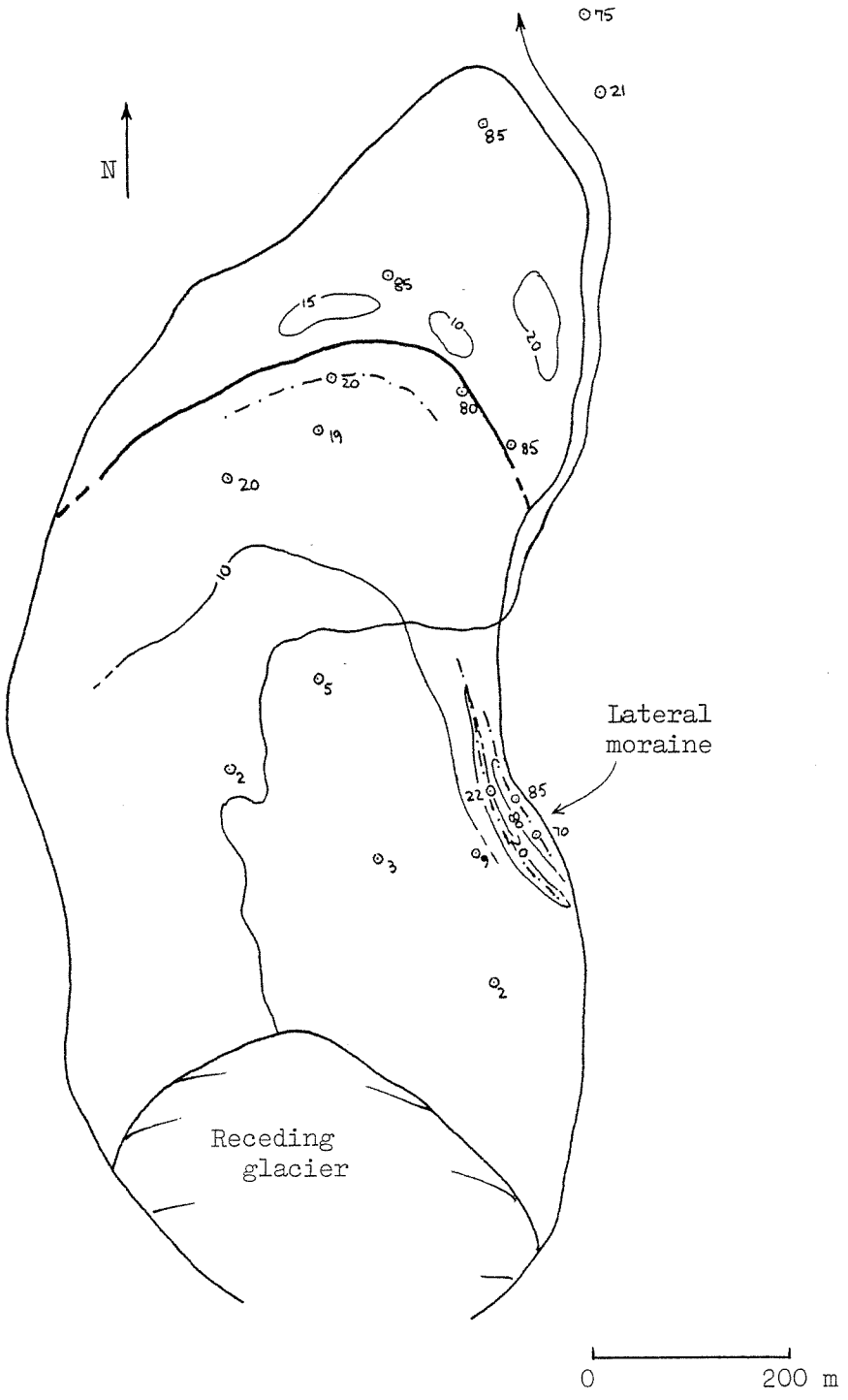

Maximum diameters of Rhizocarpon geographicum s.l. that characterize the debris lobe: 22, 85 mm.

APPENDIX C. LICHENOMETRIC MAPS

Mosquito Rock Glacier (no. 40).

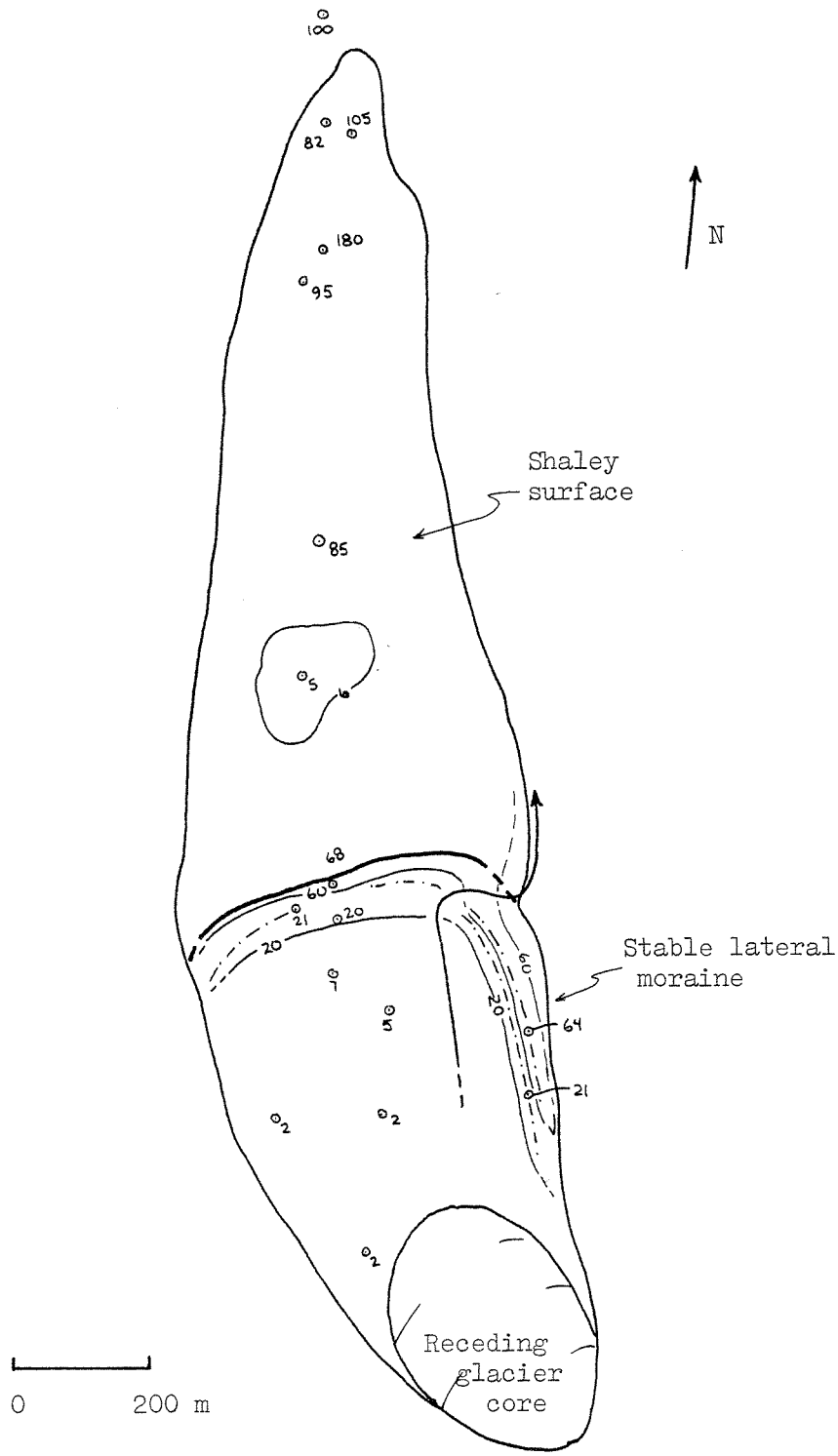

Maximum diameters of Rhizocarpon geographicum s.l. that characterize the debris lobe: 21, 68 mm.

APPENDIX C. LICHENOMETRIC MAPS

Wolverine Glacier (no. 41).

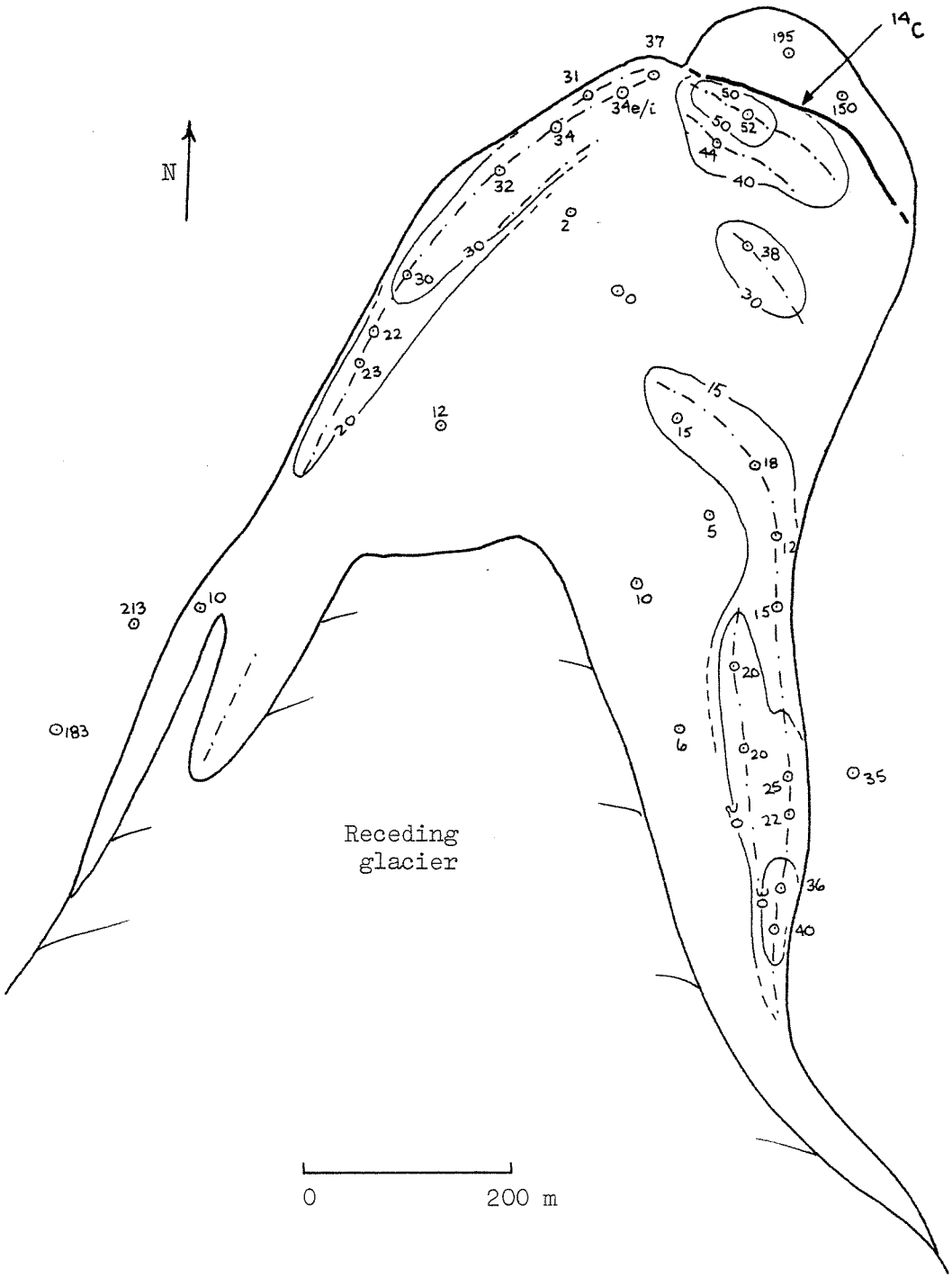

Maximum diameters of Rhizocarpon geographicum s.l. that characterize the debris lobe: 18, 25, 34, 44, 52 mm.

APPENDIX C. LICHENOMETRIC MAPS

Itikmalakpak-C Glacier (no. 48).

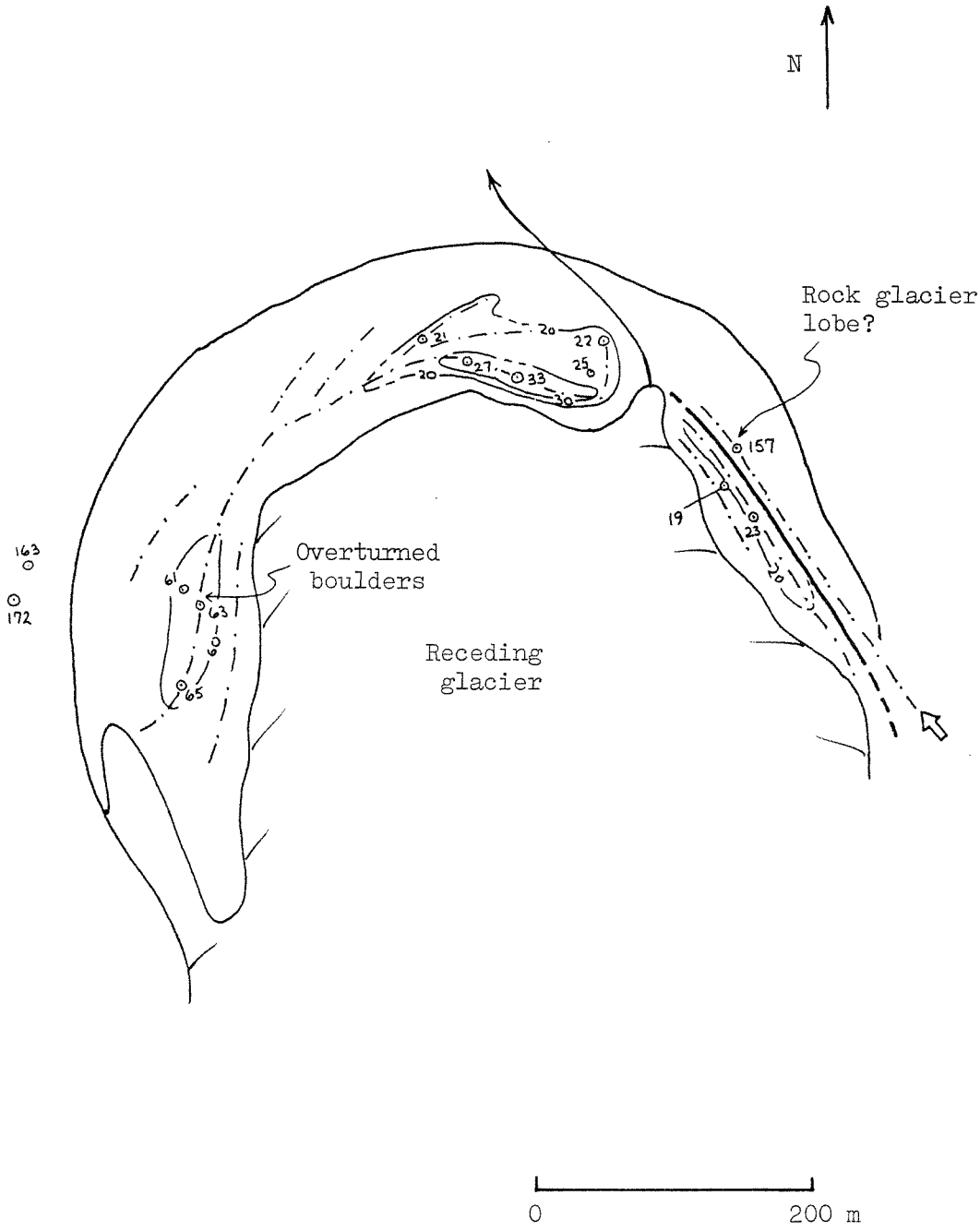

Maximum diameters of Rhizocarpon geographicum s.l. that characterize the debris lobe: 23, 33, 65 mm.

APPENDIX C. LICHENOMETRIC MAPS

Arrigetch-9 Glacier (nos. 50 and 52)

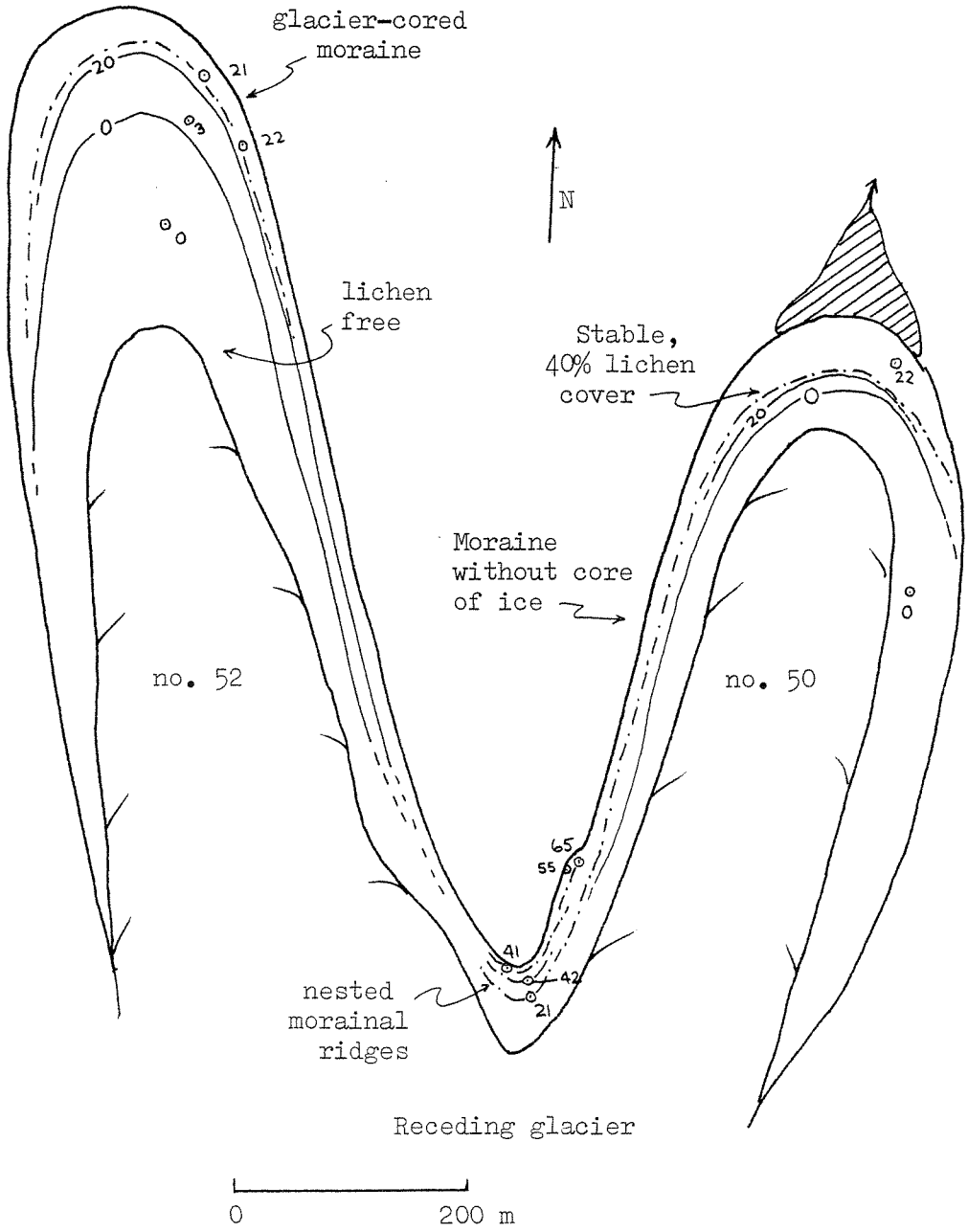

Maximum diameters of Rhizocarpon geographicum s.l. that characterize the debris lobe: 22, 42, 65 mm.

APPENDIX C. LICHENOMETRIC MAPS

Arrigetch-10 Glacier (nos. 51 and 53).

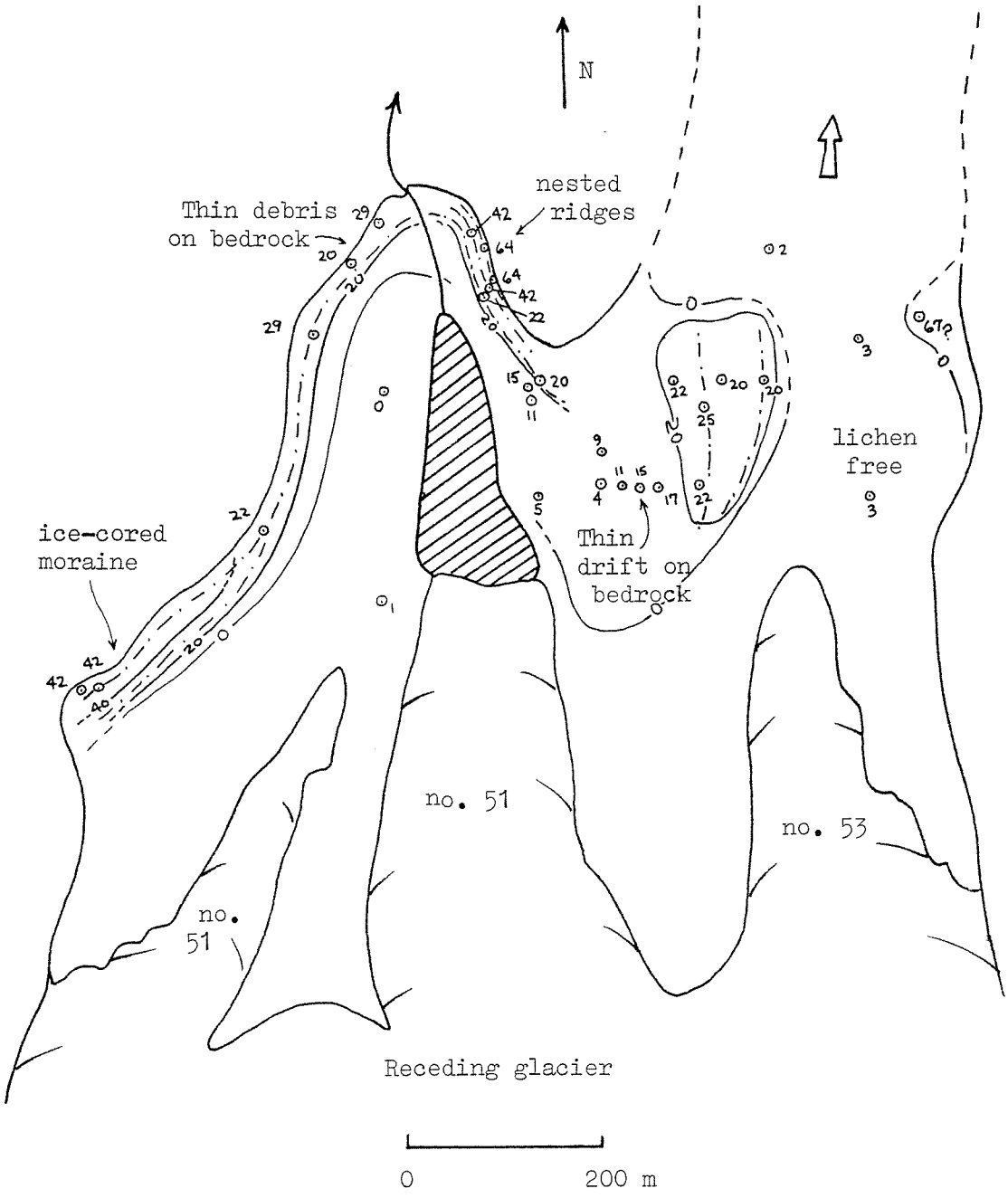

Maximum diameters of Rhizocarpon geographicum s.l. that characterize the debris lobe: 20, 25, 29, 42, 64, 65 mm.

APPENDIX C. LICHENOMETRIC MAPS

Arrigetch-1 Glacier (no.54).

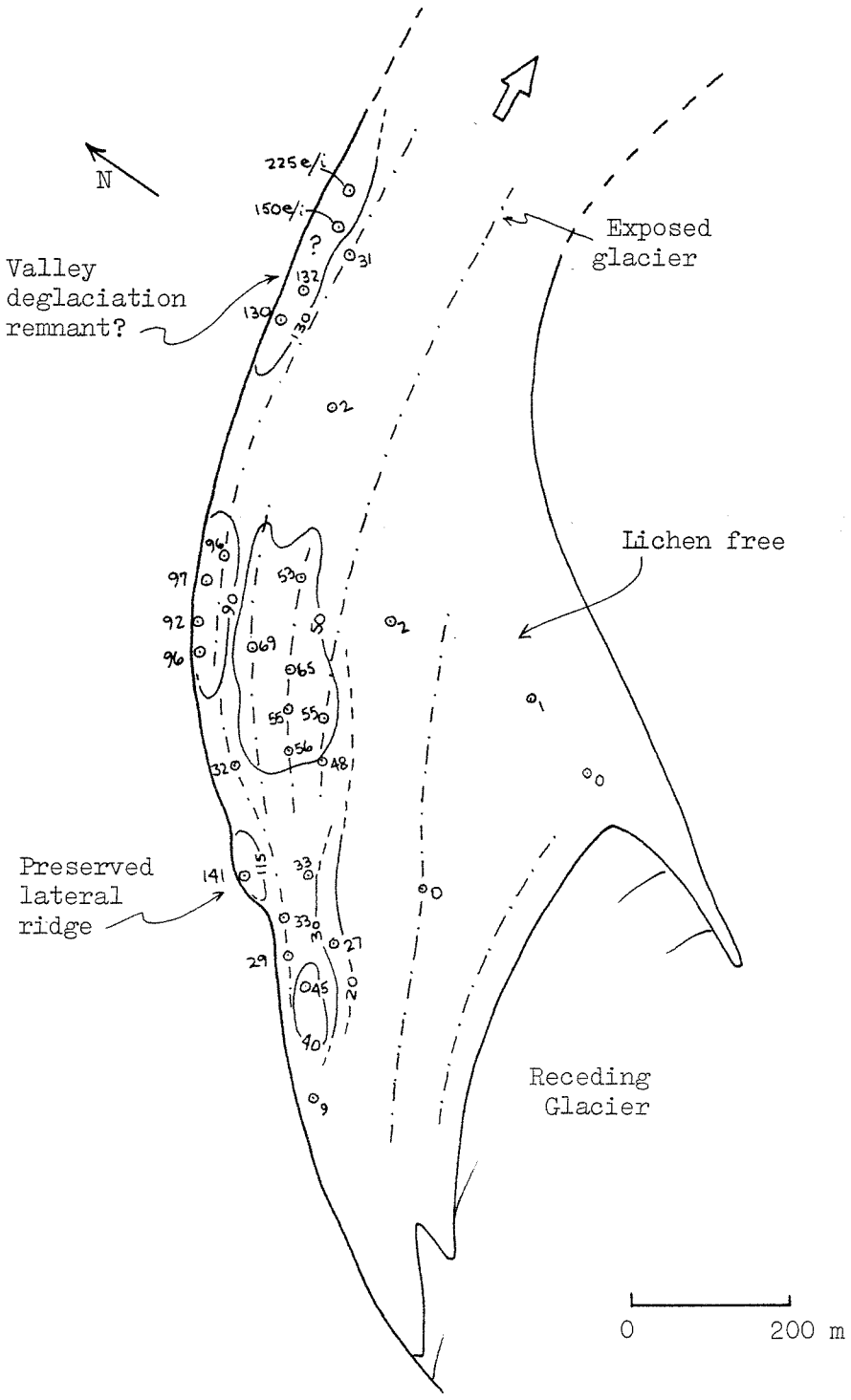

Maximum diameters of Rhizocarpon geographicum s.l. that characterize the debris lobe: 33, 45, 55?, 97, 141 mm.

APPENDIX C. LICHENOMETRIC MAPS

Arrigetch-2, 3, 4 Glacier (no. 55).

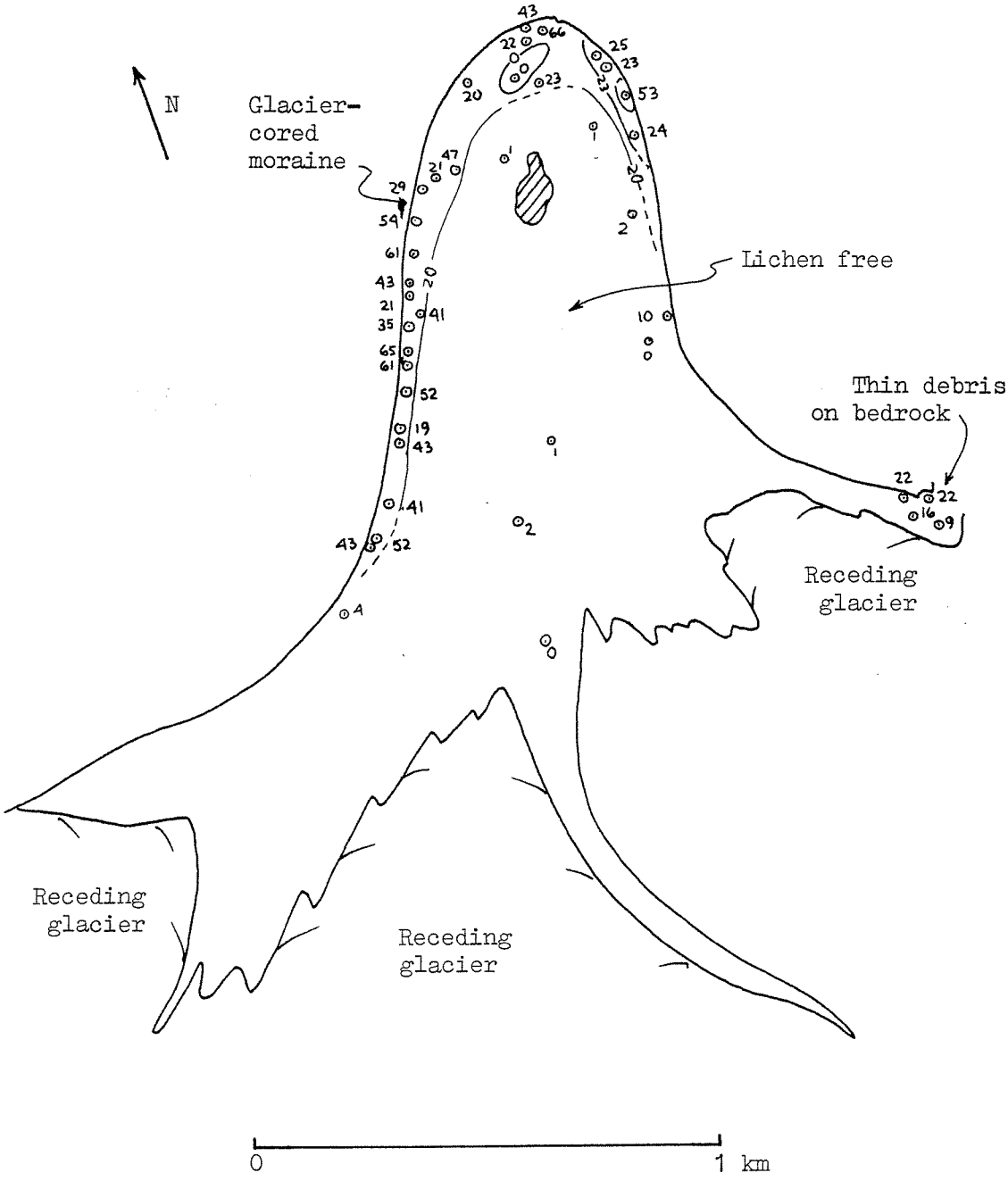

Maximum diameters of Rhizocarpon geographicum s.l. that characterize the debris lobe: 22, 25, 54, 66 mm.

APPENDIX C. LICHENOMETRIC MAPS

Arrigetch-4 East (no. 56).

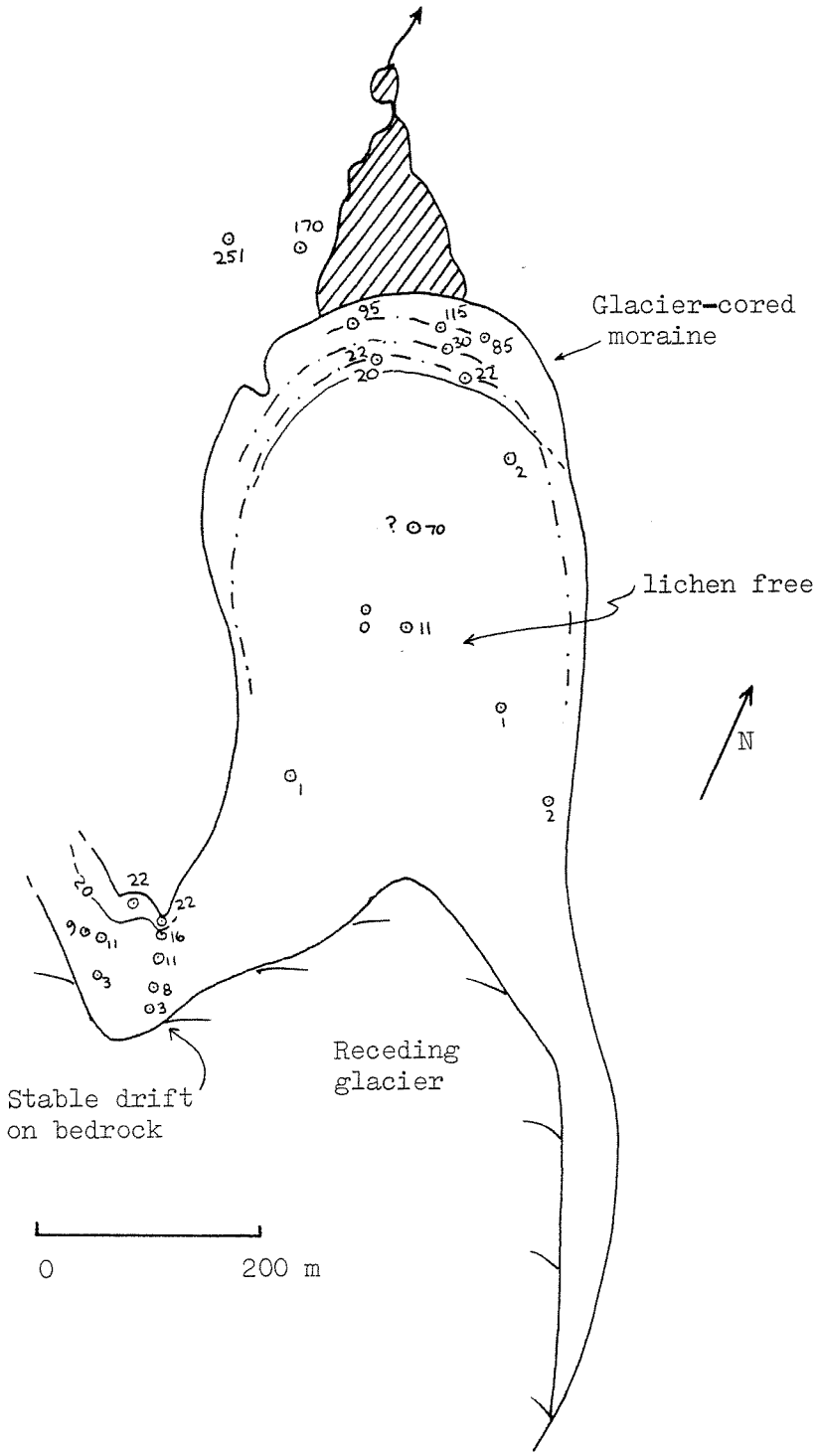

Maximum diameters of Rhizocarpon geographicum s.l. that characterize the debris lobe: 22, 95?, 115 mm.

APPENDIX C. LICHENOMETRIC MAPS

Arrigetch-11 Glacier (no. 58).

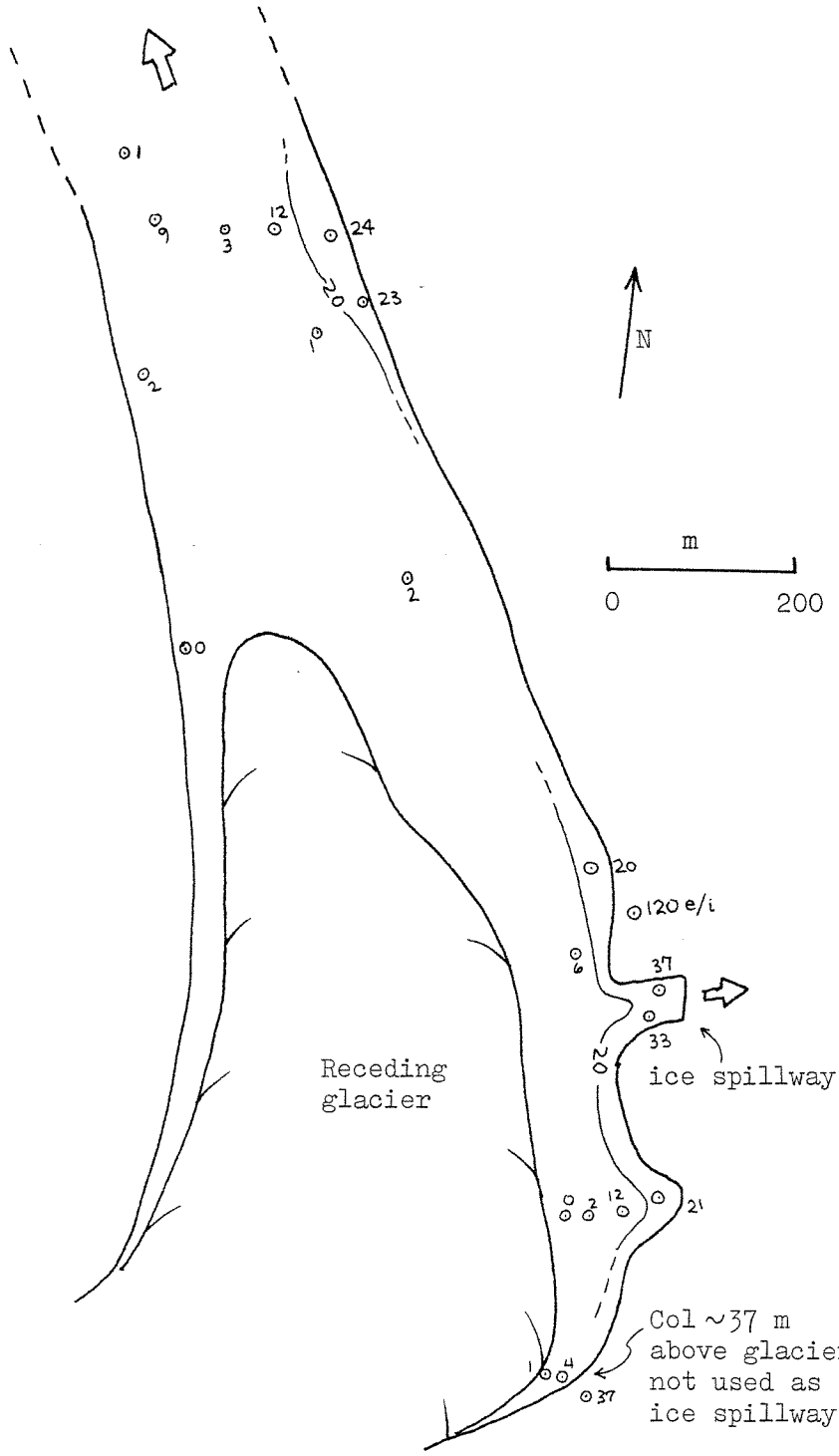

Maximum diameters of Rhizocarpon geographicum s.l. that characterize the debris lobe: 21, 24, 37 mm.

APPENDIX C. LICHENOMETRIC MAPS

Arrigetch-7 Rock Glacier (no.59).

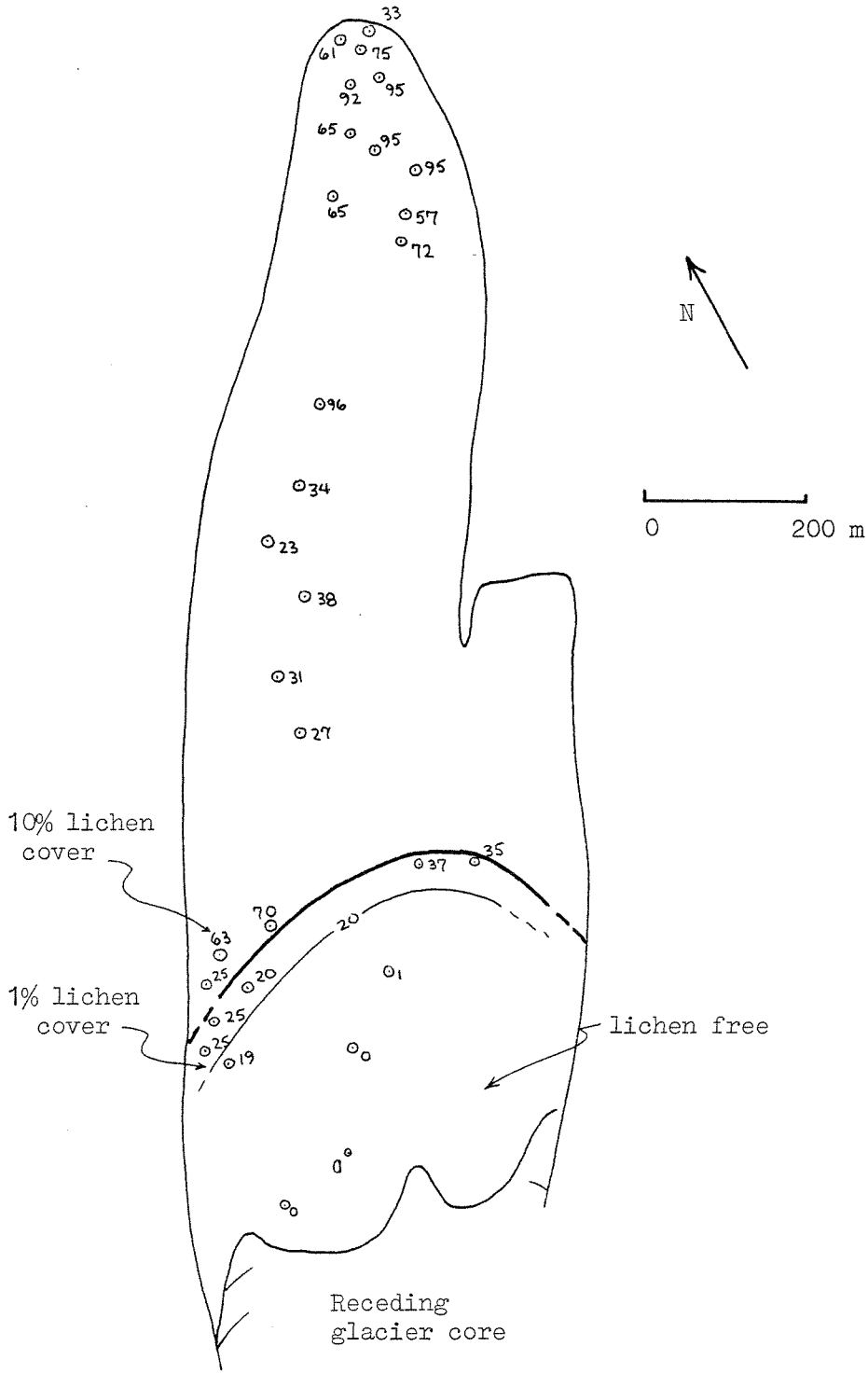

Maximum diameters of Rhizocarpon geographicum s.l. that characterize the debris lobe: 25, 37 mm.

APPENDIX D. PHOTOGRAPHIC PANORAMAS OF CIRQUE GLACIERS

During the summers of 1977 through 1980, a photographic record was continued for each glacier lichenometrically mapped. The camera was a 135 mm single lens reflex one using standard and 24 mm wide angle lenses. The locations of the photographic sites are indicated in Appendix B as enclosed dots on the "Present glacier surface" maps. The date the photographs were taken, the unofficial glacier name and designation number used in the study, and the viewing direction are noted next to each panorama. Refer to Figures 2, 3, and 4 for locations of the landforms.

CIRQUE GLACIER PANORAMAS

1. BUFFALO (view S)
   30 JULY 1979

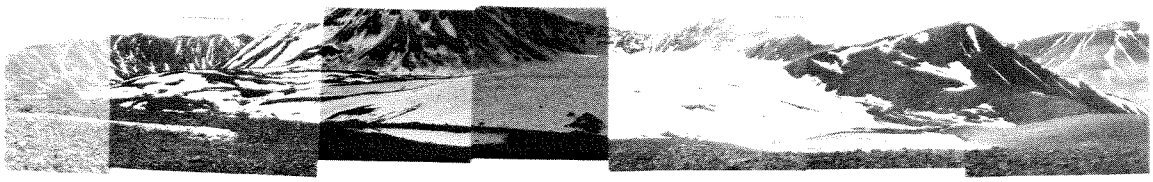

2. MARMOT (view S)
   30 JUNE 1979

3. GRIZZLY (view ESE)
   7 AUGUST 1979

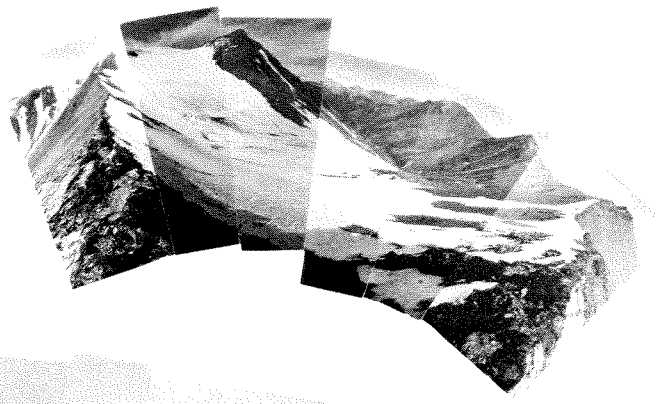

4. COYOTE (view NW)
   14 JULY 1977

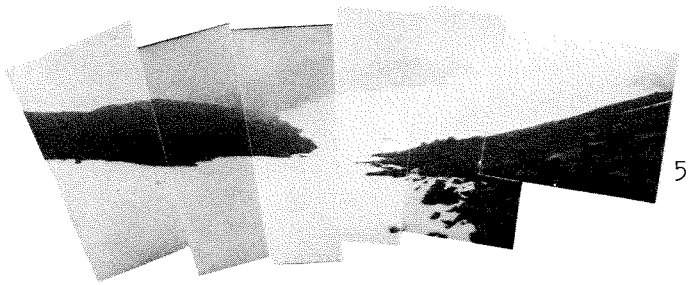

5. CARIBOU (view E)
   7 JULY 1979

CIRQUE GLACIER PANORAMAS

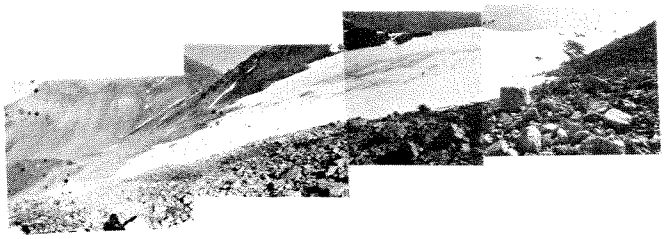

EAST (view SE)

6. RAPTOR 17 JULY 1977

WEST (view SW)

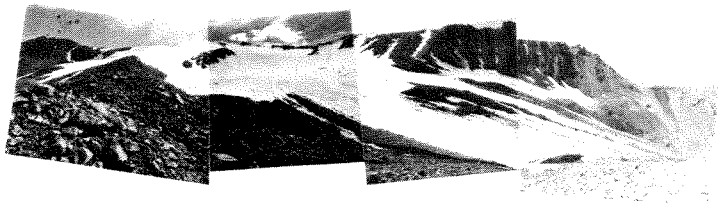

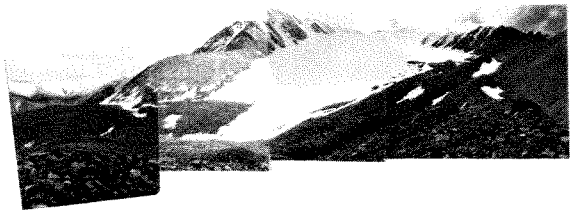

7. GOLDEN EAGLE (view E)
9 JULY 1979

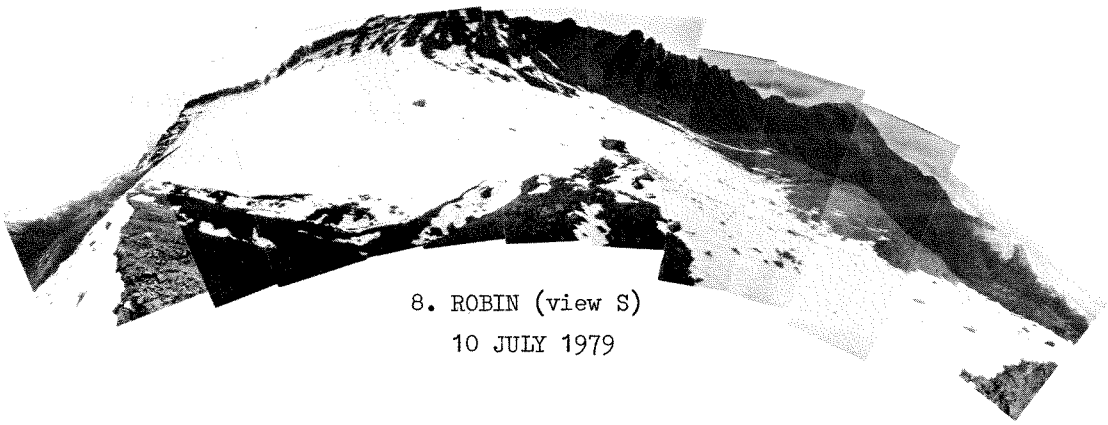

8. ROBIN (view S)
10 JULY 1979

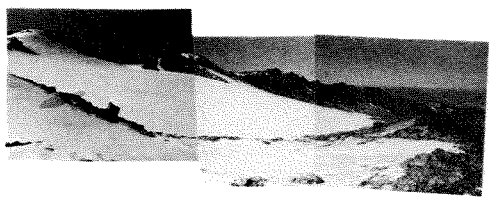

Headwall
(view W)

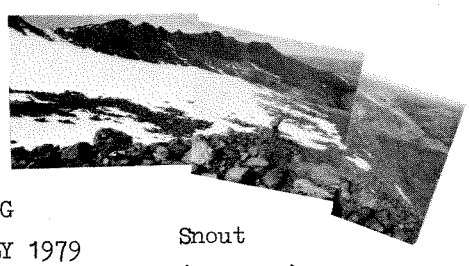

9. LEMMING
14 JULY 1979

Snout
(view NW)

CIRQUE GLACIER PANORAMAS

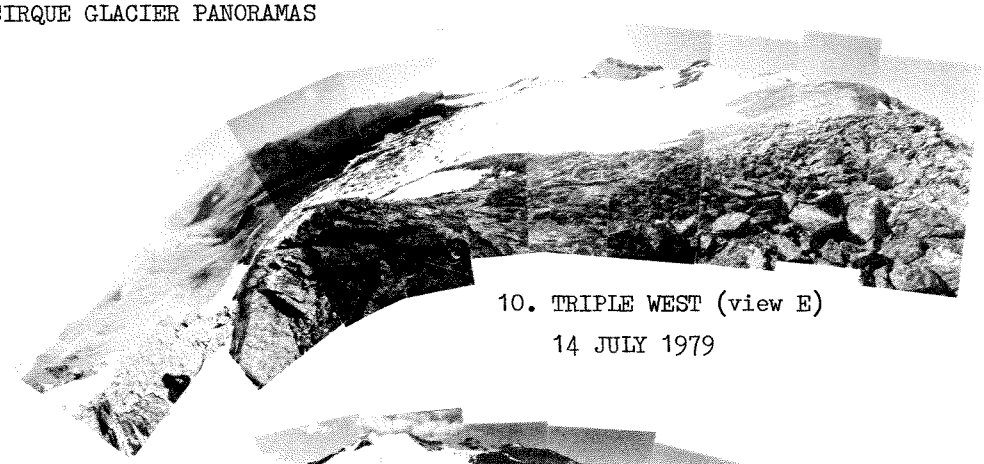

10. TRIPLE WEST (view E)
14 JULY 1979

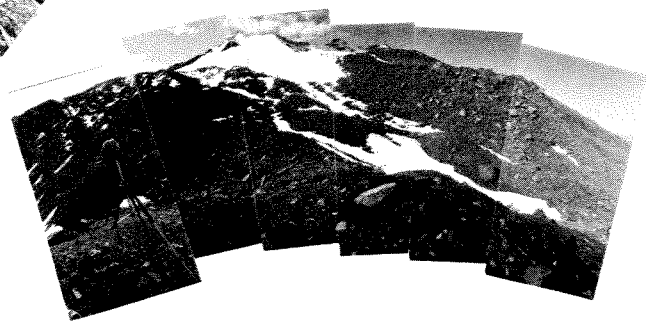

11. TRIPLE MID (view S)
13 JULY 1979

12. TRIPLE EAST (view SW)
13 JULY 1979

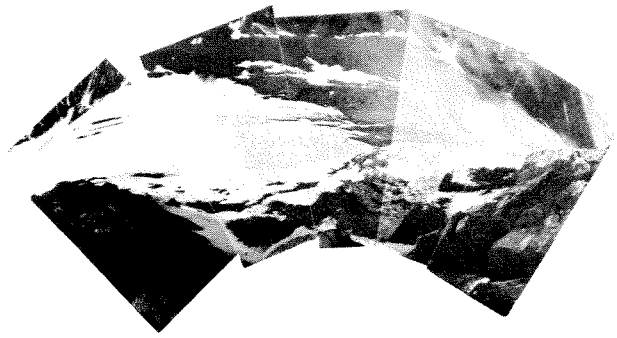

13. DALL SHEEP (view N)
10 JULY 1977

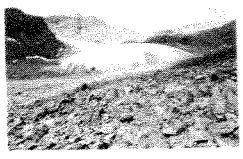

14. SNOW BUNTING
26 JULY 1977

(view W)

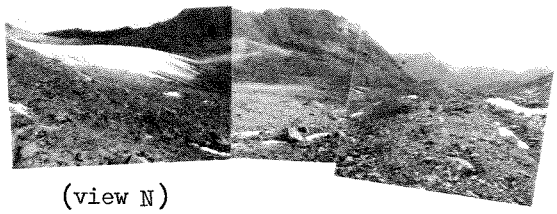

(view N)

CIRQUE GLACIER PANORAMAS

15. FOX (view E)
22 JULY 1979

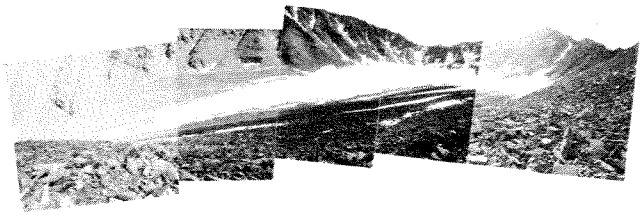

16. RAM (view SE)
20 JULY 1979

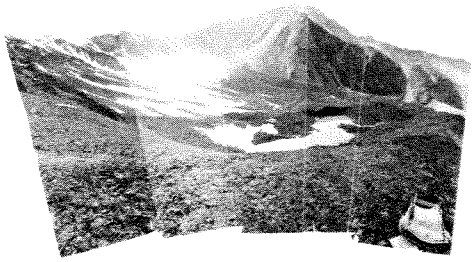

17. EWE (view W)
20 JULY 1979

18. KID (view SE)
21 JULY 1979

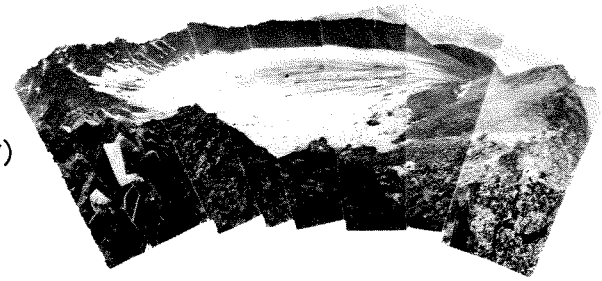

19. VOLE (view W)
21 JULY 1979

CIRQUE GLACIER PANORAMAS

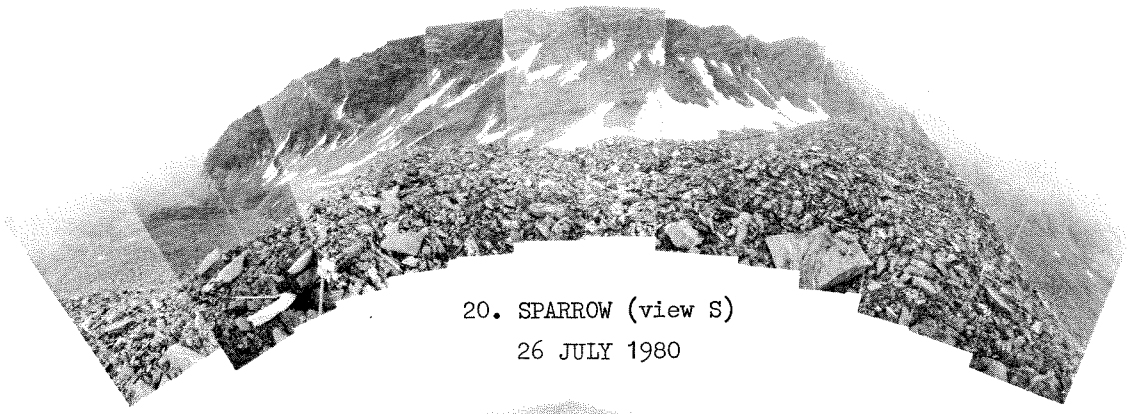

20. SPARROW (view S)
26 JULY 1980

21. RAVEN (view SWS)
26 JULY 1980

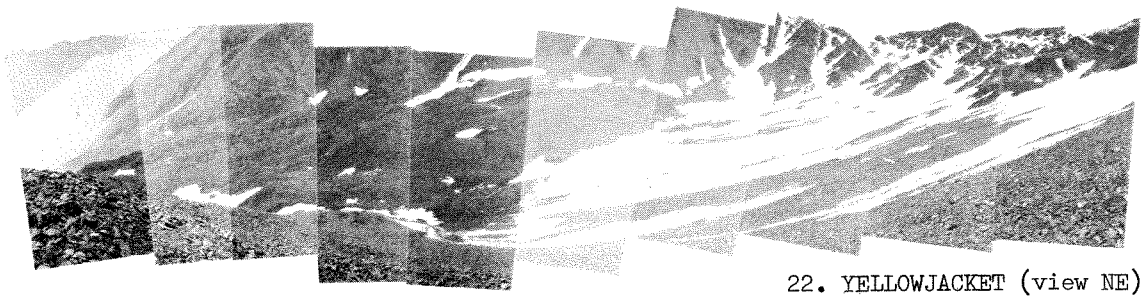

22. YELLOWJACKET (view NE)
30 JULY 1980

23. BURBOT (view S)
8 JULY 1980

CIRQUE GLACIER PANORAMAS

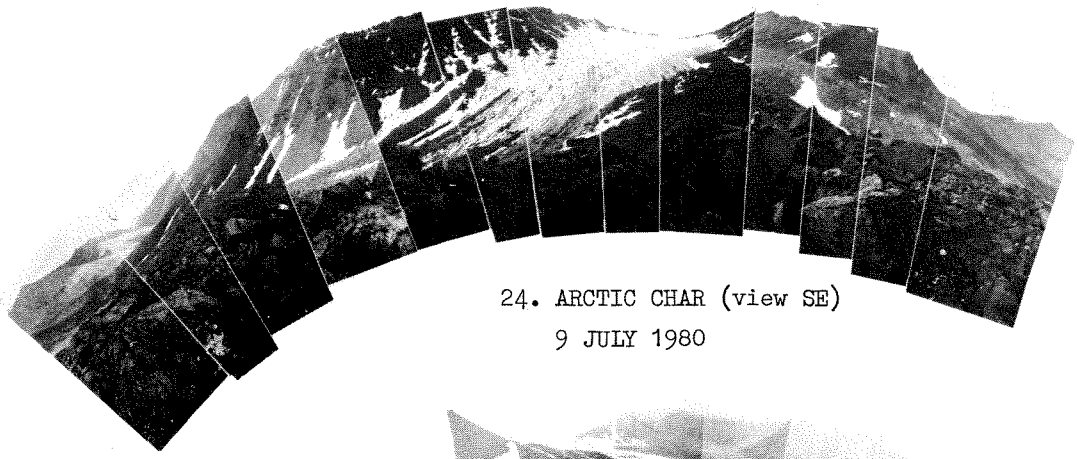

24. ARCTIC CHAR (view SE)
9 JULY 1980

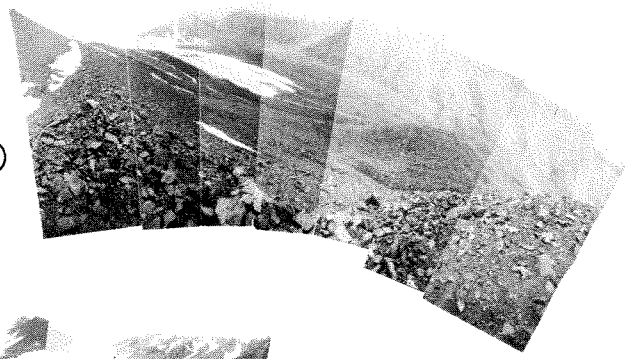

25. GRAYLING (view SW)
7 JULY 1980

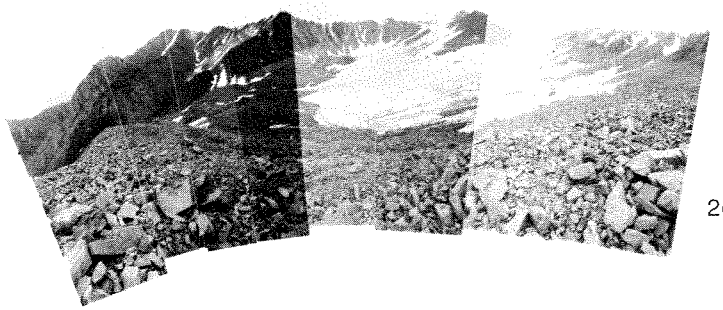

26. CISCO (view ESE)
10 JULY 1980

27. MOOSE (view N)
8 JULY 1979

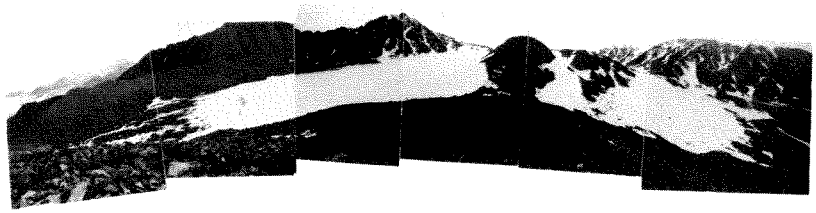

28. MUSK-OX (view S)
7 JULY 1979

CIRQUE GLACIER PANORAMAS

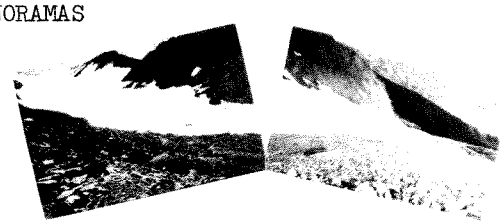

(view SW)

29. ARCTIC TERN
17 JULY 1978

(view W)

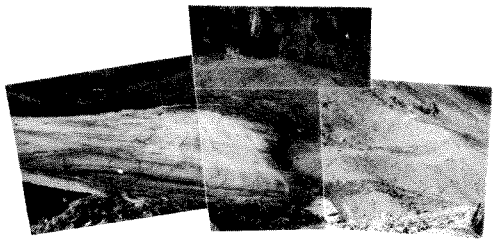

30. SNOWY OWL WEST (view N)
19 JULY 1980

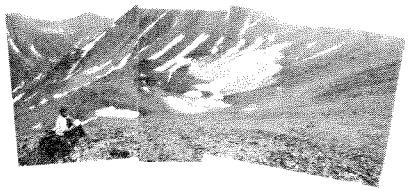

31. WOLF (view ESE)
22 JULY 1980

(view SW)

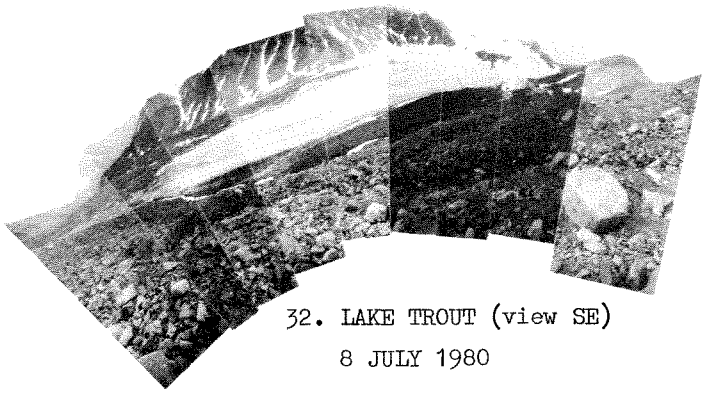

32. LAKE TROUT (view SE)
8 JULY 1980

33. TWIN
15 JULY 1978

(view NE)

34. SNOWY OWL EAST (view SW)
19 JULY 80

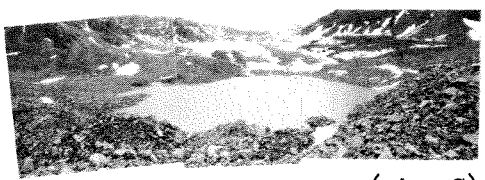

(view S)

35. HARLEQUIN DUCK
1 JULY 1980

(view W)

CIRQUE GLACIER PANORAMAS

36. Ptarmigan (view ENE)
11 JULY 1977

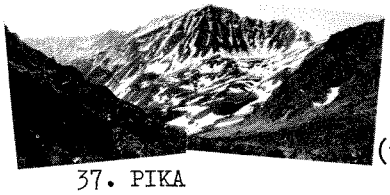

(view S)

37. PIKA
2 JULY 1977

(view NE)

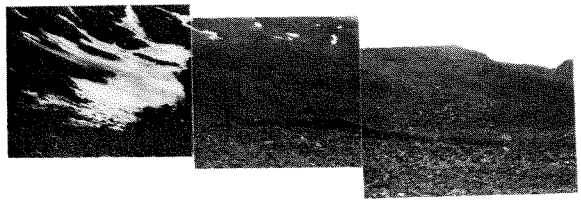

38. JAEGER (view W)
28 JULY 1978

39. PARKA SQUIRREL (view S)
21 JULY 1977

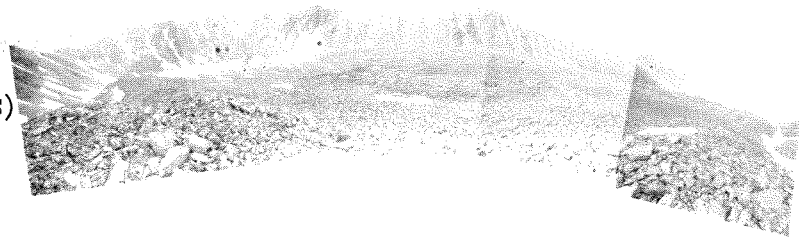

40. MOSQUITO (view SW)
18 JULY 1977

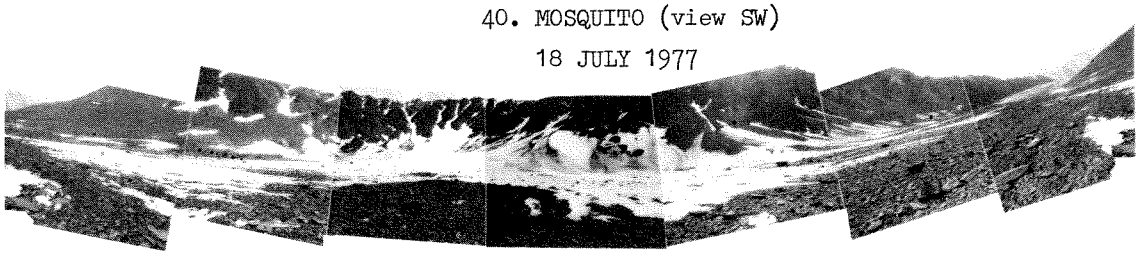

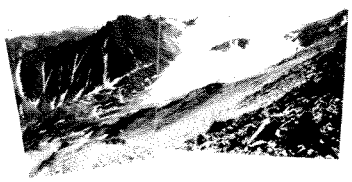

41. WOLVERINE (view SE)
16 JULY 1978

(view W)

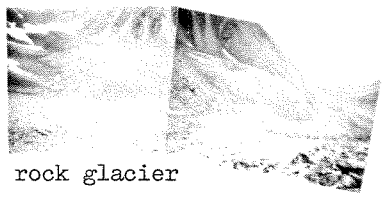

44. INUKPASAGRUK-C
24 JULY 1978
early Holocene rock glacier

CIRQUE GLACIER PANORAMAS

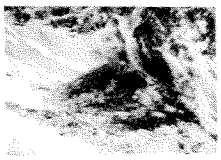

46. ITIKMALAKPAK-A (view W)
23 JULY 1978
lobate rock glacier

47. ITIKMALAKPAK-B (view W)
23 JULY 1978
lobate rock glacier

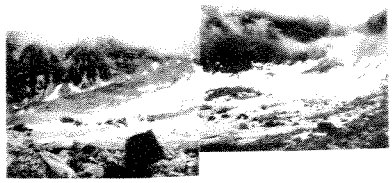

48. ITIKMALAKPAK-C (view E)
23 JULY 1978

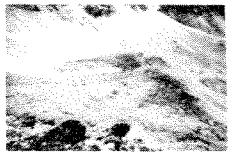

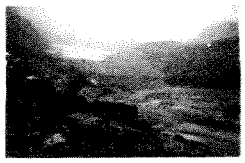

50. ARR-9E (view SSW)
20 AUGUST 1979

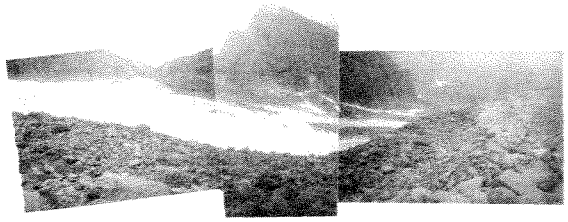

52. ARR-9W (view W)
20 AUGUST 1979

(view S)

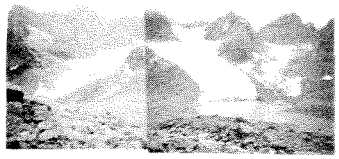

53. ARR-10E 51. ARR-10W

51. (view S)

51. (view ENE)

18 AUGUST 1979

53. (view SSE)

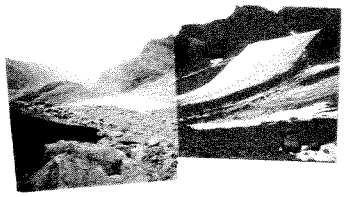

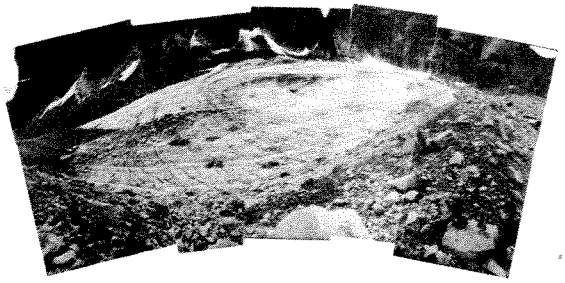

54. ARR-1 (view S)
15 AUGUST 1979

CIRQUE GLACIER PANORAMAS

55. ARR-2 (view WSW)
16 AUGUST 1979

55. ARR-2,-3,-4 (view S)
15 AUGUST 1979

55. ARR-2,-3,-4 (view SE)
15 AUGUST 1979

56. ARR-4 EAST (view SE)
15 AUGUST 1979

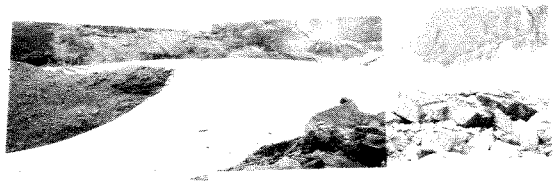

56. ARR-4 EAST (view E)
16 AUGUST 1979

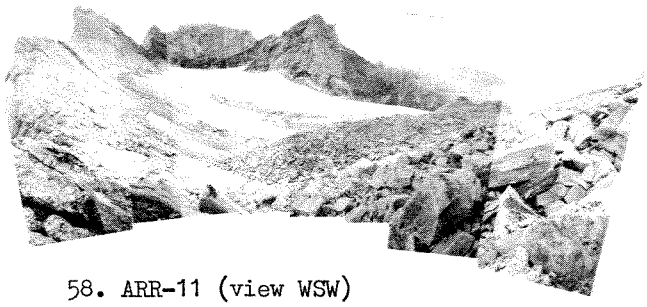

58. ARR-11 (view WSW)
18 AUGUST 1979

58. ARR-11 (view SSE)
18 AUGUST 1979

59. ARR-7 (view SSW)
14 AUGUST 1979

Appendix E. Cirque Glacier Data

(1) No.	(2) Glacier area (km^2)	(3) Neoglacial area (km^2)[a]	(4) Neoglacial Expansion (%)	(5) Type	(6) Mean glacier altitude (m)	(7) ELA AAR= 0.67 (m)[b]	(8) ELA 3/5 relief (m)[c]	(9) ELA lat. mor. (m)[d]	(10) ELA drop (m)[e]	(11) Glacier length (m)	(12) Glacier relief (m)	(13) Present past slope (°)[f]	(14) Head-wall (m)[g]	(15) Bed-rock[h]
1	2.08	2.55	23	M	1700	1660	1670	1670	40	1700	290	10/8	150	Dkss Dkm
2	0.62	1.08	74	M/Mg	1650	1600	1600	1615	50	1430	250	10/9	150	Dkm Dhs
3	0.14	0.24	80	M/Mg	1770	1725	1750	1740	45	550	180	16/17	60	Dkm
4	0.29	0.34	35	M/Mg	1860	1800	1810	1830	60	1050	340	18/18	20	Dkm Dhs
5	0.48	0.62	29	M/Mg	1880	1825	1850	1830	55	1070	355	18/18	30	Dkm Dks
6	0.76	1.00	32	M	1890	1820	1820	1800	70	1200	485	22/22	10	Dkm
7	0.46	0.61	33	M/Mg	1900	1860	1860	1860	40	1200	400	18/18	10	Dkm Dks MK
8	0.33	0.49	48	M/Mg	1855	1800	1770	1830	55	1000	225	13/14	100	Dks
9	0.53	0.66	17	M	1915	1850	1880	1920	65	1180	350	17/14	40	Dkm
10	0.49	0.64	31	M	1985	1885	1905	1950	100	830	310	20/19	40	Dkm

Appendix E. (continued)

(1)	(2)	(3)	(4)	(5)	(6)	(7)	(8)	(9)	(10)	(11)	(12)	(13)	(14)	(15)
11	0.44	0.68	55	M	1895	1815	1800	1865	80	1050	345	18/16	40	Dkm
12	0.68	0.87	28	M	1945	1880	1905	1930	65	1000	245	14/13	50	Dkm
13	0.54	0.75	40	Mg	1815	1710	1665	1705	105	1000	370	20/16	40	Dkss Dkm
14	0.69	1.04	51	Mg	1745	1720	1690	1760	25	1420	290	12/10	250	Dkm
15	0.29	0.52	79	Mg	1765	1700	1700	1765	65	590	115	11/12	215	Dkm
16	0.35	0.53	51	Mg	1720	1680	1660	1725	40	890	195	12/12	180	Dkss Dhs
17	0.29	0.54	86	Mg	1740	1665	1675	1720	75	760	150	11/11	240	Dkss Dhs Dkm
18	0.11	0.19	73	Mg	1835	1795	1810	1860	40	535	160	17/12	210	Dkm Dkss
19	0.31	0.47	52	Mg	1860	1785	1790	1820	75	890	215	14/12	160	Dkm Dkss
20	0.03	0.05	67	Mg	1800	1765	1780	1800	35	150	90	25/20	120	Dhs
21	0.07	0.20	186	Mg	1835	1765	1790	1845	70	300	130	23/15	180	Dhs
22	0.17	0.32	82	Mg	1700	1630	1640	1715	70	535	230	23/19	230	Dhw Dhs
23	0.54	0.71	31	Mg	1860	1765	1805	1845	95	1160	295	14/13	120	Dkm

Appendix E. (continued)

(1)	(2)	(3)	(4)	(5)	(6)	(7)	(8)	(9)	(10)	(11)	(12)	(13)	(14)	(15)
24	0.25	0.36	44	Mg	1735	1700	1675	1770	35	970	235	14/12	50	Dkmm Dkm
25	0.47	0.59	26	Mg	1920	1795	1850	1800	125	1180	430	20/19	120	Dhw
26	0.39	0.51	31	Mg	1860	1735	1775	1755	125	1000	400	22/20	150	Dkm Dkss
27	0.78	1.03	32	Mg	1890	1750	1845	1765	140	1550	460	17/15	100	IPMI Dkm MK
28	0.42	0.71	69	Mg/M	1810	1730	1710	1720	80	1000	300	17/18	200	Dkm
29	0.37	0.46	24	Mg	1920	1805	1850	-	115	1650	600	20/19	10	Dkm MK
30	0.42	0.62	48	Mg	1885	1785	1780	1860	100	1160	395	19/18	150	Dkmm Dkm Dkls
31	0.02	0.04	100	MG	1745	1715	1725	1740	30	180	90	26/23	100	Dkm Dhw
32	0.92	1.23	34	MG	1825	1705	1730	1770	120	1625	425	15/14	100	Dkmm Dkm
33	1.13	1.65	46	MG	1920	1755	1740	1870	165	2300	520	13/12	100	Dkm MK Dkls
34	0.39	0.70	54	MG	1870	1755	1750	1820	115	1250	310	14/16	100	Dkmm Dkm Dkls

Appendix E. (continued)

(1)	(2)	(3)	(4)	(5)	(6)	(7)	(8)	(9)	(10)	(11)	(12)	(13)	(14)	(15)
35	0.90	1.23	37	TRGC	1625	1530	1580	1560	95	2465	385	9/10	250	Dkm Dkss
36	0.25	0.43	71	TRGC	1610	1635	1600	-	+25	750	185	14/14	150	Dkm
37	0.01	0.09	-	TRGC	1660	1640	1640	-	20	50	10	10/11	200	Dkm Dhs
38	0.03	0.06	100	TRGC	1675	1640	1645	-	35	130	75	30/11	200	Dkm Dhs
39	0.09	0.45	400?	TRGC	1625	1585	1585	-	40	320	75	13/8	300	Dhs Dkss
40	0.09	0.33	267?	TRGC	1615	1575	1585	1615	40	400	60	9/8	420	Dhs
41	0.79	1.08	37	TRGC	1845	1750	1760	1810	95	1200	350	16/14	30	Dkm Dkls
48	0.14	0.24	70	MG	1685	1630	1640	1645	55	530	165	17/18	100	Dkm Dkmm
49	0.39	0.54	38	M/Mg	1560	1375	1460	1525	185	2440	520	12/13	100	Kg
50	0.42	0.62	48	M	1465	1370	1415	1430	95	1050	405	21/18	180	Kg
52				MG	1465	1345	1370	1400	120			21/19	180	

Appendix E. (continued).

(1)	(2)	(3)	(4)	(5)	(6)	(7)	(8)	(9)	(10)	(11)	(12)	(13)	(14)	(15)
51	0.54	0.97	80	M	1460	1295	1360	1340	165	1040	415	22/17	100	Kg
53				MG	1455	1295	1350	1340	160	1340	415	22/20	150	
54	0.21	0.74	250	MG	1440	1350	1330	1430	90	460	115	14/11	425	Kg
55	1.91	3.25	70	MG	1570	1345	1350	1500	235	2160	565	15/14	300	Kg
56	0.35	0.55	57	MG	1540	1375	1430	1430	165	1380	495	20/15	150	Kg
57	0.09	0.23	155	MG	1400	1345	1350	1370	55	200	90	24/13	425	Kg
58	0.45	0.75	67	MG	1465	1345	1290	1465	120	1380	365	15/17	250	Kg
59	0.09	0.28	210	TRGC	1340	1320	1300	1330	20	305	95	17/9	450	Kg

[a]Determined from lichenometric mapping.

[b]Determined planimetrically with accumulation area to ablation area ratio = 2:1.

[c]ELA determined as altitude three-fifths of the way between the backwall and end moraine.

[d]ELA determined as altitude of the upper limits of lateral moraines.

[e]Difference between mean glacier altitude and ELA determined by the AAR = 0.67 method.

Appendix E. (continued).

[f]Determined as tan (slope angle) = (12)/(11) for present surface and Neoglacial maximum surface.

[g]Estimated height of bedrock exposed in cirque cliffs (potential debris supply).

[h]see Brosgé and others (1979); Nelson and Grybeck (1980).

Rock glacier data (including cirque glacier)

(1) No.	(2) Type	(3) Total landform area (km^2)	(4) Landform affected by Neoglacial (%)	(5) Transition zone + rock glacier debris area, (km^2)	(6) Total landform length (m)	(7) Total landform relief (m)	(8) Total landform slope (°)
35	TRGC	1.52	81	0.62	3570	535	9
36	TRGC	0.58	74	0.33	1150	240	12
37	TRGC	0.26	35	0.25	700	220	17
38	TRGC	0.17	35	0.14	750	220	16
39	TRGC	0.55	82	0.46	1320	260	11
40	TRGC	0.75	44	0.67	2100	350	10

Appendix E. (continued).

(1)	(2)	(3)	(4)	(5)	(6)	(7)	(8)
41	TRGC	1.10	98	0.31	1700	450	15
44	TRGC	0.13	8?	0.13	625	130	12
59	TRGC	0.67	41	0.58	1840	385	12

APPENDIX F. TERRAIN SCREENING PROGRAM AND DATA

A FORTRAN program that uses a large matrix to determine times of sun appearance and disappearance at lat 68°N, +20° solar declination is provided. It calculates the amount of direct radiation energy received by a landform during the time(s) of sun appearance on 24 July. The format for data input and output (the same example used in Figure 6), and a program to plot 5 solar arcs and the landform horizon on a Calcomp plotter is given.

The coding scheme used to differentiate terrain screening data measured at the various glacial and periglacial landforms (Table 2), location maps of the survey sites, and raw data are provided in the appendix. Plots of the results of this analysis (see also Figs. 20, 21) are included to visually depict some relationships between the different parameters. See Appendix E for additional information.

Horizon survey sites were located on various parts of glacial and periglacial landforms. To distinguish the locations in the following table, the listed abbreviations below are used:

Designation	Location of Survey Site
CG	On relatively debris-free glacier surface
CG–M; CG–Mg; CG–MG; CG–TRGC	At debris boundary between glacier snout and the debris lobe (moraines)
M; Mg; MG; TRGC	On a Neoglacial debris lobe or at crest of its terminus
TRGB(GC)	On a glacier-cored rock glacier body
TRGS(GC)	On a glacier-cored rock glacier snout
TRGB	On a periglacial (no exposed ice core) tongue-shaped rock glacier body

TRGS	On a periglacial rock glacier snout (tongue-shaped)
LRG	On a periglacial lobate rock glacier
C	On the floor of an empty cirque
V, VH	In a fluvial valley or at the valley headwaters

The abbreviations above are further explained in Table 2.

When there is more than one survey site on a landform, the series number is followed by a letter (a, b, c, etc.). The coding scheme or series designation is summarized below with the total number of landforms surveyed given.

Landform Type	Series	Inventory
CG	000	001-008
CG-M, M, M/Mg	100	101-115
CG-Mg, Mg	200	201-219
CG-MG, MG	300	301-313
CG-TRG, TRGB(GC), TRGS(GC)	400	401-408
TRGB, TRGS	500	501-505
LRGa	600	601-619
LRGp	700	701-709
LRGi	800	801-819
C	900	901-907
V, VH	1000	1001-1004

Tables 5 and 6 contain the summarized analysis of this terrain-screening data.

```
 PROGRAM SOLAR (INPUT,OUTPUT,TAPE5=INPUT,TAPE6=OUTPUT)
C  AUTHOR: JIM ELLIS
C  DATE;   DEC 1978
C  FINAL PROJECT GEOG506
C
C     THIS PROGRAM CALCULATES FOR SELECTED SOLAR DECLINATIONS AT 68N
C  REDUCTION IN DIRECT SOLAR RADIATION DUE TO THE SCREENING BY
C  MOUNTAINOUS TERRAIN AND SLOPE/ASPECT OF THE LANDFORM.
   IT IS TO BE ACCOMPANIED BY A PLOTTING ROUTINE THAT DRAWS THE
    DECLINATION CURVES FOR 23.5,20,10,0 AND -10 DEGREES ALONG WITH
    THE LANDFORM HORIZON (PROGRAM JEPLOT).

      THIS PRESENT VERSION CALCULATES LOSS IN DIRECT RADIATION FOR
    +20 DEGREE DECLINATION ONLY.  THIS TIME IS MOST IMPORTANT AS IT
    REPRESENTS THE ABLATION SEASON AT 68N, I.E. MAY 21 AND JULY 21.
    SINCE MEASURED DIRECT RADIATION ENERGY IS NOT SYMMETRICAL ABOUT
    THE SOLAR NOON, 3 PARALLEL LINEAR ARRAYS ARE USED WHICH INDICATE
    THAT THE SPACE IS OCCUPIED BY THE SOLAR ARC ("*"), THE TIME OF
    POSITION IN THE SKY AND THE ENERGY THAT IS RECORDED IN CAL/CM2.MIN
    AT THIS POSITION ON A HORIZONTAL SURFACE.  EACH ARRAY IS 3600
    SPACES LONG, WITH EVERY 100 SPACES REPRESENTING 50 DEGREES OF
    ALTITUDE AT ONE AZIMUTH.  THE AZIMUTHS START AT 0 DEGREES (NORTH)
    AND INCREMENT CLOCKWISE AT 10 DEGREE STEPS TO 350 DEGREES.
    BY LOOPING THRU THE 3600 LINEAR ARRAY AT SEGMENTS OF 100
    A (100X36) 2D ARRAY IS SIMULATED HAVING 50 DEGREES OF ALTITUDE
    ALONG THE VERTICAL AXIS AND 360 DEGREES OF AZIMUTH ALONG THE
    HORIZONTAL AXIS. A CONTINUOUS LINE OF "*" IS MADE THRU THE
    2D ARRAY REPRESENTING THE PATH OF THE SUN.  THIS IS DONE BY
    FILLING THE APPROPRIATE SPACES FROM 0 TO 42 DEGREES ALTITUDE
    AND BACK TO 0, AS THE LOOP INCREMENTS FROM 0 AZIMUTH TO 180
    AZIMUTH AND BACK TO 350 DEGREES AZIMUTH.
       TO DIFFERENTIATE THE SUNRISE ZONE FROM THE SUNSET ZONE
    A "**" FILLER IS USED BETWEEN 0 DEGREE INCLINATION FROM THE
    HORIZON AND THE PROPER "*" SPACE ON THE SOLAR ARC.  SUNSET
    IS RECORDED BY BLANK SPACES IN THE INCLIN ARRAY.  WHEN THE
   HORIZON IS TRACKING ALONG THE DECLINATION ARC (*)
    AN ERROR MAY BE INTRODUCED INTO THE COMPUTATIONS,/
    BECAUSE OF THE LIMITED DETAIL ON THE AZIMUTH OF THE
    ARRAY STRUCTURE (ONLY DIVISIONS OF 10 DEGREES).
    THIS ONLY HAPPENS WHEN THE HORIZON TRACKS ALONG THE "*"
    FOR 30 DEGREES OR MORE, AND THIS CASE IS NOT TOO COMMON.
    CHECK WITH THE JEPLOT PICTURE OF THE HORIZON TO DETERMINE
    IF ERRORS HAVE OCCURRED.

       THE JETEST PROGRAM TALLIES SUNRISE AND SUNSET TIMES, THE
    ENERGY RECEIVED IN BETWEEN ON THE LANDFORM, AND CALCULATES AS
    A PERCENTAGE LOSS THE REDUCTION IN DIRECT RADIATION DUE TO
    SCREENING.  IT ALSO CONTAINS A SLOPE/ASPECT MATRIX THAT
    DETERMINES THE LOSS OR GAIN IN ENERGY FOR 20 DEGREE DECLINATION
    BASED ON 100% REPRESENTING THAT RECEIVED ON A HORIZONTAL
    SURFACE.  IT COMBINES THESE 2 PERCENTAGES GIVING THE TOTAL
    LOSS IN RADIATION AS A PERCENTAGE LOSS FROM 100%.

       FROM THE RUSSIAN LITERATURE (KONDRATYEV), AVERAGE VALUES
    OF DIRECT SOLAR RADIATION FALLING ON A HORIZONTAL SURFACE UNDER
    CLOUD-FREE CONDITIONS AT 68N LATITUDE WERE SUMMED FOR +20 DEGREE
    DECLINATION (20 MAY AND 20 JULY APPROXIMATELY) IN THE UNITS
```

```
MEASURED (CAL/CM2*MIN).  THESE ARE VALUES REACHED AFTER MANY
YEARS OF RECORD ACCORDING TO KONDRATYEV, AND IT APPEARS THAT
THE MAXIMUM VALUE IS REACHED MID JUNE (SUMMER SOLSTICE) WHEN
AN AVERAGE OF .90 CAL/CM2*MIN OF DIRECT SOLAR RADIATION ENERGY
WAS RECORDED ON HORIZONTAL SURFACES.  THE VALUES ATTAINED DURING
THE +20 DEGREE SOLAR DECLINATION ARC ARE LESS, OF COURSE.  THE
SUM OF THE CAL/CM2*MIN ENERGY TAKEN AT .1 HR  INTERVALS DURING
THE 24 HOUR DAY WAS DETERMINED TO BE 98.90 UNITS, AND THIS VALUE
WAS USED TO NORMALIZE THE ENERGY AND DERIVE THE % LOSS OF ENERGY
DUE TO SCREENING DURING THE 24 HR DAY. Note: CAL/CM2*MIN RAISED BY
100 TO MINIMIZE DECIMAL POINTS IN THE PROGRAM. 98.90 UNITS AT 6 MIN INTERVALS
EQUALS 593 CAL/CM2*DAY FOR +20° DECLINATION AT LAT. 68°N.
   THE DATA FILE IS JEDATA.  IT CONTAINS 44 LINES AND THEY ARE
FILLED AS FOLLOWS:
    1. THE LANDFORM HORIZON DATA IS ENTERED AT 10 DEGREE INCREMENTS
       (F4.1 FORMAT) AND IS TO BE ROUNDED TO THE NEAREST 0.5 DEGREE.
       THERE IS A CHECK FOR THIS DATA.  ONE STARTS AT 0.0 DEGREE
       AZIMUTH AND ENDS AT 350.0 AZIMUTH.
    2. LINES 37-42 ARE TO BE FILLED AS FOLLOWS:
         37. TYPE OF LANDFORM (UP TO 60 CHARACTERS)
         38. LOCATION SURFICIALLY (UP TO 60 CHARACTERS)
         39. DESIGNATION (NAME AND # TO BE USED ON PLOT; 30 CHARACT.)
         40. ALTITUDE (I4 FORMAT IN METERS)
         41. LATITUDE/LONGITUDE (UP TO 30 CHARACTERS)
         42. BEDROCK (UP TO 60 CHARACTERS)
    3. THE FINAL 2 LINES (43,44) ARE TO CONTAIN THE LANDFORM
       ASPECT AND THE SLOPE OF THE TERRAIN HOSTING IT.  ASPECT
       IS EITHER "N,NE,E,SE,S,SW,W,NW" AND IS RIGHT JUSTIFIED !)
       IN AN A2 FORMAT.  SLOPE IS IN DEGREES AND EITHER "10,20 OR
       30" (I2 FORMAT).

   REFERENCES ARE AS FOLLOWS:
KONDRATYEV,K.Y.,1969,RADIATION IN THE ATMOSPHERE,ACADEMIC PRESS.
GEIGER,R.,1965, THE CLIMATE NEAR THE GROUND,HARVARD UNIV.PRESS:
WENDLER,G. AND ISHIKAWA,N.,1974,THE EFFECT OF SLOPE,EXPOSURE AND
  MOUNTAIN SCREENING ON THE SOLAR RADIATION OF MCCALL GLACIER,
  J. GLACIOLOGY,V.13,N.68.
```

```
*******************************************************************************
```

```
C
C   DECLARE VARIABLES AND ARRAY DIMENSIONS
C   INPUT VARIABLES
    DIMENSION    INCLIN(3700),TIME(3700),ENERGY(3700),EXP(3,5),
+                HORIZN(36)
    INTEGER      X,K,I,F,M,P,TYPE,LOCAT,DESIG,ALTIT,LLONG,ROCK,
+                SLOPE,ASPECT,INCLIN,N,NE,E,SE,S,SW,W,NW,B

    REAL         HORIZ,TIME,ENERGY,EXP,HORIZN
C
    DIMENSION TYPE(6),LOCAT(6),DESIG(3),LLONG(3),ROCK(6)
```

```
C     C
C     C
C     C  OUTPUT VARIABLES
      REAL        RISE1,RISE2,ENER1,ENER2,RISE3,RISE4,ENER3,ENER4,
     +            SHADE,DURSHD,TIMES,ENERPC,SCRN,ENER,EXPPC,EXPLOS,
     +            EXPGAN,TOTAL,TTEST,ETEST,TSAVE,ESAVE
C     C
      INTEGER J,L,LSTAR,LTWO,LBLANK,H
C     C
C
C
C*************************************************************************
C
C
C        VARIABLES AND ARRAYS DEFINED
C
C     INCLIN:     ARRAY CONTAINING THE "*" FLAG FOR 20 DECLINATION
C     TIME:       ARRAY WITH UNIQUE TIME FOR THE SUN POSITION
C     ENERGY:     ARRAY WITH UNIQUE ENERGY (MEASURED) AT THE SUN POSITION
C     EXP:        ARRAY FOR SLOPE/ASPECT IMPACT ON LOSS OR GAIN OF ENERGY
C     HORIZN:     ARRAY TO HOLD THE LANDFORM'S MEASURED HORIZON
C
C     X:          COUNTER FOR THE AZIMUTH (10 DEGREE INCREMENTS)
C     K:          COUNTER
C     I:          COUNTER FOR THE 3 PARALLEL INCLIN/TIME/ENERGY ARRAYS
C     F:          COUNTER FOR SUNRISE AND SUNSET
C     M:          SLOPE VALUE IN EXP ARRAY (1 TO 3)
C     P:          ASPECT VALUE IN EXP ARRAY (1 TO 5)
C     B:          COUNTER USED IN SUNPOS SUBROUTINE TO LOOP UP (-)
C     H:          COUNTER USED IN SUNPOS TO DIFFERENTIATE SUNRISE/SET FROM
C                 INACTIVE SPACE MOVES.
C
C     TYPE:       TYPE OF LANDFORM BEING ANALYZED
C     LOCAT:      SURFICIAL LOCATION OF LANDFORM
C     DESIG:      NAME AND # ASSIGNED TO LANDFORM
C     ALTIT:      ALTITUDE OF LANDFORM IN METERS
C     LLONG:      LATITUDE/LONGITUDE OF LANDFORM
C     ROCK:       BEDROCK HOSTING THE LANDFORM
C     SLOPE:      THE SLOPE OF THE TERRAIN HOSTING THE LANDFORM
C     ASPECT:     THE DIRECTION THE LANDFORM FACES
C
C     N,NE,E,SE,S,SW,W,NW:   ASPECT OF LANDFORM
C
C     RISE1:      TIME OF FIRST SUNRISE
C     RISE2:      TIME OF FIRSE SUNSET
C     RISE3:      TIME OF SECOND SUNRISE
C     RISE4:      TIME OF SECOND SUNSET
C     ENER1:      ENERGY IN CAL/CM2*MIN AT FIRST SUNRISE TIME
C     ENER2:      ENERGY  "       "     "    "   SUNSET TIME
C     ENER3:      ENERGY  "       "     "  SECOND SUNRISE TIME
C     ENER4:      ENERGY  "       "     "    "    SUNSET TIME
C     RISE5:      TIME OF THIRD SUNRISE
C     RISE6:      TIME OF THIRD SUNSET
C     ENER5:      ENERGY IN CAL/CM2*MIN AT THIRD SUNRISE TIME
C     ENER6:      ENERGY IN      "       AT THIRD SUNSET TIME
C
```

```
C      SHADE:     HOURS OF SHADE DUE TO SCREENING
C      DURSHD:    LOSS IN DIRECT RADIATION TIME AS A %
C      TIMES:     HOURS OF SUNLIGHT ON THE LANDFORM
C      ENERPC:    PERCENTAGE OF ENERGY RECEIVED ON THE LANDFORM
C      SCRN:      LOSS IN ENERGY DUE TO SCREENING (%)
C      ENER:      TOTAL ENERGY (CAL/CM2*MIN) RECEIVED ON LANDFORM
C
C      EXPPC:     PERCENTAGE OF ENERGY RECEIVED DUE TO SLOPE/ASPECT
C      EXPLOS:        "      OF ENERGY LOSS FROM 100% DUE TO SLOPE/ASPECT
C      EXPGAN:        "       "    "   GAIN  "    "   "   "   "    "
C      TOTAL:     TOTAL LOSS IN DIRECT RADIATION ENERGY DUE TO SCREENING
C                       AND SLOPE/ASPECT EXPOSURE (%)
C
C      J:         COUNTER IN INCLIN ARRAY LOOPING
C      L:         COUNTER IN INCLIN ARRAY LOOPING
C      LSTAR:     COUNTER OF "*" INTERCEPTIONS BY HORIZON IN SUNPOS SUBROUTINE
C      LTWO:      COUNTER OF "**" INTERCEPTIONS BY HORIZON IN SUNPOS    "
C      LBLANK:    COUNTER OF " " INTERCEPTIONS BY HORIZON IN SUNPOS     "
C      TSAVE:     STORES VALUE OF SUNRISE/SET EVENT WHILE TEST FOR VALIDITY
C      ESAVE:     STORES VALUE OF ENERGY IN EVENT WHILE TEST FOR VALIDITY
C      TTEST:     TIME OF SUNRISE/SET EVENT TO BE PRINTED
C      ETEST:     ENERGY VALUE OF SUNRISE/SET TO BE PRINTED
C
C
C
C*************************************************************************
C
C

C     C
C     C  INITIALIZE VARIABLES
          X=0
          Y=0
          K=1
          F=0
          M=0
          J=0
          L=0
          P=0
          LSTAR=0
          LTWO=0
          LBLANK=0
          H=0
          B=0
          N=" N"
          NE = "NE"
          E = " E"
          SE = "SE"
          S = " S"
          SW = "SW"
          W = " W"
          NW = "NW"
          ALTIT=0
          ASPECT = 0
          SLOPE = 0
```

```
      RISE1=0.0
      RISE2=0.0
      ENER1=0.0
      ENER2=0.0
      RISE3=0.0
      RISE4=0.0
      ENER3=0.0
      ENER4=0.0
      RISE5=0.0
      RISE6=0.0
      ENER5=0.0
      ENER6=0.0
      SHADE=0.0
      DURSHD=0.0
      TIMES=0.0
      ENERPC=0.0
      ENER=0.0
      EXPPC=0.0
      EXPLOS=0.0
      SCRN=0.0
       HORIZ = 0.0
      EXPGAN=0.0
       TOTAL=0.0
      TTEST=0.0
      ETEST=0.0
      TSAVE=0.0
      ESAVE=0.0
      DO 10 I=1,3700
          INCLIN(I) = ' '
          TIME(I)   = ' '
          ENERGY(I) = ' '
10     CONTINUE
      DO 20 K=1,36
          HORIZN(K) = ' '
20     CONTINUE
      DO 35 K=1,6
          TYPE (K) = ' '
          LOCAT (K) = ' '
          ROCK (K) = ' '
35    CONTINUE
       DO 37 K = 1,3
          DESIG (K) = ' '
          LLONG (K) = ' '
37    CONTINUE
C
C
C*****************************************************************************
C
C


       I=1
       K=1
C     C
C     C
       CALL FILLSCR (INCLIN,TIME,ENERGY,I)
C     C     FILL UP THE HORIZON WITH ALTITUDES,TIME AND ENERGY OF THE SUN
```

```
C     AT SELECTED DECLINATIONS TO CALCULATE SCREENING EFFECT.
      ALSO,IT FILLS IN THE SUNSHINE PORTION OF THE DECLINATION ARC
      WITH "***" TO BUFFER RAPID CHANGES IN THE HORIZON INCLINATION
      AND CHECK THE VALIDITY OF A SUNRISE AND SUNSET.
C
C
 CALL FILLEXP (EXP,M,P)
C     FILL UP SLOPE/ASPECT EXPOSURE ARRAY FOR SELECTED SOLAR DECLINATIONS
C
C
C
C
 CALL FILLHOR (HORIZN,K,HORIZ)
C     FILL UP THE HORIZON ARRAY FOR 360 DEGREES AT 10 DEGREE INCREMENTS
C     WITH THE ALTITUDE OF THE HORIZON TO THE NEAREST 0.5 DEGREE
C     (36 HORIZON ALTITUDES PER LANDFORM ANALYZED).
C
C
C
C     COMPUTE SCREENING EFFECT.  STARTING AT 0 DEGREES, GO CLOCKWISE ON
C  THE HORIZON AT 10 DEGREE INCREMENTS AND READ IN THE HORIZON ALTITUDES
C  FROM THE HORIZN(K) ARRAY.  CHECK THE HORIZON WITH THE SUN'S POSITION
C  FOR SUNRISE AND SUNSET, ETC.
C INPUT ERROR IN FILLSCR ARRAY MAKES THE ARRAY BEGIN AT 101,RATHER
C THAN AT 1.
C
C
 K=0
 I=100
C        NOW THE ARRAY COUNTER IS SET AT THE BEGINNING OF THE INCLIN,
C    TIME AND ENERGY ARRAYS.
C
C    MOVE ALONG HORIZON AND COMPARE HORIZON TO DECLINATION. * MEANS
C  THE DATA PERTAINS TO +20 DEGREE DECLINATION.
C
  DO 90 X=10,360,10
C     FIND NEXT HORIZON ALTITUDE FOR ANALYSIS
    K=K+1
     HORIZ=HORIZN(K)
C             INCREMENT ALONG INCLIN ARRAY BY 100 (OR 10 DEGREES
C             IN THE HORIZONTAL BEARING TO FIND NEW SUN/HORIZ VALUES
      J=1+I
      L=99+J

C
C
      COMPARE THE HORIZON INCLINATION TO THE SOLAR INCLINATION AT
      THIS BEARING.  SEE IF THE SPACE ON THE DECLINATION ARRAY IS
      BLANK, "***", OR "*" IN THE SUBROUTINE SUNPOS.  FIRST EQUATE
      THE HORIZ VALUE (ALTITUDE FROM THE HORIZON) TO THE INCLINATION
      ARRAY WHICH STRUCTURALLY BEGINS AT THE OTHER END OF THE COLUMN

 I = L - (HORIZ*2)
      CALL SUNPOS (INCLIN,TIME,ENERGY,F,RISE1,RISE2,RISE3,RISE4,
     +                 ENER1,ENER2,ENER3,ENER4,I,L,J,HORIZ,
     +                 RISE5,RISE6,ENER5,ENER6)
C
```

```
C
C                    THIS SUBROUTINE CHECKS TO SEE WHAT IS OCCUPYING
C                 THE HORIZON SPACE WHEN COMPARED TO THE SOLAR ARC
C                 (EITHER A "*","**", OR " ").  IT ALLOWS A SUNRISE OR
C                 SUNSET TO OCCUR ONLY WHEN A "*" IS FOLLOWED BY A "**","*",
C                 OR " "; OR A "**" IS FOLLOWED BY A " " AND VICE VERSA!
C                 THIS MEANS THE HORIZON HAS ACTUALLY CROSSED THE SOLAR
C                 PATH.  A CHECK IS ALSO MADE TO PREVENT THE SUNRISE/SET
C                 IF THE HOIZON TOUCHES THE "*" ARC BUT DOES'T CROSS IT,
C                 OR THE HORIZON TRACKS ALONG THE "*" ARC.  IT KEEPS TRACK
C                 OF SUNRISE(S) AND SUNSET(S), TALLIES THE TIMES AND ENERGY
C                 OF EACH, AND MAKES IT READY FOR PRINTING IN THE MAIN
C                 PROGRAM.
C
C
C
C     C
C     C       FULLY INCREMENT INCLIN COLUMN TO L (BOTTOM )
C     C
   80     I=L

   90   CONTINUE
C     C
C     C
C     C     SUMMARIZE DIRECT RADIATION LOSS DUE TO SCREENING AT SELECTED DECLIN.
C     C     THE FOLLOWING IS FOR 68 N AT +20 DEGREE DECLINATION ONLY.
C     C
          TIMES= (RISE2-RISE1) + (RISE4-RISE3) + (RISE6-RISE5)
          ENER = (ENER2-ENER1) + (ENER4-ENER3) + (ENER6-ENER5)
          SHADE= 24.0 - TIMES
          DURSHD =(SHADE/24.0) * 100.0
          ENERPC = (ENER/9890.0) * 100.0
          SCRN = 100.0-ENERPC
C     C
C     C
C     C
C     C      NOW READ IN THE LANDFORM SPECIFICS AND GENERAL CHARACTERISTICS
C     C
        READ (5,100) TYPE
  100 FORMAT (6A10)
      READ (5,110) LOCAT
  110 FORMAT (6A10)
      READ (5,120) DESIG
  120 FORMAT (3A10)
      READ (5,130) ALTIT
  130 FORMAT (I4)
      READ (5,140) LLONG
  140 FORMAT (3A10)
      READ (5,150) ROCK
  150 FORMAT (6A10)
C     C
C     C
C     C
C     C     NOW COMPUTE DIRECT RADIATION LOSS DUE TO LANDFORMS EXPOSURE
C     C
        READ (5,160) ASPECT
  160   FORMAT (A2)
```

```
      READ(5,170) SLOPE
  170 FORMAT (I2)
C
C          THIS EXPOSURE IS FOR +20 DEGREE DECLINATION ONLY!
          IF (ASPECT .EQ. " N") P=1
          IF ((ASPECT .EQ. "NE") .OR. (ASPECT .EQ. "NW")) P=2
          IF((ASPECT .EQ. " W")  .OR. (ASPECT .EQ. " E"))   P=3
          IF((ASPECT .EQ. "SE") .OR. (ASPECT .EQ. "SW"))  P=4
          IF (ASPECT .EQ. " S")  P=5
C    C
          IF (SLOPE .EQ. 10)  M=1
          IF (SLOPE .EQ. 20)  M=2
          IF (SLOPE .EQ. 30)  M=3
C    C
C    C    DETERMINE %LOSS OR %GAIN FROM EXP(3,5)ARRAY
        EXPPC = EXP(M,P)
C    C
            IF (EXPPC .LE. 100.0) GO TO 190
            IF (EXPPC .GT. 100.0) GO TO 200
  190   EXPLOS = 100.0 - EXPPC
        GO TO 210
  200  EXPGAN = ABS (100.0 - EXPPC)
C    C
C    C
  210 CONTINUE
C
C        TALLY TOTAL LOSS ON LANDFORM DUE TO SCREENING AND EXPOSURE
      TOTAL = SCRN + EXPLOS - EXPGAN

C    C
C    C
C          SUMMARIZE THE LANDFORM'S CHARACTERISTICS FOR COMPARISON TO PLOT
C
      PRINT (6,500)
  500 FORMAT (1H1,3X,*SUMMARY OF LANDFORM'S CHARACTERISTICS AND DIRECT RA
     +DIATION % ENERGY LOSSES FOR +20 DECLINATION*)
C
      PRINT*," "
      PRINT*,"            TYPE:  ",TYPE
      PRINT*,"        LOCATION:  ",LOCAT
      PRINT*,"     DESIGNATION:  ",DESIG
      PRINT*,"        ALTITUDE:  ",ALTIT
      PRINT*,"        LAT/LONG:  ",LLONG
      PRINT*,"         BEDROCK:  ",ROCK
      PRINT*," "
C
      PRINT*,"     AZIMUTHS WITH INCLINATIONS FROM LANDFORM TO HORIZON"

      K=1
      X=-10
      DO 600 K=1,36
          HORIZ = HORIZN(K)
             X=X+10
      PRINT*,"     HORIZON AZIMUTH = ",X," : HORIZON ALTITUDE = ",HORIZ
  600 CONTINUE
C
      PRINT*," "
```

```
      PRINT*,"       SUNRISE1 AT ",RISE1," HRS WITH ENERGY AT: ",ENER1
      PRINT*,"       SUNSET1 AT  ",RISE2," HRS WITH ENERGY AT: ",ENER2
      PRINT*,"       SUNRISE2 AT ",RISE3," HRS WITH ENERGY AT: ",ENER3
      PRINT*,"       SUNSET2 AT  ",RISE4," HRS WITH ENERGY AT: ",ENER4
      PRINT*,"       SUNRISE3 AT ",RISE5," HRS WITH ENERGY AT: ",ENER5
      PRINT*,"       SUNSET3 AT  ",RISE6," HRS WITH ENERGY AT: ",ENER6
C
      PRINT*,"        HOURS OF SHADE DUE TO SCREENING = ",SHADE," HRS"
      PRINT*," % LOSS IN DURATION OF DIRECT RADIATION = ",DURSHD,"%"
      PRINT*,"     % LOSS IN ENERGY DUE TO SCREENING = ",SCRN,"%"
      PRINT*," "
      PRINT*," LANDFORM'S EXPOSURE (ASPECT AND SLOPE) = ",ASPECT,SLOPE
      PRINT*,"  % OF DIRECT RADIATION DUE TO EXPOSURE = ",EXPPC,"%"
      PRINT*,"       % LOSS IN ENERGY DUE TO EXPOSURE = ",EXPLOS,"%"
      PRINT*,"       % GAIN IN ENERGY DUE TO EXPOSURE = ",EXPGAN,"%"
      PRINT*," "
      PRINT*,"   TOTAL % LOSS IN DIRECT RADIATION"
      PRINT*,"   ENERGY DUE TO SCREENING AND EXPOSURE = ",TOTAL,"%"

C     C
C     C
      STOP
      END

C     C**********************************************************************
      SUBROUTINE FILLSCR (INCLIN,TIME,ENERGY,I)
C     C
C     C   THE PURPOSE IS TO FILL UP THE ARRAY (360 DEGREES ON THE HORIZON AT
C     C  10 DEGREE INTERVALS X 50 DEGREES SOLAR INCLINATION) WITH A SYMBOL
C     C  FOR THE SELECTED DECLINATION.  +20 DEGREE DECLINATION IS "*".  ALONG
C     C  WITH THIS SYMBOL, THE TIME THE SUN IS AT THIS BEARING AND % OF MAXIMUM
C     C  100% ENERGY IS ASSUMED ATTAINED AT ABOUT 21 JUNE, AND IS CALCULATED
C     C  AT ABOUT 90 CAL/CM2*MIN.
C     C
C     C  DECLARE VARIABLES AND ARRAY DIMENSIONS
C     C
      DIMENSION INCLIN(3700),TIME(3700),ENERGY(3700)
      INTEGER INCLIN,I
      REAL TIME, ENERGY
C     C
C     C
C     C  EACH COLUMN = 100 SPACES (50 DEGREES OF SOLAR INCLINATION TO THE
C     C  NEAREST 0.5 DEGREE) AND ARE STACKED ATOP EACH OTHER FOR A LINEAR ARRAY
C     C  3600 SPACES.  EACH COLUMN HAS SPACES OCCUPIED BY SYMBOLS INDICATIVE OF
C     C  OF THE SUN INCLINATION.
C     C
C     C FILL UP THE +20 DECLINATION ARC
      INCLIN(300)="*"
      TIME (300)=0.6
      ENERGY (300) = 0.0
      INCLIN (397) = "*"
      TIME (397) = 1.6
      ENERGY (397) = 10.3
      INCLIN (398) = "*"
      TIME (398) = 1.3
      ENERGY (398) = 5.1
      INCLIN (399) ="*"
      TIME (399) = 1.0
      ENERGY (399) = 1.9
      INCLIN (494) = "*"
      TIME (494) = 2.3
      ENERGY (494) = 33.2
      INCLIN (495) = "*"
      TIME (495) = 2.1
      ENERGY (495) = 24.8
      INCLIN (496) = "*"
      TIME (496) = 1.8
      ENERGY (496) = 15.2
      INCLIN (589) = "*"
      TIME (589) = 3.1
      ENERGY (589) = 84.3
```

```
      INCLIN (590) = "*"
      TIME (590) = 2.9
60    ENERGY (590) = 68.8
      INCLIN (591) = "*"
      TIME (591) = 2.8
      ENERGY (591) = 61.8
      INCLIN (592) = "*"
65    TIME (592) = 2.6
      ENERGY (592) = 49.2
      INCLIN (593) = "*"
      TIME (593) = 2.5
      ENERGY (593) = 43.5
70    INCLIN (684) = "*"
      TIME (684) = 3.8
      ENERGY (684) = 155.6
      INCLIN (685) = "*"
      TIME (685) = 3.7
75    ENERGY (685) = 143.6
      INCLIN (686) = "*"
      TIME (686) = 3.6
      ENERGY (686) = 132.2
      INCLIN (687) = "*"
80    TIME (687) = 3.5
      ENERGY (687) = 121.4
      INCLIN (688) = "*"
      TIME (688) = 3.3
      ENERGY (688) = 101.8
85    INCLIN (777) = "*"
      TIME (777) = 4.6
      ENERGY (777) = 281.1
      INCLIN (778) = "*"
      TIME (778) = 4.5
90    ENERGY (778) = 262.1
      INCLIN (779) = "*"
      TIME (779) = 4.4
      ENERGY (779) = 244.4
      INCLIN (780) = "*"
95    TIME (780) = 4.3
      ENERGY (780) = 227.6
      INCLIN (781) = "*"
      TIME (781) = 4.2
      ENERGY (781) = 211.6
100   INCLIN (782) = "*"
      TIME (782) = 4.1
      ENERGY (782) = 196.4
      INCLIN (783) = "*"
      TIME (783) = 4.0
105   ENERGY (783) = 181.9
      INCLIN (870) = "*"
      TIME (870) = 5.4
      ENERGY (870) = 478.4
      INCLIN (871) = "*"
110   TIME (871) = 5.3
      ENERGY (871) = 449.3
      INCLIN (872) = "*"
      TIME (872) = 5.2
      ENERGY (872) = 421.5
```

```
115                INCLIN (873) = "*"
                   TIME (873) = 5.1
                   ENERGY (873) = 395.0
                   INCLIN (874) = "*"
                   TIME (874) = 5.0
120                ENERGY (874) = 369.9
                   INCLIN (875) = "*"
                   TIME (875) = 4.9
                   ENERGY (875) = 345.8
                   INCLIN (876) = "*"
125                TIME (876) = 4.8
                   ENERGY (876) = 322.8
                   INCLIN (961) = "*"
                   TIME (961) = 6.2
                   ENERGY (961) = 759.6
130                INCLIN (962) = "*"
                   TIME (962) = 6.1
                   ENERGY (962) = 719.8
                   INCLIN (963) = "*"
                   TIME (963) = 6.0
135                ENERGY (963) = 681.3
                   INCLIN (964) = "*"
                   TIME (964) = 5.9
                   ENERGY (964) = 644.1
                   INCLIN (965) = "*"
140                TIME (965) = 5.8
                   ENERGY (965) = 608.3
                   INCLIN (966) = "*"
                   TIME (966) = 5.7
                   ENERGY (966) = 573.8
145                INCLIN (967) = "*"
                   TIME (967) = 5.6
                   ENERGY (967) = 540.7
                   INCLIN (968) = "*"
                   TIME (968) = 5.5
150                ENERGY (968) = 508.9
                   INCLIN (969) = "*"
                   TIME (969) = 5.4
                   ENERGY (969) = 478.4
                   INCLIN (1052) = "*"
155                TIME (1052) = 6.9
                   ENERGY (1052) = 1075.8
                   INCLIN (1053) = "*"
                   TIME (1053) = 6.8
                   ENERGY (1053) = 1026.6
160                INCLIN (1054) = "*"
                   TIME (1054) = 6.7
                   ENERGY (1054) = 978.8
                   INCLIN (1055) = "*"
                   TIME(1055) = 6.7
165                ENERGY (1055) = 978.8
                   INCLIN (1056) = "*"
                   TIME (1056) = 6.6
                   ENERGY (1056) = 932.3
                   INCLIN (1057) = "*"
170                TIME (1057) = 6.5
                   ENERGY (1057) = 887.1
```

```
                INCLIN (1058) = "*"
                TIME (1058) = 6.4
                ENERGY (1058) = 843.3
175             INCLIN (1059) = "*"
                TIME (1059) = 6.3
                ENERGY (1059) = 800.8
                INCLIN (1060) = "*"
                TIME (1060) = 6.2
180             ENERGY (1060) = 759.6
                INCLIN (1144) = "*"
                TIME (1144) = 7.5
                ENERGY (1144) = 1399.0
                INCLIN (1145) = "*"
185             TIME (1145) = 7.5
                ENERGY (1145) = 1399.0
                INCLIN (1146) = "*"
                TIME (1146) = 7.4
                ENERGY (1146) = 1341.8
190             INCLIN (1147) = "*"
                TIME (1147) = 7.3
                ENERGY (1147) = 1285.9
                INCLIN (1148) = "*"
                TIME (1148) = 7.2
195             ENERGY (1148) = 1231.4
                INCLIN (1149) = "*"
                TIME (1149) = 7.1
                ENERGY (1149) = 1178.2
                INCLIN (1150) = "*"
200             TIME (1150) = 7.1
                ENERGY (1150) = 1178.2
                INCLIN (1151) = "*"
                TIME (1151) = 7.0
                ENERGY (1151) = 1126.3
205             INCLIN (1238) = "*"
                TIME (1238) = 8.1
                ENERGY (1238) = 1770.3
                INCLIN (1239) = "*"
                TIME (1239) = 8.0
210             ENERGY (1239) = 1705.1
                INCLIN (1240) = "*"
                TIME (1240) = 7.9
                ENERGY (1240) = 1641.2
                INCLIN (1241) = "*"
215             TIME (1241) = 7.8
                ENERGY (1241) = 1578.6
                INCLIN (1242) = "*"
                TIME (1242) = 7.7
                ENERGY (1242) = 1517.4
220             INCLIN (1243) = "*"
                TIME (1243) = 7.6
                ENERGY (1243) = 1457.5
                INCLIN (1333) = "*"
                TIME (1333) = 8.8
225             ENERGY (1333) = 2263.4
                INCLIN (1334) = "*"
                TIME (1334) = 8.6
                ENERGY (1334) = 2116.5
```

```
                INCLIN (1335) = "*"
230             TIME (1335) = 8.5
                ENERGY (1335) = 2044.6
                INCLIN (1336) = "*"
                TIME (1336) = 8.4
                ENERGY (1336) = 1974.0
235             INCLIN (1337) = "*"
                TIME (1337) = 8.3
                ENERGY (1337) = 1904.8
                INCLIN (1429) = "*"
                TIME (1429) = 9.4
240             ENERGY (1429) = 2736.6
                INCLIN (1430) = "*"
                TIME (1430) = 9.2
                ENERGY (1430) = 2573.9
                INCLIN (1430) = "*"
245             TIME (1431) = 9.0
                ENERGY (1431) = 2339.0
                INCLIN (1432) = "*"
                TIME (1432) = 8.9
                ENERGY (1432) = 2339.0
250             INCLIN (1525) = "*"
                TIME (1525) = 9.9
                ENERGY (1525) = 3161.6
                INCLIN (1526) = "*"
                TIME (1526) = 9.8
255             ENERGY (1526) = 3075.0
                INCLIN (1527) = "*"
                TIME (1527) = 9.6
                ENERGY (1527) = 2904.1
                INCLIN (1528) = "*"
260             TIME (1528) = 9.5
                ENERGY (1528) = 2819.9
                INCLIN (1621) = "*"
                TIME (1621) = 10.5
                ENERGY (1621) = 3697.0
265             INCLIN (1622) = "*"
                TIME (1622) = 10.3
                ENERGY (1622) = 3516.0
                INCLIN (1623) = "*"
                TIME (1623) = 10.2
270             ENERGY (1623) = 3426.2
                INCLIN (1624) = "*"
                TIME (1624) = 10.1
                ENERGY (1624) = 3337.2
                INCLIN (1719) = "*"
275             TIME (1719) = 10.9
                ENERGY (1719) = 4066.1
                INCLIN (1720) = "*"
                TIME (1720) = 10.7
                ENERGY (1720) = 3880.6
280             INCLIN (1817) = "*"
                TIME (1817) = 11.5
                ENERGY (1817) = 4631.3
                INCLIN (1818) = "*"
                TIME (1818) = 11.2
285             ENERGY (1818) = 4347.2
```

```
                INCLIN (1916) = "*"
                TIME (1916) = 12.0
                ENERGY (1916) = 5108.0
                INCLIN (2017) = "*"
290             TIME (2017) = 12.5
                ENERGY (2017) = 5583.1
                INCLIN (2018) = "*"
                TIME (2018) = 12.8
                ENERGY (2018) = 5864.8
295             INCLIN (2119) = "*"
                TIME (2119) = 13.1
                ENERGY (2119) = 6142.0
                INCLIN (2120) = "*"
                TIME (2120) = 13.3
300             ENERGY (2120) = 6323.7
                INCLIN (2221) = "*"
                TIME (2221) = 13.5
                ENERGY (2221) = 6502.7
                INCLIN (2222) = "*"
305             TIME (2222) = 13.7
                ENERGY (2222) = 6679.2
                INCLIN (2223) = "*"
                TIME (2223) = 13.8
                ENERGY (2223) = 6766.0
310             INCLIN (2224) = "*"
                TIME (2224) = 13.9
                ENERGY (2224) = 6852.1
                INCLIN (2325) = "*"
                TIME (2325) = 14.1
315             ENERGY (2325) = 7021.6
                INCLIN (2326) = "*"
                TIME (2326) = 14.2
                ENERGY (2326) = 7105.1
                INCLIN (2327) = "*"
320             TIME (2327) = 14.4
                ENERGY (2327) = 7269.1
                INCLIN (2328) = "*"
                TIME (2328) = 14.5
                ENERGY (2328) = 7349.5
325             INCLIN (2429) = "*"
                TIME (2429) = 14.6
                ENERGY (2429) = 7428.8
                INCLIN (2430) = "*"
                TIME (2430) = 14.8
330             ENERGY (2430) = 7583.1
                INCLIN (2431) = "*"
                TIME (2431) = 15.0
                ENERGY (2431) = 7732.5
                INCLIN (2432) = "*"
335             TIME (2432) = 15.1
                ENERGY (2432) = 7805.2
                INCLIN (2533) = "*"
                TIME (2533) = 15.2
                ENERGY (2533) = 7876.6
340             INCLIN (2534) = "*"
                TIME (2534) = 15.4
                ENERGY (2534) = 8015.4
```

```
                INCLIN (2535) = "*"
                TIME (2535) = 15.5
345             ENERGY (2535) = 8082.8
                INCLIN (2536) = "*"
                TIME (2536) = 15.6
                ENERGY (2536) = 8148.9
                INCLIN (2537) = "*"
350             TIME (2537) = 15.7
                ENERGY (2537) = 8213.6
                INCLIN (2638) = "*"
                TIME (2638) = 15.9
                ENERGY (2638) = 8339.1
355             INCLIN (2639) = "*"
                TIME (2639)  = 16.0
                ENERGY (2639) = 8399.8
                INCLIN (2640) = "*"
                TIME (2640) = 16.1
360             ENERGY (2640) = 8459.2
                INCLIN (2641) = "*"
                TIME (2641) = 16.2
                ENERGY (2641) = 8517.3
                INCLIN (2642) = "*"
365             TIME (2642) = 16.3
                ENERGY (2642) = 8574.0
                INCLIN (2643) = "*"
                TIME (2643) = 16.4
                ENERGY (2643) = 8629.4
370             INCLIN (2744) = "*"
                TIME (2744) = 16.5
                ENERGY (2744) = 8683.5
                INCLIN (2745) = "*"
                TIME (2745) = 16.5
375             ENERGY (2745) = 8683.5
                INCLIN (2746) = "*"
                TIME (2746) = 16.6
                ENERGY (2746) = 8736.2
                INCLIN (2747) = "*"
380             TIME (2747) = 16.7
                ENERGY (2747) = 8787.6
                INCLIN (2748) = "*"
                TIME (2748) = 16.8
                ENERGY (2748) = 8837.7
385             INCLIN (2749) = "*"
                TIME (2749) = 16.9
                ENERGY (2749) = 8886.5
                INCLIN (2750) = "*"
                TIME (2750) = 16.9
390             ENERGY (2750) = 8886.5
                INCLIN (2751) = "*"
                TIME (2751) = 17.0
                ENERGY (2751) = 8933.9
                INCLIN (2852) = "*"
395             TIME (2852) = 17.1
                ENERGY (2852) = 8980.0
                INCLIN (2853) = "*"
                TIME (2853) = 17.2
                ENERGY (2853) = 9024.8
```

```
400                INCLIN (2854) = "*"
                   TIME (2854) = 17.3
                   ENERGY (2854) = 9068.2
                   INCLIN (2855) = "*"
                   TIME (2855) = 17.3
405                ENERGY (2855) = 9068.2
                   INCLIN (2856) = "*"
                   TIME (2856) = 17.4
                   ENERGY (2856) = 9110.3
                   INCLIN (2857) = "*"
410                TIME (2857) = 17.5
                   ENERGY (2857) = 9151.1
                   INCLIN (2858) = "*"
                   TIME (2858) = 17.6
                   ENERGY (2858) = 9190.5
415                INCLIN (2859) = "*"
                   TIME (2859) = 17.7
                   ENERGY (2859) = 9228.6
                   INCLIN (2860) = "*"
                   TIME (2860) = 17.8
420                ENERGY (2860) = 9265.4
                   INCLIN (2961) = "*"
                   TIME (2961) = 17.8
                   ENERGY (2961) = 9265.4
                   INCLIN (2962) = "*"
425                TIME (2962) = 17.9
                   ENERGY (2962) = 9300.8
                   INCLIN (2963) = "*"
                   TIME (2963) = 18.0
                   ENERGY (2963) = 9334.9
430                INCLIN (2964) = "*"
                   TIME (2964) = 18.1
                   ENERGY (2964) = 9367.7
                   INCLIN (2965) = "*"
                   TIME (2965) = 18.2
435                ENERGY (2965) = 9399.2
                   INCLIN (2966) = "*"
                   TIME (2966) = 18.3
                   ENERGY (2966) = 9429.3
                   INCLIN (2967) = "*"
440                TIME (2967) = 18.4
                   ENERGY (2967) = 9458.1
                   INCLIN (2968) = "*"
                   TIME (2968) = 18.5
                   ENERGY (2968) = 9485.6
445                INCLIN (2969) = "*"
                   TIME (2969) = 18.6
                   ENERGY (2969) = 9511.7
                   INCLIN (3070) = "*"
                   TIME (3070) = 18.6
450                ENERGY (3070) = 9511.7
                   INCLIN (3071) = "*"
                   TIME (3071) = 18.7
                   ENERGY (3071) = 9536.5
                   INCLIN (3072) = "*"
455                TIME (3072) = 18.8
                   ENERGY (3072) = 9560.0
```

```
                INCLIN (3073) = "*"
                TIME (3073) = 18.9
                ENERGY (3073) = 9582.1
460             INCLIN (3074) = "*"
                TIME (3074) = 19.0
                ENERGY (3074) = 9602.9
                INCLIN (3075) = "*"
                TIME (3075) = 19.1
465             ENERGY (3075) = 9622.4
                INCLIN (3076) = "*"
                TIME (3076) = 19.2
                ENERGY (3076) = 9640.5
                INCLIN (3177) = "*"
470             TIME (3177) = 19.4
                ENERGY (3177) = 9672.7
                INCLIN (3178) = "*"
                TIME (3178) = 19.5
                ENERGY (3178) = 9687.2
475             INCLIN (3179) = "*"
                TIME (3179) = 19.6
                ENERGY (3179) = 9701.0
                INCLIN (3180) = "*"
                TIME (3180) = 19.7
480             ENERGY (3180) = 9714.0
                INCLIN (3181) = "*"
                TIME (3181) = 19.8
                ENERGY (3181) = 9726.4
                INCLIN (3182) = "*"
485             TIME (3182) = 19.9
                ENERGY (3182) = 9738.1
                INCLIN (3183) = "*"
                TIME (3183) = 20.0
                ENERGY (3183) = 9749.3
490             INCLIN (3284) = "*"
                TIME (3284) = 20.2
                ENERGY (3284) = 9769.9
                INCLIN (3285) = "*"
                TIME (3285) = 20.3
495             ENERGY (3285) = 9779.4
                INCLIN (3286) = "*"
                TIME (3286) = 20.4
                ENERGY (3286) = 9788.1
                INCLIN (3287) = "*"
500             TIME (3287) = 20.5
                ENERGY (3287) = 9796.3
                INCLIN (3288) = "*"
                TIME (3288) = 20.7
                ENERGY (3288) = 9811.4
505             INCLIN (3389) = "*"
                TIME (3389) = 20.9
                ENERGY (3389) = 9824.8
                INCLIN (3390) = "*"
                TIME (3390) = 21.1
510             ENERGY (3390) = 9836.8
                INCLIN (3391) = "*"
                TIME (3391) = 21.2
                ENERGY (3391) = 9842.1
```

```
      INCLIN (3392) = "*"
      TIME (3392) = 21.4
      ENERGY (3392) = 9851.9
      INCLIN (3393) = "*"
      TIME (3393) = 21.6
      ENERGY (3393) = 9860.3
      INCLIN (3494) = "*"
      TIME (3494) = 21.7
      ENERGY (3394) = 9863.9
      INCLIN (3495) = "*"
      TIME (3495) = 21.9
      ENERGY (3495) = 9870.2
      INCLIN (3496) = "*"
      TIME (3496) = 22.2
      ENERGY (3496) = 9877.8
      INCLIN (3597) = "*"
      TIME (3597) = 22.4
      ENERGY (3597) = 9881.7
      INCLIN (3598) = "*"
      TIME (3598) = 22.7
      ENERGY (3598) = 9885.7
      INCLIN (3599) = "*"
      TIME (3599) = 23.0
      ENERGY (3599) = 9888.2
      INCLIN (3700) = "*"
      TIME (3700) = 23.4
      ENERGY (3700) = 9890.0
C     C
C          TO ENABLE THE PROGRAM TO HANDLE SHARP DROPS AND RISES IN THE
C          THE HORIZON, ADDITIONAL BUFFERING IS NECESSARY WITH THIS
C          THIS ALGORITHM BELOW THE +20 DECLINATION ARC (ZONE OF SUNSHINE)
C          FOR CHECKS IN SUNPOS (SUBROUTINE THAT TALLIES SUNRISE AND SUNSET
C          EVENTS).  A "***" IS USED TO FILL THE INTERIOR SPACES, AND AS WITH
C          THE "*" FILLING ROUTINE, IS IN ERROR AS FAR AS THE SPACE GOES BY
C          +100 DUE TO ORIGINAL INPUT ERROR IN THIS ARRAY.  THIS DOES NOT
C          EFFECT IN ANY WAY THE TABULATION OR TRACING OF THE ARCS!!!
C
      INCLIN(400) = "***"
      DO 10 I = 497,500
          INCLIN (I) = "***"
   10 CONTINUE
C
      DO 20 I = 594,600
          INCLIN (I) = "***"
   20 CONTINUE
      DO 30 I = 689,700
          INCLIN (I) = "***"
   30 CONTINUE

      DO 40 I = 784,800
          INCLIN (I) = "***"
   40 CONTINUE
      DO 50 I = 877,900
          INCLIN (I) = "***"
   50 CONTINUE

C
```

```
      DO 60 I = 970,1000
         INCLIN (I) = "***"
   60 CONTINUE
      DO 70 I = 1061,1100
         INCLIN (I) = "***"
   70 CONTINUE

      DO 80 I = 1152,1200
         INCLIN (I) = "***"
   80 CONTINUE
      DO 90 I = 1244,1300
         INCLIN (I) = "***"
   90 CONTINUE
      DO 100 I = 1338,1400
         INCLIN (I) = "***"
  100 CONTINUE
C
      DO 110 I = 1433,1500
         INCLIN (I) = "***"
  110 CONTINUE
      DO 120 I = 1529,1600
         INCLIN (I) = "***"
  120 CONTINUE
      DO 130 I = 1625,1700
         INCLIN (I) = "***"
  130 CONTINUE

      DO 140 I = 1721,1800
         INCLIN (I) = "***"
  140 CONTINUE
      DO 150 I = 1819,1900
         INCLIN (I) = "***"
  150 CONTINUE
C
      DO 160 I = 1917,2000
         INCLIN (I) = "***"
  160 CONTINUE
      DO 170 I = 2019,2100
         INCLIN (I) = "***"
  170 CONTINUE

      DO 180 I = 2121,2200
         INCLIN (I) = "***"
  180 CONTINUE
      DO 190 I = 2225,2300
         INCLIN (I) = "***"
  190 CONTINUE
      DO 200 I = 2329,2400
         INCLIN (I) = "***"
  200 CONTINUE
      DO 210 I = 2433,2500
         INCLIN (I) = "***"
  210 CONTINUE
      DO 220 I = 2538,2600
         INCLIN (I) = "***"
  220 CONTINUE
      DO 230 I = 2644,2700
```

```
                    INCLIN (I) = "**"
                230 CONTINUE
630                 DO 240 I = 2752,2800
                        INCLIN (I) = "**"
                240 CONTINUE
                    DO 250 I = 2861,2900
                        INCLIN (I) = "**"
635             250 CONTINUE
                    DO 260 I = 2970,3000
                        INCLIN (I) = "**"
                260 CONTINUE
                    DO 270 I = 3077,3100
640                 INCLIN (I) = "**"
                270 CONTINUE
                    DO 280 I = 3184,3200
                        INCLIN (I) = "**"
                280 CONTINUE
645                 DO 290 I = 3289,3300
                        INCLIN (I) = "**"
                290 CONTINUE
                    DO 300 I = 3394,3400
                        INCLIN (I) = "**"
650             300 CONTINUE
                    DO 310 I = 3497,3500
                        INCLIN (I) = "**"
                310 CONTINUE
              C
655                 INCLIN (3600) = "**"

              C     C
                    RETURN
                    END
```

```
C     C*************************************************************************
C     C
C     C
      SUBROUTINE FILLEXP (EXP,M,P)
C     C
C     C       SELECT A DECLINATION AND FILL UP AN ARRAY WITH VALUES OF %
C     C   DIRECT RADIATION AS COMPARED TO A HORIZONTAL SURFACE FOR 3 SLOPES
C     C   AND 5 DIRECTIONS.  THE VERTICAL COLUMN (M) HAS EITHER 10, 20 OR 30
C     C   DEGREE SLOPES, AND THE HORIZONTAL ROW HAS N, NE/NW, W/E, SE/SW AND
C     C   S DIRECTIONS FOR THE TERRAIN HOSTING THE LANDFORM.
C     C
C     C
C     C   DECLARE VARIABLES AND ARRAY DIMENSIONS
      DIMENSION EXP(3,5)
      REAL EXP
      INTEGER M,P
C     C
C     C
      EXP(1,1) = 99.0
      EXP(1,2) = 99.0
      EXP(1,3) = 100.0
      EXP(1,4) = 102.0
      EXP(1,5) = 103.0
      EXP(2,1) = 95.0
      EXP(2,2) = 94.0
      EXP(2,3) = 102.0
      EXP(2,4) = 106.0
      EXP(2,5) = 107.0
      EXP(3,1) = 87.0
      EXP(3,2) = 88.0
      EXP(3,3) = 104.0
      EXP(3,4) = 109.0
      EXP(3,5) = 109.0
      RETURN
      END
```

```
C     C
C     C
C     C
C     C**********************************************************************
C     C
C     C
C     C
      SUBROUTINE FILLHOR(HORIZN,K,HORIZ)
C     C
C     C     THIS FILLS THE HORIZON ARRAY FROM 0 TO 350 DEGREES AT 10 DEGREE
C     C  INCREMENTS TO THE NEAREST .5 DEGREE.  IT CHECKS TO SEE THAT THE
C     C  ALTITUDE IS WITHIN 0 TO 90 DEGREES AND = TO .0 OR .5 AT THE DECIMAL.
C     C
C     C
C     C    DECLARE ARRAY DIMENSIONS AND VARIABLES
C     C
      DIMENSION HORIZN (36)
      INTEGER K
      REAL HORIZ,HORIZN
C     C
C     C
      READ(5,125) (HORIZN(K), K = 1,36)
  125 FORMAT (F4.1)
         HORIZ = HORIZN(K)
C     C CHECK THE HORIZON ENTRY FOR VALIDITY
C     C
      IF ((HORIZ .GE. 0.0) .OR. (HORIZ .LE. 90.0)) GO TO 110
          PRINT*, "ERROR IN HORIZ INPUT. HORIZ =", HORIZ
         PRINT*,"ENTRY NUMBER =", K
         GO TO 110
C     C
110   IF (((HORIZ * 2) .EQ. (INT(HORIZ) * 2 + 1)) .OR. ((HORIZ * 2)
     +           .EQ. (INT(HORIZ) * 2)))GO TO 120
          PRINT*, "ERROR IN HORIZ INPUT.  HORIZ =", HORIZ
          PRINT*, " ENTRY NUMBER = ", K
          GO TO 120
C     C
120   CONTINUE
      RETURN
      END
```

```
C     C
C     C
C     C*************************************************************************
C     C
C     C
C     C
      SUBROUTINE SUNPOS (INCLIN,TIME,ENERGY,F,RISE1,RISE2,RISE3,RISE4,
     +                   ENER1,ENER2,ENER3,ENER4,I,L,J,HORIZ,
     +                   RISE5,RISE6,ENER5,ENER6)
C     C
C     C
C     C    THIS RECORDS SUNRISE/SUNSET TIMES AND ENERGY % FOR LATER ANALYSIS
C        BY KEEPING TRACK OF THE LAST SPACE IN THE 100 SPACE ARRAY THAT
C        CONTAINS A HORIZON INCLINATION WITH THE COUNTER L, THOSE TRACES
C        THAT TRACK ALONG THE "*" STRUCTURE OF THE INCLIN ARRAY WHILE
C        INCREMENTING ALONG THE HORIZON AZIMUTH AT 10 DEGREE JUMPS WILL
C        ONLY RECORD SUNRISE/SUNSET EVENTS ONCE.  ONLY TRACKS THAT LEAVE THE
C        "*" STRUCTURE WILL RECORD SUNRISE/SUNSET.
C        THE VALUES ARE SAVED (TIME AND ENERGY) BY TSAVE AND ESAVE
C        WHILE INCREMENTING TO THE NEXT 10 DEGREE AZIMUTH
C        IT CAN EITHER GO FROM A "*" SPACE TO A BLANK " " (SUNSET),
C         OR IT CAN GO TO A "**" (SUNRISE), OR TO ANOTHER "*" (NO
C         ACTION,LEAVE SUBROUTINE SUNPOS IF THIRD OR MORE "*" MET IN SUCCESSION
C         BUT IF ONLY 2ND "*", RECORD AND PRINT THE FIRST "*" VALUES FOR THE
C         EVENT.  THIS MAY BE A SOURCE OF ERROR AND ONLY BY LOOKING AT THE
C         PLOT CAN ONE TELL IF THE SUN HAS ACTUALLY SET OR RISEN WHEN TWO
C         "*" ARE MET IN SUCCESSION.  THE VAST MAJORITY OF THE TIME AN EVENT
C         WILL HAVE HAPPENED.  THIS FLAW IS INHERENT IN THE ARRAY STRUCTURE
C         AND MAKES JEPLOT USE ESSENTIAL TO SEE IF THE DATA IS SOUND).
C        THERE IS A CHECK TO ENSURE THAT ONLY SUNSET FOLLOWS SUNRISE
C        AND VICE VERSA, WHICH WILL SOMETIMES LEAD TO ERROR WHEN THE
C        HORIZON HAS BEEN TRACKING ALONG THE DECLINATION ARC "*" FOR
C        MORE THAN 30 DEGREES AND LEAVES FROM THE SAME DIRECTION IT
C        ENTERED ("BOUNCED OFF THE "*" ARC").  THE JEPLOT PICTURE MAY
C        INDICATE A SLIGHT SUNRISE/SET EVENT WHICH CANNOT BE COMPUTED
C        FROM THIS ALGOTITHM.  ADJUSTMENTS SHOULD BE MADE ACCORDING TO
C        TO THE PLOT WHEN TALLYING THE ENERGY VALUES.
C     C
C     C
C     C DECLARE VARIABLES AND ARRAY DIMENSIONS
C     C
C     C
      DIMENSION INCLIN(3700),TIME(3700),ENERGY(3700)
      INTEGER INCLIN,F,I,L,LSTAR,LTWO,LBLANK,J,B
      REAL TIME,ENERGY,RISE1,RISE2,RISE3,RISE4,ENER1,ENER2,ENER3,ENER4,
     +     TTEST,ETEST,RISE5,RISE6,ENER5,ENER6,HORIZ
C     C
C     C
C     C   COUNTER FOR SUNRISE/SUNSET RECORD
C     C       0 = MIDNIGHT
C     C       1 = SUNRISE (1ST), 2 = SUNSET (1ST)
C     C       3 = SUNRISE (2ND), 4 = SUNSET (2ND)
C
C
C-----------------------------------------------------------------------
C
C        CHECK TO SEE IF THIS SPACE IS A "*"
```

```
      IF (.NOT. (INCLIN(I) .EQ. "*")) GO TO 300
C           CHECK TO SEE IF THIS IS THE INITIAL "*" MET IN THE ARRAY
           IF (.NOT. (LSTAR .EQ. 0)) GO TO 200
C                SAVE THE VALUES OUTSIDE OF THIS CHECKING AREA
                GO TO 450
C
C
C          1. CHECK TO SEE IF PREVIOUS SPACE = "*"
  200 IF (.NOT. ((L - LSTAR) .EQ. 100)) GO TO 220
C           CHECK TO SEE IF 2 SPACES BACK IS = "*". IF SO, THEN SUNRISE
C         OR SUNSET EVENT HAS ALREADY BEEN RECORDED AND THE "*" IS TO BE
C         IGNORED (LEAVE SUNPOS IF THIRD OR MORE "*" MET IN A ROW)
C         IF NOT, PRINT THE VALUES OF THE SUNRISE
C         OR SUNSET EVENT THAT HAPPENED AS A "*" IN THE PREVIOUS SPACE.
C
          IF (.NOT.(((L-LTWO) .EQ. 200) .OR. ((L-LBLANK) .EQ. 200)))
     +         GO TO 450
C              THE ABOVE GO TO 450 ENSURES THE VALUES OF "*" IN A
C              STRING OF "*" IS KEPT CURRENT INCASE OF AN EVENT
C
C
C                 2 SPACES BACK MUST BE A "***" OR " ",SO IT PROBABLY
C                 IS AN EVENT...PRINT THE PREVIOUS "*" VALUE!
                  GO TO 470
C
C
C          2. CHECK TO SEE IF PREVIOUS SPACE = "***"
  220 IF (.NOT. ((L - LTWO) .EQ. 100)) GO TO 230
C               MEANS SUNSET MAY BE OCCURRING, SAVE VALUES
                GO TO 450
C
C          3. CHECK TO SEE IF PREVIOUS SPACE = " "
  230 IF ( .NOT. ((L - LBLANK) .EQ. 100)) GO TO 800
C                MEANS SUNRISE MAY BE OCCURRING, SAVE VALUES
                GO TO 450
C
C
C
C
C
C-----------------------------------------------------------------------
C
C          CHECK TO SEE IF THE SPACE IS FILLED WITH "***" (SUNSHINE ZONE)
C
  300 IF (.NOT. (INCLIN(I) .EQ. "***")) GO TO 400
C
C          1. CHECK TO SEE IF PREVIOUS SPACE "*", IF SO RECORD SUNRISE
C             ONLY IF SUNSET HAS OCCURRED PREVIOUSLY (F COUNTER)
      IF (.NOT. ((F.EQ.1) .OR. (F.EQ.3) .OR. (F.EQ.5))) GO TO 310
C             INCREMENT "***" COUNTER
              GO TO 510
C
  310 IF (.NOT. ((L-LSTAR) .EQ. 100)) GO TO 320
C             INSIDE OF ARC AND SUNRISE!
              GO TO 500
C
C
```

```
C          2. CHECK TO SEE IF PREVIOUS SPACE " ".  IF SO THE HORIZON
C             HAS PENETRATED THE SOLAR ARC AND IS ALREADY IN SUNSHINE.
C             RECORD THE LATEST "*" VALUES BY LOOPING UP THE LINEAR
C             INCLIN ARRAY TO THE APPROPRIATE "*" SPACE AND RECORD THESE
C             VALUES FOR PRINTING
C
  320 IF (.NOT. ((L - LBLANK) .EQ. 100))  GO TO 360
C          INSIDE OF ARC, BUT SKIPPED THE ARC VALUE.  LOOP UP TO IT
C          BY USING THE "HORIZ" VALUE INCREASING BY ITS 0.5 INCREMENT
C          TO DECREASE THE (I) VALUE BY 1, UNTIL A "*" IS FOUND.
        B = (HORIZ * 2)
        DO 330 K = B,100,1
           I = L - B
           IF (INCLIN (I) .EQ. "*")  GO TO 340
  330   CONTINUE
        GO TO 800
C
  340   GO TO 500
C
C
C          3. IF HERE, MEANS PREVIOUS SPACE "**", SO NO EVENT, INCREMENT
C             ONLY AND LEAVE SUNPOS
  360 GO TO 510
C
C
C
C-----------------------------------------------------------------------
C
C
C       CHECK TO SEE THAT SPACE IS " " (DARKNESS) AS THIS IS ALL THAT IS
C       POSSIBLE
C
C          CHECK TO SEE IF INITIAL " " OF PROGRAM, IF SO LEAVE SUNPOS
  400 IF (.NOT. (LBLANK .EQ. 0.0))   GO TO 405
C             INCREMENT ONLY THE " " INDICATOR
              GO TO 560
C
C          NOW CHECK TO SEE THAT A SUNRISE HAS HAPPENED
  405 IF (.NOT. ((F.EQ.0) .OR. (F.EQ.2) .OR. (F.EQ.4) .OR. (F.EQ.6)))
     +     GO TO 407
C
              GO TO 560
C
C
C          1. CHECK TO SEE IF PREVIOUS SPACE "*", MAY MEAN SUNSET
  407 IF (.NOT. ((L - LSTAR) .EQ. 100)) GO TO 420
C             MEANS SUNSET HAS OCCURRED,PRINT THE VALUES
              GO TO 550
C
C
C          2. CHECK TO SEE IF PREVIOUS SPACE "**", IF SO MEANS SUNSET
C             HAS OCCURRED BY HORIZON PENETRATING THE SOLAR ARC WITHOUT
C             REGISTERING ON "*".  LOOP DOWN TO THE PROPER "*" SPACE AND
C             RECORD FOR PRINTING
  420 IF (.NOT. ((L - LTWO) .EQ. 100))  GO TO 440
C             LOOP DOWN TO PROPER "*" AND PRINT
```

```
            K = I
            DO 430 I = K,L,1
                 IF (INCLIN(I) .EQ. "*") GO TO 435
  430       CONTINUE
               GO TO 800
C
C
C           HAVE FOUND PROPER VALUES, SAVE AND INCREMENT " " COUNTER
  435  GO TO 550
C
C
C           3. CHECK TO SEE IF PREVIOUS SPACE " ", IF SO LEAVE SUNPOS
  440  GO TO 560
C
C
C
C
C
C-----------------------------------------------------------------------
C
C           SAVE TIME AND ENERGY VALUES FOR NEXT INCREMENTS EVALUATION
C
  450 TSAVE = TIME(I)
      ESAVE = ENERGY (I)
C        LEAVE AND INCREMENT "*" COUNTER AT ANOTHER SITE
      GO TO 480
C
C           "**" SECTION.  H=1 USED TO DIFFERENTIATE SUNRISE/SUNSET
C                          FROM INACTIVE ONES (MORE THAN 2 "*" IN A ROW)
C                          WHILE ALWAYS INCREMENTING LSTAR COUNTER.
C
  470 H=1
      TTEST = TSAVE
      ETEST = ESAVE
      GO TO 490
C
  480 H=0
  490 LSTAR = L
C       CHECK FOR PRINT OPERATION OR LEAVE SUNPOS IMMEDIATELY
        IF (.NOT. (H .EQ. 0)) GO TO 600
              GO TO 850
C
C
C
C
C           "***" SECTION.  H=1 USED TO DIFFERENTIATE SUNRISE/SET FROM
C                           INACTIVE EVENTS WHILE ALWAYS INCREMENTING ONE
C                           COUNTER FOR "***" (LTWO)
C
  500 H=1
      TTEST = TSAVE
      ETEST = ESAVE
      GO TO 520
  510 H=0
  520 LTWO = L
C         CHECK FOR PRINT OPERATION OR LEAVE SUNPOS IMMEDIATELY
      IF (.NOT. (H .EQ. 0)) GO TO 600
```

```
          GO TO 850
C
C
C
C        "  " SECTION.  USED TO DIFFERENTIATE SUNRISE/SUNSET EVENTS FROM
C                       NONACTIVE EVENTS.  INCREMENT LBLANK COUNTER
C                       ALWAYS.
C
  550 H=1
      TTEST = TSAVE
      ETEST = ESAVE
      GO TO 570
  560 H=0
  570 LBLANK = L
      IF (.NOT. (H .EQ. 0)) GO TO 600
           GO TO 850
C
C
C-----------------------------------------------------------------------
C
C PRINTING AREA. FIRST INCREMENT SUNRISE AND SUNSET COUNTER
C
  600 F = F + 1
C
C
       IF (.NOT.(F .EQ. 1)) GO TO 610
            RISE1 = TTEST
            ENER1 = ETEST
C
  610  IF (.NOT.(F .EQ. 2)) GO TO 620
            RISE2 = TTEST
            ENER2 = ETEST
C
  620  IF (.NOT. (F .EQ. 3)) GO TO 630

            RISE3 = TTEST
            ENER3 = ETEST
C
  630  IF (.NOT. (F .EQ. 4)) GO TO 640
            RISE4 = TTEST
            ENER4 = ETEST
C
  640  IF (.NOT. (F .EQ. 5)) GO TO 650
            RISE5 = TTEST
            ENER5 = ETEST
C
  650  IF (.NOT. (F .EQ. 6)) GO TO 850
            RISE6 = TTEST
            ENER6 = ETEST
C
C
C    IF 800 USE INDICATES AN ERROR IN THE ARRAY STRUCTURE
  800 CONTINUE
      PRINT*, "MAY BE ERROR IN ARRAY STRUCTURE AT SPACE I = ",I
C
  850 CONTINUE
      RETURN


      END
```

SUMMARY OF LANDFORM'S CHARACTERISTICS AND DIRECT RDIATION % ENERGY LOSSES FOR +20 DECLINATION

TYPE: CIRQUE GLACIER OF .4 KM2 AREA AND NEGATIVE BALANCE
LOCATION: ON CONTINENTAL DIVIDE (N) AT ATIGUN PASS 0.5 KM EAST OF TAPS
DESIGNATION: GRIZZLY GLACIER
ALTITUDE: 1600
LAT/LONG: 68.13N 149.45W
BEDROCK: IN KANAYUT FM WHERE DK OVERTHRUSTS DHF PHYLLITE CIRQUE

AZIMUTHS WITH INCLINATIONS FROM LANDFORM TO HORIZON
HORIZON AZIMUTH = 0 : HORIZON ALTITUDE = 0.
HORIZON AZIMUTH = 10 : HORIZON ALTITUDE = 1.
HORIZON AZIMUTH = 20 : HORIZON ALTITUDE = 1.5
HORIZON AZIMUTH = 30 : HORIZON ALTITUDE = 2.
HORIZON AZIMUTH = 40 : HORIZON ALTITUDE = 4.
HORIZON AZIMUTH = 50 : HORIZON ALTITUDE = 4.
HORIZON AZIMUTH = 60 : HORIZON ALTITUDE = 6.5
HORIZON AZIMUTH = 70 : HORIZON ALTITUDE = 2.5
HORIZON AZIMUTH = 80 : HORIZON ALTITUDE = 4.5
HORIZON AZIMUTH = 90 : HORIZON ALTITUDE = 6.
HORIZON AZIMUTH = 100 : HORIZON ALTITUDE = 4.5
HORIZON AZIMUTH = 110 : HORIZON ALTITUDE = 5.
HORIZON AZIMUTH = 120 : HORIZON ALTITUDE = 4.
HORIZON AZIMUTH = 130 : HORIZON ALTITUDE = 11.
HORIZON AZIMUTH = 140 : HORIZON ALTITUDE = 19.
HORIZON AZIMUTH = 150 : HORIZON ALTITUDE = 22.5
HORIZON AZIMUTH = 160 : HORIZON ALTITUDE = 24.5
HORIZON AZIMUTH = 170 : HORIZON ALTITUDE = 25.
HORIZON AZIMUTH = 180 : HORIZON ALTITUDE = 25.
HORIZON AZIMUTH = 190 : HORIZON ALTITUDE = 24.5
HORIZON AZIMUTH = 200 : HORIZON ALTITUDE = 24.5
HORIZON AZIMUTH = 210 : HORIZON ALTITUDE = 24.5
HORIZON AZIMUTH = 220 : HORIZON ALTITUDE = 26.
HORIZON AZIMUTH = 230 : HORIZON ALTITUDE = 25.5
HORIZON AZIMUTH = 240 : HORIZON ALTITUDE = 25.5
HORIZON AZIMUTH = 250 : HORIZON ALTITUDE = 25.5
HORIZON AZIMUTH = 260 : HORIZON ALTITUDE = 25.5
HORIZON AZIMUTH = 270 : HORIZON ALTITUDE = 23.
HORIZON AZIMUTH = 280 : HORIZON ALTITUDE = 20.5
HORIZON AZIMUTH = 290 : HORIZON ALTITUDE = 13.5
HORIZON AZIMUTH = 300 : HORIZON ALTITUDE = 10.
HORIZON AZIMUTH = 310 : HORIZON ALTITUDE = 7.
HORIZON AZIMUTH = 320 : HORIZON ALTITUDE = 3.5
HORIZON AZIMUTH = 330 : HORIZON ALTITUDE = 2.
HORIZON AZIMUTH = 340 : HORIZON ALTITUDE = 3.5
HORIZON AZIMUTH = 350 : HORIZON ALTITUDE = 2.5

SUNRISE1 AT 1.6 HRS WITH ENERGY AT: 10.3
SUNSET1 AT 16.9 HRS WITH ENERGY AT: 8886.5
SUNRISE2 AT 18.9 HRS WITH ENERGY AT: 9582.1
SUNSET2 AT 22.2 HRS WITH ENERGY AT: 9877.8
SUNRISE3 AT 0. HRS WITH ENERGY AT: 0.
SUNSET3 AT 0. HRS WITH ENERGY AT: 0.
HOURS OF SHADE DUE TO SCREENING = 5.4 HRS
% LOSS IN DURATION OF DIRECT RADIATION = 22.5%
% LOSS IN ENERGY DUE TO SCREENING = 7.260869563218%

LANDFORM'S EXPOSURE (ASPECT AND SLOPE) = N 20
% OF DIRECT RADIATION DUE TO EXPOSURE = 95.0%
% LOSS IN ENERGY DUE TO EXPOSURE = 5.0%
% GAIN IN ENERGY DUE TO EXPOSURE = 0.%

TOTAL % LOSS IN DIRECT RADIATION
ENERGY DUE TO SCREENING AND EXPOSURE = 12.26086956522%

JEDATA FORMAT

```
 0.0
 1.0
 1.5
 2.0
 4.0
 4.0
 6.5
 2.5
 4.5
 6.0
 4.5
 5.0
 4.0
11.0
19.0
22.5
24.5
25.0
25.0
24.5
24.5
24.5
26.0
25.5
25.5
25.5
25.5
23.0
20.5
13.5
10.0
 7.0
 3.5
 2.0
 3.5
 2.5
CIRQUE GLACIER OF .4 KM2 AREA AND NEGATIVE BALANCE
ON CONTINENTAL DIVIDE (N) AT ATIGUN PASS 0.5 KM EAST OF TAPS
GRIZZLY GLACIER
1600
68.13N 149.45W
IN KANAYUT FM WHERE DK OVERTHRUSTS DHF PHYLLITE CIRQUE
 N
20
```

```
      PROGRAM SUNPLT (INPUT,OUTPUT,TAPE5=INPUT,TAPE6=OUTPUT)
C
C     AUTHOR: JAMES ELLIS
C     DATE:   DEC 1978
C     FINAL PROJECT GDEG506
C
C
C     THIS CALCOMP PLOTTING ROUTINE IS TO BE USED IN CONJUNCTION WITH THE
C   PROGRAM JETEST.  THE DATA FILE CONTAINS THE PATHS OF THE SUN AT 68N
C   LATITUDE FOR DECLINATIONS OF 23.5,20,10,0,-10 DEGREES.  THE HORIZON
C   ABOUT A LANDFORM IS ENTERED IN THE LAST 38 SPACES OF THE DATA FILE
C   (JEDATP) WITH THE LANDFORM DESIGNATION IN THE 39TH SPACE.  USE EDIT
C   MODE TO ENTER THE DESIRED 36 HORIZON COORDINATES AND 2 REQUIRED CALCOMP
C   VALUES AFTER THE "PERMANENT" DECLINATION COORDINATES WHICH TAKE UP THE
C   FIRST 140 SPACES OF THE DATA FILE (I.E. AFTER EDIT MODE IS ATTAINED,
C   TYPE "S;140" AND FILL IN 39 LINES.  THE ARRAY LINES ARE TO BE FILLED
C   IN AN (F5.1,5X,F4.1) MANNER,EG. "340.0     36.5" MEANS THE AZIMUTH OF
C   340 DEGREES HAS A HORIZON OF 36.5 DEGREES INCLINATION.  THE HORIZON IS
C   ENTERED AT EVERY 10 DEGREE INCREMENTS, STARTING AT N (0  DEGREES).
C
C     THE PLOT IS 5" BY 6" WITH THE 5 SOLAR PATHS IN BLACK INK AND THE
C   LANDFORM HORIZON PATH IN RED FROM 0 TO 360 DEGREES ALONG THE HORIZON.
C   THIS ENABLES THE CALCULATIONS ABOUT LOSS IN DIRECT RADIATION AND SUNRISE/
C   SUNSET TIMES OBTAINED IN JETEST TO BE CHECKED.
C
C     JEJCLP IS THE JCL FILE.  JEPLOT IS THE PROGRAM FILE.  JEDATP IS THE
C   DATA FILE.  DESIGNATION IN THE JEDATP FILE SHOULD COINCIDE WITH THE
C   DESIGNATION IN THE JETEST'S DATA FILE (JEDATA).
C
C
C
C
      DIMENSION  XJUNE(39),YJUNE(39),XMAY(39),YMAY(39),XAPR(27),YAPR(27)
     +          ,XMAR(21),YMAR(21),XFEB(15),YFEB(15),XHORIZ(39),
     +           YHORIZ(39)
C
C
      INTEGER K,NUM
C
C
      CALL PLOTS
C        READ IN THE 23.5 DEGREE DECLINATION (JUNE 21)
C
      READ (5,100) (XJUNE(K),YJUNE(K),K=1,39)
  100 FORMAT (F5.1,5X,F4.1)
      CALL PLOT (1.0,1.0,-3)
C
C        DRAW A 6" HORIZONTAL AXIS AND 5" VERTICAL AXIS
C
      CALL AXIS (0.0,0.0,23HDIRECTION ALONG HORIZON,-23,6.0,0.0,
     +           0.0,60.0)
      CALL AXIS (0.0,0.0,25HSOLAR/HORIZON INCLINATION,25,
     +           5.0,90.0,0.0,10.0)
C
      CALL LINE (XJUNE,YJUNE,37,1,0,0)
C
```

```
C         READ IN THE 20 DEGREE DECLINATION (MAY21,JULY21)
C
      READ (5,200) (XMAY(K),YMAY(K),K=1,39)
  200 FORMAT (F5.1,5X,F4.1)
      CALL LINE (XMAY,YMAY,37,1,0,0)
C
C
C         READ IN THE 10 DEGREE DECLINATION (APR16,AUG28)
C
      READ (5,300) (XAPR(K),YAPR(K),K=1,27)
  300 FORMAT (F5.1,5X,F4.1)
      CALL LINE (XAPR,YAPR,25,1,0,0)
C
C
C         READ IN THE 0 DEGREE DECLINATION (MAR21,SEP23)
C
      READ (5,400) (XMAR(K),YMAR(K),K=1,21)
  400 FORMAT (F5.1,5X,F4.1)
      CALL LINE (XMAR,YMAR,19,1,0,0)
C
C
C         READ IN THE -10 DEGREE DECLINATION (FEB23,OCT20)
C
      READ (5,500) (XFEB(K),YFEB(K),K=1,15)
  500 FORMAT (F5.1,5X,F4.1)
      CALL LINE (XFEB,YFEB,13,1,0,0)
C
C
C         READ IN THE LANDFORM HORIZON AND PLOT IN RED
C
      CALL NEWPEN(2)
      READ (5,600) (XHORIZ(K),YHORIZ(K),K=1,39)
  600 FORMAT (F5.1,5X,F4.1)
      CALL LINE (XHORIZ,YHORIZ,37,1,0,0)
C
      CALL NEWPEN(1)
C
C
C         THIS DESIGNATION NUMBER ALLOWS COORDINATION WITH JESUN PROGRAM
C
      READ (5,700) NUM
  700 FORMAT (I1)
C
C
C         COMMENCE LABELLING THE GRAPH
C
      CALL SYMBOL (0.5,7.5,0.14,29HSCREENING OF DIRECT RADIATION,0.0,29)
      CALL SYMBOL (1.5,7.1,0.14,15HAT 68N LATITUDE,0.0,15)
      CALL SYMBOL (0.7,6.5,0.14,24HLANDFORM DESIGNATION:   ,0.0,24)
      CALL NUMBER (-0.0,-0.0,0.14,NUM,0.,-1)
C
C         ANNOTATE THE DECLINATION CURVES
      CALL SYMBOL (2.9,4.6,0.07,5H+23.5,0.0,5)
      CALL SYMBOL (2.9,4.2,0.07,3H+20,0.0,3)
      CALL SYMBOL (2.9,3.2,0.07,3H+10,0.0,3)
      CALL SYMBOL (3.0,2.2,0.07,1H0,0.0,1)
      CALL SYMBOL (2.9,1.2,0.07,3H-10,0.0,3)
```

```
C
C        INDICATE TRACE COLOR MEANING
      CALL SYMBOL (3.2,5.5,0.07,36HSOLAR DECLINATION PATHS: BLACK TRACE,
     +             0.0,36)
      CALL SYMBOL (3.3,5.2,0.07,27HLANDFORM HORIZON: RED TRACE,
     +             0.0,27)
      CALL SYMBOL (3.6,4.9,0.07,33HTIME ON +20 SOLAR ARC AND HORIZON,
     +             0.0,33)
C
C          ANNOTATE THE TIMES ON THE DECLINATION CURVE
C
      CALL SYMBOL (0.5,0.10,0.091,1H2,0.0,1)
      CALL SYMBOL (1.0,0.76,0.091,1H4,0.0,1)
      CALL SYMBOL (1.4,1.67,0.091,1H6,0.0,1)
      CALL SYMBOL (1.85,2.85,0.091,1H8,0.0,1)
C
      CALL SYMBOL (2.55,3.75,0.091,2H10,0.0,2)
      CALL SYMBOL (2.9,4.05,0.091,2H12,0.0,2)
      CALL SYMBOL (3.4,3.75,0.091,2H14,0.0,2)
      CALL SYMBOL (4.0,2.85,0.091,2H16,0.0,2)
      CALL SYMBOL (4.45,1.67,0.091,2H18,0.0,2)
C
      CALL SYMBOL (4.9,0.76,0.091,2H20,0.0,2)
      CALL SYMBOL (5.3,0.10,0.091,2H22,0.0,2)
      CALL SYMBOL (5.05,0.05,0.091,2H20,0.0,2)
      CALL SYMBOL (4.55,0.05,0.091,2H18,0.0,2)
      CALL SYMBOL (4.05,0.05,0.091,2H16,0.0,2)
C
      CALL SYMBOL (2.9,1.05,0.091,2H12,0.0,2)
      CALL SYMBOL (1.9,0.05,0.091,1H8,0.0,1)
      CALL SYMBOL (1.4,0.05,0.091,1H6,0.0,1)
      CALL SYMBOL (0.9,0.05,0.091,1H4,0.0,1)

C
C
      CALL EFPLOT
C
      STOP
      END
```

SCREENING OF DIRECT RADIATION

AT 68N LATITUDE

LANDFORM DESIGNATION: 0

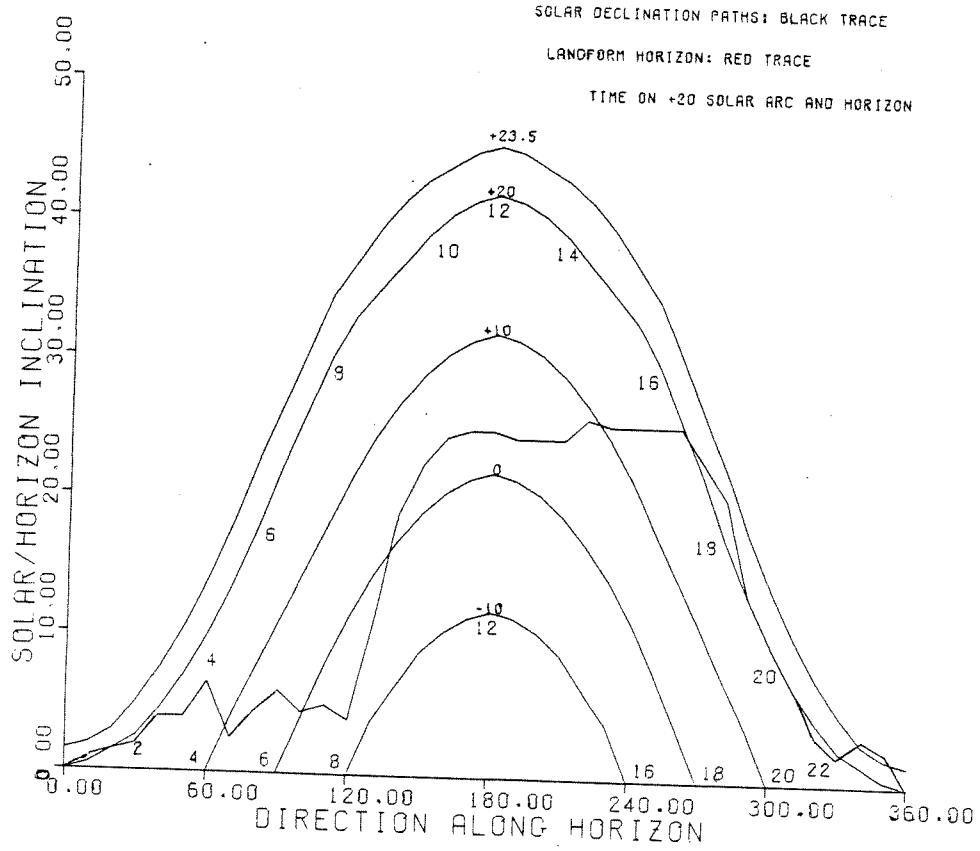

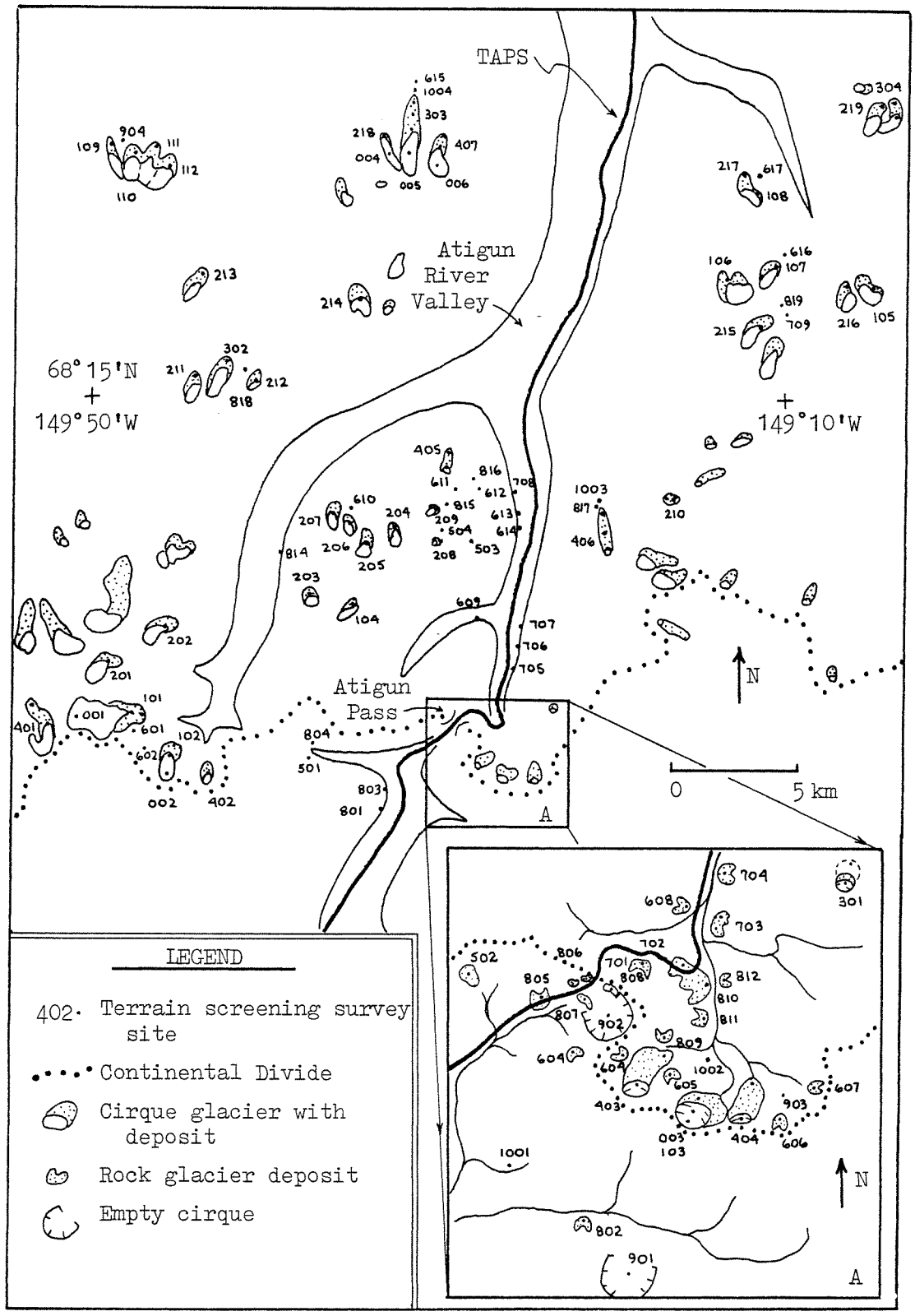
TAPS
Atigun River Valley
Atigun Pass
68° 15' N
149° 50' W
149° 10' W
N
0
5 km
A
LEGEND
402. Terrain screening survey site
Continental Divide
Cirque glacier with deposit
Rock glacier deposit
Empty cirque

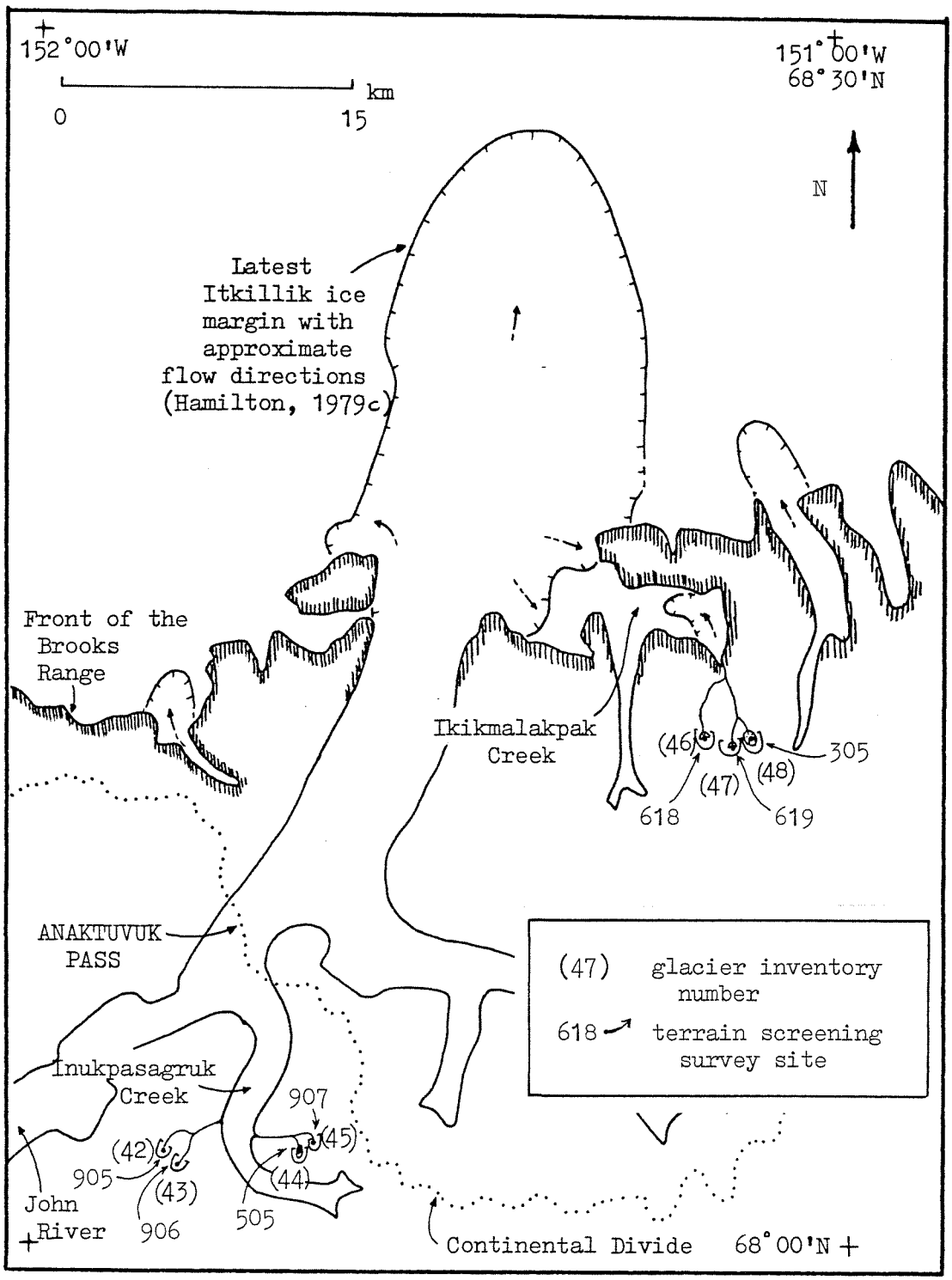
152°00'W
151°00'W
68°30'N
0
15
km
N
Latest Itkillik ice margin with approximate flow directions (Hamilton, 1979c)
Front of the Brooks Range
Ikikmalakpak Creek
(46)
(47)
(48)
305
618
619
ANAKTUVUK PASS
Inukpasagruk Creek
907
(45)
(42)
905
(43)
906
(44)
505
John River
Continental Divide
68°00'N
(47) glacier inventory number
618 terrain screening survey site

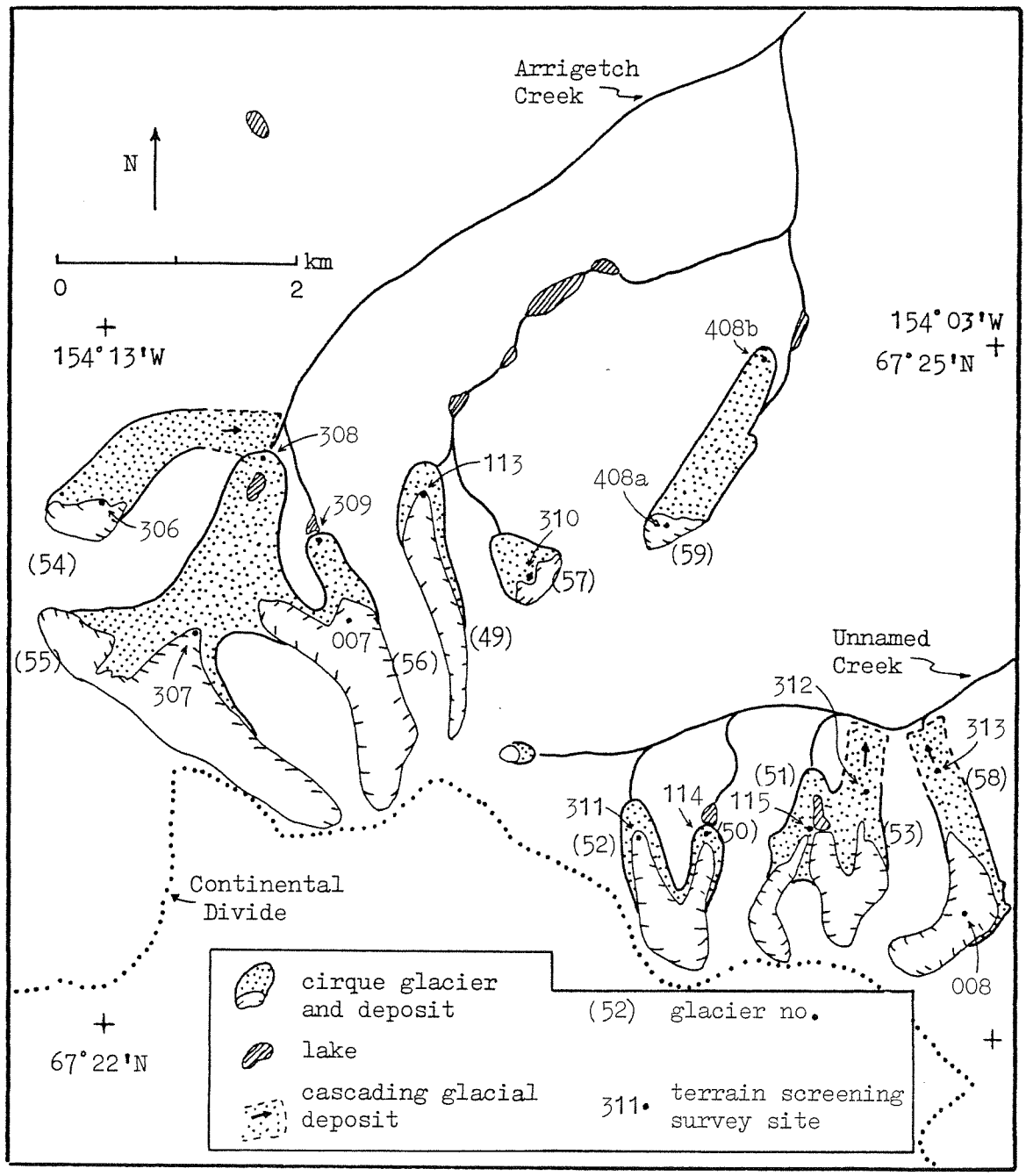
Arrigetch Creek
N
km
0
2
154°13'W
67°22'N
154°03'W
67°25'N
308
306
309
113
310
408b
408a
(54)
(57)
(59)
(55)
307
007
(56)
(49)
Unnamed Creek
312
313
(58)
(51)
311
(52)
114
115
(50)
(53)
Continental Divide
008
cirque glacier and deposit
lake
cascading glacial deposit
(52) glacier no.
311. terrain screening survey site

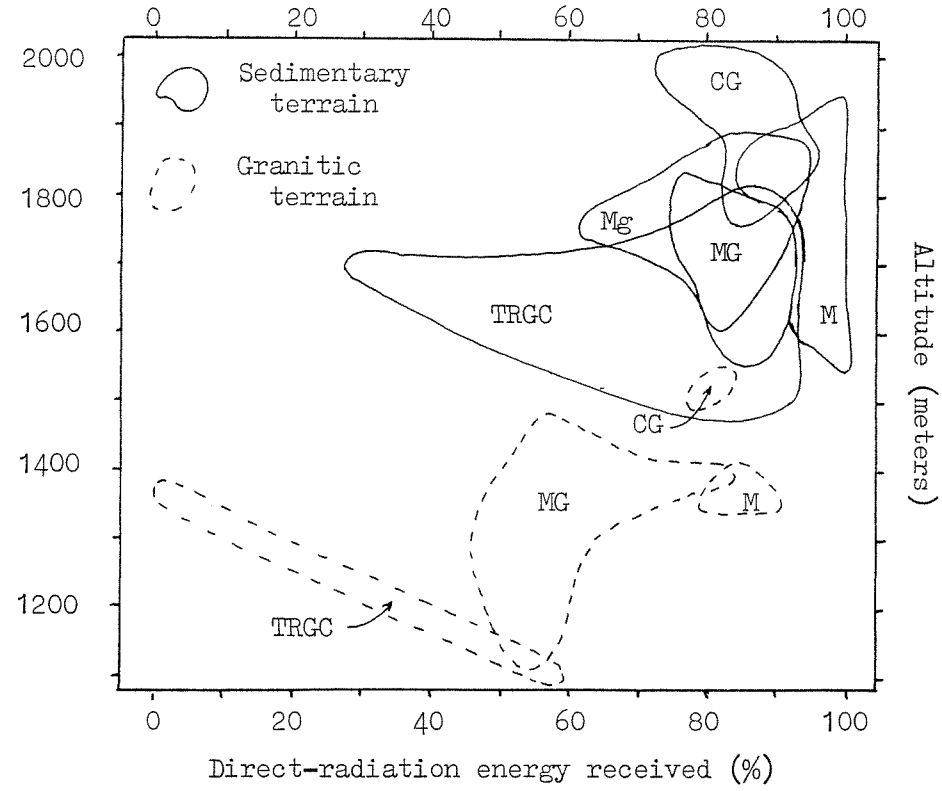
0
20
40
60
80
100
2000
1800
1600
1400
1200
Sedimentary terrain
Granitic terrain
CG
Mg
MG
M
TRGC
CG
MG
M
TRGC
Altitude (meters)
Direct-radiation energy received (%)

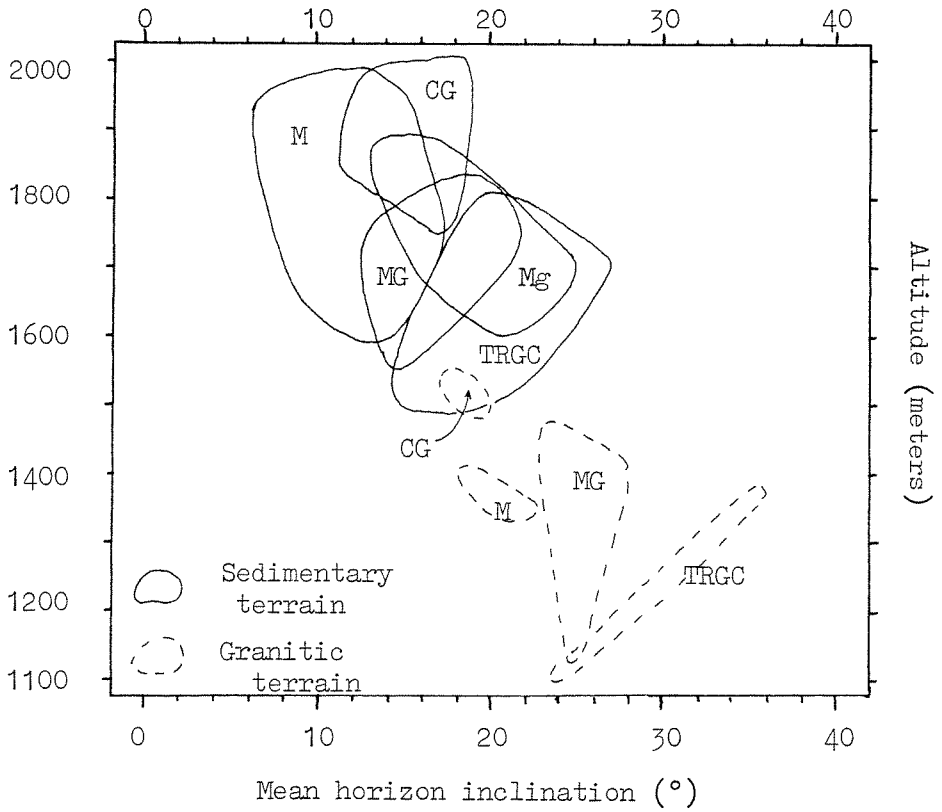
0
10
20
30
40
2000
1800
1600
1400
1200
1100
M
CG
MG
Mg
TRGC
CG
MG
M
TRGC
Sedimentary terrain
Granitic terrain
Altitude (meters)
Mean horizon inclination (°)

Appendix F. Terrain screening data.

Series: 000

(1) Site no./ Glacier no.[a]	(2) Lat/Long	(3) Survey site altitude (m)	(4) Type of survey site	(5) Duration of sun (hr)	(6) Direct energy blocked (%)	(7) Landform aspect /slope (°)	(8) Gain/ loss exposure (%)[b]	(9) Total energy receipt (%)	(10) Mean horizon (°)	(11) Max horizon (°)	(12) Bed-rock[c]
001/1	68 08.8/149 51	1750	CG	15.3	-4.6	E/10	0	95.4	11.6±5.3	20.5	Dkss Dkm
002/2	68 06.7/149 46	1660	CG	14.2	-16.1	N/10	-1	83.9	16.8±9.1	29.5	Dkm
003a/3	68 06.7/149 26	1820	CG	15.2	-10.7	N/20	-5	84.3	15.2±11.8	19.5	Dkm
003b/3	68 06.8/149 26	1760	CG	18.0	-7.3	N/20	-5	87.7	12.4±10.4	26.0	Dkm
004/29	68 20.3/149 34	1900	CG	13.5	-20.7	NW/20	-6	73.3	18.2±11.4	33.0	Dkm
005/33	68 20.5/149 32	1875	CG	18.2	-6.3	N/15	-3	90.7	12.7±8.3	25.0	Dkm Dkls
006/41	68 20.0/149 31	1800	CG	12.1	-13.7	N/15	-3	83.3	18.0±8.9	30.5	Dkm
007/56	67 23.8/154 00	1400	CG	12.2	-20.2	N/10	-1	78.8	19.2±8.4	34.0	Kg
008/58	67 22.6/154 03	1435	CG	12.4	-16.1	NE/10	-1	82.9	17.7±10.4	35.5	Kg

Appendix F. (continued).

Series: 100

(1)	(2)	(3)	(4)	(5)	(6)	(7)	(8)	(9)	(10)	(11)	(12)
101a/1	68 08.1/149 48	1570	CG-M	15.6	-3.8	NE/10	-1	95.2	12.4±6.0	26.0	Dkss
101b/1	68 08.1/149 48	1500	M	14.1	-6.5	E/0	0	93.5	13.8±6.2	22.5	Dkss
102a/2	68 07.3/149 46	1540	CG-M	18.7	-1.1	N/15	-3	95.9	10.3±5.9	23.5	Dkm Dhs
102b/2	68 07.9/149 46	1450	M	18.8	-1.0	S/5	0	100	9.6±4.6	22.5	Dkm Dhs
103/3	68 06.8/149 26	1700	M	18.3	-11.6	N/10	-1	87.4	11.6±8.2	24.5	Dkm
104[a]/4	68 10.2/149 36	1720	CG-M	14.2	-14.1	N/10	-1	84.9	16.3±7.7	26.5	Dkm Dhs
105/5	68 17.4/149 05	1815	CG-M	20.4	-0.4	N/10	-1	98.6	10.4±8.8	25.0	Dkm Dks
106[a]/6	68 17.2/149 13	1770	CG-M	16.3	-7.9	N/20	-5	87.1	13.0±8.8	25.5	Dkm
107/7	68 17.9/149 11	1720	CG-M	14.5	-8.6	N/10	-1	90.4	19.3±8.4	29.5	Dkm Dks Mk
108/8	68 19.5/149 12	1800	CG-M	16.2	-4.0	N/10	-1	95.0	13.6±8.5	27.0	Dks
109/9	68 20.5/149 49	1740	CG-M	16.9	-6.7	N/20	-5	88.3	12.7±9.4	25.0	Dkm
110/10	68 20.2/149 48	1815	CG-M	21.6	-1.5	N/10	-1	97.5	9.3±8.7	23.5	Dkm

Appendix F. (continued).

(1)	(2)	(3)	(4)	(5)	(6)	(7)	(8)	(9)	(10)	(11)	(12)
111/11	68 20.3/149 47	1645	CG-M	22.1	-0.2	N/10	-1	98.8	9.0±7.8	21.0	Dkm
112/12	68 20.1/149 46	1830	CG-M	22.3	0	N/0	0	100	6.5±6.4	16.5	Dkm
113[a]/49	67 24.3/154 09	1300	CG-M?	14.5	-15.2	N/10	-1	83.8	18.7±11.1	37.5	Kg
114/50	67 22.9/154 06	1250	CG-M	12.2	-18.7	N/10	-1	80.3	22.0±9.8	36.0	Kg
115/51	67 22.9/154 05	1250	CG-M	14.7	-10.6	N/0	0	89.4	20.2±10.1	36.5	Kg
Series: 200											
201[a]/13	68 04.0/149 50	1630	CG-Mg	12.9	-10.1	NE/20	-6	83.9	17.6±9.3	34.5	Dkss Dkm
202[a]/14	68 10.0/149 46	1600	CG-Mg	13.3	-9.2	NE/10	-1	89.8	16.1±8.0	30.5	Dkm
203/15	68 10.8/149 38	1720	CG-Mg	12.9	-11.3	NE/10	-1	87.7	16.0±8.0	27.0	Dkm
204/16	68 12.2/149 33	1650	CG-Mg	13.5	-17.0	N/10	-1	82.0	19.5±9.0	31.0	Dkss Dhs
205/17	68 11.8/149 35	1650	CG-Mg	8.6	-28.9	N/20	-5	66.1	20.9±10.2	31.0	Dkss Dhs Dkm
206/18	68 12.3/149 36	1770	CG-Mg	15.2	-12.3	NE/20	-6	81.7	16.1±10.4	31.5	Dkm Dkss

Appendix F. (continued).

(1)	(2)	(3)	(4)	(5)	(6)	(7)	(8)	(9)	(10)	(11)	(12)
207/19	68 12.5/149 36	1770	CG-Mg	16.7	-4.8	N/10	-1	94.2	13.3±7.4	23.0	Dkm Dkss
208/20	68 11.8/149 30	1740	CG-Mg	12.7	-20.8	NE/10	-1	78.2	17.9±11.6	33.5	Dhs
209/21	68 12.5/149 31	1780	CG-Mg	12.1	-16.3	E/10	+1	84.7	16.5±12.0	33.0	Dhs
210a/22	68 12.9/149 17	1600	CG-Mg	12.7	-16.9	NE/10	-1	82.1	24.5±9.9	36.5	Dhw Dhs
210b/22	68 13.0/149 18	1510	Mg	11.5	-16.9	NW/10	-1	82.1	20.9±7.6	32.5	Dhw Dhs
211/23	68 15.5/149 44	1680	Mg	12.4	-11.5	N/20	-5	83.5	16.9±5.5	30.0	Dkmm Dkm
212/24	68 15.4/149 41	1650	CG-Mg	8.3	-32.7	N/20	-5	62.3	19.3±10.5	35.0	Dkmm Dkm
213/25	68 17.2/149 44	1680	Mg	12.8	-10.3	NE/10	-1	88.7	18.0±7.5	26.5	Dhw
214/26	68 17.3/149 35	1660	CG-Mg	9.5	-23.6	N/10	-1	75.4	20.0±7.7	29.0	Dkm Dkmm
215[a]/27	68 16.8/149 12	1660	CG-Mg	14.5	-8.9	NE/10	-1	90.1	17.5±6.9	25.5	IPMI Dkm MK
216/28	68 17.2/149 08	1675	CG-Mg	15.7	-5.4	N/20	-5	89.6	16.1±8.3	28.0	Dkm Dks
217/8	68 19.7/149 13	1740	CG-Mg	13.4	-14.5	N/20	-5	80.5	17.1±9.7	30.5	Dks

Appendix F. (continued).

(1)	(2)	(3)	(4)	(5)	(6)	(7)	(8)	(9)	(10)	(11)	(12)
218/29	68 20.6/149 34	1660	CG-Mg	10.5	-19.1	N/10	-1	79.9	19.8±8.4	31.0	Dkm Mk
219/30	68 21.4/149 05	1680	CG-Mg	12.0	-14.5	N/15	-3	82.5	19.6±8.7	33.5	Dkmm Dkm Dkls
Series: 300											
301a/31	68 08.7/149 23	1680	CG-MG	13.1	-16.3	N/10	-1	82.7	20.3±12.4	36.5	Dkm Dhw
301b/31	68 08.9/149 23	1620	TRG?	14.8	-7.4	N/10	-1	91.6	13.8±8.9	25.0	Dkm Dhw
302/32	68 16.0/149 42	1550	MG	14.9	-7.0	N/10	-1	92.0	13.9±5.8	24.5	Dkmm Dkm
303a/33	68 21.2/149 32	1660	CG-MG	16.6	-5.1	N/15	-3	91.9	13.5±6.3	22.0	Dkm MK Dkls
303b/33	68 21.4/149 32	1585	MG	16.7	-9.3	N/15	-3	87.7	12.8±7.6	25.5	"
303c/33	68 21.6/149 32	1460	MG	14.3	-10.9	N/20	-5	84.1	14.5±8.1	24.5	"
304a/34	68 21.2/149 04	1720	CG-MG	11.0	-18.6	N/20	-5	76.4	18.3±6.8	28.5	Dkmm Dkm Dkls

Appendix F. (continued).

(1)	(2)	(3)	(4)	(5)	(6)	(7)	(8)	(9)	(10)	(11)	(12)
304b/34	68 21.5/149 04	1580	MG	10.6	-18.2	N/10	-1	80.8	19.7±6.3	30.0	Dkmm Dkm Dkls
305[a]/48	68 13.2/151 06	1615	CG-MG	13.5	-22.2	N/10	-1	76.8	20.7±12.5	35.5	Dkm Dkmm
306/54	67 24.3/154 13	1300	CG-MG	13.2	-14.4	N/10	-1	84.6	23.6±10.8	37.0	Kg
307/55	67 23.7/154 12	1280	CG-MG	10.1	-23.9	NE/10	-1	75.1	23.4±9.7	41.0	Kg
308/55	67 24.5/154 12	1035	MG	6.4	-43.8	N/10	-1	55.2	24.9±8.5	43.0	Kg
309/56	67 24.2/154 11	1190	MG	6.6	-41.8	N/20	-5	53.2	26.4±9.7	42.0	Kg
310[a]/57	67 24.0/154 08	1360	CG-MG	7.6	-42.7	NW/10	-1	56.3	23.6±11.4	45.5	Kg
311/52	67 22.8/154 07	1300	CG-MG	8.2	-37.6	N/10	-1	61.4	27.6±14.0	52.0	Kg
312/53	67 23.0/154 04	1130	MG	8.7	-42.8	N/20	-5	52.2	25.6±14.2	48.5	Kg
313/58	67 22.9/154 03	1220	MG	7.4	-46.9	NW/20	-5	48.1	26.1±15.2	52.5	Kg
Series: 400											
401a/35	68 08.0/149 53	1460	CG-TRG	12.4	-14.1	N/10	-1	84.9	20.1±7.2	84.9	Dkm Dkss

Appendix F. (continued).

(1)	(2)	(3)	(4)	(5)	(6)	(7)	(8)	(9)	(10)	(11)	(12)
401b/35	68 08.5/149 53	1420	TRGS(GC)	13.9	-7.2	NW/10	-1	91.8	17.4±6.8	27.5	Dkm Dkss
402/36	68 06.9/149 44	1510	CG-TRG	8.7	-28.1	N/10	-1	70.9	19.9±8.0	29.0	Dkm
403a/37	68 07.0/149 28	1680	CG-TRG	15.3	-8.5	NE/10	-1	90.5	20.5±11.7	35.5	Dkm
403b/37	68 07.3/149 27	1500	TRGS(GC)	13.3	-11.5	E/10	0	88.5	19.3±7.9	28.0	Dkm Dhs
404a/38	68 06.7/149 26	1700	CG-TRG	13.5	-7.8	N/20	-5	87.2	19.4±11.8	38.5	Dhs Dkm
404b/38	68 07.1/149 26	1500	TRGS(CG)	14.4	-7.9	N/20	-5	87.1	15.4±7.4	27.0	"
405a[a]/39	68 13.5/149 30	1585	CG-TRG	12.4	-13.6	N/10	-1	85.4	20.0±11.3	35.0	Dhs Dkss
405b/39	68 14.0/149 30	1400	TRGS(CG)	11.2	-19.5	N/10	-1	79.5	15.4±8.3	30.0	"
406a/40	68 11.6/149 20	1600	CG-TRG	3.8	-69.8	N/10	-1	29.2	26.6±13.2	41.0	Dhs
406b/40	68 12.1/149 20	1525	TRGB(GC)	10.3	-19.8	N/10	-1	79.2	17.4±7.7	27.0	"
406c/40	68 12.6/149 20	1430	TRGS(GC)	8.3	-30.4	N/20	-5	64.6	21.6±7.9	33.0	"
407a/41	68 20.4/149 30	1680	CG-TRG	11.8	-13.6	N/10	-1	85.4	17.4±7.3	28.0	Dkm Dkls
407b/41	68 20.6/149 30	1585	TRGS(GC)	11.1	-16.3	N/20	-5	78.7	17.1±7.1	26.0	"

Appendix F. (continued).

(1)	(2)	(3)	(4)	(5)	(6)	(7)	(8)	(9)	(10)	(11)	(12)
408a/59	67 24.2/154 07	1270	CG-TRG	1.5	-99.0	NE/20	-	1	35.4±14.6	50.5	Kg
408b/59	67 24.9/154 06	1000	TRGS(CG)	8.4	-41.6	NE/10	-1	57.4	23.7±12.7	44.0	Kg
Series: 500											
501	68 07.2/149 37	1280	TRGSi	15.7	-7.8	E/10	0	92.2	15.1±6.2	25.5	Dkm
502	68 07.9/149 32	1585	TRGBa	11.0	-17.6	SE/15	+4	85.9	19.5±11.3	34.5	Dkm
503	68 12.2/149 29	1400	TRGSa	14.1	-7.8	N/15	-3	89.2	21.0±8.6	34.0	Dhs
504	68 12.3/149 30	1620	TRGBi	11.1	-30.6	E/10	0	69.4	19.3±12.5	39.5	Dhs
505[a]/44	68 02.4/151 40	1295	TRGBi	8.1	-48.9	N/10	-1	50.1	24.6±13.1	41.5	Dkm Dkmm
Series: 600											
601	68 07.9/149 48	1660	LRGa	16.6	-2.6	N/20	-5	92.4	11.7±8.1	30.5	Dkm Dkss
602	68 07.6/149 46	1430	LRGa	14.4	-7.4	N/20	-5	87.6	15.0±6.8	28.0	Dhs

Appendix F. (continued).

(1)	(2)	(3)	(4)	(5)	(6)	(7)	(8)	(9)	(10)	(11)	(12)
603	68 07.9/149 29	1645	LRGa	11.3	-27.0	NW/20	-6	67.0	20.4±12.9	37.0	Dkm
604	68 07.3/149 28	1660	LRGa	12.9	-17.6	E/20	+2	84.4	19.7±10.2	33.5	Dkm
605	68 07.1/149 27	1570	LRGa	14.9	-7.0	N/20	-5	88.0	17.4±9.8	36.0	Dhs
606	68 06.7/149 25	1700	LRGa	13.6	-24.1	NW/20	-6	69.9	19.1±12.2	35.0	Dkss Dkm
607	68 07.0/149 24	1720	LRGa	11.9	-28.1	W/20	+2	73.9	20.6±12.5	38.0	Dkss
608	68 08.5/149 27	1200	LRGa	10.3	-20.0	E/20	+2	82.0	17.3±7.9	30.5	Dhs
609	68 10.1/149 27	1080	LRGa	16.3	-3.3	N/20	-5	91.7	15.5±8.0	30.5	Dhw
610	68 12.4/149 36	1740	LRGa	13.3	-17.6	E/20	+2	84.4	18.0±11.2	35.0	Dkss
611	68 13.2/149 31	1495	LRGa	10.9	-39.1	NE/20	-6	54.9	22.0±14.5	41.0	Dhs
612	68 13.3/149 27	1350	LRGa	9.4	-50.8	N/20	-5	44.2	23.6±12.7	43.5	Dhs
613	68 13.4/149 25	1050	LRGa	10.0	-26.1	E/20	+2	75.9	16.7±10.7	38.5	Dhs
614	68 12.8/149 25	1000	LRGa	10.7	-22.5	E/20	+2	79.5	17.5±10.4	36.5	Dhs
615	68 21.8/149 32	1430	LRGa	9.1	-33.5	W/20	+2	68.5	20.5±11.8	39.5	MII
616	68 18.2/149 11	1645	LRGa	12.8	-13.6	SE/20	+6	92.4	18.1±10.2	33.0	MII MK

Appendix F. (continued).

(1)	(2)	(3)	(4)	(5)	(6)	(7)	(8)	(9)	(10)	(11)	(12)
617	68 19.7/149 12	1630	LRGa	17.1	-2.1	N/20	-5	92.9	15.9±10.8	35.0	Dks Dkm
618[a]/46	68 13.5/151 09	1830?	LRGa	18.1	-6.1	NW/20	-6	87.9	14.5±11.2	32.5	Dkm Dkmm
619[a]/47	68 13.2/151 08	1450	LRGa	14.9	-11.8	N/20	-5	83.2	21.2±10.6	33.5	Dkm Dkmm
Series: 700											
701	68 07.9/149 29	1525	LRGp	12.6	-10.5	S/20	+7	96.5	20.3±12.4	40.5	Dkm
702	68 08.0/149 28	1400	LRGp	16.0	-5.5	N/20	-5	89.5	16.4±9.7	34.0	Dkm
703a	68 08.3/149 26	1200	LRGp	11.4	-16.3	W/20	+2	86.7	18.2±8.6	39.0	Dhw
703b	68 08.4/149 26	1230	LRGp	9.4	-27.8	W/20	+2	74.2	19.6±9.8	38.5	Dhw
704	68 08.8/149 26	1200	LRGp	8.6	-30.7	W/20	+2	71.3	18.5±10.2	36.5	Dhs
705	68 09.0/149 26	1140	LRGp	8.8	-30.0	W/20	+2	72.0	18.2±10.2	36.0	Dhs
706	68 09.5/149 26	1115	LRGp	9.9	-27.0	W/20	+2	75.0	17.9±10.2	36.0	Dhs
707	68 10.1/149 25	1080	LRGp	11.6	-19.7	W/20	+2	82.3	14.9±8.9	33.0	Dhs Dhw
708	68 13.5/149 26	1050	LRGp	9.5	-28.9	E/20	+2	73.1	16.3±10.6	36.0	Dhs

Appendix F. (continued).

(1)	(2)	(3)	(4)	(5)	(6)	(7)	(8)	(9)	(10)	(11)	(12)
709	68 16.9/149 10	1525	LRGp	7.5	-40.4	NW/20	-6	53.6	20.3±10.7	42.5	Dkm
Series: 800											
801	68 06.1/149 32	1130	LRGi	12.3	-12.0	SE/30	+9	97.0	13.9±9.2	31.0	Dkm? Dhs
802	68 05.8/149 29	1200	LRGi	14.9	-6.0	N/20	-5	89.0	19.5±10.0	38.5	Dhs
803	68 06.5/149 32	1190	LRGi	11.0	-18.7	E/30	+4	85.3	15.9±7.7	32.0	Dhs
804	68 07.5/149 38	1310	LRGi	11.9	-12.8	S/10	+3	90.2	18.2±7.2	30.0	Dkm
805	68 07.7/149 30	1370	LRGi	13.7	-7.4	E/30	+4	96.6	18.8±9.3	35.5	Dkm
806	68 07.9/149 29	1460	LRGi	13.8	-7.2	S/20	+7	99.8	19.2±11.2	38.5	Dkm
807	68 07.7/149 29	1480	LRGi	12.7	-12.4	NE/30	-12	75.8	20.4±9.9	36/5	Dkm
808	68 07.8/149 28	1500	LRGi	10.0	-25.6	W/30	+4	78.4	19.5±10.5	38.5	Dkm
809	68 07.4/149 27	1480	LRGi	12.8	-12.1	S/20	+7	74.9	22.2±11.0	39.0	Dkm
810	68 07.8/149 26	1230	LRGi	8.8	-33.0	E/20	+2	69.0	18.2±9.5	37.0	Dkm
811	68 07.6/149 26	1310	LRGi	9.2	-27.2	E/20	+2	74.8	19.5±9.7	39.0	Dkm

Appendix F. (continued).

(1)	(2)	(3)	(4)	(5)	(6)	(7)	(8)	(9)	(10)	(11)	(12)
812	68 07.9/149 26	1230	LRGi	10.8	-22.5	W/20	+2	79.5	20.2±8.9	36.0	Dhw
813	68 08.0/149 27	1250	LRGi	12.0	-12.7	NE/30	-12	75.3	18.0±8.8	35.5	Dkm Dkss
814	68 11.9/149 40	1190	LRGi	11.6	-15.2	W/10	0	84.8	16.3±8.2	36.0	Dkm
815	68 12.7/149 31	1705	LRGi	11.4	-14.9	S/10	+3	88.1	19.6±10.9	36.0	Dhs
816	68 13.4/149 27	1340	LRGi	13.9	-11.3	SE/20	+6	94.7	20.5±9.2	33.5	Dkss
817	68 12.9/149 21	1220	LRGi	6.5	-43.2	E/30	+4	60.8	24.6±8.7	37.5	Dhs
818	68 15.6/149 41	1570	LRGi	9.1	-27.6	N/0	0	72.4	18.9±9.5	34.0	Dkm
819	68 16.9/149 11	1525	LRGi	11.8	-17.6	SW/20	+6	88.4	21.0±8.6	33.5	Dkm
Series: 800											
901	68 05.5/149 28	1480	C	11.7	-17.7	N/10	-1	81.3	20.9±8.9	30.0	Dhs
902	68 07.7/149 29	1450	C	11.2	-19.3	N/10	-1	79.7	22.0±9.4	33.5	Dkm
903	68 07.0/149 25	1600	C	14.1	-13.4	W/5	0	86.6	17.4±9.8	30.5	Dkss Dkm
904	68 20.3/149 50	1690	C	15.9	-10.2	N/10	-1	88.8	17.3±10.7	33.0	Dkm

Appendix F. (continued).

(1)	(2)	(3)	(4)	(5)	(6)	(7)	(8)	(9)	(10)	(11)	(12)
905[a]/42	68 02.5/151 50	1450	C	13.3	-17.3	N/10	-1	81.7	21.7±9.8	32.0	Dkm Dkmm
906[a]/43	68 02.1/151 49	1370	C	9.7	-30.3	N/10	-1	68.7	21.6±8.7	31.0	Dkm Dkmm
907[a]/45	68 02.7/151 39	1385	C	10.7	-26.2	N/0	0	73.8	22.8±8.4	35.0	Dkm Dkmm
Series: 1000											
1001	68 05.3/149 30	1160	VH	14.4	-7.6	S/5	+2	94.4	12.4±6.1	23.5	Dhs
1002	68 07.4/149 26	1360	VH	11.1	-16.3	N/10	-1	82.7	18.3±6.6	27.0	Dkm Dhs Dkss
1003	68 12.9/149 21	1220	VH	6.5	-43.2	N/10	-1	56.8	24.6±8.7	37.5	Dhs
1004	68 21.8/149 32	1400	VH	8.0	-32.6	N/10	-1	65.4	21.6±9.4	31.5	Dkm MK Dkls

[a]Survey site horizon determined trigonometrically from topographic sheets.

[b]See Table 3 for aspect/slope conversion to direct radiation energy values.

[c]See Brosgé and others (1979); Nelson and Grybeck (1980).

Appendix G. Statistical Analysis and Data

In order to determine if any single variable was capable of distinguishing between the preassigned groups of glacial and periglacial landforms (listed in Table 2), the mean value of a variable for one group was compared to the mean of another (Appendix Fig. 1a). The comparison of two samples or groups against one another involved the F-test to determine equality of variances followed by the t-test to determine if, and at what level, there was a significant statistical difference between the means of a variable representing the two groups of landforms (Davis, 1973). A 95% confidence level was applied for these comparisons.

The second level of investigation involved plotting the values of two variables on linear-scaled graph paper while coding the different landform groups (Appendix Fig. 1b). This promoted distinctions and highlighted overlaps between groups. Also plotting two variables enhances examining the concept that these glacial and periglacial landforms form a continuum or sequence of transitional facies (Currey, 1969; Madole, 1972; Whalley, 1974). Where trends were graphically apparent, simple linear correlation was performed providing the correlation coefficient (r) which assesses the degree of relationship between two variables (Till, 1971). Its significance for a given number of samples can be derived from Murdoch and Barnes (1974, Table 10). Linear regression lines were calculated by the least-squares method when a significant relationship did exist in order to quantify a rate of change along a continum of glacial/periglacial landforms (Till, 1971).

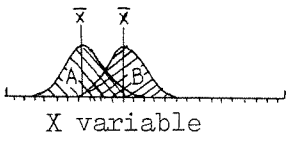

a) Univariate analysis.

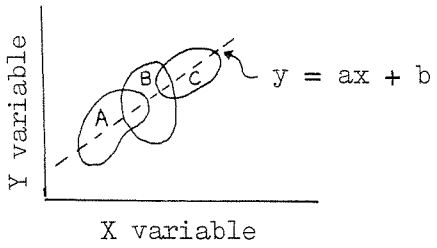

b) Bivariate analysis.

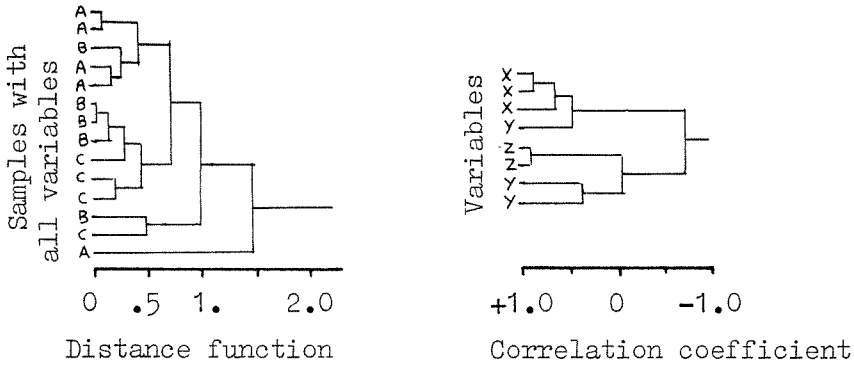

c) Multivariate cluster analysis of samples and variables.

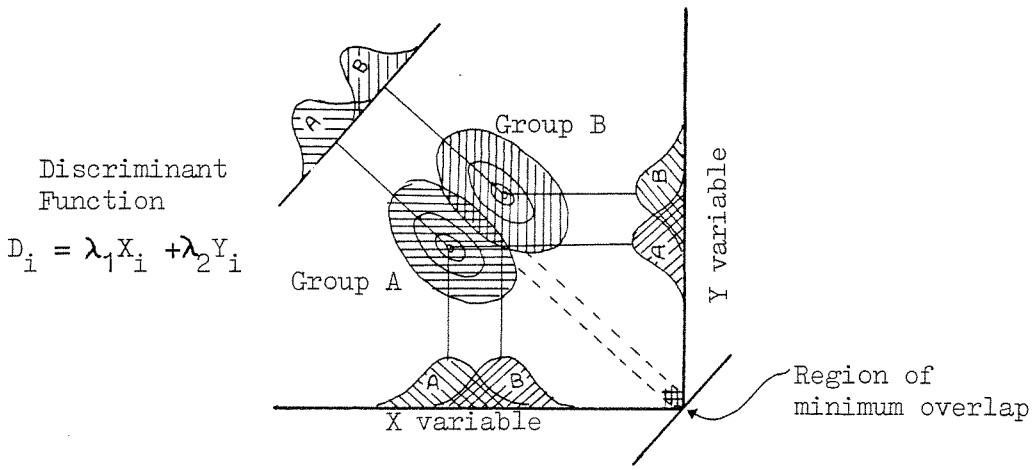

d) Multivariate linear discriminant analysis of two groups (modified after Davis, 1973, p. 444 and May, 1971).

Two multivariate techniques (see Andrews and Estabrook, 1971) were utilized to analyze, classify, and discriminate glacial and periglacial landforms. The first technique, cluster analysis, requires no a priori classification of individual landforms into groups; classification of samples into groups is based solely on a logical pair-by-pair comparison of distance between the variables (Appendix Fig. 1c; Parks, 1966; Hartigan, 1977). The distance measure is the Euclidean distance, the square root of the sum of squares of the differences between the variables for two cases or two landforms. Hartigan (1977) specifies each case (or landform with its variables) is initially considered to be in a cluster of its own. At each step the two clusters with the shortest distance between them are combined (amalgamated) and treated as one cluster. This process of combining clusters continues until all the cases are combined into one cluster. This algorithm is called average distance. The advantage of cluster analysis is that two principal restrictions in conventional statistical analysis do not apply; specifically, the sample does not have to be representative of the general population and there are no implications of cause and effect or a relationship of dependent and independent variables (Parks, 1966).

Linear discriminant analysis was the second multivariate technique used (Klecka, 1975). It was applied to distinguish between two or three groups of glacial landforms. Four variables were selected that measured characteristics on which the groups were expected to differ. Discriminant analysis finds the linear combination of these variables which produces the maximum difference between the previously-defined groups (Appendix Fig. 1d; Davis, 1973). If

a discriminant function(s) is found which produces a significant difference, it can be used to classify other glacial landforms of unknown type to one of the original groups (May, 1972; Davis, 1973). In this study, the score(s) of the discriminant function(s) is used to indicate which glacial landform would be favored to develop in a cirque environment given four environmental and morphometric parameters.

Unlike cluster analysis, linear discriminant analysis requires assumptions about the nature of the data, such as randomness of observations, normal distribution of variables, and equal variance-covariance matrices within the groups (Davis, 1973). Given these assumptions, tests of significance for the discriminant function may developed which are often of major theoretical significance (Klecka, 1975). The relative contributions of the four discriminating variables to the function, the relative ability of each function to separate landform groups, and the percent of "known" groups correctly classified are provided in the SPSS Discriminant Analysis program (Klecka, 1975). These are utilized to further analyze the environment of glacial landforms.

A final objective of this multivariate study is cluster analysis of variables (Hartigan, 1977). It was utilized to measure similarity or correlation coefficients between the variables (ranges from -1.0 to +1.0, Appendix Fig. 1c). Amalgamation of the variables follows the procedure outlined above for cluster analysis of samples. The method enables detection and measurement of highly correlated variables which can then be eliminated to reduce the number of

variables being considered or analyzed for cause and effect relationships. It also detects uncorrelated or poorly correlated variables which are then used to achieve near-orthogonality of data, a property desired for variables utilized in linear discriminant analysis (see Parks, 1966).

The landforms were grouped for statistical analysis as shown in Table 2. In addition, the 43 glacial debris lobes mapped in the sedimentary terrain of Atigun and Anaktuvuk Passes were distinguished and compared to the 11 analyzed in the granitic terrain of the Arrigetch Peaks. The variables used are shown in Table 7.

Statistical information and the data for Linear Discriminant Analyses 1-3 are provided (see Figs. 22-24; Tables 8-10). The data for Cluster Analysis 1 and 2 (see Figs. 25, 27, Tables 11-12) are also provided. Cluster Analysis 1 considered only the landforms with glaciers upslope, and averaged the data from multiple survey sites (Appendix F) to give one value for each landform in each category, except for Robin Glacier (no. 8) where "If" and "Mg" lobes were considered separately. Cluster Analysis 2 utilized the 64 survey sites on periglacial landforms (Appendix F).

The cluster diagrams and data for three other analyses are provided. These analyses utilized all the terrain-screening sites even if they were multiple on the same landform to detect shading correlations. There were 143 survey sites: 66 on glacial landforms in the sedimentary terrain of Atigun and Anaktuvuk (Cluster Analysis 3); 13 on glacial landforms in the granitic Arrigetch (combined with

the sedimentary glacial data for Cluster Analysis 4); and 64 on periglacial landforms. All 143 sites were clustered in Analysis 5.

The five terrain-screening variables (HEADINCL, HEADMAX, EXPOSURE, SUNHR, SUNENER; Table 7) were used together and/or with the variables LATITUDE and ALTITUDE in Cluster Analyses 2, 3, 4, and 5. Cluster Analyses 3 and 4 demonstrate that glacial landform exposure, the gain or loss in direct radiation energy due to landform slope and aspect, has little correlation with latitude, altitude, or even terrain screening in the central Brooks Range. Cluster Analysis 5 demonstrates correlations of variables to be intermediate in value to those attained on previous analyses and intermixing of most glacial and periglacial landforms, suggesting an overall uniformity of terrain screening in alpine areas for different types of deposits. However, non ice-cored moraines (MS) in sedimentary terrain and glacier-cored deposits (MGI, TRGI) in the granitic Arrigetch tend to be clustered into two groups, separated from the periglacial landforms; the environments of these two glacial deposits are obviously unique.

Appendix G (continued).

SAMPLE DISCRIMINANT ANALYSIS 1 FOR BROOKS RANGE

FILE NONAME (CREATION DATE = 81/02/09.)
SUBFILE MORAIN GLAMOR GLATRG

- D I S C R I M I N A N T A N

ON GROUPS DEFINED BY SUBFILE

43 (UNWEIGHTED) CASES WERE PROCESSED.
0 OF THESE WERE EXCLUDED FROM THE ANALYSIS.
43 (UNWEIGHTED) CASES WILL BE USED IN THE ANALYSIS.

NUMBER OF CASES BY GROUP

SUBFILE	NUMBER OF CASES UNWEIGHTED	WEIGHTED	LABEL	
1	12	12.0	SUBFILE	MORAIN
2	24	24.0	SUBFILE	GLAMOR
3	7	7.0	SUBFILE	GLATRG
TOTAL	43	43.0		

GROUP MEANS

SUBFILE	NSUN	NELA	NHEAD	NLAT
1	93.29167	1793.33333	58.33333	68.25683
2	62.58750	1736.54167	153.91667	68.24742
3	79.75714	1622.14286	221.42857	68.16214
TOTAL	85.11395	1734.88372	136.23256	68.23942

GROUP STANDARD DEVIATIONS

SUBFILE	NSUN	NELA	NHEAD	NLAT
1	5.38609	88.24896	49.14419	.06961
2	7.66439	47.76480	81.62423	.06387
3	11.63241	69.81267	121.85081	.07900
TOTAL	9.30774	84.18721	97.57191	.07667

POOLED WITHIN-GROUPS COVARIANCE MATRIX WITH 40 DEGREES OF FREEDOM

	NSUN	NELA	NHEAD	NLAT
NSUN	62.05181			
NELA	47.96347	4164.567		
NHEAD	-13.70156	-2610.942	6722.255	
NLAT	.9146280E-02	3.136478	-2.965173	.5500309E-02

POOLED WITHIN-GROUPS CORRELATION MATRIX

	NSUN	NELA	NHEAD	NLAT
NSUN	1.00000			
NELA	.09413	1.00000		
NHEAD	-.02121	-.49228	1.00000	
NLAT	.01566	.65418	-.46764	1.00000

Appendix C (continued).

```
SAMPLE DISCRIMINANT ANALYSIS 1 FOR BROOKS RANGE                          81/
FILE   NONAME   (CREATION DATE = 81/02/09.)
SUBFILE    MORAIN      GLAMOR      GLATRG

- - - - - - - - - - - - - - - - - - - - - - -  D I S C R I M I N A N T  A N A L

ON GROUPS DEFINED BY SUBFILE

ANALYSIS NUMBER        1
DIRECT METHOD-  ALL VARIABLES PASSING THE TOLERANCE TEST ARE ENTERED.
     MINIMUM TOLERANCE LEVEL.....................  .00100
CANONICAL DISCRIMINANT FUNCTIONS

     MAXIMUM NUMBER OF FUNCTIONS.................  2
     MINIMUM CUMULATIVE PERCENT OF VARIANCE....  100.00
     MAXIMUM SIGNIFICANCE OF WILKS  LAMBDA....  1.0000

PRIOR PROBABILITY FOR EACH GROUP IS  .33333

                                                  CANONICAL DISCRIMINANT FUNCTIONS

                                 PERCENT OF   CUMULATIVE     CANONICAL  =  AFTER
FUNCTION   EIGENVALUE             VARIANCE     PERCENT     CORRELATION  =  FUNCTION
                                                                        =      0
    1*        1.30165              86.84        86.84        .7520163  =      1
    2*         .19722              13.16       100.00        .4056714  =

     * MARKS THE   2 FUNCTION(S) TO BE USED IN THE REMAINING ANALYSIS.

 WILKS  LAMBDA   CHI-SQUARED    D.F.   SIGNICANCE
 =      .3629003      39.025       8        .0000
 =      .8352684       6.9301      3        .0742


STANDARDIZED CANONICAL DISCRIMINANT FUNCTION COEFFICIENTS

                FUNC  1     FUNC  2
NSUN             .49323      -.55371
NELA             .77513      -.87663
NHEAD           -.45270      -.62116
NLAT            -.48048      -.20468

CANONICAL DISCRIMINANT FUNCTIONS EVALUATED AT GROUP MEANS (GROUP CENTROIDS)

   GROUP        FUNC  1     FUNC  2
     1          1.54075      -.33601
     2          -.25277      -.36818
     3         -1.77464       .68289

SYMBOLS USED IN TERRITORIAL MAP

SYMBOL   GROUP   LABEL
   1         1   SUBFILE   MORAIN
   2         2   SUBFILE   GLAMOR
   3         3   SUBFILE   GLATRG
   *             GROUP CENTROIDS
```

Appendix G (continued).

DATA USED IN LINEAR DISCRIMINANT ANALYSIS 1

```
RUN NAME          SAMPLE DISCRIMINANT ANALYSIS 1 FOR BROOKS RANGE
VARIABLE LIST     NSUN,NELA,NHEAD,NLAT
INPUT MEDIUM      CARD
INPUT FORMAT      FIXED(5X,F4.1,5X,F4.0,5X,F3.0,5X,F6.3)
DISCRIMINANT      GROUPS=SUBFILES/VARIABLES=NSUN,NELA,NHEAD,NLAT/
                  ANALYSIS=NSUN,NELA,NHEAD,NLAT/
                  PRIORS=.20,.60,.20/
OPTIONS           5,7,9,10
STATISTICS        1,2,3,4,5
READ INPUT DATA                                          GLACIER NO.
      94.0      1660       150       68.133              1
      97.5      1600       150       68.117              2
      87.4      1725       60.       68.133              3
      84.9      1800       20.       68.172              4
      98.6      1625       30.       68.263              5
      87.1      1820       10.       68.287              6
      90.4      1660       10.       68.300              7
      95.0      1600       100       68.325              8(M)
      88.3      1650       40.       68.333              9
      97.5      1685       40.       68.333              10
      98.8      1815       40.       68.333              11
      100.      1880       50.       68.333              12
      93.6      1710       400       68.150              13
      91.8      1720       250       68.167              14
      87.7      1700       215       68.175              15
      82.0      1680       180       68.200              16
      66.1      1740       240       68.197              17
      81.7      1795       210       68.207              18
      79.2      1765       120       68.200              20
      94.2      1765       160       68.207              19
      84.7      1765       180       68.208              21
      82.1      1630       230       68.215              22
      83.5      1765       120       68.253              23
      62.3      1700       50.       68.255              24
      88.7      1795       120       68.283              25
      75.4      1735       150       68.287              26
      90.1      1750       100       68.280              27
      89.6      1730       200       68.287              28
      80.5      1800       100       68.325              8(Mg)
      76.6      1805       10.       68.342              29
      84.5      1765       150       68.350              30
      82.7      1715       100       68.169              31
      92.0      1705       100       68.258              32
      87.7      1755       100       68.353              33
      78.6      1755       100       68.350              34
      76.8      1640       100       68.220              48
      88.4      1530       250       68.153              35
      70.9      1635       150       68.125              36
      89.5      1640       200       68.117              37
      87.1      1640       200       68.125              38
      82.4      1585       300       68.217              39
      57.5      1575       420       68.200              40
      82.5      1750       30.       68.338              41
FINISH
```

Appendix G (continued).

SAMPLE DISCRIMINANT ANALYSIS 2 FOR BROOKS RANGE

FILE NONAME (CREATION DATE = 61/02/09.)
SUBFILE MORAIN GLAMOR GLATRG

- D I S C R I M I N A N T A N

ON GROUPS DEFINED BY SUBFILE

43 (UNWEIGHTED) CASES WERE PROCESSED.
0 OF THESE WERE EXCLUDED FROM THE ANALYSIS.
43 (UNWEIGHTED) CASES WILL BE USED IN THE ANALYSIS.

NUMBER OF CASES BY GROUP

SUBFILE	NUMBER OF CASES UNWEIGHTED	WEIGHTED	LABEL	
1	12	12.0	SUBFILE	MORAIN
2	24	24.0	SUBFILE	GLAMOR
3	7	7.0	SUBFILE	GLATRG
TOTAL	43	43.0		

GROUP MEANS

SUBFILE	NSUN	NHEAD	NDROP	NAREA
1	93.29167	58.33333	80.41667	.61500
2	62.58750	139.54167	81.45833	.58125
3	79.75714	221.42857	46.42857	.52429
TOTAL	85.11395	129.65116	69.86372	.63721

GROUP STANDARD DEVIATIONS

SUBFILE	NSUN	NHEAD	NDROP	NAREA
1	5.38609	49.14414	17.38054	.59791
2	7.06435	64.42858	36.75935	.37347
3	11.63241	121.65081	36.02246	.45865
TOTAL	9.30774	89.04517	35.81514	.46156

POOLED WITHIN-GROUPS COVARIANCE MATRIX WITH 40 DEGREES OF FREEDOM

	NSUN	NHEAD	NDROP	NAREA
NSUN	62.05181			
NHEAD	-23.04189	5276.156		
NDROP	67.77269	-750.7478	1143.315	
NAREA	1.015054	1.247522	6.845960	.2100933

POOLED WITHIN-GROUPS CORRELATION MATRIX

	NSUN	NHEAD	NDROP	NAREA
NSUN	1.00000			
NHEAD	-.04026	1.00000		
NDROP	.25445	-.30561	1.00000	
NAREA	.28113	.03746	.44172	1.00000

SAMPLE DISCRIMINANT ANALYSIS 2 FOR BROOKS RANGE 81/

FILE NONAME (CREATION DATE = 81/02/09.)
SUBFILE MORAIN GLAMOR GLATRG

- D I S C R I M I N A N T A N A L

ON GROUPS DEFINED BY SUBFILE

ANALYSIS NUMBER 1

DIRECT METHOD- ALL VARIABLES PASSING THE TOLERANCE TEST ARE ENTERED.

MINIMUM TOLERANCE LEVEL.................. .00100

CANONICAL DISCRIMINANT FUNCTIONS

MAXIMUM NUMBER OF FUNCTIONS.............. 2
MINIMUM CUMULATIVE PERCENT OF VARIANCE... 100.00
MAXIMUM SIGNIFICANCE OF WILKS LAMBDA.... 1.0000

PRIOR PROBABILITY FOR EACH GROUP IS .33333

CANONICAL DISCRIMINANT FUNCTIONS

FUNCTION	EIGENVALUE	PERCENT OF VARIANCE	CUMULATIVE PERCENT	CANONICAL CORRELATION	-	AFTER FUNCTION	WILKS LAMBDA	CHI-SQUARED	D.F.	SIGNICANCE
					-	0	.3498737	40.432	8	.0000
1*	1.32282	85.16	85.16	.7546445	-	1	.8126927	7.9850	3	.0463
2*	.23048	14.84	100.00	.4327902	-					

* MARKS THE 2 FUNCTION(S) TO BE USED IN THE REMAINING ANALYSIS.

STANDARDIZED CANONICAL DISCRIMINANT FUNCTION COEFFICIENTS

	FUNC 1	FUNC 2
NSUN	.62736	-.09147
NHEAD	-.79367	-.37441
NDROP	-.66959	.90477
NAREA	.37022	-.34636

CANONICAL DISCRIMINANT FUNCTIONS EVALUATED AT GROUP MEANS (GROUP CENTROIDS)

GROUP	FUNC 1	FUNC 2
1	1.76149	-.11509
2	-.57275	.33552
3	-1.05598	-.95306

SYMBOLS USED IN TERRITORIAL MAP

SYMBOL	GROUP	LABEL
1	1	SUBFILE MORAIN
2	2	SUBFILE GLAMOR
3	3	SUBFILE GLATRG
*		GROUP CENTROIDS

Appendix G (continued).

DATA USED IN LINEAR DISCRIMINANT ANALYSIS 2 AND 3 (INCLUDE LAST 11 LINES FOR 3 WHICH PERTAIN TO THE ARRIGETCH PEAKS)

```
RUN NAME          SAMPLE DISCRIMINANT ANALYSIS 3 FOR BROOKS RANGE
VARIABLE LIST     NSUN,NHEAD,NDROP,NAREA
INPUT MEDIUM      CARD
SUBFILE LIST      NORAIN(12)GLAMOR(24)GLATRG(7)
INPUT FORMAT      FIXED(5X,F4.1,5X,F3.0,5X,F3.0,3X,F4.2)
DISCRIMINANT      GROUPS=SUBFILES/VARIABLES=NSUN,NHEAD,NDROP,NAREA/
                  ANALYSIS=NSUN,NHEAD,NDROP,NAREA/
OPTIONS           5,7,9,10
STATISTICS        1,2,3,4,5
READ INPUT DATA
```

				GLACIER NO.
94.0	150	40.	2.55	1
97.5	150	50.	1.08	2
87.4	60.	45.	0.24	3
84.9	20.	60.	0.34	4
98.6	30.	55.	0.62	5
87.1	10.	70.	1.00	6
90.4	10.	40.	0.61	7
95.0	100	55.	0.49	8(M)
88.3	40.	65.	0.66	9
97.5	40.	100	0.64	10
96.9	40.	80.	0.68	11
100.	50.	65.	0.87	12
83.6	40.	105	0.75	13
91.8	250	25.	1.04	14
87.7	215	65.	0.52	15
82.0	180	40.	0.53	16
66.1	240	75.	0.54	17
81.7	210	40.	0.19	18
94.2	180	75.	0.47	19
76.2	120	35.	0.05	20
84.7	180	70.	0.20	21
82.1	230	70.	.32	22
83.5	120	95.	0.71	23
62.3	50.	35.	0.36	24
88.7	120	125	0.59	25
75.4	150	125	0.51	26
90.1	100	140	1.03	27
89.6	200	80.	0.71	28
80.5	100	55.	0.49	8(Mg)
76.6	100	115	0.46	29
84.5	150	100	0.62	30
82.7	100	30.	0.04	31
92.	100	120	1.23	32
87.7	100	165	1.65	33
78.6	100	115	0.70	34
76.8	100	55.	0.24	48
88.4	250	95.	1.23	35
70.9	150	0.	0.43	36
89.5	200	20.	0.09	37
87.1	200	35.	0.06	38
82.4	300	40.	0.45	39
57.5	420	40.	0.33	40
82.5	30.	95.	1.08	41
85.9	100	165	0.54	49
80.3	180	95.	0.62	50
89.4	100	165	0.97	51
52.2	150	160	0.97	53
84.6	425	90.	0.74	54
65.1	300	235	3.25	55
53.2	150	165	0.55	56
52.3	425	55.	0.23	57
48.1	250	120	0.75	58
29.2	450	20.	0.28	59
61.4	180	120	0.62	52

```
FINISH
```

Appendix G (continued).

```
SAMPLE DISCRIMINANT ANALYSIS 3 FOR BROOKS RANGE
FILE   NONAME   (CREATION DATE = 81/02/09.)
SUBFILE   SED        GRANIT

- - - - - - - - - - - - - - - - - - - - D I S C R I M I N A N T   A N
ON GROUPS DEFINED BY SUBFILE

          54 (UNWEIGHTED) CASES WERE PROCESSED.
          0 OF THESE WERE EXCLUDED FROM THE ANALYSIS.
          54 (UNWEIGHTED) CASES WILL BE USED IN THE ANALYSIS.

NUMBER OF CASES BY GROUP

                NUMBER OF CASES
SUBFILE      UNWEIGHTED     WEIGHTED   LABEL
    1            43           43.0    SUBFILE   SED
    2            11           11.0    SUBFILE   GRANIT
TOTAL            54           54.0

GROUP MEANS

SUBFILE        NSUN          NHEAD          NDROP          NAREA
    1       65.11395      129.65116      69.66372        .63721
    2       63.76182      246.36364     126.18182        .86545
TOTAL       60.76852      153.42593      81.75926        .68370

GROUP STANDARD DEVIATIONS

SUBFILE        NSUN          NHEAD          NDROP          NAREA
    1        9.30774       69.04517       35.61514        .46156
    2       19.16903      133.56816       61.73624        .82520
TOTAL       14.60107      109.09068       47.93035        .55309

POOLED WITHIN-GROUPS COVARIANCE MATRIX WITH        52 DEGREES OF FREEDOM

          NSUN          NHEAD          NDROP          NAREA
NSUN     140.6375
NHEAD   -443.0003       9635.083
NDROP    133.1690      -1656.542       1769.001
NAREA     1.725592      -4.407186       11.81048       .3030180

POOLED WITHIN-GROUPS CORRELATION MATRIX

          NSUN          NHEAD          NDROP          NAREA
NSUN     1.00000
NHEAD    -.37667       1.00000
NDROP     .26691       -.40722        1.00000
NAREA     .26433       -.08073         .51012        1.00000
CORRELATIONS WHICH CANNOT BE COMPUTED ARE PRINTED AS 99.0.
```

```
SAMPLE DISCRIMINANT ANALYSIS 3 FOR BROOKS RANGE                                          61
FILE      NONAME    (CREATION DATE =  81/02/09.)
SUBFILE   SED            GRANIT

- - - - - - - - - - - - - - - - - - - - -   D I S C R I M I N A N T   A N A L
ON GROUPS DEFINED BY SUBFILE

ANALYSIS NUMBER          1
DIRECT METHOD-  ALL VARIABLES PASSING THE TOLERANCE TEST ARE ENTERED.
     MINIMUM TOLERANCE LEVEL..................   .00100
CANONICAL DISCRIMINANT FUNCTIONS
     MAXIMUM NUMBER OF FUNCTIONS..............   1
     MINIMUM CUMULATIVE PERCENT OF VARIANCE...   100.00
     MAXIMUM SIGNIFICANCE OF WILKS  LAMBDA....   1.0000

PRIOR PROBABILITY FOR EACH GROUP IS  .50000

                                           CANONICAL DISCRIMINANT FUNCTIONS

                        PERCENT OF  CUMULATIVE    CANONICAL  -   AFTER
FUNCTION  EIGENVALUE     VARIANCE     PERCENT    CORRELATION -  FUNCTION

   1*        1.46718     100.00       100.00      .7711543   :     0
    * MARKS THE   1 FUNCTION(S) TO BE USED IN THE REMAINING ANALYSIS.

    WILKS  LAMBDA  CHI-SQUARED   D.F.  SIGNICANCE
    : .4053210      45.154        4       .0000

STANDARDIZED CANONICAL DISCRIMINANT FUNCTION COEFFICIENTS
               FUNC  1

NSUN           .62388
NHEAD        -.52452
NORCF        -.90868
NAREA          .11568

CANONICAL DISCRIMINANT FUNCTIONS EVALUATED AT GROUP MEANS (GROUP CENTROIDS)
   GROUP       FUNC   1

     1          .60119
     2        -2.35069
```

Appendix G (continued).

```
/PROBLEM    TITLE IS 'BROOKS RANGE VARIABLES'.
/INPUT      VARIABLES ARE 10.
            FORMAT IS '(A4,8(F5.1,3X),F5.1)'.
/VARIABLE   NAMES ARE ID,HEADINCL,HEADMAX,SUNHR,SUNENER,HEADEXP,
            NLOSIZE,ICESLOPE,ELADROP,EXPANICE.
            LABELS ARE ID.
/END
```

CASE NO.										
1	MS	13.1	24.2	14.5	94.0	150.	2.55	10.	40.	23.
2	MS	10.0	23.0	18.7	97.5	150.	1.08	10.	50.	74.
3	MS	11.6	24.5	18.3	87.4	60.	0.24	16.	45.	80.
4	MS	16.3	26.5	14.2	84.9	20.	0.34	18.	60.	35.
5	MS	10.4	25.0	20.4	96.6	30.	0.62	10.	55.	29.
6	MS	13.0	25.5	16.3	87.1	10.	1.00	22.	70.	32.
7	MS	19.3	29.5	14.5	90.4	10.	0.61	18.	40.	33.
8	MS	13.6	27.0	16.2	95.0	100.	0.49	13.	55.	48.
9	MS	12.7	25.0	16.9	88.3	40.	0.66	17.	65.	17.
10	MS	9.3	23.5	21.6	97.5	40.	0.64	20.	100.	31.
11	MS	9.0	21.0	22.1	98.8	40.	0.68	18.	80.	55.
12	MS	6.5	16.5	22.3	100.0	50.	0.87	14.	65.	28.
13	MI	18.7	37.5	14.5	85.8	100.	0.54	12.	185.	38.
14	MI	22.0	36.0	12.2	80.3	180.	0.62	21.	95.	48.
15	MI	20.2	36.5	14.7	89.4	100.	0.97	22.	165.	80.
16	MGS	17.6	34.5	12.9	83.9	40.	0.75	20.	105.	40.
17	MGS	16.1	30.5	13.3	91.8	250.	1.04	12.	25.	51.
18	MGS	16.0	27.0	12.9	87.7	215.	0.52	11.	65.	79.
19	MGS	19.5	31.0	13.5	82.0	180.	0.53	12.	40.	51.
20	MGS	20.9	31.0	8.6	66.1	240.	0.54	11.	75.	86.
21	MGS	16.1	31.5	15.2	81.7	210.	0.19	17.	40.	73.
22	MGS	13.3	23.0	16.7	94.2	160.	0.47	14.	75.	52.
23	MGS	17.9	33.5	12.7	79.2	120.	0.05	30.	35.	67.
24	MGS	16.5	33.0	12.1	84.7	180.	0.20	23.	70.	166.
25	MGS	22.7	34.5	12.1	82.1	230.	0.32	23.	70.	82.
26	MGS	16.9	30.0	12.4	83.5	120.	0.71	14.	95.	31.
27	MGS	19.3	35.0	8.3	62.3	50.	0.36	14.	35.	44.
28	MGS	18.0	26.5	12.8	88.7	120.	0.59	20.	125.	26.
29	MGS	20.	29.0	9.5	75.4	150.	0.51	22.	125.	31.
30	MGS	17.5	25.5	14.5	90.1	100.	1.03	17.	140.	32.
31	MGS	16.1	28.0	15.7	69.6	200.	0.71	17.	80.	69.
32	MGS	17.1	30.5	13.4	80.5	100.	0.49	13.	55.	48.
33	MGS	19.8	31.0	10.5	79.9	10.	0.46	20.	115.	24.
34	MGS	19.6	33.5	12.0	84.5	150.	0.62	19.	100.	48.
35	MGS	20.3	36.5	13.1	82.7	100.	0.04	26.	30.	100.
36	MGS	13.9	24.5	14.9	92.0	100.	1.23	15.	120.	34.
37	MRS	13.5	24.5	15.9	87.7	100.	1.65	13.	165.	46.
38	MGS	19.0	29.3	10.8	78.6	100.	0.70	14.	115.	54.
39	MGS	20.7	35.5	13.5	76.8	100.	0.24	17.	55.	70.
40	MGI	27.6	52.0	8.2	61.4	180.	0.62	21.	120.	48.
41	MGI	25.6	49.5	8.7	52.2	150.	0.97	22.	160.	80.
42	MGI	23.6	37.0	13.2	84.6	425.	0.74	14.	90.	250.
43	MGI	24.2	42.0	3.3	65.1	300.	3.25	15.	235.	70.
44	MGI	26.4	42.0	6.6	53.2	150.	0.55	20.	165.	57.
45	MGI	23.6	45.5	7.6	52.3	425.	0.23	24.	55.	155.
46	MGI	26.1	52.5	7.4	48.1	250.	0.75	15.	120.	67.
47	RGS	19.9	31.5	13.2	84.4	250.	1.23	9.	95.	37.
48	RGS	19.9	29.0	8.7	70.9	150.	0.43	13.	0.	71.
49	RGS	19.9	32.0	14.3	89.5	200.	0.09	14.	20.	400.
50	RGS	17.4	33.0	14.0	87.1	200.	0.06	18.	35.	100.
51	RGS	17.7	32.5	11.8	82.4	300.	0.45	12.	40.	400.
52	RGS	21.9	33.5	7.5	57.5	420.	0.33	9.	40.	267.
53	RGS	17.5	24.2	11.7	82.5	30.	1.21	10.	60.	37.
54	RGI	24.6	47.5	4.8	29.2	450.	0.28	14.	20.	210.

DATA FOR CLUSTER ANALYSIS 1 OF ALL GLACIAL LANDFORMS

MS, MGS, RGS are sedimentary terrain glacial deposits.

MI, MGI, RGI are granitic terrain glacial deposits.

MRS is Twin Glacier.

Appendix G (continued).

CLUSTER ANALYSIS 1: See Table 11.

VARIABLE NAME	NO.	OTHER BOUNDARY OF CLUSTER	NUMBER OF ITEMS IN CLUSTER	DISTANCE OR SIMILARITY WHEN CLUSTER FORMED
HEADINCL	2	5	9	29.51
HEADMAX	3	2	2	55.04
HEADEXP	6	10	2	64.69
EXPANICE	10	2	4	71.23
ICESLOPE	8	2	5	58.66
NEDSIZE	7	9	2	73.76
ELADROP	9	2	7	51.33
SUNHR	4	5	2	93.51
SUNENER	5	2	9	29.51

CLUSTER ANALYSIS 2: See Table 12.

VARIABLE NAME	NO.	OTHER BOUNDARY OF CLUSTER	NUMBER OF ITEMS IN CLUSTER	DISTANCE OR SIMILARITY WHEN CLUSTER FORMED
HEADINCL	2	6	7	41.55
HEADMAX	3	2	2	73.37
LAT	7	2	3	54.05
EXPOSURE	5	2	4	51.81
SUNHR	4	6	3	63.45
SUNENER	6	4	2	84.31
ALTITUDE	8	2	7	41.55

Appendix G (continued).

DATA FOR CLUSTER ANALYSIS 2
ON PERIGLACIAL LANDFORMS

```
/PROBLEM    TITLE IS 'SLD          PERIGLACIAL VARIABLES'.
/INPUT      VARIABLES ARE 8.
            FORMAT IS '(A4,5(5X,F4.1),5X,F6.3,5X,F5.0)'.
/VARIABLE   NAMES ARE ID,HEADINCL,HEADMAX,SUNHR,
            EXPOSURE,SUNENER,LAT,ALTITUDE.
            LABELS ARE ID.
/END
```

TRGI	15.1	25.5	15.7	100.	92.2	66.120	1260.
TRGA	19.5	34.5	11.0	104.	85.9	66.132	1585.
TRGA	21.0	34.0	14.1	97.0	89.2	66.203	1400.
TRGI	19.3	39.5	11.1	100.	69.4	66.205	1620.
TRGI	24.6	41.5	8.10	99.0	50.1	66.040	1295.
LRGA	11.7	30.5	16.6	95.0	92.4	66.132	1660.
LRGA	15.0	28.0	14.4	95.0	87.6	66.127	1430.
LRGA	20.4	37.0	11.3	94.0	67.0	66.132	1645.
LRGA	19.7	33.5	12.9	102.	84.4	66.122	1660.
LRGA	17.4	36.0	14.9	95.0	88.0	66.118	1570.
LRGA	19.1	35.0	13.6	94.0	69.5	66.112	1700.
LRGA	20.6	38.0	11.9	102.	73.9	66.117	1720.
LRGA	17.3	30.5	10.3	102.	82.0	66.142	1200.
LRGA	15.5	30.5	16.3	95.0	91.7	66.168	1080.
LRGA	16.0	35.0	13.3	102.	64.4	66.207	1740.
LRGA	22.0	41.0	10.9	94.0	54.9	66.220	1495.
LRGA	23.1	43.5	9.40	95.0	44.2	66.221	1350.
LRGA	16.7	30.5	10.0	102.	75.9	66.223	1050.
LRGA	17.5	36.5	10.7	102.	79.5	66.213	1000.
LRGA	20.5	39.5	9.10	102.	68.5	66.363	1430.
LRGA	18.1	33.0	12.6	106.	92.4	66.303	1645.
LRGA	15.9	35.0	17.1	95.0	92.5	66.328	1630.
LRGA	14.5	32.5	16.1	94.0	87.9	66.229	1830.
LRGA	21.2	33.5	14.9	95.0	83.2	66.220	1450.
LRGP	20.3	40.5	12.6	107.	96.5	66.132	1525.
LRGP	16.4	34.0	16.0	95.0	89.5	66.133	1400.
LRGP	18.2	39.0	11.4	102.	86.7	66.136	1200.
LRGP	19.6	38.5	9.40	102.	74.2	66.140	1230.
LRGP	18.5	36.5	8.60	102.	71.3	66.147	1200.
LRGP	18.2	36.0	8.80	102.	72.0	65.150	1140.
LRGP	17.9	36.0	9.90	102.	75.0	66.158	1115.
LRGP	14.9	33.0	11.6	102.	82.3	66.168	1080.
LRGP	16.3	36.0	8.50	102.	73.1	66.225	1050.
LRGP	20.3	42.5	7.50	94.0	53.6	66.262	1525.
LRGI	13.9	31.0	12.3	109.	97.0	66.102	1130.
LRGI	19.5	38.5	14.9	95.0	89.0	66.097	1200.
LRGI	15.9	32.0	10.9	104.	85.3	66.106	1190.
LRGI	18.2	30.0	11.9	103.	90.2	66.125	1310.
LRGI	18.8	35.5	13.7	104.	96.6	66.123	1370.
LRGI	19.2	38.5	13.8	107.	99.6	66.132	1460.
LRGI	20.4	36.5	12.7	86.0	75.8	66.125	1420.
LRGI	19.5	35.5	10.0	104.	78.4	66.130	1500.
LRGI	22.2	39.0	12.8	107.	74.9	66.123	1420.
LRGI	18.2	37.0	8.80	102.	69.0	66.145	1230.
LRGI	19.5	39.0	9.20	102.	74.6	66.127	1310.
LRGI	20.2	36.0	10.8	102.	79.5	66.132	1290.
LRGI	18.0	35.5	12.0	88.0	75.3	66.133	1250.
LRGI	16.3	36.0	11.6	100.	84.0	66.145	1190.
LRGI	19.6	36.0	11.4	103.	88.1	66.217	1705.
LRGI	20.5	33.5	13.9	106.	94.7	66.223	1340.
LRGI	24.6	37.5	6.50	104.	60.6	66.215	1220.
LRGI	18.9	34.0	9.10	100.	72.4	66.260	1570.
LRGI	21.0	33.5	11.8	106.	88.4	66.662	1525.
C	20.9	30.5	11.7	99.0	81.3	66.042	1480.
C	22.0	33.5	11.2	99.0	79.7	66.126	1450.
C	17.4	30.5	13.7	100.	66.6	66.117	1000.
C	17.3	33.0	15.9	99.0	88.8	66.338	1690.
C	21.0	32.0	13.3	99.0	81.7	66.042	1450.
C	21.6	31.0	9.70	95.0	68.7	66.035	1370.
C	22.8	35.0	10.7	100.	73.8	66.045	1365.
VH	12.4	23.5	14.4	102.	94.4	66.066	1160.
VH	18.3	27.0	11.1	99.0	82.7	66.173	1360.
V	24.6	37.5	6.50	99.0	56.8	66.215	1220.
V	21.6	31.5	8.00	99.0	65.4	66.363	1400.

Appendix G (continued).

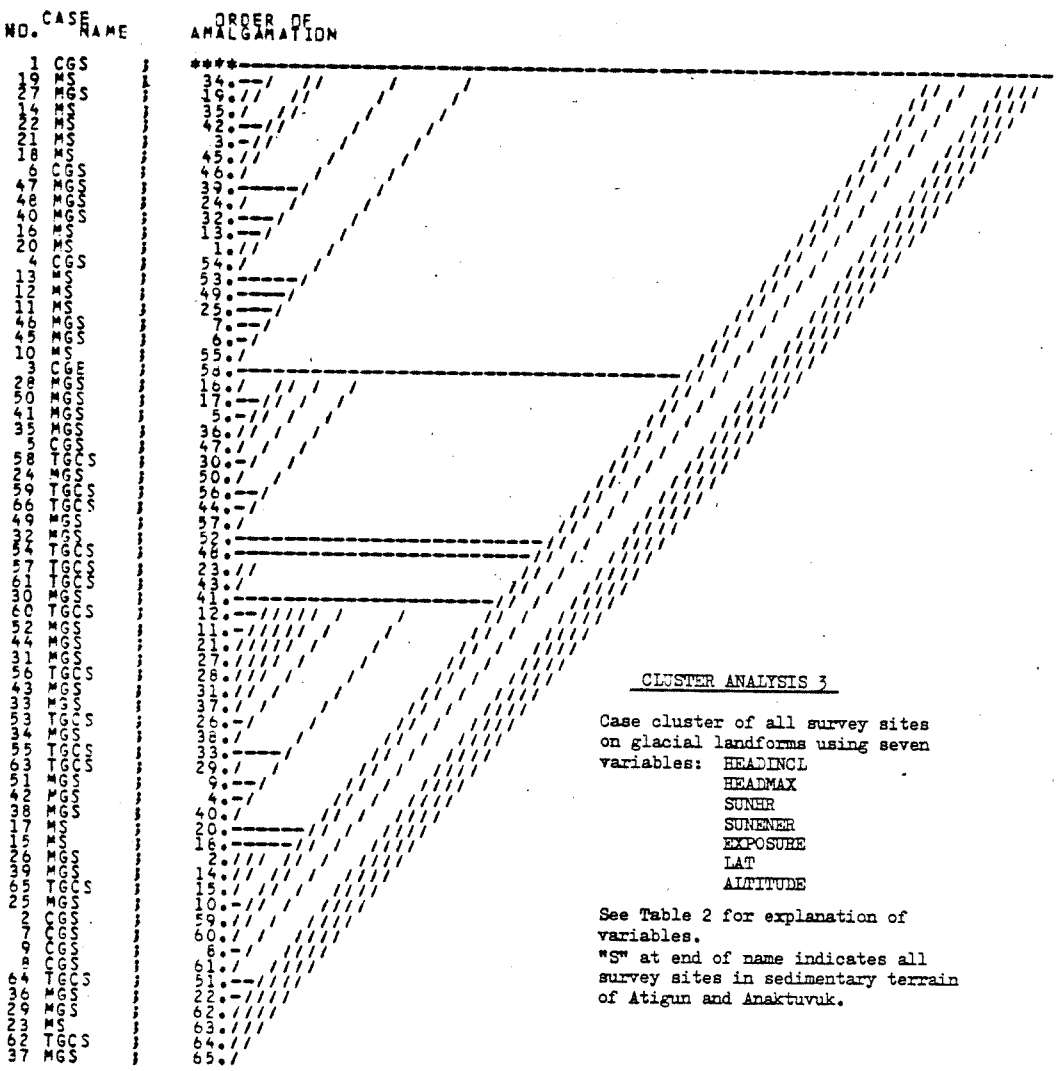

Appendix G (continued).

TREE PRINTED OVER CORRELATION MATRIX (SCALED 0-100).
CLUSTERING BY AVERAGE DISTANCE METHOD.

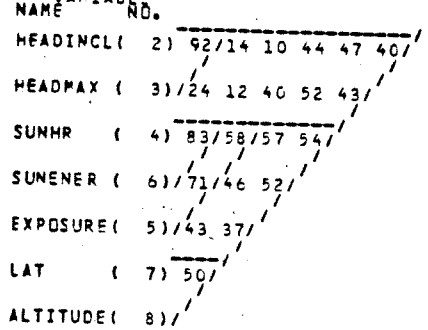

CLUSTER ANALYSIS 3

Variable cluster on all survey sites on glacial landforms in sedimentary terrain using seven variables.

See Table 2 for explanation of variable names.

THE VALUES IN THIS TREE HAVE BEEN SCALED 0 TO 100 ACCORDING TO THE FOLLOWING TABLE

VALUE ABOVE	CORRELATION	VALUE ABOVE	CORRELATION
0	-1.000	50	.000
5	-.900	55	.100
10	-.800	60	.200
15	-.700	65	.300
20	-.600	70	.400
25	-.500	75	.500
30	-.400	80	.600
35	-.300	85	.700
40	-.200	90	.800
45	-.100	95	.900

NAME	VARIABLE NO.	OTHER BOUNDARY OF CLUSTER	NUMBER OF ITEMS IN CLUSTER	DISTANCE OF SIMILARITY WHEN CLUSTER FORMED
HEADINCL	2	8	7	32.98
HEADMAX	3	2	2	92.73
SUNHR	4	8	5	48.72
SUNENER	6	4	2	83.57
EXPOSURE	5	4	3	65.09
LAT	7	8	2	50.56
ALTITUDE	8	2	7	32.98

Appendix G (continued).

```
/PROBLEM    TITLE IS 'SED GLA-PERIGLA CASE CLUSTER'.
/INPUT      VARIABLES ARE 8.
            FORMAT IS '(A4,5(5X,F4.1),5X,F6.3,5X,F5.0)'.
/VARIABLE   NAMES ARE ID, HEADINCL, HEADMAX, SUNHR,
            EXPOSURE,SCREENER,LAT,ALTITUDE.
            LABELS ARE ID.
/END
```

DATA FOR CLUSTER ANALYSES 3 AND 4 USING 7 OR 5 (delete LAT & ALT) VARIABLES

```
CCSS  11.6  20.0  15.3  100.   95.4  68.145  1750.
CCGS  16.8  29.5  14.2  99.0   63.9  68.112  1660.
CCGG  15.2  29.5  15.2  95.0   84.3  68.112  1620.
CCGG  12.4  26.0  16.0  95.0   87.7  68.113  1760.
CCGG  16.2  33.0  13.5  94.0   73.3  68.338  1400.
CCGG  12.7  25.0  16.2  97.0   90.7  68.344  1675.
CCGG  18.0  30.5  22.5  97.0   83.3  68.333  1800.
CCGG  19.2  34.0  20.7  99.0   78.6  69.397  1460.
CCGG  17.7  35.5  20.1  99.00  82.5  68.377  1435.
CKMS  12.4  26.0  15.6  99.00  95.2  68.135  1570.
CKMS  13.6  22.5  14.1  100.   93.5  68.133  1500.
CKMS  10.3  23.5  18.7  97.0   95.7  68.132  1740.
CKMS  9.60  22.5  18.8  101.   100.   68.132  1450.
CKMS  11.6  24.5  18.3  99.0   87.4  68.113  1700.
CKMS  16.3  26.5  14.2  99.0   84.9  68.170  1720.
CKMS  13.0  25.5  16.3  95.0   87.1  69.267  1770.
CKMS  19.3  29.5  14.5  99.0   90.4  68.265  1720.
CKMS  10.4  25.0  20.4  99.0   98.6  68.260  1615.
CKMS  13.6  27.0  16.2  99.0   92.0  68.325  1800.
CKMS  12.7  25.0  16.9  95.0   88.3  68.342  1740.
CKMS  9.30  23.5  21.6  99.00  97.5  68.337  1815.
CKMS  9.00  21.0  22.1  99.0   96.8  69.336  1645.
CKMS  6.50  16.5  22.3  100.   100.   68.335  1630.
CSSS  17.6  34.5  12.9  94.00  83.4  69.067  1690.
CSSS  16.2  30.5  13.3  99.00  89.8  68.167  1600.
CSSS  16.0  27.0  12.9  99.00  87.7  68.160  1720.
CSSS  13.3  23.0  16.7  99.00  94.2  68.208  1770.
CSSS  16.1  31.5  15.2  94.00  81.7  68.265  1770.
CSSS  20.1  31.0  6.60  95.00  66.1  68.197  1650.
CSSS  19.9  31.0  13.5  99.00  82.0  68.263  1650.
CSSS  17.9  33.5  12.7  99.00  78.2  68.177  1740.
CSSS  16.5  33.0  12.1  101.   64.7  68.208  1750.
CSSS  24.5  36.5  12.7  99.00  82.1  68.215  1600.
CSSS  20.9  32.5  11.5  99.00  82.4  68.217  1510.
CSSS  16.9  30.0  12.4  95.00  83.5  68.256  1680.
CSSS  19.3  35.0  8.30  95.00  62.3  68.257  1650.
CSSS  18.0  26.5  12.8  99.00  86.7  68.287  1660.
CSSS  20.0  29.0  9.50  99.00  75.4  68.288  1660.
CSSS  17.5  25.2  14.5  99.00  90.1  68.260  1690.
CSSS  16.1  23.0  15.7  95.00  89.6  68.267  1675.
CSSS  17.1  30.5  13.4  95.00  80.5  68.328  1740.
CSSS  19.8  31.0  10.5  99.00  79.9  68.343  1660.
CSSS  19.3  33.5  12.0  97.00  82.5  68.317  1600.
CSSS  20.3  36.5  13.1  99.00  82.7  68.145  1690.
CSSS  13.8  25.0  14.5  99.00  91.6  68.146  1620.
CSSS  13.5  24.5  14.9  99.00  92.0  68.257  1550.
CSSS  13.5  22.0  16.6  97.00  91.9  68.353  1660.
CSSS  12.5  25.5  16.7  97.00  87.7  68.357  1585.
CSSS  14.5  24.5  14.3  95.00  84.1  68.360  1460.
CSSS  18.3  28.5  11.0  95.00  70.4  68.353  1720.
CSSS  19.7  30.0  10.5  99.00  80.8  68.358  1590.
CSSS  20.7  35.5  13.5  99.00  79.8  68.220  1615.
TGCI  20.1  35.0  12.4  99.00  89.4  68.133  1460.
TGCI  17.4  27.5  13.9  99.00  91.8  68.142  1420.
TGCI  19.9  29.0  8.70  99.00  70.5  68.115  1510.
TGCI  20.5  35.5  15.3  99.00  90.5  68.117  1600.
TGCI  16.3  26.0  13.3  100.   68.5  68.122  1500.
TGCI  19.4  36.5  13.5  95.00  87.2  68.116  1700.
TGCI  15.4  27.0  10.4  95.00  87.1  68.116  1500.
TGCI  20.0  35.0  12.4  99.00  89.4  68.265  1550.
TGCI  15.4  30.00  11.2  99.00  77.5  68.190  1400.
TGCI  26.6  41.0  3.30  99.00  29.2  68.193  1600.
TGCI  17.4  27.00  10.3  99.0   79.2  68.202  1525.
TGCI  21.6  33.0  8.30  95.00  64.6  68.210  1430.
TGCI  17.4  25.0  11.4  99.00  85.4  68.340  1680.
TMII  17.1  26.0  11.1  95.00  78.7  68.343  1550.
TMII  22.0  36.0  12.2  99.00  80.3  67.382  1250.
TMII  18.7  37.5  14.6  99.0   63.2  67.405  1300.
TMII  20.2  36.5  14.7  100.   69.4  67.382  1250.
TMGI  23.6  37.0  13.2  99.00  84.6  67.405  1500.
TMGI  23.4  41.0  10.1  99.00  75.1  67.395  1280.
TMGI  24.9  43.0  6.40  99.00  55.2  67.406  1035.
TMGI  26.4  42.0  6.00  95.00  53.2  67.403  1190.
TMGI  23.6  45.5  7.80  99.0   56.3  67.400  1360.
TMGI  27.5  52.0  6.20  99.00  61.4  67.380  1300.
TMGI  25.6  46.5  6.70  95.00  52.2  67.383  1130.
TMGI  26.1  52.5  7.40  95.00  46.1  67.382  1220.
TGCI  35.4  50.5  1.50  99.00  1.00  67.403  1270.
TGCI  23.7  44.0  8.40  99.0   57.4  67.415  1000.
```

Appendix G (continued).

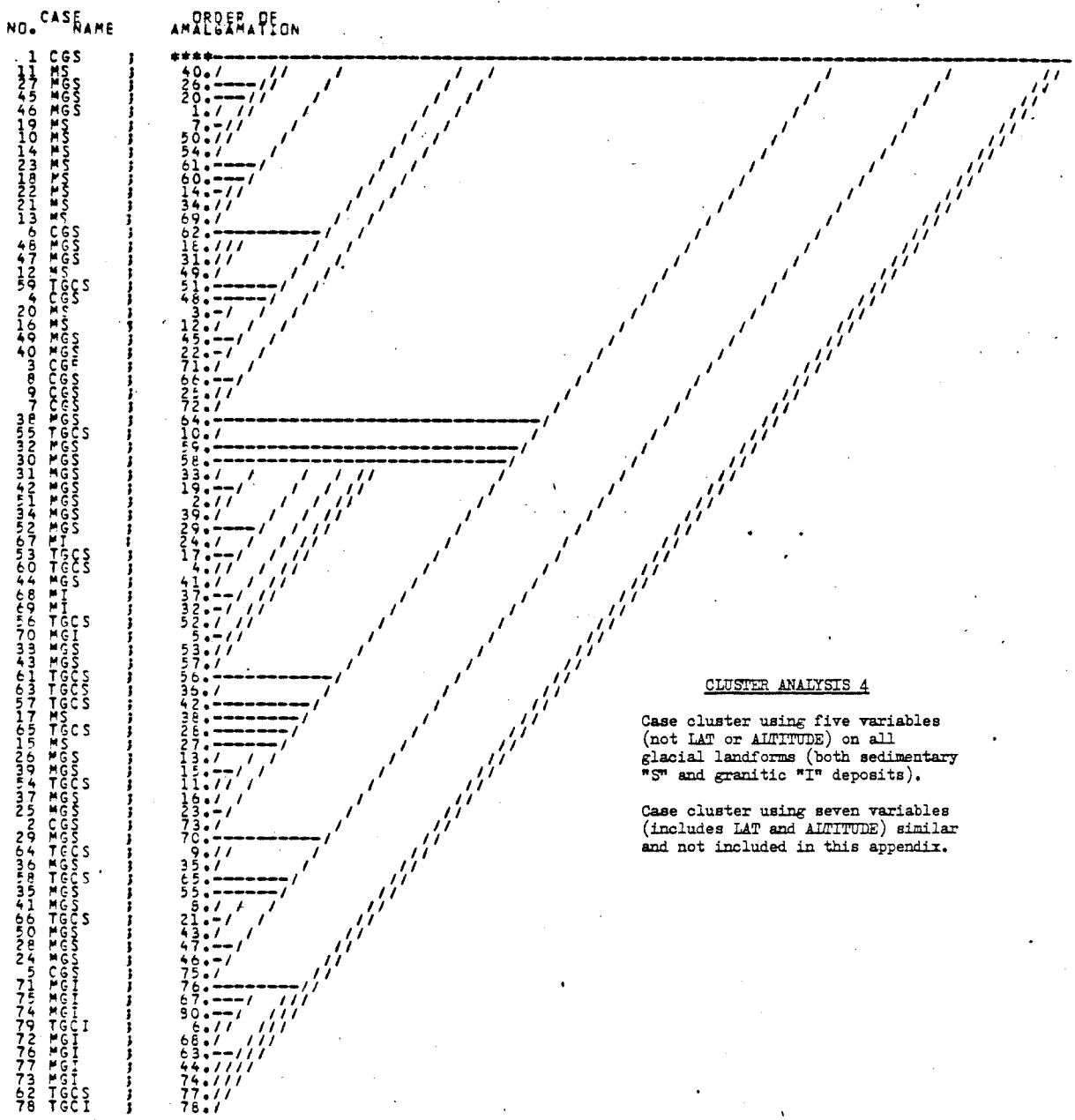

Appendix G (continued).

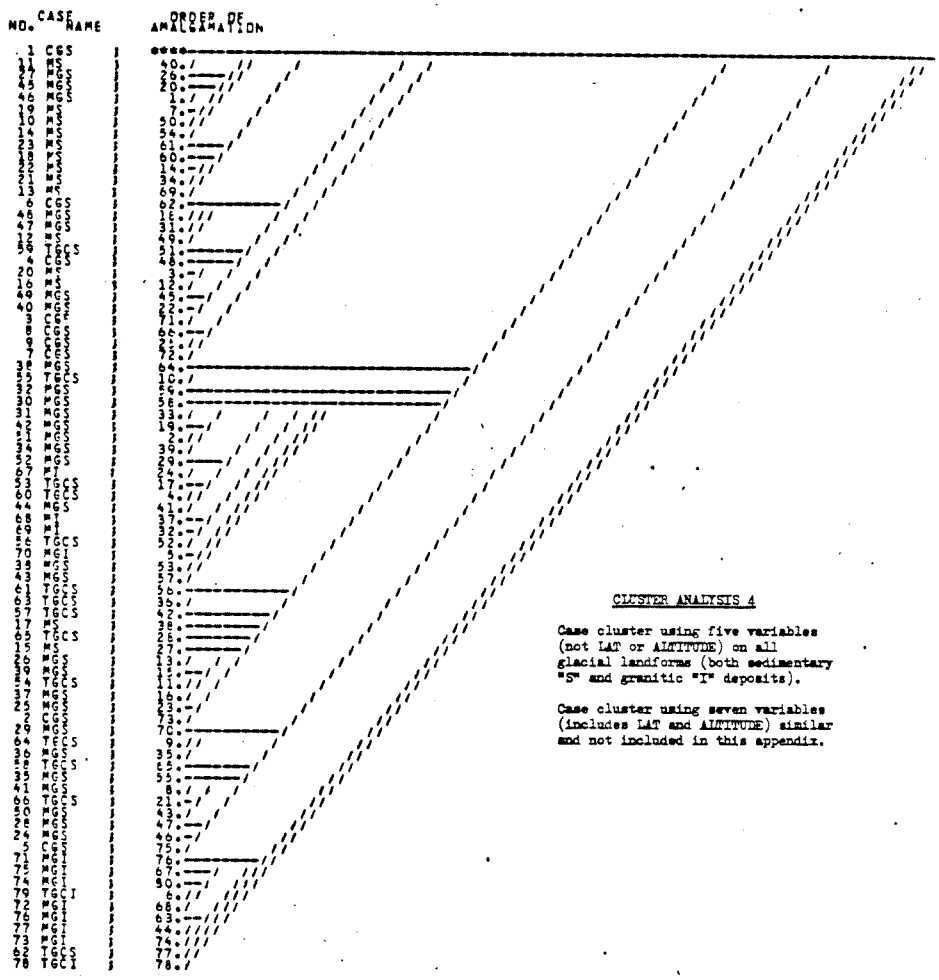

TREE PRINTED OVER CORRELATION MATRIX (SCALED 0-100).
CLUSTERING BY AVERAGE DISTANCE METHOD.

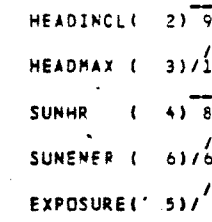

CLUSTER ANALYSIS 4

Variable cluster using five variables on all glacial landforms in both sedimentary and granitic terrain.

Case cluster included in this appendix.

See Table 2 for variable explanation.

THE VALUES IN THIS TREE HAVE BEEN SCALED 0 TO 100
ACCORDING TO THE FOLLOWING TABLE

VALUE ABOVE	CORRELATION	VALUE ABOVE	CORRELATION
0	-1.000	50	.000
5	-.900	55	.100
10	-.800	60	.200
15	-.700	65	.300
20	-.600	70	.400
25	-.500	75	.500
30	-.400	80	.600
35	-.300	85	.700
40	-.200	90	.800
45	-.100	95	.900

NAME	VARIABLE NO.	OTHER BOUNDARY OF CLUSTER	NUMBER OF ITEMS IN CLUSTER	DISTANCE OR SIMILARITY WHEN CLUSTER FORMED
HEADINCL	2	5	5	21.56
HEADMAX	3	2	2	95.08
SUNHR	4	5	3	63.31
SUNENER	6	4	2	89.35
EXPOSURE	5	2	5	21.56

TREE PRINTED OVER CORRELATION MATRIX (SCALED 0-100).
CLUSTERING BY AVERAGE DISTANCE METHOD.

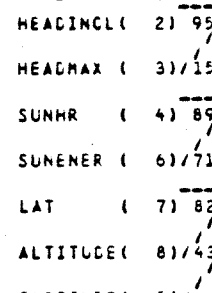

CLUSTER ANALYSIS 4

Variable cluster using seven variables on all glacial landforms in both sedimentary and granitic terrain.

Case cluster not included in this appendix.

See Table 2 for variable explanation.

THE VALUES IN THIS TREE HAVE BEEN SCALED 0 TO 100
ACCORDING TO THE FOLLOWING TABLE

VALUE ABOVE	CORRELATION	VALUE ABOVE	CORRELATION
0	-1.000	50	.000
5	-.900	55	.100
10	-.800	60	.200
15	-.700	65	.300
20	-.600	70	.400
25	-.500	75	.500
30	-.400	80	.600
35	-.300	85	.700
40	-.200	90	.800
45	-.100	95	.900

NAME	VARIABLE NO.	OTHER BOUNDARY OF CLUSTER	NUMBER OF ITEMS IN CLUSTER	DISTANCE OR SIMILARITY WHEN CLUSTER FORMED
HEADINCL	2	5	7	20.93
HEADMAX	3	2	2	95.08
SUNHR	4	5	5	53.79
SUNENER	6	4	2	89.35
LAT	7	6	2	82.44
ALTITUDE	8	4	4	74.24
EXPOSURE	5	2	7	20.93

TREE PRINTED OVER CORRELATION MATRIX (SCALED 0-100).
CLUSTERING BY AVERAGE DISTANCE METHOD.

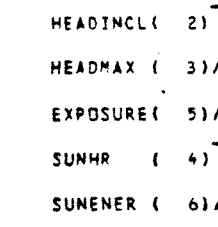

CLUSTER ANALYSIS 5

Variable cluster of all survey sites (143) on glacial and periglacial landforms in the central Brooks Range using five variables.

Case cluster not included. Landforms intermixed except for MS and MGI deposits.

See Table 2 for variable explanation.

THE VALUES IN THIS TREE HAVE BEEN SCALED 0 TO 100
ACCORDING TO THE FOLLOWING TABLE

VALUE ABOVE	CORRELATION	VALUE ABOVE	CORRELATION
0	-1.000	50	.000
5	-.900	55	.100
10	-.800	60	.200
15	-.700	65	.300
20	-.600	70	.400
25	-.500	75	.500
30	-.400	80	.600
35	-.300	85	.700
40	-.200	90	.800
45	-.100	95	.900

NAME	VARIABLE NO.	OTHER BOUNDARY OF CLUSTER	NUMBER OF ITEMS IN CLUSTER	DISTANCE OR SIMILARITY WHEN CLUSTER FORMED
HEADINCL	2	6	5	26.99
HEADMAX	3	2	2	91.31
EXPOSURE	5	2	3	53.01
SUNHR	4	6	2	86.63
SUNENER	6	2	5	26.99

TREE PRINTED OVER CORRELATION MATRIX (SCALED 0-100).
CLUSTERING BY AVERAGE DISTANCE METHOD.

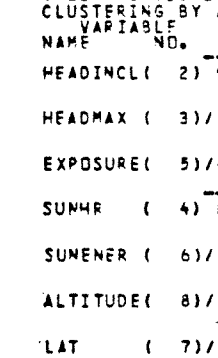

CLUSTER ANALYSIS 5

Variable cluster of all survey sites (143) on glacial and periglacial landforms in the central Brooks Range using seven variables.

Case cluster not included. Landforms intermixed except for Arrigetch ("I") and "MS" deposits.

See Table 2 for variable explanation.

THE VALUES IN THIS TREE HAVE BEEN SCALED 0 TO 100
ACCORDING TO THE FOLLOWING TABLE

VALUE ABOVE	CORRELATION	VALUE ABOVE	CORRELATION
0	-1.000	50	.000
5	-.900	55	.100
10	-.800	60	.200
15	-.700	65	.300
20	-.600	70	.400
25	-.500	75	.500
30	-.400	80	.600
35	-.300	85	.700
40	-.200	90	.800
45	-.100	95	.900

NAME	VARIABLE NO.	OTHER BOUNDARY OF CLUSTER	NUMBER OF ITEMS IN CLUSTER	DISTANCE OR SIMILARITY WHEN CLUSTER FORMED
HEADINCL	2	7	7	29.76
HEADMAX	3	2	2	91.31
EXPOSURE	5	2	3	53.01
SUNHR	4	7	4	65.74
SUNENER	6	4	2	86.63
ALTITUDE	8	4	3	72.09
LAT	7	2	7	29.76

APPENDIX H. SOILS DATA

A location map of soil sample sites in the Atigun Pass area and soil profile descriptions are provided; soil profiles are correlated with the estimated age of the surface (0 to 12,500 yr B.P.). The soil profiles are formatted as follows:

Soil Profile No.

1. Geographic position.

2. Physiographic position; altitude (a.s.l.)

3. Drainage

4. Vegetation cover.

5. Estimated age of surface as determined from lichenometry, horizontal stratigraphy, and other relative dating techniques (Appendix I) or extrapolated from radiocarbon dates on late Pleistocene moraines (Hamilton, 1979b).

6. Parent bedrock of till.

7. Remarks.

8. Profile description

Horizon	Depth (cm)	Description

The profile descriptions are organized as follows: color (dry and moist); texture; consistence (dry, moist, wet); pH; K, N, P; effervesence with dilute HCl; miscellaneous data; horizon boundary. Soil pH, potassium (K), nitrogen (N), and Phosphorous (P) tests were made in the field with simple chemical kits and color charts to determine their relative dating potential. The K, N, and P determinations were made at only six sites spanning 12,500 years; no detectable

change was noted.

Terminology for the soil profile descriptions was derived from the Soil Conservation Service Soil Survey Staff (1975), except for "Cox" and "Cn" (see Fig. 37 for definitions). There is not enough laboratory data to justify using the "Seventh Approximation" soil taxonomy nomenclature (order, suborder, and great group) for these soil profiles. However, it appears most Neoglacial soils on the cirque moraines are Pergelic cryorthents (Soil Survey Staff, 1975, p. 196), those on early Holocene rock glacier lobes are Pergelic cryochrepts (Soil Survey Staff, 1975, p. 247-248), and those at lower elevations and on late Pleistocene moraines are perhaps best described as Pergelic cryochrepts or Pergelic cryoborolls (Everett and Parkinson, 1977). Those late Pleistocene moraines south of the Continental Divide and Atigun Pass and on the West Fork North Fork Chandalar Shelf may be Pergelic cryoborolls with calcic horizons (soil sites 6, 7).

The bedrock parent material of the till was determined from Brosgé and others (1979) and field observations. The bedrock map units noted in the following soil profiles are partially described by Brosgé as follows:

Hunt Fork Shale (Upper Devonian)

Dhw — Wacke member - mostly (50 to 80 percent) grayish green, brown and black micaceous manganiferous clay shale and shaley siltstone. Interbedded with limonitic quartzitic and quartz-chert wacke; green fine-grained wacke.

Dhs — Shale member - dark-gray to medium gray, fissile, lam-

inated clay shale and slate, silty shale and slate, and micaceous sandstone. Interbedded with as much as 25 percent brown-weathering and orange-weathering sandstone.

Kanayut Conglomerate (Upper Devonian)

Dkm — Mostly gray- to rusty orange-weathering conglomerate, quartzite, and sandstone; units of shale, siltstone, and impure sandstone.

Dks — Mostly shale, shaley siltstone, and thin-bedded sandstone and quartzite; minor conglomerate.

Dkls — Mostly (60 to 80 percent) red, grayish green and manganiferous brown shale containing thin beds of sandstone.

Dkss — Generally brown and gray weathering, thin, tabular-bedded, slightly calcareous limonitic sandstone, interbedded with black shale and ironstone.

Kayak Shale (Mississippian)

Mk — Mostly black, fissile clay shale and silty shale.

Lisburne Group, Undivided (Pennsylvannian and Mississippian)

IPMl — Gray limestone and dolomite, shaley limestone, nodular chert.

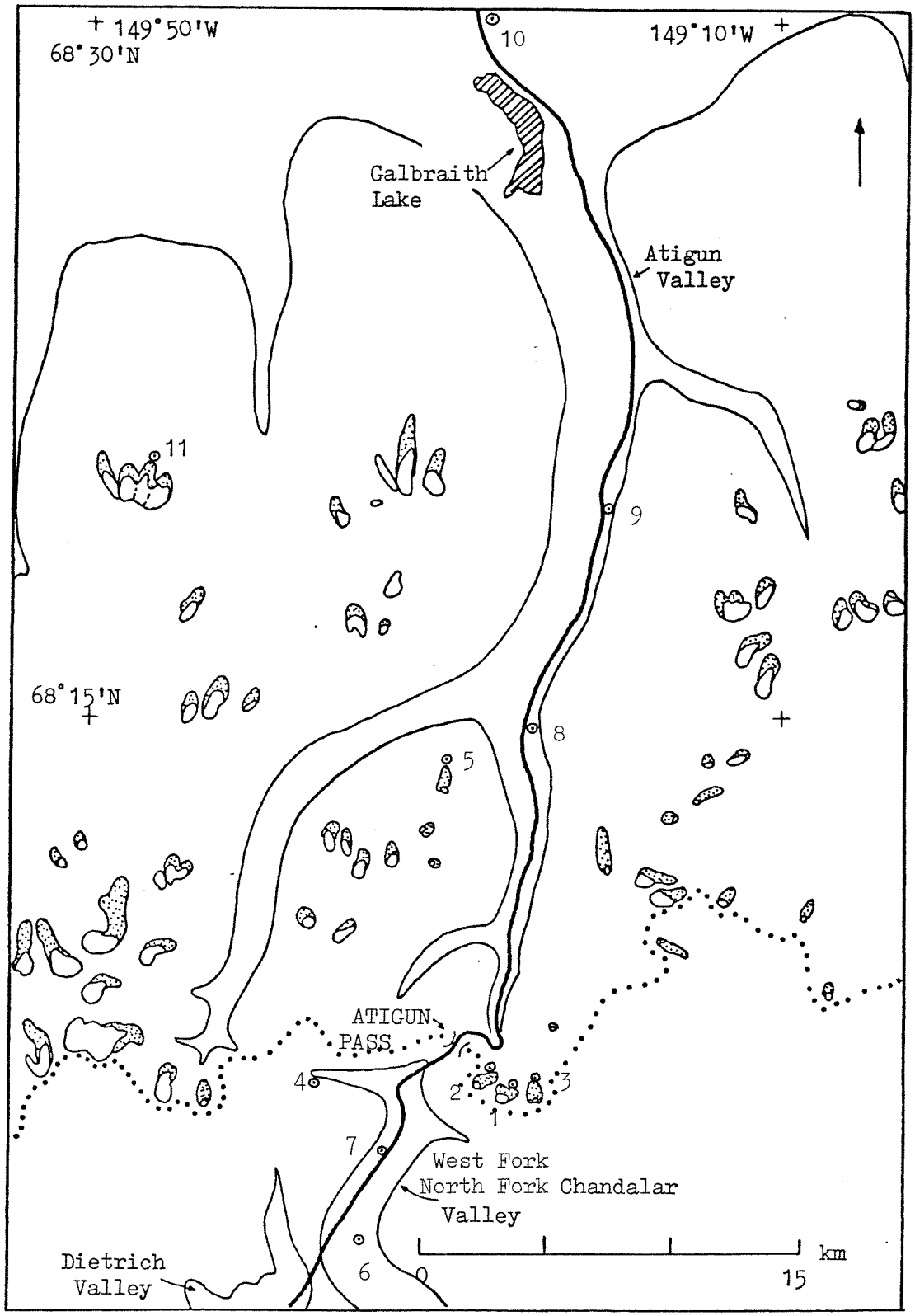

Appendix H. Location map of soil pits.

APPENDIX H.

Soil Profile 1a

1. Grizzly Glacier, youngest Neoglacial debris.
2. Crest of bouldery transverse ridge (unstable glacier-cored), 4 m from the ice margin; 1720 m.
3. well drained.
4. none
5. till from Dkm.
6. <10 years.
7. Site analyzed at 10 cm depth by Ellis (1978, Appendices A-E, Sample site 1) and Bruen (1980); frost churning of ridge witnessed since summer of 1977; broken, angular sandstone clasts common.
8. Profile Description:

Horizon	Depth (cm)	Description
Cn	0 - >20	Light olive brown (2.5Y 5/4), moist (2.5 Y 5/4); stoney sandy loam, sand 75%, fines 25%; hard (dry), friable (moist), slightly sticky and non plastic (wet); pH = 7.7; High K, very low N, low P; very slight effervescence.

Soil Profile 1b

1. Grizzly Glacier, youngest Neoglacial debris.
2. Crest of bouldery ridge; 10 m from ice margin; 1720 m.
3. well drained.
4. none.
5. till from Dkm; most clasts have rusty orange surfaces from iron oxidation (Brosgé and others, 1979).
6. <10 years.
7. none.
8. Profile Description.

Horizon	Depth (cm)	Description
Cn	0 - >20	Light yellowish brown (2.5Y 6/4), moist (2.5Y 6/6); stoney sandy loam, sand 69%, fines 31%; hard (dry), friable (moist), slightly sticky and non plastic (wet); pH = 6.2.

Soil Profile 1c

1. Grizzly Glacier; youngest Neoglacial debris.
2. crest of glacier-cored, bouldery ridge; 10 m from ice margin; 1720 m.
3. well drained.
4. none.
5. till from Dhs.
6. <10 years.
7. none.
8. Profile description:

Horizon	Depth (cm)	Description
Cn	0 - >20	Gray (2.5Y 5/0), moist (2.5Y 4/0); stoney sandy loam, sand 75%, fines 25%; very hard (dry), friable (moist), slightly sticky and slightly plastic (wet); pH = 7.6.

Soil Profile 1d

1. Grizzly Glacier; oldest Neoglacial ridge.
2. crest of stable, bouldery ridge; 1710 m.
3. well drained.
4. lichens, sedges, mosses, grasses.
5. till from Dkm, Dhs.
6. ~2000 lichenometric years.
7. abundant shale/phyllite clasts throughout profile.
8. Profile description:

Horizon	Depth (cm)	Description
O1	2 - 0	Organic mat
Cox	0 - 21	Light yellowish brown (2.5Y 6/4), moist (10YR 5/2); stoney loamy sand, sand 68%, fines 32%; friable (moist), slightly sticky and non plastic (wet); pH = 6.0; slight effervescence on undersides of clasts where caliche build-up evident; clear wavy boundary.
Cn	21 - >30	Olive (5Y 5/3), moist (5Y 5/1); stoney loamy sand, sand 68%, fines 32%; slightly hard (dry), loose (moist), non sticky and non plastic (wet); pH = 7.5; high K, very low N, low P.

Soil Profile 2a

1. Pika Rock Glacier (glacier-cored) headward supraglacial debris.
2. Debris layer <0.5 m thick over ice core; 1635 m.
3. moderately well drained.
4. none.
5. talus from Dkm headwall.
6. <10 years.
7. none.
8. Profile description:

Horizon	Depth (cm)	Description
Cn	0 - >20	Grayish brown (2.5Y 5/2), moist (2.5Y 4/2); stoney sandy loam, sand 76%, fines 24%; slightly hard (dry), very friable (moist), slightly sticky and non plastic (wet); pH = 7.9.

Soil Profile 2b

1. Pika Rock Glacier (glacier-cored); highest Neoglacial ridge.
2. crest of transverse bouldery ridge; 1640 m.
3. well drained.
4. sparse lichen cover.
5. till of Dkm.
6. ~400 lichenometric years.
7. eluviation or periglacial sorting may occur from 3 to 11 cm depth as little matrix is evident. Cox sample from 15 cm depth.
8. Profile description:

Horizon	Depth (cm)	Description
01	1 - 0	Organic mat.
Cox	0 - 18	Grayish brown (2.5Y 5/2), moist (5Y 4/2); stoney sandy loam, sand 69%, fines 31%; slightly hard (dry), very friable (moist); slightly sticky and slightly plastic (wet); pH = 6.6; gradual broken boundary.
Cn?	18 - >32	Grayish brown (2.5Y 5/2), moist (5Y 5/2); stoney sandy loam, sand 73%, fines 27%; slightly hard (dry), very friable (moist), slightly sticky and slightly plastic (wet); pH = 7.3.

Soil Profile 2c

1. Pika Rock Glacier (glacier-cored) downslope debris snout.
2. crest of subdued ridge; 4 m upslope of active rock glacier front; 1500 m.
3. well drained.
4. lichens, mosses, grasses, sedges.
5. till from Dkm.
6. ~8000 years?
7. Surface has subtle relief; boulders ~50% buried; Cn sample obtained 3 m below crest of rock glacier front in unweathered debris.
8. Profile description.

Horizon	Depth (cm)	Description
01	4 - 0	Organic mat; granules sorted underneath flat cobbles and boulders.
A	0 - 17	Brown (10YR 5/3), moist (10YR 4/3); stoney sandy loam, sand 66%, fines 34%; hard (dry), friable (moist), sticky and slightly plastic (wet); pH = 6.4; gradual wavy boundary.
Cox	17 - >55	Grayish brown (10YR 5/2), moist (5Y 4/2); stoney sandy loam, sand 68%, fines 32%; slightly hard (dry), friable (moist), slightly sticky and slightly plastic (wet); pH = 6.8; no effervescence.
Cn	~300	Grayish brown (10YR 5/2), moist (10YR 4/1); stoney sandy loam, sand 74%, fines 26%; slightly hard (dry), friable (moist), slightly sticky and slightly plastic (wet); pH = 7.8.

Soil Profile 3a

1. Jaeger Rock Glacier (glacier-cored) supraglacial debris near headwall.
2. Less than 0.5 m thick debris layer on glacier core; 1645 m.
3. well drained.
4. none.
5. talus accumulations from Dhs headwall.
6. <10 years.
7. sample was saturated in the field.
8. Profile description:

Horizon	Depth (cm)	Description
Cn	0 - >15	Dark gray (10YR 4/1), moist (10YR 4/1); stoney sandy loam, sand 64%, fines 36%; slightly hard (dry), friable (moist), slightly sticky and slightly plastic (wet); pH = 7.5.

Soil Profile 3b

1. Jaeger Rock Glacier (glacier-cored) highest Neoglacial ridge.
2. crest of bouldery transverse ridge; 1645 m.
3. well drained.
4. sparse lichen cover, thin moss mat.
5. ~400 lichenometric years.
6. till from Dhs.
7. none.
8. Profile description:

Horizon	Depth (cm)	Description
01	1 - 0	Organic mat.
Cox	0 - 4	Grayish brown (10YR 5/2), moist (7.5YR 3/1); stoney sandy loam, sand 59%, fines 41%; slightly hard (dry), friable (moist), slightly sticky and slightly plastic (wet); pH = 6.8; limonitic coatings on some clasts; gradual broken boundary.
Cn	4 - >40	Dark brown (10YR 4/1), moist (7.5YR 3/0); stoney sandy loam, snad 65%, fines 35%; slightly hard (dry), firm (moist), slightly sticky and slightly plastic (wet); pH = 7.8.

Soil Profile 3c

1. Jaeger Rock Glacier (glacier-cored) most distal ridge in transition zone.
2. crest of transverse ridge; 1630 m.
3. well drained.
4. lichens, mosses, sedges.
5. ~2000 lichenometric years.
6. till from Dhs.

7. Boulders ~40% buried; exposed boulder corners rounded; only tough sandstone/conglomerate boulders evident on surface.
8. Profile description:

Horizon	Depth (cm)	Description
01	2.5 - 0	Organic mat.
A	0 - 6.5	Grayish brown (10YR 5/2), moist (7.5YR 3/2); stoney sandy loam, sand 62%, fines 38%; soft (dry), friable (moist), slightly sticky and plastic (wet); pH = 6.2; abundant roots; abrupt smooth boundary.
Cox	6.5 - 38	Gray (10YR 5/1), moist (10YR 4/1); stoney sandy loam, sand 64%, fines 36%; slightly hard (dry), friable (moist), sticky and plastic (wet); pH = 6.8; underneath some cobbles are concentrations of granules (periglacial sorting?); diffuse, wavy boundary.
Cn or IICox	38 - >68	Gray (10YR 5/1), moist (10YR 4/1); stoney sandy clay loam, sand 58%, fines 42%; very hard (dry), friable (moist), sticky and plastic (wet); pH = 7.0; saturated.

Profile 3d

1. Jaeger Rock Glacier (glacier-cored) downslope debris snout.
2. crest of transverse ridge; 7 m upslope of active front; 1525 m.
3. well drained.
4. lichens, mosses, grasses, and sedges.
5. till from Dhs.
6. ~8000 years?
7. Sandstone/conglomerate stones extensive on surface, but Dhs shale/phyllite material dominates soil pit; Cn sample obtained ~35 m below downslope crest of rock glacier front inside meltwater tunnel.
8. Profile description:

Horizon	Depth (cm)	Description
01	3.5 - 0	Organic mat

(continued)

A	0 - 9	Brown (10YR 5/3), moist (10YR 3/2); stoney sandy loam, sand 58%, fines 42%; firm (moist), sticky and plastic (wet); pH = 6.4; no effervescence; diffuse broken boundary.
B	9 - 52	Grayish brown (2.5Y 5/2), moist (2.5Y 4/1); stoney sandy loam, sand 52%, fines 48%; firm (moist), very sticky and very plastic (wet); pH = 7.5; slight effervescence on undersides of cobbles and pebbles; roots present; diffuse wavy boundary.
Cox	52 - >80	Grayish brown (10YR 5/2), moist (7.5YR 4/0); stoney sandy clay loam, sand 72%, fines 38%; slightly hard (dry), firm (moist), slightly sticky and plastic (wet); pH = 7.5; no effervesence.
Cn	~3500	Grayish brown (10YR 5/2), moist (10YR 4/1); stoney sandy clay loam, sand 61%, fines 39%; slightly hard (dry), firm (moist), slightly sticky and plastic (wet); pH = 8.0.

Soil Profile 4

1. Spider tongue-shaped rock glacier (inactive) downslope debris snout.
2. Crest of stoney ridge; 1250 m.
3. well drained.
4. Dryus-lichen community.
5. Diamicton from Dhs; platey sandstone cobbles dominate surface.
6. ~9000 years?
7. Profile may be missing the A horizon due to deflation (sequence may be O1-A-Cox or O1-B-Cox?)
8. Profile description:

Horizon	Depth (cm)	Description
O1	4 - 0	Organic mat
A or B	0 - 19	Yellowish brown (10YR 5/4), moist (10YR 3/4); stoney sandy loam, sand 65%, fines 35%; soft (dry), firm (moist), sticky and plastic (wet); pH = 4.8; gradual wavy boundary.

(continued)

Cox	19 - >75	Brown (10YR 5/3), moist (10YR 3/3); stoney sandy loam, sand 75%, fines 25%; slightly hard (dry), firm (moist), slightly sticky and slightly plastic (wet); pH = 6.4 at 45 cm, pH = 6.7 at 75 cm; no effervesence; clasts oxidized throughout, corners rounded.

Soil Profile 5a

1. Parka Squirrel Rock Glacier (glacier-cored) supraglacial debris on ice core near headwall.
2. Debris layer <0.8 m thick; site near glacier bergshrund; 1615 m.
3. Well drained.
4. none
5. till from MK and Dkm.
6. ~10 years.
7. none
8. Profile description:

Horizon	Depth (cm)	Description
Cn?	0 - >20	Gray (10YR 5/1), moist (2.5Y 4/2); stoney sandy loam, sand 77%, fines 23%; soft (dry), firm (moist), non-sticky and non plastic (wet); pH = 6.9; may be slightly weathered talus from headwall.

Soil Profile 5b

1. Parka Squirrel Rock Glacier (glacier-cored) Neoglacial lateral ridge in transition zone.
2. Crest of lateral bouldery ridge; 1600 m.
3. well drained.
4. sparse lichen cover, some moss.
5. Till from Dkm and MK.
6. ~400 lichenometric years.
7. Adjacent to outermost lateral ridge of transition zone (soil profile 5c); site analyzed at 10 cm depth by Ellis (1978, Appendix A, sample site 9).
8. Profile description:

Horizon	Depth (cm)	Description
Cox	0 - 10	Brown (10YR 5/3), moist (2.5Y 3/2); stoney sandy loam, sand 74%, fines 26%; slightly hard (dry), firm (moist), nonsticky and nonplastic (wet); pH = 7.7; gradual irregular boundary.
Cn	10 - >50	Grayish brown (10YR 5/2), moist (5Y 3/2); stoney sandy loam, sand 75%, fines 25%; slightly hard (dry), firm (moist), nonsticky and nonplastic (wet); pH = 8.0.

Soil Profile 5c

1. Parka Squirrel Rock Glacier (glacier-cored) outermost Neoglacial lateral ridge.
2. crest of bouldery ridge; 1600 m.
3. well drained.
4. lichens, mosses, sedges, and grasses.
5. till from Dkm and MK.
6. ~2500 lichenometric years
7. Adjacent to ~400 year old ridge (soil profile 5b); site analyzed at 10 cm depth by Ellis (1978, Appendices A-E, Sample site 8).
8. Profile description:

Horizon	Depth (cm)	Description
01	3 - 0	Organic mat.
A	0 - 10	Brown (10YR 5/3), moist (2.5Y 4/2); stoney sandy loam, sand 61%, fines 39%; soft (dry), firm (moist), slightly sticky and plastic (wet); pH = 6.4; gradual irregular boundary.
Cox	10 - >50	Grayish brown (10YR 5/2), moist (10YR 3/2); stoney sandy loam at 20 cm: sand 68%, fines 32%, slightly hard (dry), firm (moist), slightly sticky and slightly plastic (wet); stoney sandy loam at 50 cm: sand 65%, fines 35%; hard (dry), firm (moist) slightly sticky and slightly plastic; pH = 7.7.

Soil Profile 5d

1. Parka Squirrel Rock Glacier (glacier-cored) downslope debris snout.
2. Crest of stable ridge ~20 m upslope of active rock glacier front; 1400 m.
3. well drained.
4. lichens, mosses, grasses, sedges.
5. till from Dkm and MK.
6. ~8000 years?
7. grab sample.
8. Profile description:

Horizon	Depth (cm)	Description
01	3 - 0	Organic mat.
A	0 - >15	Grayish brown (10YR 5/2), moist (2.5Y 5/2); stoney sandy loam, sand 65%, fines 35%; slightly hard (dry), friable (moist); slightly sticky and plastic; pH = 6.8; frost heaving marked at surface.

Soil Profile 6

1. N.F.W.F. Chandalar River latest Itkillik (late Pleistocene) medial (?) moraine.
2. Crest of ~60 m high ridge; 1000 m.
3. well drained.
4. Dryus-lichen community.
5. till from Dkm and Dhs.
6. ~12,500 years.
7. site dug in middle of non sorted polygon.
8. Profile description:

Horizon	Depth (cm)	Description
01	3 - 0	Organic mat.
A	0 - 6	Dark yellowish brown (10YR 3/4), moist (10YR 3/3); stoney sandy loam, sand 76%, fines 24%; soft (dry), firm (moist), nonsticky and slightly plastic (wet); pH = 6.2 at 4 cm, pH = 5.3 at 7.5 cm; soil more basic near roots; ~20% of horizon organic roots; abrupt smooth boundary.

(continued)

B	6 - 23	Light yellowish brown (10YR 6/4), moist (10YR 5/4); stoney sandy loam, sand 68%, fines 32%; slightly hard (dry), firm (moist), slightly sticky and slightly plastic (wet); pH = 5.0; gradual wavy boundary.
Cca	23 - >50	Light brownish gray (10YR 6/2), moist (2.5Y 4/2); stoney sandy clay loam, sand 63%, fines 37%; hard (dry), friable (moist), sticky-very sticky and plastic (wet); pH = 6.7; caliche increases with depth.

Soil Profile 7

1. N.F.W.F. Chandalar River latest Itkillik ground drift near inactive pingo (10 m east of TAPS haul road).
2. Crest of washed (?) till mound that stands ~1 m above surroundings; 1000 m.
3. well drained.
4. Dryus-lichen community.
5. till from Dkm and Dhs.
6. ~12,500 years
7. Lower limit of caliche ~110 cm; section exposed along west bank of river.
8. Profile description:

Horizon	Depth (cm)	Description
01	3.5 - 0	Organic mat.
A	0 - 6	Yellowish brown (10YR 5/4), moist (10YR 4/2); stoney sandy loam, sand 56%, fines 44%; soft (dry), friable (moist), slightly sticky and plastic (wet); pH = 5.3; gradual broken boundary.
B	6 - 20	Light yellowish brown (10YR 6/4), moist (10YR 5/6); stoney sandy loam, sand 67%, fines 33%; soft (dry), friable (moist), slightly sticky and slightly plastic (wet); pH = 5.4; gradual wavy boundary.

(continued)

Cca	20 - 110	Light yellowish brown (10YR 6/4), moist (10YR 5/6); caliche build-up on undersides of cobbles and pebbles; strongly effervescent; clear wavy boundary.
Cox	110 - >140	Gray (10YR 5/1), moist (5Y 4/1); stoney loamy sand, sand 85%, fines 15%; slightly hard (dry), loose (moist), nonsticky and nonplastic (wet); pH = 7.7; silt coatings on granules.

Soil Profile 8

1. Till mounds at confluence of East- and West-Atigun River.
2. Crest of 4 m-high mounds; 900 m.
3. well drained.
4. Dryus-lichen community, grasses, some willow shrubs.
5. till from Dkm, Dhs, Dhw.
6. ~12,500 years.
7. Conglomerate boulders ~50% buried below surface; chert pebbles etched to ~5 mm relief; corners of exposed and buried boulders rounded; see Ellis (1978) Appendices A and E, sample site 15).
8. Profile description:

Horizon	Depth (cm)	Description
01	6 - 0	Organic mat.
A	0 - 24	Yellowish brown (10YR 5/4), moist (10YR 4/3); stoney sandy loam, sand 61%, fines 39%; soft (dry), firm (moist), slightly sticky and slightly plastic (wet); pH = 5.4; high K, very low N, low P; high organic content; abrupt smooth boundary.
B	24 - 53	Brown-dark brown (7.5YR 4/4), moist (10YR 5/2); stoney sandy loam, sand 55%, fines 45%; soft (dry), firm (moist), sticky and plastic (wet); pH = 5.2; pH increases to 6.8 near roots; roots to 56 cm depth; gradual irregular boundary.

(continued)

Cca	53 - >90	Pale brown (10YR 6/3), moist (10YR 4/1?); stoney sandy loam, sand 57%, fines 43%; slightly hard (dry), firm (moist), sticky and very plastic; pH = 6.8; caliche on undersides of cobbles.

Soil Profile 9

1. Latest Itkillik lateral moraine along base of east wall of Atigun valley
2. Site along crest, section exposed due to slumping; 885 m.
3. well drained topographically but water ponded on ridge.
4. tussocks, willow shrubs.
5. till largely derived from red shale/siltstone units associated with massive marker bed (Dkmm) of Dkm member which forms valley wall.
6. ~12,500 years.
7. Dkmm crops out above this site giving pronounced red color; site analyzed at 10 cm depth by Ellis (1978, Appendices A-E, sample site 12).
8. Profile description:

Horizon	Depth (cm)	Description
O1	7 - 0	Organic mat.
A	0 - 23	Reddish brown (2.5YR 5/4), moist (2.5YR 4/4); stoney sandy loam, sand 52%, fines 48%; hard (dry), friable (moist), sticky and plastic (wet); granular structure; pH = 6.8; gradual wavy boundary.
B2t	23 - 87	Weak red (10R 4/3), moist (10R 4/3); stoney clay, sand 26%, fines 74%; extremely hard (dry), friable (moist), very sticky and very plastic (wet); well-developed prismatic structure; pH = 6.5; limonitic ghosts, oxidation rinds on clasts; slight effervescence, clay skins along ped faces; diffuse broken boundary.
IICox	87 - >160	Reddish brown (5YR 4/3), moist (2.5YR 4/2); stoney sandy clay loam, sand 51%, fines 49%; very hard (dry), friable (moist), slightly sticky and very plastic; pH = 6.8; no effervescence.

Soil Profile 10

1. Latest Itkillik Galbraith Lake end moraine.
2. crest of subdued ridge; 915 m.
3. well drained.
4. Dryus-lichen community
5. till from IPMI, MK, Kanayut Conglomerate and Hunt Fork Shale.
6. ~12,500 years
7. Ridge apparently was washed by meltwater during late Pleistocene deglaciation. Substantial percent of fines in O, A, and B may have been introduced by eolian influx and pedogenic processes. End moraine sampled at 10 cm depth ~100 m west of this site by Ellis (1978, Appendices A-E, sample site 18).
8. Profile description:

Horizon	Depth (cm)	Description
O1	3.5 - 0	Organic mat.
A	0 - 17	Yellowish brown (10YR 5/4), moist (7.5YR 4/4); stoney sandy clay loam, sand 54%, fines 46%; soft (dry), friable (moist), sticky and moist (wet); pH = 4.7; high K, very low N, low P; clear wavy boundary.
ACox	17 - 42	Brown (10YR 5/3), moist (10YR 3/3); stoney sandy loam, sand 71%, fines 29%; soft (dry), firm (moist), slightly sticky and slightly plastic; pH = 5.2; gradual wavy boundary.
Cox	42 - 69	Brown (10YR 5/3), moist (7.5YR 5/2); loamy sand, sand 81%, fines 19%; slightly hard (dry), loose (moist), nonsticky and nonplastic (wet); pH = 6.4; no effervescence; basal portion of washed till?; diffuse smooth boundary.
IICox	69 - >82	Pale brown (10YR 6/3), moist (2.5Y 4/4); stoney sandy clay loam, sand 52%, fines 48%; very hard (dry), firm (moist), sticky and plastic (wet); pH = 6.4; unwashed till?

Soil Profile 11a

1. Triple Glacier Neoglacial end moraine.
2. Crest of ridge; 1800 m.
3. well drained.
4. sparse lichen cover.
5. till from Dkm, red siltstone dominates moraine surface.
6. ~400 lichenometric years.
7. none.
8. Profile description:

Horizon	Depth (cm)	Description
Cox	0 - >15	Weak red (2.5YR 5/2), moist (10R 3/2); stoney sandy clay loam, sand 58%, fines 42%; hard-very hard (dry), firm (moist), sticky and plastic (wet); pH = 6.8; medium K, very low N, very low P.

Soil Profile 11b

1. Thin, latest Itkillik ground drift downslope of Triple Glacier Neoglacial complex.
2. Center of periglacially-sorted terrace; 1750 m.
3. well drained ?
4. Dryus-lichen cover and moss.
5. drift of Dkm.
6. ~12,500 years.
7. grab sample.
8. Profile description:

Horizon	Depth (cm)	Description
01	4 - 0	Organic mat.
A	0 - >12	Light brown (7.5YR 6/4), moist (2.5YR 4/2); stoney clay, sand 36%, fines 64%; very hard (dry), firm (moist), very sticky and very plastic (wet); pH = 5.5; high K, very low N, very low P.

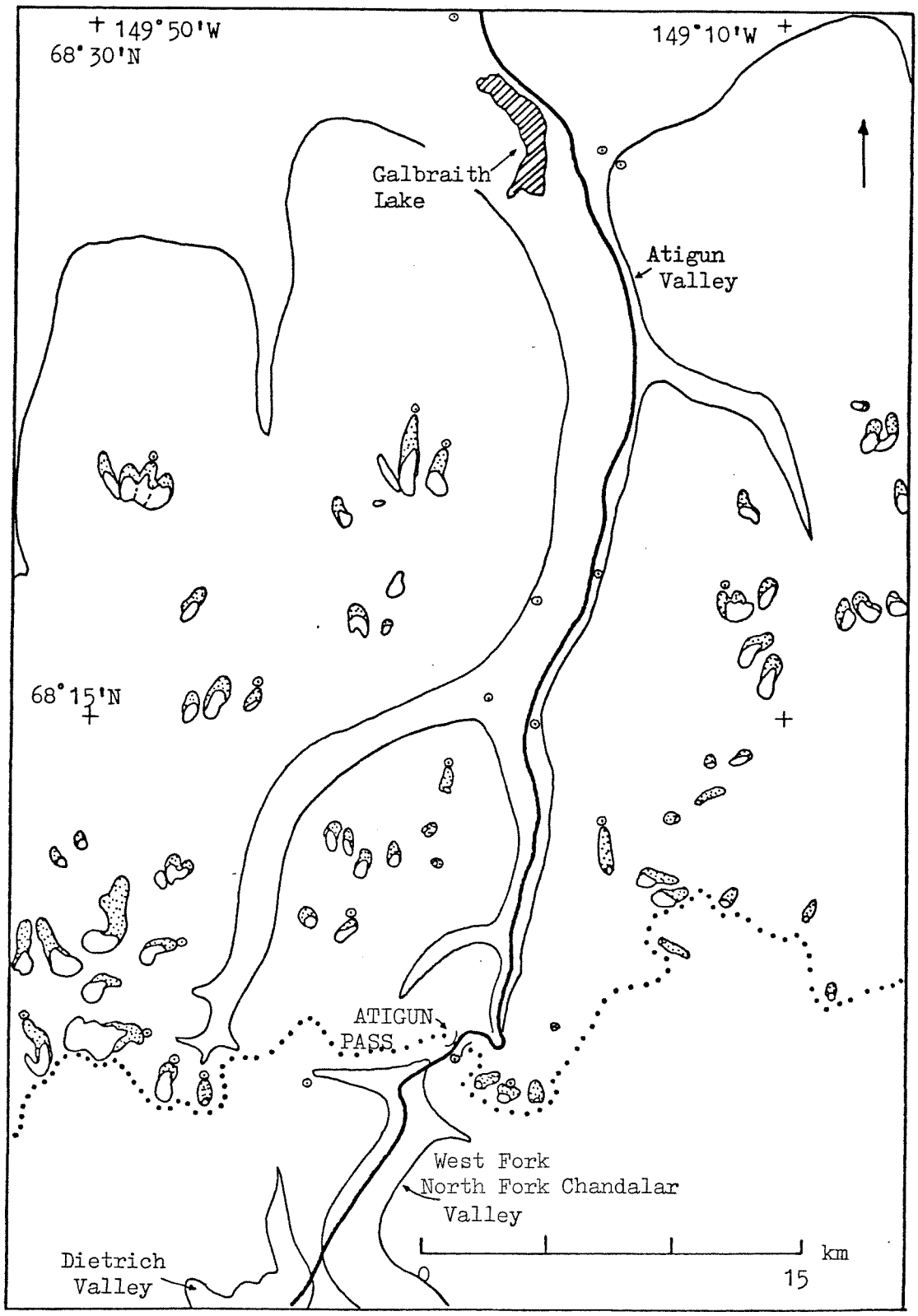

Appendix I. Location map of weathering rind and pebble relief sample sites.

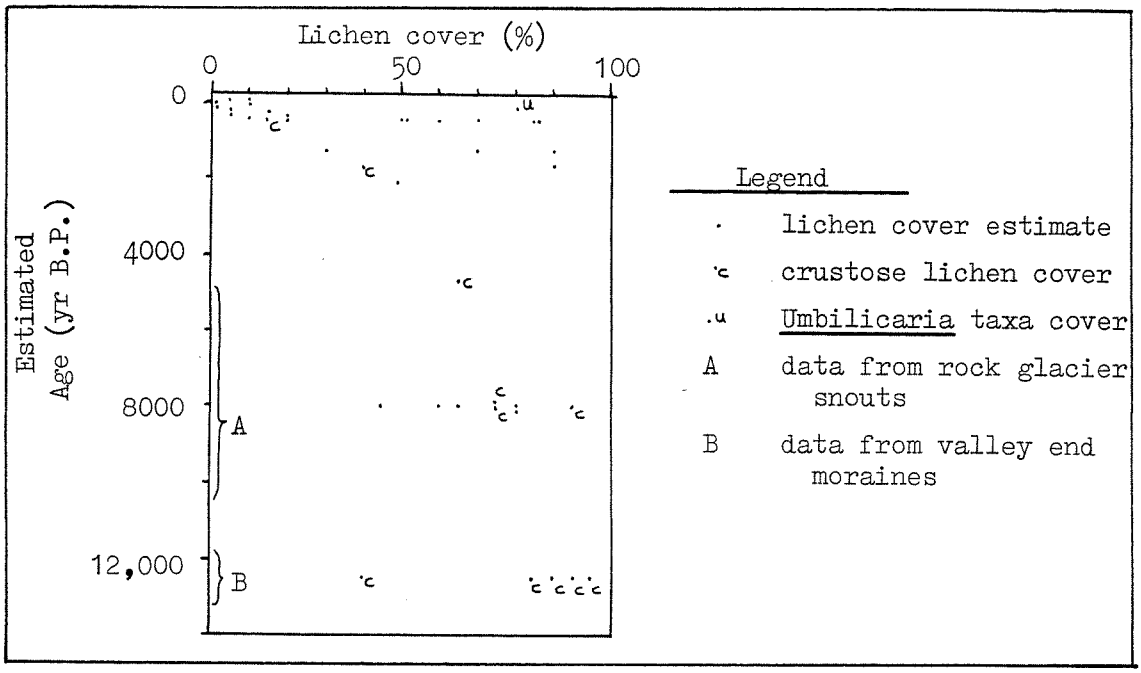

Appendix I. Summation of preliminary lichen cover data from sedimentary terrain of Atigun and Anaktuvuk Passes.

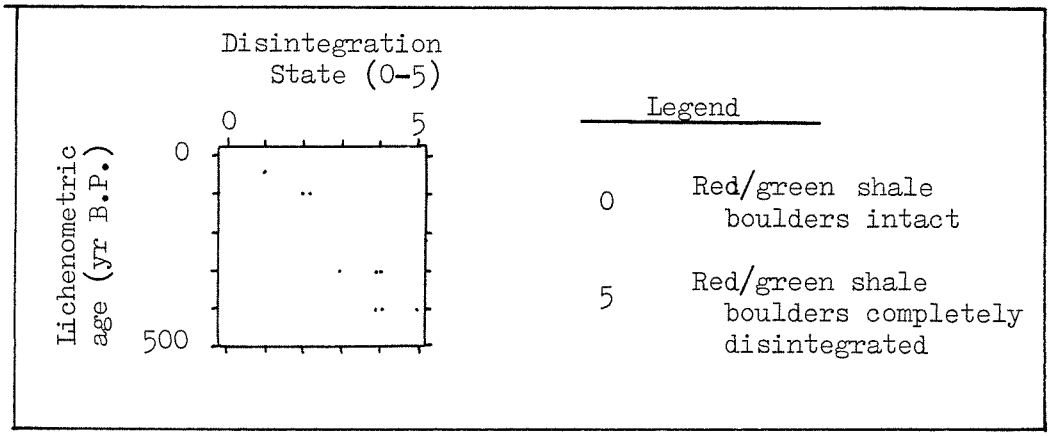

Appendix I. Summation of red and green shale disintegration with time. Shale from the middle member of the Kanayut Conglomerate (Dkm, Brosgé and others, 1979).

APPENDIX J. HORIZON-MEASURING INSTRUMENTATION

Lightness, ease of set-up and take-down, and utilization of equipment normally associated with field work (a Brunton compass and photographic tripod with adjustable legs) are the chief advantages of this horizon-measuring system. It is especially useful where topographic maps are of small scale and not field checked, and information at a specific point or landform is desired. The accompanying diagrams show the components and their assembly on the tripod.

The Brunton compass holder is made from a light sheet of aluminum with three holes (a-c): (a) is for the threaded screw on the tripod platform, (b) allows the user to read the inclination scale when the Brunton is fixed in the holder, and (c) allows the user access to the inclination bubble-adjustment lever on the outside of the Brunton case. At the top of the tripod there must be a threaded bolt in the extension tube that when disassembled provides a site for the azimuth plate to be attached. This thin aluminum plate is scribed at equal intervals through 360° which allows easy computerization of the horizon measurements (10°, 15°, or 20° increments).

This incremented azimuth plate is attached to the tripod and aligned parallel to the Brunton holder. The bubble in the Brunton is next used to set the tripod parallel to the zenith or perpendicular to the horizontal plane. When the extension tube is aligned vertical, the azimuth plate and Brunton holder are aligned north by use of the Brunton magnetic compass. After fixing the orientation of the tripod head, the Brunton can be inserted vertically into the holder.

Appendix J. (continued)

A. Exploded view of components

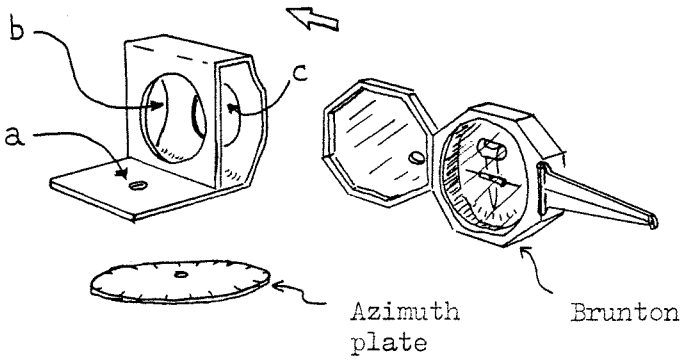

B. Instrument ready for measurements

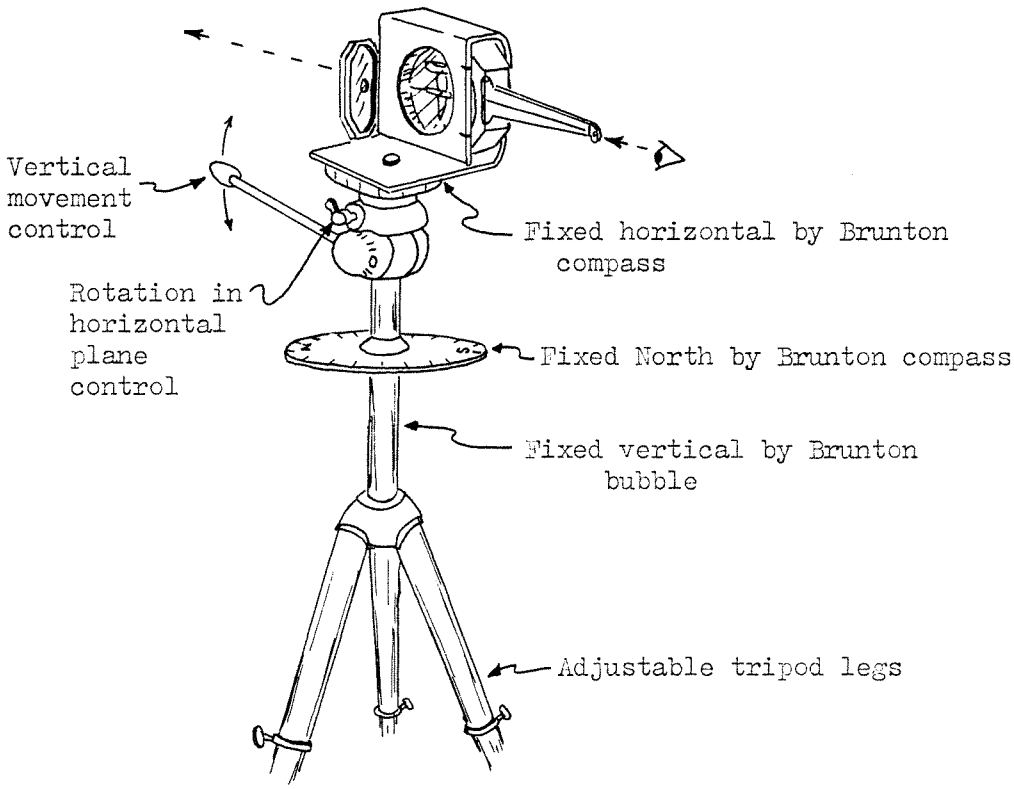

Readings to the surrounding horizon are made by aiming the Brunton toward the top of the horizon, fixing the tripod head, and leveling the bubble and reading the vertical angle by use of the hinged mirror. The first reading will be in the North direction. The large levers and friction action of camera tripod heads make aiming of the Brunton through its sight and opening in the mirror easy, even in inclement weather. The accuracy is largely operator dependent, and compares favorably with theodolite measurements. Readings were made at 0.5° increments in this study for inclinations.

The readings are made through 360° at a uniform interval. One should redo the initial reading at the end of the survey to detect changes in the instrument's alignment and make appropriate corrections. The readings can be plotted in the field on graph paper and this horizon trace superimposed with a chosen solar path to determine time(s) of sunrise(s) and sunset(s); this will give solar duration. The associated energy values for the selected solar path can be tabulated with time during the day (see Appendix F) and these energy values will allow determination of the direct radiation energy received at that survey site while the user is still in the field.

Appendix J. Brunton holder schematic for horizon-measuring instrumentation.